

Vehicle Dynamics

Compendium for Course MMF062

steady state cornering, driver tries to keep constant path radius $\frac{m}{s}$

Parameter	Value
0.1° vehicle YawRate [0.1°deg/s]	16 $\frac{m}{s}$
vehicleSpeed [m/s]	8 $\frac{m}{s^2}$
vehicleLateralAcceleration [m/(s*s)]	6.75 deg
vehicleLongitudinalAcceleration [m/(s*s)]	30 $\frac{deg}{s}$
road wheel steering angle [deg]	5.25 deg

Preface 2015

This edition has various changes and additions. Some of these are: brush model with parabolic pressure distribution, typical numerical data for heavy vehicle, added “2.3.1 Tyre design and function”, “4.5.3.2 (Example of) Explicit form model”, more about tyre relaxation, introduction of neutral steering point, introduction of steady state roll-over wheel lift diagram. Thanks to Anton Albinsson, Edo Drenth (VCC), Gunnar Olsson (LeanNova), Manjurul Islam, Mathias Lidberg, Mats Jonasson (VCC), Niklas Fröjd (Volvo GTT), Ola Benderius, Pär Pettersson, and Zuzana Nedelkova among other.

Bengt Jacobson, Göteborg, 2015

Preface 2014

This edition has various small changes and additions. The largest changes are: Function definitions added and major update of section 1.2, 3.1.1, 4.1.1, 5.1.1.

Thanks to Lars Almfelt from Chalmers, Jan Andersson from VCC, Kristoffer Tagesson from Volvo GTT and Gunnar Olsson from Leannova and Karthik Venkataraman.

Bengt Jacobson, Göteborg, 2014

Preface 2013

This edition has various small changes and additions. The largest additions were in: Functional architecture, Smaller vehicles, Roll-over, Pendulum effect in lateral load transfer and Step steer.

Thanks to Gunnar Olsson from LeanNova, Mathias Lidberg, Marco Dozza, Andrew Dawkes from Chalmers, Erik Coelingh from Volvo Cars, Fredrik Bruzelius from VTI, Edo Drenth from Modelon, Mats Sabelström, Martin Petersson and Leo Laine from Volvo GTT.

Bengt Jacobson, Göteborg, 2013

Preface 2012

A major revision is done. The material is renamed from “Lecture notes” to “Compendium”. Among the changes it is worth mentioning: 1) the chapters about longitudinal, lateral and vertical are more organised around design for vehicle functions, 2) a common notation list is added, 3) brush tyre model added, 4) more organised and detailed about different load transfer models, and 5) road spectral density roughness model is added.

Thanks to Adithya Arikere, John Aurell, Andrew Dawkes, Edo Drenth, Mathias Lidberg, Peter Nilsson, Gunnar Olsson, Mats Sabelström, Ulrich Sander, Simone Sebben, Kristoffer Tagesson, Alexey Vdovin and Derong Yang for review reading.

Bengt Jacobson, Göteborg, 2012

Preface 2011

Material on heavy vehicles is added with help from John Aurell. Coordinate system is changed from SAE to ISO. Minor additions and changes are also done.

Bengt Jacobson, Göteborg, 2011

Preface 2007

This document was developed as a result of the reorganization of the Automotive Engineering Master’s Programme at Chalmers in 2007. The course content has been modified in response to the redistribution of vehicle dynamics and power train education.

These lecture notes are based on the original documents developed by Dr Bengt Jacobson. The text and examples have been reformatted and edited but the author is indebted to the contribution of Dr Jacobson.

Rob Thomson, Gothenburg, 2007

Cover picture, left column, from top: Test of lane change support for combination-vehicle A-double in VTI’s simulator, Chalmers’ Saab93 test vehicle in steady state cornering at AstaZero, and Tilt table test of timber trailer at Volvo GTT.

This compendium is also available as pdf file at <http://pingpong.chalmers.se/public/courseld/5512/lang-en/publicPage.do>.

© Copyright: Chalmers University of Technology, Bengt Jacobson

Contents

1	INTRODUCTION	11
1.1	About this compendium	11
1.2	Attributes and Functions	12
1.2.1	Attributes	12
1.2.2	Functions	14
1.2.2.1	Seeing versus Blind functions	14
1.2.2.2	Dynamic versus Driver-informing functions	15
1.2.2.3	Other categorisations	15
1.2.3	Requirements	16
1.2.4	Models, methods and tools	16
1.3	Technical References	17
1.3.1	Engineering	17
1.3.2	General modelling, drawing and mathematics	17
1.3.3	Notations	20
1.3.4	From general “Mechanical engineering”	24
1.3.4.1	Free-body diagrams	24
1.3.4.2	Operating conditions	25
1.3.5	Verification methods with real vehicles	26
1.3.6	Verification methods involving theoretical simulation	26
1.3.7	Tools & Methods	27
1.3.8	Coordinate Systems	29
1.3.9	Terms with special meaning	32
1.3.10	Architectures	34
1.3.10.1	Reference architecture of vehicle functionality	34
1.4	Heavy truck versus passenger cars	35
1.4.1	General differences	36
1.4.2	Vehicle dynamics differences	36
1.5	Smaller vehicles	36
1.6	Automotive engineering	38
1.7	Typical numerical data	39
1.7.1	For passenger vehicle	39
1.7.2	For heavy vehicle	40
2	VEHICLE INTERACTIONS	43
2.1	Introduction	43
2.2	Introduction to Tyre Terminology	43
2.2.1	Wheel angles	44
2.2.1.1	Steering angle	44
2.2.1.2	Camber (Angle)	44
2.2.1.3	Caster Angle	44
2.2.1.4	Toe Angle	45
2.2.1.5	Steering axis inclination	45
2.3	Tyre Construction	45
2.3.1	Tyre design and function	47

2.4	Longitudinal Properties of Tyres	49
2.4.1	Tyre Rolling and Radii	49
2.4.2	The Rolling Resistance of Tyres	51
2.4.2.1	Variation of rolling resistance	52
2.4.3	Longitudinal forces	55
2.4.3.1	Tyre brush model for longitudinal slip	56
2.4.3.2	Empirical tyre models	60
2.4.3.3	Tyre with both rolling resistance and slip	62
2.4.3.4	Relaxation	63
2.5	Lateral Properties of Tyres	64
2.5.1	Tyre brush model for lateral slip	64
2.5.2	Empirical tyre models	66
2.5.3	Influence of vertical load	67
2.5.4	Relaxation	69
2.5.5	Other effects than lateral force due to lateral slip	69
2.5.5.1	Overturning moment	69
2.5.5.2	Tyre self-aligning moment	70
2.5.5.3	Camber force	70
2.6	Combined Longitudinal and Lateral Slip	71
2.7	Vertical Properties of Tyres	76
2.8	Tyre wear	77
2.9	Vehicle Aerodynamics	77
2.9.1	Longitudinal wind velocity	77
2.9.2	Lateral wind velocity	78
2.10	Driver interactions with vehicle dynamics	78
2.10.1	Open-loop and Closed-loop Manoeuvres	79
2.10.2	Pedals	80
2.10.3	Steering	81
2.11	Traffic interactions with vehicle dynamics	81
3	LONGITUDINAL DYNAMICS	83
3.1	Introduction	83
3.1.1	References for this chapter	83
3.2	Steady State Functions	83
3.2.1	Propulsion System	83
3.2.1.1	Prime movers	84
3.2.1.2	Transmissions	85
3.2.1.2.1	Main transmissions	86
3.2.1.2.2	Distribution transmissions	86
3.2.1.3	Energy buffers	87
3.2.2	Traction diagram	87
3.2.3	Driving Resistance	88
3.2.4	Top speed *	89
3.2.5	Starting with slipping clutch	90
3.2.6	Steady state load distribution	90
3.2.7	Friction limit	91
3.2.8	Uphill performance	92
3.2.8.1	Start-ability *	92
3.2.8.2	Grade-ability *	93
3.2.8.3	Towing capacity *	93

3.3	Functions over longer events	94
3.3.1	Driving cycles	94
3.3.2	Other ways of defining the driving event	96
3.3.2.1	Driving pattern	96
3.3.2.2	Transport task/Operating cycle	96
3.3.3	Rotating inertia effects	97
3.3.4	Traction diagram with deceleration	99
3.3.5	Fuel or energy consumption *	100
3.3.6	Emissions *	103
3.3.7	Tyre wear *	103
3.3.8	Range *	103
3.3.9	Acceleration reserve *	103
3.3.10	Load Transfer, without delays from suspension	104
3.3.11	Acceleration – simple analysis	106
3.3.11.1	Acceleration performance *	106
3.3.11.2	Solution using integration over time	106
3.3.11.3	Solution using integration over speed	108
3.4	Functions in shorter events	108
3.4.1	Typical test manoeuvres	109
3.4.2	Deceleration performance	109
3.4.2.1	Braking efficiency *	109
3.4.2.2	Braking Distance *	109
3.4.2.3	Stopping Distance *	110
3.4.3	(Friction) Brake system	110
3.4.4	Pedal Response *	111
3.4.5	Pedal Feel *	111
3.4.6	Brake proportioning	111
3.4.7	Body heave and pitch due to longitudinal wheel forces	113
3.4.8	Load Transfer including suspension linkage effects	116
3.4.8.1	Load Transfer model with Pitch Centre	117
3.4.8.2	Load Transfer model with Axle Pivot Points	117
3.4.8.3	Steady state heave and pitch due to longitudinal wheel forces	118
3.4.8.4	Examples of real suspension design	119
3.4.8.5	Additional phenomena	119
3.4.9	Dive at braking *	120
3.4.10	Squat at propulsion *	120
3.4.11	Anti-dive and Anti-squat designs	120
3.4.12	Deceleration performance *	121
3.4.13	Acceleration performance *	123
3.5	Control functions	123
3.5.1	Longitudinal Control	123
3.5.2	Longitudinal Control Functions	123
3.5.2.1	Pedal driving *	123
3.5.2.2	Cruise Control and Adaptive Cruise Control (CC and ACC) *	124
3.5.2.3	Anti-lock Braking System, ABS *	124
3.5.2.4	Electronic Brake Distribution, EBD *	125
3.5.2.5	Traction Control, TC *	126
3.5.2.6	Engine Drag Torque Control, EDC *	126
3.5.2.7	Automatic Emergency Brake, AEB *	126
3.5.3	Longitudinal Motion Functionality shown in a reference architecture	128

4 LATERAL DYNAMICS 131

4.1	Introduction	131
-----	--------------	-----

4.1.1	References for this chapter	131
4.2	Low speed manoeuvrability	132
4.2.1	Path with orientation	132
4.2.2	Vehicle and wheel orientations	133
4.2.3	Steering System	133
4.2.3.1	Chassis steering geometry	133
4.2.3.2	Steering system forces	134
4.2.4	One-track models	137
4.2.5	Ideally tracking wheels and axles	139
4.2.6	One-track model for low speeds, with Ackerman geometry	140
4.2.7	Turning circle *	142
4.2.8	Swept path width and Swept Area *	143
4.2.9	Off-tracking *	144
4.2.10	Steering effort *	144
4.2.11	One-track model for low speeds, with non-Ackerman geometry	145
4.2.12	One-track model for low speeds, with trailer	148
4.3	Steady state cornering at high speed	148
4.3.1	Steady state driving manoeuvres	148
4.3.2	Steady state one-track model	150
4.3.2.1	Relation δf , v_x and R	153
4.3.2.2	Relation δf , v_x and β	153
4.3.2.3	Relation v_x , R and β	154
4.3.2.4	Simpler model	154
4.3.3	Under-, Neutral- and Over-steering *	155
4.3.3.1	Understeering as built-in measure	155
4.3.3.2	Understeering as varying with steady state lateral acceleration	156
4.3.3.3	Understeering as variable during a transient manoeuvre	157
4.3.3.4	Neutral steering point	158
4.3.4	How to design for a desired understeer gradient	159
4.3.4.1	Tyre design, inflation pressure and number of tyres	159
4.3.4.2	Roll stiffness distribution between axles	160
4.3.4.3	Steering system compliance	160
4.3.4.4	Side force steer gradient	160
4.3.4.5	Roll steer gradient	161
4.3.4.6	Camber steer	161
4.3.4.7	Toe angle	161
4.3.4.8	Wheel Torque effects	162
4.3.4.9	Transient vehicle motion effects on yaw balance	162
4.3.4.10	Some other design aspects	162
4.3.5	Normalized required steering angle	163
4.3.5.1	Critical and Characteristic speed *	163
4.3.6	Steady state cornering gains *	164
4.3.6.1	Yaw Rate gain	165
4.3.6.2	Curvature gain	165
4.3.6.3	Lateral Acceleration gain	166
4.3.6.4	Side slip gain as function of speed	166
4.3.7	Manoeuvrability and Stability	167
4.3.8	Handling diagram	167
4.3.9	Steady state cornering at high speed, with Lateral Load Transfer	169
4.3.9.1	Load transfer between vehicle sides	169
4.3.9.2	Body heave and roll due to lateral wheel forces	170
4.3.9.2.1	Steady-state roll-gradient *	172
4.3.9.3	Lateral load transfer	172
4.3.9.3.1	Load Transfer model with Wheel Pivot Points	172
4.3.9.3.2	Load Transfer model with Axle Roll Centres	173
4.3.9.4	Influence of anti-roll bars	177
4.3.9.5	Axle suspension system	178

4.3.9.6	Lateral load transfer influence on steady state handling	180
4.3.10	Steering feel *	181
4.3.11	Roll-over in steady state cornering	181
4.3.11.1	Roll-over threshold definitions	182
4.3.11.2	Static Stability Factor, SSF	183
4.3.11.3	Steady-state cornering roll-over	184
4.3.11.3.1	Model with fore/aft symmetry	184
4.3.11.3.2	Model without fore/aft symmetry	185
4.3.11.3.3	Using a transient model for steady-state roll-over	185
4.3.11.4	Roll-over and understeering/propulsion	186
4.4	Stationary oscillating steering	186
4.4.1	Stationary oscillating steering tests	186
4.4.2	Transient one-track model	187
4.4.2.1	Simpler model	191
4.4.2.3	Validity of solution	192
4.4.3	Steering frequency response gains *	193
4.4.3.1	Single frequency response	193
4.4.3.2	Lateral Velocity and Yaw Rate response	196
4.4.3.3	Lateral Acceleration response	198
4.4.3.4	Other responses to oscillating steering	199
4.4.3.5	Random frequency response	199
4.5	Transient handling	199
4.5.1	Transient driving manoeuvres	200
4.5.2	Transient one-track model, without Lateral load transfer	201
4.5.3	Transient model, with Lateral load transfer	203
4.5.3.1	(Example of) Mathematical model	203
4.5.3.2	(Example of) Explicit form model	207
4.5.4	Step steering response *	213
4.5.4.1	Mild step steering response	213
4.5.4.2	Violent step steering response	214
4.5.5	Long heavy vehicle combinations manoeuvrability measures	214
4.5.5.1	Rearward Amplification *	215
4.5.5.2	Off-tracking *	216
4.5.5.3	Yaw Damping *	216
4.6	Lateral Control Functions	217
4.6.1	Lateral Control Design	217
4.6.2	Lateral Control Functions	217
4.6.2.1	Lane Keeping Aid, LKA *	217
4.6.2.2	Electronic Stability Control, ESC *	218
4.6.2.3	Roll Stability Control, RSC *	220
4.6.2.4	Lateral Collision Avoidance, LCA *	220
5	VERTICAL DYNAMICS	221
5.1	Introduction	221
5.1.1	References for this chapter	221
5.2	Suspension System	222
5.3	Stationary oscillations theory	224
5.3.1	Time domain and time frequency domain	225
5.3.1.1	Mean Square (MS) and Root Mean Square (RMS) of variable	225
5.3.1.2	Power Spectral Density and Frequency bands	226
5.3.1.2.1	Differentiation of PSD	227
5.3.1.3	Transfer function	227
5.3.2	Space domain and Space frequency domain	228
5.3.2.1	Spatial Mean Square (MS) and spatial Root Mean Square (RMS) of variable	229

5.3.2.2	Spatial Power Spectral Density and Frequency bands	230
5.4	Road models	230
5.4.1	One frequency road model	231
5.4.2	Multiple frequency road models	231
5.4.2.1	Transfer function from road spectrum in spatial domain to system response in time domain	234
5.5	One-dimensional vehicle models	235
5.5.1	One-dimensional model without dynamic degree of freedom	235
5.5.1.1	Response to a single frequency excitation	236
5.5.1.2	Response to a multiple frequency excitation	237
5.5.2	One dimensional model with one dynamic degree of freedom	238
5.5.2.1	Response to a single frequency excitation	238
5.5.3	One dimensional model with two degrees of freedom	242
5.5.3.1	Response to a single frequency excitation	244
5.5.3.2	Simplified model	247
5.6	Ride comfort *	248
5.6.1	Single frequency	248
5.6.2	Multiple frequencies	249
5.7	Fatigue life *	253
5.7.1	Single frequency	253
5.7.2	Multiple frequencies	253
5.8	Road grip *	254
5.8.1	Multiple frequencies	254
5.9	Variation of stiffness and damping	255
5.9.1	Varying suspension stiffness	255
5.9.2	Varying suspension damping	256
5.9.3	Varying unsprung mass	257
5.9.4	Varying tyre stiffness	257
5.10	Two dimensional oscillations	258
5.10.1	Bounce (heave) and pitch	259
5.10.2	Bounce (heave) and roll	261
5.11	Transient vertical dynamics	261
5.12	Other excitation sources and functions	262
	BIBLIOGRAPHY	221
	INDEX	266

1 INTRODUCTION

1.1 About this compendium

This compendium is intended for first-time-studies studies of vehicle dynamics. At Chalmers University of Technology this is in the course “MMF062 Vehicle Dynamics”. The compendium covers more than actually included in the course; both in terms of subsystem designs, which not necessarily has to be fully understood in order to learn the vehicle level; and in terms of some teasers for more advanced studies of vehicle dynamics. Therefore, the compendium can also be useful in general vehicle engineering courses, e.g. in the Chalmers course “TME121 Engineering of Automotive Systems”; and as an introduction to more advance courses, which at Chalmers is the course “TME102 Vehicle Dynamics Advanced”.

The overall objective of the compendium is to contribute to education of automotive engineers with good skills to design for, and verify, requirements on complete vehicle level functions, regarding vehicle dynamics or motion.

The compendium focus on road vehicles, both passenger cars and commercial vehicles. Smaller road vehicles, such as bicycles and single-person cars, are only very briefly mentioned. It should be mentioned that a lot of ground-vehicle types are not covered at all, such as: off-road/construction vehicles, tracked vehicles, horse wagons, hovercrafts or railway vehicles.

The vehicle can be seen as a component (or sub-system) in a superior transport system, consisting of vehicles with drivers, other road users and roads with wind and weather. A vehicle is also, in itself, a system, within which many components (or sub-systems) interact. In order to approach the vehicle dynamics in a structured way, the course is divided into the following parts:

- Longitudinal dynamics (e.g. propulsion and braking sub-systems)
- Lateral dynamics (e.g. steering sub-systems)
- Vertical dynamics (e.g. suspension sub-systems)

These 3 parts are found as chapters 3-5, and the goal is that the compendium should lead all the way to “functions”. Functions are needed for requirement setting, design and verification. The overall order within the compendium is that models/methods/tools needed to understand the functions are placed before the functions.

It is important to qualitatively understand the characteristics of the vehicle’s sub-systems and, from this, learn how to quantitatively analyse the vehicle’s behaviour. These skills support the overall goal of engineering design for desired attributes and functions, see Section 1.2.

The reader of this compendium is assumed to have knowledge of mathematics and mechanics, to the level of a Bachelor of Engineering degree. Previous knowledge in dynamic systems, e.g. from Control Engineering courses, is often useful. There are no prerequisites on previous knowledge in automotive engineering, because basic vehicle components (or sub-systems) are presented to the necessary level of detail. This could be considered as unnecessary repetition for some readers. References and suggestions for further reading are provided and readers are directed to these sources of information for a deeper understanding of a specific topic.

1.2 Attributes and Functions

Development of a vehicle is driven by requirements which come from:

- Use case based needs of the customer/users
- Legislation and rating from the authorities and consumer organisation, and
- Engineering constraints from the manufacturer's platform/architecture on which it to certain vehicle should be built.

One way of organising most of those, in particular the first ones, is to define **Attributes** and **Functions**. The terms are not strictly defined and may vary between vehicle manufacturers and over time. With this said, it is assumed that the reader understand that the following is an approximate and simplified description.

In this compendium, both attributes and functions implicitly concern the **complete vehicle**; not the sub-systems within the vehicles and not the superior level of the transportation system with several vehicles in a road infrastructure.

Attributes and Functions are used to establish processes and structures for requirement setting and verification within a vehicle engineering organisation. Such processes and structures are important to enable a good overall design of such a complex product as a vehicle intended for mass production at affordable cost for the customers/users. Figure 1-1 tries to give an overview, with reference to the well-known V-model, how a vehicle program generally is organised. The figure is idealized in many ways. First, one have more levels of functions and subsystems. Secondly, it is difficult to keep such a clean hierarchical order between functions and subsystems. Thirdly and most conceptually difficult, is the fact that each subsystem gets requirements from many functions as showed by the dashed lines; this makes the complexity explode.

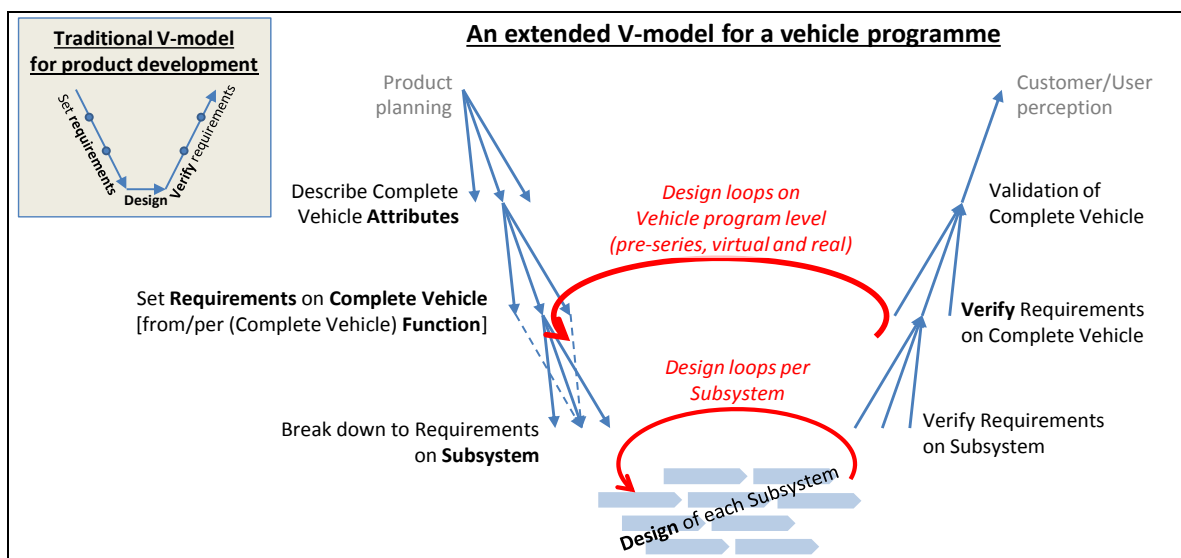


Figure 1-1: V-model applied to a vehicle program.

1.2.1 Attributes

An attribute is a high-level aspect of how the user of the vehicle perceives the vehicle. Attributes which are especially relevant for Vehicle Dynamics are listed in Table 1.1. The table is much generalised and the attributes in it would typically need to be decomposed into more attributes when used in the engineering organisation of an OEM. Also, not mentioned in the table, are

INTRODUCTION

attributes which are less specific for vehicle dynamics, such as **Affordability** (low cost for user), **Quality** (functions sustained over vehicle lifetime), **Styling** (appearance, mainly visual), etc.

Attributes can be seen as one way to categorise or group functions, especially useful for an OEM organisation and vehicle development programs. Functions can, in turn, be seen as one way to group requirements. **Legal** requirements are often, but not always, possible to trace back to primarily one specific attribute. Requirements arising from company-internal **platform and architecture constraints** are often more difficult to trace in that way. Hence, legal and platform/architecture can be seen as two “attribute-like requirement container”, beside the other user-derived attributes.

Table 1.1: Attributes

Attribute	Description	Abbreviation
Transport Efficiency	<p>This attribute means to maximize transport output and minimize costs for transportation. Transport output can be measured in <i>person · km</i> or <i>ton · km</i>. The costs are mainly energy costs and time, but also wear/life time of vehicle parts influence. The attribute is most important for commercial vehicles, but becomes increasingly important also for passenger vehicles. The attribute is mainly addressing long-term vehicle usage pattern, typically 10 min to 10 hours. There are different ways to define such usages, e.g. (Urban / Highway / Mixed) driving cycles. So far, the attribute is mainly required and assessed by the vehicle customers/users.</p> <p>The attribute can also be seen to include “Environmental Efficiency”, which means low usage of natural resources (mainly energy) and low pollution, per performed transport task. This is to a large extent required and assessed by society/legislation.</p>	E
Safety	<p>Minimizing risk of property damages, personal injuries and fatalities both in vehicle and outside, while performing the transportation. This attribute is to a large extent required and assessed by society/legislation. In some markets, mainly developed countries, it is also important for vehicle customers/users.</p>	S
Driving Dynamics	<p>How the driver experiences driving, from relaxed transport driving (comfort) to active driving (sensation). Driving Dynamics contains sub-attributes as:</p> <ul style="list-style-type: none"> • Driveability, Handling and Road-holding describes how the vehicle responds to inputs from driver and disturbances, and how driver gets feedback from vehicle motion e.g. through steering feel. (It can be noted that same response aspects are similarly important for a “virtual driver”, i.e. a control algorithm doing some automatic/autonomous control.) Driveability often refers to longitudinal (acceleration, braking gear shifting). Handling and Road-holding often refer to lateral manoeuvres. • Performance describes how the vehicle can perform at the limits of its capabilities; acceleration, deceleration or cornering. Most often, it refers to longitudinal limitations due to propulsion and brake systems limitations. • Ride comfort. Ride comfort often refers to vibrations and harshness of the occupants’ motion, primarily vertical but secondly longitudinal. So, V and H in NVH (=Noise, Vibration and Harshness) is included. If expanding to “comfort” it would include also N (noise) and compartment air conditioning, but these sub-attributes are less related to vehicle dynamics. <p>This attribute is to a large extent required and assessed by the vehicle customers/users, both through own experience but to a large extent indirectly via assessments by experts, e.g. in motor journals.</p>	D

1.2.2 Functions

A function supplies certain functionality to the customer/user of the vehicle. A function is more specific than an attribute, which is needed to set (quantitative) requirements, see Section 1.2.3. The (complete vehicle) function does not primarily stipulate any specific subsystem. However, the realisation of a function, in one particular vehicle programme, normally only engages a limited subset of all subsystems. So, the function will there pose requirements on that subsystem. Hence, it is easy to mix up whether a function originates from an attribute or a subsystem. One way to categorise functions is to let each function belong to the subsystem which it mainly implies requirements on rather than the source attribute. Categorizing functions by subsystems tends to lead to “carry-over” function realisations from previous vehicle program, which can be good enough in many cases. Categorizing functions by source attribute facilitates more novel function realisations, which can be motivated in other cases.

The word “function” has appeared very frequently lately along with development of electrically controlled systems. The function “Accelerator pedal driving” in Section 3.5.2.1 has always been there, but when the design of it changed from mechanical cable and cam to electronic communication and computational algorithms (during 1990’s) it became much more visible as a function, sometimes referred to as “electronic throttle”. The point is that the main function was there all the time, but the design was changed. The change of design enabled, or was motivated by, improvement of some sub-functions, e.g. idle speed control which works better in a wider range of engine and ambient temperature.

At some places, the compendium emphasizes the functions by adding an **asterisk “*”** in section heading and a **“Function definition”** in the following typographic form:

*Function definition: **{The Function}** is the {Measure} ... for {Fixed Conditions} and certain {Parameterized Conditions}.*

The {Measure} should be one unambiguously defined measure, such as time, velocity or force. The {Fixed Conditions} should be unambiguously defined and quantified conditions for the vehicle and its surroundings. The keyword “certain” identifies the {Parameterized Conditions}, which are not fixed in this definition, but need to be fixed before using the Function definition for requirement setting. The {Measure} is ideally a continuous, objective and scalar quantity, subjected for setting a requirement on. A requirement can then be: “{Measure} shall be =, ≈, > or < {value*unit}”, see more in Section 1.2.3.

Since the term “Function” is defined very broadly in the compendium, these definitions become very different. One type of Function definition can be seen in beginning of Section “3.2.4 Top speed”, which includes a well-defined measure. Another type of Function definition is found in Section “3.5.2.3 Anti-lock Braking System, ABS” and “4.3.3 Under-, Neutral- and Over-steering”. Here, the definitions are more on free-text format, and an exact measure is not so well defined.

The compendium defines functions on complete vehicle level, i.e. not cascaded to requirements on specific sub-systems.

There are different ways of categorising functions, where of two are shown below.

1.2.2.1 Seeing versus Blind functions

This categorisation is relevant for control functions and environment sensors.

1.2.2.1.1 Seeing functions

These functions use information about the (vehicle’s) environment, sensed through camera, radar, etc. Normally, these functions do something instead of the driver, e.g. brake, accelerate or steer the vehicle. The driver is important mainly in two ways: the driver’s actions can be used to identify when

the driver needs help (e.g. when he has not identified a threat in the environment), then an automatic intervention is triggered; the driver's action can also be used to identify when the driver wants to take back control, then the automatic intervention is cancelled. Examples of these functions are Automatic Emergency Brake, Lane Departure Warning and Forward Collision Warning.

1.2.2.1.2 Blind functions

These are functions which do not rely on information about the environment, but only about the vehicle itself. ABS and ESC are examples of blind functions.

1.2.2.2 **Dynamic versus Driver-informing functions**

This categorisation is relevant for control functions and driver interface.

1.2.2.2.1 Dynamic functions

These functions change the dynamics of the vehicle, using actuators such as brake system, propulsion system and steering system. Normally, the functions help the driver to control the vehicle motion and path/trajectory in the desired way. The driver's actions are then interpreted as requests to the control functions. Also, sensing of vehicle's state and environment can be used to further improve the interpretation of driver's intention, and/or to correct a control error. The control is then performed by vehicle motion actuation, e.g. changing engine torque, brake torque or steering angle. In today's vehicles, the vehicle motion is mainly measured by the vehicle's speeds and accelerations, but in future one could expect that also environment sensors will give inputs to actual motion/position versus object in the environment. Examples of these functions are ABS, ESC and AEB, see Section 3.5.2 and 4.6.2.

1.2.2.2.2 Driver-informing functions

These are functions which do not change the dynamics of the vehicle. Instead, they might actuate audio, visual or haptic (touch) warnings to driver. Examples of these functions can be Forward Collision Warning (FCW), Lane Departure Warning (LDW) and Blind Spot Detection (BSD). FCW is mentioned in Section 3.5.2.7. LDW is a function that warns the driver via visual, audio and/or haptic signals when the vehicle is tending to drift out of the lane. BSD is a function which warns when there is a vehicle beside and behind the subject vehicle (in the "blind spot" for the driver).

1.2.2.2.3 Un-categorized

There are interventions which are both of information type and dynamic, or difficult to categorize. Such as a superimposed steering-wheel torque in a traditional steering system. It will actually steer the vehicle if driver does not hold on to steering wheel. Alternatively, if driver holds steering wheel fixed, it would just result in a haptic force in driver's hand.

Similar difficulties to categorize could appear with "active pedals", but such solutions are hardly on market yet.

1.2.2.3 **Other categorisations**

There are also other ways of categorizing functions:

- Grouping in **(sub-)systems** on which the function imply main part of its requirements, such as brake system and steering system.
- Grouping in those who are realized solely mechanically and those who **involve electronics**.
- Grouping in "**customer functions**" and "**support functions**". Support functions are typically used by many customer functions, see Section "1.3.10.1 Reference architecture of vehicle functionality".
- Grouping in **standard and option** in the vehicle program or platform.

One thing to remember about the concept of functions is that there are always several ways of breaking down the total package of functions in a vehicle into a finite list of functions. Also, one can define sub-functions as being parts of superior functions. A function can also be relying on another function by needing input, or demanding actuation from the other. To summarise, defining separate functions as parts in the whole vehicle is not very precise, although it is helpful when trying to organise a combined hardware and software development process.

1.2.3 Requirements

A requirement shall be measurable. A requirement on complete vehicle level is typically formulated as: “*The vehicle shall ... {< or > or =} {number} {unit}*”. Examples:

- The vehicle shall accelerate from 50 to 100 km/h on level road in <5 s when acceleration pedal is fully applied.
- The vehicle shall decelerate from 100 to 0 km/h on level road in <35 m when brake pedal is fully applied, without locking any rear wheel.
- The vehicle shall turn with outermost wheel edge on a diameter <11m when turning with full-lock steering at low speed.
- The vehicle shall have a characteristic speed of 70 km/h (± 10 km/h) on level ground and high-friction road conditions and any recommended tyres.
- The vehicle shall give a weighted RMS-value of vertical seat accelerations <1.5 m/s² when driving on road with class B according to ISO 8608 in 100 km/h.
- The vehicle shall keep its body above a 0.1 m high peaky two-sided bump when passing the bump in 50 km/h.

In order to limit the amount of text and diagrams in the requirements it is useful to refer to ISO and OEM specific standards. Also, it is often good to include the purpose, and/or a use case, when documenting the requirement.

The above listed requirements stipulate the function of the vehicle, which is the main approach in this compendium. Alternatively, a requirement can stipulate the design of the vehicle, such as “The vehicle shall weigh <1600 kg” or “The vehicle shall have a wheel base of 2.5 m”. The first type (above listed) can be called *Performance based requirement*. The latter type can be called *Design based requirement* or *Prescriptive requirement* and such are rather “means” than “functions”, when seen in a function vs mean hierarchy. It is typically desired that legal requirements are Performance based, else they would limit the technology development in society.

1.2.4 Models, methods and tools

The attributes, functions and requirements are top level entities in vehicle development process. But in order to define/formulate them, design for them and verify them, the engineers need knowledge in terms of models, methods and tools.

As mentioned above, some sections in the compendium have an asterisk “*” in the section heading, to mark that they explain a function, which can be subject for complete vehicle requirement setting. The remaining section, without an asterisk “*”, are there to give the necessary knowledge (models, methods, tools, etc.) to understand the function. It is the intention that the necessary knowledge for a certain function appears before that function section. One example is that the Sections “3.2.1 Propulsion System”, “3.2.2 Traction diagram” and “3.2.3 Driving Resistance” are placed before Section “3.2.4 Top speed *”.

The functions only appear in Chapter 3, Chapter 4 and Chapter 5.

1.3 Technical References

This section introduces notations. The section also covers some basic disciplines, methods and tools. Parts of this section probably repeat some of the reader's previous education.

1.3.1 Engineering

Engineering Design or Engineering (in Swedish "Ingenjörsvetenskap", in German "Ingenieurwissenschaften"), is not the same as Analysis, Inverse analysis and (Nature) Science, see Figure 1-2. In education, it is often easiest to do Analysis (or Inverse Analysis). However, in a product based subject, such as Vehicle Dynamics, it is important to keep in mind that the ultimate use of the knowledge is Engineering, which is to propose and motivate the design and actual values of design parameters of a product. The distinction between Analysis and Inverse Analysis can only be made if there is a natural direction (input or output) of interface signals.

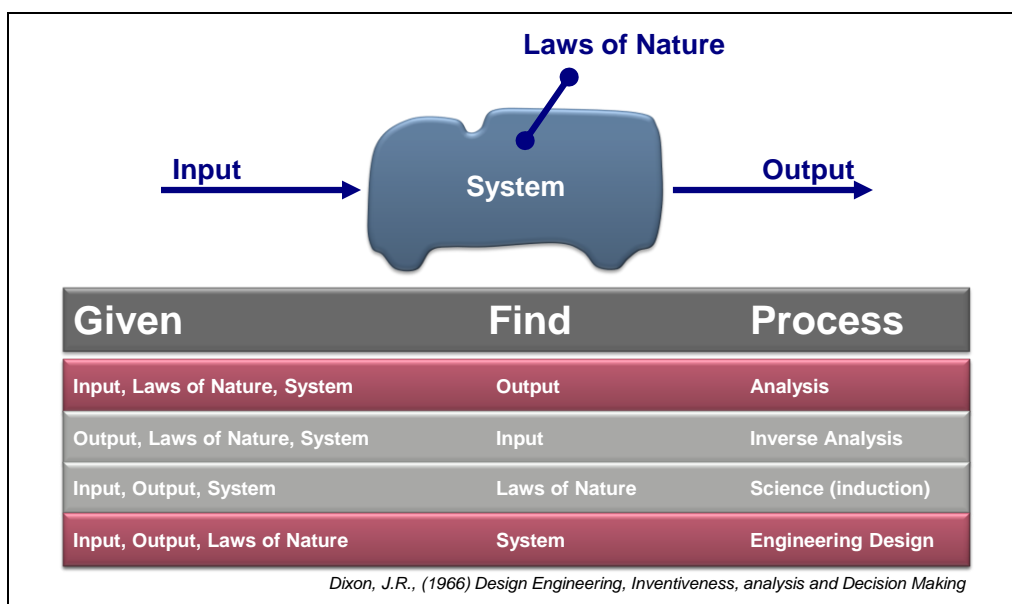


Figure 1-2: Distinction between Engineering and its neighbouring activities.

Picture from Stefan Edlund, Volvo Trucks.

1.3.2 General modelling, drawing and mathematics

A model is a representation of something during a certain event or course of events, such as the model of the motion of a car during acceleration from stand-still to 100 km/h. Models are always based on assumptions, approximations and simplifications. However, when using models as a tool for solving a particular problem, the models at least have to be able to reproduce the problem one is trying to solve. Also, models for engineering have to reflect design changes (e.g. changed parameters or input signals) in a representative way, so that new designs can be proposed which solve/reduce the problem. Too advanced models tend to be a disadvantage, since they produce a lot of data.

The modelling focused in vehicle dynamics (and many related areas) has no well-established name, but some alternative names are: *functional models*, one-dimensional models, system models, dae-model, ode-models, etc. Functional models are typically multi-domain type, involving mechanics, hydraulics, pneumatics, electric, control algorithms, etc. Functional models typically lumps or discretises possible continuous parts of the system. Examples of modelling methods which are very

INTRODUCTION

seldom directly used for functional models are: Finite Elements, Computational Fluid Dynamics, CAD geometry models, etc.

One can identify the modelling in different stages in the overall process of engineering:

- **Engineering design task**, which describes which design decisions for a certain system (an existing product or a concept/drawing) that is needed. Also, requirements on how the system should work have to be present.
- **Analysis task** is formulated, and a plan of how the result of this analysis task can support the actual design decisions.
- **Physical model**, in sketches (or thoughts & words, but sketches are really recommended!). It clarifies assumptions for different parts of the system, e.g. rigid/elastic and inertial/massless. How one model here should be based on what phenomena is needed to be captured, so it might depend on both which system you model and what the analysis task is.
- **Mathematical model** (or *Declarative* model), in equations. Basically, it is about finding exactly the right number of equations, not too many and not too few. Here, the assumptions are transformed into equations. For dynamic systems, the equations form a “DAE” (Differential-Algebraic system of Equations). It is seldom necessary to introduce derivatives with respect to other independent variables, such as positions, i.e. one does seldom need PDE (Partial Differential Equations). The general form of a DAE:

$$f_z(\dot{z}, z, u, t) = \mathbf{0}; \quad y = g_z(z, u, t); \quad u = u(t);$$

where z are the dependent variables, u are the input variables, y the output variables and t is time (independent variable).

Note that the DAE is generally on implicit form with respect to calculating the state derivatives, as opposed to explicit form below. Note also that it is not only a question of finding suitable equations, but also to decide *parameterisation*, which is how parameters relate to each other. The parameterisation has to reflect a “fair” comparison between different design parameters, which often requires a lot of experience of the product and the full set of requirements on the vehicle.

Also, *selection of output variables* is important so that output variables are enough to evaluate the requirements on the system. Selecting more might drive unnecessary complex models.

- **Explicit form model** (or *Imperative* model) is the equations rearranged to an (explicit) form or an algorithm to calculate the state derivatives. You probably recognize this from solving “ODE” (Ordinary Differential Equations) or “IVP” (Initial Value Problems). The general form is:

$$\dot{x} = f_x(x, u, t); \quad y = g_x(x, u, t); \quad u = u(t);$$

where x is the state variables and y the output variables.

- **Analysis** or calculation. Several methods can be used depending of the analysis task, e.g.:
 - *Simulation* (e.g. Initial value problem, IVP or End value problem, EVP). There are many advanced pre-programmed integration methods and tools which one can rely on without knowing the details. It is often enough to know that the concept is similar to the simplest of them, “Euler forward”, in which the state variables are updated in each time step as follows:

$$\begin{aligned} \dot{x}_{now} &= f(x(t_{now}), u(t_{now}), t_{now}); \\ x(t_{now} + \Delta t) &= x(t_{now}) + \Delta t \cdot \dot{x}_{now}; \end{aligned}$$

Note: Simulation corresponds to running experiments in real world, while the 3 previous steps corresponds to building a real test object and instrument it.

- *Methods for linear systems*, e.g. for studying stationary oscillation, eigen-oscillations, step response, etc. With a linearized model, it is also possible to find explicit solutions over time.

INTRODUCTION

- *Optimization*. Either optimizing a finite number of defined design parameters or time trajectories. Optimization is not further addressed in this compendium.
- **Synthesis** of the numerical result. Understand and interpret analysis results, including judge validity of model assumptions and parameterizations.
- **Solution**, in terms of a concrete proposal of design, such as numerical parameter value, drawing/control algorithm, ...

In this process description, we can identify 3 modelling steps with 3 different kinds of models: Physical model, Mathematical model and Explicit form model. The compendium spends most effort on the first 2 of those, because the last step is more about mathematical science than vehicle engineering.

A **variable** is something that varies in time. **Constants** and **parameters** are not varying, with the distinction that a parameter does not change during the manoeuvre/experiment studied, but can be changed between subsequent manoeuvres/experiments with the same model. Typical constant is pi or gravity. Typical parameter is vehicle mass or road friction co-efficient.

A variable can be used as **state variable**, which means that it is given initial values and then updated through integration along the time interval studied. Which variables to use as state variables is **not** strictly defined by the physical (or mathematical) model. For mechanical systems, one often uses positions and velocities of bodies as state variables, but it is quite possible and sometimes preferable, to use forces in compliances (springs) and velocities of bodies as state variables. With mass/spring system as simple example, the two alternatives becomes $[\dot{v} = F/m; F = c \cdot x; \dot{x} = v;]$ and $[\dot{v} = F/m; \dot{F} = c \cdot v; x = F/c;]$, respectively.

Systems can be modelled with **Natural causality**. For mechanical systems, this is when forces on the masses (or motion of the compliance's ends) are prescribed as functions of time. Then the velocities of the masses (or forces of the compliances) become state variables and have to be solved through time integration. The opposite is called **Inverse dynamics** and means that velocities of masses (or forces of compliances) are prescribed. For instance, the velocity of a mass can be prescribed and then the required forces on the mass can be calculated through time differentiation of the prescribed velocity. Cf. Analysis and Inverse Analysis in Figure 1-2.

Drawing is a very important tool for understanding and explaining. Beyond normal drawing rules for engineering drawings, it is also important to draw motion and forces. The notation for this is proposed in Figure 1-3.

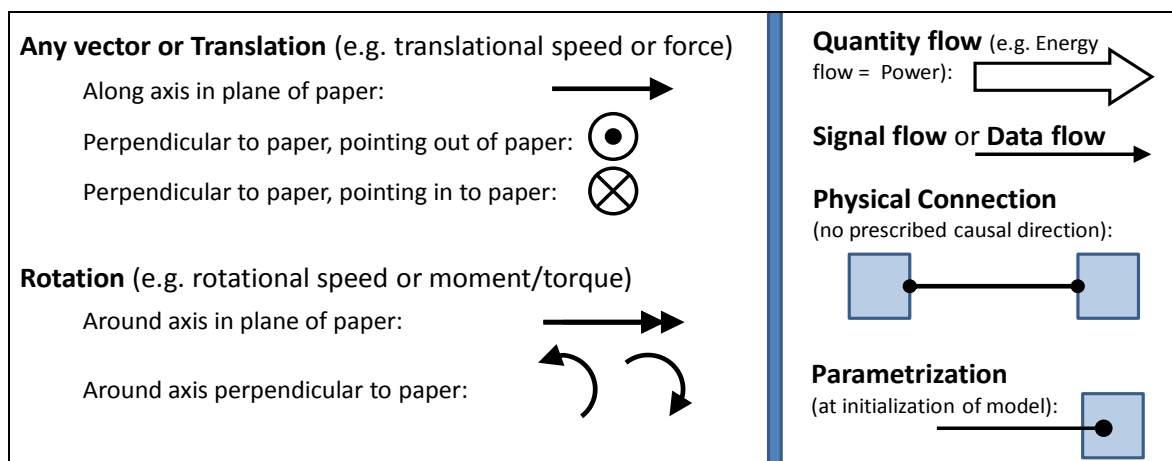


Figure 1-3: Arrow like notation. Left: For motion and forces in drawings. Right: Other

It is often necessary to include more than just speeds and forces in the drawings. In vehicle dynamics these could be: power flow and signal flows. These are often natural to draw as arrows

When connecting components with signal flow, the resulting diagram is a *data flow diagram*. Physical components and physical connections can be included in such diagram. It should be noted that a *flow charts* and (*discrete*) *state diagram* represents a quite different type of diagram, even if they may look similar; here an arrow between two blocks does not represent data flow from one component to another, but stepping from one state or operation to another.

1.3.3 Notations

Generally, a variable is denoted **x or $x(t)$** , where t is the independent variable time. In contexts where one means that variable's value at a certain time instant, t_0 , it can be denoted **$x(t_0)$** . In contexts where one means the variable's time history over a whole time interval (infinitely many values), it can be denoted **$x(.)$** .

Differentiation (of x) with respect to time (t): $\frac{dx}{dt} = \dot{x} = der(x)$.

Vectors exist of two kinds: **Geometrical vector** (or physical vector, or spatial vector), denoted by \vec{v} , and **mathematical vector**, denoted $[v_x;v_y]$. The geometrical vector is the true vector, while the mathematical is a representation of it, in a certain coordinate system. Matrices are denoted with brackets, e.g. $[A]$. Row vectors are denoted with parentheses, e.g. (a) .

Parentheses shall be used to avoid ambiguity, e.g. $(a/b) \cdot c$ or $a/(b \cdot c)$, not $a/b \cdot c$.

Multiplication symbol ($*$ or \cdot) shall be used to avoid ambiguity, e.g. $a \cdot bx$, not abx (assuming bx is one variable, not two). Stringent use of multiplication symbol enables use of variables with more than one token, cf. programming. Stringent use of multiplication symbol reduces the risk of ambiguity when using operators, e.g. it shows the difference between $f(x)$ and $f \cdot (x)$.

An **interval** has a notation with double dots. Example: Interval between a and b is denoted $a..b$.

An **explanation**, between two consecutively following steps in a derivation of equations is written within $\{ \}$ brackets. Example: $x + y = \{a + b = b + a\} = y + x$ or $x + y = 7 \Rightarrow \{a + b = b + a\} \Rightarrow y + x = 7$.

An **inverse function** is denoted with -1 as superscript, e.g. $y = f(x); \Leftrightarrow x = f^{-1}(y)$.

Fourier and Laplace **transforms** are denoted $\mathcal{F}(f(t))$ and $\mathcal{L}(f(t))$, respectively.

1.3.3.1 Notation list

Table 1.2 shows notation of parameters, variables and subscripts used in this compendium. The intention of this compendium is to follow International Standards (ISO8855). Some alternative notations are also shown, to prepare the reader for other frequently used notation in other literature.

The list does not show the order of subscripting, e.g. whether longitudinal (subscript x) force (notation F) on rear axle (subscript r) should be denoted F_{rx} or F_{xr} . The intention in this compendium is to order subscript with the physical vehicle part (here rear axle) as first subscript and the specification (longitudinal, x) as second: F_{rx} . If there is also further detailed specifications, such as coordinate system, e.g. wheel coordinate (subscript w), it would be the third subscript: F_{rxw} .

INTRODUCTION

Table 1.2: Notation

Categorization		Notation			Unit	Description / Note	
Engineering	Sub category	Subject for notation	in code	by hand	Alternatives		
1. General	Basic	(Shaft) Torque	T	T	M	Nm	
1. General	Basic	Coefficient of friction	mu	μ	mue, muh	1=N/N	
1. General	Basic	Damping coefficient	d	d	c, k, D	N/(m/s) or Nm/(rad/s)	
1. General	Basic	Density	roh	ρ			
1. General	Basic	Efficiency	eta	η		1=W/W	Ratio between useful/output power and used/input power
1. General	Basic	Energy	E	E	W	Nm=J	
1. General	Basic	Force	F	F	f	N	
1. General	Basic	Gravity	g	g		m/s ²	9.80665 average on Earth
1. General	Basic	Height	h	h	H		
1. General	Basic	Imaginary unit	j	j	i	-	j* j=-1
1. General	Basic	Mass	m	m	M	kg	
1. General	Basic	Mass moment of inertia	J	J	I	kg*m ²	Subscript can be given to denote around which axis
1. General	Basic	Moment (of forces)	M	M	T	Nm	Not for shaft torque
1. General	Basic	Power	P	P		W=Nm/s=J/s	
1. General	Basic	Ratio	r	r	u, i (ISO8855)	Nm/(Nm) or (rad/s)/(rad/s)	Ratio between input and output rotational speed, or output and input torque, in a transmission
1. General	Basic	Rotational speed	w	ω	@	rad/s	
1. General	Basic	Shear stress	tau	τ		N/m ²	
1. General	Basic	Stiffness coefficient	c	c	C, k, K	N/m or Nm/rad	
1. General	Basic	Strain	eps	ϵ		m/m	
1. General	Basic	Translational speed	v	v	V	m/s	
1. General	Basic	Wave length	lambda	λ		m	
1. General	Basic	Width	W	W	w	m	Can be track width, vehicle width, tyre width, ...
1. General	Dynamics	(Time) Frequency	f	f		1/s=periods/s	
1. General	Dynamics	Angular (time) frequency	w	ω	@	rad/s	
1. General	Dynamics	Angular spatial frequency	W	Ω		rad/m	
1. General	Dynamics	Dependent variables in a dynamic system	z	z		<various>	Both state variables and output variables
1. General	Dynamics	Input variables in a dynamic system	u	u		<various>	
1. General	Dynamics	Mean Square value	MS	MS			
1. General	Dynamics	Output variables in a dynamic system	y	Y		<various>	
1. General	Dynamics	Power spectral density	G	Φ	PSD		
1. General	Dynamics	Root Mean Square value	RMS	RMS			
1. General	Dynamics	Spacial frequency as radians per travelled distance	W	Ω		rad/m	
1. General	Dynamics	Spatial frequency	f_s	f_s		1/m=periods/m	
1. General	Dynamics	States variables in a dynamic system	x	x		<various>	
1. General	Dynamics	Time	t	t	t, T	s	The independent variable in a dynamic system
1. General	Operators	Transfer function	H	H		<not applicable>	
2. Vehicle	1. General	Air resistance coefficient	cd	c_d	Cd	1	
2. Vehicle	1. General	Cornering stiffness or lateral tyre stiffness	C _y	C_y	C _α	N/rad or N/1	$dF_y/d\alpha = dF_y/ds_y$ at $\alpha=s_y=0$
2. Vehicle	1. General	Longitudinal tyre stiffness	C _x	C_x		N/1	df_{yw}/ds_x at $s_x=0$

INTRODUCTION

Categorization		Notation				Unit	Description / Note
Engineering	Sub category	Subject for notation	in code	by hand	Alternatives		
2. Vehicle	1. General	Mass	m	m	M	kg	
2. Vehicle	1. General	Rolling resistance coefficient	f	f		1=N/N	
2. Vehicle	1. General	Track width	W	W		m	
2. Vehicle	1. General	Tyre stiffness	C	C	c	N/1	dF/ds at $s=0$
2. Vehicle	1. General	Understeer gradient	Ku	K_u	K_{us}, k_{us}, U (ISO8855)	N/(N/rad) = rad/(m/s ²)	
2. Vehicle	1. General	Vehicle side slip angle	b	β	β	rad	If no subscript, undefined or CoG
2. Vehicle	1. General	Wheel base	L	L	l, l_f+l_r, WB	m	
2. Vehicle	1. General	Wheel radius	R	R	r, R_w	m	
2. Vehicle	2. Road	Curvature	kappa	κ	ρ_{oh}, ρ	rad/m=1/m	road or path
2. Vehicle	2. Road	Curve radius	R	R	r, ρ_{oh}, ρ	m	road or path
2. Vehicle	2. Road	Road bank angle	pxr	ϕ_{xr}			Positive when right side of ground is lower than left side ground
2. Vehicle	2. Road	Road inclination angle	pyr	ϕ_{yr}		rad	Positive downhill
2. Vehicle	2. Road	Vertical Position of road	zr	z_z	z, Z	m	
2. Vehicle	3. Motion	Vehicle acceleration, decomposed in vehicle coordinates in vehicle frame	a_x, a_y, a_z	$[a_x, a_y, a_z]$		m/(s*s)	
2. Vehicle	3. Motion	Vehicle acceleration, in world frame	dervx, dervy, der vz	$\dot{v}_x, \dot{v}_y, \dot{v}_z$	der (vx), der (vy), der (vz)	m/(s*s)	
2. Vehicle	3. Motion	Vehicle position	$x=[x, y, z]$	$[x, y, z]$	$r=[r_x, r_y, r_z], [X, Y, Z]$	m	Often referring to Center of Gravity, CoG
2. Vehicle	3. Motion	Vehicle speed	$v=[v_x, v_y, v_z]$	$[v_x, v_y, v_z]$	V_x, V_y, V_z	m/s	speed in inertial frame, decomposed in vehicle coordinates
2. Vehicle	4. Forces	Forces and moments on vehicle	$F = [F_x, F_y, F_z, M_x, M_y, M_z]$	$[F_x, F_y, F_z, M_x, M_y, M_z]$		[N, N, N, Nm, Nm, Nm]	From ground, air, towed units, colliding objects, etc. May appear also as reduced, e.g. for in road plane dynamics: $F=[F_x, F_y, M_z]$
2. Vehicle	4. Forces	Forces on one wheel, axle or side from ground	$[F_{ix}, F_{iy}, F_{iz}]$	$[F_{ix}, F_{iy}, F_{iz}]$	lowercase f	N	Subscript "i" is placeholder for particular wheel, axle or side. May appear also extended with moments: $[F_x, F_y, F_z, M_x, M_y, M_z]$
2. Vehicle	4. Forces	Forces on one wheel, axle or side from ground	$[F_{ixv}, F_{iyv}, F_{izv}]$	$[F_{ixv}, F_{iyv}, F_{izv}]$	lowercase f	N	in vehicle coordinate system
2. Vehicle	4. Forces	Forces on one wheel, axle or side from ground	$[F_{ixw}, F_{iyw}, F_{izw}]$	$[F_{ixw}, F_{iyw}, F_{izw}]$	lowercase f	N	in wheel coordinate system
2. Vehicle	5. Angles	Camber angle	g	g	gamma, γ	rad	Sign convention might be positive when either of "rotated as wheel roll angle" or "leaning outward vs vehicle body".
2. Vehicle	5. Angles	Low speed or Ackermann speed steering wheel angle	dswA	δ_{swA}		rad	The angle required for a certain vehicle path curvature at low speeds
2. Vehicle	5. Angles	Roll, pitch, yaw angle	$p = [p_x, p_y, p_z]$	$[\phi_x, \phi_y, \phi_z]$	$[\phi, \theta, \psi]$	rad	Zero when horizontal or when perpendicular to ground
2. Vehicle	5. Angles	Roll, pitch, yaw angular speed	$w = [w_x, w_y, w_z]$	$[\omega_x, \omega_y, \omega_z]$	$[\dot{\phi}, \dot{\theta}, \dot{\psi}], [\dot{\phi}, \dot{\theta}, \dot{\Omega}]$	rad/s	
2. Vehicle	5. Angles	Steering angle	d	δ	delta	rad	May refer to steering wheel, road wheel or axle
2. Vehicle	5. Angles	Steering angle of road wheels	drw	δ_{rw}	RWA	rad	Normally an average of angles on front axle

INTRODUCTION

Categorization		Subject for notation	Notation		Unit	Description / Note	
			Recommended	Alternatives			
Engineering	Sub category		in code	by hand			
2. Vehicle	5. Angles	Steering angle of steering wheel	dsw	δ_{sw}	SWA	rad	
2. Vehicle	6. Slip	Tyre (lateral) slip angle	a	α	alpha	rad	a=arctan(sy)
2. Vehicle	6. Slip	Tyre lateral slip	sy	s_y		1=(m/s)/(m/s)	sy=tan(a)
2. Vehicle	6. Slip	Tyre longitudinal slip	sx	s_x	K, -K	1=(m/s)/(m/s)	
2. Vehicle	6. Slip	Tyre slip	s	s		1=(m/s)/(m/s)	
2. Vehicle	7. Subscript	axle	a	a		<not applicable>	used e.g. as Ca=cornering stiffness for any axle
2. Vehicle	7. Subscript	centre of gravity	CoG	CoG	COG, cog, CG, cg	<not applicable>	
2. Vehicle	7. Subscript	front	f	f	F, 1	<not applicable>	Often used as double subscript, e.g. fr=front right
2. Vehicle	7. Subscript	inner	i	i		<not applicable>	Often means with respect to curve
2. Vehicle	7. Subscript	left	l	l	L	<not applicable>	Often used as double subscript, e.g. fl=front left
2. Vehicle	7. Subscript	outer	o	o		<not applicable>	Often means with respect to curve
2. Vehicle	7. Subscript	rear	r	r	R, 2	<not applicable>	Often used as double subscript, e.g. rr=rear right
2. Vehicle	7. Subscript	road	r	r		<not applicable>	
2. Vehicle	7. Subscript	road wheel	rw	rw	RW	<not applicable>	E.g. drw=road wheel steering angle
2. Vehicle	7. Subscript	sprung mass	s	s		<not applicable>	
2. Vehicle	7. Subscript	steering wheel	sw	sw	SW, H (ISO8855)	<not applicable>	E.g. dsw=steering wheel angle
2. Vehicle	7. Subscript	unsprung mass	u	u	us	<not applicable>	
2. Vehicle	7. Subscript	vehicle	v	v		<not applicable>	used e.g. as F1v to denote wheel force on wheel 1 in vehicle coordinates
2. Vehicle	7. Subscript	wheel	w	w		<not applicable>	used e.g. as F1w to denote wheel force on wheel 1 in wheel coordinates
3. Subsystem in vehicles	1. Propulsion	Engine torque	Te	T_e		Nm	
3. Subsystem in vehicles	2. Brake						
3. Subsystem in vehicles	3. Steering	Steering wheel torque	Tsw	T_{sw}	SWT	Nm	
3. Subsystem in vehicles	4. Suspension	Caster angle	CA			rad	
3. Subsystem in vehicles	4. Suspension	Caster offset	c			m	
3. Subsystem in vehicles	4. Suspension	Kingpin inclination angle	KPI			rad	
3. Subsystem in vehicles	4. Suspension	Pneumatic trail	t			m	

1.3.4 From general “Mechanical engineering”

Vehicle dynamics originates from mechanical engineering. Therefore, it is important to be familiar with the following basic relationships:

- Energy = time integral of Power
- [Torque or Moment] = Force · Lever
- Power = Torque · Rotational speed *or* Power = Force · Translational speed
- (Torque) Ratio = Output torque / Input torque
- (Speed) Ratio = Input speed / Output speed
- Efficiency = Output power / Input power *or, in a wider meaning,* Efficiency = Useful / Used

1.3.4.1 Free-body diagrams

An example of a free-body diagram is given in Figure 1-4.

Division into sub-systems is often needed, e.g. to implement moment less connection points or other models of the vehicle internal behaviour. The sub-system split typically goes through:

- Connection point between towing unit and towed unit (interface quantities: 2D position, 2D speed and 2D force)
- Driveshaft close to each wheel (interface quantities: 1D angle and 1D torque)
- Surface between driver’s hand and steering wheel (interface quantities: 1D angle and 1D torque)

The free-body diagram is an important step between system model and equilibrium equations. Relevant notes for this are:

- A short-cut that can be taken when drawing the diagram is to assume forces are already in equilibrium, which makes one equilibrium equation unnecessary. An example of this could be to use F_{zf} instead of F_{zf0} in Figure 1-4, which would make it pointless to set up the vertical force equilibrium for the front axle ($F_{zf} - F_{zf} = 0$).
- In the free-body diagram, one draws arrows and names them. These are typically to mark forces and speeds. You can either use a standard sign rule and let mathematics decide the sign (‘+’ or ‘-’) of the variable, or, try to “feel” which direction the force or speed will have and define your arrows and names according to this, to get positive numerical values. It is a matter of taste which is best, but it is recommended that care is taken – it is very easy to make sign mistakes.

You will notice that most mechanical models set up in Vehicle Dynamics are basically combinations of (Static or Dynamic) Equilibrium, Compatibility and Constitutive relationships:

- (Static) Equilibrium (using Newtonian mechanics):
 - Sum of forces in one direction = 0
 - Sum of moments around an axis in one direction = 0
- Dynamic equilibrium (or “Equation of motion” or “Newton’s 2nd law”):
 - Sum of forces (including “fictive forces” = “d’Alambert forces”) in one direction = 0, **or** sum of forces in one direction = Mass * Acceleration in the forces’ direction
 - Sum of moments (including “fictive moments”) in one direction = 0, **or** sum of moments in one direction = Moment of inertia * Rotational acceleration in the moment’s direction
 - If fictive forces or moments are included on equation left-hand side, it is recommended that they are introduced in the free-body diagram (see dashed force arrow in Figure 1-4). These forces shall be opposite to the positive direction of acceleration and act through the centre of gravity.

INTRODUCTION

- (An alternative to Newtonian mechanics is Lagrange mechanics, which is sometimes an easier way to find the same equations.)
- Compatibility: Relation between positions or velocities, e.g. "Speed=Radius*Rotational speed" for a rotating wheel
- Constitutive relations: Relation between forces and positions or between forces and velocities, e.g.
 - "Force = constant * deformation" for a linear spring
 - "Force = constant * deformation speed" for a linear damper
 - "Force = constant * sign(sliding speed)" for a dry friction contact

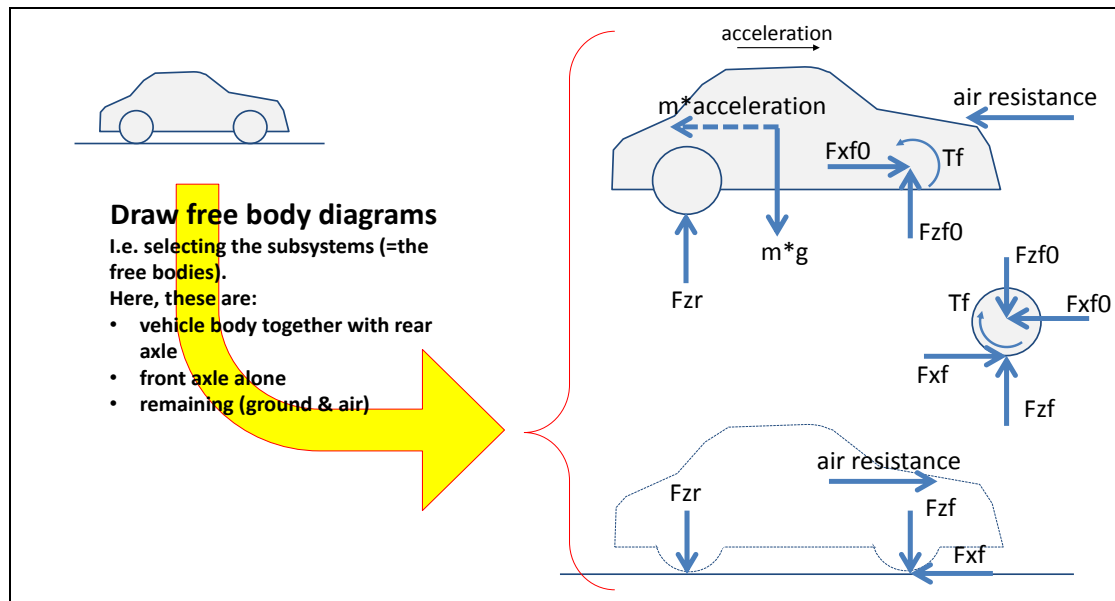


Figure 1-4: Free body diagram. The dashed arrow is a "fictive force".

1.3.4.2 Operating conditions

The operating conditions of a vehicle lend expressions from general dynamics, as listed below.

- **(Static)** conditions, meaning that vehicle is standing still, are seldom relevant to analyse. Static means that the all velocities are zero, i.e. that all positions are constant.)
- **Steady State** operation means that time history is irrelevant for the quantities studied. Seen as a manoeuvre over time, the studied quantities are constant.
- **Transient** manoeuvres means that time history is relevant; i.e. there are delays, represented by "state variables" when simulated.
- **Stationary (oscillation)** manoeuvre is a special case of transient, where cyclic variations continues over long time with a constant pattern. This pattern is often assumed to be harmonic, meaning that the variable varies in sinus and cosine with constant amplitudes and phases. An example is sinusoidal steering, where also the vehicle response is harmonic if steering amplitude is small enough to assume the vehicle response is governed by a linear dynamic system.
- **Quasi-static** and **Quasi-steady state** are terms with a more diffuse meaning, which refers rather to analysis methods than the actual operation/manoeuvre. It is used when the analysis neglects the dynamics of a variable which normally is a state variable. An example is when constant non-zero deceleration is assumed, but speed is not changed; then the dynamics "der(speed)=acceleration" is neglected, and speed is instead prescribed.

1.3.5 Verification methods with real vehicles

Methods which are helpful and frequently used for vehicle dynamics are listed in this section.

1.3.5.1 Testing in real traffic

Driving on public roads in real traffic is the most realistic way to verify how a vehicle actually works. It can be used for completely new vehicle models; or new systems, mounted on old models. The drivers can be either ordinary drivers (FOT=Field Operational Test) or test drivers (expeditions). A general existing vehicle population can also be studied by collecting data, e.g. as Accident Statistics Databases.

1.3.5.2 Testing on test track

For vehicles and systems which are not yet allowed on public roads, or tests which are very severe or need a high degree of repeatability, test are carried out at test tracks. There are specialized test tracks for certain conditions, such as hot climate or slippery surfaces.

1.3.6 Verification methods involving theoretical simulation

The following are examples of methods containing theoretical simulation to some extent:

1.3.6.1 HIL = Hardware in the loop simulation

The hardware is often one or several ECUs (Electronic Control Units). If several ECUs are tested, the hardware can also contain the communication channel between them, e.g. a CAN bus. The hardware is run with real-time I/O to simulation model of the remaining system (vehicle, driver and environment).

In some cases, there is also mechanical hardware involved, such as if the ECU is the brake system ECU, the actual hydraulic part of the brake system can also be included in the HIL set-up, a so called "wet brake ECU HIL".

1.3.6.2 SIL = Software in the loop simulation

The software is often one or several computer programs (intended for download in electronic control units). The software is run with synchronized time-discrete I/O to a simulation model of the remaining system (vehicle, driver and environment).

The software is often used in compiled format (black box format) so that the supplier of the software can retain his intellectual property.

1.3.6.3 MIL = Model in the loop simulation

The model, or more correctly, a control algorithm, is a conceptual form of the computer programs (intended for download in electronic control units). The control algorithm is run with I/O to a simulation model of the remaining system (vehicle, driver and environment).

The control algorithms can appear in compiled format so that the supplier of the control algorithms can retain his intellectual property. Then it is hard to tell the difference between MIL and SIL.

1.3.6.4 Simulator = Driver in the loop simulation

This is when a real human, not a driver model, uses real driver devices (pedals, steering wheel) to influence a simulation model of the remaining system (vehicle and environment). The loop is closed by giving the human feedback through display of what would be visible from driver seat, including

views outside windscreen. Feedback can be further improved by adding a motion platform to the driver's seat, sound, vibrations in seat, steering wheel torque, etc.

1.3.6.5 AR = Augmented Reality

This is a new method. A typical example is: A real driver drives a real vehicle on a real road/test track. Some additional (virtual/simulated) traffic objects are presented to driver, e.g. on a head-up display. The same objects can be fed into the control functions, as if they were detected by the vehicles camera/radar, which enables functions such as automatic braking to be triggered.

1.3.7 Tools & Methods

(Computer) Tools are helpful, and frequently used for vehicle dynamics. Some descriptions and typical uses is also given.

1.3.7.1 General mathematics tools

Examples of tool: Matlab, Matrixx, Python

We will take Matlab as example. Matlab is a commercial computer program for general mathematical analysis. It is developed by Mathworks Inc.

Solve linear systems of equations, $A*x=b$

```
>> x=inv(A)*b;
```

Solve non-linear systems of equations, $f(x)=0$

```
>> x=fsolve('f',...);
```

Parameter optimization (may be used for trajectory optimization, if trajectory is parameterised)

```
>> (x,fval) = fmincon('f',x0,...)
```

Solve ODE (=“systems of Ordinary Differential Equations”) as initial value problems, $dx/dt=f(t,x)$, given $x(0)$

```
>> x=ode23('f',x0,...);
```

Find Eigen vectors (V) and Eigen values (D) to linear systems: $D*V=A*V$

```
>> [V,D]=eig(A);
```

Matlab is mainly numerical, but also has a symbolic toolbox:

```
>> syms x a; Eq='a/x+x=0'; solve(Eq,x)
ans = (-a)^(1/2)
      -(-a)^(1/2)
>> diff('a/x+x',x)
ans = 1 - a/x^2
>> int('x^3+log(x)',x)
ans = (x*(4*log(x) + x^3 - 4))/4
```

Some simple Matlab code will be used to describe models in this compendium.

1.3.7.2 Block diagram based simulation tools

Examples of tools: Simulink, Systembuild

We will take Simulink as example. Graphical definition of non-linear systems of ODE, if known on explicit form $dx/dt=f(t,x)$. An example of how the corresponding graphical model may look is given in Figure 1-5.

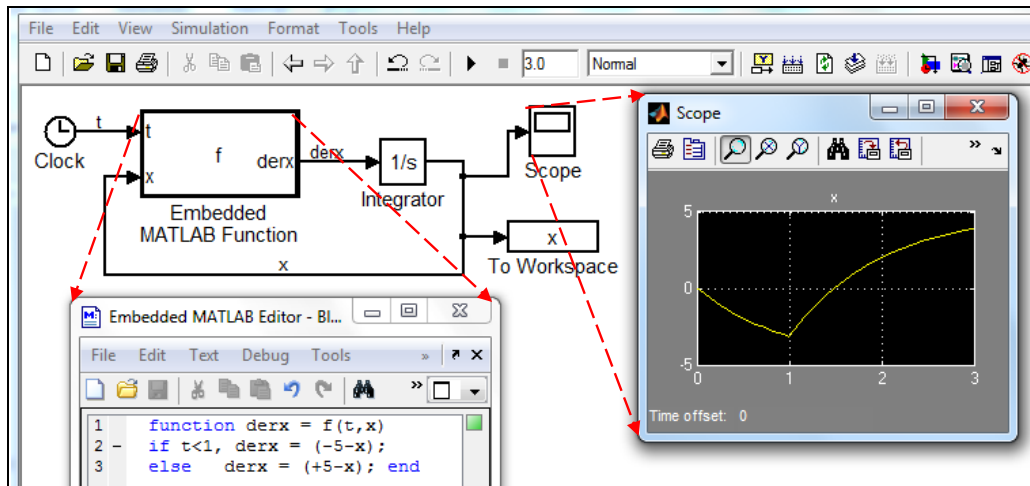


Figure 1-5: Graphical model of dynamic system $\dot{x} = f(t, x)$; using Simulink.

Simulink is designed for designing/modelling signal processing and control design. It can also be used for modelling the physics of the controlled systems.

There are no dedicated vehicle dynamics tools/libraries from Mathworks (but there are in-house developed specific libraries in automotive companies).

From this type of tools it is often possible to automatically generate real time code, which is more and more used instead of typing algorithms. It can be used for rapid prototyping of control functions, or even for generation of executable code for production ECUs.

1.3.7.3 Vehicle dynamics specialized simulation tools

Examples of tools: CarMaker, veDYNA, CarSim.

These tools are specialized for vehicle dynamics. They contain purpose-built (not necessary complete 3D mechanics) and relatively advanced models of vehicles, drivers and scripts for test manoeuvres. They often have an interface to Simulink, so that the user can add in their own models.

1.3.7.4 MBS tools

Examples of tools: Adams, Simpack, LMS Virtual Lab

These are general 3D mechanics modelling and simulation tools, so called MBS (Multi-Body Simulation) tools. As one example, Adams contains libraries of general bodies, joints and force elements. But there are toolboxes in Adams for vehicle dynamics, where template models and special components (such as tyre models and driver models) are available for vehicles dynamics. The models are very advanced and accurate for 3D mechanics, and there are import/export interfaces to Simulink.

1.3.7.5 Modelica based modelling tools

Examples of tools: Dymola, Maplesim, System-Modeler, AMESim, Optimica Studio, Jmodelica, OpenModelica

Modelica is not a tool but a globally standardized format for dynamic models on DAE form (see Mathematical/Declarative modelling in Section 1.3.2). There are a number of tools which supports this format.

The model format itself is non-causal and symbolic. There is one equation part and one declaration part in a model. An example of model is given in Figure 1-6.

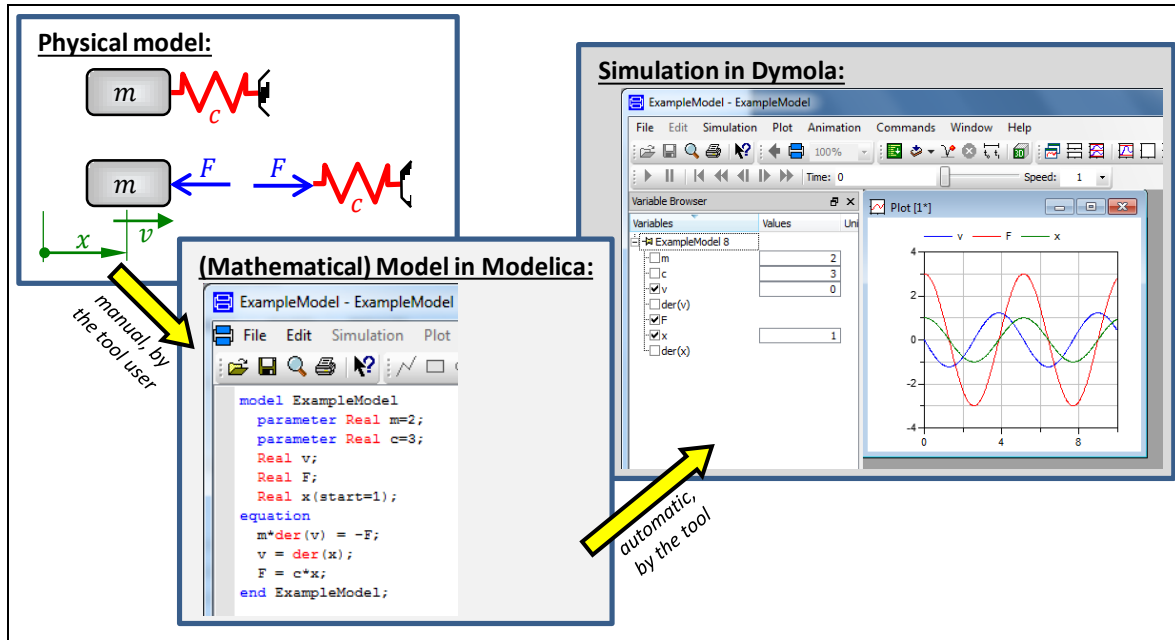


Figure 1-6: Example of model in Modelica forma (using the tool Dymola).

The model format is also object oriented, which means that libraries of model components are facilitated. These are often handled with graphical representation, on top of the model code. There are some open-source libraries for various physical domains, such as hydraulic, mechanics, thermodynamics and control. There are also commercial libraries, where we find vehicle dynamics relevant components: Vehicle Dynamics Library and Powertrain Library.

Some simple Modelica code will be used to describe models in this compendium.

In one way, Mathematical modelling (Declarative modelling) is more efficient than Explicit form modelling (Imperative modelling), since the engineer does not need to spend time on symbolic/algebraic manipulation of the equations. In this compendium, most modelling is done with Mathematical modelling. On the other hand, an Explicit form model has the value of capturing the causality, i.e. the cause-to-effect chain. The causality can sometimes facilitate the understanding and in that way help the engineer, which is why at least one and rather complete model is shown as Explicit form model, see Section 4.5.3.2.

1.3.8 Coordinate Systems

A vehicle's (motion) degrees of freedom are named as in marine and aerospace engineering, such as heave, roll, pitch and yaw, see Figure 1-7. Figure 1-7 also defines the 3 main geometrical planes, such as transversal plane and symmetry plane. For ground vehicles, the motion in ground plane is often treated as the primary motion, which is why longitudinal, lateral and yaw are called in-ground-plane degrees of freedom. The remaining degrees of freedom are referred to as out-of-ground-plane.

The consistent use of parameters that describe the relevant positions, velocities, accelerations, forces, and moments (torques) for the vehicle are critical. Unfortunately there are sometimes disparities between the nomenclature used in different text books, scientific articles, and technical reports. It is important to recognize which coordinate system is being applied and realize that all conventions will provide the same results as long as the system is used consistently. Two predominant approaches are encountered: the International Standards Organisation (ISO) and the Society of Automotive Engineers (SAE). Both ISO, (ISO8855), and SAE, (SAEJ670), are right handed systems. Figure 1-8 shows the vehicle fixed coordinate systems for these two standards. This

INTRODUCTION

compendium uses ISO, which also seems to be the trend globally. The new edition of (SAEJ670) now also recognises an optional use of z-up.

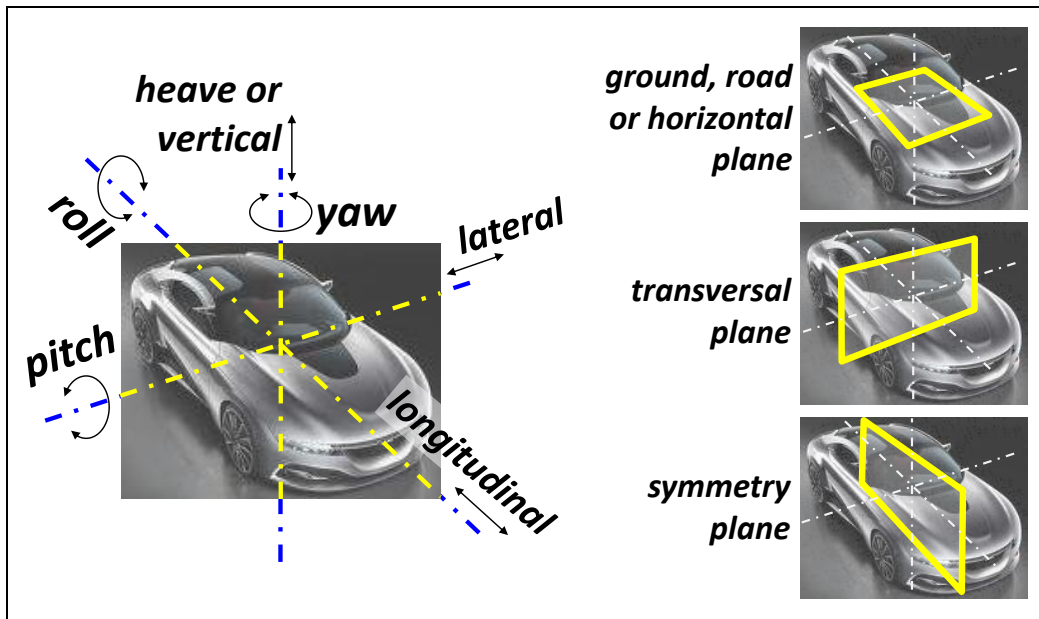


Figure 1-7: Vehicle (motion) degrees of freedom and important planes.

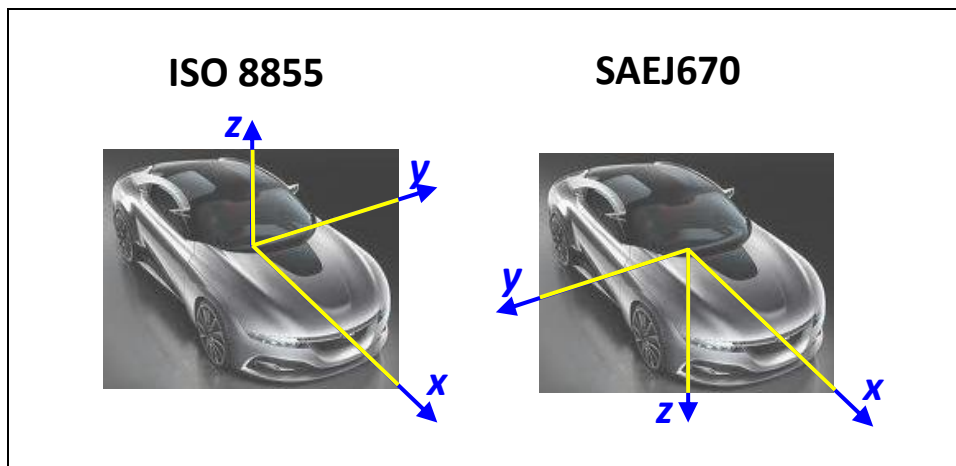


Figure 1-8: ISO and SAE coordinate systems

The distinction of vehicle fixed and inertial (= earth fixed = world fixed) coordinate systems is important. Figure 1-9 depicts the four most relevant reference frames in vehicle dynamics: the inertial, vehicle, wheel corner and wheel reference frames. All these different coordinate systems allow for the development of equations of motion in a convenient manner.

The orientation of the axes of an inertial coordinate system is typically either along the vehicle direction at the beginning of a manoeuvre or directed along the road or lane. Road or lane can also be curved, which calls for curved longitudinal coordinate.

Origin for a vehicle fixed coordinate system is often centre of gravity of the vehicle, but other points can be used, such as mid of front axle, mid of front bumper, outer edge of body with respect to certain obstacle, etc. Positions often need to be expressed for centre of lane, road edge, other moving vehicle, etc.

INTRODUCTION

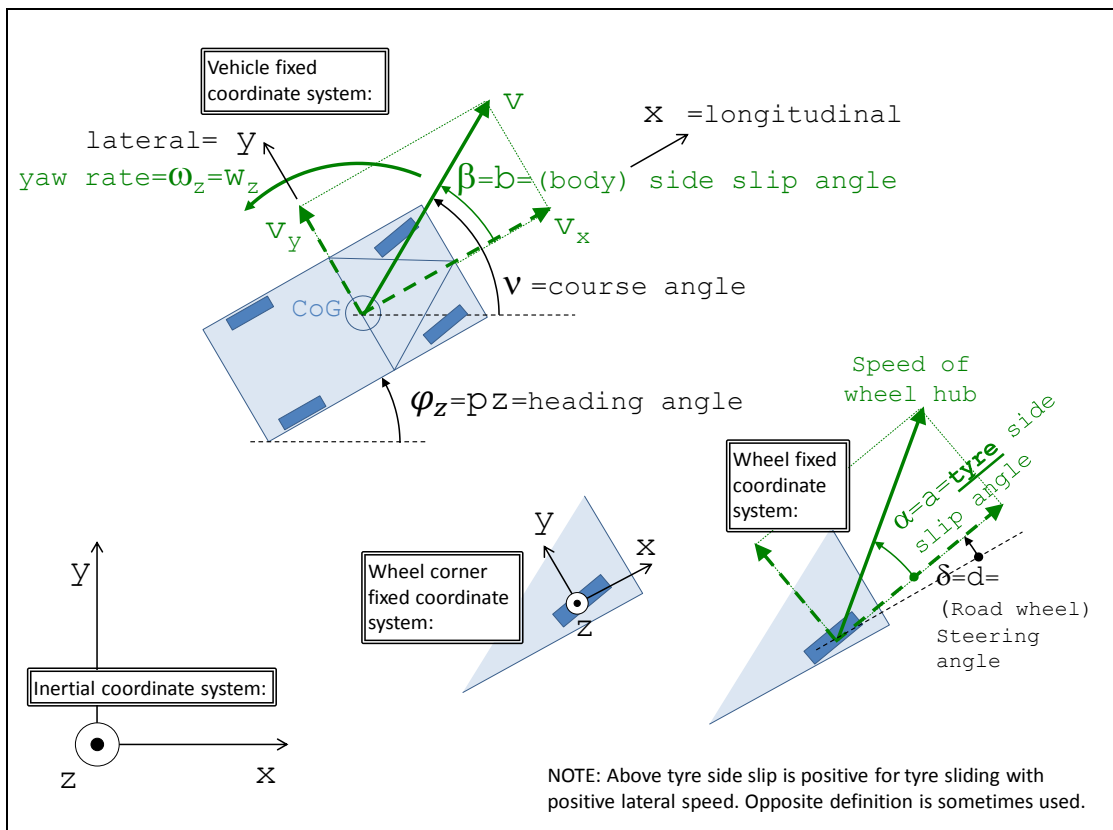


Figure 1-9: Coordinate systems and motion quantities in ground plane

In ISO and Figure 1-9, tyre side-slip is defined so that it is positive for positive lateral speed. This means that lateral forces on the wheel will be negative for positive side-slip angles. Some would rather want to have positive force for positive angle. Therefore, one can sometimes see the opposite definition of tyre side-slip angles, as e.g. in (Pacejka, 2005). It is called the “modified SAE” or “modified ISO” sign convention. This compendium does not use the modified sign convention in equations, but some diagrams are drawn with force-slip-curve in first quadrant. Which is preferable is simply a matter of taste.

Often there is a need to number each unit/axle/wheel. The numbering in Figure 1-10 is proposed. It should be noted that non-numeric notations are sometimes used, especially for two axle vehicles without secondary units. Then front=f, rear=r. Also to differentiate between sides, l=left and r=right.

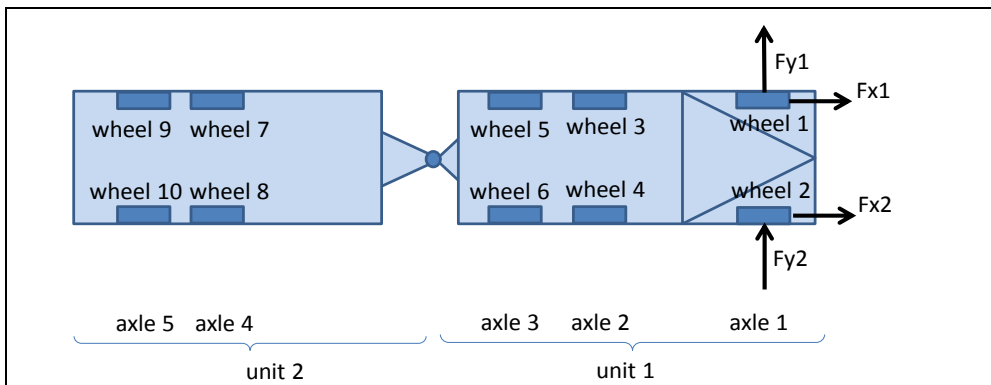


Figure 1-10: Proposed numbering of units, axles and wheels. Example shows a truck with trailer.

1.3.9 Terms with special meaning

1.3.9.1 Load levels

The weight of the vehicle varies through usage. For many vehicle dynamic functions it is important to specify the level, which is these definitions are important to know and use.

Kerb weight is the total weight of a vehicle with standard equipment, all necessary operating consumables (e.g., motor oil and coolant), a full tank of fuel, while not loaded with either passengers or cargo. Kerb weight definition differs between different governmental regulatory agencies and similar organizations. For example, many European Union manufacturers include a 75 kilogram driver to follow European Directive 95/48/EC.

Payload is the weight of carrying capacity of vehicle. Depending on the nature of the mission, the payload of a vehicle may include cargo, passengers or other equipment. In a commercial context, payload may refer only to revenue-generating cargo or paying passengers.

Gross Vehicle Mass (GVM) is the maximum operating weight/mass of a vehicle as specified by the manufacturer including the vehicle's chassis, body, engine, engine fluids, fuel, accessories, driver, passengers and cargo but excluding that of any trailers.

Other load definitions exist, such as:

- **“Design Weight”** (typically Kerb with 1 driver and 1 passenger, 75 kg each, in front seats)
- **“Instrumented Vehicle Weight”** (includes equipment for testing, e.g. out-riggers)

For vehicle dynamics it is often also relevant to specify where in the vehicle the load is placed.

1.3.9.2 Open loop and Closed loop manoeuvres

Depending on the drivers operation, one can differ between **Open loop** and **Closed loop** manoeuvres, see Section 2.10.1.

1.3.9.3 Objective and subjective measures

Two main categories of finding measures are:

- An **Objective** measure is a measure calculated in a defined and unique way from data which can be logged in a simulation or from sensors in a real test.
- A **Subjective** measure is a measure based on the test driver's judgement (e.g. on a scale 1-10) from a real test or driving simulator test.

One generally strives for objective measures, but many relevant functions are difficult to capture objectively, such as Steering feel and Comfort in transient jerks.

1.3.9.4 Path, Path with orientation and Trajectory

A **path** can be $x(y)$ or $y(x)$ for centre of gravity where x and y are coordinates in the road plane. To cope with all paths, it is often necessary to use a curved path coordinate instead, s , i.e. $x(s)$ and $y(s)$. The vehicle also has a varying orientation, $\varphi_z(x)$ or $\varphi_z(s)$, which often is often relevant, but the term “path” does necessarily include this. In those cases, it might be good to use an expression **“path with orientation”** instead.

A **trajectory** is a more general term than a path and it brings in the dependence of time, t . One typical understanding is that trajectories can be $[x(t); y(t); \varphi_z(t)]$. But also other quantities, such as steering angle or vehicle propulsion force can be called trajectory: $\delta(t)$ and $F_x(t)$, respectively. The word “trace” is sometimes used interchangeably with trajectory.

1.3.9.5 Stable and Unstable

Often, in the automotive industry and vehicle dynamics, the words “stable” and “unstable” have a broad meaning, describing whether high lateral slip on any axle is present or not. In more strict physics/mathematical nomenclature, “unstable” would be more narrow, meaning only exponentially increasing solution, which one generally finds only at high rear axle side-slip.

It is useful to know about this confusion. An alternative expression for the wider meaning is “loss of control” or “loss of tracking”.

1.3.9.6 Subject and object vehicle

The **subject vehicle** is the vehicle that is studied. Often this is a relevant to have a name for it, since one often study one specific vehicle, but it may interact with other in a traffic situation. Alternative names are **host vehicle**, **ego vehicle** or simply **studied vehicle**.

If one particular other vehicle is studied, it can be called **object vehicle** or **opponent vehicle**. A special case of object vehicle is **lead vehicle** which is ahead of, and travels in same direction as, subject vehicle. Another special case is **on-coming vehicle** which is ahead of, and travels in opposite direction as, subject vehicle.

1.3.9.7 Active Safety and ADAS

The expression *Active Safety* is used a lot in Automotive Engineering. There are at least two different usages:

- Active Safety can refer to the vehicle’s ability to avoid accidents, including both functions where the driver is in control (such as ABS and ESC, but also steering response) and functions with automatic interventions based on sensing of the vehicle surroundings (such as AEB and LKA). See http://en.wikipedia.org/wiki/Active_safety. Active Safety can even include static design aspects, such as designing the wind shield and head light for good vision/visibility.
- Alternatively, Active Safety can refer to only the functions with automatic interventions based on sensing of the vehicle surroundings. In those cases it is probably more specific to use Advanced Driver Assistance Systems (ADAS) instead, see http://en.wikipedia.org/wiki/Advanced_Driver_Assistance_Systems. ADAS does not only contain safety functions, but also comfort functions like CC and ACC.

1.3.9.8 Autonomous driving

Functions that off-load the driver the direct tasks during driving can be sorted under Autonomous driving. Fully autonomous driving, e.g. transportation without human driver on-board, is probably a far future vision. On the other hand, it is already a reality that some portion of the driving tasks are autonomous in the latest vehicle on the market, such as Adaptive cruise control, see Section 3.5.2.2, and Lane Keeping Aid, see Section 4.6.2.1. If both those are active at the same time, we have already autonomous driving in some sense. Today’s version of these systems normally have a way to hand-back responsibility to driver rather immediately in hazardous situations. Future autonomous driving functions will need to always have a safe-stop function. The way to compete between vehicle manufacturers will probably be to avoid hand-backs (maximize up-time) and to allow as long “hand-back times” as possible. So, vehicle dynamics will be important in the development, especially for safety reasons for autonomous driving in higher speeds; hazardous situations where human driver selects to take back the driving.

1.3.10 Architectures

Vehicles are often designed in platforms, i.e. parts of the design solutions are reused in several variants. Typical variants may be different model years or different propulsion system. To be able to reuse solutions, the vehicles have to be built using the same *architecture*.

A **mechanical** architecture may include design decisions about certain type of wheel suspension on front and rear axle. An **electrical and electronic** architecture may include design decisions about electric energy supply system (battery voltage etc.) and electronic hardware for computers (Electronic Control Units, ECUs) and how they are connected in networks, such as Controller Area Network, CAN.

That the mechanical architecture influences vehicle dynamics functions is rather obvious. However, it is noteworthy that also the electronic architecture also is very important for the vehicle dynamics, through all electronic sensors, actuators and control algorithms. One example of this importance is the ABS control of the friction brake actuators. Architectures for functions are therefore motivated, see Section 1.3.10.1.

1.3.10.1 Reference architecture of vehicle functionality

As the number of electronically controlled functions increase, the need for some sort of reference architecture for vehicle functionality, or “Functional Architecture”, becomes necessary to meet fast introduction of new functionality and to manage different variety of vehicle configurations. A reference architecture is a set of design decisions about how functions interact with each other (e.g. signalling between control functions). An older expression which is related to functional architecture is cybernetics. Examples (from Vehicle Dynamics functional domain) of modern expressions which are related are Integrated Chassis Control (GM), Integrated Vehicle Dynamics Control (Ford), Complete Vehicle Control (Volvo) and Vehicle Dynamics Integrated Management (Toyota). The authors of the compendium claim that there is no exact and generally well accepted definition of such architecture. However, it becomes more and more essential, driven by increasing content of electronic control in vehicles. One way to visualize a reference architecture is given in Figure 1-11.

In order to be able to formulate design rules in reference architecture of functionality the following are relevant questions:

- Which physical vehicle quantities should be represented on the interface between Sensors and Actuators on one side and Vehicle Level Functionality on the other?
- Partitioning within a reference architecture of vehicle motion functionality could be realised as shown in Figure 1-11. Different Layers/Domains are defined:
 - Motion Support Device Layer: This includes the devices/actuators that can generate vehicle motion. This layer is also consisting sensors which could include the capability and status of each device e.g. max/min wheel torque.
 - Vehicle Motion Layer: This includes the Energy management, powertrain coordination, brake distribution, and vehicle stability such as ESC, ABS. This layer also estimates the vehicle states e.g. v_x , v_y , w_z . In addition this layer would be able to give vehicle level capability of max/min acceleration and their derivative.
 - Traffic Situation Layer: Interpret the immediate surrounding traffic which the vehicle is in. Automated driving assistance functions such as adaptive cruise control, collision avoidance, and lane steer support are typical functions.
 - Vehicle Environment: Includes surrounding sensors mounted on vehicle but also communication with other vehicles (V2V) and infrastructure (V2I) and map information.

INTRODUCTION

- Human Machine Interface: This includes the sensors/buttons which the driver use to request services from the vehicle's embedded motion functionality.
- Formalisation of different types of:
 - Blocks, e.g. Controller, Signal Fusion, Arbitrator, and Coordinator.
 - Signals, e.g. Request, Status and Capability.
 - Parameters used in Functional blocks, e.g. Physical parameter and Tuning parameter.

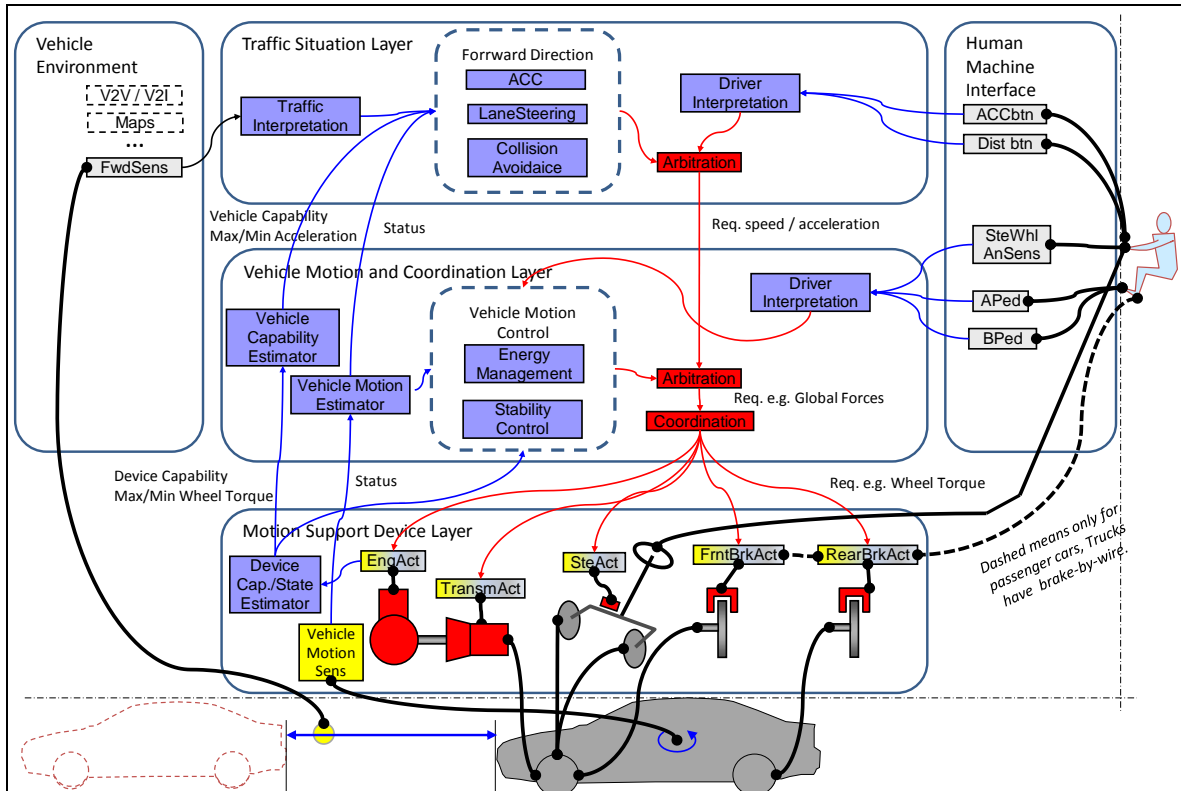


Figure 1-11: One example of reference architecture of vehicle motion functionality. Red arrows: Requests, Blue arrow: Information, Black lines with dot-ends: physical connection.

The functionality is then allocated to ECUs, and signals allocated to network communication. The reference architecture can be used for reasoning where the allocation should be done. Which functionality is sensitive for e.g. time delay and thus should be allocated in the same ECU. Detailed control algorithm design is not stipulated by a reference architecture. Instead the reference architecture assists how detailed control algorithms be managed in the complete problem of controlling the vehicle motion. Whether representation of solutions of Functional Safety (ISO 26262, etc.) is represented in a reference architecture of functionality can vary.

1.4 Heavy truck versus passenger cars

Passenger cars are relatively well known to most people and they seldom appear in very complex combinations. But heavy trucks are less well known and appear in vehicle combinations with many more units. Hence the following overview of the differences and most common units is given.

1.4.1 General differences

Trucks are normally bought by companies, not private persons. Each truck is bought for a specialized transport task. Life, counted in covered distance, for trucks is typically 10 times passenger cars. The life time cost of fuel is normally 5 times the vehicle cost, compared to passenger car where these costs are about equal. The cost for driver salary is a part of mileage cost, typically same magnitude as fuel cost. If investment cost for vehicle and repairs are distributed over travelled distance, these are typically also of same magnitude. So, the cost for a transport typically comes from one third fuel, one third driver salary and one third vehicle investment and repairs.

1.4.2 Vehicle dynamics differences

A truck has 5..10 times less power installed per vehicle weight. Trucks have their centre of gravity much higher, meaning that roll-over occurs at typically 4 m/s² lateral acceleration, as compared to around 10 m/s² for passenger cars. Trucks have centre of gravity far behind mid-point between axles, where passenger cars have it approximately symmetrical between the axles. Trucks are often driven with more units after, see Figure 1-12. The weight of the load in a truck can be up to 2..4 times the weight of the empty vehicle, while the maximum payload in passenger cars normally are significantly lower than the empty car weight. Trucks often have many steered axles, while passenger cars normally are only steered at front axle.






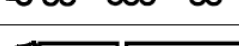

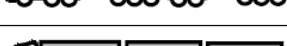
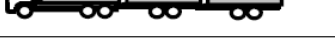
Conventional Combination Vehicles	Tractor-Semitrailer (Tractor-ST)	16.5 m/40 ton	
	Truck-Center Axle Trailer (Tractor-CAT)	18.75 m/40 ton	
	Truck-Full Trailer (Truck-FT)	18.75 m/40 ton	
Existing Longer Combination Vehicles	Tractor-Link Semitrailer-Semitrailer (B-Double)	25.25 m/60 ton	
	Tractor-Semitrailer-Center Axle Trailer (Tractor-ST-CAT)	25.25 m/60 ton	
	Truck-Dolly-Semitrailer (Truck-Dolly-ST)	25.25 m/60 ton	
Prospective Longer Combination Vehicles	Tractor-Semitrailer-Dolly-Semitrailer (A-Double)	31.5 m/80 ton	
	Truck-Duo Center Axle Trailer (Truck-Duo CAT)	27.5 m/66 ton	
	Truck-Dolly-Link Semitrailer-Semitrailer (Truck-B-Double)	34 m/90 ton	

Figure 1-12: An overview over conventional and longer combinations. From (Kharrazi , 2012).

1.5 Smaller vehicles

This section is about smaller vehicles, meaning bicycles, electric bicycles, motorcycles and 1-2 person car-like vehicles. The latter group refers to vehicles which are rare today, but there is a logic reasoning why they could become more common in the future: Increasing focus on energy consumption and congestion in cities can be partly solved with such small car-like vehicles, of which the Twizy in Figure 1-13 is a good example. All vehicles in Figure 1-13 can be referred to as Urban

INTRODUCTION

Personal Vehicle (UPVs), because they enable personalised transport in urban environments. The transport can be done with low energy consumption per travelled person and distance, compared to today's passenger cars. The transport can be done with high level of flexibility and privacy for the travelling persons, compared to today's public transportation.

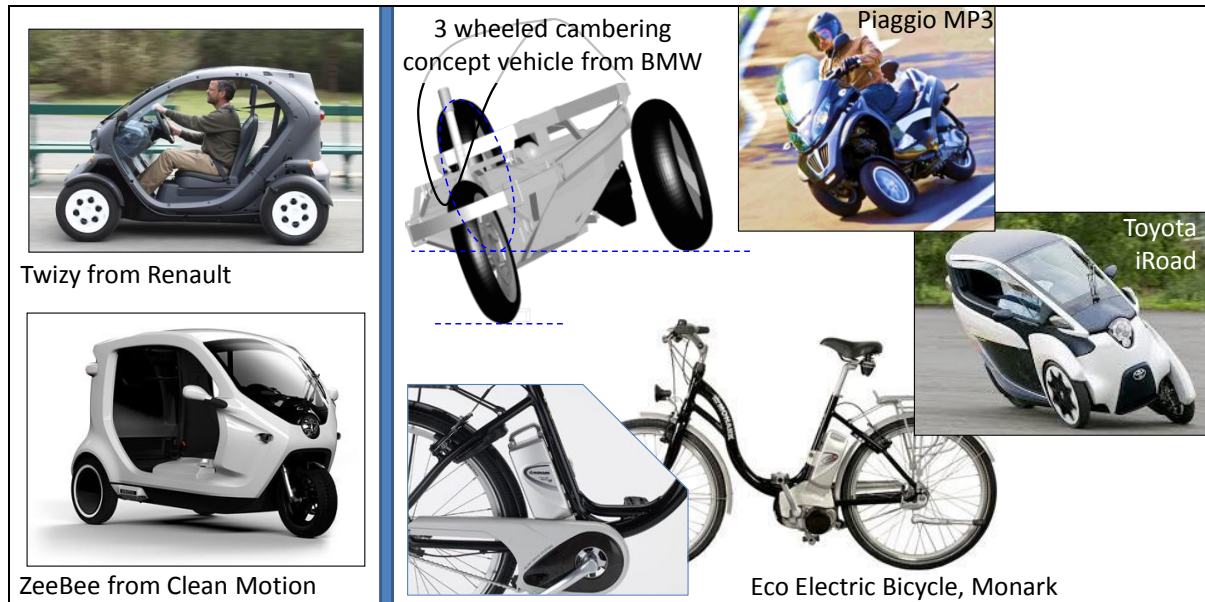


Figure 1-13: Examples of Urban Personal Vehicles. Left: “Roll-stiff”. Right: “Cambering”. From www.motorstown.com, www.cleanmotion.se, www.monarkexercise.se, www.nycscootering.com.

New solutions as in Figure 1-13 may require some categorization.

- Climate and user type: Sheltered or open.
- Transport and user type: Short travels (typically urban, 5-10 km, 50 km/h) or long travels (typically inter-urban, 10-30 km, 100 km/h).
- Chassis concept:
 - Narrow (e.g. normal bicycles and motorcycles) or wide (at least one axle with 2 wheels, resulting in 3-4 wheels on the vehicle).
Note that UPVs in both categories are typically still less wide than passenger cars.
 - Roll moment during cornering carried by suspension roll stiffness or roll moment during cornering avoided by vehicle cambering. The first concept can be called “Roll-stiff vehicle”. The second concept can be called “Cambering vehicle” or “Leaning vehicle”. 1-tracked are always Cambering vehicles. 2-tracked are normally Roll-stiff, but there are examples of Cambering such (see upper right in Figure 1-13).
 - (This compendium does only consider vehicles which are “Pitch-stiff”, i.e. such that can take the pitch moment during acceleration and braking. Examples of vehicles not considered, “Pitching vehicles”, are: one-wheeled vehicles as used at circuses and two-wheeled vehicles with one axle, such as Segways.)

Note that also Roll-stiff Vehicles camber while cornering, but only **slightly** and **outwards** in curve, while Cambering Vehicles above refer to **significant** cambering and **inwards** in curve.

Cambering Vehicles is more intricate to understand when it comes to how wheel steering is used. As a reference: In Roll-stiff Vehicles, the wheel suspension takes the roll-moment (keeps the roll balance), which means that driver can use wheel steering solely for making the vehicle steer (follow an intended path). In Cambering Vehicles, the driver has to use the wheel steering for both keeping

INTRODUCTION

the roll balance and follow the intended path. This means one control for two purposes, which calls for one more control. The additional control used comes from that the driver can move the CoG of the vehicle (including driver) laterally. So, the driver of a Cambering Vehicle has to use a combination of wheel steering and CoG moving for a combination of maintaining roll balance and following the intended path.

Smaller vehicles might have significantly different vehicle dynamics in many ways:

- Influence of driver weight is larger than for other vehicle types. This especially goes for bicycles, where driver weight can be typically 5 times larger than the vehicles own weight. Drivers not only change the total inertia properties, but they can also actively use their weight and move it during driving.
- Ratio between CoG height and wheel base is likely to be larger than passenger cars and trucks. This gives a larger longitudinal load transfer during acceleration and braking. Some concepts might even have the risk of “pitch-over”.
- For 2-tracked UPVs, the ratio between CoG height and track width is likely to be larger than passenger cars, rather like trucks, because it is likely that one want to keep swept area low for UPVs.
 - If Roll-stiff, this gives a larger lateral load transfer and roll angles during cornering. The risk for roll-over is also likely to be larger than passenger cars.
 - If Cambering, this opens for the risk for slide (“roll-over inwards in curve”, so called “low-sider”), which is known from motorcycles.
- For future UPVs it is possible that the part costs need to be kept low, as compared to passenger cars. This, and the fact that new inexperienced OEMs might show up on market, might lead to low-cost and/or unproven solutions appear for the vehicle design. This might be a challenge for driving experience and (driver and automated) active safety.
- Positive, for safety, is that future UPVs can have significantly lower top speed than passenger cars. However, the acceleration performance up to this top speed might be high, e.g. due to electric propulsion, which might cause new concerns for city traffic with surrounding.

1.6 Automotive engineering

This section is about a larger area than Vehicle Dynamics. It is about the context where Vehicle Dynamics is mainly applied.

OEM means Original Equipment Manufacturer and is, within the automotive industry, used for a company whose products are vehicles. OEM status is a legal identification in some countries.

In the automotive industry, the word Supplier means supplier to an OEM. There are Tier1 suppliers, Tier2 suppliers, etc. A Tier1 supplies directly to an OEM. A Tier2 supplies to a Tier1 and so on. Primarily, suppliers supply parts and systems to the OEMs, but suppliers can also supply competence, i.e. consultant services.

From an engineering view it is easy to think that an OEM only does Product Development and Manufacturing. But it is good to remember that there is also Marketing & Sales, After Sales, etc. However, Product Development is the main area where the vehicles are designed. It is typically divided into Powertrain, Chassis, Body, Electrical and Vehicle Engineering. Vehicle Dynamics competence is mainly needed in Chassis and Powertrain.

On supplier side, Vehicle Dynamics competence is mainly needed for system suppliers that supplies propulsion, brake, steering and suspension systems.

Except for OEMs and suppliers, Vehicle Dynamics competence is also needed at some governmental legislation and testing as well as research institutes.

There are engineering associations for automotive engineering. FISITA (Fédération Internationale des Sociétés d'Ingénieurs des Techniques de l'Automobile, www.fisita.com) is the umbrella organisation for the national automotive societies around the world. Examples of national societies are IMechE (United Kingdom), JSAE (Japan), SAE (USA), SAE-C (Kina), SATL (Finland), SIA (France), SVEA (Sweden, www.sveafordon.com) and VDI FVT (Germany). There is a European level association also, EAEC.

1.7 Typical numerical data

The purpose of the tables in this section is to give approximate numerical values of parameters. Vehicle parameters are often dependent of each other; changing one leads to that it is suitable to change others. The parameters are given with the intention to be consistent with each other, for each vehicle example. The tables balances between being generic and specific, which is difficult. Therefore, please consider the table as very approximate.

Table 1.3: Typical data, common for typical passenger cars and heavy trucks

Parameter	Notation	Typical Value	Unit
Air density	ρ	1	kg/(m ³)
Earth gravity	g	9.80665	m/(s*s)
Road friction, at dry asphalt	μ	1.0	N/N
Road friction, at wet asphalt		0.6	
Road friction, at snow		0.3	
Road friction, at wet ice		0.1	
Tyre cornering stiffness, normalized with vertical load	C	10	(N/rad)/N = (N/1)/N

1.7.1 For passenger vehicle

Table 1.2 gives typical numerical data for a medium sized passenger car.

INTRODUCTION

Table 1.4: Typical data for a passenger vehicle

Group/Type	Parameter	Notation	Typical Value	Unit	Note / Typical / Range / Relation to other
1. General	Length, bumper to bumper		5.00	m	
1. General	Longitudinal distance from CoG to front axle	lf	1.3	m	40-50% of wheel base: lf=0.55*L;
1. General	Mass	m	1700	kg	
1. General	Moment of inertia for yaw rotation	Jzz	2900	kg*m*m	Radius of gyration is slightly less (0.9) than half wheel base: =m*(0.9*L/2)^2
1. General	Unsprung mass	mus	200	kg	Sum of 4 wheels with suspensions
1. General	Track width	W	1.70	m	
1. General	Wheel base	L	2.90	m	
2. Systems	Engine inertia		0.5	kg*m*m	
2. Systems	Transmission ratio, highest gear		5.00	rad/rad= Nm/Nm	Engine to wheel. In magnitude of 5.
2. Systems	Transmission ratio, lowest gear		10.00	rad/rad= Nm/Nm	Engine to wheel. In magnitude of 10.
2. Systems	Brake proportioning, front/rear		70/30	N/N or Nm/Nm	Often tuned so that braking both axles when braking 0.8*g
2. Systems	Rolling resistance		0.01	N/N	
2. Systems	Steering ratio		16	rad/rad	Steering wheel to Road wheel
2. Systems	Wheel radius		0.30	m	
2. Systems	Wheel rotational inertia		0.5	kg*m*m	For one wheel
3. Longitudinal	Projected area in a transversal view	Afront	2.2	m^2	For calculation of air resistance
3. Longitudinal	Aerodynamic coefficients	cd, clf, clr	0.31, 0.10, 0.07	1	For calculation of longitudinal resistance and lift force over front and rear axle
5. Vertical	Suspension heave stiffness (without roll)	cs	100 000	N/m	Vertical stiffness at wheel. Sum of 4 wheels. So that bounce frequency f is between 1 and 2 Hz: sqrt(c/ms)=f*2*pi;
5. Vertical	Suspension roll stiffness, only from anti-roll-bars	carb	14 000	N/m	Vertical stiffness at wheel. Sum of both axles.
5. Vertical	Suspension damping	ds	13 000	N/(m/s)	Wheel rate. Sum of 4 wheels. Some 40..60% of critical damping: d = (0.4..0.6)*2*sqrt(c*m); 2..3 times softer in compression than rebound.
5. Vertical	Tyre vertical stiffness	ct	250 000	N/m	For one wheel

1.7.2 For heavy vehicle

Compared to passenger cars, trucks differs much more in size and configuration, see Figure 1-12. Also, a certain individual vehicle also differs much more between empty and fully loaded. So, Figure 1-14 and Table 1.5 are really to be seen only as an example. Globally, "Tractor with Semitrailer" is the most common vehicle, which is why it is used as example.

INTRODUCTION

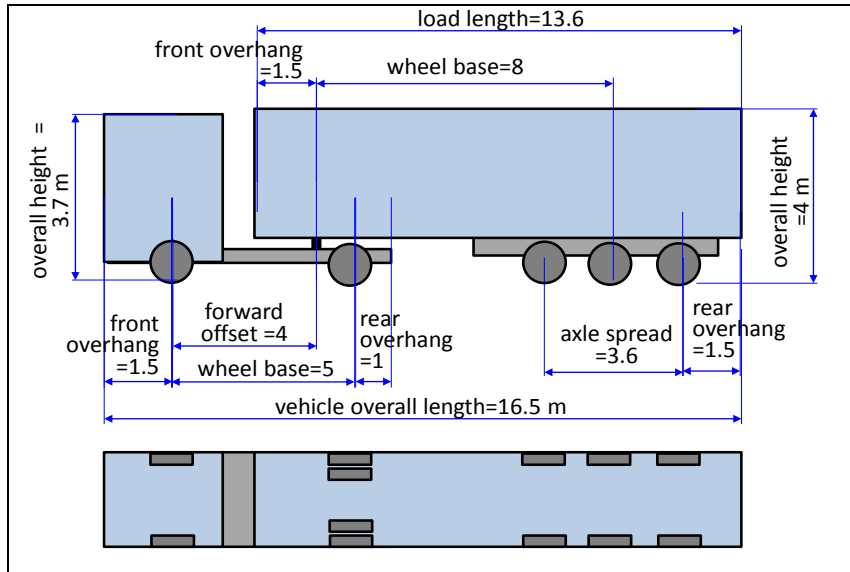


Figure 1-14: Typical data for a heavy vehicle, exemplified with “Tractor with Semi-trailer”

Table 1.5: Typical data for a heavy vehicle, exemplified with “Tractor with Semi-trailer”

Group/Type	Parameter	Typical Value		Unit	Note / Typical / Range / Relation to other
		Empty	With max payload		
Trackwidth	Trackwidth, centre-to-centre for single tyres	2.25		m	Outer tyre edge 2.55
Tractor	CoG height	1.00		m	
Semitrailer	CoG height	1.00	2.00	m	
Vehicle	CoG height	1.00	2.00	m	
Tractor	Mass (total), tractor	7500		kg	
Semitrailer	Mass (total), semi-trailer	10000	32500	kg	
Tractor	Moment of yaw inertia	22500		kg*m*m	Around unit CoG
Semitrailer	Moment of yaw inertia	150000	500000	kg*m*m	Around unit CoG
Tractor	Unsprung mass	1700		kg	Sum of all axles at unit
Semitrailer	Unsprung mass	2400		kg	Sum of all axles at unit
Wheels	Wheel radius	0.50		m	0.4-0.5
Wheels	Wheel rotational inertia	10.0		kg*m*m	For one wheel, single tyre
Tyres	Rolling resistance	0.005		N/N	Or less, 0.003
Propulsion	Engine max power	370		kNm/s=kW	
Propulsion	Engine inertia	5		kg*m*m	
Propulsion	Transmission ratio, highest gear	3		1=rad/rad= Nm/Nm	Engine to wheel
Propulsion	Transmission ratio, lowest gear	30			Engine to wheel
Steering	Steering ratio	20		rad/rad	Steering wheel to Road wheel
Vehicle	Projected area in a transversal view	10.0		m ²	For calculation of air resistance
Vehicle	Aerodynamic coefficient	0.4		1	c _d coefficient in aero dynamic resistance formula

INTRODUCTION

2 VEHICLE INTERACTIONS

2.1 Introduction

The study of vehicle dynamics starts with the interfaces between the vehicle and its environment, see Figure 2-1. The vehicle tyres are the primary structures to transfer loads that produce desired motions (vehicle weight, acceleration, steering, braking) and undesired disturbances (road vibrations, road bumps, etc.). Additionally, the aerodynamic loads on the vehicle will create forces and moments that are often undesirable (wind resistance, side gusts, etc.) but can sometimes be exploited for better contact with the road (down-force). An example of extreme interactions to the vehicle is the impact forces from a crash. An interaction of another kind, but still very influencing, is the driver.

The main focus of this chapter is to present the general characteristics of the tyres to start the process of qualitatively and quantitatively studying the other vehicle systems (steering, propulsion, suspension). Initial first order models will be presented with a brief interaction of combined loading.

General aerodynamic load calculations are presented but further discussion of aerodynamic loads are outside the scope of this compendium. Driver interaction is briefly mentioned. Traffic interactions with the vehicle are also briefly mentioned. Interaction with other road-users (collisions) is not covered.

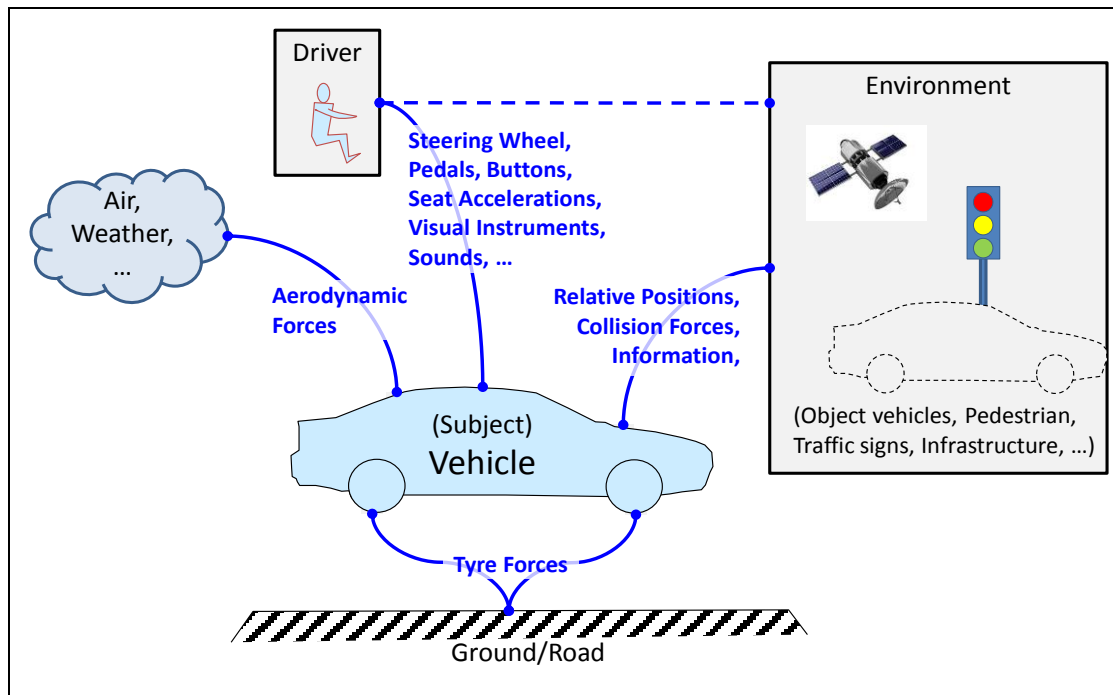


Figure 2-1: Interactions of the vehicle

2.2 Introduction to Tyre Terminology

The tyre (or wheel) should be analysed in its own coordinate system, see Figure 2-2. There are many different quantities and terms presented in Figure 2-2 and all are relevant for vehicle dynamics analysis. Fortunately some terms dominate the analyses presented in this course. The three forces, F_x , F_y , and F_z , are obviously necessary for any free body diagrams of the loads on the vehicle. Following these parameters, the term R_l represents the loaded (deflected) or rolling radius of the

tyre needed to identify how the loads are applied relative to the spin axis of the vehicles. Terms critical to the main topics in this course are:

- Longitudinal Dynamics: Torques about the spin axis.
- Lateral Dynamics: Slip angle: α
- Vertical Dynamics: Vertical Load: F_z

Other parameters presented in Figure 2-2 will have some influence on the theories developed in the coming chapters and will be discussed as appropriate.

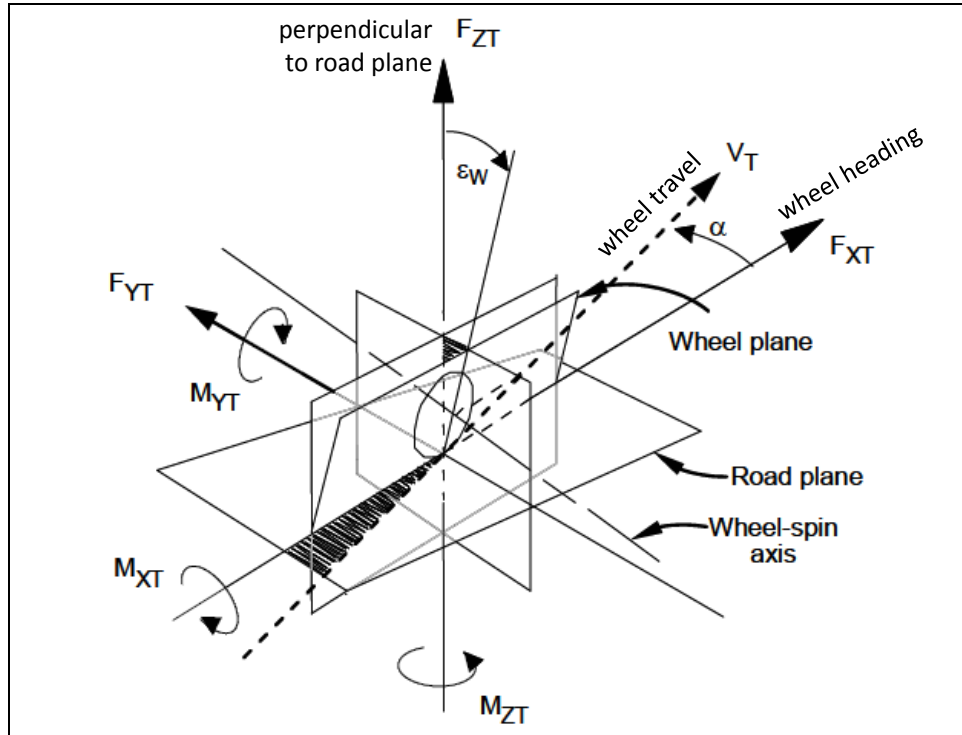


Figure 2-2: Tyre Coordinate System according to ISO

2.2.1 Wheel angles

2.2.1.1 Steering angle

A wheel's steering angle is the angle between the wheel plane and the longitudinal axis of the vehicle. Steering angle can be defined for one wheel or one axle, using averaging of left and right wheel.

2.2.1.2 Camber (Angle)

Camber or Camber angle is the angle between the wheel plane and the vertical, positive when the top of the wheel leans outward. (This definition of sign is only applicable for axles with two wheels. For instance, it is not applicable for motorcycles.) Camber generates lateral forces and gives tyre wear. See also Section 0.

2.2.1.3 Caster Angle

The angle in a side-view between the steering axis and the vertical axis is called Caster angle. It is positive if the top of the steering axis is inclined backwards. Caster angle provides an additional aligning torque, see Section 0 and Section 4.2.3.2, and changes the camber angle when the wheel is steered.

2.2.1.4 Toe Angle

Toe angle (or toe-in) is defined for an axle with two wheels (not for a single wheel), as the difference between right and left wheel's steering angles. Toe angle is positive if front ends of the wheels are pointing inward. Hence, toe can be called toe-in. Negative toe can be called toe-out. Toe angle generates opposing lateral forces on each side.

The toe angles vary with the tyre forces, due to suspension linkage geometry and elasticity in suspension bushings. This means that there is a *static toe angle* (when a vehicle parked in workshop, with a certain load and not tyre forces in ground plane) has one value, while *actual toe angle* (in a particular moment during a manoeuvre) has another value.

Zero toe gives low rolling resistance and low tire wear. Theoretically, toe-out on front axle and toe-in on rear axle makes the vehicle most yaw stable (less over-steered). Tone-in on front axle makes vehicle more yaw agile and improves on-centre steering feel. Normal design choice is toe-in on both axles, and more on front axle.

2.2.1.5 Steering axis inclination

Steering axis inclination (or Kingpin inclination) is defined for a wheel with its suspension linkage (not for an isolated wheel). The angle in a front view between the steering axis (or Kingpin) and the vertical axis is called Kingpin inclination. See Section 4.2.3.2.

2.3 Tyre Construction

The tyres of a vehicle have the following tasks:

- Carry the static load
- Generate brake, traction and lateral forces
- Isolate vertical disturbances, for comfort, road grip and reduction of suspension fatigue
- Roll with minimum energy loss, particle emissions and noise emission

Before discussing the mechanics of tyre and road interactions, the physical structure of the wheel assembly should be understood. Consisting of a steel rim and an inflated rubber toroid, pneumatic tyres were invented and patented by Robert William Thomson in 1845 and are essentially the only type of tyre found on motor vehicles today.

The physical construction of the tyre carcass affects the response of the tyre to different road loadings. The carcass is a network of fabric and wire reinforcement that gives the tyre the mechanical strength. The structure of the carcass can be divided into different types of tyres: BIAS-PLY, BIAS-PLY BELTED, and RADIAL-PLY. Bias-ply tyres were the first types of pneumatic tyres to be used on motor vehicles. Radial ply tyres followed in 1946 and became the standard for passenger car tyres. Figure 2-3 shows the main features of these tyre types.

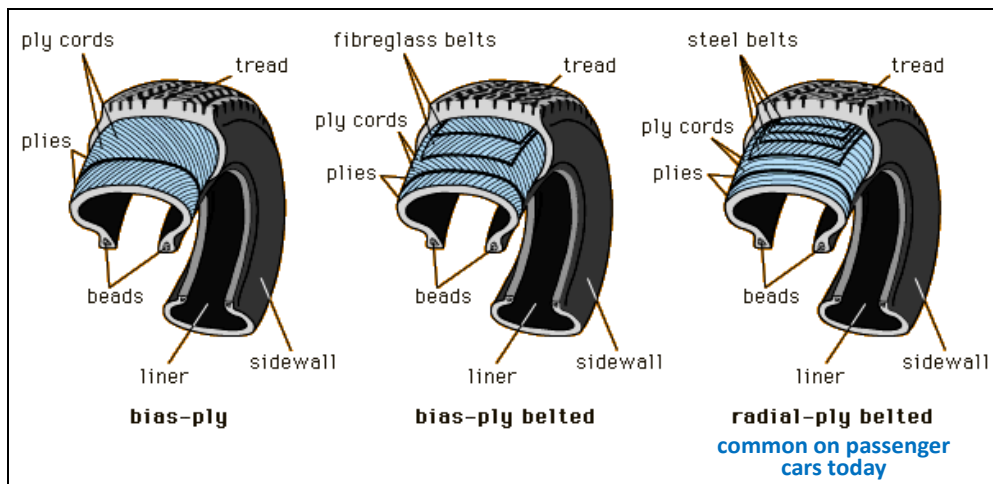


Figure 2-3: Common Tyre Constructions, from (Encyclopædia Britannica Online, 2007)

Note how the bias-ply constructions have textile structures oriented at an angle to the tyre centreline along the x-z plane. This angle is referred to as the crown angle and is further illustrated in Figure 2-4. Note the textile orientation for the bias-ply and radial tyres. Also note the difference in crown angles between the two tyre constructions. This difference plays an important part in the rolling resistance characteristics of the tyre which is Section 2.4.

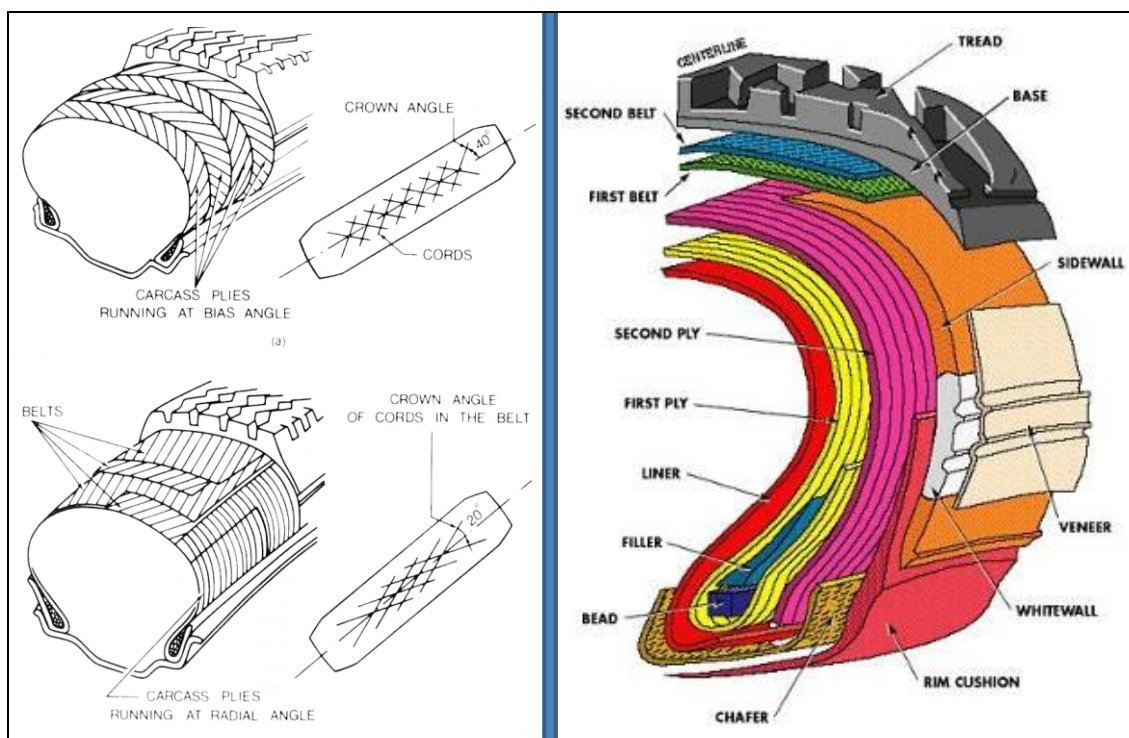


Figure 2-4: Left: Carcass Construction, (Wong, 2001). Left top: Bias-ply construction. Left bottom: Radial construction. Right: Radial Tyre Structure, (Cooper Tire & Rubber Co., 2007)

The tyre components have been constructed to provide the best tyre performance for different loading directions. A trade-off must be made between handling performance and comfort, between acceleration and wear, as well as between rolling resistance and desired friction for generating forces in ground plane. Some of the tyre components have an important role in vehicle performance. For example, the radial tyre components are presented in more detail in Figure 2-4. The rubber

components and patterns incorporated in the tread are critical to the friction developed between the tyre and road under all road conditions (wet, dry, snow, etc.). Friction is most relevant in longitudinal and lateral vehicle dynamics. The belts define the circumferential strength of the tyre and thus braking and acceleration performance. The sidewall and plies define the lateral strength of the tyre and thus influence the lateral (cornering) performance of the vehicle. The sidewall as well as the inflation pressure are also significant contributors to the vertical stiffness properties of the tyre and affect how the tyre transmits road irregularities to the remainder of the vehicle. It becomes clear that a tyre that has strong sidewalls will support cornering at the cost of vertical compliance – reducing the comfort in the vehicle.

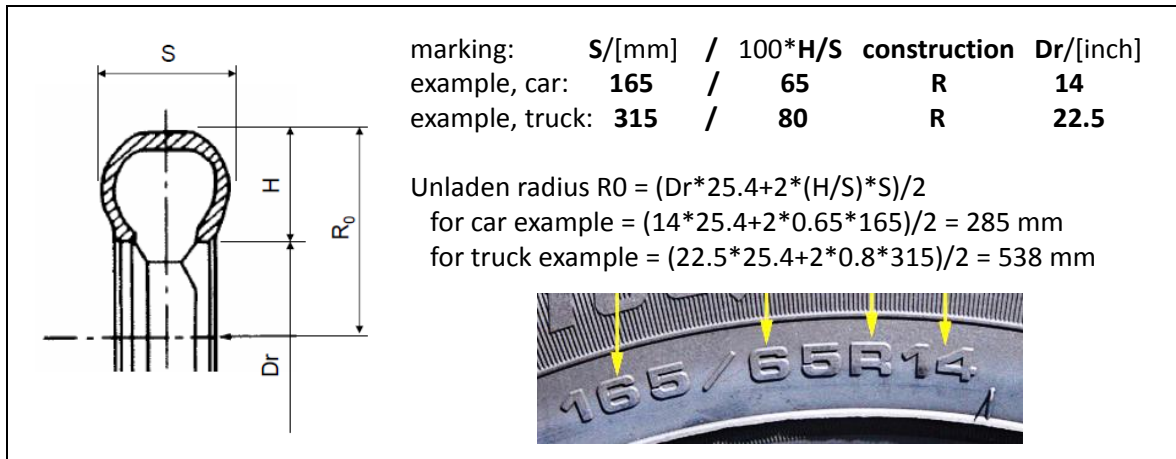


Figure 2-5: Tyre marking (radial tyre)

2.3.1 Tyre design and function

This section differs between design and function as well as between parameters and variables. It assumes observations over time; i.e. time is the independent variable, i.e. variables vary with time. It can be noted that, in another problem context, some of the quantities could switch between parameters and variables. One example is a design optimization, where basically all design parameters becomes variables (are varied) in the optimization.

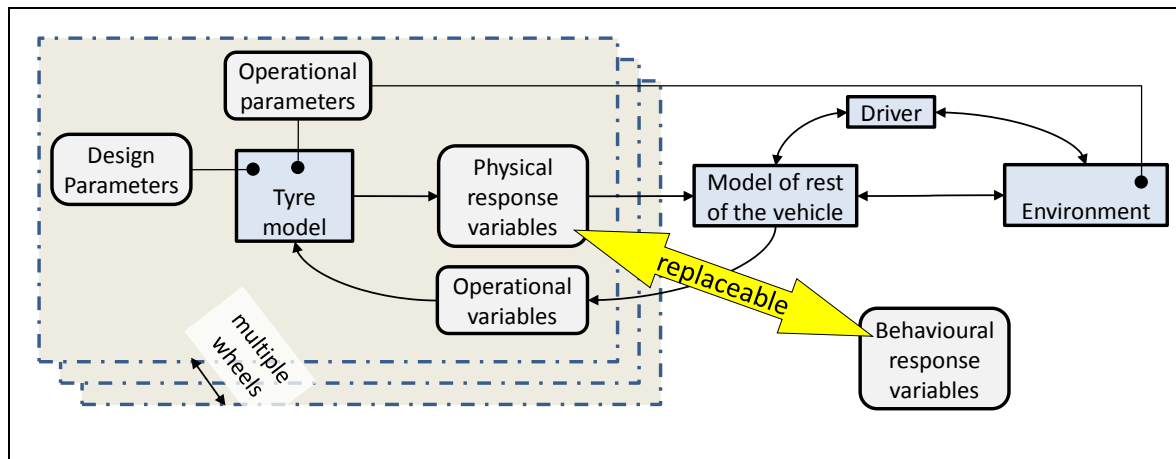


Figure 2-6: How tyre models can come into a model context.

2.3.1.1 Design parameters

We limit ourselves to today’s traditional pneumatic tyres. Then the design is captured by:

- Carcass/Material: Rubber quality and plies arrangement.

- Tread/Grooves: Groove pattern, Groove depth, Tread depth, Spikes pattern (if spikes)
- Main dimensions: Outer radius, Width, Aspect ratio
- Installation parameters: Inflation pressure

2.3.1.2 Operational parameters

These are operating conditions which vary slowly, and in this description assumed to be constant during one manoeuvre/driving cycle. These are:

- Road surface (dry/wet, asphalt/gravel/snow/ice, ...),
- Road compliance and damping (hard/soft, ...),
- Wear state of tyre,
- Age of tyre,
- Temperature

2.3.1.3 Operational variables

These are operating conditions which vary quickly, and in this description assumed to be variable in time during one manoeuvre/driving cycle. These are:

- Longitudinal speed,
- Tyre slip (s_x, s_y , see Equation [2.2]),
- Vertical tyre force, (F_z , see Figure 2-2)
- Camber angle

Tyre forces in road plane (F_x, F_y) can be given instead of tyre slip. Another alternative is to give the corresponding actuation, e.g. wheel shaft torque and wheel steering angle relative to wheel course angle. With those setups, the response variables in Section 2.3.1.4.

Vertical tyre force can be modelled as arbitrarily varying in time or as an offset amplitude for different frequencies where offset is from a mean value. The mean value would then be a parameter instead of a variable. The latter alternative can be more efficient if simulating a longer driving cycle, where following each road wave would be very computational inefficient.

2.3.1.4 Responses

Response refers to response to both Design changes and Operation changes.

2.3.1.4.1 Physical response (variables)

The variables from tyre model to model of rest of the vehicle is essential the forces and moments, see Figure 2-2:

- Longitudinal and lateral forces (F_x, F_y)
- Roll moment or Overturning moment (M_x)
- Rolling resistance moment (M_y)
- Spin moment or Aligning moment (M_z)

Other responses are:

- Wear rate [worn rubber mass or tread depth per time unit]

2.3.1.4.2 Behavioural response (variables)

The Responses can be modelled as Behavioural variables instead:

- Slip characteristics (C_{sx} , C_{sy} , peak friction coefficient, ... or other parameters in physical or empirical tyre slip model, as in Section 2.4.3.2)
- Rolling resistance coefficient
- Vertical stiffness and damping
- Wear coefficient
- Relaxation length, ...

When working with Behavioural instead of Physical, the distinction between variables and parameters become less clear. So, we can see the same list of quantities as parameters instead of variables.

2.4 Longitudinal Properties of Tyres

The forces in ground plane, in the tyre's contact patch, depend on the tyre's construction, the type of road surface and the operating states (velocities and vertical force). This section treats the main phenomena of tyre mechanics that influence the tyre-longitudinal force. The tyre can be under braking, free rolling or traction.

The whole wheel, including the tyre, can be seen as a transmission from rotational mechanical energy to translational mechanical energy. The shaft is on the rotating side; where we find rotational speed, ω , and torque, T . The shaft torque T is then the sum of torque on the propulsion shaft and torque on the brake disk or drum. The wheel hub is on the translator; where we find translating speed, v_x , and force, $F_{hub,x}$. See Figure 2-7.

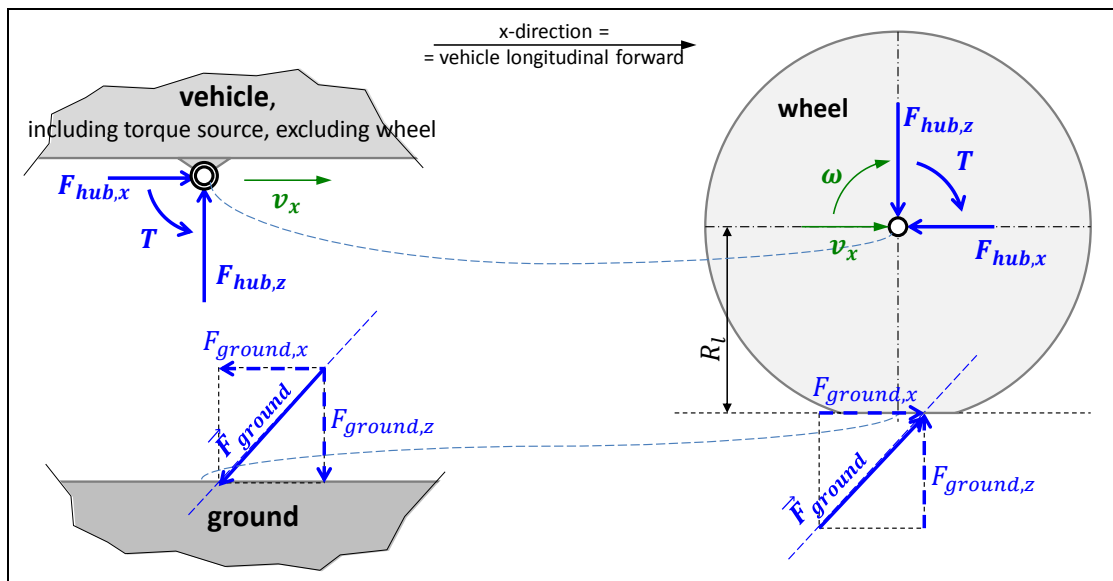


Figure 2-7: A wheel as a transmission from rotational $[\omega; T]$ to translational $[v_x; F_{hub,x}]$.

2.4.1 Tyre Rolling and Radii

In all fundamental engineering mechanics, the radius of an object that rolls without sliding is a compatibility link between the translational velocity and angular velocity as shown in Figure 2-8 a). This relationship does not hold when the tyre is deflected as in Figure 2-8 b). Not even the deflected radius can be assumed to be a proportionality constant between angular and translational velocity, since the tyre contact surface slides, or slips, versus the ground. Then, an even truer picture of a

rolling tyre looks like Figure 2-8 c), where the deformation at the leading edge also is drawn. This means that v_x is only $\approx R_l \cdot \omega$ and $\approx R_o \cdot \omega$ for limited slip levels.

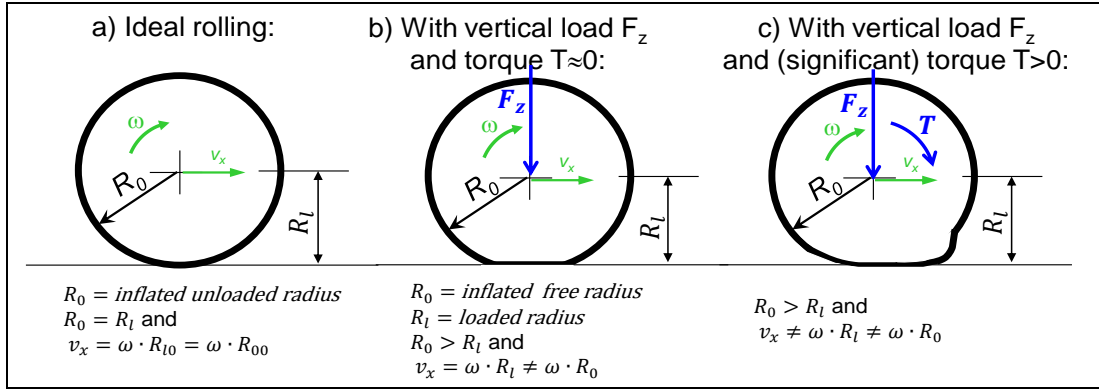


Figure 2-8: Radius and speed relations of a rolling tyre R_0 and R_l do not have exactly the same numerical values across a), b) and c).

There is a difference speed between tyre and the road surface. The ratio between this speed and a reference speed is defined as the “tyre slip”. The reference speed can be the translational speed of the tyre or the circumferential speed of the tyre depending on the application. For a driven wheel, the longitudinal (tyre) slip is often defined as:

$$s_x = \frac{R \cdot \omega - v_x}{|R \cdot \omega|}; \quad [2.1]$$

For braked wheels it is often defined as:

$$s_x = \frac{R \cdot \omega - v_x}{|v_x|}; \quad [2.2]$$

Averaging the reference speed gives the third variant in Eq [2.3]. This is actually possible to argue for physically as we will see in Section 2.4.3.1.

$$s_x = \frac{R \cdot \omega - v_x}{|R \cdot \omega + v_x|/2}; \quad [2.3]$$

With the definition in Equation [2.3], the following transformation falls out:

$$\omega = \begin{cases} = \frac{2 + s_x}{2 - s_x} \cdot \frac{v_x}{R}; & \text{if } R \cdot \omega + v_x > 0 \Rightarrow \text{if } v_x > 0; \\ = \frac{2 - s_x}{2 + s_x} \cdot \frac{v_x}{R}; & \text{if } R \cdot \omega + v_x < 0 \Rightarrow \text{if } v_x < 0; \end{cases} \quad [2.4]$$

Whether one should use $R \cdot \omega$ or v_x or something else as reference speed (the denominators in Equations [2.1]..[2.3]), is not obvious and is discussed in Section 2.4.3.

It is also not obvious which R to use in Equations [2.1]..[2.3], e.g. R_0 or R_l . However, this compendium recommends R_0 , rather than R_l , because R_0 is a better average value of the radius around the tyre and the tyre’s circumference is tangentially stiff so speed has to be same around the circumference.

Sometimes one defines a third radius, the Rolling Radius = $(v_x/\omega)|_{T=0}$, i.e. a speed ratio with dimension length, between translator and rotating speeds, measured when the wheel is un-driven.

This radius can be used for relating vehicle longitudinal speed to wheel rotational speed sensors, e.g. for speedometer or as reference speed for ABS and ESC algorithms. The Rolling radius is normally between R_0 and R_l .

Yet another approach is to use the $R = (v_x/\omega)|_{F_x=0}$, i.e. the ratio when the wheel is pure rolling.

Using $R = (v_x/\omega)|_{T=0}$ or $R = (v_x/\omega)|_{F_x=0}$ in the slip definitions shifts $F_x(s_x)$ curve and $T(s_x)$ curve, see more in Section 2.4.3.3.

The variable s_x is the longitudinal slip value, sometimes also denoted as κ . When studying braking, one sometimes uses the opposite sign definition, so that the numerical values of slip becomes positive. It is used to model the longitudinal, traction or braking, tyre force in Section 2.4.3.

2.4.2 The Rolling Resistance of Tyres

The rolling resistance force is defined as the loss of longitudinal force on the vehicle body, as compared to the longitudinal force, which would have been transferred with an ideal wheel. The Rolling Resistance Coefficient, f_r , is the rolling resistance force divided by the normal force, F_z . Assuming force equilibria in longitudinal and vertical direction, $F_{hub,z} = F_{ground,z} = F_z$ and $F_{hub,x} = F_{ground,x} = F_x$, see Figure 2-7.

$$f_r = \frac{\frac{T}{R_l} - F_x}{F_z} \quad [2.5]$$

F_x denotes the longitudinal force on the wheel, T denotes the applied torque and R_l denotes the tyre radius. For a free rolling tyre, where $T = 0$, f_r becomes simply $-F_x/F_z$. One often see definitions of f_r which assumes free rolling tyre; but Eq [2.5] is more generally useful.

Regarding which radius to use, it should rather be R_l than R_0 , because R_l represents the lever for the longitudinal tyre force around the wheel hub.

A free body diagram of the forces on the wheel can be used to explain the rolling resistance. Consider Figure 2-9 which represents a free rolling wheel under steady state conditions. The inertia of the wheel is neglected.

The main explanation model of rolling resistance for pneumatic tyres on hard flat surfaces is that the pressure distribution is biased towards the edge towards which the wheel is rolling. Damping and friction, see Figure 2-9, is the main reason for this and it is not dependent on the longitudinal force. Same figure also shows the off-centre effect, which is directly influenced by the longitudinal force. The force offset, e , explains f_r . Additional to what is shown in Figure 2-9 one can motivate even higher e , by including other effects, such as wheel bearing loss, brake disk drag and aerodynamic torque loss.

Longitudinal and vertical force equilibria are already satisfied, due to assumptions above. However, moment equilibrium around wheel hub requires:

$$T - F_x \cdot R_l - F_z \cdot e = 0 \Rightarrow F_x = \frac{T}{R_l} - F_z \cdot \frac{e}{R_l}; \quad [2.6]$$

An analysis of this result is that the force F_x which pushes the vehicle body forward is the term T/R_l (arising from the applied propulsion or brake torque T), minus the term $F_z \cdot e/R_l$. The term can be seen as a force F_{roll} and referred to as the rolling resistance force. The dimensionless ratio e/R expression is the rolling resistance coefficient, f_r :

$$f_r = \frac{e}{R_l}; \quad [2.7]$$

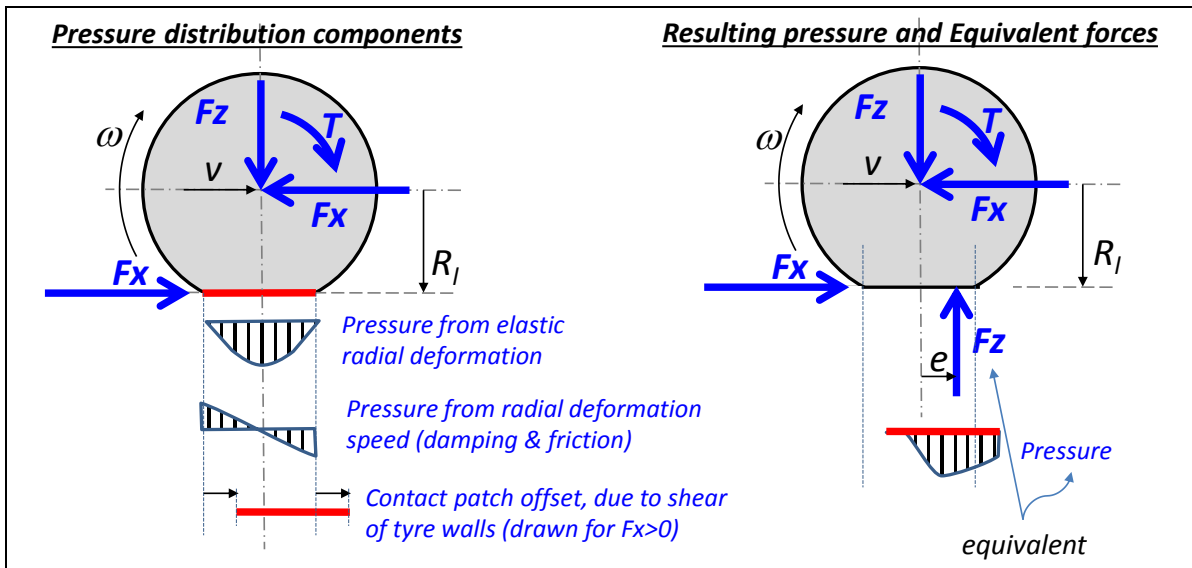


Figure 2-9: Normal force distribution on a tyre. The measure e is the force offset.

Eq [2.7] is a definition of rolling resistance coefficient based assumed physical mechanisms internally in the tyre with road contact. Rolling resistance coefficient can also be defined based on quantities which are measurable externally, see Eq [2.5]. Sometimes one see $f_r = -F_x/F_z$ as a definition, but that is not suitable since it assumes absence of torque.

It is important to refer to this phenomenon as rolling **resistance** as opposed to rolling **friction**. It is not friction in the basic sense of friction, because $F_x \neq -f_r \cdot F_z$ except for the special case when un-driven wheel ($T = 0$).

Figure 2-10 shows an un-driven wheel, which is a special case of a driven wheel.

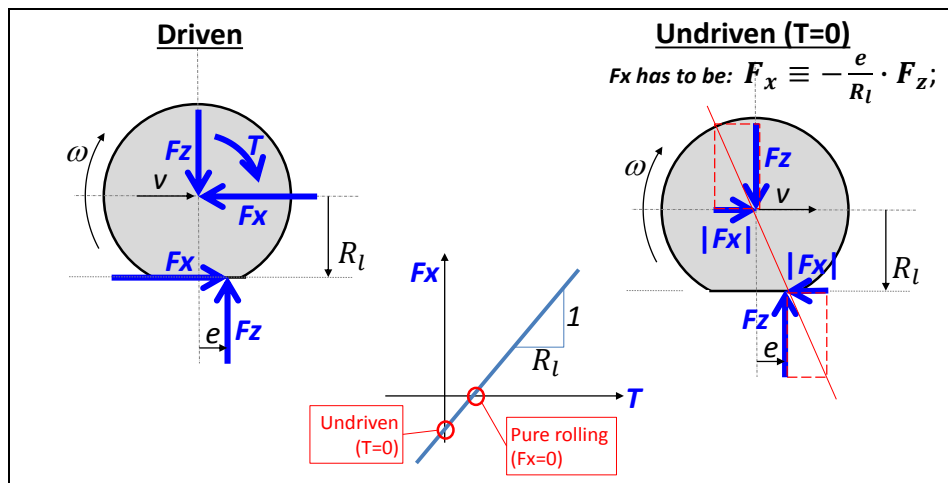


Figure 2-10: Driven wheel with rolling resistance, special cases "Un-driven" and "Pure rolling".

2.4.2.1 Variation of rolling resistance

Several factors will affect the rolling resistance of tyres. Design factors:

VEHICLE INTERACTIONS

- Tyre material. Natural rubber often gives lower rolling resistance.
- Radial tyres have more flexible sides, giving lower rolling resistance also bias ply have a greater crown angle causing more internal friction within the tyre during deflection.
- Geometry:
 - Diameter. Large wheels often have lower coefficient of rolling resistance
 - Width
 - Groove depth
 - Tread depth

Usage factors, long term varying:

- Higher inflation pressure gives lower rolling resistance on hard ground but higher rolling resistance on soft ground (and vice versa), see Figure 2-11 and Figure 2-12.
- Wear. Worn tyres have lower rolling resistance than new ones (less rubber to deform).

Usage factors, short term varying:

- Tyre loads (traction, braking and lateral forces)
- Speed. Rolling resistance increases with vehicle speed due to rubber hysteresis and air drag.
- High temperatures give low rolling resistance. Tyres need to roll approximately 30 km before the rolling resistance drop to their lowest values.
- Road/ground material. Asphalt, gravel, snow, etc.

Figure 2-11 shows how widely the rolling resistance changes due to different road/ground material and inflation pressures. As can be expected, a range of values exist depending on the specific tyre and surface materials investigated. On hard ground, the rolling resistance decreases with increased inflation pressure, which is in-line with the explanation model used above, since higher pressure intuitively reduces the contact surface and hence reduces e . On soft ground the situation is reversed, which requires a slightly different explanation model, see Figure 2-12. On soft ground, the ground is deformed so that the wheel rolls in a “local uphill slope” with inclination angle φ . Intuitively, a higher inflation pressure will lead to more deformation of the ground, leading to a steeper φ .

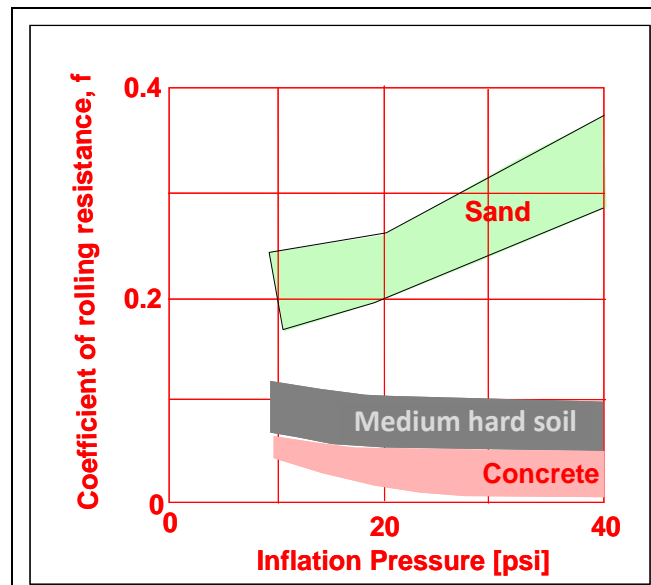


Figure 2-11 : Range of Coefficient of Rolling Resistance for different road/ground material

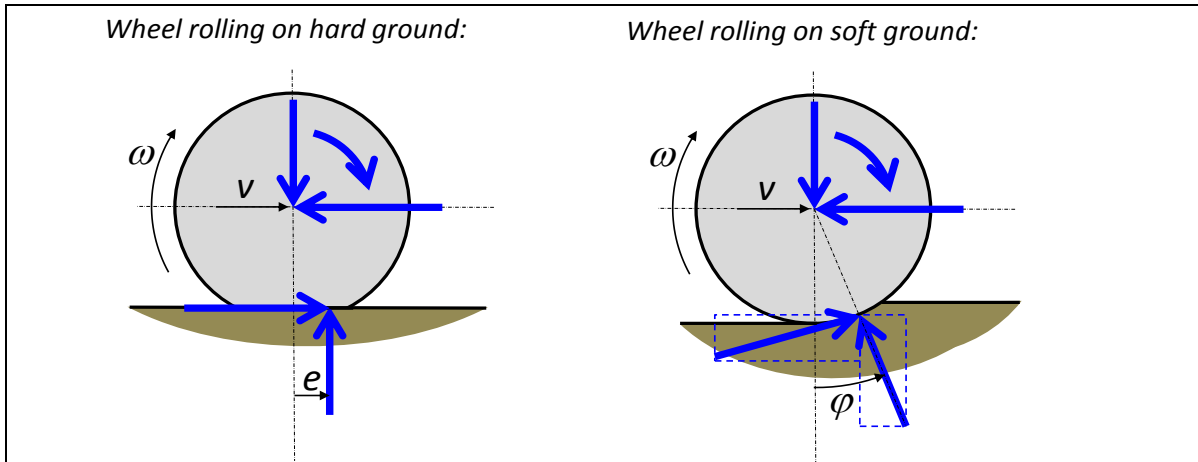


Figure 2-12 : Rolling resistance explanation model for hard and soft ground.

As an example, Figure 2-13 shows the influence of tyre construction and speed on rolling resistance. The sudden increase in rolling resistance at high speed is important to note since this can lead to catastrophic failure in tyres. The source of this increase in rolling resistance is a high energy standing wave that forms at the trailing edge of the tyre/road contact.

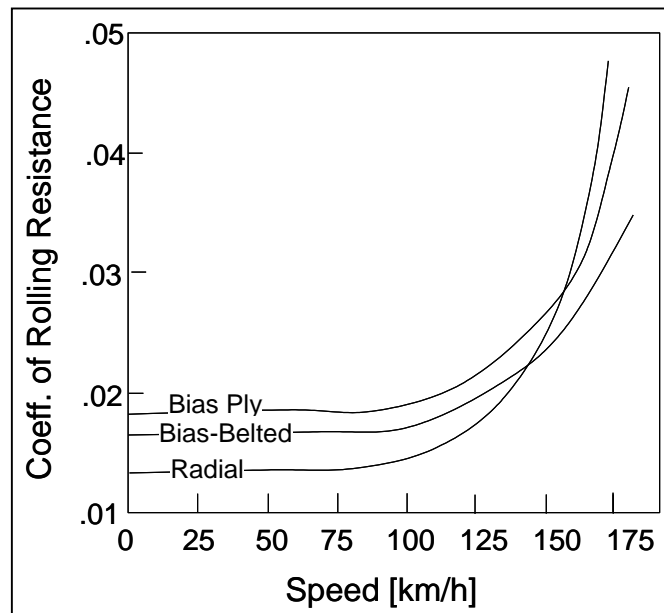


Figure 2-13: Rolling Resistance Values for Tyre Type and Operating Speed, (Gillespie, 1992)

There are some empirical relationships derived for the tyre's rolling resistance. It is advisable to refer to the tyre manufacturer's technical specifications when exact information is required. This type of information is usually very confidential and not readily available. Some general relationships have been developed, from (Wong, 2001):

Radial-ply passenger car tyres: $f_r = 0.0136 + 0.04 \cdot 10^{-6} \cdot v^2$
 Bias-ply passenger car tyres: $f_r = 0.0169 + 0.19 \cdot 10^{-6} \cdot v^2$
 Radial-ply truck tyres: $f_r = 0.006 + 0.23 \cdot 10^{-6} \cdot v^2$
 Bias-ply truck tyres: $f_r = 0.007 + 0.45 \cdot 10^{-6} \cdot v^2$

There is a weak variation with speed which can be ignored for lower speeds. As seen in Figure 2-13, the influence of speed on rolling resistance is constant up to about 100 km/h. Trucks tyres have a

much lower rolling resistance (approximately half). Tyres have developed in that way for trucks, because their fuel economy is so critical.

There is also a dependency on longitudinal force, see Figure 2-14. RRC increases when positive force, since the shearing of the sidewall moves the contact forward and the shearing decreases the wheel radius. For negative forces, these two effects have opposite influence, so the change is less for negative force.

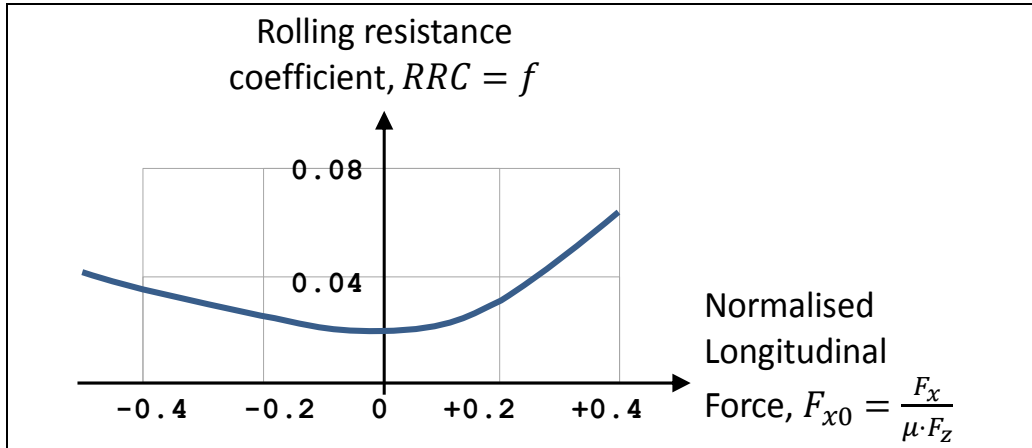


Figure 2-14 : Rolling resistance dependency of longitudinal tyre force. Inspired by (Wong, 2001)

Rolling resistance is a torque loss. Other torque losses, which can be included or not in tyre rolling resistance, are:

- Losses associated with friction in gear meshes,
- drag losses from oil in the transmission,
- wheel bearing torque losses, and
- drag losses from aerodynamic around the wheel.

These should, as rolling resistance, be subtracted from propulsion/brake torque when calculating T in Figure 2-10. However, sometimes they are included as part of the tyres rolling resistance coefficient, which is somewhat misleading even if it works if done correctly. The wheel bearing torque losses are special in that they are rather proportional to vertical load on the wheel, and hence it is rather natural to include them in rolling resistance coefficient. The aerodynamic losses due to wheel rotation are special since they vary with wheel rotational speed, meaning that they (for constant vertical load) are relevant to include when studying the variation of rolling resistance coefficient with vehicle speed. A summarizing comment is that one has to be careful with where to include different torque losses, so that they are included once and only once.

One should note that torque losses as discussed above are not the only losses which affect energy efficiency of the vehicle. There are also speed losses: speed losses in the wheel slip and speed losses in slipping clutch and torque converters. These cannot be modelled as rolling resistance.

2.4.3 Longitudinal forces

The longitudinal force (tangential to tyre circumference) between the tyre and road is critical to vehicle propulsion and braking performance.

First compare the friction characteristics for a translating block of rubber and a rolling wheel of rubber. Figure 2-2 shows the basic differences between classical dry-friction, or Coulomb friction, models and the basic performance of a rolling tyre. Experiments have shown that the relative speed between the tyre and the road produces a frictional force that has an initial linear region that builds

to a peak value. After this peak is achieved, no further increase in the tangential (friction) force is possible. There is not always a peak value, which is shown by the dashed curve in the figure.

The slope in the right diagram will be explained below, using the so called “tyre brush model”.

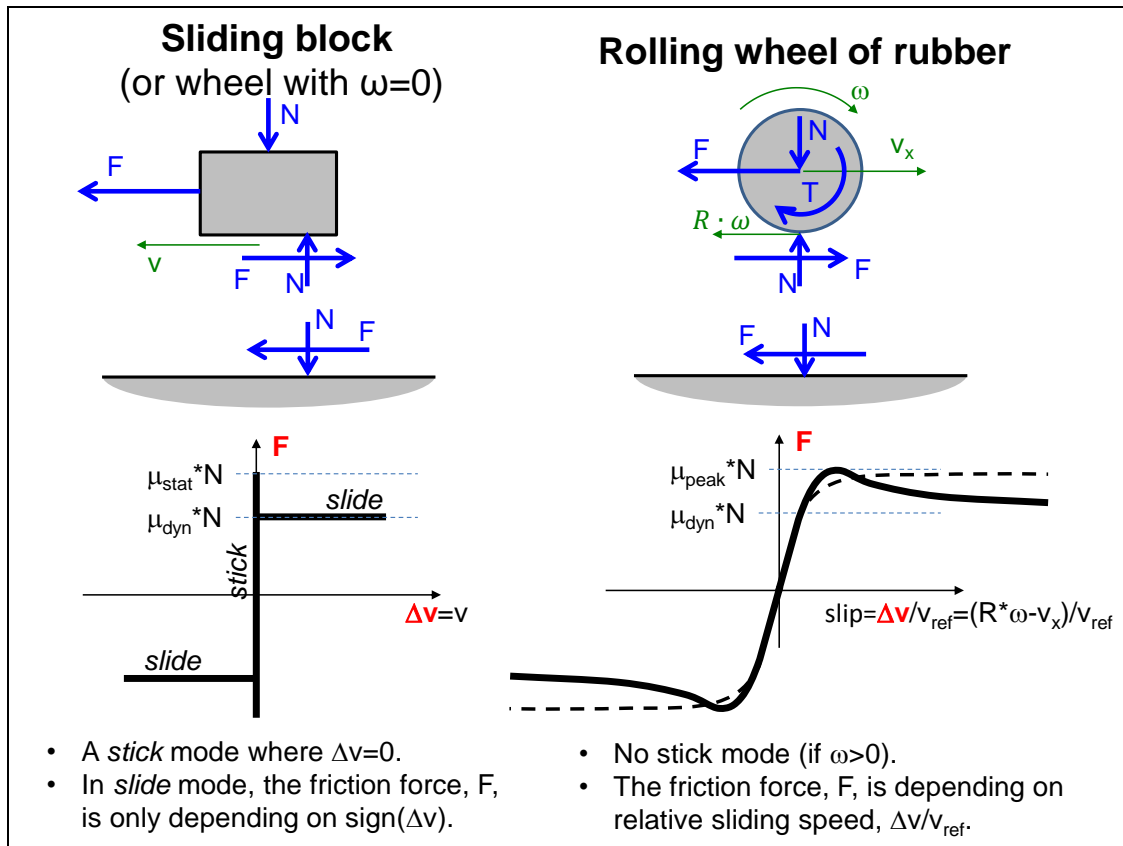


Figure 2-15: Friction characteristics

2.4.3.1 Tyre brush model for longitudinal slip

The brush model is a physically-based model that uses shear stress and dry friction at a local level, i.e. for each contact point in the contact patch.

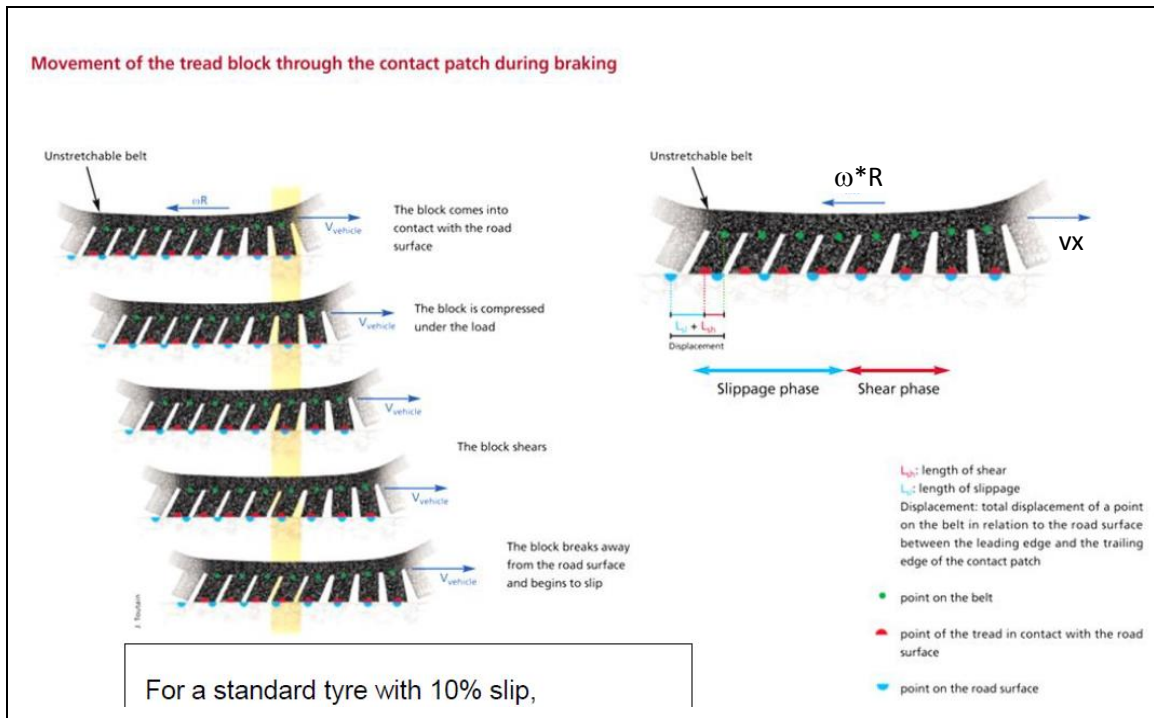


Figure 2-16: Picture of physical model of tyre, a so called “Brush model”. From Michelin.

Below shows a simplified version, using the following assumptions:

- Sliding and shear stress only in **longitudinal** direction (as opposed to combined longitudinal and lateral)
- Constant and known **pressure distribution**. (As opposed to using a contact mechanics based approach, which can calculate pressure distribution over the whole contact. For instance, one can use Hertz contact theory, which would motivate parabolic pressure distribution and contact length proportional to $F_z^{1/2}$ for line contact or $F_z^{1/3}$ for point contact.)
- No difference between **static and dynamic** coefficient of friction
- Only studying the **steady state conditions**, as opposed to including the transition between operating conditions. Steady state as opposed to stationary variations, which would arise for driving on undulated road.

These assumptions lead to a model as drawn in Figure 2-17.

The lines between tyre and road are sheared rubber elements, fixed to the wheel and having a friction contact to the ground. The shear stress of the element develops as in Hooke’s law, see Equation [2.8].

$$\tau = G \cdot \gamma; \tau = \text{shear stress}; G = \text{shear modulus}; \gamma = \text{shear angle}; \quad [2.8]$$

When a rubber element enters the contact patch, it lands un-deformed, $\gamma = 0$. The further into contact, along coordinate ξ , we follow the element, the more sheared will it become. Since the ground end of the element sticks to ground, the increase becomes proportional to the speed difference Δv and the time t it takes to reach that coordinate, $t(\xi)$:

$$\gamma = \frac{\Delta v \cdot t(\xi)}{H} = \frac{(R \cdot \omega - v_x) \cdot t(\xi)}{H};$$

where $t(\xi) = \xi/v_{Transport}$ and $v_{Transport} \approx \frac{|R \cdot \omega + v_x|}{2}$; [2.9]

Combining these equations yields the following, where the slip s_x can be identified:

$$\tau = \frac{G}{H} \cdot \underbrace{\frac{(R \cdot \omega - v_x)}{|R \cdot \omega + v_x|/2}}_{s_x} \cdot \xi; \quad [2.10]$$

This expression for shear stress only holds until the ξ where the friction limit is reached, ξ_c . At larger $\xi > \xi_c$, the rubber element will slide with a constant $\tau = \mu \cdot p$. Hence, the total force is the sum of two integrals as follows:

$$\begin{aligned} F_x &= W \cdot \int_0^L \tau \cdot d\xi = W \cdot \int_0^{\xi_c} \frac{G}{H} \cdot s_x \cdot \xi \cdot d\xi + W \cdot \int_{\xi_c}^L \mu \cdot p \cdot d\xi = \\ &= \frac{W \cdot G \cdot s_x}{H} \cdot \frac{\xi_c^2}{2} + W \cdot \mu \cdot p \cdot (L - \xi_c); \\ &\text{where } \xi_c = \frac{\mu \cdot p \cdot H}{G \cdot s_x} ; p \cdot W \cdot L = F_z \end{aligned} \quad [2.11]$$

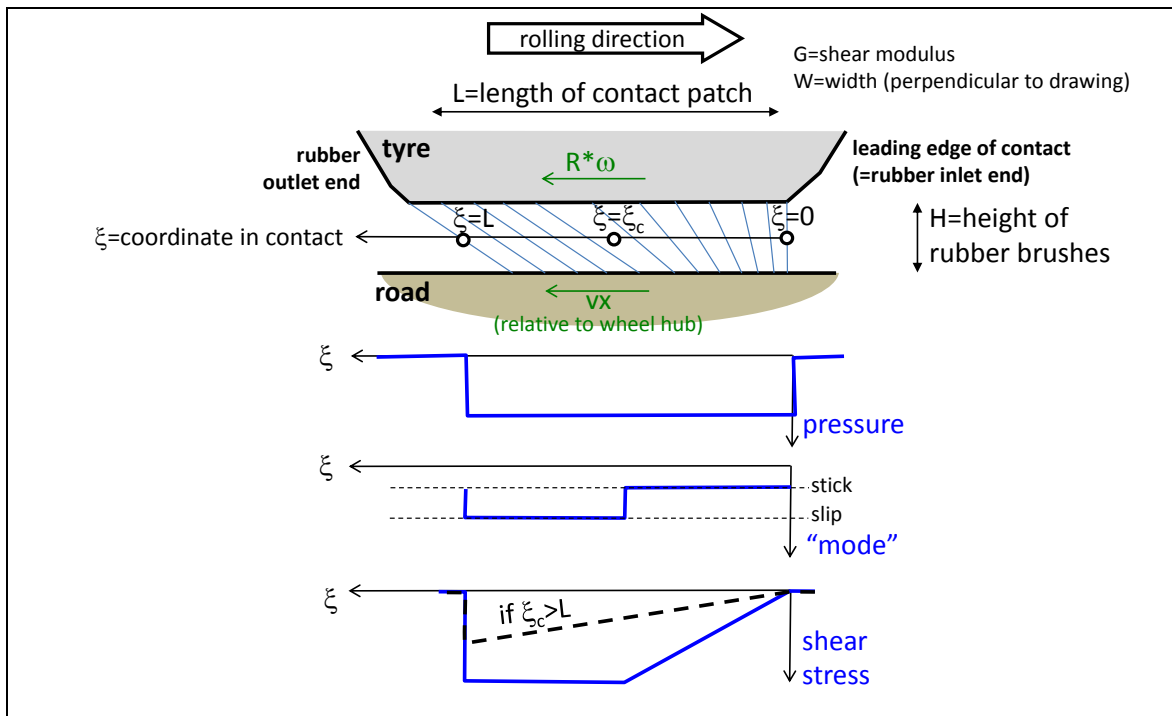


Figure 2-17: Physical model for deriving brush model for longitudinal slip. Speeds are relative to hub translational motion (not relative to ground). Drawn for $R \cdot \omega > v_x$.

Equation [2.11] is only valid for s_x corresponding to $0 < \xi_c < L$. Otherwise, the simpler Equation [2.10] can be used. This and further simplification of Equation [2.11] leads to:

$$F_x = \begin{cases} = \frac{G \cdot W \cdot L^2}{2 \cdot H} \cdot s_x; & \text{for } |s_x| \leq \frac{\mu \cdot F_z \cdot H}{G \cdot W \cdot L^2} \Leftrightarrow |F_x| \leq \frac{\mu \cdot F_z}{2} \\ = \text{sign}(s_x) \cdot \mu \cdot F_z \cdot \left(1 - \frac{\mu \cdot F_z \cdot H}{2 \cdot G \cdot W \cdot L^2} \cdot \frac{1}{|s_x|}\right); & \text{else} \end{cases}$$

or, equivalent:

$$F_x = \begin{cases} = C_x \cdot s_x; & \text{for } |s_x| \leq \frac{\mu \cdot F_z}{2 \cdot C_x} \Leftrightarrow |F_x| \leq \frac{\mu \cdot F_z}{2}; \\ = \text{sign}(s_x) \cdot \mu \cdot F_z \cdot \left(1 - \frac{\mu \cdot F_z}{4 \cdot C_x} \cdot \frac{1}{|s_x|}\right); & \text{else} \end{cases}$$

where $C_x = \frac{G \cdot W \cdot L^2}{2 \cdot H}$;

[2.12]

The shape of this curve becomes as shown in Figure 2-18.

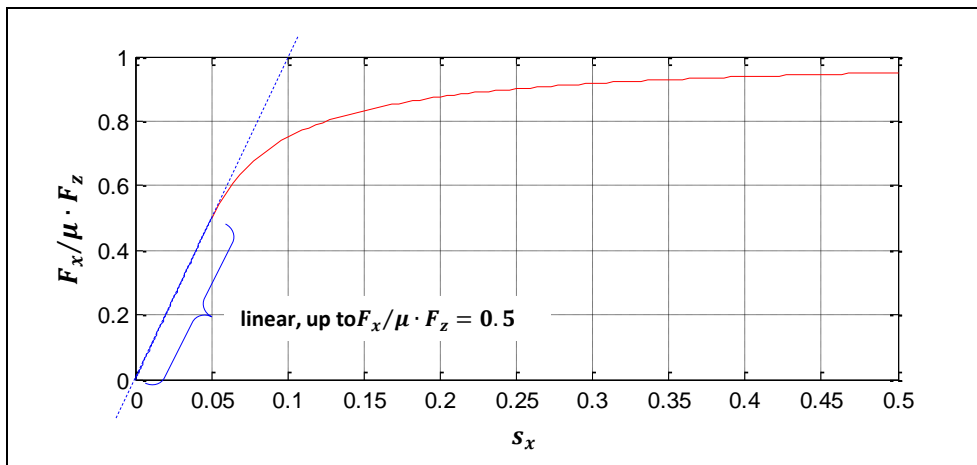


Figure 2-18: Shape of force/slip relation derived with brush model (assuming constant pressure distribution, etc.).

Figure 2-28 shows similar plots but with certain physically realistic assumptions about of parameters in the brush model (W, H, G, etc.). With a brush height, H=2 cm, the slope of the curve becomes in the correct magnitude, which makes it credible that the brush model actually models the most significant mechanisms in a proper way.

The brush model can be extended as indicated above, see e.g. References (Pacejka, 2005) and (Svendenius, 2007). Similar behaviour can also be derived assuming other physical models, e.g. models using tangential stress instead of shear stress. Reference (Wong, 2001) shows such an alternative to the brush model.

In summary for many models (and tests!) the following is a good approximation for small longitudinal slip (and constant normal load):

$$F_x = C_x \cdot s_x$$

[2.13]

For the brush model, or any other model which describes $F_x(s_x)$, one can define the “Longitudinal tyre (slip) stiffness” C_x , which have the unit $N = N/1 = N / \left(\frac{m/s}{m/s}\right)$. It is the derivative of force with respect to slip. In many cases one means the derivative at $s_x=0$:

$$C_x = \left(\frac{\partial}{\partial s_x} F_x \right) \Big|_{s_x=0} \quad [2.14]$$

Note that C_x is not a stiffness in the conventional sense, force/deformation. The tyre also have such a conventional stiffness, defined by force and deformation of a not rotating wheel. Often, it is obvious which stiffness is relevant, but to be unambiguous one can use the wording: “slip stiffness [N/1]” and “deformation stiffness [N/m]”.

Equation [2.12] proposes that longitudinal stiffness (at $s_x=0$) varies with G , W , L and H . For specified tyre and inflation pressure, these are approximately constant, except for L . Length L vary with vertical load, F_z , which makes longitudinal stiffness vary with vertical load. This is true also for “lateral tyre stiffness” and it is an important variation. This is further discussed in Section 2.5.3.

2.4.3.1.1 Brush model with parabolic pressure distribution

A parabolic pressure distribution can be assumed, instead of constant:

$$p(x) = \frac{3 \cdot F_z}{2 \cdot L} \cdot \left(1 - \left(\frac{x}{L/2} \right)^2 \right); \quad [2.15]$$

If we do the corresponding derivation, e.g. assuming a stick and slip zones, an equation for the force function of slip can be derived:

$$F_x = \begin{cases} \text{sign}(s_x) \cdot \left(C_x \cdot |s_x| - \frac{C_x^2 \cdot |s_x|^2}{3 \cdot \mu \cdot F_z} + \frac{(C_x \cdot |s_x|)^3}{27 \cdot (\mu F_z)^2} \right); & \text{for } |s_x| < \frac{3 \cdot \mu \cdot F_z}{C_x} \Leftrightarrow |F_x| \leq \mu \\ = \text{sign}(s_x) \cdot \mu \cdot F_z; & \text{else} \end{cases} \quad [2.16]$$

where $C_x = \text{function}(G, W, L, H)$;

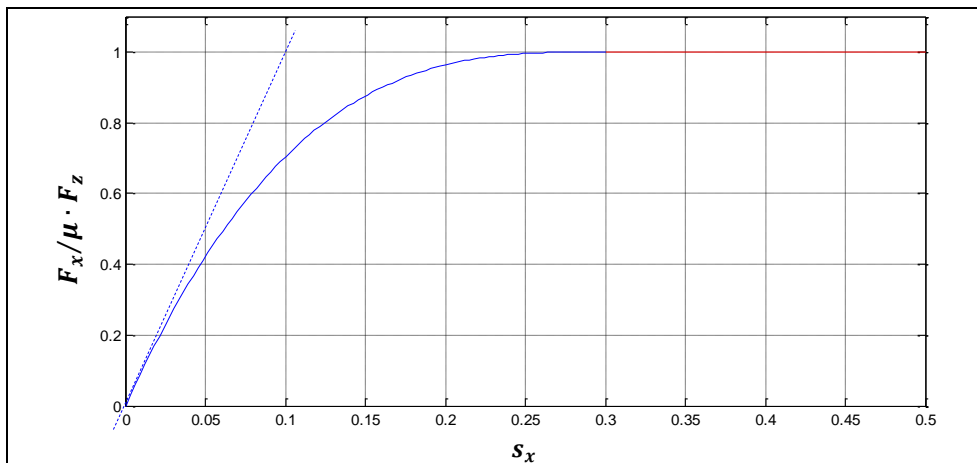


Figure 2-19: Shape of force/slip relation derived with brush model, assuming parabolic pressure distribution.

It should be noted that this model will not have any linear part.

2.4.3.2 Empirical tyre models

The brush model is a physical model which explains the principles of how the forces are developed. However, if a model is required which is numerically accurate to a certain tyre, one often uses a

fitted curve instead of Equation [2.12]. To limit the number of parameters to fit, one often uses a mathematical curve approximation, using trigonometric and exponential formulas.

2.4.3.2.1 Magic Formula Tyre Model

Probably the most well-known curve fit is called “Magic Formula” and it was proposed in (Bakker, 1987). This approach uses trigonometric functions to curve fit the experimental data. The curve fit has the general form:

$$\begin{aligned}
 y(x) &= D \cdot \sin(C \cdot \arctan(B \cdot x - E \cdot (B \cdot x - \arctan(B \cdot x)))); \\
 Y(x) &= y(s) + S_V; \\
 x &= X + S_H;
 \end{aligned}
 \tag{2.17}$$

Where B is a stiffness parameter, C is a shape parameter, D is a peak value parameter, and E is a curvature parameter describing the curve. The variable x is the tyre slip value. The parameters S_V and S_H simply shifts the curve so that it passes through the origin. The relationship between these parameter and the tyre slip/friction relation is shown in Figure 2-20.

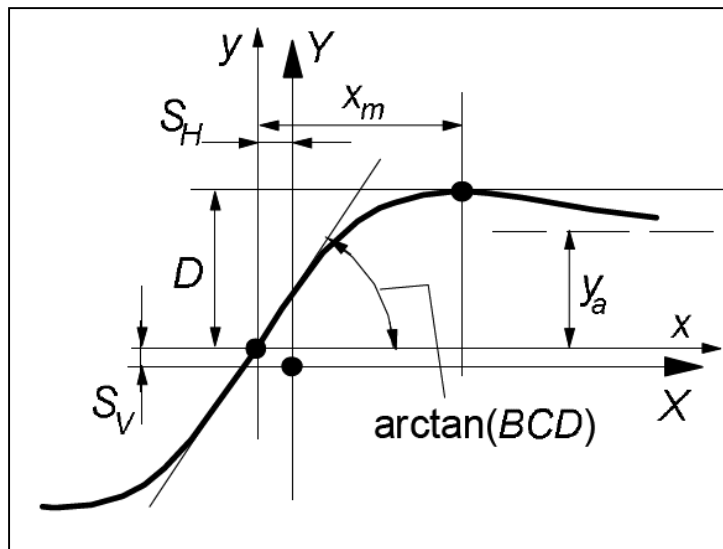


Figure 2-20: Magic Formula Tyre Parameters, (Pacejka, 2005)

2.4.3.2.2 TM-Easy Tyre Model

Since Equation [2.17] is a curve fit, it can be applied to any type of data with similar characteristics and can thus be used to describe other loading behaviour of the tyre such as lateral stiffness and self-aligning torque. These parameters will be discussed in later sections. Other curve fitting approaches to friction/slip modelling are possible such as the TM-Easy, (Hirschberg, et al., 2002), tyre model shown in Figure 2-21.

2.4.3.2.3 Other Tyre Models

There are many more models with different degree of curve fitting to experimental data. However, one can often have use for very simple curve fits, such as:

- Linearized: $F_x = C_x \cdot s_x$
- Linearized and saturated: $F_x = \text{sign}(s_x) \cdot \min(C_x \cdot |s_x|; \mu \cdot F_z)$

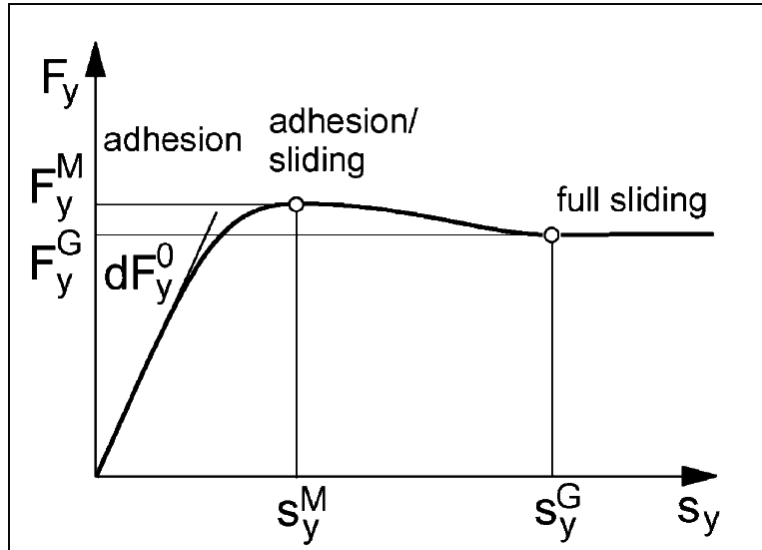


Figure 2-21: TM-Easy Tyre Model, (Hirschberg, et al., 2002)

2.4.3.3 Tyre with both rolling resistance and slip

So far, the models in Section 2.4.3 has not included rolling resistance. As we regard rolling resistance as a torque, not a force, it does not affect the $F_x(s_x)$ curve. But it does move the $T(s_x)$ curve upwards, and if wheel is rolling rearwards, the curve moves downwards, see Figure 2-22. The $F_x(s_x)$ curve is normally the suitable view for vehicle level studies, while the $T(s_x)$ curve is sometimes needed for involving a model of the propulsion system. As mentioned in Section 2.4.1, one can select R in slip definition so that the $F_x = 0$ for $s_x = 0$, as shown in Figure 2-22. This compendium claims this is the most appropriate if one does not know R . As also mentioned in Section 2.4.1, one can alternatively select R in slip definition so that the $T = 0$ for $s_x = 0$. This compendium claims that it is less appropriate and that using $T = F_x(s_x) \cdot R_l + \text{sign}(\omega) \cdot \frac{f}{R} \cdot F_z$ is better.

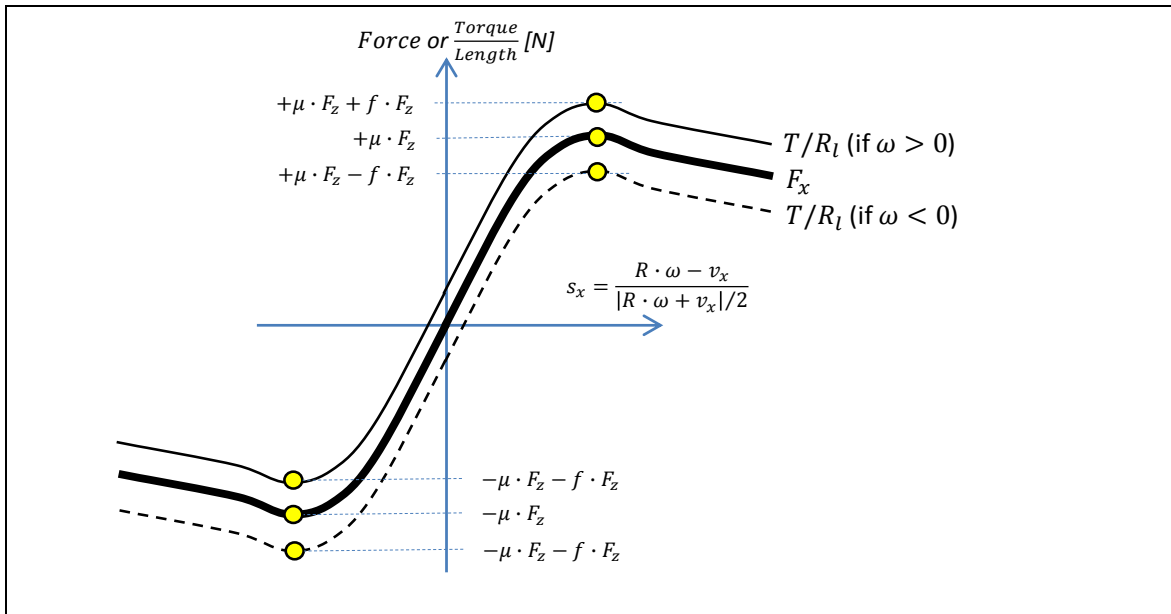


Figure 2-22: Longitudinal tyre force (F_x) and normalized wheel torque (T/R_l) including both rolling resistance and slip.

2.4.3.4 Relaxation

Both the physical and empirical tyre models discussed above are based on the assumption of steady state condition in the contact patch, meaning steady state deformation pattern and macro-slip zone for the rubber in the tyre. The transients between different steady state conditions involve finding a new such steady state. The fact that the change takes some time is referred to as relaxation. In many Vehicle Dynamics studies, the relaxation is such a quick process that it can be assumed to take place instantaneously, i.e. the $F_x(s_x)$ curve can be used. Generally one can need to model the transients in: slip (v_x and/or ω), vertical force (F_z) and/or surface conditions (e.g. expressed in varying μ).

A driving situation where slip varies a lot is when a vehicle starts from stand-still with initially undeformed tyres (no shear stress). For $v_x = \omega = 0$, the slip becomes undefined and the physical explanation is that it takes some degree of rotation of the wheel before the rubber elements reach their state of stress and deformation. During this transient there are other physical phenomena that are involved, namely the dynamics of building up a force or stress in an elastic part.

A dynamic equation of this type is needed: $\dot{F} = \text{stiffness} \cdot (R \cdot \omega - v_x)$. A common way to model this phenomenon is to add a first order delay of the force:

$$\dot{F}_x = A \cdot (f(s_x, F_z, \mu, \dots) - F_x);$$

where $f(s_x, F_z, \mu, \dots)$ is the force according to a steady state model, e.g. Eq [2.12] and $A = \frac{v_{Transport}}{L_r} = \frac{|R \cdot \omega + v_x|/2}{L_r}$ or $A = \frac{v_x}{L_r}$ or $A = \frac{R \cdot \omega}{L_r}$ and L_r is the relaxation length, which is a fraction ($\approx 25.50\%$) of tyre circumference.

[2.18]

One can also express the delay in delaying the slip, as follows:

$$F_x = f(s_{x,delayed}, F_z, \mu, \dots);$$

$$\dot{s}_{x,delayed} = A \cdot (s_x - s_{x,delayed});$$

where $f(s_{x,delayed}, F_z, \mu, \dots)$ is the force according to a steady state model, e.g. Eq [2.12] and A is as defined in Eq [2.18].

[2.19]

A physical motivation for this relaxation model is given in Reference (Rill, 2006). This identifies the relaxation length as the relation between tyre slip stiffness [N/((m/s)/(m/s))] and tyre longitudinal stiffness [N/m].

One non-physical behaviour of the model in Eq [2.18] is that it can give $F_x > \mu \cdot F_z$ transiently, when F_z and/or μ is quickly decreasing. This calls for rather using Eq [2.9] or, if using Eq [2.8], limit the integration of \dot{F}_x to F_x to $\mu \cdot F_z$. Another way to capture the phenomena of varying F_z is given in Chapter 7 in Reference (Pacejka, 2005) and it is to add a term dependent of $\frac{\partial F_x}{\partial F_z} \cdot \dot{F}_z$.

Introducing this delay can be motivated both for better description of fast transients and for avoiding singularities, caused by $v_{Transport}$ close to zero. With $f(s_x, F_z, \mu, \dots) = f(s_x) = C_x \cdot s_x$; as from Eq [2.13], the singularity disappears as follows, starting from Eq [2.18]:

$$\begin{aligned} \dot{F}_x &= A \cdot (f(s_x) - F_x) = \frac{v_{Transport}}{L_r} \cdot (C_x \cdot s_x - F_x) = \\ &= \frac{v_{Transport}}{L_r} \cdot \left(C_x \cdot \frac{R \cdot \omega - v_x}{v_{Transport}} - F_x \right) = \frac{C_x}{L_r} \cdot (R \cdot \omega - v_x) - \frac{v_{Transport}}{L_r} \cdot F_x = \\ &= \{e.g.\} = \frac{C_x}{L_r} \cdot (R \cdot \omega - v_x) - \frac{|R \cdot \omega + v_x|/2}{L_r} \cdot F_x; \end{aligned}$$

[2.20]

2.5 Lateral Properties of Tyres

After a vehicle starts moving, controlling the direction of travel becomes a high priority for the operator. For wheeled vehicles, the primary mode to control travel direction is to change the orientation of the tyre, i.e. to apply a steering angle. Tyres generate a lateral force when they are oriented at an angle different to the direction of the vehicle motion. The tyre typically deforms as in Figure 2-23.

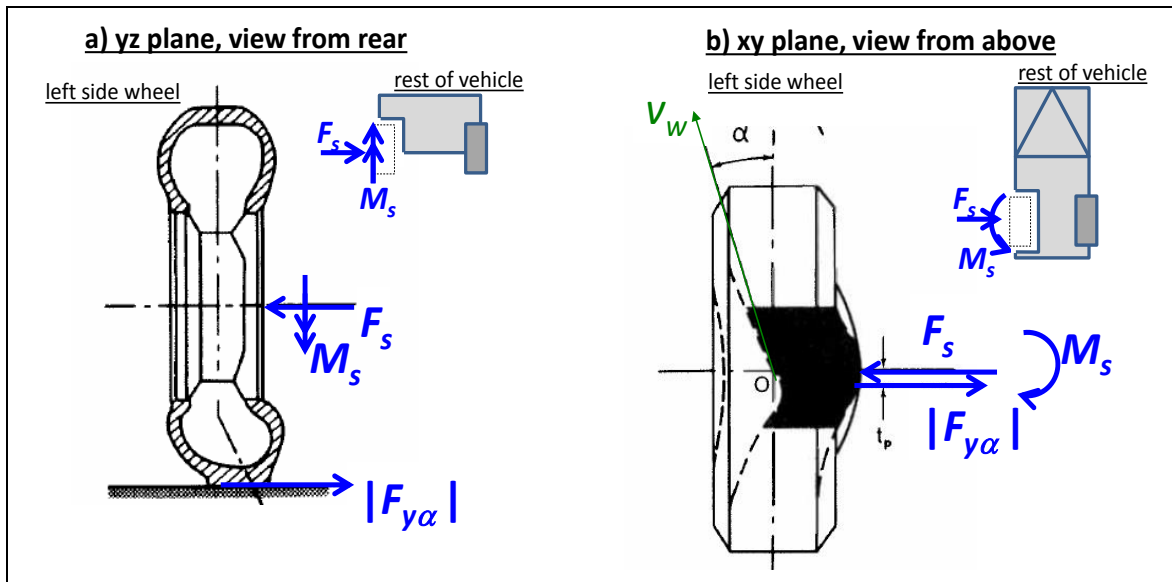


Figure 2-23: Deformation of a Cornering Tyre, (Clark, 1971)

It is essential to distinguish between the steering angle and (lateral or side) slip angle of the tyre. Lower right part of Figure 1-9 shows this difference. The steering angle, δ or d , is the angle between vehicle longitudinal direction and tyre longitudinal direction. The slip angle, α or a , is the angle between tyre longitudinal direction and the tyre translational velocity (=wheel hub velocity).

The relation between the lateral force of a tyre and the tyre side slip angle is typically as shown in Figure 2-25. The behaviour of the curve is similar to that exhibited for longitudinal forces Figure 2-20 and Figure 2-21. It becomes even more similar if lateral slip angle is replaced by lateral slip, $s_y = \tan(\alpha)$.

2.5.1 Tyre brush model for lateral slip

With corresponding simplification as in Section 2.4, we now use the brush model to also explain the lateral properties. Figure 2-24 shows the model for lateral slip and should be compared to Figure 2-17. The differences are that the model for lateral slip has the deformation of the rubber elements perpendicular to drawing.

The model equations become very similar, and the expression for how lateral force varies with lateral slip becomes:

$$F_y = \begin{cases} = -\frac{G \cdot W \cdot L^2}{2 \cdot H} \cdot s_y; & \text{for } |s_y| \leq \frac{\mu \cdot F_z \cdot H}{G \cdot W \cdot L^2} \Leftrightarrow |F_y| \leq \frac{\mu \cdot F_z}{2} \\ = -\text{sign}(s_y) \cdot \mu \cdot F_z \cdot \left(1 - \frac{\mu \cdot F_z \cdot H}{2 \cdot G \cdot W \cdot L^2} \cdot \frac{1}{|s_y|}\right); & \text{else} \end{cases}$$

or, equivalent:

$$F_y = \begin{cases} = -C_y \cdot s_y; & \text{for } |s_x| \leq \frac{\mu \cdot F_z}{2 \cdot C_y} \Leftrightarrow |F_y| \leq \frac{\mu \cdot F_z}{2}; \\ = -\text{sign}(s_y) \cdot \mu \cdot F_z \cdot \left(1 - \frac{\mu \cdot F_z}{4 \cdot C_y} \cdot \frac{1}{|s_y|}\right); & \text{else} \end{cases}$$

$$\text{where } C_y = \frac{G \cdot W \cdot L^2}{2 \cdot H};$$

[2.21]

where the lateral slip, s_y , is defined as:

$$s_y = \frac{v_y}{|R \cdot \omega + v_x|/2}$$

[2.22]

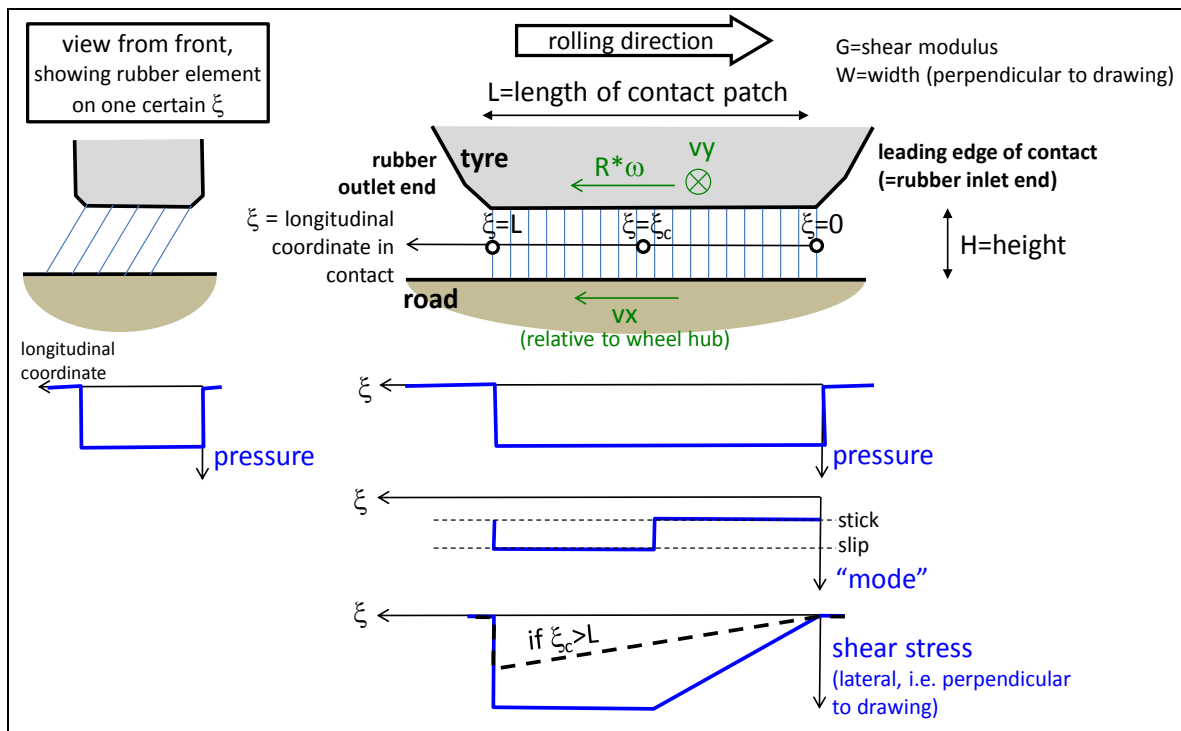


Figure 2-24: Physical model for deriving brush model for lateral slip.

Notes:

- The slip is the sliding speed in lateral direction, divided by the same "transport speed" as for longitudinal slip, i.e. the longitudinal transport speed.
- There is a minus sign appearing, because of sign conventions.
- The slip definition in Equation [2.22] is not consistent with the earlier mentioned relation $s_y = \tan(\alpha) = v_y/v_x$. One can identify two different lateral slip:

- “Lateral **wheel slip**” = $s_{y,wheel} = v_{y,wheel}/v_{x,wheel}$, which is defined by how wheel hub moves over ground: $s_{y,wheel} = s_{y,wheel}(v_{x,Vehicle}, v_{y,Vehicle}, \omega_{z,Vehicle})$
- “Lateral **tyre slip**” = $s_{y,tyre} = v_y/(|R \cdot \omega + v_x|/2)$, valid for the constitutive relation: $F_y = F_y(s_{y,tyre})$.

These names are not well established, but invented in this compendium for writing about it. If $R \cdot \omega = v_x$ (no longitudinal slip), these two slips are the same. (This compendium does almost not consider combined slip, why no further distinction is made between these two slip definitions. Combined slip is briefly covered in Section 2.6.)

- For a linearization, Eq [2.22] tells that the most correct way is that lateral force is $F_y \propto s_y$, not $F_y \propto \alpha$. Often one find $F_y \propto \alpha$ as starting point in the literature, but this compendium uses $F_y \propto s_y$.
(The advantage with using $F_y \propto \alpha$ is that the vehicle dynamics equations becomes linear in v_y and ω_z , e.g. see derivation of Equation [4.53]. However, the compendium proposes that the tyre model itself should be linearized as $F_y \propto s_y$ and, only when linear dynamic model is needed, one deliberately and consciously approximate $s_y \approx \alpha$. The result is the same when no longitudinal slip, but there is a risk that one don't realize that longitudinal tyre slip has been assumed small.)

In summary for many models (and tests!) the following is a good approximation for small lateral and longitudinal slip (and constant normal load):

$$F_y = -C_y \cdot s_y; \quad \text{or} \quad F_y = -C_\alpha \cdot \alpha; \quad [2.23]$$

For the brush model, or any other model which describes $F_y = F_y(s_y)$ or $F_y = F_y(\alpha)$, one can define the “Lateral tyre stiffness” or “Tyre Cornering Stiffness”, C_y or C_α , which have the unit N/1 or N/rad. It is the derivative of force with respect to slip or slip angle. Reference (ISO8855) defines the cornering stiffness as C_α for slip angle=0:

$$C_\alpha = -\left(\frac{\partial F_y}{\partial \alpha}\right)\Bigg|_{\alpha=0} = C_y = -\left(\frac{\partial F_y}{\partial s_y}\right)\Bigg|_{s_y=0} \quad [2.24]$$

The minus is added to get positive values on C_α and C_y .

When using only small slip, it does not matter if the cornering stiffness is defined as the slope in an F_y versus α diagram or F_y versus $s_y = \tan(\alpha)$ diagram. Therefore, the notation for cornering stiffness varies between C_α and C_y . Cornering stiffness has the unit N which can be interpreted as $N = N/1 = N/\left(\frac{m/s}{m/s}\right)$ or $N = N/rad$.

“Cornering Compliance” is sometimes used instead of “Cornering stiffness”. Cornering compliance is simply the inverted quantity, the unit being $1/N$ or rad/N .

2.5.2 Empirical tyre models

The cornering tyre forces initially exhibit a linear relation with the slip angle. A non-linear region is then exhibited up to a maximum value. In Figure 2-25, the maximum slip angle is only 16 degrees (or $s_y = \tan(16 \text{ deg}) = 0.29$) and one can expect that the tyre forces will drop as the slip angle approaches 90 degrees. The general form of the lateral force versus slip angle curve is also suitable for the Magic Formula, TM-Easy, or similar curve fitting approach when sufficient test data is available.

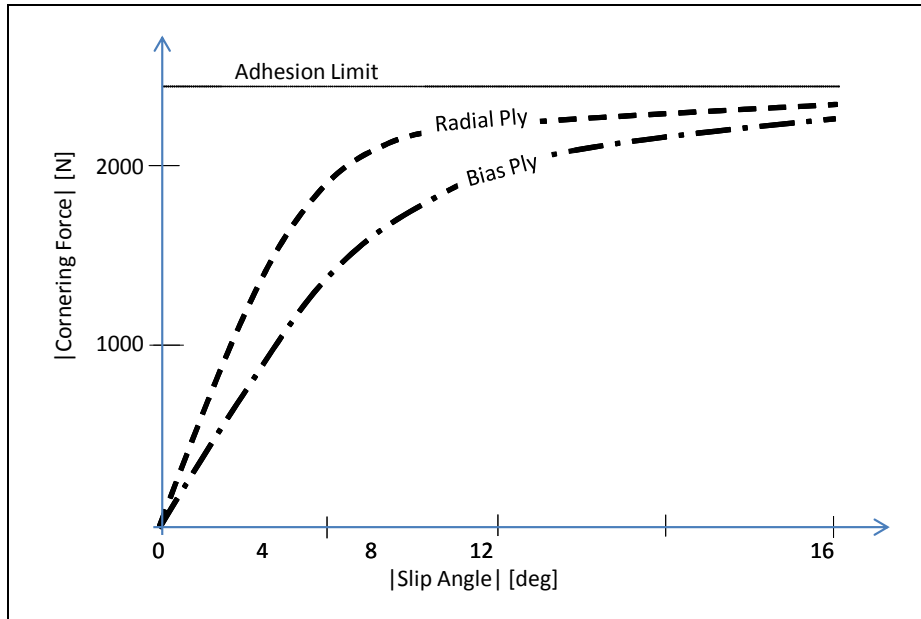


Figure 2-25: Cornering Forces of Tyres

2.5.3 Influence of vertical load

As discussed for longitudinal slip and the rolling resistance behaviour of tyres, the vertical load on the tyre affects the force generation. The general behaviour of the tyre’s cornering performance as the vertical load changes is presented in Figure 2-26. These figures show that the cornering stiffness is influenced by vertical load. One term is used to describe the dependence of cornering stiffness on vertical load: cornering coefficient, and is defined as:

$$CC_{\alpha} = \frac{F_z}{C_{\alpha}}$$

[2.25]

The influence of vertical tyre force on the generated lateral forces is an important aspect of vehicle performance in cornering and will be further discussed in 4.

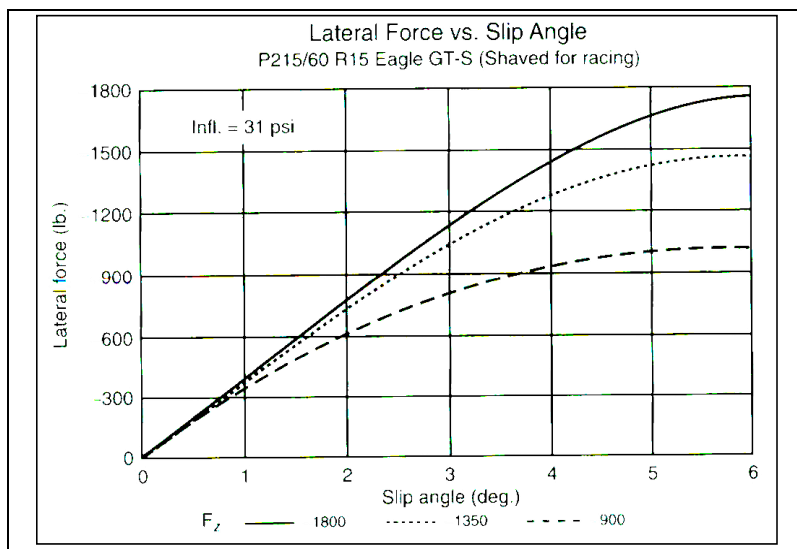


Figure 2-26: Left: Influence of Vertical Load on Lateral Force, (Gillespie, 1992). Right: Cornering stiffness versus vertical load

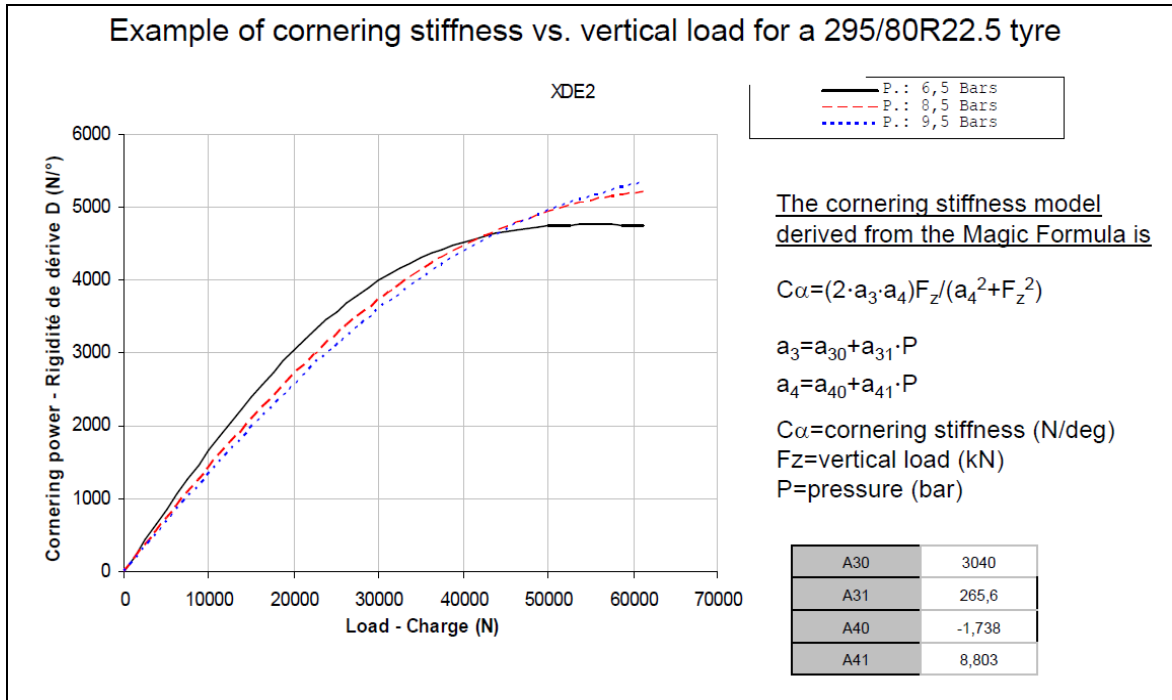


Figure 2-27: Cornering stiffness versus vertical load

A variation of cornering stiffness with vertical load can be explained using the brush model and a contact patch length, L, which varies with tyre normal load, F $_z$. From contact theories such as Hertz’s contact theory, one can motivate $F_z \propto L^a = L^2$ (line contact) or $F_z \propto L^a = L^3$ (for point contact). An extreme assumption, that the tyre is a membrane with an inside inflation pressure, gives $F_z \propto L^a = L^1$. These can be inserted as $L = k \cdot \sqrt[a]{F_z}$ in Equation [2.12]:

$$\frac{F_x}{\mu \cdot F_z} = \begin{cases} = \frac{G \cdot W \cdot k^2 \cdot F_z^{\left(\frac{2}{a}-1\right)}}{2 \cdot H \cdot \mu} \cdot s_x; & \text{for } \frac{|F_x|}{\mu \cdot F_z} \leq \frac{1}{2} \\ = 1 - \frac{\mu \cdot H}{2 \cdot G \cdot W \cdot k^2 \cdot F_z^{\left(\frac{2}{a}-1\right)}} \cdot \frac{1}{s_x}; & \text{else} \end{cases} \quad [2.26]$$

An equivalent reasoning for the lateral tyre force can be done starting from Equation [2.21].

In Figure 2-28, the tyre characteristics are plotted for a=2 and a=3 and varying vertical force. We see that if $a > 2$, the degressive characteristics, as in Figure 2-26 and Figure 2-27, can be explained. Since a tyre is more like a line contact (width constant, a=2) or even a membrane (a=1), it is not likely that the contact length variation is the whole explanation of the degressive stiffness.

Another mechanism which could influence the stiffness is that the pressure distribution is not uniform (as assumed in equations above) and it most likely varies with vertical load. A distribution which goes from triangular to uniform when F $_z$ increases would explain a degressive stiffness. This compendium does not derive the brush model for non-uniform pressure distribution, so this is left as an unproven hypothesis.

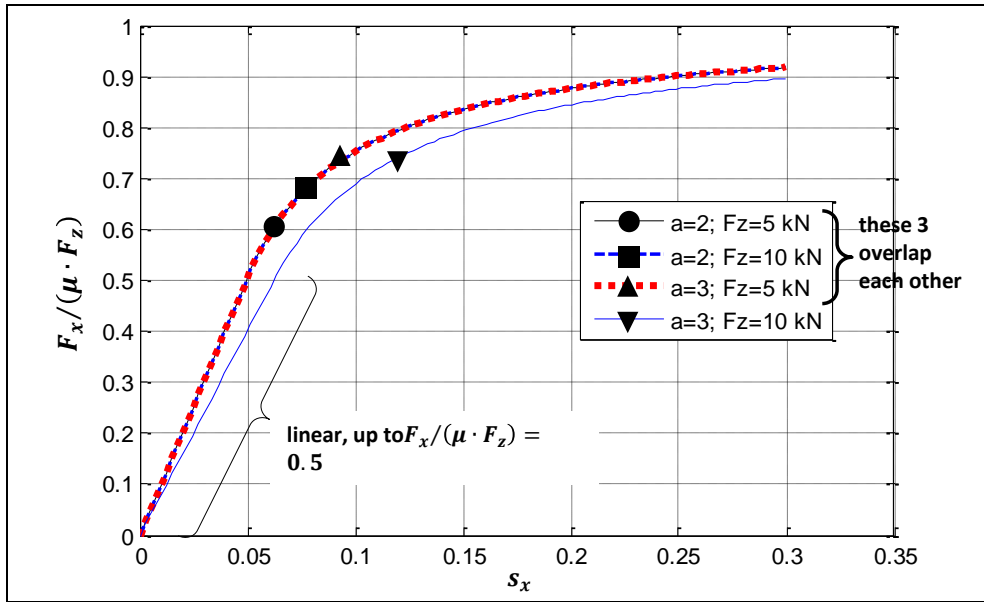


Figure 2-28: Shape of force/slip relation derived with brush model (assuming constant pressure distribution, etc). Parameter a is varied between 2 to 3. Other data used: $W=0.15$ m, $H=0.02$ m, $\mu=1$, $G=0.6e6$ N/m² and k tuned so that $L=0.15$ m when $Fz=5$ kN.

2.5.4 Relaxation

As for longitudinal, there is a delay in how fast the steady state conditions can be reached, which is sometimes important to consider. A similar model, as for longitudinal is to add a first order delay of the force:

$$F_y = f(s_{y,delayed});$$

$$\dot{s}_{y,delayed} = A \cdot (s_y - s_{y,delayed});$$

where $f(s_{y,delayed})$ is the force according to a steady state model, e.g. Eq [2.21] and $A = \frac{v_{Transport}}{L_r} = \frac{|R \cdot \omega + v_x|/2}{L_r}$ or $A = \frac{v_x}{L_r}$ or $A = \frac{R \cdot \omega}{L_r}$ and L_r is the relaxation length, which is a fraction (≈ 25 ..50%) of tyre circumference.

[2.27]

Most reasoning in Section 2.4.3.4 is applicable also for lateral relaxation.

2.5.5 Other effects than lateral force due to lateral slip

The deformations of the tyre during cornering are quite complex when compared to the case of pure longitudinal motion, see Figure 2-23. Hence, there are more effects than simply a lateral force. Some of these will be discussed in the following.

2.5.5.1 Overturning moment

The contact patch is deflected laterally from the centre of the carcass. This creates an overturning moment M_x due to the offset position of the normal force. The lateral force F_y also contributes to the overturning moment.

2.5.5.2 Tyre self-aligning moment

(This section has large connection with Section 4.2.3.2 Steering system forces.)

In the lowest diagram in Figure 2-24, one can see that shear stress is concentrated to the outlet side of the contact patch for small slip angles. So the equivalent lateral force acts behind the centre of wheel rotation for small slip angles. As seen in Figure 2-23 b) it acts at a position t_p behind the wheel's y axis. This distance is referred to as the pneumatic trail, see Figure 4-5, and the resulting moment of the lateral force acting on the ground and the reaction of wheel on the suspension creates a moment, M_z , which is an aligning torque. More commonly the moment M_z is referred to as the self-aligning moment since it (with a positive caster offset) tends to align the tyre to zero tyre slip angle. The reason why pneumatic trail can become slightly negative is because pressure centre is in front of wheel centre, see Figure 2-9.

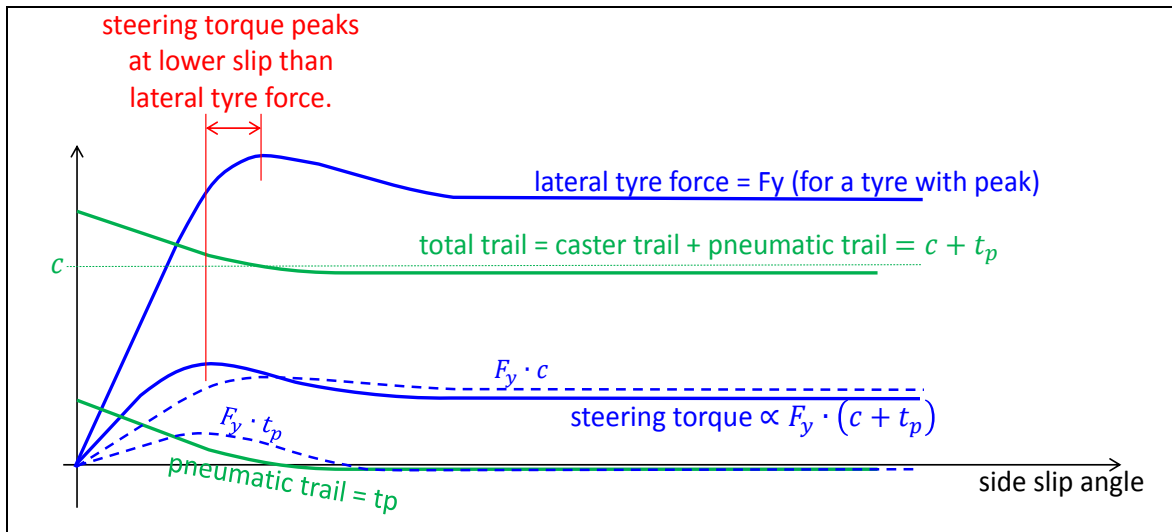


Figure 2-29: General Response of Steering torque to Side slip angle. Tyre self-aligning moment = $F_y \cdot t_p$ is one part of the steering moment.

Figure 2-29 shows the combined response of lateral force and slip angle. It is interesting to note that the steering torque reaches a peak before the maximum lateral force capacity of the tyre is reached. It can be used by drivers to find, via steering wheel torque, a suitable steering angle which gives a large lateral force but still does not pass the peak in lateral force.

2.5.5.3 Camber force

Camber force (also called Camber thrust) is the lateral force caused by the cambering of a wheel. One explanation model is shown in Figure 2-30. It is that Camber force is generated when a point on the outer surface of a leaning (cambered) and rotating tyre, that would normally follow a path that is elliptical when projected onto the ground, is forced to follow a straight path due to friction with the ground. This deviation towards the direction of the lean causes a deformation in the tyre tread and carcass that is transmitted to the vehicle as a force in the direction of the lean. Another explanation model is that the tyre "climbs" sideways as the inlet edge is directed, because there is more stick and less slip in the inlet edge as compared to the outlet edge; see brush model.

Camber thrust is approximately linearly proportional to camber angle for small angles: Camber thrust = $F_{yc} = C_\gamma \cdot \gamma$. The camber stiffness, C_γ , is typically 5-10 % of the cornering stiffness and opposite sign.

The camber force is superimposable for small lateral slip and small camber angle. The approximative Eq [2.23], can then be developed to:

$$F_y = F_{y,SideSlip} + F_{y,Camber} = C_y \cdot s_y + C_\gamma \cdot \gamma; \quad \text{or} \quad F_y = C_\alpha \cdot \alpha + C_\gamma \cdot \gamma \quad [2.28]$$

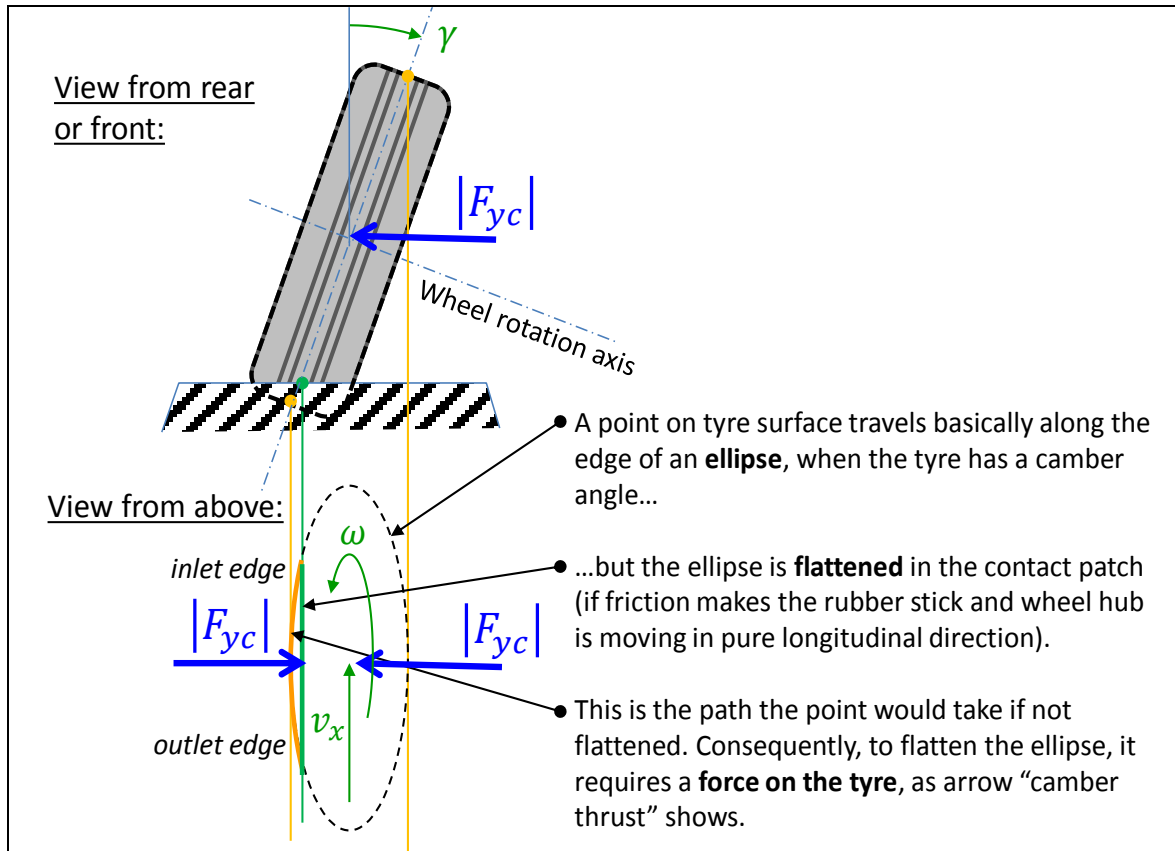


Figure 2-30: Camber thrust

There is also a rotation perpendicular to the ground due to the camber. The total rotation vector of the wheel is directed along the wheel rotation axis. The component of this vector that is perpendicular to ground creates friction moment which steers the wheel towards the side it tilts; on a cambering vehicle like a bicycle, the wheel is steered "into the fall", which counteracts falling.

2.6 Combined Longitudinal and Lateral Slip

The operation of motor vehicles often involves a combination of turning, braking, and steering actions. Hence, the performance of the tyre under combined (tyre) slip is important.

If the tyre has isotropic adhesion properties in the lateral and longitudinal direction, then one can start an analysis assuming that the maximum force generated by the tyre is fixed by the maximum resultant friction force, $\mu \cdot F_z$.

$$F_{xy}^2 = F_x^2 + F_y^2 \leq (\mu \cdot F_z)^2 \Rightarrow \left(\frac{F_x}{F_z}\right)^2 + \left(\frac{F_y}{F_z}\right)^2 \leq \mu^2 \quad [2.29]$$

Equation [2.29] can be plotted as a circle, called the "Friction Circle". Since the lateral and longitudinal properties are not really isotropic (due to carcass deflection, tread patterns, camber, etc) the shape may be better described as a "Friction Ellipse" or simply "Friction limit".

When not cornering, the tyre forces are described by a position between -1 (braking) and +1 (acceleration) along the Y-axis. Note that the scales of both axes are normalized to the maximum value for friction.

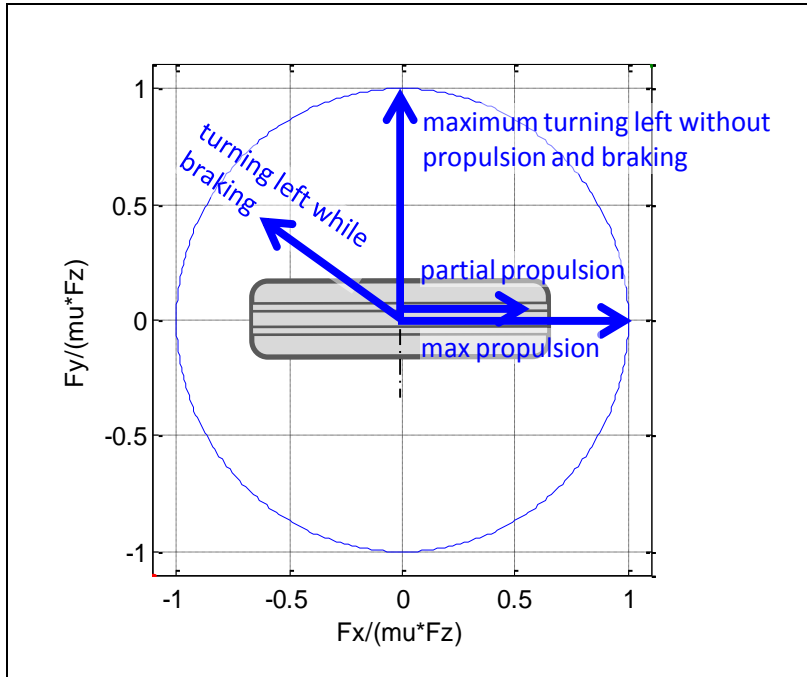


Figure 2-31: Friction Circle with some examples of tyre friction utilization.

The “actuation” of the wheel means the propulsion, braking and steering (and sometimes suspension control) of the wheel. An ideal actuation allows all conditions within the boundaries of the friction circle to be achieved anytime during a vehicle manoeuvre. An example of limitation in actuation is a wheel on a non-steered rear axle. They cannot access any of the lateral parts of the circle; unless the vehicle slides laterally.

At the boundary of the friction circle, tyres become more sensitive to changes in slip. It is therefore extra important to model the direction of the force in relation to shear deformation and relative slip motion in the tyre contact patch. Here, isotropic shear and friction properties are assumed:

$$\frac{\text{lateral sliding speed}}{\text{longitudinal sliding speed}} = \frac{v_y}{R \cdot \omega - v_x} = -\frac{F_y}{F_x} \quad [2.30]$$

Significant testing and modelling work have been undertaken to quantify the relationship between tyre slip (s_x and s_y , or s_x and α) and tyre forces. As an example, Figure 2-32 presents one method to present the maximum lateral force for different longitudinal slips. Note that each line represents a constant slip angle and that the maximum lateral force occurs for a slip angle between 10 and 18 degrees. Also the maximum value for longitudinal slip does not occur at zero, but for a slight braking condition (around 0.05).

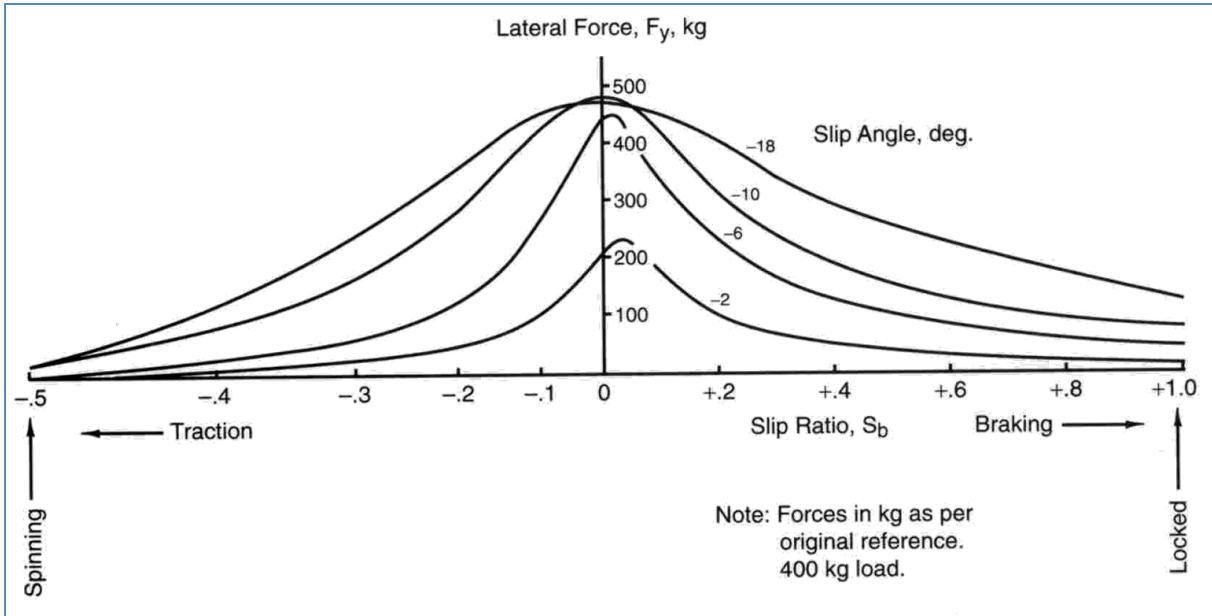


Figure 2-32: Combined Longitudinal and Lateral Slip

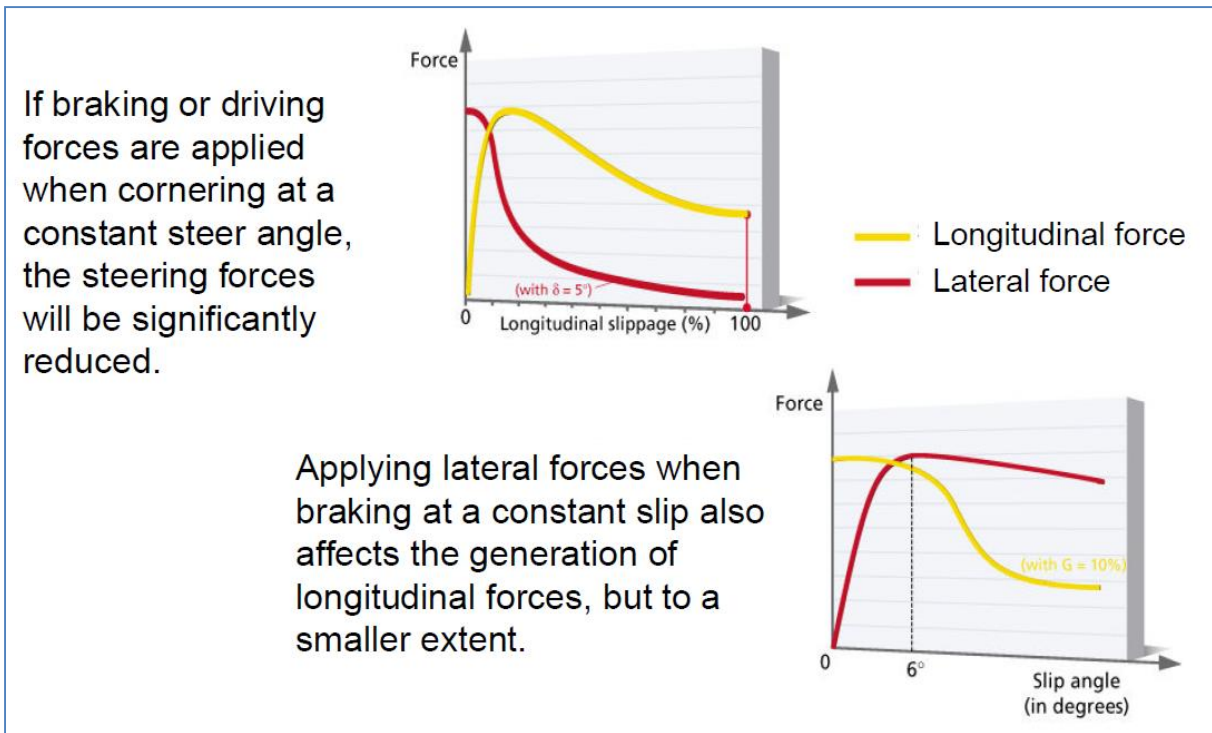


Figure 2-33: Effects of combined longitudinal and lateral utilization of friction.

2.6.1.1 Physically consistent combined slip model

A simple but physically consistent combined slip model can be expressed using “effective slip, s ”, as shown in Equation [2.31]. The function f using arctan, given as example, does NOT then reflect a drop in friction after macro slip has started in the contact patch.

$$\left\{ \begin{array}{l}
 F_x = \frac{+s_x}{s} \cdot F_{xy}; \text{ and } F_y = \frac{-s_y}{s} \cdot F_{xy}; \\
 s^2 = s_x^2 + s_y^2; \\
 s_x = \frac{R_w \cdot \omega - v_x}{v_{Transport}}; \text{ and } s_y = \frac{v_y}{v_{Transport}}; \\
 v_{Transport} = \{e.g.\} = \frac{|R_w \cdot \omega + v_x|}{2}; \\
 F_{xy} = \mu \cdot F_z \cdot f(s); \\
 f(s) = \{e.g.\} = \frac{2}{\pi} \cdot \arctan\left(C_0 \cdot \frac{2}{\pi} \cdot s\right); \\
 \text{or } f(s) = \{e.g.\} = \min\left(\frac{C_0}{\mu} \cdot s; 1\right); \\
 C_0 \approx \{\text{typically}\} \approx 20 \text{ [non-dimensional]}; \\
 \text{or } f(s) = \{\text{Eq [2.12] and [2.21]}\} = \min\left(\frac{C_0}{\mu} \cdot s; 1\right); \\
 C_0 \approx \{\text{typically}\} \approx 20 \text{ [non-dimensional]};
 \end{array} \right. \quad [2.31]$$

In simulation models, it is often so that ω, v_x, v_y are known, in which case the Equation [2.31] is already on explicit form. However, the model becomes singular if $v_{Transport}$ is close to zero (happens usually only at stand-still, or unusually other conditions with $R_w \cdot \omega = -v_x$). Some other model has to be switched in during these conditions. If s becomes close to zero (no tyre forces in road plane), the model in Equation [2.31] might also seem singular, but it is only a problem if one calculate s before dividing with s . Instead, one can express the tyre forces in ground plane as linear with sliding speeds ($R_w \cdot \omega - v_x$ and v_y). If using $f(s) = \{e.g.\} = \min\left(\frac{C_0}{\mu} \cdot s; 1\right)$, Equation [2.31] can be rewritten as Equation [2.32].

$$\begin{aligned}
 F_x &= \frac{+s_x}{s} \cdot F = \\
 &= \left\{ \text{small } s \Rightarrow \frac{C_0}{\mu} \cdot s < 1 \Leftrightarrow s < \frac{\mu}{C_0} \right\} = \frac{+s_x}{s} \cdot \mu \cdot F_z \cdot \frac{C_0}{\mu} \cdot s = +F_z \cdot C_0 \cdot s_x; \\
 F_y &= \frac{-s_y}{s} \cdot F = \{\text{similar}\} = -F_z \cdot C_0 \cdot s_y;
 \end{aligned} \quad [2.32]$$

2.6.1.2 Brush model for combined slip

The brush model can be applied also for combined slip. If doing that, the expression for F_{xy} in Eq [2.32] can be used as F_{xy} in Eq [2.31].

$$F_{xy} = \begin{cases} = \frac{G \cdot W \cdot L^2}{2 \cdot H} \cdot s; & \text{for } |s| \leq \frac{\mu \cdot F_z \cdot H}{G \cdot W \cdot L^2} \Leftrightarrow |F_{xy}| \leq \frac{\mu \cdot F_z}{2} \\ = \mu \cdot F_z \cdot \left(1 - \frac{\mu \cdot F_z \cdot H}{2 \cdot G \cdot W \cdot L^2} \cdot \frac{1}{s}\right); & \text{else} \end{cases}$$

Or, equivalent:

$$F_{xy} = \begin{cases} = C_{xy} \cdot s; & \text{for } |s| \leq \frac{\mu \cdot F_z}{2 \cdot C_{xy}} \Leftrightarrow |F_{xy}| \leq \frac{\mu \cdot F_z}{2} \\ = \mu \cdot F_z \cdot \left(1 - \frac{\mu \cdot F_z}{4 \cdot C_{xy}} \cdot \frac{1}{s}\right); & \text{else} \end{cases}$$

Or, equivalent:

$$F_{xy} = \begin{cases} = C_0 \cdot \mu \cdot F_z \cdot s; & \text{for } |s| \leq \frac{1}{2 \cdot C_0} \Leftrightarrow |F_{xy}| \leq \frac{\mu \cdot F_z}{2} \\ = \mu \cdot F_z \cdot \left(1 - \frac{1}{4 \cdot C_0} \cdot \frac{1}{s}\right); & \text{else} \end{cases}$$

[2.33]

In the same way, the brush model in Eq [2.16] in section 2.4.3.1.1, can be used in combined slip.

2.6.1.3 An approximate combined slip model

A combined model for cases when one knows F_x without involving s_x is shown in Equation [2.34]. This is not completely physically motivated, but works relatively well. One can consider it as a mathematical scaling inspired by the friction circle.

$$F_y \approx \sqrt{1 - \left(\frac{F_x}{\mu \cdot F_z}\right)^2} \cdot F_{y0}; \quad \text{where } F_{y0} = F_y|_{s_x=0}$$

[2.34]

2.6.1.4 Relaxation

The models above for combined slip assume steady state conditions. For separate longitudinal and lateral slip, there is a delay in how fast the steady state conditions can be reached, which is sometimes important to consider. A similar model, as for longitudinal and lateral, is to add a first order delay of the force:

$$[F_x; F_y] = f(s_{x,delayed}; s_{y,delayed});$$

$$[\dot{s}_{x,delayed}; \dot{s}_{y,delayed}] = [A_x \cdot (s_x - s_{x,delayed}); A_y \cdot (s_y - s_{y,delayed})];$$

where $f(s_{x,delayed}; s_{y,delayed})$ is the force according to a steady state model, e.g. Eq [2.33] and $[A_x; A_y]$ are relaxation lengths, as defined in Eq [2.18] and Eq [2.27].

[2.35]

Most reasoning in Section 2.4.3.4 is applicable also for combined slip relaxation.

Generally, the models become more stable the less state variables one uses, which can be a reason to not model relaxation. For combined slip, there is also a possible to model with one instead of two state variables. This is to model relaxation (delay) only of the force magnitude (or total slip) while letting the force direction be without delay. This is shown in the following equation, using force as state variable:

$$\dot{F}_{xy} = A \cdot (f(s_{xy}, F_z, \mu, \dots) - F_{xy});$$

$$[F_x; F_y] = \begin{bmatrix} +s_x \\ s \\ -s_y \\ s \end{bmatrix} \cdot F_{xy};$$

where $f(s_{xy}, F_z, \mu, \dots)$ is the force according to a steady state model, e.g. Eq [2.33] and A_{xy} is a combined relaxation length, averaging the ones defined in Eq [2.18] and Eq [2.27].

[2.36]

2.7 Vertical Properties of Tyres

The most important vertical property of a tyre is probably the stiffness. It mainly influences the vertical dynamics, see 5. For normal operation, the vertical force of the tyre can be assumed to vary linearly with vertical deflection. If comparing a tyre with different pressures, the stiffness increases approximately linear with pressure. See Figure 2-34.

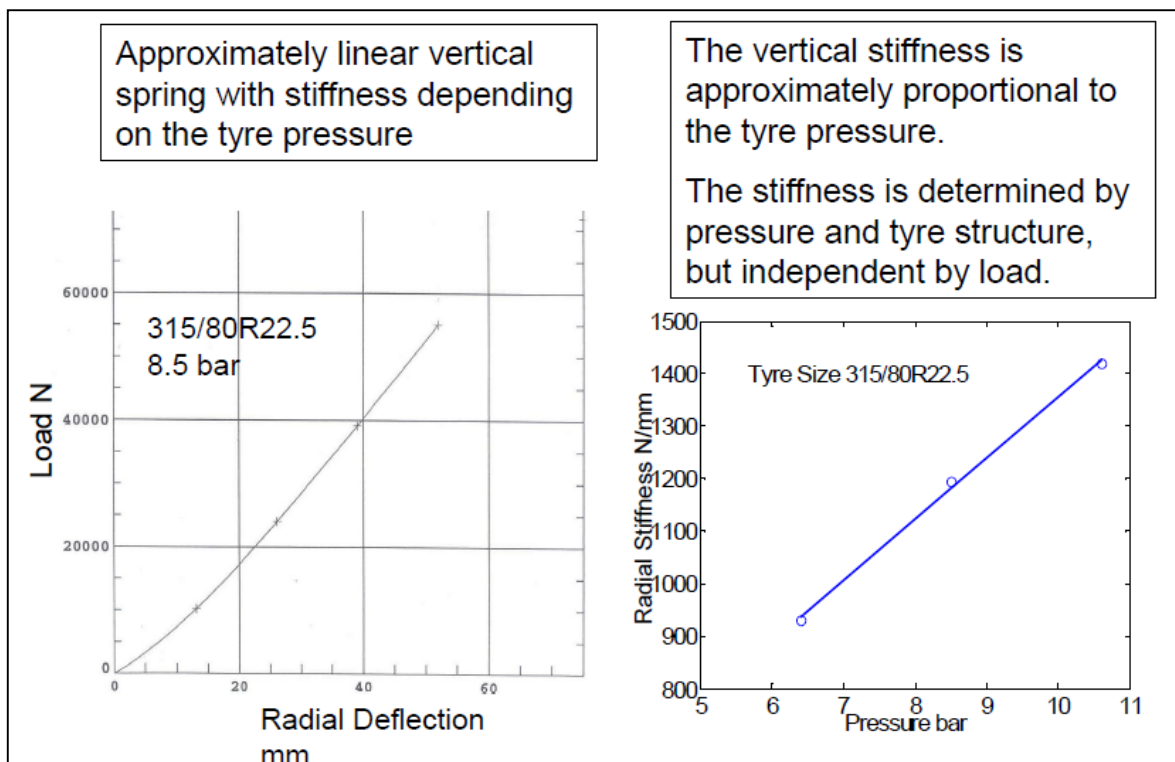


Figure 2-34: Vertical properties of a truck tyre.

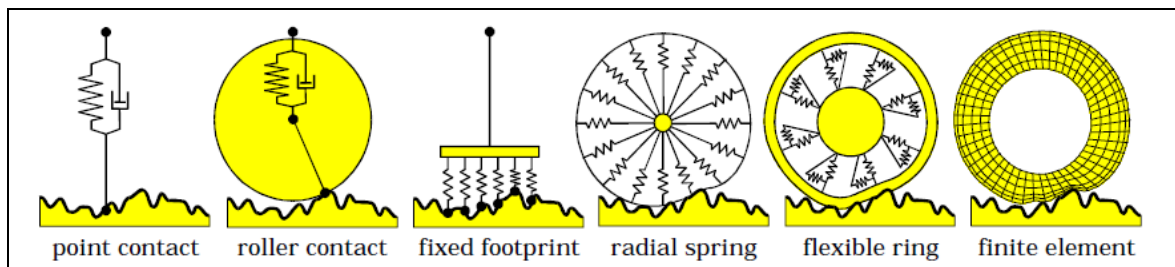


Figure 2-35: Different tyre models which will filter road irregularities differently. Picture from Peter Zegelaar, Ford Aachen.

2.8 Tyre wear

There are many other aspects of tyres, for instance the wear. Wear models are often based around the Archard's (or Reye's) wear hypothesis: worn material is proportional to work done by friction, i.e. friction force times sliding distance. Wear rate (worn material per time) is therefore friction force times sliding speed. Different approaches to apply this to tyres and expanding to temperature dependency etc. is found for instance in Reference (Grosch, et al., 1961). A generalization of *WearRate* [in mass/s or mm tread depth/s], for one certain tyre at constant temperature, becomes as follows:

$$\begin{aligned} \text{WearRate} &\propto \text{FrictionForce} \cdot \text{SlidingSpeed} \Rightarrow \\ \Rightarrow \text{WearRate} &= k \cdot F \cdot \Delta v \approx k \cdot (C \cdot s) \cdot (s \cdot v_{Transport}) \approx k \cdot C \cdot s^2 \cdot v_x; \end{aligned} \quad [2.37]$$

where $F = \sqrt{F_x^2 + F_y^2}$; $s = \sqrt{s_x^2 + s_y^2}$; $v_{Transport}$ defined as in Eq [2.9]
and
 k is a constant for a certain tyre with a certain temperature, rolling on a certain road surface.

2.9 Vehicle Aerodynamics

The flow of air around the vehicle body produces different external forces and moments on the vehicle. Considerable research and engineering has been carried out, and the fluid mechanics will not be covered in this course. However practical first order models for aerodynamics forces have been established and are presented here.

2.9.1 Longitudinal wind velocity

The most relevant force of interest in this course is the resistance force to forward motion, aerodynamic drag $F_{x,air}$, which is proportional to the square of the longitudinal component of the wind speed relative to the vehicle, $v_{x,rel}$. For aerodynamic loads resisting forward motion of the vehicle, the Equation [2.38] can be used. The parameters c_d , ρ and A_{front} represent the drag coefficient, the air density and a reference area, respectively. The reference area is the area of the vehicle projected on a vehicle transversal plane.

$$F_{x,air} = -\frac{1}{2} \cdot c_d \cdot \rho \cdot A_{front} \cdot v_{x,rel}^2; \quad [2.38]$$

Typical values of drag coefficients (cd) for cars can be found from sources such as: (Robert Bosch GmbH, 2004), (Barnard, 2010) and (Hucho, 1998). These coefficients are derived from coast down tests, wind tunnel tests or CFD (Computational Fluid Dynamics) calculations. For light vehicles (cars, SUVs, pick-up trucks) the air resistance can often be neglected for city traffic up to 30-50 km/h, but not at highway speeds.

Since a car structure moving through the air is not unlike an aircraft wing, there are also aerodynamic lift forces. Considering the forward motion only, a lift force and pitch moment will develop. This affects the normal loads on front and rear axle, and consequently the tyre to road grip. Hence, it affects the lateral stability.

$$\begin{aligned} F_{z,air} &= \frac{1}{2} \cdot c_l \cdot \rho \cdot A_{front} \cdot v_{x,rel}^2; \\ M_{y,air} &= \frac{1}{2} \cdot c_{pm} \cdot \rho \cdot A_{front} \cdot L_c \cdot v_{x,rel}^2; \end{aligned} \quad [2.39]$$

The coefficient c_l represents the lift characteristics of the vehicle. The lift force is here assumed to act through the centre of gravity. The c_{pm} (pitch moment coefficient) and L_c (characteristic length, usually wheelbase) must be reported together.

With identical effect on the (rigid) vehicle body one can replace the lift force in centre of gravity, $F_{z,air}$, and the pitch moment, $M_{y,air}$, with lift forces at two different longitudinal positions, typically over each axle:

$$\begin{aligned} F_{air,fz} &= \frac{1}{2} \cdot c_{lf} \cdot \rho \cdot A_{front} \cdot v_{x,rel}^2; \\ F_{air,rz} &= \frac{1}{2} \cdot c_{lr} \cdot \rho \cdot A_{front} \cdot v_{x,rel}^2; \end{aligned} \quad [2.40]$$

The coefficients c_{lf} and c_{lr} are lift coefficient over front and rear axle, respectively. Relations between Equation [2.39] and Equation [2.40] are: $c_l = c_{lf} + c_{lr}$; and $c_{pm} = (c_{lr} - c_{lf}) \cdot L_c$.

2.9.2 Lateral wind velocity

When the wind comes from the side, there can be direct influences on the vehicle lateral dynamics. Especially sensitive are large but light vehicles (such as buses or vehicles with unloaded trailers). The problem can be emphasized by sudden winds (e.g. on bridges or exiting a forested area). Besides direct effects on the vehicle lateral motion, side-winds can also disturb the driver through disturbances in the steering wheel feel.

Similar expressions to the longitudinal loads are derived for lateral forces and from side-winds.

$$F_{y,air} = \frac{1}{2} \cdot c_s \cdot \rho \cdot A \cdot v_{y,rel}^2 \quad [2.41]$$

$$M_{z,air} = \frac{1}{2} \cdot c_{ym} \cdot \rho \cdot A \cdot L_c \cdot v_{y,rel}^2 \quad [2.42]$$

The speed $v_{y,rel}$ is the lateral component of the vehicle velocity relative to the wind. Note that A and L_c may now have other interpretations and values than in Equations [2.38]-[2.40].

2.10 Driver interactions with vehicle dynamics

The driver interacts with the vehicle mainly through steering wheel, accelerator pedal and brake pedal. In addition to these, there are clutch pedal, gear stick/gear selector, in some vehicles, and various buttons, etc., see Figure 2-36, but we focus here on the first 3 mentioned.

The driver is also a medium through which other road-users and traffic objects interact with a vehicle. The driver sees and hears what happens in traffic and acts accordingly, see Figure 2-37 and Figure 2-1.

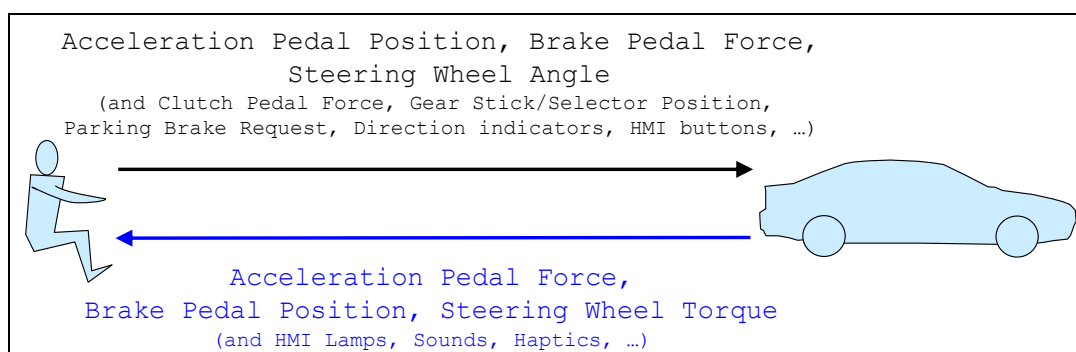


Figure 2-36: Commonly assumed causality (direction of cause and effect).

Driver's control of vehicle dynamics, or vehicle motion including position, can be discussed in longitudinal and lateral. The longitudinal is about how driver uses his vision to determine pedal operation. Looming (optical expansion of an object in the driver's field of view) is often used as a cause for how driver pushes the pedals. The optical flow (the pattern of apparent motion of objects, surfaces, and edges in the driver's field of view) is often used as a cause for highest comfortable speed.

2.10.1 Open-loop and Closed-loop Manoeuvres

Two common expressions used in analysing vehicle dynamics are "Open-loop" and "Closed-loop". These concepts are used to describe how the vehicle control systems are manipulated in a "driving" event.

An **open-loop** manoeuvre refers to the case where the driver controls (steering wheel, brake pedal and accelerator pedal) are operated in a specific sequence, i.e. as functions of time. A typical case is a sine wave excitation of the steering wheel. The time history of the steering wheel angle is defined as a function that is independent of the road environment or driver input. This type of manoeuvre is a practical design exercise to study the steering response of the system, but has little relation to a real-world driving case. Theoretical simulation and real testing with a steering robot are examples of how such studies can be made.

A **closed-loop** manoeuvre refers to the case when (human) driver feedback via driver controls is included. This represents real-world driving better. In real vehicle or driving simulator testing, a real driver is used. This enables collection of the drivers' subjective experience. In cases of theoretical simulation, a "driver-model" is needed. A driver-model can have varying levels of complexity but in all cases simulates the response of a human driver to different effects, such as lateral acceleration, steering wheel torque, various objects appearing outside the vehicle, etc.

A test with real vehicle, carried out with a steering-robot (and/or pedal robot) can also be called closed-loop if the robot is controlled with a control algorithm which acts differently depending on the vehicle states, i.e. if the algorithm is a driver model.

The concepts of open- and closed-loop control are demonstrated in Figure 2-37. The important difference to note is that in open-loop control there is no feedback to the driver. The figure also shows a "Virtual driver" which represents today's automatic functions based on environment sensing, such as adaptive cruise control, which adapts speed to a vehicle ahead. Closed loop control incorporates the different types of feedback to the driver. Drivers automatically adapt to the different feedback. Understanding driver response to different feedback, and expressing it in mathematical descriptions, is an active area of research, particularly for driver support functions.

The boxes "Suspension, Linkage, Wheels" and "Vehicle body" in the diagram are the main focus for this course. The mechanics relating the wheels' transfer of forces between the road and vehicle are

the critical elements to study in introductory vehicle dynamics. In a first order analysis the influence of the suspension and steering components can be ignored as long as the mechanical components are not undergoing extensive deflections.

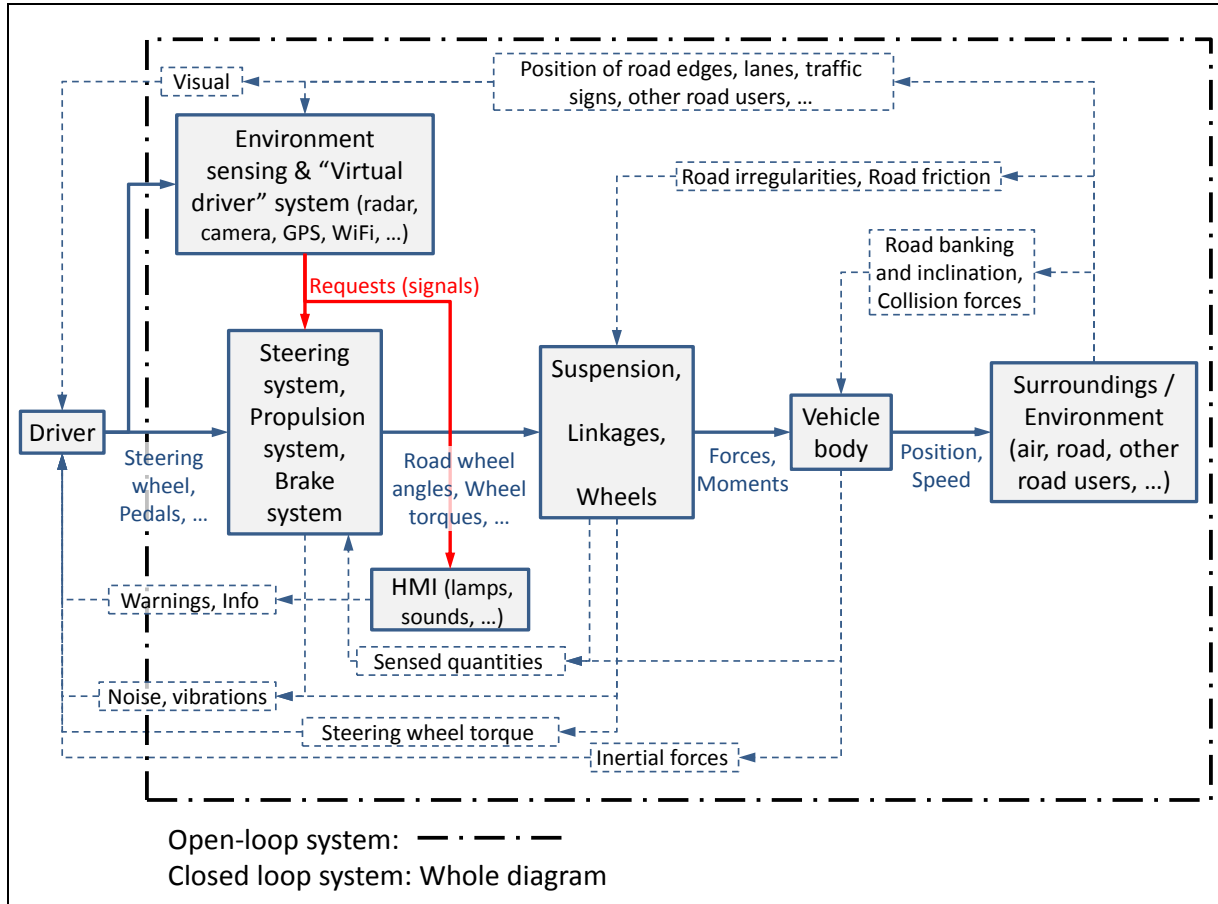


Figure 2-37: Open and closed loop representations of vehicle dynamic systems

2.10.2 Pedals

Each pedal has both pedal position and pedal force as communication channels to the driver.

In broad terms, the accelerator pedal position is interpreted by a control system as a certain requested engine torque, which means a certain wheel shaft torque on the propelled axle/axes. In some advanced solutions, one could think of using accelerator pedal force as a feedback channel from vehicle to driver.

In broad terms, the brake pedal force gives a certain friction brake torque application on each axle. In some advanced solutions, one could think of changing brake pedal position versus force characteristics as a feedback channel from vehicle to driver. But already with traditional (hydraulic) brake systems for passenger cars, the brake pedal gives a feedback to driver in that ABS interventions is felt.

For electric and hybrid vehicles the brake pedal can typically influence the propulsion system as well, in that at low levels of pedal braking, the electric propulsion motors give negative wheel shaft torque. This is for regenerating energy. Regenerative braking can even be engaged at low levels of accelerator pedal position.

The propulsion and brake systems are to some extent also described in 3. LONGITUDINAL DYNAMIC.

2.10.3 Steering

The driver interacts with steering wheel through two channels, steering wheel angle and steering wheel torque.

A frequently used model is that the driver decides a steering wheel angle and expects a certain steering wheel torque, T_{sw} , feedback. Only in extreme situations, the causality is modelled the other way, e.g. studying what happens if driver takes hands-off, i.e. steering wheel torque =0. However, it should be noted that, from neuromuscular point-of-view, it is not motivated to model a driver as controlling the torque or forces, but only the position.

In a broad view, the angles of the road wheels are functions of steering wheel angle, independent of forces and torques in the steering system. Further, the steering wheel torque is a function of the lateral force on the front axle, possibly scaled down with assistance from the power steering or steering servo. Some more detailed aspects on the two latter sentences are discussed below. See more about steering system in Section 4.2.3.

2.11 Traffic interactions with vehicle dynamics

Other road-users and traffic objects interact with a vehicle via the driver, as mentioned in Section 2.10, but also directly via environment sensors on-board the vehicle, see Figure 2-37. These sensors give information to a “virtual driver”, which consists of control algorithms which can request basically the same as a driver can (steering, brake, propulsion systems). Functions of this type were categorized as both “Seeing” and “Dynamic” in Section 1.2.

As mentioned in Section 1.2, the same environment information is also the base for functions that stimulates the driver to act, through functions categorized as both “Seeing” and “Driver informing”. These do not have a direct interface to the vehicle, but interact via the driver.

VEHICLE INTERACTIONS

3 LONGITUDINAL DYNAMICS

3.1 Introduction

The primary purpose of a vehicle is transportation, which requires longitudinal dynamics. The chapter is organised with one group of functions in each section as follows:

- 3.2 Steady State Function
- 3.3 Functions over longer events
- 3.4 Functions in shorter events
- 3.5 Control functions

Most of the functions in “3.5 Control functions”, but not all, could be parts of “3.4 Functions in shorter events”. However, they are collected in one own section, since they are special in that they partly rely on software algorithms.

There are a lot of propulsion related functions, originating from the attribute Driving dynamics. Examples of such, not covered in this compendium are:

- Off-road accessibility: Ability to pass obstacles of different kind, such as uneven ground, extreme up- and down-hills, mud depth, snow depth, etc.
- Shift quality: Quick and smooth automatic/automated gear shifts
- Shunt & shuffle: Absence from oscillation for quick pedal apply, especially accelerator pedal.

3.1.1 References for this chapter

- *“Chapter 23. Driveline” in Reference (Ploechl, 2013).*
- *“Chapter 24. Brake System Dynamics” in Reference (Ploechl, 2013).*
- *“Chapter 27 Basics of Longitudinal and Lateral Vehicle Dynamics” in Reference (Ploechl, 2013).*

3.2 Steady State Functions

Functions as top speed and grade-ability are relevant without defining a certain time period. For such functions it is suitable to observe the vehicle in steady state, i.e. independent of time. Those functions are therefore called steady state functions, in this compendium.

The main subsystems that influences here are the propulsion system, see Section 3.2.1, and the (Friction) Brake system, see Section 3.4.3.

3.2.1 Propulsion System

A generalisation of the propulsion system is given in Figure 3-1, along with a specific example of a conventional type. The component “Energy buffer” refers to an energy storage that can “buffer” energy during vehicle operation. This means that an energy buffer can not only be emptied (during propulsion), but also refilled by regenerating energy from the vehicle during deceleration. A fuel tank is an energy storage, but not an energy buffer. Also, a battery which can only be charged from the grid, and not from regenerating deceleration energy, is not an Energy buffer.

Note that the approach in Figure 3-1 is one-dimensional: we consider neither the differential between left and right wheel on the driven axle nor distribution between axles. Instead, we sum up the torques at all wheels and assume same rotational speed.

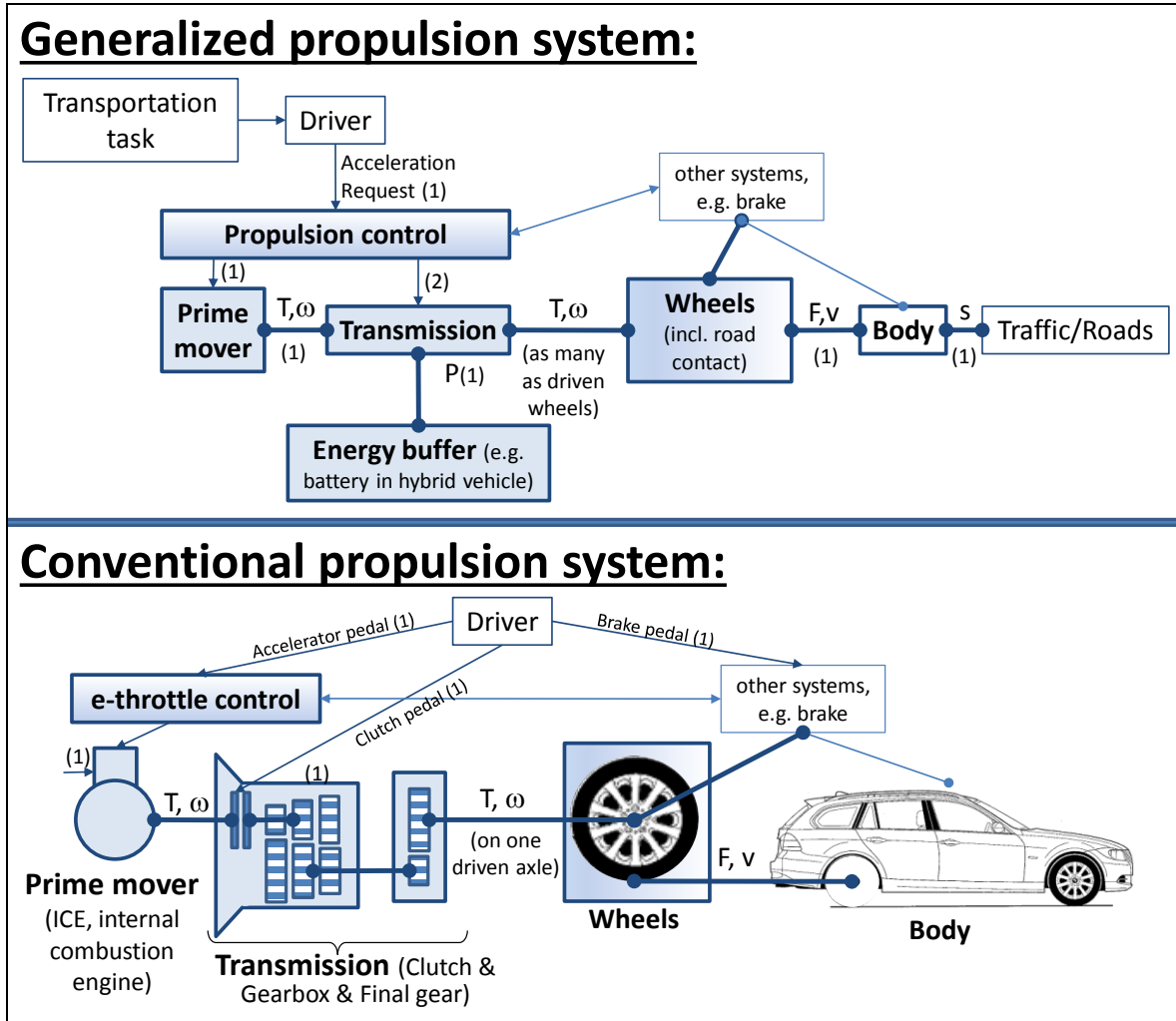


Figure 3-1: Propulsion system

3.2.1.1 Prime movers

The conversion of stored energy to power occurs in the prime mover, see Figure 3-1. Details of the conversion processes and transmission of power to the tyres are not covered in this compendium. Some basic background is still necessary to describe the longitudinal performance of the vehicle. The main information that is required is a description of the torque applied to the wheels over time and/or as a function of speed. Sketches of how the maximum torque varies with speed for different prime movers (internal combustion engine (ICE), electric motor or similar) are shown in Figure 3-2 and Figure 3-3. The torque speed characteristics vary dramatically between electric and internal combustion engines. Also, gasoline and diesel engines characteristics vary.

The curve for electric motors in Figure 3-2 shows that the main speciality, compared to ICEs, is that their operation range is nearly symmetrical for negative speeds and torques. However, the curve should be taken as very approximate, since electric motors can work at higher torque for short periods of time. The strong time duration dependency makes electric motors very different to ICEs from a vehicle dynamics point of view. Other properties that makes them special are quick and accurate response, well known actual torque and that it is much more realistic to divide them into several smaller motors, which can operate on different wheels/axles.

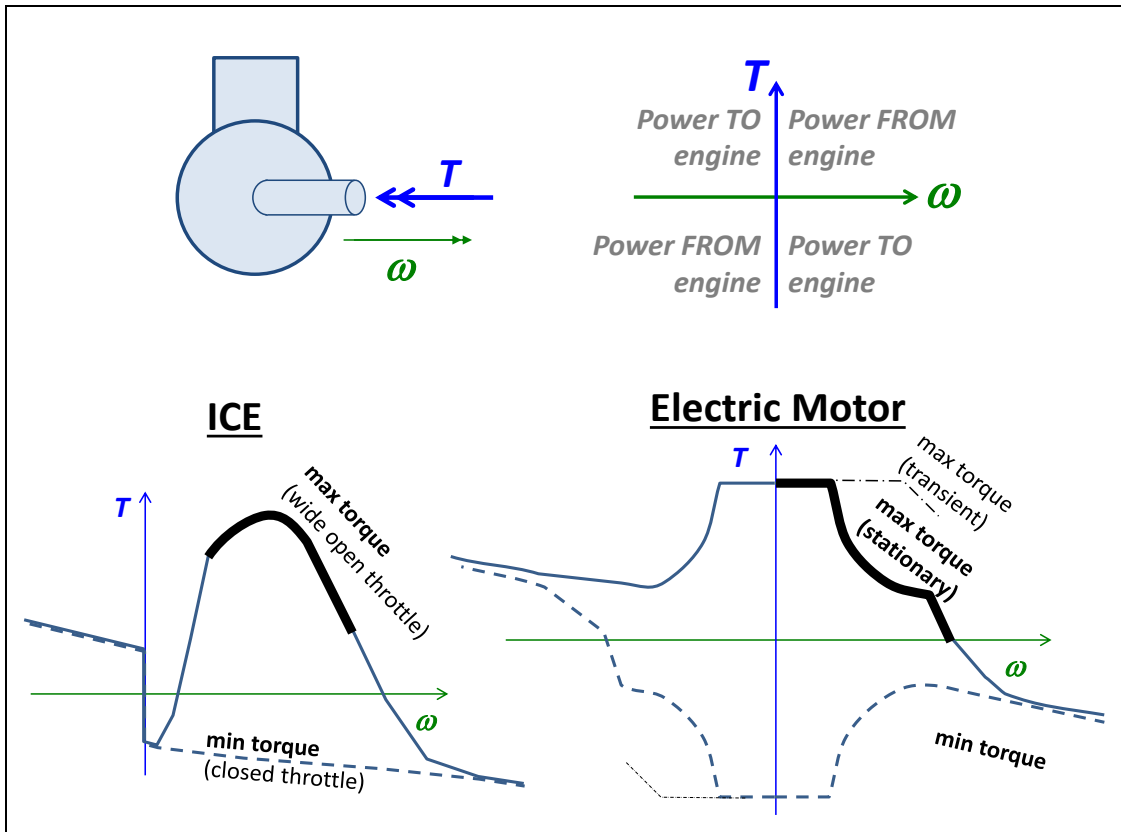


Figure 3-2: Torque Characteristics of Prime Movers

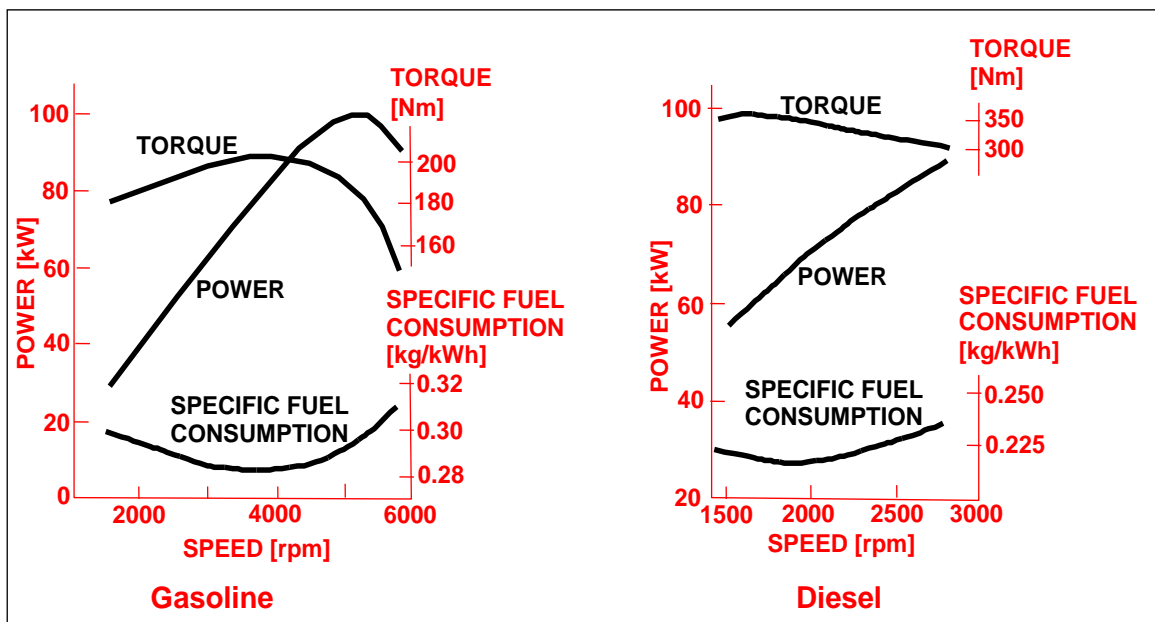


Figure 3-3: Engine Characteristics for Gasoline and Diesel Engines, at maximum torque capability. Typical values for passenger car.

3.2.1.2 Transmissions

In some contexts “transmission” means the 1-dimensional transmission of rotational mechanical power from an input shaft to one output shaft. These are covered in Section 3.2.1.2.1

In other contexts, “transmission” means the system that distributes the energy to/from an energy buffer and to/from multiple axles and/or wheels. These are covered in Section 3.2.1.2.2.

3.2.1.2.1 Main transmissions

An example of such transmission is a stepped gearbox, which can be modelled e.g. as:

$$\begin{aligned} T_{out} &= r \cdot T_{in} \cdot \eta_{CoggMeshes} - \Delta T_{Bearings} \cdot \text{sign}(\omega_{out}); \\ \omega_{out} &= \frac{\omega_{in}}{r}; \\ r &= r_1, r_2, \dots, r_N; \quad r \neq 0; \end{aligned} \quad [3.1]$$

Eq [3.1] is not valid for neutral gear (then there is no speed equation, but instead two torque equations: $T_{out} = -\Delta T_{outBearings} \cdot \text{sign}(\omega_{out})$; and $T_{in} = \Delta T_{inBearings} \cdot \text{sign}(\omega_{in})$);

For any 1-dimensional transmission of rotational mechanical power between two rotating shafts, the total efficiency, $\eta_{total} = P_{out}/P_{in} = T_{out} \cdot \omega_{out}/(T_{in} \cdot \omega_{in})$; is depending on operating condition. If assuming a nominal ratio, r , the total efficiency can be decomposed in $\eta_{total} = \eta_T \cdot \eta_\omega$; where $\eta_T = T_{out}/(r \cdot T_{in})$; and $\eta_\omega = \omega_{out}/(\omega_{in}/r)$;

Clutches and torque converters can also be part of models of main transmissions.

3.2.1.2.2 Distribution transmissions

The distribution to energy buffer and multiple axles and/or wheels can basically be done in two ways:

- Distribute in certain fractions of (rotational) speed. A (rotationally) rigid shaft between left and right wheel is one example of this. We find this in special vehicles, such as go-carts, and in more common vehicles when a differential lock is engaged. There are 3 shafts in such an axle: input to the axle and two outputs (to left and right wheel). The equations will be:

$$\begin{aligned} \omega_{in} &= \omega_{left}; \\ \omega_{in} &= \omega_{right}; \\ T_{in} &= T_{left} + T_{right}; \end{aligned} \quad [3.2]$$

- Distribute in certain fraction of torque. This requires some type of planetary gear arrangement. A conventional (open) differential gear is one example of this, where the equations will be:

$$\begin{aligned} \omega_{in} &= \frac{\omega_{left} + \omega_{right}}{2}; \\ T_{left} &= T_{right}; \\ T_{in} &= T_{left} + T_{right}; \end{aligned} \quad [3.3]$$

Generally speaking, the open differential is rather straight-forward to use in most vehicle dynamics analysis: The speeds are given by vehicle motion (e.g. curve-outer wheel runs faster than curve-inner wheel, defined by vehicle yaw rate and track width). The torques are defined by the differential, as half of the propulsion torque at each side.

Also, a locked differential, it is generally more complex to analyse. Here, the wheels are forced to have same rotational speed and, in a curve, that involves the tyre longitudinal slip characteristics. The solution involves more equations with shared variables.

So, open/locked differential is the basic concept choice. But there are additions to those: One can build in friction clutches which are either operated automatically with mechanical wedges or similar or operated by control functions. One can also build in electric motors which moves torque from one wheel to the other. However, the compendium does not intend to go further into these designs.

Part of the distribution transmissions are also shafts. If oscillations is to be studied, these has to be modelled as energy storing compliances: $\dot{T} = c \cdot (\omega_{in} - \omega_{out})$.

3.2.1.3 Energy buffers

Energy buffers in vehicles are today often electro-chemical batteries. However, other designs are possible, such as flywheels and hydrostatic accumulators. A simple model of a buffer is as follows:

$$\dot{E} = \begin{cases} = (P_{in} - P_{out}) \cdot \eta_{charge}; & \text{for } P_{in} > P_{out}; \\ = (P_{in} - P_{out})/\eta_{use}; & \text{else}; \end{cases} \quad [3.4]$$

where $P_{in} = T_{in} \cdot \omega_{in}$; and $P_{out} = T_{out} \cdot \omega_{out}$;

Including how the buffer is connected, one more equation can be found: Typically $\omega_{in} = \omega_{out}$; or $T_{in} = T_{out}$.

The model uses stored energy, E . For batteries one often uses state of charge, SoC , instead. Conceptually, $SoC = E/E_{max}$; where E_{max} is a nominal maximum charge level.

A first approximation of the efficiencies, can be $\eta_{charge} = \eta_{use} = constant < 1$, but typically the efficiency is dependent of many things, such as $P_{in} - P_{out}$. The model above does not consider any leakage when buffer is "resting": $P_{in} = P_{out}$.

3.2.2 Traction diagram

The force generated in the prime mover is transmitted through a mechanical transmission to the wheel which then generates the propulsive forces in the contact patch between tyre and road. In an electric in-wheel motor, the transmission can be as simple as a single-step gear. In a conventional vehicle it is a stepped transmission with several gear ratios (i.e. a gearbox). Then, the drivetrain can be drawn as in Figure 3-4. The torque and rotational speed of the engine is transformed into force and velocity curves via the mechanical drivetrain and driven wheel. The result is a Traction diagram. The transformation follows the following formula, if losses are neglected:

$$F = ratio \cdot \frac{T}{WheelRadius}; \quad \text{and} \quad v = WheelRadius \cdot \frac{\omega}{ratio}; \quad [3.5]$$

A traction diagram for a truck is given in Figure 3-5, which also shows that there will be one curve for each gear.

Losses in transmission can be included by using equations including loss models for transmission, such as:

$$\begin{aligned} \text{Replace } F &= ratio \cdot \frac{T}{radius}; \quad \text{with } F = \eta_T \cdot ratio \cdot \frac{T}{radius}; \quad \text{where } \eta_T \leq 1; \\ \text{Replace } v &= radius \cdot \frac{\omega}{ratio}; \quad \text{with } v = \eta_\omega \cdot radius \cdot \frac{\omega}{ratio}; \quad \text{where } \eta_\omega \leq 1; \\ \text{where } \eta_{total} &= \frac{P_{vehicle}}{P_{engine}} = \frac{F \cdot v}{T \cdot \omega} = \eta_T \cdot \eta_\omega \leq 1 \end{aligned} \quad [3.6]$$

This will basically move the curves in the first quadrant slightly downwards and to the left.

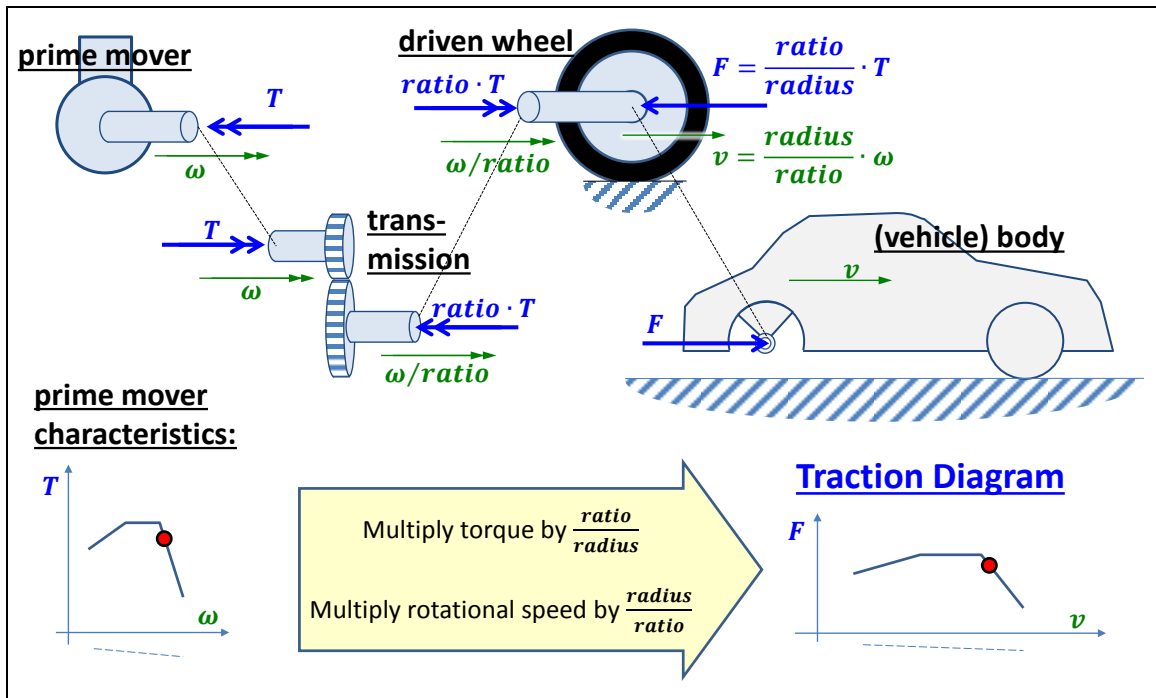


Figure 3-4: Construction of Traction Diagram, i.e. diagram for transmission of torque to longitudinal force on vehicle.

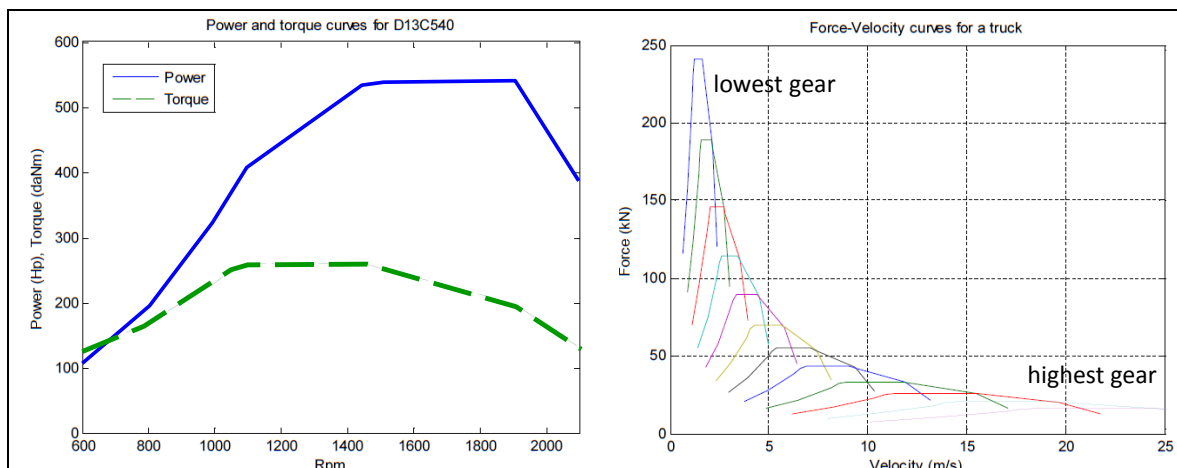


Figure 3-5: Example of engine map and corresponding traction diagram map from a truck. (D13C540 is an I6 diesel engine of 12.8-litre and 540 hp for heavy trucks.)

Tyre rolling friction is a loss mechanism, which on its own yields $\eta_{\omega} = 1$ and $\eta_T < 1$. Tyre longitudinal slip is a loss mechanism, which on its own yields $\eta_{\omega} < 1$ and $\eta_T = 1$. See Section 2.4.

A traction diagram is a kind of one degree of freedom graphical model. The diagram can be extended with, e.g., the longitudinal force from the brake system.

3.2.3 Driving Resistance

From studying Figure 3-5 one could extrapolate that a very low transmission ratio, i.e., a very high gear, we would enable almost infinite speed. We know that this is not possible. Something obviously limits the top speed: the limit comes from "driving resistance". As presented in Chapter 2, there are tyre rolling-resistance forces and aerodynamic driving-resistance forces. Also, there can be an

additional resistance force to be considered when going uphill: the grade or gravitational load on the vehicle. This resistance can also be negative, i.e. act as propulsion down-hill. The formula for driving resistance becomes as follows, using Equation [2.38]. Notation f means rolling resistance coefficient.

$$F_{resistance} = m \cdot g \cdot \sin(\varphi) + f \cdot m \cdot g \cdot \cos(\varphi) + \frac{1}{2} \cdot c_d \cdot \rho \cdot A \cdot (v_x - v_{wind,x})^2 \quad [3.7]$$

Superimposing the external loads on the Traction Diagram allows us to identify when the “demands” can be met by the “supply”. As seen in Figure 3-6, the combination of external resistance loads and the internally generated drive forces can be presented on the same figure. The resulting intersection of supply (prime mover) and demand (driving resistance) identifies the top speed of the vehicle. These results hold only for steady state (no acceleration) conditions.

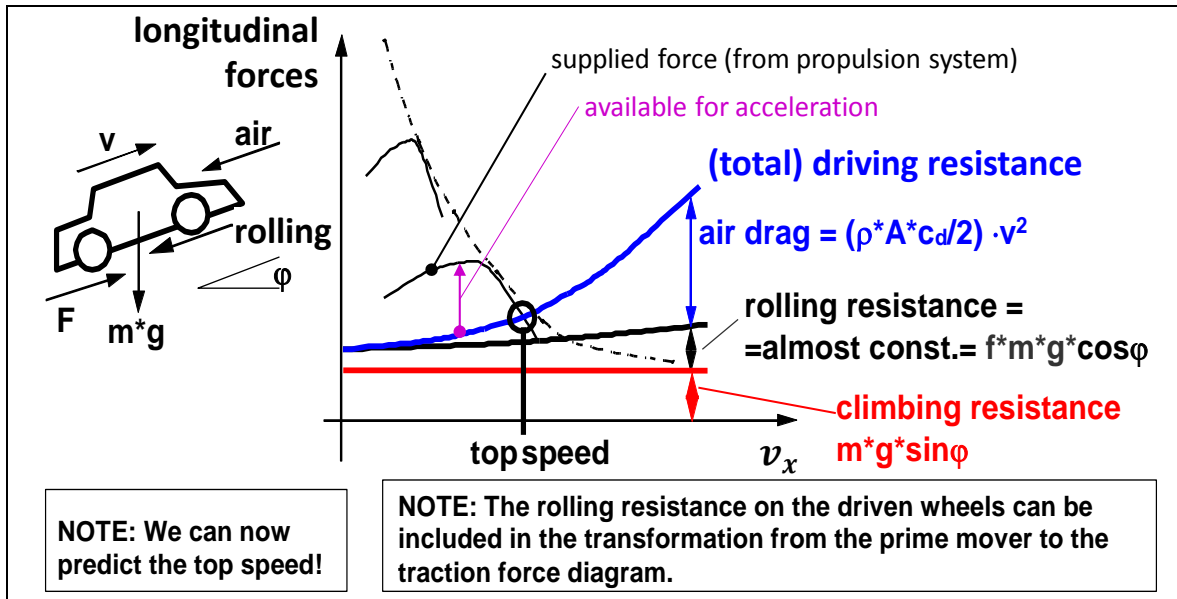


Figure 3-6: Top speed can be found from Traction diagram with Driving Resistance curves. Head wind speed, $v_{wind,x}$, is assumed to be zero. Note that “rolling” actually is a moment loss on the wheels, why it is more correct to let it influence the “supplied force curve” for driven axles and the driving resistance curve for the non-driven axles, see Figure 3-9.

As seen in Figure 3-6, the acceleration can be identified as a vertical measure in the traction diagram, divided by the mass. However, one should be careful when using the traction diagram for more than steady state driving. We will come back to acceleration performance later, after introducing the two effects “Load transfer” and “Rotating inertia effect”.

There are more driving-resistance effects than covered in Equation [3.7]. One example is that lateral tyre forces may have components in longitudinal direction, such as when the vehicle is making a turn or if one axle have a significant toe-in.

3.2.4 Top speed *

*Function definition: **Top speed** is the maximum longitudinal forward speed the vehicle can reach and maintain on level and rigid ground without head-wind.*

The top speed can be read out from a traction diagram with driving resistance, see Figure 3-6. Top speed is the speed where the sum of all driving resistance terms is equal to the available propulsion forces.

3.2.5 Starting with slipping clutch

As seen in previous traction diagrams, there is no available positive propulsion force at zero speed. This means that the diagram can still not explain how we can start a vehicle from stand-still.

The concepts in Figure 3-4 were used to create the force-velocity diagram in Figure 3-7. It shows the smooth curve of a Continuous Variable ratio Transmission (CVT) in comparison to the stepped transmission. The CVT is the ideal situation for the engine since it can always let the engine work at a maximum power or minimum fuel consumption (minimum for the momentarily required power). If the CVT has unlimited high ratio, it can actually have a non-zero propulsion force at zero vehicle speed. Without losses, this force would be infinite, but in reality it is limited, but still positive, so the vehicle can start from stand-still.

A stepped transmission, as well as a CVT with limited ratio range, instead needs a clutch to enable starting from vehicle stand-still. This is shown in Figure 3-7. The highest force level on each curve can be reached at all lower vehicle speeds, because the clutch can slip. It requires the clutch to be engaged carefully to the torque level just below the maximum the engine can produce. In traditional automatic transmissions the slipping clutch is replaced with a hydrodynamic torque converter, to enable start from stand-still.

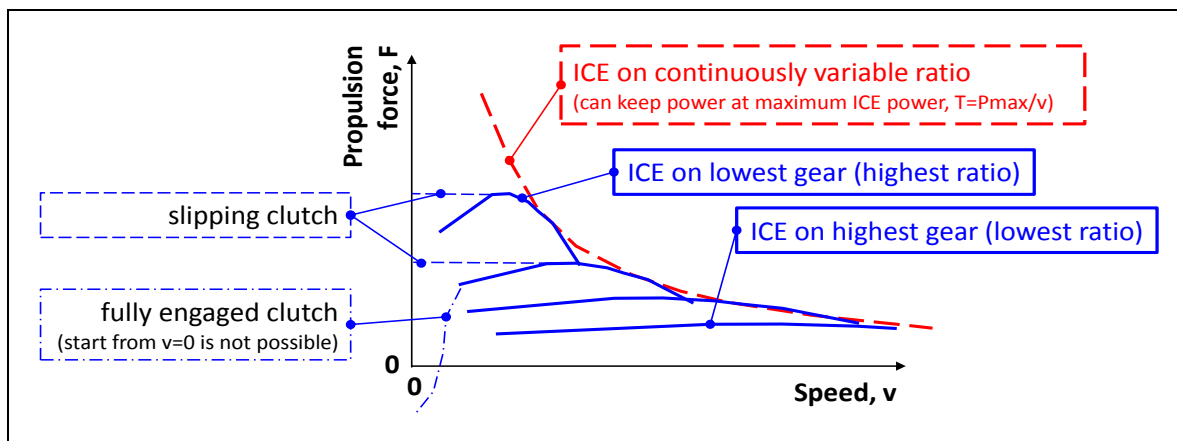


Figure 3-7: Force/Speed Curves for a Multiple Gear Transmission and for CVT.

3.2.6 Steady state load distribution

The vehicle performance discussed previously does not rely on knowing the distribution of (vertical) load between the axles. To be able to introduce limitations due to road friction, this distribution must be known. Hence we set up the free-body diagram in Figure 3-8.

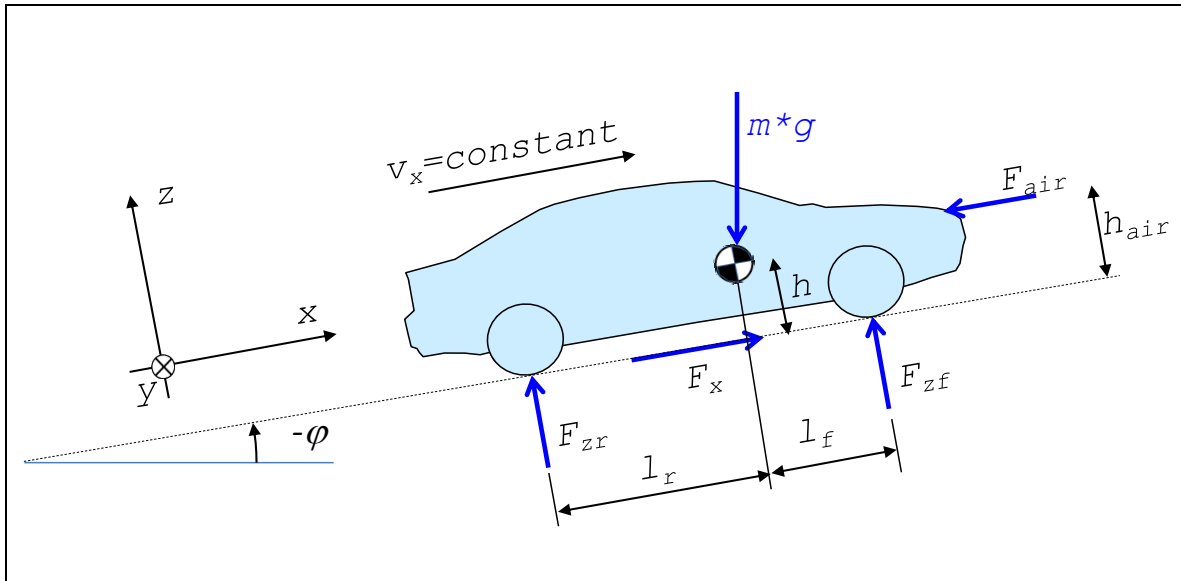


Figure 3-8: Free Body Diagram for steady state vehicle. With ISO coordinate system, the road gradient is negative when downhill. (Rolling resistance is included in F_x .)

From the free-body diagram we can set up the equilibrium equations as follows and derive the formula for load on front and rear axle:

Moment equilibrium, around rear contact with ground:

$$F_{zf} \cdot (l_f + l_r) - m \cdot g \cdot (l_r \cdot \cos(-\varphi) - h \cdot \sin(-\varphi)) + F_{air} \cdot h_{air} = 0 \Rightarrow$$

$$\Rightarrow F_{zf} = m \cdot g \cdot \frac{l_r \cdot \cos(\varphi) + h \cdot \sin(\varphi)}{l_f + l_r} - F_{air} \cdot \frac{h_{air}}{l_f + l_r}$$

Moment equilibrium, around front contact with ground:

$$-F_{zr} \cdot (l_f + l_r) + m \cdot g \cdot (l_f \cdot \cos(-\varphi) + h \cdot \sin(-\varphi)) + F_{air} \cdot h_{air} = 0 \Rightarrow$$

$$\Rightarrow F_{zr} = m \cdot g \cdot \frac{l_f \cdot \cos(\varphi) - h \cdot \sin(\varphi)}{l_f + l_r} + F_{air} \cdot \frac{h_{air}}{l_f + l_r}$$

[3.8]

For most vehicles and reasonable gradients one can neglect $h \cdot \sin(\varphi)$ since it is $\ll |l_f \cdot \cos(\varphi)| \approx |l_r \cdot \cos(\varphi)|$.

3.2.7 Friction limit

With a high-powered propulsion system, there is a limitation to how much the vehicle can be propelled, due to the road friction limit. It is the normal load and coefficient of friction, which limits this. For a vehicle which is driven only on one axle, it is only the normal load on the driven axle, $F_{z,driven}$, that is the limiting factor:

$$F_x = \min(F_{x,PropSyst} ; \mu \cdot F_{z,driven})$$

[3.9]

One realises, from Figure 2-10, that the rolling resistance on the driven axle works as a torque loss and that the road friction limitation will be limiting $T_{eng} \cdot ratio - e \cdot F_{z,driven}$ rather than limiting $T_{eng} \cdot ratio$. Expressed using the rolling resistance coefficient, f_{roll} , gives:

$$F_x = \min(F_{x,PropSyst} ; \mu \cdot F_{z,driven}) =$$

$$= \min\left(\frac{T_{eng} \cdot ratio}{radius} - f_{roll} \cdot F_{z,driven} ; \mu \cdot F_{z,driven}\right) \quad [3.10]$$

This is shown in the traction diagram in Figure 3-9, where it should also be noted that the rolling resistance curve only consists of the rolling resistance on the non-driven axles. See also Figure 2-10.

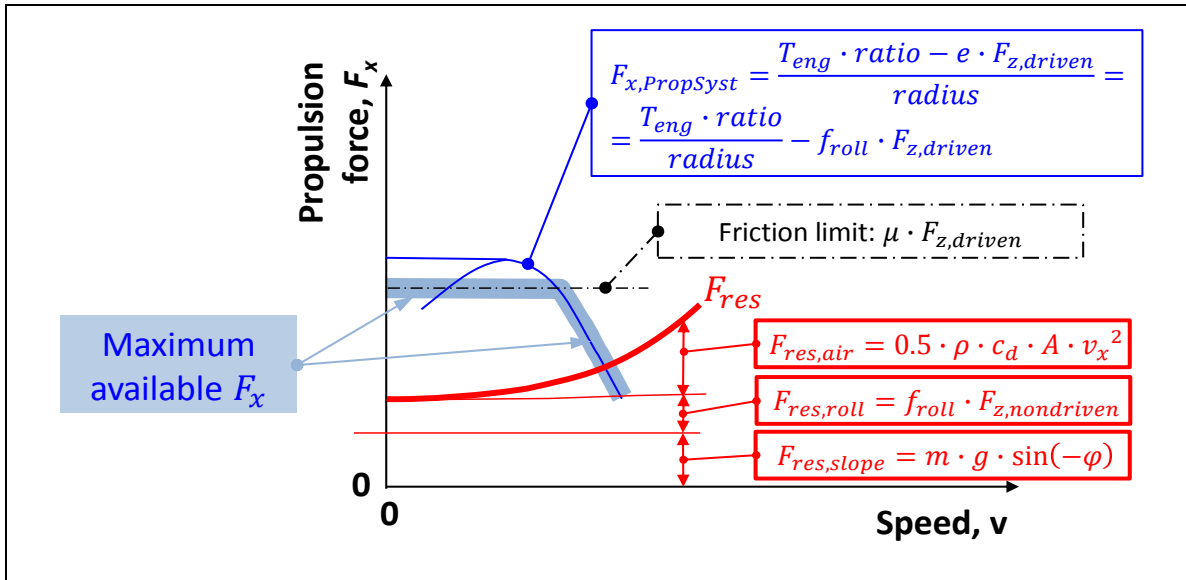


Figure 3-9: Traction diagram with Road Friction limitation and Driving Resistance curves.

3.2.8 Uphill performance

3.2.8.1 Start-ability *

*Function definition: **Start-ability** is the maximum grade that a vehicle is capable to start in and maintain the forward motion at a certain road friction level and a certain load. (Reference (Kati, 2013))*

Figure 3-10 shows how we find the start-ability in the traction diagram.

To allow clutch or tyres to slip, is not very practical, because there will be a lot of wear and heat in the slipping clutch or tyre. Hence, Figure 3-10 also shows also the case when we require absence of slip in clutch and tyre **in the end of the starting sequence**. Then the start-ability is slightly reduced. The reduction is however very small, since the resistance curves does not change very much during this small speed interval (the resistance curves in the figure have exaggerated slope; the air resistance can typically be neglected for start-ability).

However, in practice the energy loss (heat, wear) in clutch and tyre should be limited also **during the starting sequence**. This can limit the start-ability more severely than the slope of the resistance curves, but it is not easily shown in the traction diagram, since it is limited by energy losses in clutch or tyre, which is a time integral of $T \cdot \omega_{clutch}$ and $T_{wheel} \cdot \omega_{wheel}$.

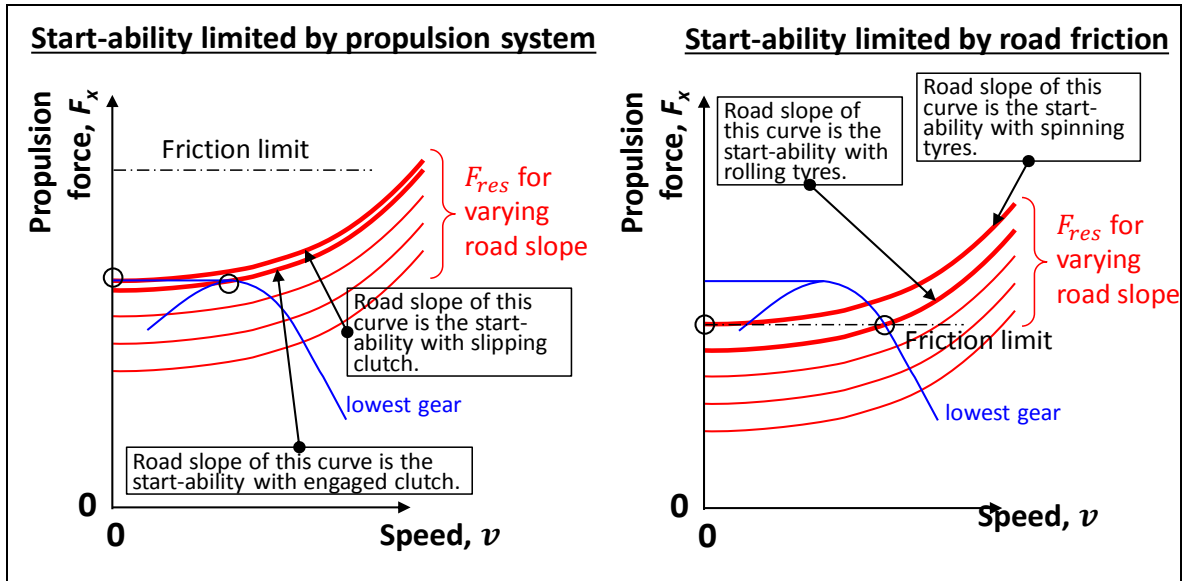


Figure 3-10: How Start-ability is read-out from Traction diagram.

3.2.8.2 Grade-ability *

Function definition: **Grade-ability** is the maximum grade that a vehicle is capable to maintain the forward motion on an uphill road at a certain constant speed, at a certain road friction level and with a certain load. (from Reference (Kati, 2013))

Figure 3-11 shows how we find the start-ability in the traction diagram. For vehicles with high installed propulsion power per weight, the road friction can be limiting, but this is not visualised in Figure 3-11. Since the speeds are higher than for start-ability, the air resistance cannot be neglected.

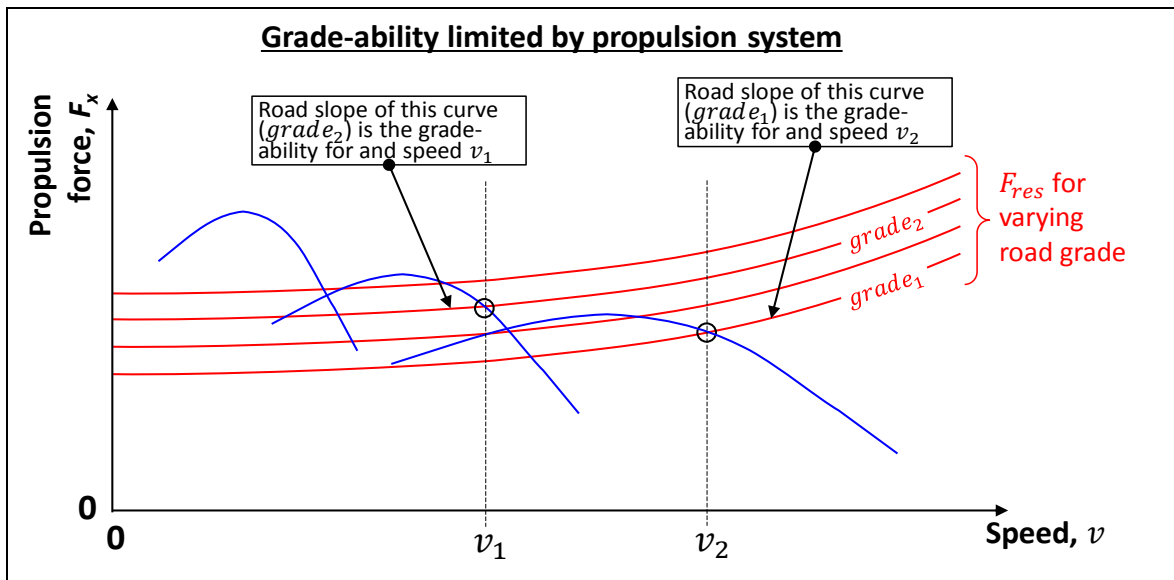


Figure 3-11: How Grade-ability is read-out from Traction diagram.

3.2.8.3 Towing capacity *

Function definition: **Towing capacity** is the maximum vehicle-external longitudinal force the vehicle can have on its body and start and maintain a certain forward speed at a certain road friction and a certain up-hill gradient.

The driving situation for defining towing capacity is similar to the one for defining grade-ability. Towing capacity describes how much load the vehicle can tow, P_x in Figure 3-12, on a certain up-hill gradient. Since towing a load is more relevant as part of a longer transport mission, it is normally also for a particular constant speed, typically in range 80 to 100 km/h. Since the speed is that large, the air resistance may not be neglected. It is also important consider air resistance of the trailer and that axle loads can change, which changes both friction limitation and rolling resistance. A free-body diagram is shown in Figure 3-12. It is noticeable, that there can also be an additional air resistance of the trailer which will influence in a test of Towing capacity.

For pure off-road vehicles and agriculture tractors, the term “towing” can mean the maximum pulling force at very low forward speeds at level ground. This is related but different to the above described towing capacity for road vehicles.

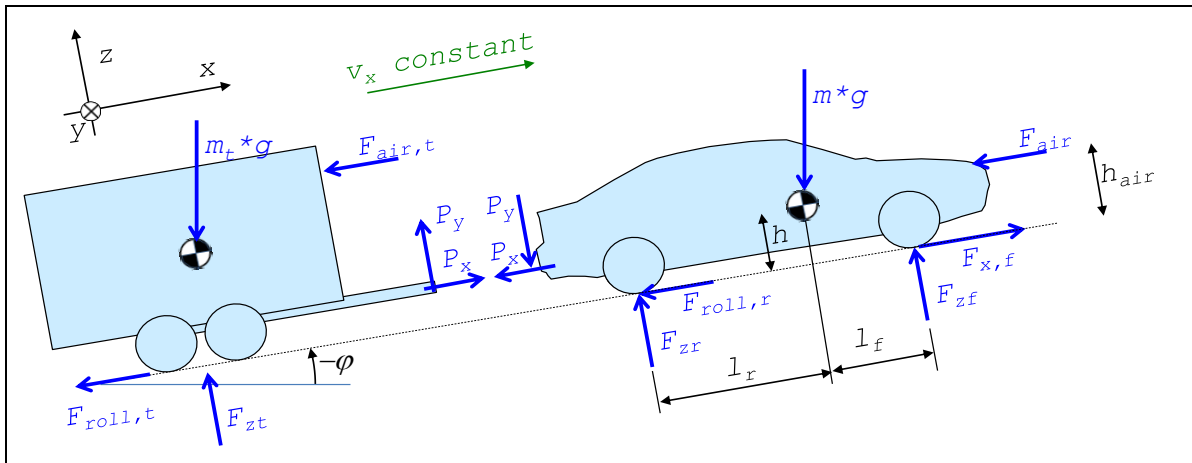


Figure 3-12: Towing Loads. The towing vehicle is front axle driven.

3.3 Functions over longer events

Functions as fuel or energy consumption and emissions are relevant only over certain but longer periods of driving, typically some seconds (typically ≥ 10 s) to hours of driving. There are different ways of defining such driving events.

3.3.1 Driving cycles

One way to define a longer event is a so called driving cycle; where the relevant variables are pre-scribed as function of time. At least on defines speed as a function of time. Examples of commonly used driving cycles are given in Figure 3-13 and Figure 3-14. In addition, it can also be relevant to give road inclination as function of time. Engine temperature and selected gear as functions of time may also be defined. For hybrid vehicles, the possibility to regenerate energy via electric machines is limited in curves, so curvature radius can also be prescribed as function of time. For heavy vehicles, the weight of transported goods can be another important measure to prescribe.

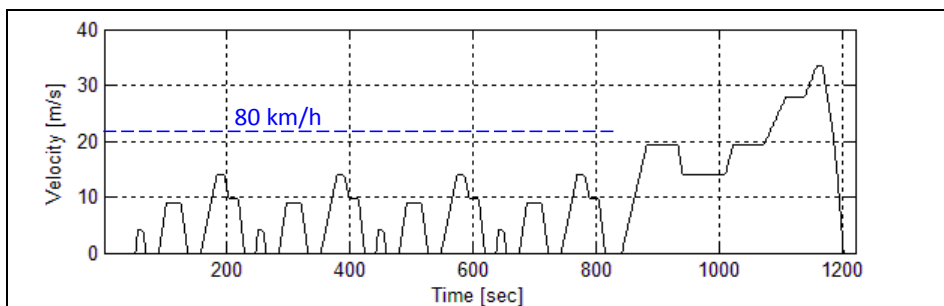


Figure 3-13: New European Driving Cycle (NEDC). From (Boerboom, 2012)

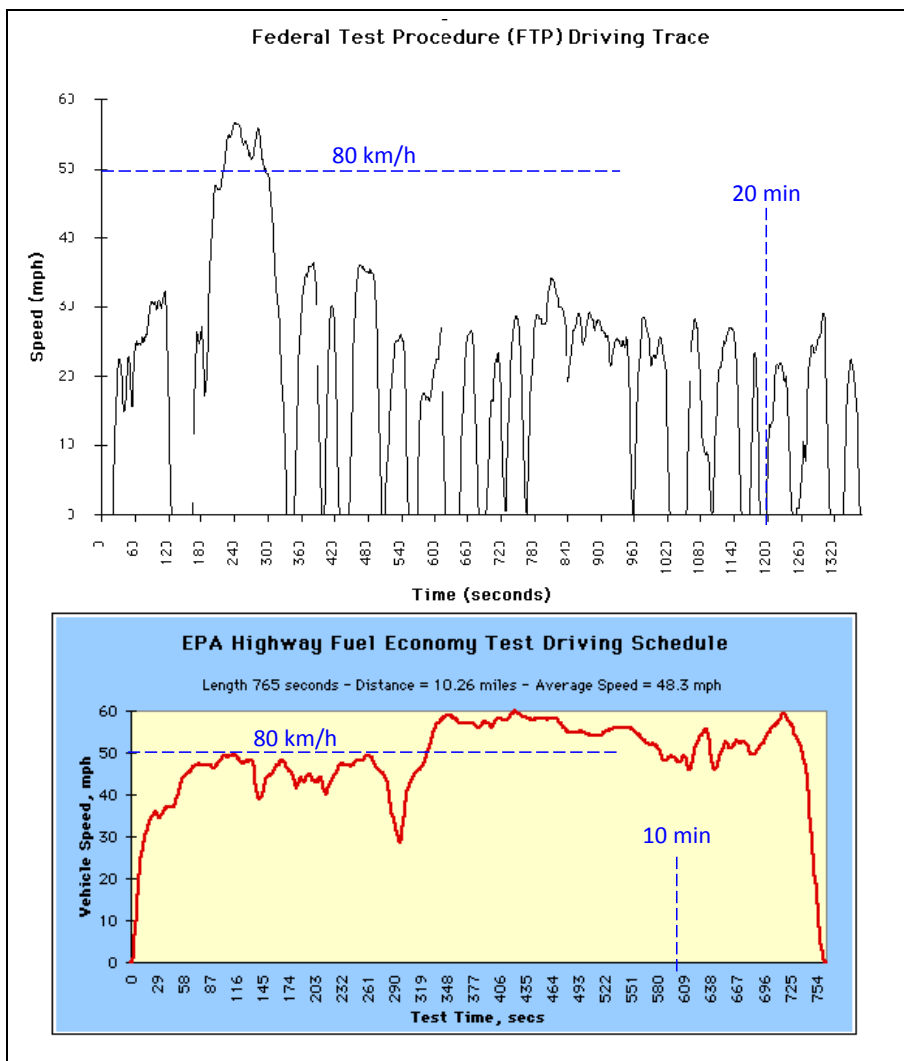


Figure 3-14: Top: FTP cycle from <http://www.epa.gov/oms/reg/ld-hwy/ftp-rev/ftp-tech.pdf>.
Bottom: HFTP cycle from <http://www.epa.gov/nvfel/methods/hwfetdds.gif>.

FTP and HFTP are examples of cycles derived from logging actual driving, mainly used in North America. NEDC is an example of a “synthetically compiled” cycle, mainly used in Europe. Worldwide harmonized Light duty driving Test Cycle (WLTC) is a work with intention to be used world-wide, see Figure 3-15. WLTC exists in different variants for differently powered vehicle [power/weight].

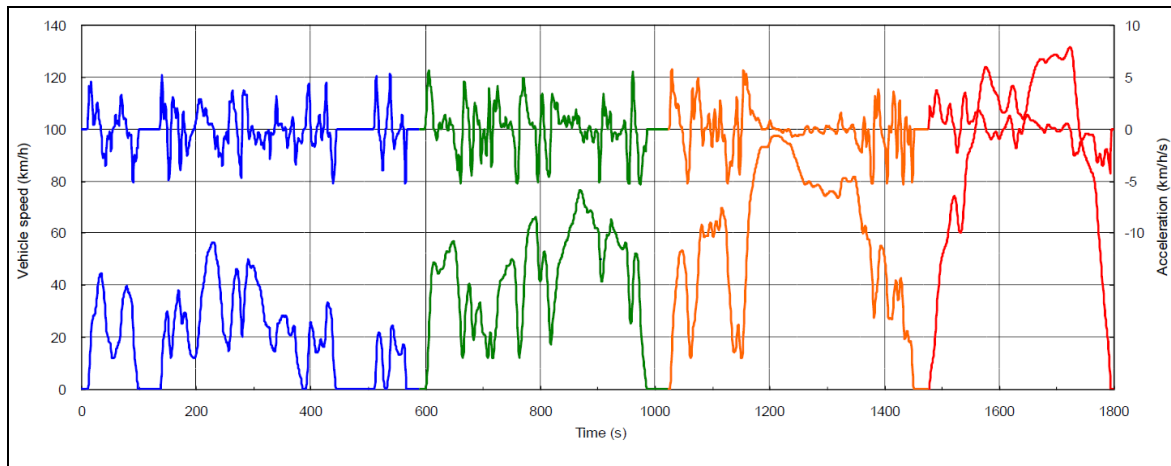


Figure 3-15: WLTC cycle from <http://www.unece.org>.

3.3.2 Other ways of defining the driving event

Alternative ways of defining the driving event are:

3.3.2.1 Driving pattern

A driving cycle can be condensed into a 2-dimensional function of speed and acceleration, as shown in Figure 3-16. This figure is simply a scatter plot showing which combinations are most common, but can also be converted to durations (in seconds or fractions of total time) for different intervals of combination of speed and acceleration. This is a less advanced and less realistic description of the transport task. With this method one does not need any dynamic vehicle model at all and there will be no influence of the time history from the original driving cycle.

Driving patterns can use more than 2 dimensions, such as [speed, acceleration, road gradient]. In principle, they can also use less than 2 dimensions, maybe only [speed].

3.3.2.2 Transport task/Operating cycle

Desired speed, road inclination, weight of transported goods etc are defined in position rather than time. For stops along the route, the stop duration or departure time has to be separately defined. This is a more advanced and realistic description of the vehicle usage. It can be extended to include operation at stand-still, e.g. idle and loading/unloading cargo.

Theoretical analyses of such vehicle usage require some kind of driver model. A consequence is that different driver models will give different results, e.g., different fuel consumption due to different driver preferred acceleration. Hence, the driver model itself can be seen as a part of the vehicle usage definition.

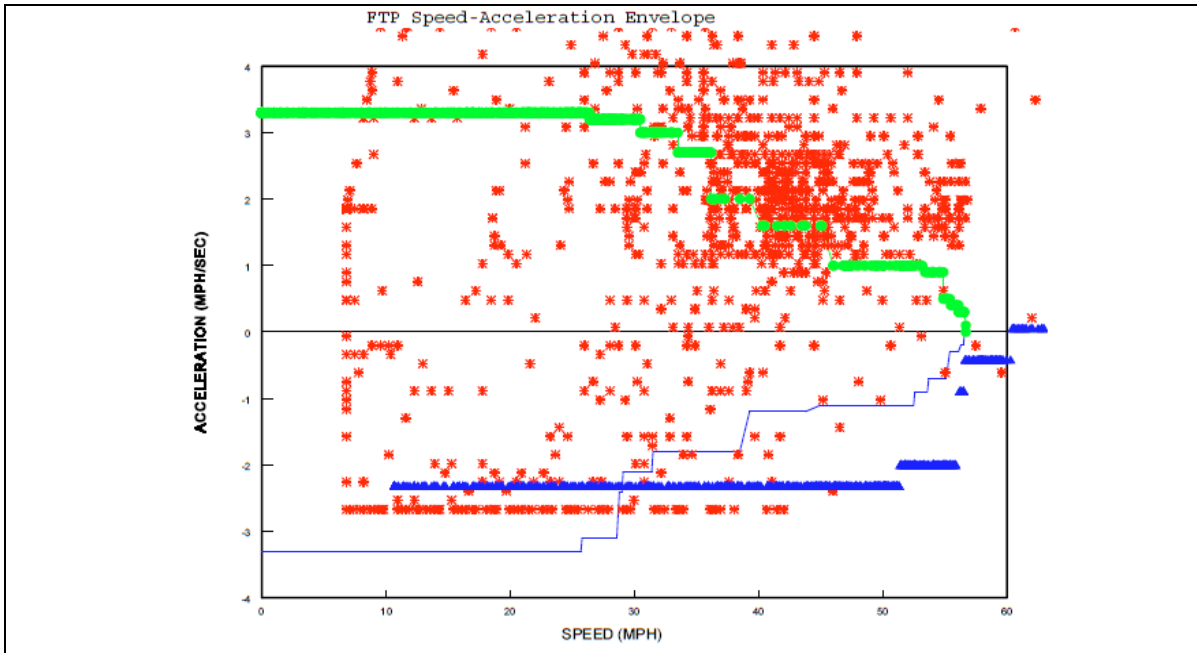


Figure 3-16: FTP cycle converted to a Driving pattern, i.e. a distribution of operating duration in speed and acceleration domain. From <http://www.epa.gov/oms/regs/ld-hwy/ftp-rev/ftp-tech.pdf>.

3.3.3 Rotating inertia effects

In Figure 3-6 it was shown that the acceleration cannot be found directly as a force difference (distance between curves) divided by vehicle mass. This is because the Traction Diagram does not contain any dynamics, and dynamics are more complicated than simply accelerating the vehicle mass. The phenomenon that occurs is referred to here as “rotating inertia effect”. The rotating part of the propulsion system, e.g. engine and wheels, must be synchronically accelerated with the vehicle mass. This “steals” some of the power from the propulsion system. This affects the required propulsion force when following accelerations in a driving cycle.

Consider a wheel rolling which is ideally rolling (no slip), with a free-body diagram and notations as in Figure 3-17. Setting up 2 equilibrium equations and 1 compatibility equation gives:

$$\begin{aligned} m \cdot \dot{v} &= F; \\ J \cdot \dot{\omega} &= T - F \cdot R; \\ v &= R \cdot \omega \Rightarrow \dot{v} = R \cdot \dot{\omega}; \end{aligned}$$

[3.11]

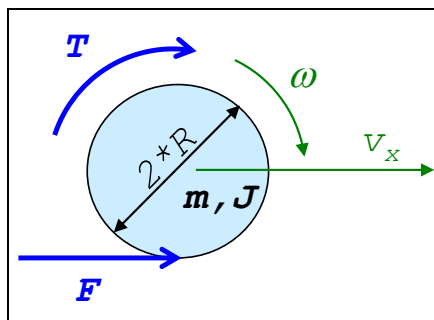


Figure 3-17: Rolling wheel

Assume that we know torque T and want to compare this with the situation without rotational inertia:

$$m \cdot \dot{v} = \frac{T}{R}; \quad \text{and} \quad F = \frac{T}{R}; \quad [3.12]$$

Then we use the compatibility equation to eliminate ω in Equation [3.11], which then becomes:

$$k \cdot m \cdot \dot{v} = \frac{T}{R}; \quad \text{and} \quad F = \frac{1}{k} \cdot \frac{T}{R};$$

where $k = \frac{m + J/R^2}{m} = \frac{m + J_{transf}}{m};$ [3.13]

Thus, we can see the effect of the rotating inertia as making the mass a factor k larger and making the reaction force correspondingly lower. We call the factor k the “rotational inertia coefficient”.

In a vehicle propulsion system, there are rotational inertias mainly at two places:

- Rotating inertias before transmission, i.e. elements rotating with the same speed as the engine: J_e
- Rotating inertias after transmission, i.e. elements rotating with same speed as the wheel: J_w

The effective mass, $k \cdot m$, will be dependent on the gear ratio as well:

$$k \cdot m = m + \frac{J_w}{R^2} + \frac{J_e \cdot ratio^2}{R^2}; \quad [3.14]$$

Typically for a passenger car, $k=1.4$ in the first gear and $k=1.1$ in the highest gear. So, in the first gear, approximately one third of the engine torque is required to rotationally accelerate the driveline, and only two thirds is available for accelerating the vehicle!

When the clutch is slipping, there is no constraint between engine speed and vehicle. The term with J_e disappears from Equation [3.14]. If the wheel spins, both rotational terms disappear.

We can now learn how to determine acceleration from the Traction Diagram, see Figure 3-18.

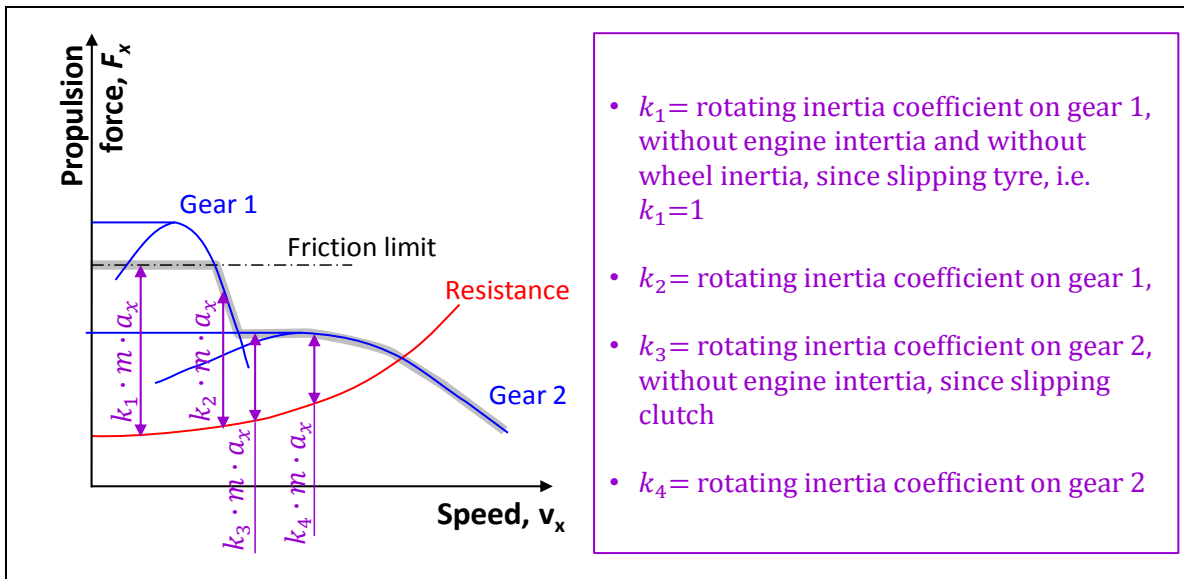


Figure 3-18: Acceleration in Traction Diagram. Rotating inertia effects are shown assuming that the engine is run on its maximum curve and the gear (or slipping clutch) for highest acceleration is selected.

3.3.4 Traction diagram with deceleration

The cases 1-4 in Figure 3-18 assumes that the engine is running on its maximum torque curve, which is not generally necessary during a certain driving cycle. Instead, the accelerations are often more modest, meaning that two gears are often used. Then one can generally find an engine operating point between the maximum and minimum curve of the engine, see Figure 3-2.

When the driving cycle shows a deceleration which is larger than can be achieved with resistance force, we need to brake with a combination of engine braking and friction brakes. If only friction braking is used, it can be with engaged or disengaged clutch. That influences the rotating inertia coefficient by using or not using the J_e term in Equation [3.14], respectively.

The traction diagram can be extended to also cover engine braking and friction braking. However, the friction brake system is seldom limiting factor for how negative the longitudinal force can be. But the road friction is, see Figure 3-19.

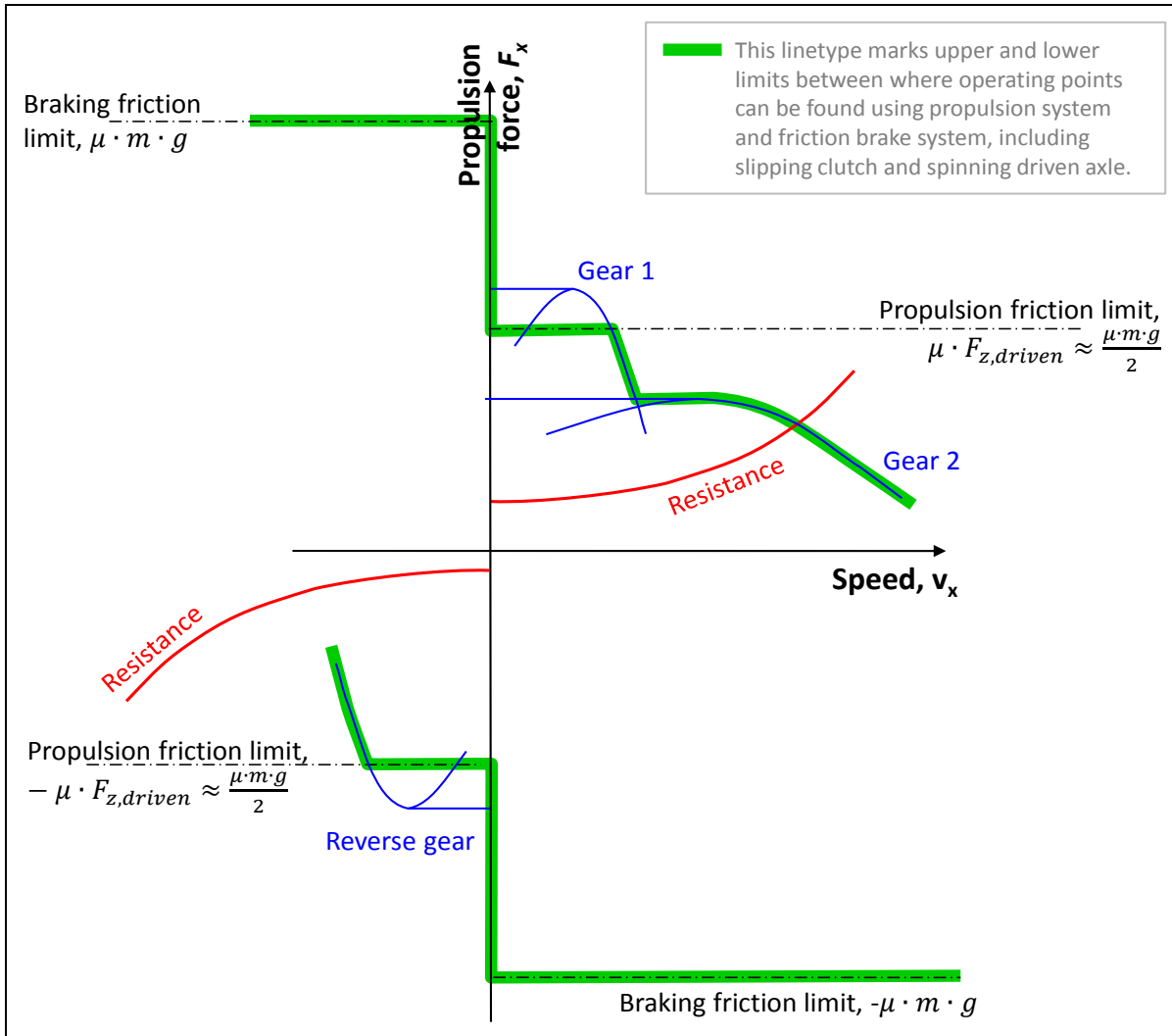


Figure 3-19: Traction Diagram including both maximum and minimum propulsion. One of two axles is assumed to be driven, which limits propulsion to approximately half of braking friction limit. Up-hill slope is assumed, which is seen as asymmetric resistance.

3.3.5 Fuel or energy consumption *

*Function definition: **Fuel (or Energy) Consumption** is the amount of fuel [kg or litre] (or energy [J]) consumed by the vehicle per performed transportation amount. Transportation amount can e.g. be measured in km, person*km, ton*km or m³*km. The vehicle operation has to be defined, e.g. with a certain driving cycle (speed as function of time or position), including road gradient, cargo load, road surface conditions, etc.*

The consumption arises in the prime mover. The consumption is dependent on the operating point in the speed vs torque diagram, or map, for the prime mover. Each point have a consumption rate [g/s] or [Nm/s=W], but it is often given as a specific consumption or an efficiency. Specific consumption is the consumption rate divided with output power= speed*torque; for a fuel consuming prime mover this leads to the unit [(g/s)/(Nm/s)] or [g/J] or [g/(Ws)] or [g/(kWh)]. Efficiency is, conceptually, the inverse of specific consumption; "out/in" instead of "in/out". The units for efficiency becomes [W/W=1]. An example of a map for an ICE is given in Figure 3-20. Maps with similar function can be found for other types of prime movers, such as the efficiency map for an electric motor, see Figure 3-21.

Figure 3-20 and Figure 3-21 also show that the efficiencies can be transformed to the traction diagram. The maps for different gears partly overlap each other, which show that an operating point of the vehicle can be reached using different gears. The most fuel or energy efficient way to select gear is to select the gear which gives the lowest specific fuel consumption, or highest efficiency. Such a gear selection principle is one way of avoiding specifying the gear selection as a function over time in the driving cycle. For vehicles with automatic transmission, that principle can be programmed into the control algorithms for the transmission.

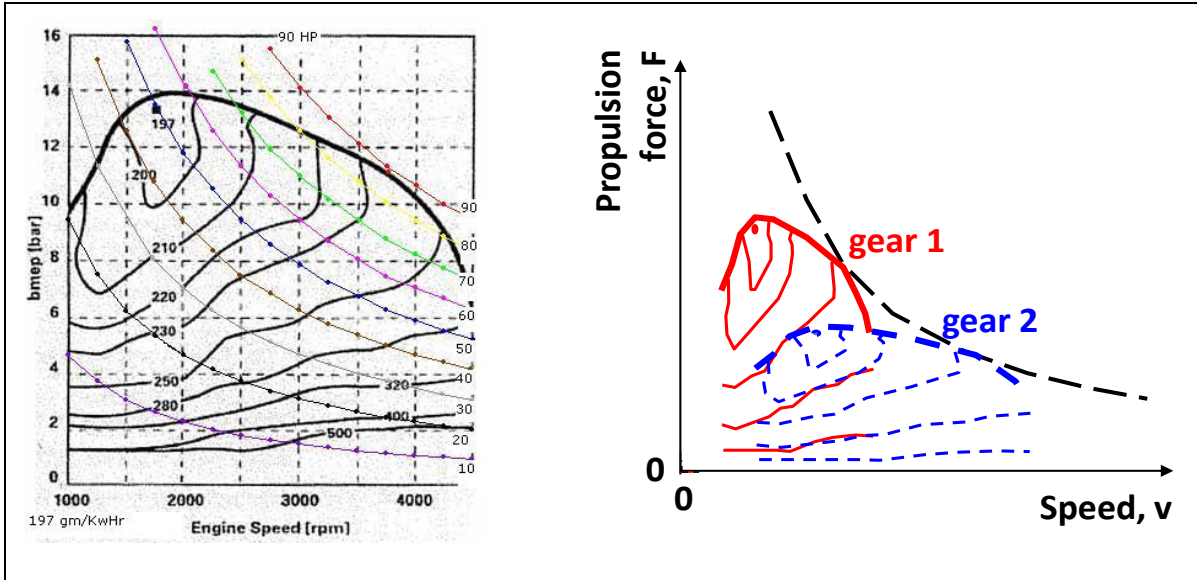


Figure 3-20: Left: Fuel consumption map. Curves show where specific fuel consumption $[g/(kW \cdot h)]$ is constant. For a specific fuel, this is proportional to $1/\text{efficiency}$. Right: Specific fuel consumption curves can also be transformed in Traction Diagram, for a given gear.

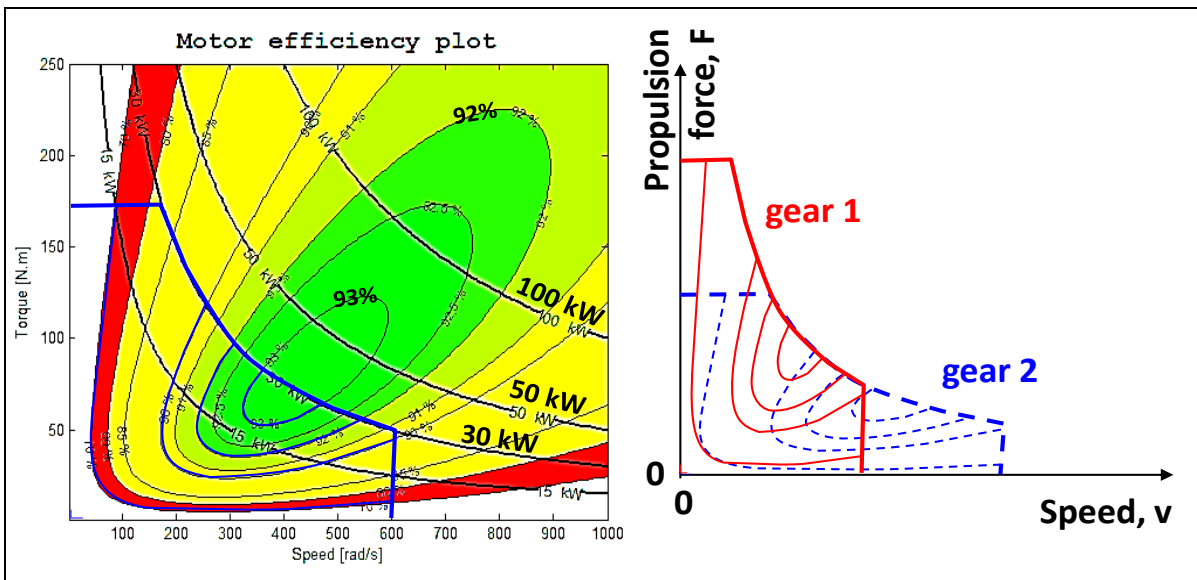


Figure 3-21: Left: Efficiency map for a typical brushless DC motor, from (Boerboom, 2012). Elliptic curves show where efficiency is constant. Right: The efficiency curves can also be transformed in Traction Diagram, for a given gear.

How to predict the consumption for a vehicle during a certain driving cycle is rather straight-forward using what has been presented earlier in this chapter. Since a driving cycle is a prediction of how the vehicle is moving, it actually stipulates the acceleration of a mass, which calls for an “inverse

dynamics” analysis. In such analysis one assumes that the driving cycle is met exactly, which means that both required wheel speed and required wheel torque can be calculated for each time instant. Then, via a propulsion and brake system model, the corresponding fuel consumption in the engine can also be found for each time instant. A summary of such an inverse dynamic algorithm for prediction of fuel or energy consumption is given in Equation [3.15].

For each time step in the driving cycle:

- Calculate operating point for vehicle (speed and acceleration) from driving cycle. Acceleration is found as slope of $v(t)$ curve. Other quantities, such as road slope, also needs to be identified;
- Select gear (and clutch state, tyre spin, friction brake state, etc) to obtain this operating point. Select also friction brake, especially for operating points which can be reached using only friction brake. If the vehicle has an energy buffer, regenerative braking is also an option;
- Calculate required actuation from propulsion system on the driven wheel, i.e. rotational speed and shaft torque;
- Calculate backwards through propulsion system, from wheel to prime motor. It gives the operating point for prime mover (rotational speed and torque);
- Read prime mover consumption [in kg/s or $W=J/s$, not specific consumption, not efficiency] from prime mover consumption map;
- Sum up consumption [in kg or J] with earlier time steps, e.g. using the Euler forward integration method:
 $AccumulatedConsumption = AccumulatedConsumption + Consumption * TimeStepLength;$

end;

[3.15]

The final accumulated consumption [in kg or J] is often divided by the total covered distance in the driving cycle, which gives a value in kg/km or J/km. If the fuel is liquid, it is also convenient to divide by fuel density, to give a value in litre/(100*km). It can also be seen as a value in m^2 , which is the area of the “fuel pipe” which the vehicle “consumes” on the way.

We should note that the calculation scheme in Equation [3.15] does not always guarantee a solution. An obvious example is if the driving cycle prescribes such high accelerations at such high speeds that the propulsion system is not enough, i.e. we end up outside maximum torque curve in engine diagram. This is often the case with “inverse dynamic” analysis, i.e. when acceleration of inertial bodies is prescribed and the required force is calculated. An alternative is to do a (fully) dynamic analysis, which means that a driver model calculates the pedals in order to follow the driving cycle speed as closely as possible, but not exactly. Inverse dynamic analysis is more computational efficient, but limits what can phenomena that can be modelled in the propulsion and brake system. Inverse dynamics and dynamic simulations are sometimes referred to as backward and forward analysis, respectively; see Reference (Wipke, o.a., 1999).

For hybrid vehicles with energy buffers the same driving cycle can be performed but with quite different level of energy in the buffer after completing the driving cycle. Also, the level when starting the driving cycle can be different. This can make it unfair to compare energy efficiency only by looking at fuel consumption in kg/km or litre/km.

If the driving event is given in some other way than a driving cycle, see Section 3.3.2, the prediction method have to be somewhat different.

Driving cycles are used for legislation and rating for passenger cars. For commercial vehicles, the legislation is done for the engine alone, and not for the whole vehicle.

3.3.6 Emissions *

Function definition: As Energy consumption, but amount of certain substance instead of amount of energy.

There are emission maps where different emission substances (NO_x, HC, etc) per time or per produced energy can be read out for a given speed and torque. This is conceptually the same as reading out specific fuel consumption or efficiency from maps like in Figure 3-20 and Figure 3-21. A resulting value can be found in mass of the emitted substance per driven distance.

Noise is also sometimes referred to as emissions. It is not relevant to integrate noise over the time for the driving cycle, but maximum or mean values can have relevance. Noise emissions are very peripheral to vehicle dynamics.

3.3.7 Tyre wear *

*Function definition: **Tyre wear** is the worn out tyre tread depth on a vehicle per performed transportation amount. Transportation amount can be measured as for Energy consumption. Tyre wear as a vehicle function has to consider all tyres on the vehicle, e.g. as maximum over the wheels (assuming that all tyres are changed when one is worn out) or average (assuming that single tyres are exchanged when worn out).*

There are models for tyre wear (e.g. outputting “worn tread depth per time”), see Equation [2.37]. For a certain driving cycle we can integrate the *WearRate* [in mass/s or mm tread depth/s], over time similar to energy consumption rate, which becomes worn material [in mass or mm tread depth]. The wear rate per wheel is a function of the total slip, so it can include both longitudinal slip (propulsion and brake) and lateral slip (from cornering and toe angles).

Generally, the worn material will be different for different axles, or wheels, so a tyre change strategy might be necessary to assume to transform the worn material on several axles into one cost. The cost will depend on whether one renews all tyres on the vehicle at once or if one change per axle. The tyre wear is a cost which typically sums up with energy cost and cost of transport time (e.g. driver salary, for commercial vehicles).

3.3.8 Range *

*Function definition: **Range** [km] is the inverted value of Energy consumption [kg/km, litre/km or J/km], and multiplied with fuel tank size [kg or litre] or energy storage size [J].*

The range is how far the vehicle can be driven without refilling the energy storage, i.e. filling up fuel tank or charging the batteries from the grid. This is in principle dependent on how the vehicle is used, so the driving cycle influences the range. In principle, the same prediction method as for energy consumption and substance emissions can be used. In the case of predicting range, you have to integrate speed to distance, so that you in will know the travelled distance.

3.3.9 Acceleration reserve *

*Function definition: **Acceleration reserve** is the additional acceleration the vehicle will achieve within a certain time (typically 0.1..1 s) without manual gear-shifting by pressing accelerator pedal fully, when driving in a certain speed on level ground without head-wind. For vehicles with automatic transmissions or CVTs the certain time set can allow automatic gear-shift (or ratio-change) or not. The reserve can also be measured in propulsion force.*

In general terms, the lowest consumption is found in high gears. However, the vehicle will then tend to have a very small reserve in acceleration. It will, in practice, make the vehicle less comfortable and

less safe to drive in real traffic, because one will have to change to a lower gear to achieve a certain higher acceleration. The gear shift gives a time delay. Figure 3-22 shows one way of defining a momentary acceleration reserve. The reserve becomes generally larger the lower gear one selects.

A characteristic of electric propulsion systems is that an electric motor can be run at higher torque for a short time than stationary, see Figure 3-2. On the other hand, the stationary acceleration reserve is less gear dependent, since an electric motor can work at certain power levels in large portions of its operating range.

One can calculate the acceleration reserve at each time instant over a driving cycle. However, integration of acceleration reserve, as we did with fuel, emissions and wear, makes less sense. Instead, a mean value of acceleration reserve tells something about the vehicle's driveability. Minimum or maximum values can also be useful measures.

Acceleration reserve was above described as limited by gear shift strategy. Other factors can be limiting, such as energy buffer state of charge for parallel hybrid vehicles or how much overload an electric machine can take short term, see right part of Figure 3-22.

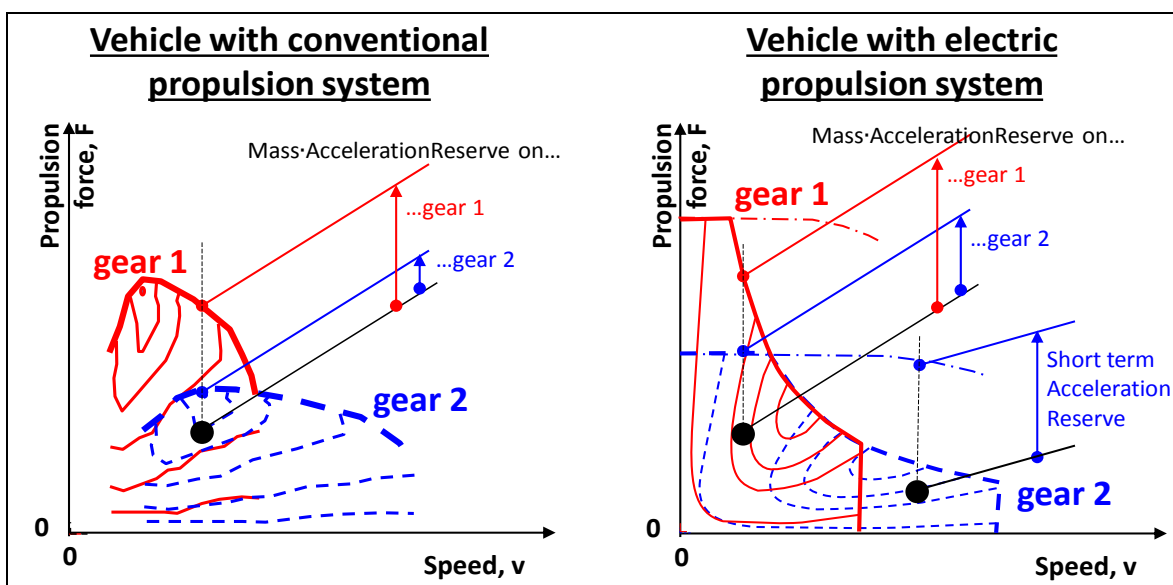


Figure 3-22: Acceleration reserves for different gears. Large dots mark assumed operating points, each with its acceleration reserve shown.

3.3.10 Load Transfer, without delays from suspension

It is useful to understand longitudinal load transfer because unloading one axle often limits the traction and braking. This is because the propulsion and brake systems are normally designed such that axle torques cannot always be ideally distributed. We start with the free-body diagram in Figure 3-23, which includes acceleration, a_x .

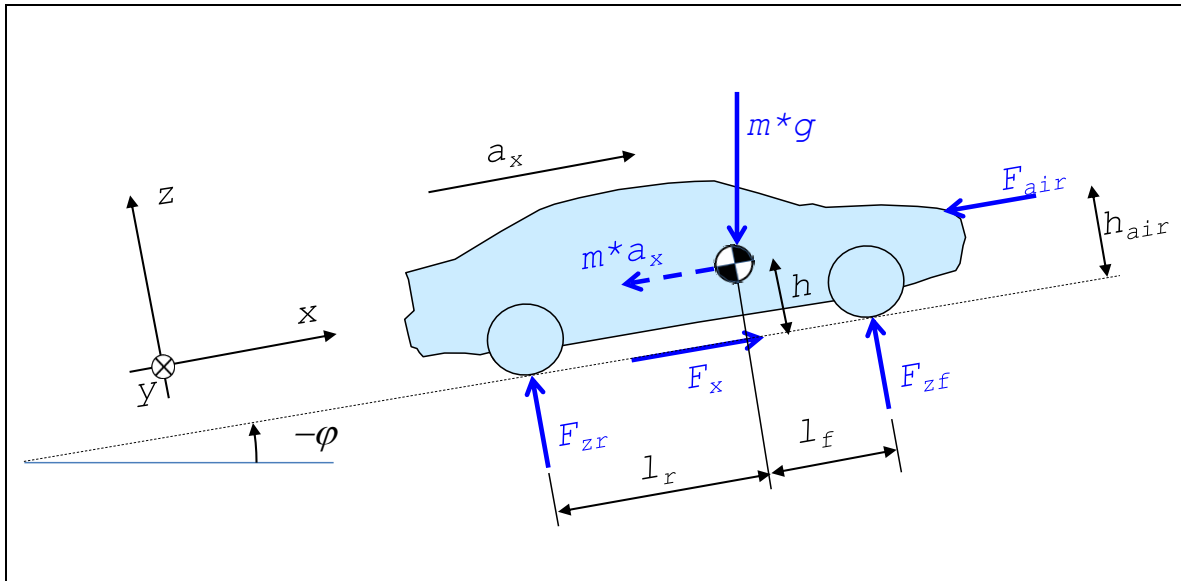


Figure 3-23: Free Body Diagram for accelerating vehicle. (Rolling resistance included in F_x .)

Note that the free-body diagram and the following derivation is very similar to the derivation of Equation [3.8], but we now include the fictive force $m \cdot a_x$.

Moment equilibrium, around rear contact with ground:

$$F_{zf} \cdot (l_f + l_r) - m \cdot g \cdot (l_r \cdot \cos(-\varphi) - h \cdot \sin(-\varphi)) + F_{air} \cdot h_{air} + m \cdot a_x \cdot h = 0 \Rightarrow$$

$$\Rightarrow F_{zf} = m \cdot \left(g \cdot \frac{l_r \cdot \cos(\varphi) + h \cdot \sin(\varphi)}{l_f + l_r} - a_x \cdot \frac{h}{l_f + l_r} \right) - F_{air} \cdot \frac{h_{air}}{l_f + l_r}$$

[3.16]

Moment equilibrium, around front contact with ground:

$$-F_{zr} \cdot (l_f + l_r) + m \cdot g \cdot (l_f \cdot \cos(-\varphi) + h \cdot \sin(-\varphi)) + F_{air} \cdot h_{air} + m \cdot a_x \cdot h = 0 \Rightarrow$$

$$\Rightarrow F_{zr} = m \cdot \left(g \cdot \frac{l_f \cdot \cos(\varphi) - h \cdot \sin(\varphi)}{l_f + l_r} + a_x \cdot \frac{h}{l_f + l_r} \right) + F_{air} \cdot \frac{h_{air}}{l_f + l_r}$$

These equations confirm what we know from experience, the front axle is off-loaded under acceleration with the load shifting to the rear axle. The opposite occurs under braking.

The load shift has an effect on the tyre's grip. If one considers the combined slip conditions of the tyre (presented in Chapter 2), a locked braking wheel limits the amount of lateral tyre forces. The same is true for a spinning wheel. This is an important problem for braking as the rear wheels become off-loaded. This can cause locking of the rear wheels if the brake pressures are not adjusted appropriately.

Consider the different conditions for a vehicle where either the front axle or rear axle is locked.

Figure 3-24 shows the vehicle response of the vehicle with a small disturbance and one locked axle.

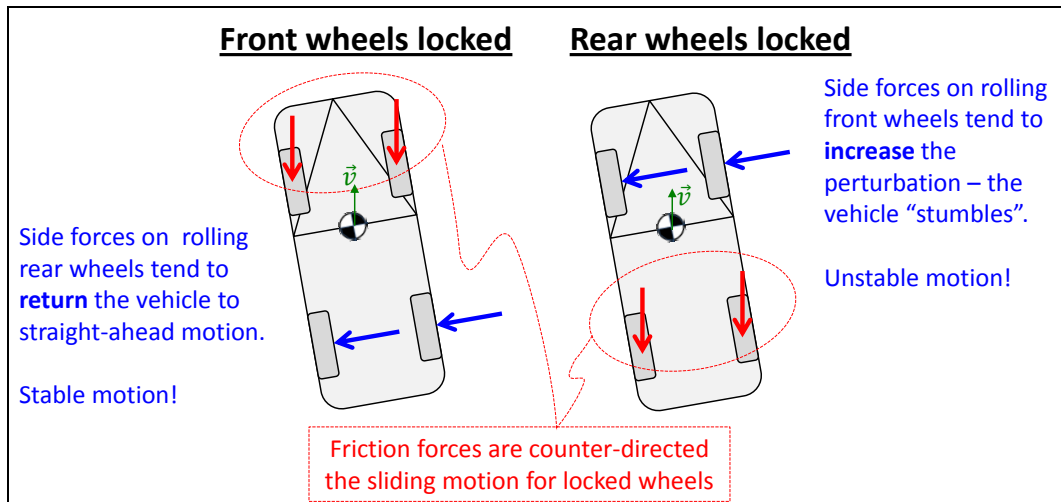


Figure 3-24: Locked Axle Braking. Same reasoning works for acceleration, if replacing “locked” with “large longitudinal tyre slip”.

Thus:

- A vehicle with **locked front** wheels will have a **stable** straight-ahead motion. However, steering ability is lost.
- A vehicle with **locked rear** wheels will be **unstable**. It turns around and ends up in stable sliding, i.e. with the rear first.

Usually, it is preferred that the front wheels lock first. But it is of course also important that both axles are used as much as possible during braking, to improve braking efficiency. Hence, there are trade-offs when designing the brake torque distribution.

3.3.11 Acceleration – simple analysis

3.3.11.1 Acceleration performance *

*Function definition: **Acceleration performance** is the time needed to, with fully applied accelerator pedal, increase speed from a certain speed to another certain higher speed, at certain road friction on level ground without head-wind and certain load.*

Acceleration events will be considered in Section 3.4, as being shorter events, where more dynamic aspects become important. If we are only interested in an approximate analysis of acceleration performance, and typically over a longer acceleration (0-100 km/h over 5..10 s), we can do a simpler analysis.

3.3.11.2 Solution using integration over time

A front-wheel-drive passenger car with a stepped gearbox should accelerate from 0 to 100 km/h. A Matlab code is given in Equation [3.17], which simulates the acceleration uphill from stand-still, using simple numerical integration. The code calculates the possible acceleration in each of the gears, and one mode with slipping clutch. In each time step it selects that which gives the highest acceleration. The numerical data and results are not given in the code, but some diagrams are shown in Figure 3-25. The code is not fully documented, only using equations so far presented in this compendium.

LONGITUDINAL DYNAMIC

```

dt=0.1; t_vec=[0:dt:10]; vx_vec(1)=0;
for i=1:length(t_vec)
    vx=vx_vec(i);
    Fres=m*g*sin(p)+froll*m*g*cos(p)+0.5*roh*A*cd*vx*vx;

    %if gear 1 (clutch engaged)
    ratio=ratios(1);
    we=vx*ratio/radius;
    Te=interpl(Engine_w,Engine_T,we);
    Fx=Te*ratio/radius;
    ax=(Fx-Fres)/(m+(Jw+Je*(ratio^2))/(radius^2));
    Fzf=m*(g*lr/(lf+lr)-ax*h/(lf+lr));
    if Fx>mu*Fzf
        Fx=mu*Fzf;
        ax=(Fx-Fres)/m;
    end
    ax1=ax;

    %if gear 2 (clutch engaged)
    ratio=ratios(2);
    ... then similar as for gear 1
    ax2=ax;

    %if gear 3 (clutch engaged)
    ratio=ratios(3);
    ... then similar as for gears 1 and 2
    ax3=ax;

    %if clutch slipping on gear 2
    ratio=ratios(2);
    wc=vx*ratio/radius; %speed of output side of clutch
    Te=max(Engine_T);
    we=Engine_w(find(Engine_T>=Te)); %engine runs on speed where max
torque
    Fx=Te*ratio/radius;
    ax=(Fx-Fres)/(m+Jw/(radius^2));
    Fzf=m*(g*lr/(lf+lr)-ax*h/(lf+lr));
    if Fx>mu*Fzf
        Fx=mu*Fzf;
        ax=(Fx-Fres)/m;
    end
    if wc>we %if vehicle side (wc) runs too fast, we cannot slip on
clutch
        ax=-inf;
    end
    ax0=ax;

    [ax,gear_vec(i)]=max([ax0,ax1,ax2,ax3]);
    vx_vec(i+1)=vx+ax*dt;
end

```

[3.17]

Phenomena that are missing in this model example are:

- Gear shifts are assumed to take place instantly, without any duration
- The option to use slipping clutch on 1st and 3rd gear is not included in model
- The tyre slip is only considered as a limitation at a strict force level, but the partial slip is not considered. The code line “we=vx*ratio/radius;” is hence not fully correct. Including the slip, the engine would run at somewhat higher speeds, leading to that it would lose its torque earlier, leading to worse acceleration performance. The calculation scheme in Equation [3.17] would be much less explicit.
- Load transfer is assumed to take place instantly quick; Suspension effects as described in Section 3.3 are not included.

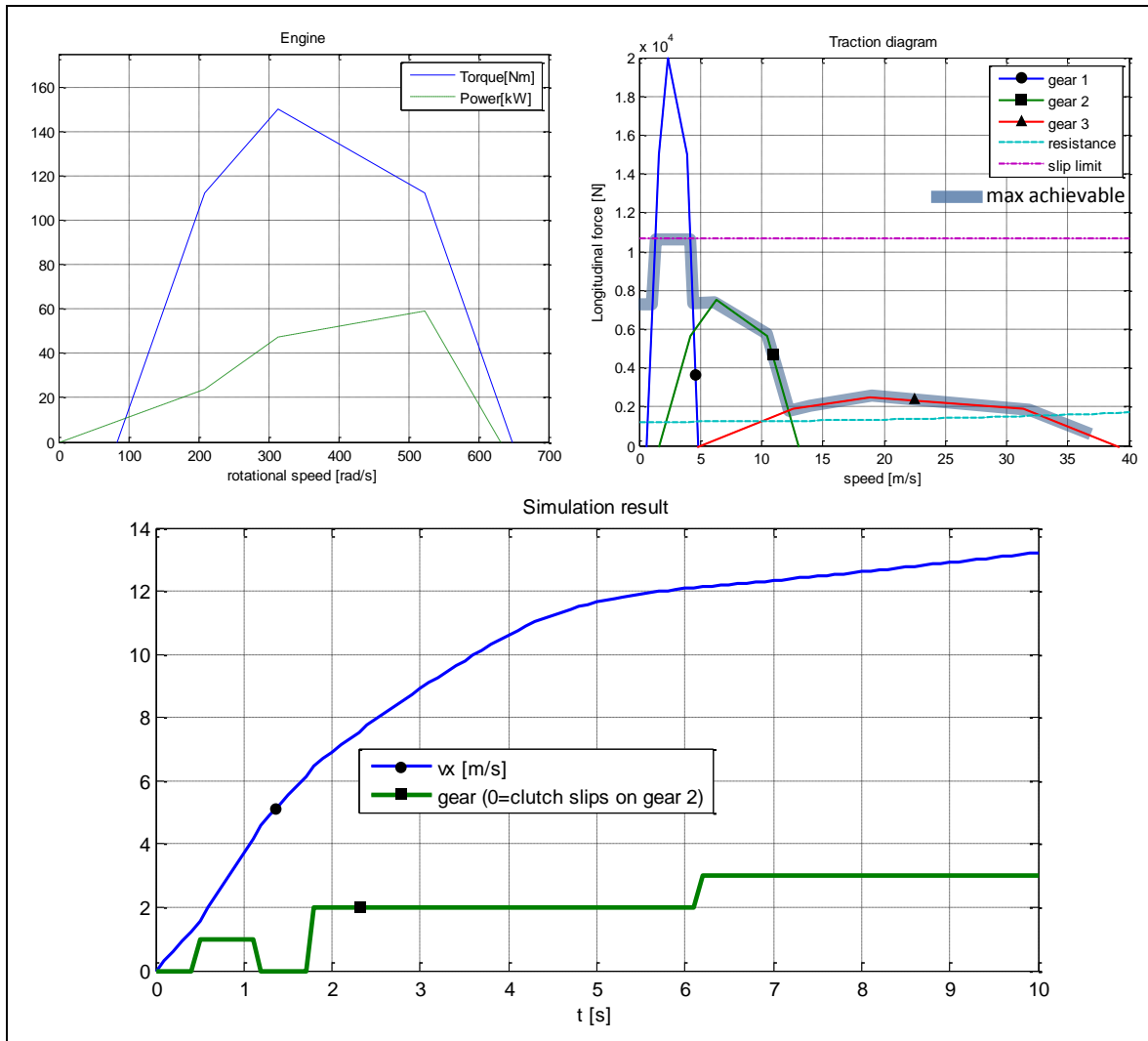


Figure 3-25: Example of simulation of acceleration, using the code in Equation [3.17].

3.3.11.3 Solution using integration over speed

An alternative way to calculate how speed varies with time is to separate the differential equation as follows:

$$\begin{aligned}
 m \cdot a &= m \cdot \frac{dv}{dt} = F(v) - F_{res}(v); \Rightarrow \\
 \Rightarrow \frac{m \cdot dv}{F(v) - F_{res}(v)} &= dt \Rightarrow \int_0^v \frac{m \cdot dv}{F(v) - F_{res}(v)} = \int_0^t dt \Rightarrow t = \int_0^v \frac{m \cdot dv}{F(v) - F_{res}(v)};
 \end{aligned}
 \tag{3.18}$$

Now, the time is calculated by means of integration over speed, as opposed to integration over time. If simple mathematic functions are used to describe $F(v)$ and $F_{res}(v)$ the solution can potentially be mathematically explicit, but the previous integration over time is more general and works for more advanced models.

3.4 Functions in shorter events

This section targets models and methods to define and predict functions in a certain and shorter time frame, typically 0.5 to 5 seconds. It can be both acceleration and deceleration. (Friction) Brake

system and phenomena as load transfer then becomes important, why these are presented early. But first, some typical driving manoeuvres are presented.

3.4.1 Typical test manoeuvres

When applying the longitudinal actuator systems (propulsion system and brake system) there are a couple of different situations which are typical to consider:

- Straight line maximum braking from, typically 100 km/h to stand-still for passenger cars.
- Braking in curve with significant lateral acceleration, see References (ISO, 2006) and (ISO, 2011).
- Straight line acceleration, typically 0 to 100 km/h and 80-100 km/h.
- Accelerating in curve with significant lateral acceleration.

For these four main situations, one can also vary other, typically:

- At high road friction and at low friction, often called “hi-mu” and “lo-mu”
- At different road friction left and right, often called “split-mu”
- At sudden changes in road friction, called “step-mu”
- At high speed, typically 200 km/h, for checking stability
- At different up-hill/down-hill gradients
- At different road banking (slope left to right)

Braking of heavy trucks is special in that their load varies a lot and that they often have towed units. Depending on brake distribution between the units, the longitudinal forces in the couplings may push or pull. When braking in a curve, this also leads to an extra influence on the lateral dynamics.

A braked wheel or axle develops a longitudinal force, F_x , counter-acting the rotation of the wheel. F_x is limited by the road friction: $|F_x|_{max} = \mu \cdot F_z$. (NOTE: $|F_x|_{max}$ is **not** $\mu \cdot F_z - f_r \cdot F_z$, see Figure 2-10.)

Braking coefficient = $-F_x/F_z$, is a property defined for an axle (or a single wheel) = brake force/normal load. It can be seen as the utilized friction coefficient. A suitable notation can be μ_{util} . The coefficient should not be mixed up with friction coefficient, μ ; the relation between them is $\mu_{util} \leq \mu$.

3.4.2 Deceleration performance

There are some different functions that measures braking performance or deceleration performance.

3.4.2.1 Braking efficiency *

*Function definition: **Braking Efficiency** is the ratio of vehicle deceleration and the best brake-utilized axle (or wheel), while a certain application level of the brake pedal at a certain speed straight ahead, at certain road friction on level ground without head-wind and certain load at a certain position in the vehicle.*

In equation form, the Braking Efficiency becomes = $\frac{-a_x/g}{\max_{\text{axles}} \mu_{util}}$; If Braking Efficiency=1=100%, the distribution of braking is optimal.

3.4.2.2 Braking Distance *

*Function definition: **Braking Distance** is the distance travelled during braking with fully applied brake pedal from a certain speed straight ahead to another certain lower speed, at certain road friction on level ground without head-wind and certain load at a certain position in the vehicle.*

For passenger cars one typically brakes fully from 100 km/h and then the braking distance is typically around 40 m (average deceleration 9.65 m/s^2). For a truck it is typically longer, 51..55 m ($7.5..7 \text{ m/s}^2$).

3.4.2.3 Stopping Distance *

*Function definition: **Stopping Distance** is the distance travelled from that an obstacle becomes visible to driver have taken the vehicle to stand-still. Certain conditions, as for Braking Distance, have to be specified, but also a certain traffic scenario and a certain driver to be well defined.*

Stopping Distance is the braking distance + the “thinking/reaction distance”, which depends on the speed and the reaction time. The reaction time of a driver is typically 0.5..2 seconds.

3.4.3 (Friction) Brake system

Generally speaking, there are several systems that can brake a vehicle:

- Service brake system (brake pedal and ABS/ESC controller, which together applies brake pads to brake discs/drums)
- Parking brake (lever/button that applied brake pads to brake discs/drums, normally on rear axle)
- Engine braking (ICE run at high speeds generate a negative propulsion)
- Electric machines (machines can be used symmetrical, i.e. both for positive and negative torques)
- Retarders, or auxiliary brakes, for heavy vehicles
- Large steering angles will actually decelerate the vehicle

This section is about Friction brakes, meaning Service brakes and Parking brake. In vehicle dynamics perspective these have the following special characteristics:

- In practice, Friction brakes are unlimited in force since they can lock the wheels for most driving situations and road friction (ICE and electric motors are often limited by their maximum power, since it is often smaller than available road friction.)
- Friction brakes can only give torque in opposite direction to wheel rotation. (Electric motors can brake so much that wheel spins rearwards.)
- Friction brakes can hold the vehicle at exact standstill. (If using electric machines for holding stand-still in a slope, a closed loop control would be necessary, resulting in that vehicle “floats” a little.)

The basic design of a passenger car brake system is a hydraulic system is show in Figure 3-26. Here, the brake pedal pushes a piston, which causes a hydraulic pressure (pressure = pedal force/piston area), The hydraulic pressure is then connected to brake callipers at each wheel, so that a piston at each wheel pushes a brake pad towards a brake disc (disc force = pressure * piston area). The brake torque on each wheel is then simply: torque = number of friction surfaces * disc coefficient of friction * disc force * disc radius. (Normally, there are 2 friction surfaces, since double-acting brake callipers.) By selecting different piston area and disc radii at front and rear, there is a basic hydro mechanical brake distribution ratio between front and rear axle. There is normally two circuits for redundancy.

Brake systems for heavy trucks are generally based on pneumatics, as opposed to hydraulics.

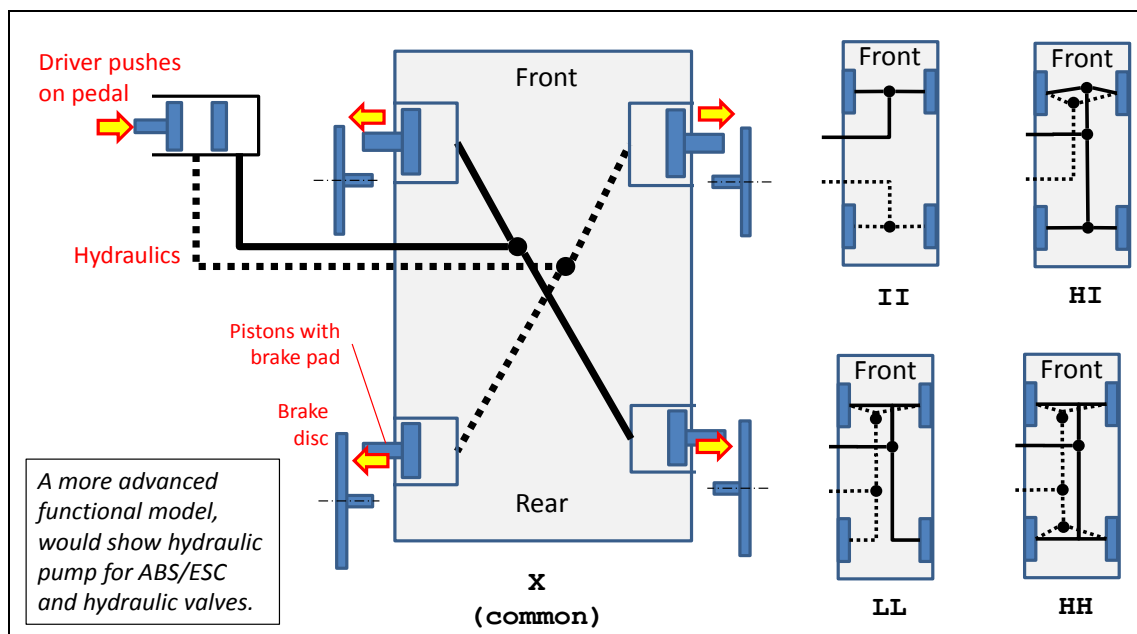


Figure 3-26: Principles for a hydraulic brake system, which is conventional on passenger cars.

3.4.4 Pedal Response *

Function definition: Accelerator pedal response is how vehicle acceleration varies with accelerator pedal position, for a certain vehicle speed and possibly certain gear, on level ground without pressing the brake pedal.

Function definition: Brake pedal response is how vehicle deceleration varies with brake pedal force, for a certain vehicle speed, on level ground without pressing the accelerator pedal.

These functions, together with the functions in Section 3.4.5, enable the driver to operate the vehicle longitudinally with precision and in an intuitive and consequent way. The requirements based on above function definitions, are typically that the translation of pedal position (or force) to vehicle acceleration (or deceleration) should be consistent, progressive and oscillation-free.

For accelerator pedal steps, there should be enough acceleration, but also absence of “shunt and shuffle” (driveline oscillations). When accelerator pedal is suddenly lifted off, there shall be certain deceleration levels, depending on vehicle speed and gear selected.

3.4.5 Pedal Feel *

Function definition: Accelerator pedal feel is the pedal’s force response to pedal position.

Function definition: Brake pedal feel is the pedal’s position response to pedal force.

These functions, together with the functions in Section 3.4.4, enable the driver to operate the vehicle longitudinally with precision and in an intuitive and consequent way.

3.4.6 Brake proportioning

The basic function of a brake system is that brake pressure (hydraulic on passenger cars and pneumatic on trucks) is activated so that it applies brake pads towards brake discs or drums. In a first approximation, the pressure is distributed with a certain fraction on each axle. For passenger cars this is typically 60..70% front and the remaining rear, where percentage is calculated in axle torque.

If neglecting air resistance and slope in Equation [3.16], the vertical axle loads can be calculated as function of deceleration (=ax). An ideal brake distribution would be if each axle always utilize same fraction of friction: $F_{fx}/F_{fz} = F_{rx}/F_{rz}$. This requirement gives the optimal F_{fx} and F_{rx} as:

$$\frac{F_{fx}}{\mu \cdot F_{fz}} = \frac{F_{rx}}{\mu \cdot F_{rz}} \Rightarrow \frac{F_{fx}}{F_{rx}} = \frac{F_{fz}}{F_{rz}} \Rightarrow \frac{F_{fx}}{F_{rx}} = \frac{m \cdot \left(g \cdot \frac{l_r}{l_f + l_r} - a_x \cdot \frac{h}{l_f + l_r} \right)}{m \cdot \left(g \cdot \frac{l_f}{l_f + l_r} + a_x \cdot \frac{h}{l_f + l_r} \right)} = \frac{g \cdot l_r - a_x \cdot h}{g \cdot l_f + a_x \cdot h};$$

$$F_{fx} + F_{rx} = m \cdot a_x;$$

$$\Rightarrow F_{fx} = m \cdot a_x \cdot \frac{g \cdot l_r - a_x \cdot h}{g \cdot (l_f + l_r)}; \quad \text{and} \quad F_{rx} = m \cdot a_x \cdot \frac{g \cdot l_f + a_x \cdot h}{g \cdot (l_f + l_r)};$$

[3.19]

Equation [3.19] is plotted for some variation in centre of gravity height and longitudinal position in Figure 3-27.

The proportioning is done by selecting pressure areas for brake callipers, so the base proportioning will be a straight line, marked as “Hydrostatic brake proportioning”. For passenger cars, one typically designs this so that front axle locks first for friction below 0.8 for lightest vehicle load and worst variant. For heavier braking than 0.8*g, or higher (or front-biased) centre of gravity, rear axle will lock first, if only designing with hydrostatic proportioning..

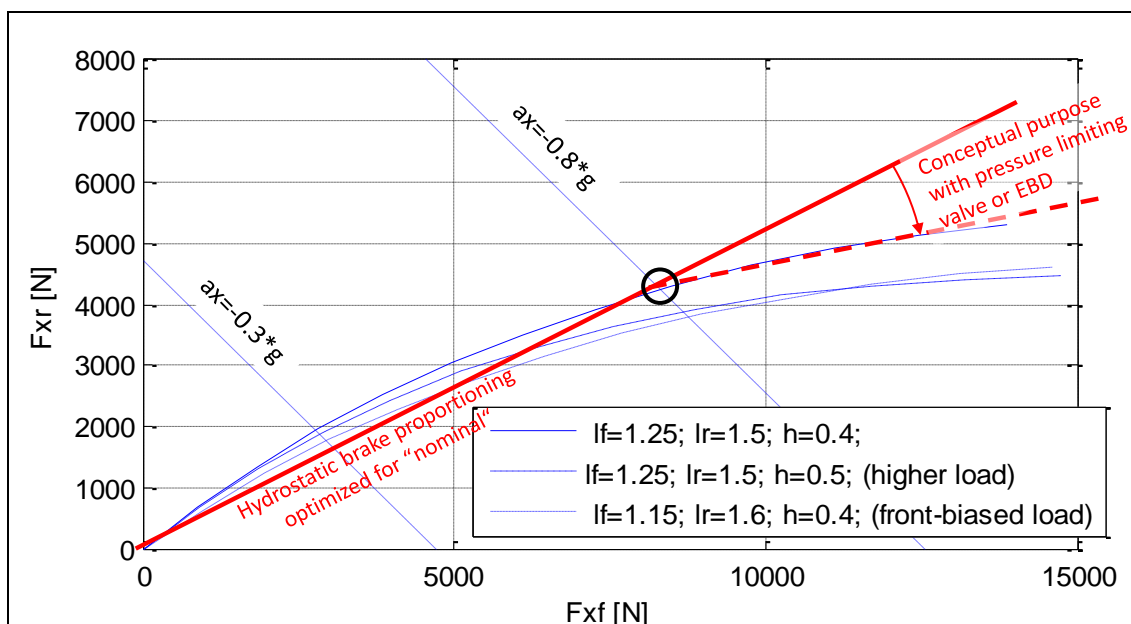


Figure 3-27: Brake Proportioning diagram. The curved curves mark optimal distribution for some variation in position of centre of gravity.

To avoid rear axle lock up, one restricts the brake pressure to the rear axle. This is done by pressure limiting valve, brake pads with pressure dependent friction coefficient or Electronic Brake Distribution (EBD). In principle, it bends down the straight line as shown in Figure 3-27. With pressure dependent values one gets a piece-wise linear curve, while pressure dependent friction coefficient gives a continuously curved curve. EBD is an active control using same mechatronic actuation as ABS. EBD is the design used in today’s passenger cars, since it comes with ABS, which is now a legal requirement on most markets.

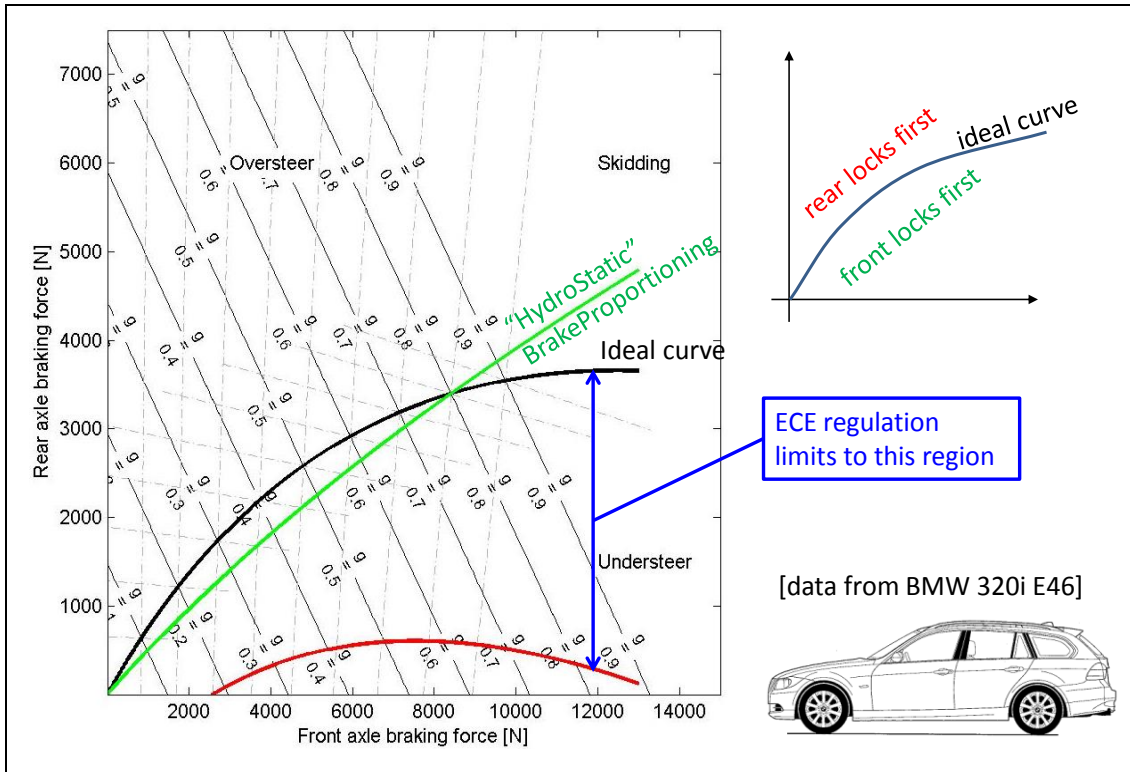


Figure 3-28: Brake Proportioning. From (Boerboom, 2012).

3.4.7 Body heave and pitch due to longitudinal wheel forces

Additional to that the axle vertical loads change due to acceleration a_x , there are also change in displacement (heave and pitch). In the following section, a model assuming “quasi-steady state” will be derived, see Figure 3-29. This assumption means that the accelerations and speeds are constant, except for in longitudinal direction. The model is approximately valid for heave and pitch during such a constant braking and acceleration. The model differs between the “unsprung mass” (wheels and the part of the suspension that does not heave) and the “sprung mass” or “body” (parts that heaves and pitches as one rigid body).

It is especially noted that the model in Figure 3-29 models the suspension in a very trivial way; purely vertical. It can be seen as a very trivial (suspension) linkage. The model will be further developed in Section 3.4.8, to model linkage in the suspension better, which allows validity for transients braking and acceleration. It will also generally improve the validity also for quasi-steady state acceleration or braking.

There is no damping included in model, because their forces would be zero, since there is no displacement velocity, due to the “quasi-steady-state” assumption. As constitutive equations for the compliances (springs) we assume that displacements are measured from a static conditions and that the compliances are linear. The road is assumed to be smooth, i.e. $z_{fr} = z_{rr} = 0$.

$$F_{zf} = F_{zf0} + c_f \cdot (z_{\overline{ff}} - z_f) \quad \text{and} \quad F_{zr} = F_{zr0} + c_r \cdot (z_{\overline{ff}} - z_r)$$

where $F_{zf0} + F_{zr0} = m \cdot g$ and $F_{zf0} \cdot l_f - F_{zr0} \cdot l_r = 0$

[3.20]

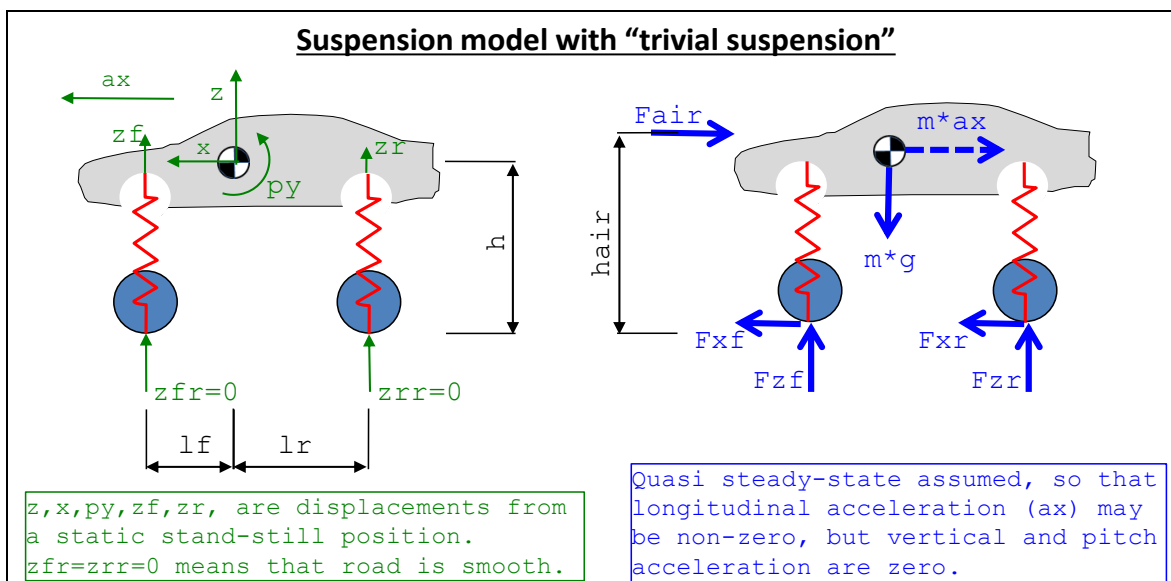


Figure 3-29: Model for quasi-steady state heave and pitch due to longitudinal accelerations.

Suspension design is briefly discussed at these places in this compendium: Section 3.4.7, Section 4.3.9.5 and Section 5.2.

The stiffnesses c_f and c_r are the effective stiffnesses at each axle. The physical spring may have another stiffness, but its effect is captured in the effective stiffness. An example of different physical and effective stiffness is given in Figure 3-30. Note that the factor $(a/b)^2$ is not the only difference between effective and physical stiffness, but the effective can also include compliance from other parts than just the spring, such as bushings and tyre. A common alternative name for the effective stiffness is axle rate, or wheel (spring) rate if measured per wheel. There will also be a need for a corresponding effective damping coefficient, see Section 3.4.8.2, or wheel (damping) rate.

We see already in free-body diagram that F_{xf} and F_{xr} always act together, so we rename $F_{xf} + F_{xr} = F_{xw}$, where w refers to wheel. This and equilibrium give:

$$\begin{aligned} -F_{air} - m \cdot a_x + F_{xw} &= 0; \\ m \cdot g - F_{zf} - F_{zr} &= 0; \\ F_{zr} \cdot l_r - F_{zf} \cdot l_f - F_{xw} \cdot h - F_{air} \cdot (h_{air} - h) &= 0; \end{aligned} \quad [3.21]$$

Compatibility, to introduce body displacements, z and p_y , gives:

$$z_f = z - l_f \cdot p_y; \quad \text{and} \quad z_r = z + l_r \cdot p_y; \quad [3.22]$$

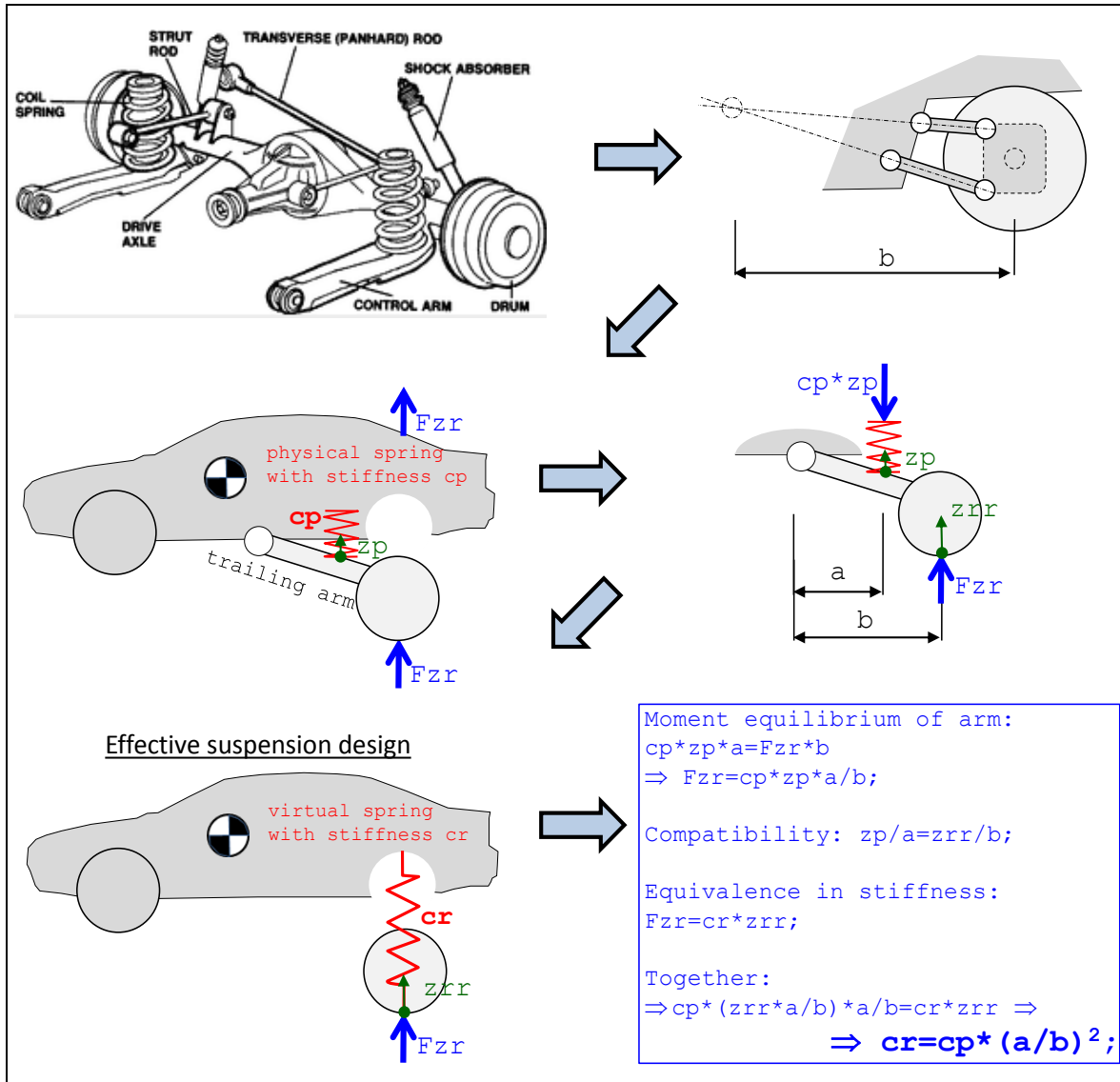


Figure 3-30: From physical suspension design to effective stiffness. Upper left: From http://www.procarcare.com/icarumba/resourcecenter/encyclopedia/icar_resourcecenter_encyclopedia_suspsteer3.asp.

Combining constitutive relations, equilibrium, compatibility and renaming $F_{xf} + F_{xr} = F_{xw}$, where w refers to wheel), gives, as Matlab script:

```
clear, syms zf zr Fzf Fzr Fzf0 Fzr0 ax z py
sol=solve( ...
    'Fzf=Fzf0-cf*zf', ...
    'Fzr=Fzr0-cr*zr', ...
    'Fzf0+Fzr0=m*g', ...
    'Fzf0*lf-Fzr0*lr=0', ...
    '-Fair-m*ax+Fxw=0', ...
    'm*g-Fzf-Fzr=0', ...
    'Fzr*lr-Fzf*lf-Fxw*h-Fair*(hair-h)=0', ...
    'zf=z-lf*py', ...
    'zr=z+lr*py', ...
    zf, zr, Fzf, Fzr, Fzf0, Fzr0, ax, z, py);
```

[3.23]

The solution from Matlab script in Equation [3.23] becomes:

$$\begin{aligned}
 a_x &= \frac{F_{xw} - F_{air}}{m}; \\
 z &= -\frac{c_f \cdot l_f - c_r \cdot l_r}{c_f \cdot c_r \cdot (l_f + l_r)^2} \cdot (F_{xw} \cdot h + F_{air} \cdot (h_{air} - h)) \\
 p_y &= -\frac{c_f + c_r}{c_f \cdot c_r \cdot (l_f + l_r)^2} \cdot (F_{xw} \cdot h + F_{air} \cdot (h_{air} - h))
 \end{aligned}
 \tag{3.24}$$

In agreement with intuition and experience the body dives (positive pitch) when braking (negative F_{xw}). Further, the body centre of gravity is lowered (negative z) when braking and weaker suspension front than rear ($c_f \cdot l_f < c_r \cdot l_r$), which is normally the chosen design for cars.

The air resistance force is brought into the equation. It can be noted that for a certain deceleration, there will be different heave and pitch depending on how much of the decelerating force that comes from air resistance and from longitudinal wheel forces. But, as already noted, heave and pitch does not depend on how wheel longitudinal force is distributed between the axles.

3.4.8 Load Transfer including suspension linkage effects

In previous model of load transfer, see Section 3.3.10, we assumed nothing about the transients of transfer (vertical wheel) loads between front and rear axle. So, if we study longer events when the wheel force is applied and then kept constant for a longer time (1-5 s), it is often a good enough model. But if the wheel forces vary more, we need to capture the transients better. Then it is important to consider that the linkage can transfer some of the wheel longitudinal forces. When studying the transients, it is also relevant to consider the damping.

Another reason for doing a better model than in Section 3.3.10 can be that one is interested in the displacements, heave and pitch, which are not covered in the model in Section 3.3.10.

There are basically two modelling ways to include the suspension in the load transfer: through a pitch centre or through a pivot point for each axle, see Figure 3-31.

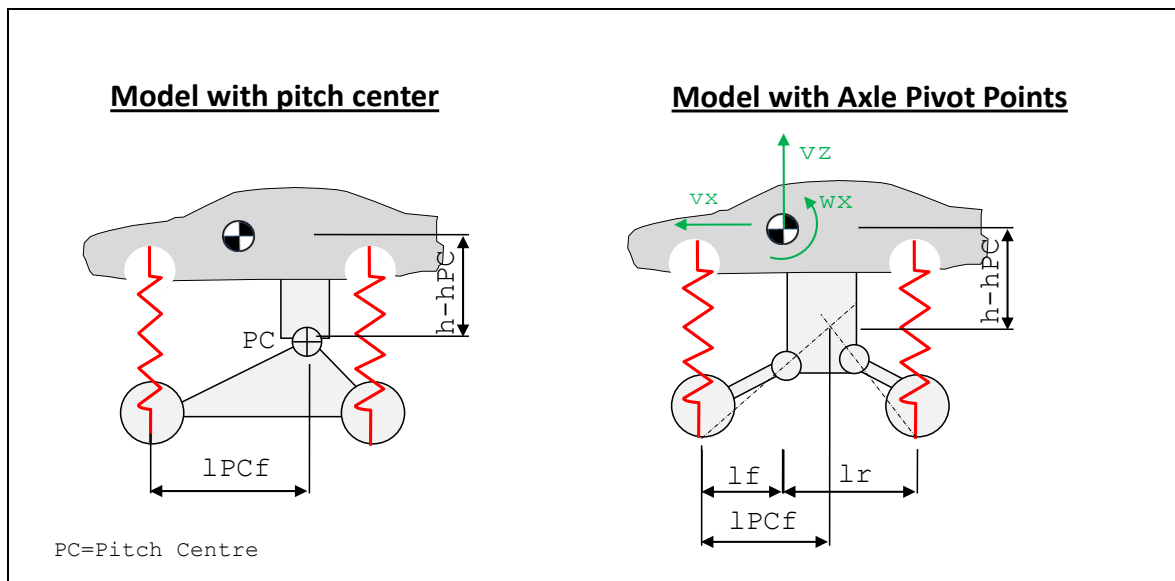


Figure 3-31: Models for including suspension effects in longitudinal load transfer

3.4.8.1 Load Transfer model with Pitch Centre

This model will not be deeply presented in this compendium. It has drawbacks in that it has only one suspended degree of freedom. Also, it does not take the distribution of longitudinal wheel forces between the axles into account. These shortcomings are not very important for studying dive and squat, but they are essential when studying rapid individual wheel torque changes in time frames of 0.1 s, such as studying ABS or traction control. So, since the model with axle pivot points is more generally useful and not much more computationally demanding (and probably more easy intuitively), that model is prioritized in this compendium.

3.4.8.2 Load Transfer model with Axle Pivot Points

Behold the free-body diagram in Figure 3-32. The road is assumed to be flat, $z_{fr} = z_{rr} \equiv 0$. In free-body diagram for the rear axle, P_{xr} and P_{zr} are reaction forces in the pivot point. F_{sr} is the force in the elasticity, i.e. where potential spring energy is stored. The torque T_{sr} is the shaft torque, i.e. from the propulsion system. No torque from friction brake is visible in this free-body diagram, since such appears as internal torque between brake pad and brake calliper, which both are within the free laid rear axle.

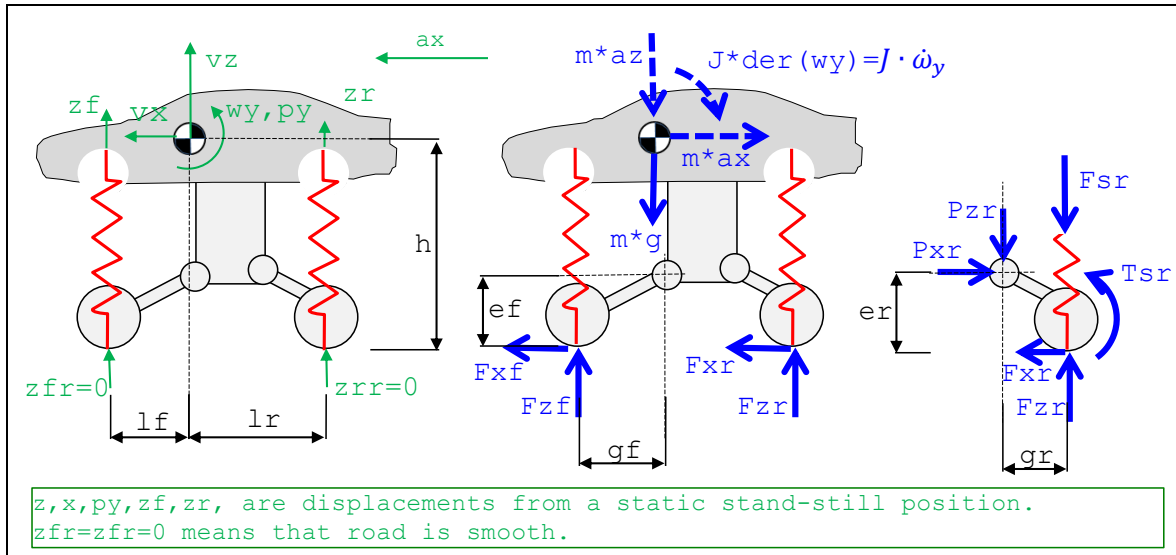


Figure 3-32: Free-body diagram for model with Axle Pivot Points

We assume that displacements are measured from the forces F_{sf0} and F_{sr0} , respectively, and that the compliances are linear. The total constitutive equations become:

$$F_{sf} = F_{sf0} + c_f \cdot (z_{ff} - z_f) \quad \text{and} \quad F_{sr} = F_{sr0} + c_r \cdot (z_{ff} - z_r) \quad [3.25]$$

Now, there are two ways of representing the dynamics in spring-mass systems: Either as second order differential equations in position or first order differential equations in velocity and force. We select the latter, because it is easier to select suitable initial values. Then we need the differentiated versions of the compliances constitutive equations:

$$\dot{F}_{sf} = 0 + c_f \cdot (\dot{z}_{ff} - \dot{z}_f) = -c_f \cdot v_{zf} \quad \text{and} \quad \dot{F}_{sr} = 0 + c_r \cdot (\dot{z}_{ff} - \dot{z}_r) = -c_r \cdot v_{zr} \quad [3.26]$$

Even if damping is not drawn in Figure 3-32, for graphical clarity, we will include it in the model. The damper forces are denoted F_{df} and F_{dr} . They will appear in the equilibrium equations quite similar to F_{sf} and F_{sr} . Note that the damping coefficients, d_f and d_r , are the effective ones, i.e. the ones

defined at the wheel contact point with ground, as opposed to the physical ones defined for the actual physical damper. C.f. effective stiffness in Section 3.4.7.

$$F_{df} = d_f \cdot (\dot{z}_{\text{eff}} - \dot{z}_f) = -d_f \cdot v_{zf} \quad \text{and} \quad F_{dr} = d_r \cdot (\dot{z}_{\text{eff}} - \dot{z}_r) = -d_r \cdot v_{zr} \quad [3.27]$$

Now, 3 equilibria for whole vehicle and one moment equilibria around pivot point for each axle gives:

$$\begin{aligned} -m \cdot \dot{v}_x + F_{xf} + F_{xr} &= 0; \\ -m \cdot \dot{v}_z - m \cdot g + F_{zf} + F_{zr} &= 0; \\ -J \cdot \dot{\omega}_y + F_{zr} \cdot l_r - F_{zf} \cdot l_f - (F_{xf} + F_{xr}) \cdot h &= 0; \\ (F_{zr} - F_{sr} - F_{dr}) \cdot g_r - F_{xr} \cdot e_r + T_{sr} &= 0; \\ (F_{sf} + F_{df} - F_{zf}) \cdot g_f - F_{xf} \cdot e_f + T_{sf} &= 0; \end{aligned} \quad [3.28]$$

Compatibility, to connect to body displacements, z and py , gives:

$$\begin{aligned} z_f &= z - l_f \cdot p_y; \quad \text{and} \quad z_r = z + l_r \cdot p_y; \\ v_{zf} &= v_z - l_f \cdot \omega_y; \quad \text{and} \quad v_{zr} = v_z + l_r \cdot \omega_y; \\ \dot{z} &= v_z; \quad \text{and} \quad \dot{p}_y = \omega_y; \end{aligned} \quad [3.29]$$

By combining constitutive relations, equilibrium and compatibility we can find explicit function so that:

$$\begin{aligned} \text{StateDerivatives} &= \text{function}(\text{States}, \text{Inputs}); \\ \text{States} &= [v_x \quad v_z \quad \omega_y \quad F_{sf} \quad F_{sr} \quad z \quad p_y]; \\ \text{StateDerivatives} &= [\dot{v}_x \quad \dot{v}_z \quad \dot{\omega}_y \quad \dot{F}_{sf} \quad \dot{F}_{sr} \quad \dot{z} \quad \dot{p}_y]; \\ \text{Inputs} &= [F_{xf} \quad F_{xr} \quad T_{sf} \quad T_{sr}]; \end{aligned} \quad [3.30]$$

Equation [3.30] can be solved with well-established methods for numerical ode solution, if *Inputs* are known as functions of time and initial values of *States* are known. Such simulation of Equation [3.30] is shown in Section 3.4.12.

3.4.8.3 Steady state heave and pitch due to longitudinal wheel forces

If we study long term quasi-steady state (all derivatives zero, except \dot{v}_x) for the model described in Section 3.4.8.2 we find a model comparable with the model in Section 3.4.7. but also correct steady state displacements, heave and pitch. For this reason we set all time derivatives equal to zero except $der(v_x) = a_x$, in Equations [3.25] to [3.29]. The reasons why we keep a_x at the “quasi-steady state” assumption, which is that longitudinal acceleration (a_x) may be non-zero, but vertical and pitch acceleration are zero. This means that damper forces are zero. We also neglect air resistance force for clarity of equations. Equation [3.25] becomes, in Matlab format:

```
clear, syms zf zr Fzf Fzr Fsf0 Fsr0 ax Fsf Fsr z py
sol=solve( ...
    'Fsf=Fsf0-cf*zf', 'Fsr=Fsr0-cr*zr', ...
    'Fsf0+Fsr0=m*g', 'Fsf0*lf-Fsr0*lr=0', ...
    '-m*ax+Fxf+Fxr=0', ...
    '-m*0-m*g+Fzf+Fzr=0', ...
    '-J*0+Fzr*lr-Fzf*lf-(Fxf+Fxr)*h=0', ...
    '(Fzr-Fsr-0)*gr-Fxr*er+Tsr=0', '(Fsf0-Fzf)*gf-Fxf*ef+Tsf=0', ...
    'zf=z-lf*py', 'zr=z+lr*py', ...
    zf, zr, Fzf, Fzr, Fsf0, Fsr0, ax, Fsf, Fsr, z, py);

%results:
% ax = (Fxf + Fxr)/m
```

```
% z = -(Tsr*cf*gf*lf^2 - Tsf*cr*gr*lr^2 + Tsr*cf*gf*lf*lr -
Tsf*cr*gr*lf*lr - Fxr*cf*er*gf*lf^2 + Fxf*cr*ef*gr*lr^2 +
Fxf*cf*gf*gr*h*lf + Fxr*cf*gf*gr*h*lf - Fxf*cr*gf*gr*h*lr -
Fxr*cr*gf*gr*h*lr - Fxr*cf*er*gf*lf*lr +
Fxf*cr*ef*gr*lf*lr)/(cf*cr*gf*gr*(lf + lr)^2)

% py = -(Tsr*cf*gf*lf + Tsr*cf*gf*lr + Tsf*cr*gr*lf + Tsf*cr*gr*lr +
Fxf*cf*gf*gr*h + Fxr*cf*gf*gr*h + Fxf*cr*gf*gr*h + Fxr*cr*gf*gr*h -
Fxr*cf*er*gf*lf - Fxf*cr*ef*gr*lf - Fxr*cf*er*gf*lr -
Fxf*cr*ef*gr*lr)/(cf*cr*gf*gr*(lf + lr)^2)
```



The solution should be compared with corresponding solution in Equation [3.24]. One can see that ax is in complete alignment between the two models. Then, a general reflection is that the displacement, z and py, in Equation [3.31] follows a complex formula, but that they are dependent on how the $F_{xw} = F_{xf} + F_{xr}$ is applied: both dependent on distribution between axles and dependent on how much of the axle forces (F_{xf} and F_{xr}) that are actuated with shaft torques (T_{sf} and T_{sr} , respectively). In Figure 3-35, dashed lines show the quasi-steady state solutions from Equation [3.24].

3.4.8.4 Examples of real suspension design

In Figure 3-32, some kind of “trailing arm” is drawn both for front and rear axle. For rear axle, that is a realistic design even if other designs are equally common. However, for front axle a so called McPherson suspension is much more common, see Figure 3-33.

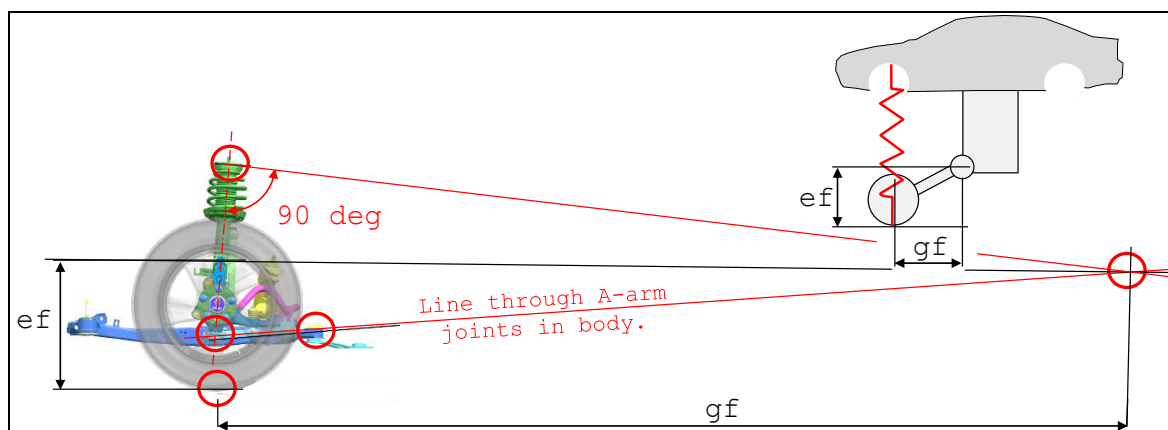


Figure 3-33: Example of typical front axle suspension, and how pivot point is found. The example shows a McPherson suspension. From Gunnar Olsson, LeanNova.

3.4.8.5 Additional phenomena

It is relevant to point out the following, which are not modelled in this compendium:

- **Stiffness and damping** may be dependent of **wheel (vertical) displacement** and **wheel steering angle**. One way of inserting this in the model is to make the coefficients varying with spring force, which is a measure of how much compressed the suspension is. Here, non-linearities within spring working range, as well as bump stops, can be modelled. Also, **position of pivot points (or pitch and roll centres)** can be dependent of wheel displacement steering angle.
- Dampers are often **deformation direction dependent**, i.e. different damping coefficients are suitable to use for compression and rebound. Typical is 2..4 times softer (smaller d [N/(m/s)]) in compression than in rebound.

3.4.9 Dive at braking *

*Function definition: **Dive at braking** is pitch angle change that the vehicle body experience when brake pedal is applied to a certain deceleration level, from driving straight ahead. Either the peak or steady state pitch angle can be addressed.*

Now, study the suspension at front axle in Figure 3-32. When the axle is braked, F_{xf} will be negative and push the axle rearwards, i.e. in under the body. The front of the vehicle will then be lifted as in pole jumping. This means that this design counter-acts the (transient) dive of the front. (Only the transient dive will be reduced, while the dive after a longer time of kept braking is dependent only on the stiffnesses according to Equation [3.24].) The design concept for front axle suspension to place the pivot point behind axle and above ground is therefore called “anti-dive”.

If the braking is applied without shaft torque T_{sf} , a good measure of the Anti-dive mechanism is e_f/g_f . This is the normal way for braking, since both the action and reaction torque acts on the axle. For in-board brakes, or braking via propulsion shaft, the reaction torque is not taken within the axle, but the reaction torque is taken by the vehicle body. The action torque T_{sf} then appears in the equilibrium equation for the axle, as shown in Equation [3.28]. If we neglect the wheel rotational dynamics for a while, we can insert $T_{sf} = F_{xf} \cdot R_w$ in the equation with T_{sf} in Equation [3.28]:

$$\begin{aligned} (F_{sf} + F_{df} - F_{zf}) \cdot g_f - F_{xf} \cdot e_f + T_{sf} &= 0; \text{ with } T_{sf} = F_{xf} \cdot R_w; \Rightarrow \\ \Rightarrow (F_{sf} + F_{df} - F_{zf}) \cdot g_f - F_{xf} \cdot e_f + F_{xf} \cdot R_w &= 0; \Rightarrow \\ \Rightarrow (F_{sf} + F_{df} - F_{zf}) \cdot g_f - F_{xf} \cdot (e_f - R_w) &= 0; \end{aligned} \quad [3.32]$$

We can then see that a good measure of the Anti-dive mechanism is $(e_f - R_w)/g_f$ instead.

3.4.10 Squat at propulsion *

*Function definition: **Squat at propulsion** is pitch angle change that the vehicle body experience when accelerator pedal is applied to a certain acceleration level, from driving straight ahead. Either the peak or steady state pitch angle can be addressed.*

Now, study the suspension at rear axle in Figure 3-32. When the axle is propelled, F_{xr} will push the axle in under the body. This means that this design reduces the rear from squatting (transiently). The design concept for rear axle suspension to place the pivot point ahead of axle and above ground is therefore called “anti-squat”.

3.4.11 Anti-dive and Anti-squat designs

With Anti-dive front and Anti-squat rear, we avoid front lowering at braking and rear lowering at acceleration, respectively. But how will the designs influence the parallel tendencies: that rear tend to lift at braking and front then to lift at propulsion? Well, they will luckily counteract also these: Braking at rear axle will stretch the rear axle rearwards and upwards relative to the body. When propelling the front axle, the propulsion force will stretch the front axle forwards and upwards relative to the body. (If one brakes at one axle and propels at the other, the reasoning is not valid. This mode may seem irrelevant, but could be desired for a hybrid vehicle with ICE on front axle and electric motor on rear axle, if one would like to charge batteries “via the road”. This is an example of that novel designs may rise new issues.)

In summary: Anti-dive and anti-squat refer to the front diving when braking and the rear squatting when acceleration. Anti-dive and anti-squat can be measured in fractions: Anti-dive for $=e_f/g_f$ or $(e_f - R_w)/g_f$ and Anti-squat= e_r/g_r or $(e_r - R_w)/g_r$. Normal values are typically 0.05..0.15.

The fractions, or percentages, can be seen as slope of lines from wheel contact to pivot points, as shown in Figure 3-34.

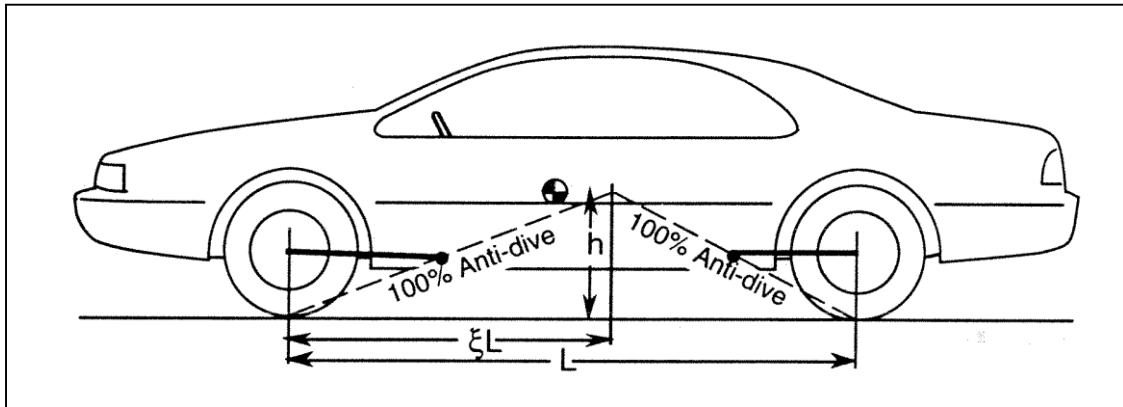


Figure 3-34: Anti-Dive Geometry, (Gillespie, 1992)

3.4.12 Deceleration performance *

Function definition: See Section 3.4.2.2.

Deceleration performance can now be predicted, including the suspension mechanisms. It is a very important function, and every decimetre counts when measuring braking distance in standard tests like braking from 100 to 0 km/h. The active control of the brake torques (ABS function) is then very important, and this is so fast dynamics that the suspension mechanisms of Anti-lift and Anti-dive influences. The position of the load in the vehicle will influence, since it influences the load transfer.

We will now set up a mathematical model, see Equation [3.33], which shows how the normal forces change during a braking event. It is based on the physical model in Figure 3-32. Driving resistance contributes normally with a large part of the deceleration, but we will neglect this for simplicity, just to show how the suspension mechanism works. The equations in the model are presented in the dynamic modelling standardized format “Modelica”, and are hence more or less identical to Equation [3.26] to [3.29].

```

Fxf = if 1 < time and time < 3 then -0.4*m*g else 0;
Fxr = if 3 < time and time < 7 then -0.4*m*g else 0;
Tsf/Rw = 0;
Tsr/Rw = if 5 < time and time < 7 then -0.4*m*g else 0;

// Motion equations:
der(z) = vz;
der(py) = wy;

// Consitutive equations for the springs:
der(Fsf) = -cf*vzf;
der(Fsr) = -cr*vzr;

// Consitutive equations for the dampers:
Fdf = -df*vzf;
Fdr = -dr*vzr;

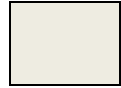
// (Dynamic) Equilibrium equations:
-m*der(vx) + Fxf + Fxr = 0;
-m*der(vz) - m*g + Fzf + Fzr = 0;
-Jy*der(wy) + Fzr*lr - Fzf*lf - (Fxf + Fxr)*h = 0;
(Fzr - Fsr - Fdr)*gr - Fxr*er + Tsr = 0;
(Fsf + Fdf - Fzf)*gf - Fxf*ef + Tsf = 0;

//Compatibility:
zf = z - lf*py;
    
```

[3.33]

LONGITUDINAL DYNAMIC

$$\begin{aligned} z_r &= z + l_r \cdot p_y; \\ v_{zf} &= v_z - l_f \cdot w_y; \\ v_{zr} &= v_z + l_r \cdot w_y; \end{aligned}$$



The simulation results are shown in Figure 3-35. It shows a constant deceleration, but it is changed how the decelerating force is generated. At time=3 s, there is a shift from braking solely on front axle to solely on rear axle. The braking is, so far, only done with friction brakes, i.e. generating torque by taking reaction torque in the axle itself. At time=5 s, there is a shift from braking with friction brakes to braking with shaft torque. It should be noted that if we shift axle or shift way to take reaction torque, gives transients even if the deceleration remains constant.

One can also see, at time=1 s, that the normal load under the braked axle first changes in a step. This is the effect of the Anti-dive geometry. Similar happens when braking at rear axle, due to the Anti-squat geometry. Since brake performance is much about controlling the pressure rapidly, the transients are relevant and the plots should make it credible that it is a control challenge to reach a high braking efficiency.

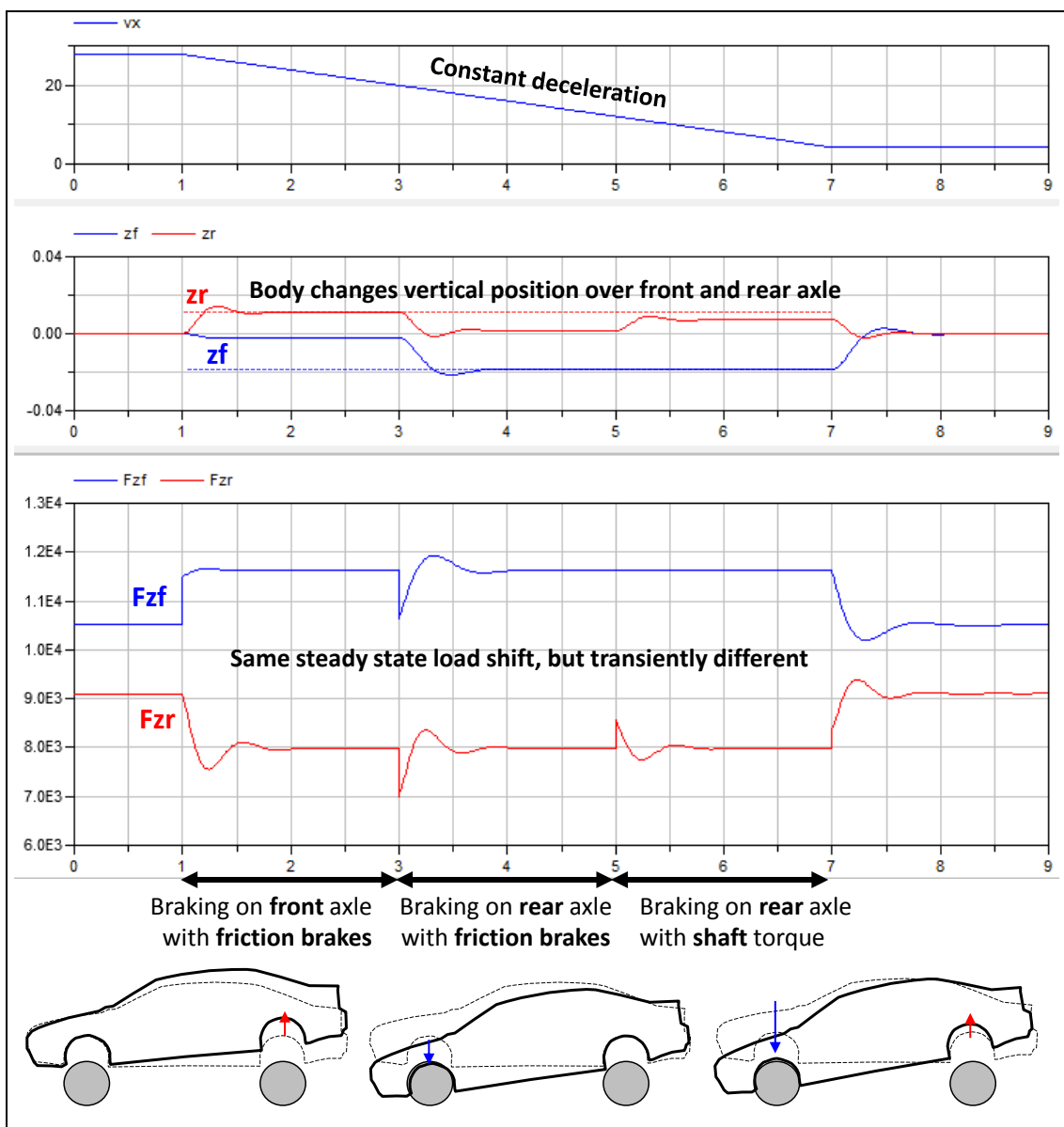


Figure 3-35: Deceleration sequence with constant vehicle deceleration, but changing between different ways of actuation. Dashed lines are solutions from Equation [3.24].

3.4.13 Acceleration performance *

Function definition: See Section 3.3.11.1.

The model presented in Equation [3.33] can also be used to predict acceleration performance in a more accurate way compared to Section 3.3.11. Especially, the more accurate model is needed when propelling or braking on the limit of tyre to road adhesion, since the normal load of each tyre then is essential. It is a challenge to control the propulsion and brake wheel torques to utilize the varying normal loads under each axle.

3.5 Control functions

Some control functions will be presented briefly. There are more, but the following are among the most well-established ones. First, some general aspects on control are given.

3.5.1 Longitudinal Control

Some of the most important sensors available and used for longitudinal control are:

- **Wheel Speed Sensors, WSS.** For vehicle control design, one can often assume that “sensor-close” software also can supply information about longitudinal vehicle speed.
- **Vehicle body inertial sensors.** There is generally a yaw rate gyro and a lateral accelerometer available, but sometimes also a longitudinal accelerometer. The longitudinal accelerometer is useful for longitudinal control and longitudinal velocity estimation.
- **Pedal sensors.** Accelerator pedal normally has a position sensor and brake pedal force can be sensed via brake system main pressure sensor. Heavy vehicles often have both a brake pedal position and brake pressure sensors.
- High specification modern vehicles have **environment sensors** (camera, radar, GPS with electronic map, etc.) that can give information (relative distance and speed, etc.) about objects ahead of subject vehicle. It can be both fixed objects (road edges, curves, hills, ...) and moving objects (other road users, animals, ...).
- Information about what actuation that is **actually applied at each time instant** is available, but it should be underlined that the confidence in that information often is questionable. Information about axle propulsion torque is generally present, but normally relies on imprecise models of the whole combustion process and torque transmission, based on injected amount of fuel and gear stick position. (Electric motors can typically give better confidence in estimation, especially if motor is close to the wheel without too much transmission in between.) Wheel individual friction brake torque is available, but normally rely on imprecise models of the brake systems hydraulic/pneumatic valves and disc friction coefficient, based on brake main cylinder pressure.
- Information about what **actuation levels that are possible** upon request (availability or capability) is generally not so common. It is difficult to agree of general definitions of such information, because different functions have so different needs, e.g. variations in accepted time delay for actuation.

3.5.2 Longitudinal Control Functions

3.5.2.1 Pedal driving *

Function definition: See Section 3.4.4.

These functions, Pedal Response *, are often not seen as comparable with other control functions, but they become more and more relevant to define as such, since both accelerator and brake pedals tend to be electronically controlled, and hence they become increasingly tuneable. Also, more and more functions, such as those below in section 3.5.2, will have to be arbitrated with the pedals.

In modern passenger vehicles, Accelerator pedal is normally electronically controlled but the Brake pedal is basically mechanical. In modern heavy commercial vehicles, both functions are electronically controlled.

The functions in Section “3.4.5 Pedal Feel *” are normally not actively controlled, but in there are concept studies with active pedals, where also the pedal feel can be actively changed to give feedback to driver.

3.5.2.2 Cruise Control and Adaptive Cruise Control (CC and ACC) *

*Function definition: **Cruise Control, CC**, controls the vehicle’s longitudinal speed. Driver can activate the function and decide desired speed.*

*Function definition: **Adaptive Cruise Control, ACC**, is an addition to CC. ACC controls the vehicle’s time gap to a lead vehicle. Driver can activate the function and decide desired gap. When there is no lead vehicle, CC controls the vehicle’s speed.*

The purpose of CC is to keep the vehicle at a driver selected longitudinal speed, while driver not pushes the accelerator pedal. The actuator used is the propulsion system. In heavy vehicles also the braking system (both retarders and service brakes) is used to maintain or regulate the vehicle speed.

ACC is an addition to CC. The purpose of ACC is to keep a safe distance to the lead vehicle (vehicle ahead of subject vehicle). ACC uses also friction brake system as actuator, but normally limited to a deceleration of 2.4 m/s².

CC is normally only working down to 30..40 km/h. ACC can have same limitation, but with good forward looking environment sensors, brake actuators and speed sensing, it can be allowed all the way down to stand-still.

3.5.2.3 Anti-lock Braking System, ABS *

*Function definition: **Anti-lock Braking System, ABS**, prohibits driver to lock the wheels while braking. The wheel brake torques requested are limited by ABS in a way that each individual wheel’s longitudinal slip stays above a certain (negative) value. An extended definition of ABS also includes vehicle deceleration requested by other functions than pedal braking, such as AEB. ABS only uses friction brake as actuator.*

The purpose of ABS is to avoid losing vehicle brake force due to that the tyre force curve drops at high slips AND to leave some friction for steering and cornering, see Sections 2.4, 0 and 2.6. ABS is a wheel slip closed loop control, active when driver brakes via brake pedal. It keeps the slip above a certain value, typically -15..-20 %. ABS uses the friction brakes as actuator.

Each wheel is controlled individually, but all wheels speed sensors contribute to calculation of vehicle longitudinal speed (which is needed to calculate actual slip value). In the ABS function, it may be included how slip are distributed between the wheels, such as normally the front axle is controlled to a slip closer to locking than the rear axle. Also, a sub function called “select-low” which means that the wheel closest to locking decides the pressure also for the other wheel at the same axle. Select-low is typically used at rear axles.

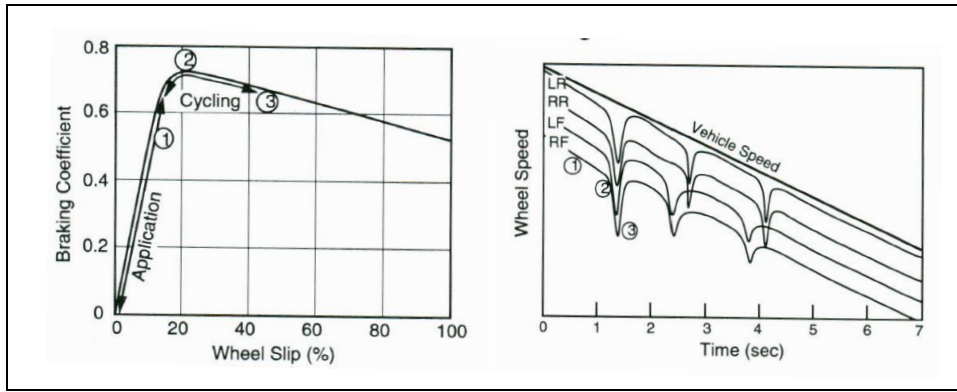


Figure 3-36: ABS control. Principle and control sequence

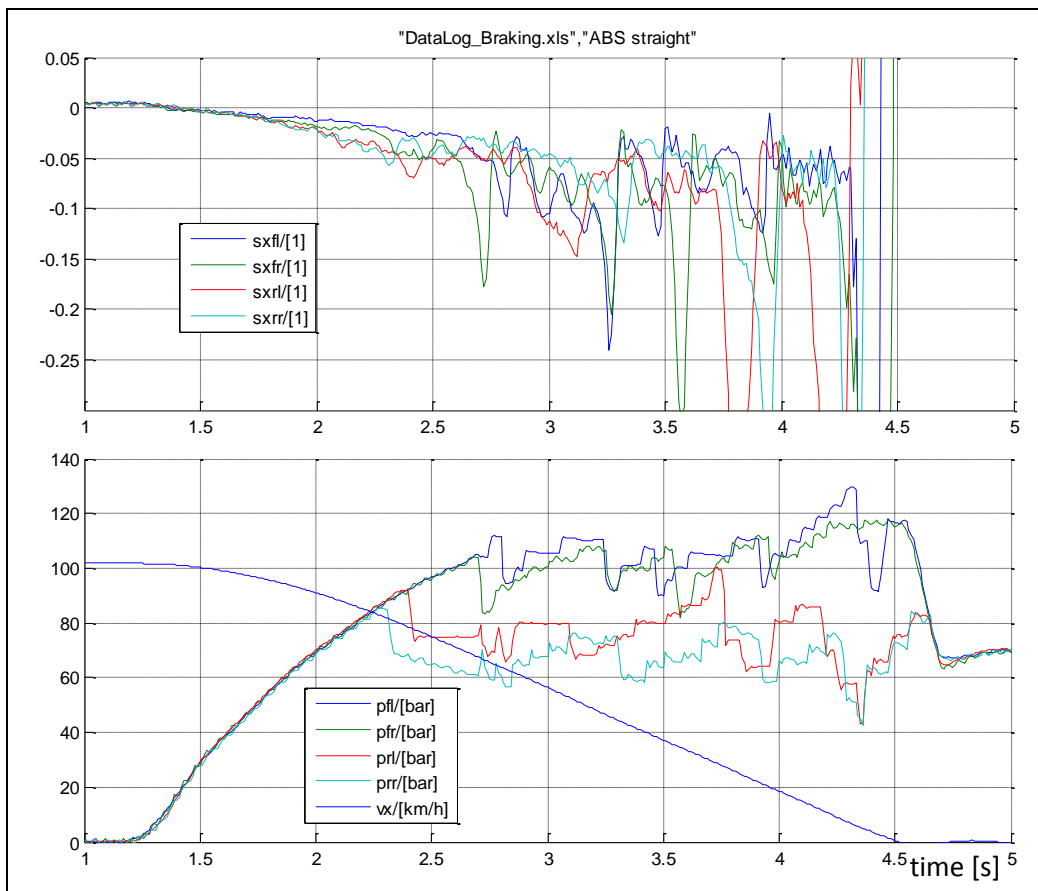


Figure 3-37: ABS control, Data log from passenger car test.

3.5.2.4 Electronic Brake Distribution, EBD *

*Function definition: **Electronic Brake Distribution** prohibits driver to over-brake the rear axle while braking. An extended definition of EBD also includes vehicle deceleration requested by other functions than pedal braking, such as AEB. EBD only uses friction brake as actuator.*

With a fix proportioning between front and rear axle braking, there is a risk to over-brake rear axle when friction is very high, since rear axle is unloaded so much then. Before electronic control was available, it was solved by hydraulic valves, which limited the brake pressure to rear axle when pedal force became too high. In today's cars, where electronic brake control is present thanks to legislation of ABS, the software base function EBD fulfils this need. In heavy vehicles, pneumatic valves are used

that limits the brake pressure in relation to the rear axle load (deflection of mechanical spring suspension or air pressure in air suspension).

There are other side functions enabled by having ABS on-board. Such are “select low”, which means that the brake pressure to both wheels on an axle is limited by the one with lowest pressure allowed from ABS. So, if one wheel comes into ABS control, the other gets the same pressure. This is most relevant on rear axle (to reduce risk of losing side grip) but one tries to eliminate the need of it totally, because it reduces the brake efficiency when braking in curve or on different road friction left/right.

It is often difficult to define strict border between functions that is a part of ABS and which is part of EBD, which is why sometimes one say ABS/EBD as a combined function.

3.5.2.5 Traction Control, TC *

*Function definition: **Traction Control** prohibits driver to spin the driven axle(s) in positive direction while accelerating. An extended definition of TC also includes vehicle acceleration requested by other functions than pedal braking, such as CC. TC uses both friction brakes and propulsion system as actuators.*

The purpose of Traction Control is to maximise traction AND to leave some friction for lateral forces for steering and cornering. Traction control is similar to ABS, but for keeping slip below a certain value, typically +(15..20)%.

Traction control can use different ways to control slip, using different actuators. One way is to reduce engine torque, which reduces slip on both wheels on an axle if driven via differential. Another way is to apply friction brakes, which can be done on each wheel individually. Vehicles with propulsion on several axles can also redistribute propulsion from one axle to other axles, when the first tends to slip. Vehicles with transversal differential clutch or differential lock can redistribute between left and right wheel on one axle.

3.5.2.6 Engine Drag Torque Control, EDC *

*Function definition: **Engine Drag Torque Control** prohibits over-braking of the driven axle(s) while engine-braking. EDC uses both friction brakes and propulsion system as actuators.*

The purpose of Engine Drag Torque Control is as the purpose of ABS, but the targeted driving situation is when engine braking at low road friction, when engine drag torque otherwise can force the wheels to slip too much negative. Similarly to ABS, it keeps the slip above a certain negative value. However, it does it by increasing the engine torque from negative (drag torque) to zero (or above zero for a short period of time).

3.5.2.7 Automatic Emergency Brake, AEB *

*Function definition: **Automatic Emergency Brake** decelerates vehicle without driver having to use brake pedal when probability for forward collision is predicted as high.*

The purpose of AEB is to eliminate or mitigate collisions where subject vehicle collides with a lead vehicle. AEB uses friction brake system as actuator, up to full brake which would be typically 10 m/s². An AEB system is often limited by that it cannot be designed to trigger too early, because driver would be disturbed or it could actually cause accidents. Therefore, in many situations, AEB will rather mitigate than avoid collisions. (The A in the abbreviation AEB can be for either of “Automatic”, “Autonomous” or “Advanced”.)

Conceptually, an AEB algorithm can be assumed to know physical quantities as marked in Figure 3-38. The quantity time-to-collision, TTC, can then be defined as $TTC = x_o / (v_x - v_{ox})$, which means the time within a collision will appear if no velocities changes. TTC can also be seen as the “time gap” to the lead vehicle.

AEB function shall, continuously, decide whether or not to trigger AEB braking. AEB shall intervene by braking when driver can be assumed to collide without intervention. If no other information, this can be predicted as when driver can NOT avoid by normal driving. Avoidance manoeuvres that have to be considered are (normal) deceleration and (normal) lateral avoidance to the left and to the right.

What to assume as normal driving is a question of tuning; here the following limits are used $|\dot{v}_x| < a_{xn} = e.g. 4 \text{ m/s}^2$ and $|\dot{v}_y| < a_{yn} = e.g. 6 \text{ m/s}^2$. A physical model based algorithm can start from the following simple models:

- Normal **deceleration** ($\dot{v}_x = -a_{xn} = -4 \text{ m/s}^2$) leads to **collision if**:

$$\min_{t > 0} (x_o(t)) < 0 \Rightarrow \min_{t > 0} \left(x_o + v_{ox} \cdot t - \left(v_x \cdot t + a_{xn} \cdot \frac{t^2}{2} \right) \right) < 0 \Rightarrow$$

$$\Rightarrow \left(x_o + v_{ox} \cdot t - \left(v_x \cdot t + a_{xn} \cdot \frac{t^2}{2} \right) \right) \Big|_{t = \frac{v_{ox} - v_x}{a_{xn}}} < 0 \Rightarrow$$

$$\Rightarrow x_o - \frac{1}{2 \cdot (-a_{xn})} \cdot (v_x - v_{ox})^2 < 0 \Rightarrow \frac{x_o}{v_x - v_{ox}} = \mathbf{TTC} < \frac{v_x - v_{ox}}{2 \cdot (-a_{xn})} = \frac{v_x - v_{ox}}{8};$$
- Normal **avoidance to the left** ($\dot{v}_y = a_{yn} = 6 \text{ m/s}^2$) leads to **collision if**:

$$\left(y_{ol}(t) + \frac{w}{2} \right) \Big|_{x_o=0} < 0 \Rightarrow \left(y_{ol} - a_{yn} \cdot \frac{t^2}{2} + \frac{w}{2} \right) \Big|_{t = \frac{x_o}{v_x - v_{ox}}} < 0 \Rightarrow$$

$$\Rightarrow \frac{x_o}{v_x - v_{ox}} = \mathbf{TTC} < \sqrt{2 \cdot \frac{y_{ol} + w/2}{a_{yn}}} = \{e.g.\} = \sqrt{\frac{0.6 + 1.8/2}{3}} \approx 0.4 \text{ s};$$
- Normal **avoidance to the right** ($\dot{v}_y = -a_{yn} = -6 \text{ m/s}^2$) leads to **collision if**:

$$\dots \Rightarrow \frac{x_o}{v_x - v_{ox}} = \mathbf{TTC} < \sqrt{2 \cdot \frac{-y_{or} - w/2}{a_{yn}}} = \sqrt{\frac{-y_{or} + w/2}{3}};$$
- Assuming that the AEB intervention decelerates the vehicle with $-\dot{v}_x = a_{xAEB} = -8 \text{ m/s}^2$, a forward collision can be avoided if AEB intervenes AND if:

$$\dots \Rightarrow \frac{x_o}{v_x - v_{ox}} = \mathbf{TTC} > \frac{v_x - v_{ox}}{2 \cdot (-a_{xAEB})} = \frac{v_x - v_{ox}}{16};$$

Figure 3-38 shows a diagram where different condition areas are marked. The sectioned area shows where AEB will be triggered, using above rules. The smaller of the sectioned areas shows where it also will be possible to trigger AEB so timely that a collision is actually avoided; with the assumed numbers, this is for speeds up to 6.4 m/s ≈ 23 km/h.

The reasoning above is very simplified. Additional information can improve effectiveness of AEB, such as knowing if a lateral avoidance on one side of object vehicle is blocked, whether the object vehicle is decelerating and what the road friction is. Also, the reasoning is only valid for vehicles driving in straight path with no lateral relative velocity. The vehicle dynamics model used is simply a point mass with predicted constant velocity and certain assumed acceleration capability, which of course can be extended a lot; both with taking actual accelerations into account and more advanced vehicle dynamics models.

AEB is on market and legal requirement for both passenger vehicles and heavy vehicles.

Related functions are, e.g. extra force assistance in brake pedal when driver steps quickly onto brake. Another related function is automatic braking triggered by a first impact and intended to mitigate or avoid secondary accident events, starts to appear at market, see Reference (Yang, 2013). In semantic meaning this could be seen as AEB, but they are normally not referred to as AEB; AEB normally refers to functions that use environment sensors (forward directed radar, camera, etc).

When designing and evaluating AEB, it is important to also know about the function Forward Collision Warning, FCW. FCW is a function that warns the driver via visual and/or audio signals when a forward collision is predicted. FCW is typically triggered earlier than AEB.

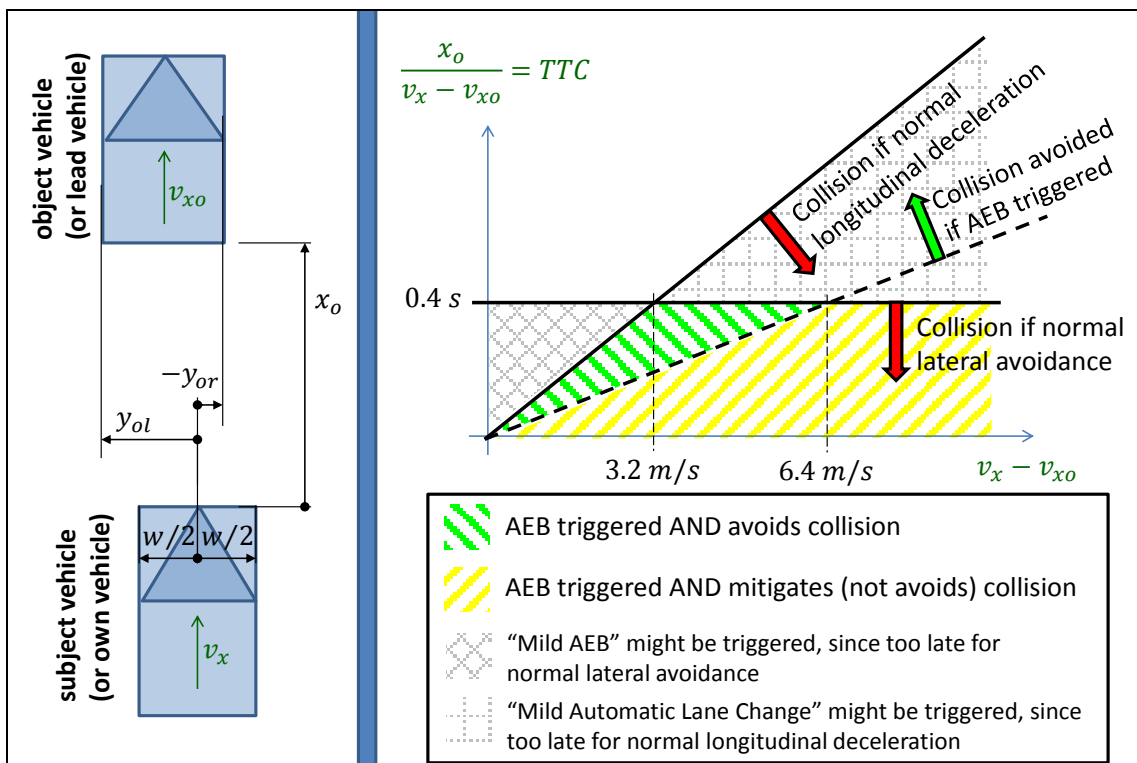


Figure 3-38: Left: Quantities known for an AEB algorithm in the subject vehicle, assuming forward directed camera or radar. Right: Model based decision of triggering AEB and effectiveness of AEB if triggered.

3.5.3 Longitudinal Motion Functionality shown in a reference architecture

All control functions controls have to cooperate and they have to be transferable between platforms and vehicle variants. It is very complex to take all functions into consideration, but with a scope limited to the longitudinal Motion functionality Figure 3-39 can be drawn as a solution within the reference architecture.

By using a reference architecture it can be illustrated that Adaptive Cruise control and cruise control can be seen as part of Traffic Situation Layer (ACC=CC if no vehicle ahead). The Traffic Situation Layer has the purpose and scope to understand the ego vehicle’s surrounding traffic by looking at e.g. Forward Sensors. The forward looking sensor is in this case part of Vehicle Environment sensors.

Vehicle Motion and Coordination Layer would include the arbitration of Driver’s Acceleration and Brake pedal input and Traffic functionality, see Figure 3-39. In addition, Vehicle Motion and Coordination Layer would perform the powertrain coordination and brake distribution. The coordinated requests are then sent to Motion Support Device Layer.

The Human Machine Interface would include the services available for the driver to activate or request, E.g. ACC activation to Traffic Situation or Deceleration by pressing the brake pedal.

LONGITUDINAL DYNAMIC

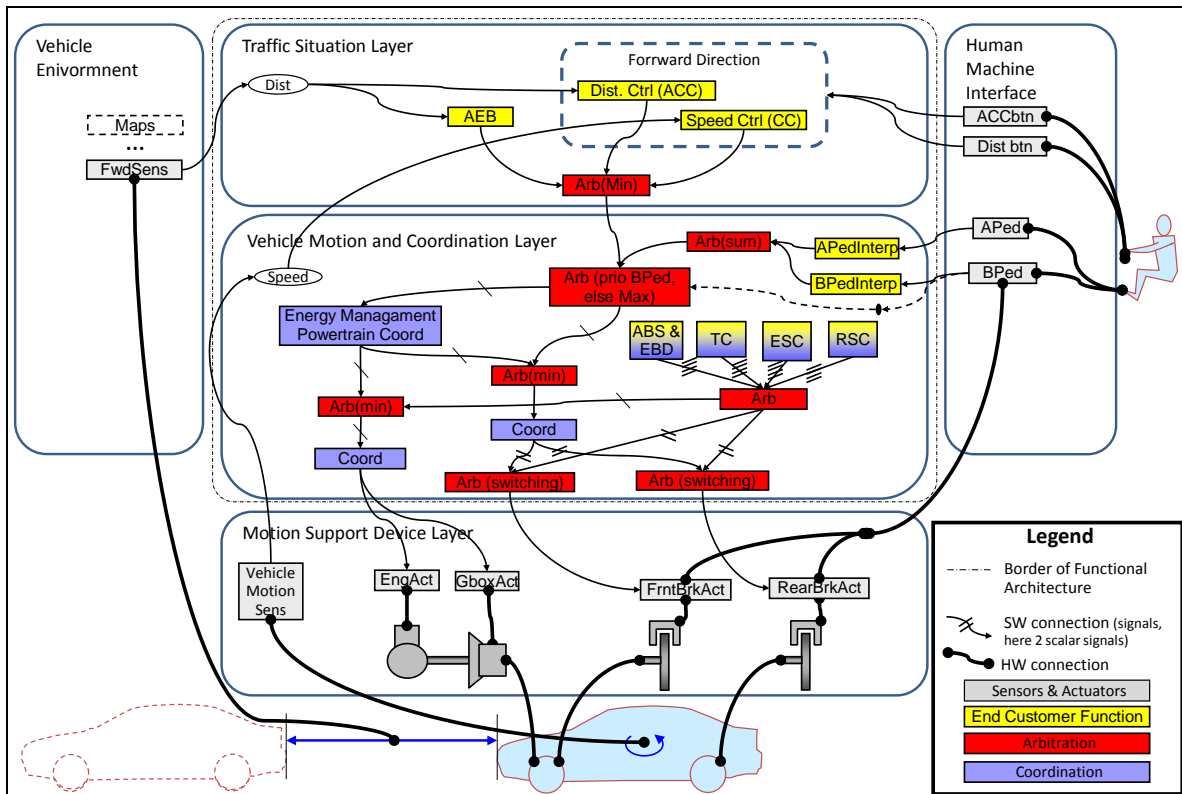


Figure 3-39: Functional architecture for conventional front axle driven passenger car. Mainly longitudinal functions (plus ESC, RSC) are shown, e.g. no steering. Cf Figure 1-11.

If a reference architecture is used, it can assist function developers from OEM's Electrical, Powertrain, and Chassis departments and suppliers to have a common view of how vehicle's embedded motion functionality is intended to be partitioned and to understand how different functions relate and interact with each other and what responsibilities they have.

4 LATERAL DYNAMICS

4.1 Introduction

The lateral motion of a vehicle is needed to follow the roads' curves and select route in intersections as well as to laterally avoid obstacles that appear. The vehicle needs to be steerable. With some simplification, one can say that lateral dynamics is about how steerable the vehicle is for different given longitudinal speeds. Vehicle steering is studied mainly through the vehicle degrees of freedom: yaw rotation and lateral translation.

A vehicle can be steered in different ways:

- Applying steering angles on, at least one, road wheel. Normally both of front wheels are steered.
- Applying longitudinal forces on road wheels. Either unsymmetrical between left and right side of vehicle, e.g. one sided braking, or deliberately use up much friction longitudinally on one axle in a curve, so that that axle loses lateral force.
- Articulated steering, where the axles are fixed mounted on the vehicle but the vehicle itself can bend.

The chapter is organised with one group of functions in each section as follows:

- 4.2 Low speed manoeuvrability
- 4.3 Steady state cornering at high speed
- 4.4 Stationary oscillating steering
- 4.5 Transient handling
- 4.6 Lateral Control Functions

Most of the functions in "4.6 Lateral Control Functions", but not all, could be parts of "4.5 Transient handling". However, they are collected in one own section, since they are special in that they partly rely on software algorithms.

The lateral dynamics of vehicles is often experienced as the most challenging for the new automotive engineer. Longitudinal dynamics is essentially motion in one plane and rectilinear. Vertical dynamics may be 3 dimensional, but normally the displacements are small and in this compendium the vertical dynamics is mainly studied in one plane as rectilinear. However, lateral dynamics involves analysis of motion in the vehicle coordinate system which introduces curvilinear motion since the coordinate system is rotating as the vehicle yaws.

The turning manoeuvres of vehicles encompass two concepts. Handling is the driver's perception of the vehicle's response to the steering input. Cornering is usually used to describe the physical response (open-loop) of the vehicle independent of how it influences the driver.

4.1.1 References for this chapter

- *"Chapter 25 Steering System" in Reference (Ploechl, 2013).*
- *"Chapter 27 Basics of Longitudinal and Lateral Vehicle Dynamics" in Reference (Ploechl, 2013).*

4.2 Low speed manoeuvrability

This section is about operating vehicles in low speeds, including stand-still and reverse. Specific for low speed is that inertial effects can be neglected, i.e. one can assume that left hand side in motion equation ($Mass \cdot LateralAcceleration = sum\ of\ Forces$) is zero.

In low speed, one often needs to find the path with orientation and understand the steering system and how tyres can be modelled to track ideally. This, and the resulting one-track model for low speeds, is described in Sections 4.2.1, ...,4.2.6.

4.2.1 Path with orientation

The path and path with orientation was introduced in Section 1.3. The path, in global coordinate system, is related to vehicle speeds, in vehicle fix coordinates, as given in Figure 4-1 and Equation [4.1].

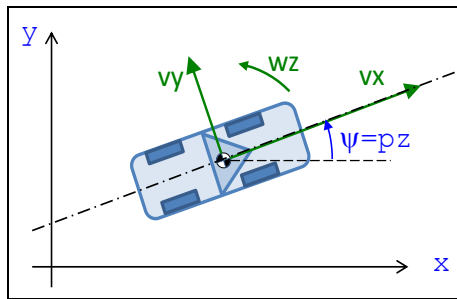


Figure 4-1: Model for connecting “path with orientation” to speeds in vehicle coordinate system.

$$\begin{bmatrix} \dot{x} \\ \dot{y} \end{bmatrix} = \begin{bmatrix} \cos(\psi) & -\sin(\psi) \\ \sin(\psi) & \cos(\psi) \end{bmatrix} \cdot \begin{bmatrix} v_x \\ v_y \end{bmatrix};$$

$$\dot{\psi} = \omega_z$$

[4.1]

Knowing $(v_x(t), v_y(t), \omega_z(t))$, we can determine “path with orientation” $(x(t), y(t), \psi(t))$, by time integration of the right hand side of the equation. Hence, the positions are typically “state variables” in lateral dynamics models.

It should be noted that in some problems, typically manoeuvring at low speed, the real time scale is of less interest. Then, the problem can be treated as time independent, e.g. by introducing a coordinate, s , along the path, as in Equation [4.2].

$$x' = \frac{v_x}{\dot{s}} \cdot \cos(\psi) - \frac{v_y}{\dot{s}} \cdot \sin(\psi);$$

$$y' = \frac{v_y}{\dot{s}} \cdot \cos(\psi) + \frac{v_x}{\dot{s}} \cdot \sin(\psi);$$

$$\psi' = \frac{\omega_z}{\dot{s}};$$

where prime notes differentiation with respect to s

[4.2]

Here, \dot{s} can be thought of like an arbitrary time scale, with which all speeds are scaled. One can typically chose $\dot{s} = 1 [m/s]$. However, in this compendium we will keep notation t and the dot notation for derivative.

4.2.2 Vehicle and wheel orientations

For steered wheels, there are often reason to translate forces and velocities between vehicle coordinate system and wheel coordinate system, see Figure 4-2 and Equation [4.3].

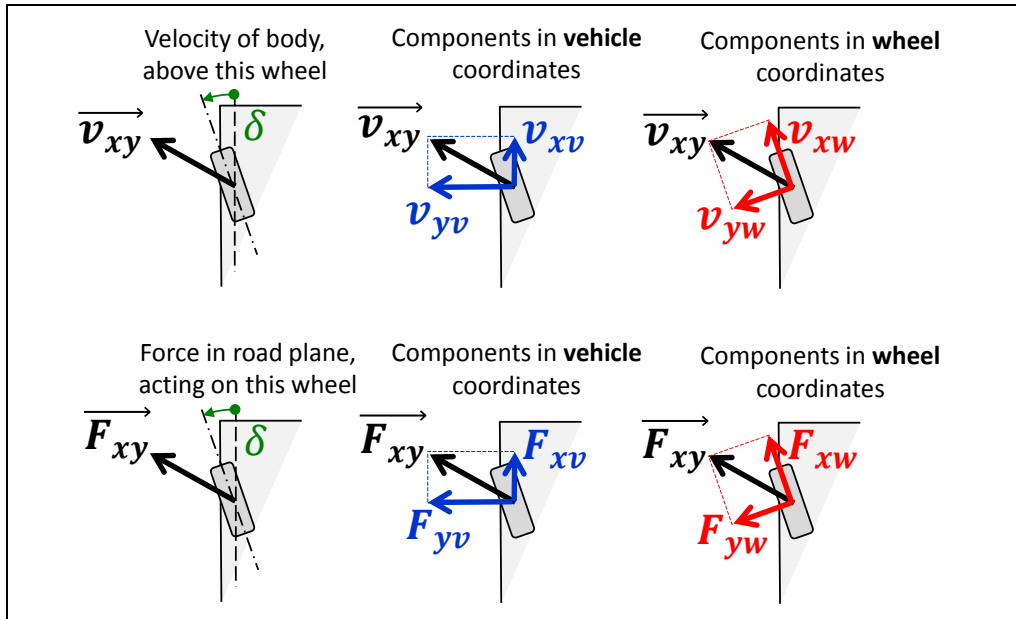


Figure 4-2: Transformation between forces and velocities in vehicle coordinate system and wheel coordinate system.

Transformation from wheel coordinates to vehicle coordinates:

$$\begin{bmatrix} v_{xv} \\ v_{yv} \end{bmatrix} = \begin{bmatrix} \cos(\delta) & -\sin(\delta) \\ \sin(\delta) & \cos(\delta) \end{bmatrix} \cdot \begin{bmatrix} v_{xw} \\ v_{yw} \end{bmatrix}; \text{ and } \begin{bmatrix} F_{xv} \\ F_{yv} \end{bmatrix} = \begin{bmatrix} \cos(\delta) & -\sin(\delta) \\ \sin(\delta) & \cos(\delta) \end{bmatrix} \cdot \begin{bmatrix} F_{xw} \\ F_{yw} \end{bmatrix};$$

Transformation from vehicle coordinates to wheel coordinates:

$$\begin{bmatrix} v_{xw} \\ v_{yw} \end{bmatrix} = \begin{bmatrix} \cos(\delta) & \sin(\delta) \\ -\sin(\delta) & \cos(\delta) \end{bmatrix} \cdot \begin{bmatrix} v_{xv} \\ v_{yv} \end{bmatrix}; \text{ and } \begin{bmatrix} F_{xw} \\ F_{yw} \end{bmatrix} = \begin{bmatrix} \cos(\delta) & \sin(\delta) \\ -\sin(\delta) & \cos(\delta) \end{bmatrix} \cdot \begin{bmatrix} F_{xv} \\ F_{yv} \end{bmatrix};$$

[4.3]

4.2.3 Steering System

The steering system is here referred to the link between steering wheel and the road wheel's steering, on the steered axle. It is normally the front axle that is steered. Driver's interaction is two-folded, both steering wheel angle and torque, which is introduced in Section 2.10. In present section, we will focus on how wheel steering angles are distributed between the wheels.

4.2.3.1 Chassis steering geometry

The most basic intuitive relation between the wheels steering angles is probably that all wheels rotation axes always intersect in one point. This is called Ackermann geometry and is shown Figure 4-3. The condition for having Ackermann geometry is, for the front axle steered vehicle that:

$$\left. \begin{aligned} \frac{1}{\tan(\delta_i)} &= \frac{R_r - w/2}{L}; \\ \frac{1}{\tan(\delta_o)} &= \frac{R_r + w/2}{L}; \end{aligned} \right\} \Rightarrow \frac{1}{\tan(\delta_o)} = \frac{1}{\tan(\delta_i)} + \frac{w}{L}; \quad [4.4]$$

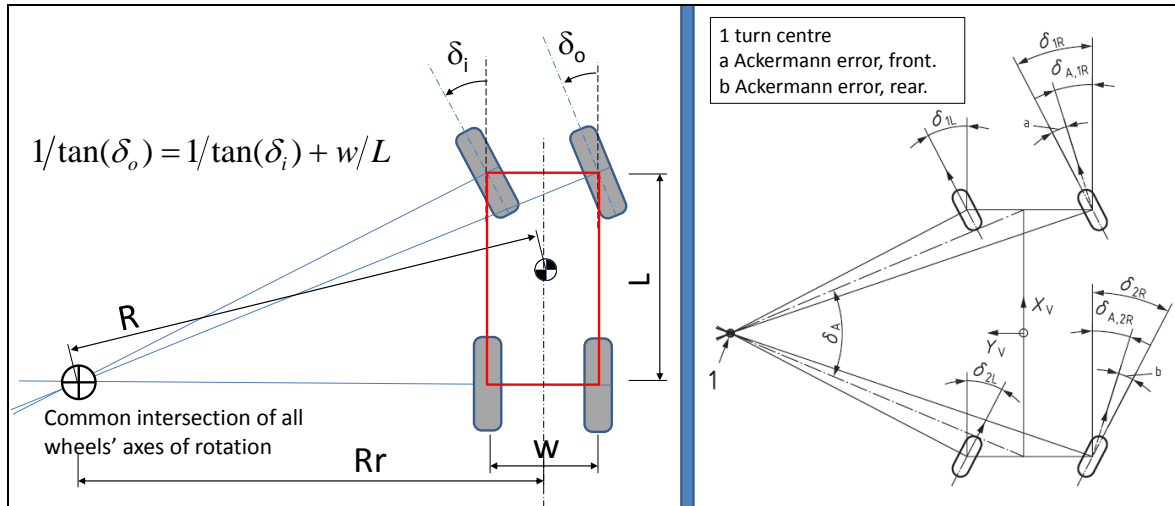


Figure 4-3: Ackermann steering geometry. Left: One axle steered. Right: Both axles steered and including “Ackermann errors”. From (ISO8855).

The alternative to Ackermann steering geometry is parallel steering geometry, which is simply that $\delta_i = \delta_o$. Note that Ackermann geometry is defined for a vehicle, while parallel steering is defined for an axle. This means that, for a vehicle with 2 axles, each axle can be parallel steered, which means that the vehicle is non-Ackermann steered. However, the vehicle can still be seen as Ackermann steered with respect to mean steering angles at each axle.

For low-speed, Ackermann gives best manoeuvrability and lowest tyre wear. For high-speed, Parallel is better in both aspects. This is because vehicles generally corner with a drift outwards in curves, which means that the instantaneous centre is further away than Ackermann geometry assumes, i.e. more towards optimal for parallel. Hence the chosen geometry is normally somewhere between Ackermann and parallel.

Practical arrangement to design the steering geometry is shown in Figure 4-7. The design of linkage will also make the transmission from steering wheel angle to road wheel steering angle non-linear. This can lead to different degrees of Ackerman steering for small and large steering wheel angles.

In traditional steering systems, the steering wheel angle has a monotonically increasing function of the steering angle of the two front axle road wheels. This relation is approximately linear with a typical ratio of 15..17 for passenger cars. For trucks the steering ratio is typically 18..22. Differences between left and right wheels are discussed in 4. In some advanced solutions, steering on other axles is also influenced (multiple-axle steering, often rear axle steering). There are also advanced solutions for adding an additional steering angle to the basic steering ratio gives, so called AFS=Active Front Steering.

4.2.3.2 Steering system forces

(This section has large connection with Section 2.5.5.2 Tyre self-aligning moment.)

The steering wheel torque, T_{sw} , should basically be a function of the tyre/road forces, mainly the wheel-lateral forces. This gives the driver a haptic feedback of what state the vehicle is in. The

torque/force transmission involves a servo actuator, which helps the driver to turn the steering system, typically that assists the steering wheel torque with a factor varying between 1 and 10, but less for small T_{sw} (highway driving) than large T_{sw} (parking), see Figure 4-4. Here, the variation in assistance is assumed to be hydraulic and follows a so called boost curve. At $T_{sw} = 0$, the assistance is $\approx 0.45/0.55 \approx 1$ and for $T_{sw} = 4 \text{ Nm}$, it is $\approx 0.9/0.1 \approx 10$.

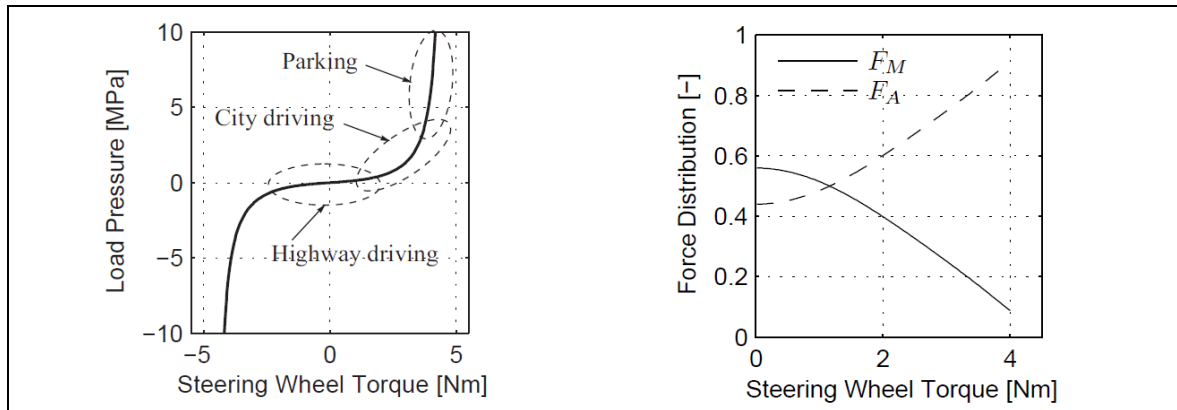


Figure 4-4: Left: Boost Curve with different working areas depending on the driving envelope. Right: Torque distribution between manual torque, F_M , and assisting torque, F_A , depending on applied steering wheel torque. From Reference (Rösth, 2007).

For vehicle dynamics, one important effect of a steered axle, is that the lateral force on the axle tries to align the steering in the direction that the body (over the steered axle) moves, i.e. towards a zero tyre side slip. This is designed in via the sign of the caster trail, see Figure 4-5. Also, asymmetry in longitudinal tyre forces (wheel shaft torques and/or brake torques) affects the steering wheel torque. This is analysed in the following.

On a steered axle, there is a *Steering axis* (or *Kingpin axis*) around which the wheel is rotated when it is steered. The steering axis intersects with the ground plane at a point which normally has an offset from the contact patch centre, both longitudinally and laterally. The offsets are called *Castor offset at ground* and *Steering axis offset at ground*, respectively, see Figure 4-5. (Steering axis offset at ground is sometimes called *Scrub radius*, but that is also used for the resulting distance of both offsets, so it is an ambiguous name.) This figure also defines *Normal steering axis offset at wheel centre*. We will use the 3 latter measures to explain why steering is affected by differences in shaft torque left/right, differences in brake torque left/right, and lateral wheel forces. The steering axis distance from wheel centre in side view, is called *Castor offset at wheel centre*.

Often, the actual forces between tyre and ground are not in the exact centre of the nominal contact patch, which also creates “effective” version of caster offset and scrub radius. For instance, the *Pneumatic trail* adds to the Castor offset at ground due to the lateral force distribution being longitudinally offset from nominal contact point; so that the lever becomes not only s , but $s+t$. The moment, T_{steer} , on steering system (around Steering axis, turning towards increasing steering angle) is affected by tyre forces on a steered axle as in Equation [4.5].

Castor offset at ground is, on passenger vehicles, 15-20 mm (at motorcycles approximately 100 mm). On rear wheel driven passenger vehicles it can typically be 5 mm, due to higher Castor Angle which gives a beneficial higher Camber angle gain at cornering. On a front wheel driven passenger vehicle a non-zero caster offset is not chosen due to drive axle lateral displacement.

(Notations in Equation [4.5] are defined in Figure 4-5.)

$$\begin{aligned}
 T_{steer} &= \frac{-(T_{b1} + T_{s1})}{R} \cdot s \cdot \cos(KPI) + \frac{-T_{s1}}{R} \cdot R \cdot \sin(KPI) + \\
 &+ \frac{(T_{b2} + T_{s2})}{R} \cdot s \cdot \cos(KPI) + \frac{T_{s2}}{R} \cdot R \cdot \sin(KPI) + \\
 &+ (-1) \cdot (F_{y1} \cdot (c + t_1) + F_{y2} \cdot (c + t_2)) \cdot \cos(CA) = \\
 &= \frac{T_{b2} - T_{b1}}{R} \cdot s \cdot \cos(KPI) + \frac{T_{s2} - T_{s1}}{R} \cdot k - (F_{y1} \cdot (c + t_1) + F_{y2} \cdot (c + t_2)) \cdot \cos(CA);
 \end{aligned}$$

[4.5]

The equation shows that difference in both brake torque and shaft torque affects steering. So does the sum of lateral forces. For reducing torque steer and disturbances from one-sided longitudinal forces due to road irregularities, kingpin offset, scrub radius different road friction should be as small as possible, but it is limited by geometrical conflicts between brake disc, bearing, damper, etc.

Positive scrub radius contributes to self-centring, thanks to lifting the car body, see below. Negative scrub radius compensates for split- μ braking, or failure in one of the brake circuits. Hence, the scrub is a balance between these two objectives. Scrub radius is often slightly negative on modern passenger cars. Scrub radius is often positive on trucks, maybe 10 cm, due to packaging.

The geometry in Figure 4-6 shows one part of the lifting effect. This is that if steering angle is changed from zero, it lifts the vehicle slightly which requires a steering torque. One can see this as a kind of “return spring effect”. Figure 4-6 shows how KPI and scrub radius causes the vehicle body to lift a distance $s''' = s \cdot \cos(KPI) \cdot (1 - \cos(|\varphi_{steer}|)) \cdot \sin(KPI)$. This will require a work $T_{steer} \cdot \varphi_{steer} = F_{iz} \cdot s'''$. This leads to an T_{steer} (additional to Eq [4.5]) as follows:

$$\begin{aligned}
 (\text{additional}) T_{steer} &= \sum_{i=\text{left and right}} \frac{F_{iz} \cdot s'''}{\varphi_{steer}} = \\
 &= \frac{s \cdot \cos(KPI) \cdot (1 - \cos(|\varphi_{steer}|)) \cdot \sin(KPI)}{\varphi_{steer}} \cdot F_{axle,z,i}
 \end{aligned}$$

[4.6]

It should be noted that Eq [4.6] is not complete with respect to all “returning effects”. There are also effects from Castor angle and Caster trail as well as that the tyre has a width and radius. However, in total, these give rise to a returning steering torque which is depending on the steering angle.

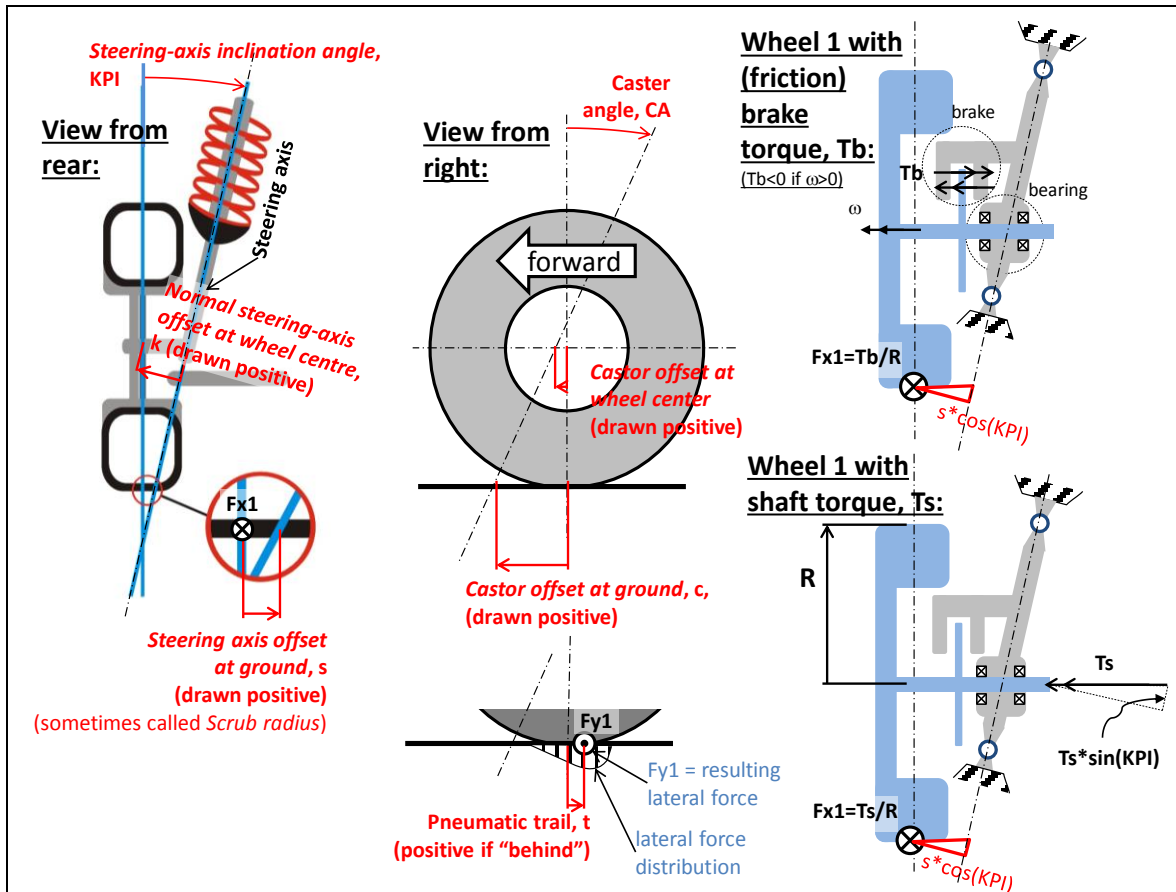


Figure 4-5: Steering geometry and offsets.

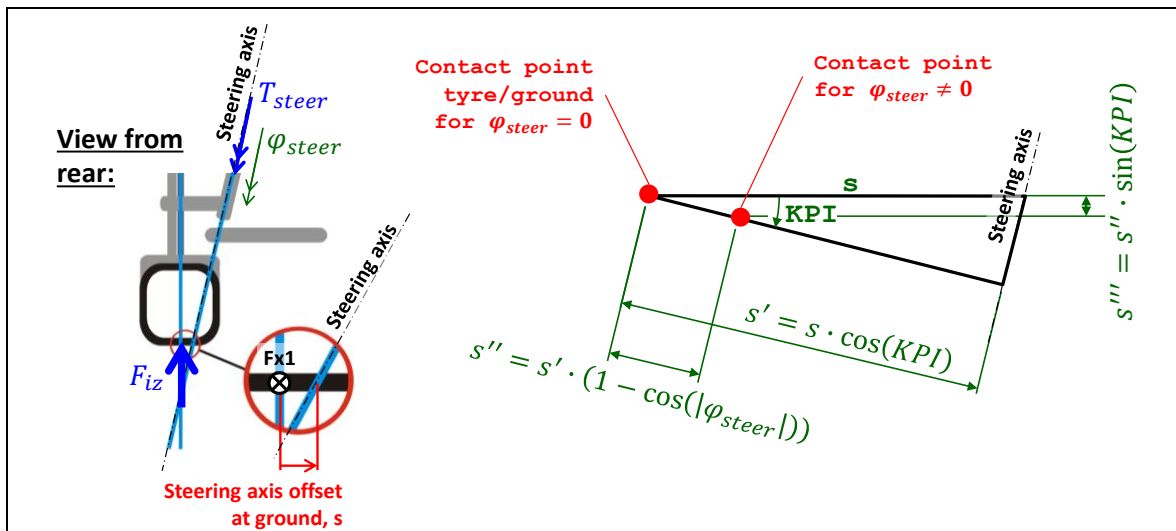


Figure 4-6: Lift effect due to steering angle and positive Steering axis offset at ground.

4.2.4 One-track models

When conducting analyses of the vehicle cornering response, it is useful to combine the effects of all tyres on the axle into one virtual tyre. This assumption, referred to as the one-track model (or single-track model or bicycle model), facilitates understanding but can also capture most important phenomena. A one-track model of a two-axle vehicle is shown in Figure 4-8. One-track model for truck with trailer is exemplified in Figure 4-9.

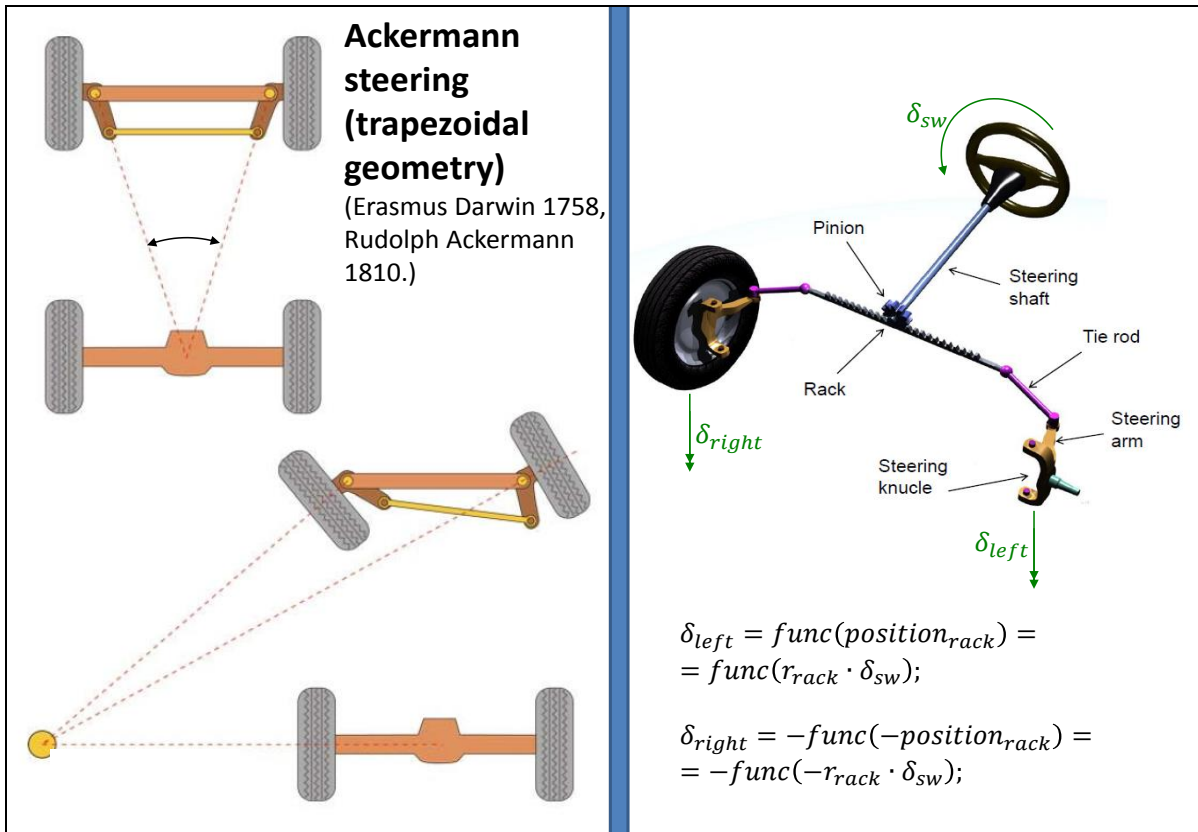


Figure 4-7: Example of Trapezoidal Steering. Left: Conceptual use of steering arms. Right: More exact design, common today. From Gunnar Olsson, LeanNova.

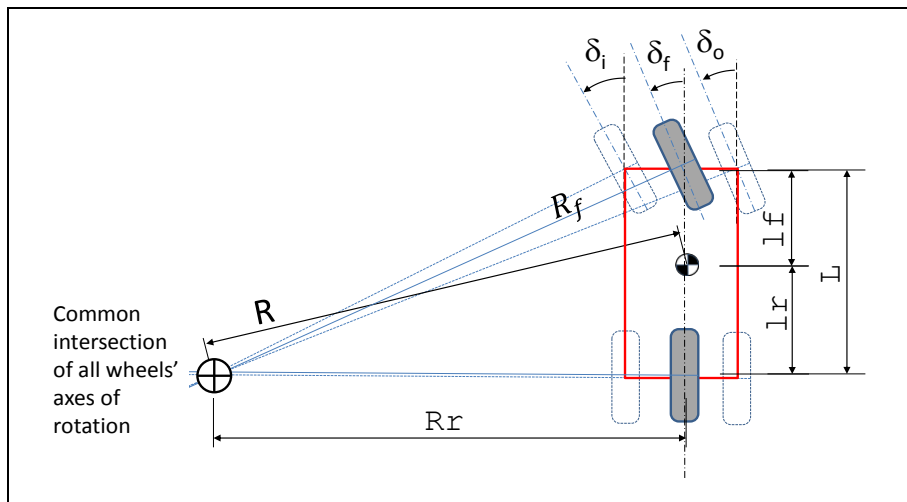


Figure 4-8: Collapsing to one-track model.

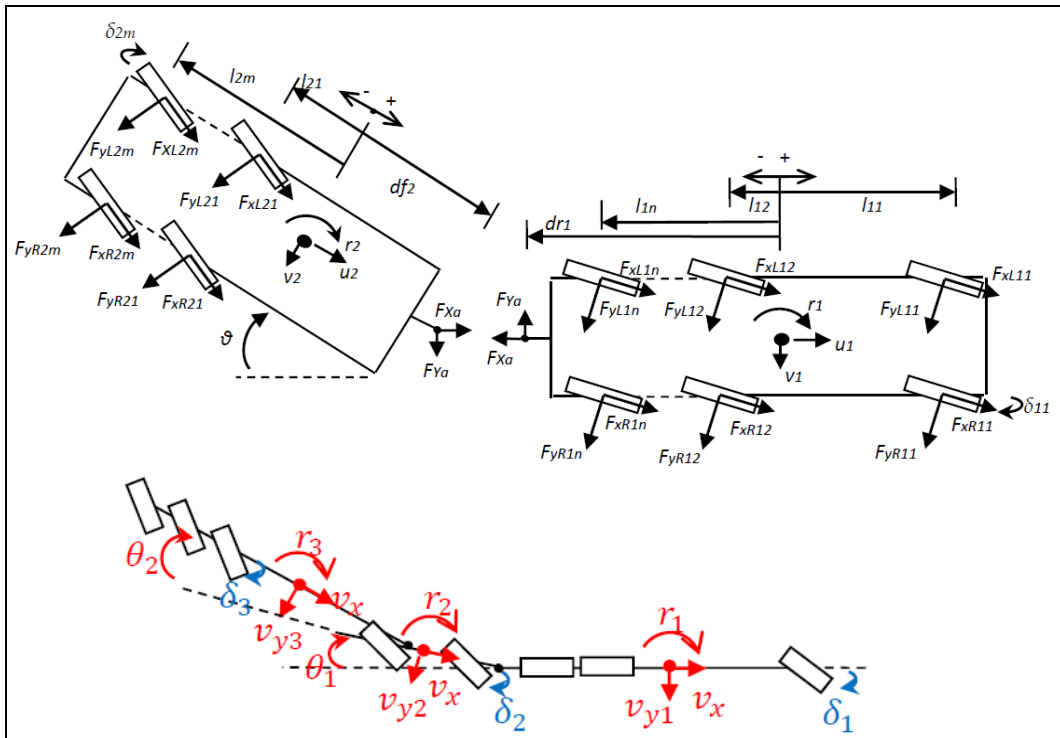


Figure 4-9: Upper: Two-track model of truck with trailer. Lower: One-track model of a truck with a trailer (not exactly same vehicle combination as above). In SAE coordinate system. From (Kharrazi, 2012).

Phenomena which one-track models not capture are, e.g.:

- Large deviations from Ackerman geometry within an axle.
- Varying axle cornering stiffness due to lateral load shift and axle propulsion/braking, see Section 4.3.
- Additional yaw moment due to non-symmetrical wheel torque interventions, such as ESC interventions.

These effects can, however, be approximately captured with a one-track vehicle model, extended with sub-models for the axles. The axle sub-models, can propagate the varying cornering stiffnesses and yaw moments to the superior one-track vehicle model.

4.2.5 Ideally tracking wheels and axles

In Section 0, lateral slip models for tyres were introduced. It is the constitutive equation $F_y = -C_y \cdot s_y$. If the tyre force, F_y , is small compared to cornering stiffness, C_y , one would expect side slip, s_y , to be very small. If this assumption is taken to its extreme, one get something we can call “ideal tracking” for a tyre or for an axle, which is that side slip is zero and side force can be any (finite) value. For low speed this is often a good enough model of the tyre. The validity of this assumption is limited by when lateral force becomes large with respect to available lateral force, $\mu \cdot F_z$. Hence, the speed border between low speed and high speed is lowered on low road friction.

Models using ideally tracking wheels are sometimes referred to as “kinematic models”. However, a strictly kinematic model does not contain the forces at all, why validity cannot be checked.

The assumption about ideally tracking wheel or axle is a constitutive assumption, although that the equation (tyre lateral speed=tyre side slip=0) does not couple force and speed, but only stipulates speed. If forces should be calculated, it has to be done using the equilibrium.

4.2.6 One-track model for low speeds, with Ackerman geometry

Low speed manoeuvres are characterised by that the inertial forces are neglected, i.e. $m \cdot a = 0$. If the geometry is according to Ackermann, it is reasonable to assume ideal tracking axles. This means that the intersection point of the wheels rotational axes coincides with the instantaneous centre of vehicle rotation in ground plane. We can there through connect steering angles and path radius. For the model in Figure 4-8 this connection becomes:

$$\left. \begin{aligned} \tan(\delta_f) &= \frac{L}{R_r}; \\ R^2 &= R_r^2 + l_r^2; \end{aligned} \right\} \Rightarrow \delta_f = \arctan\left(\frac{L}{\sqrt{R^2 - l_r^2}}\right) \cdot \text{sign}(R) \approx \frac{L}{\sqrt{R^2 - l_r^2}} \cdot \text{sign}(R) \approx \frac{L}{R}; \quad [4.7]$$

where $R > 0$ means that instantaneous centre of rotation is left of the vehicle

To get a more complete model, where more variables can be extracted, we can set up the model in Figure 4-10.

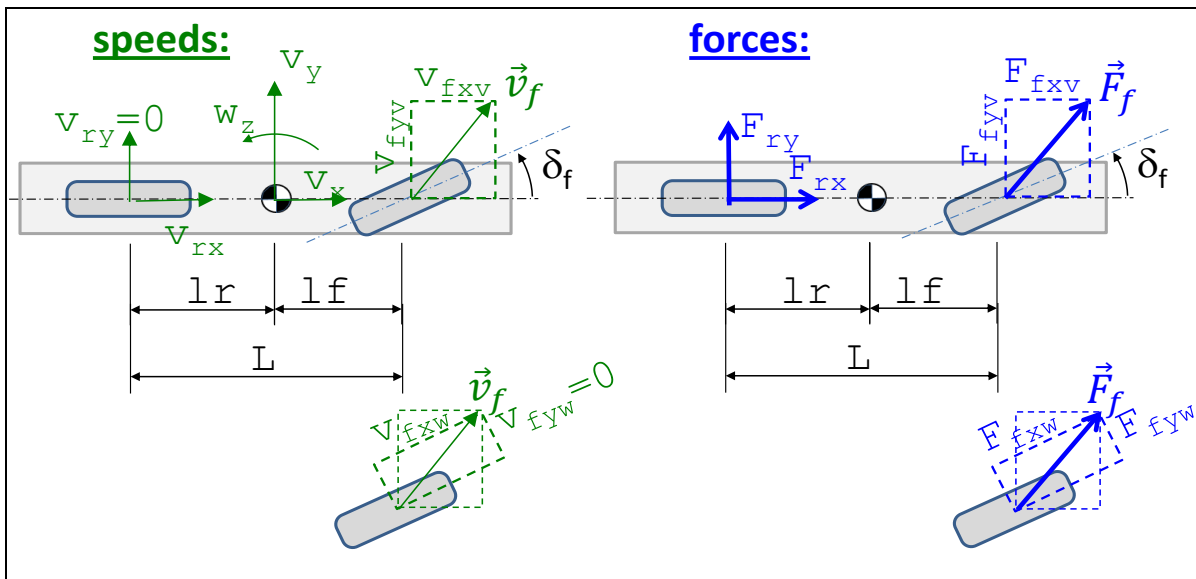


Figure 4-10: One-track model with ideally tracking axles. Lower view of front wheel shows conversion between wheel and vehicle coordinate systems.

The “physical model” in Figure 4-10 gives the following “mathematical model”:

Equilibrium (longitudinal, lateral and yaw-rotational):

$$\begin{aligned} 0 &= F_{fxv} + F_{rx}; \\ 0 &= F_{fyv} + F_{ry}; \\ 0 &= F_{fyv} \cdot l_f - F_{ry} \cdot l_r; \end{aligned}$$

Transformation between vehicle and wheel coordinate systems:

$$\begin{aligned} F_{fxv} &= F_{fxw} \cdot \cos(\delta_f) - F_{fyw} \cdot \sin(\delta_f); \\ F_{fyv} &= F_{fxw} \cdot \sin(\delta_f) + F_{fyw} \cdot \cos(\delta_f); \\ v_{fxv} &= v_{fxw} \cdot \cos(\delta_f) - v_{fyw} \cdot \sin(\delta_f); \\ v_{fyv} &= v_{fxw} \cdot \sin(\delta_f) + v_{fyw} \cdot \cos(\delta_f); \end{aligned}$$

[4.8]

Compatibility:

$$\begin{aligned}v_{fxv} &= v_x; \\v_{fyv} &= v_y + l_f \cdot \omega_z; \\v_{rx} &= v_x; \\v_{ry} &= v_y - l_r \cdot \omega_z;\end{aligned}$$

Ideal tracking (Constitutive relation, but without connection to forces):

$$\begin{aligned}v_{fyw} &= 0; \\v_{ry} &= 0;\end{aligned}$$

Path with orientation:

$$\begin{aligned}\dot{x} &= v_x \cdot \cos(\varphi_z) - v_y \cdot \sin(\varphi_z); \\ \dot{y} &= v_y \cdot \cos(\varphi_z) + v_x \cdot \sin(\varphi_z); \\ \dot{\varphi}_z &= \omega_z;\end{aligned}$$

Prescription of steering angle operation:

$$\delta_f = \begin{cases} (35 \cdot \pi/180) \cdot \sin(0.5 \cdot 2 \cdot \pi \cdot t); & \text{if } t < 4.5; \\ 35 \cdot \pi/180; & \text{else} \end{cases}$$

Rear axle undriven, which gives drag from roll resistance:

$$F_{rx} = -100;$$

The “Compatibility” in Eq [4.8] neglects the influence of steering axis offsets at ground, see Section 4.2.3.2. The terms neglected are of the type *LateralOffset* · δ ; in the equation for v_{fxv} and *LongitudinalOffset* · δ in the equation for v_{fyv} . This is generally well motivated for normal road vehicles, except for quick steering when vehicle is stand-still.

Equation [4.8] is written in Modelica format in Equation [4.9]. Comments are marked with //. The subscript v and w refers to vehicle coordinate system and wheel coordinate system, respectively. The actual assumption about ideal tracking lies in that $v_{fyw} = v_{ry} = 0$. Global coordinates from Figure 4-1 is also used.

```
//Equilibrium:
0 = Ffxv + Frx;
0 = Ffyv + Fry;
0 = Ffyv*lf - Fry*lr;

//Ideal tracking (Constitutive relation, but without connection to
forces):
vfyw = 0;
vry = 0;

//Compatibility:
vfxv = vx;
vfyv = vy + lf*wz;
vrx = vx;
vry = vy - lr*wz;

//Transformation between vehicle and wheel coordinate systems:
Ffxv = Ffxw*cos(df) - Ffyw*sin(df);
Ffyv = Ffxw*sin(df) + Ffyw*cos(df);
vfxv = vfxw*cos(df) - vfyw*sin(df);
vfyv = vfxw*sin(df) + vfyw*cos(df);

//Path with orientation:
der(x) = vx*cos(pz) - vy*sin(pz);
der(y) = vy*cos(pz) + vx*sin(pz);
der(pz) = wz;
```

[4.9]

```
// Prescription of steering angle:
df = if time < 4.5 then (35*pi/180)*sin(0.5*2*pi*time) else 35*pi/180;
//Rear axle undriven, which gives drag from roll resistance:
Frx = -100;
```

The longitudinal speed is a parameter, $v_x=10$ km/h. A simulation result from the model is shown in Figure 4-11. It shows the assumed steering angle function of time, which is an input. It also shows the resulting path, $y(x)$. The variables x, y, p_z are the “state variables” of this simulation.

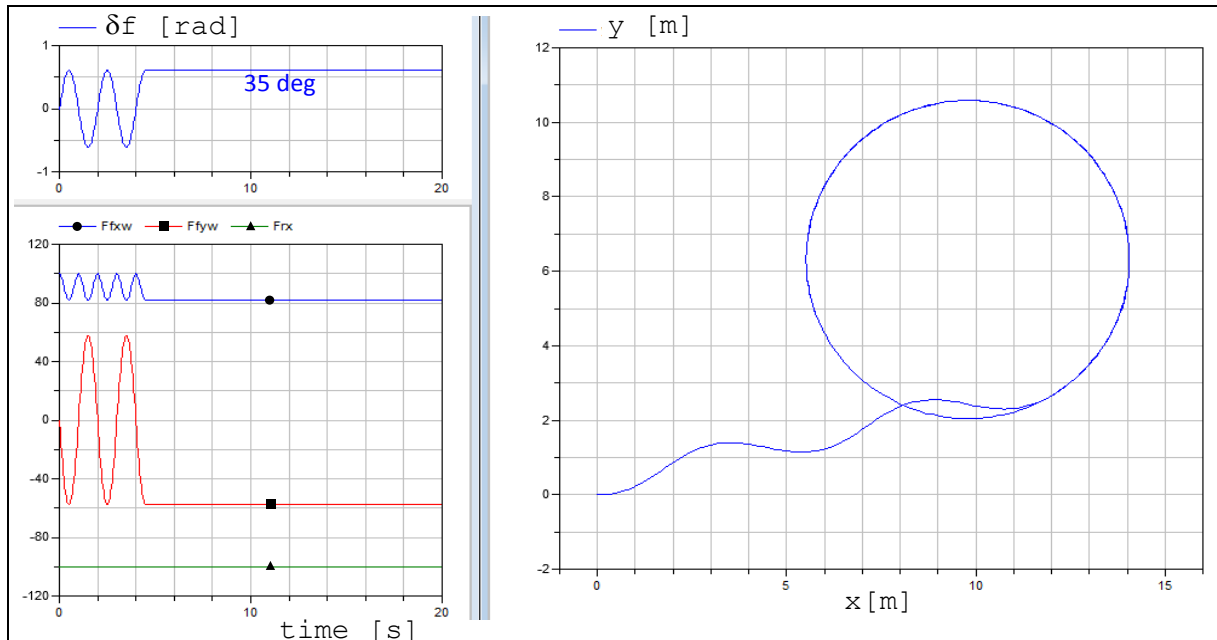


Figure 4-11: Simulation results of one-track model with ideal tracking.

The variables x, y, p_z are the only “state variables” of this simulation. If not including the path model (Equation [4.1]), the model would actually not be a differential equation problem at all, just an algebraic system of equations. That system of equations could be solved isolated for any value of steering angle without knowledge of time history. These aspects are the same for the steady state model in section 4.3.2.

A driving resistance of 100 N is assumed on the rear axle ($F_{rx} = -100$);. This is to exemplify that forces does not need to be zero, even if forces normally are not so interesting for low speed manoeuvres. Anyway, one should note that the speeds and forces are not coupled, since there are no inertial forces modelled. The modelling of forces is really a preparation for the case where we don’t have Ackerman geometry. For a two-axle one-track model we always have Ackermann geometry, because there is always an intersection point between the front and rear wheels rotational axes.

4.2.7 Turning circle *

*Function definition: **Turning diameter** is the diameter of the smallest possible circular path obtained steady state at low speed, measured to a certain point at the vehicle. The certain point can be either outer-most point on wheel (Kerb Turning diameter) or outer-most point on body (Wall Turning diameter).*

The turning circle (or turning diameter) is the diameter of the smallest circular turn that the vehicle is capable of making at low speed. The value should be as low as possible to enable best manoeuvrability in e.g. U-turns.

The end of the simulation in Figure 4-11 is made with constant steering angle. If we assume that it is the maximum steering angle, the circle actually shows the turning circle (diameter) for centre of gravity. If we add the path for the outermost wheels, we get the kerb or kerb-to-kerb turning circle diameter, see Figure 4-12. If we add the path for the outermost point at the vehicle body we get the wall or wall-to-wall turning circle diameter, also shown in Figure 4-12. The outermost point at the vehicle body is normally the front outer corners of the vehicle body, i.e. the outer front bumper end.

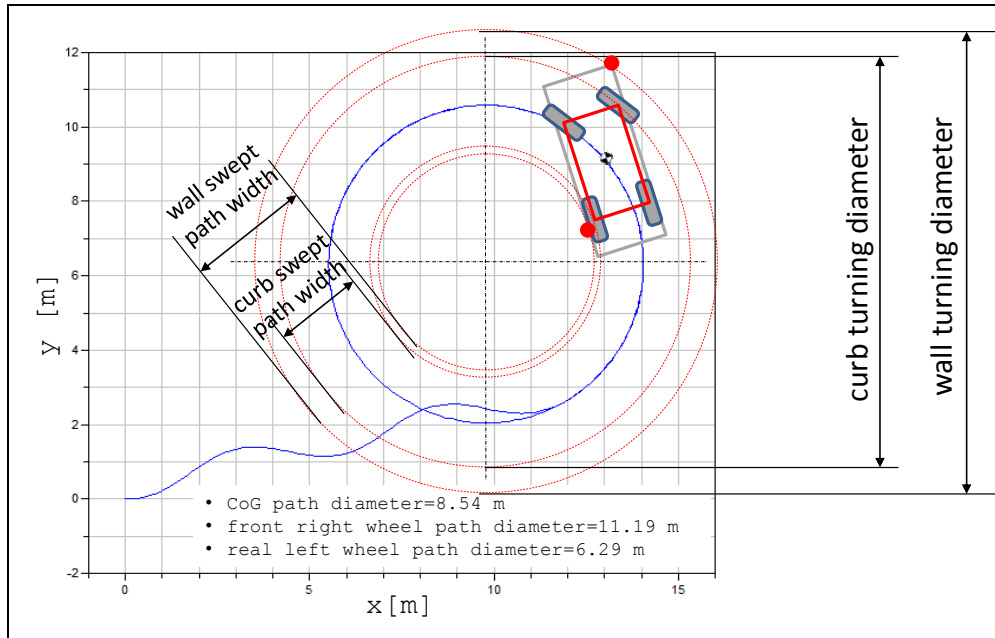


Figure 4-12: Adding paths for wheels and body points, on top of result in Figure 4-11.

Turning circle can also be defined for high speed, but it is more conventional to talk about curvature gain, which is not curvature at maximum steering angle, but the curvature per steering angle, see Section 4.2.12.

4.2.8 Swept path width and Swept Area *

*Function definition: **Swept path width** is the distance between the outermost and innermost trajectories of wheels (or body edges). The trajectories are then from a certain turning or lane change manoeuvre at a certain speed.*

*Function definition: **Swept path area** is the area between the outermost and innermost trajectories in the definition of Swept path width.*

For manoeuvrability, there is a function which is complementary to turning radius diameter. It is “Swept path width” (SPW), see Figure 4-12. It can occur as a kerb and wall version as well as turning circle radius can. It is the distance between the outermost and innermost wheel/point on the vehicle. The SPW should be as small as possible for improving manoeuvrability.

Another way of measuring approximately the same is “Swept Area”, which is the area between the outer and inner circle in Figure 4-12. Again, one can differ between kerb and wall version of this measure.

“Swept path width” and “Swept Area” is often used for low vehicle speeds. For higher speeds it is more common to talk about off-tracking, see next section.

4.2.9 Off-tracking *

*Function definition: **Off-tracking** is the distance between the outermost and innermost trajectories of centre points of the axles. The trajectories are then from a certain turning or lane change manoeuvre at a certain speed.*

Another measure of manoeuvrability is “Off-tracking”, see Figure 4-13. It is like swept area width, but for the centre point of the axles. It is also used for higher speeds, and then the rear axle can track on a larger circle than front axle.

Off-tracking is most relevant for vehicles with several units, such as truck with trailer. Off-tracking for driving several rounds in a circle is well defined since it is a steady state, but seldom the most relevant. Often, it is a more relevant to set requirements on off-tracking when driving from straight, via curve with certain radius, to a new straight in a certain angle from the first straight, e.g. 90 degrees. A way to predict off-tracking for this is to simulate with time integration, even if no traditional dynamics (mass inertia times acceleration) is modelled. The states in such simulation are the path coordinates with orientation (x, y, φ_z) .

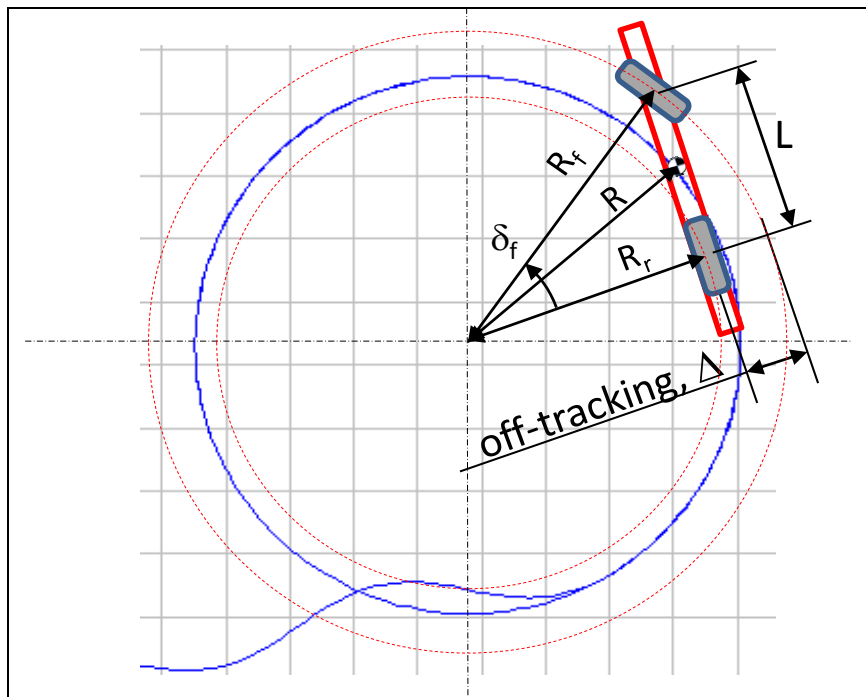


Figure 4-13: Adding one-track model, on top of result in Figure 4-11.

From geometry in Figure 4-13 on can find an expression for off-tracking at low speed:

$$\begin{aligned} \Delta &= R_f - R_r = \frac{R_r}{\cos(\delta_f)} - R_r = R_r \cdot \left(\frac{1}{\cos(\delta_f)} - 1 \right) = \sqrt{R^2 - l_r^2} \cdot \left(\frac{1}{\cos(\delta_f)} - 1 \right) \approx \\ &\approx R \cdot \left(\frac{1}{\cos(\delta_f)} - 1 \right) \approx R \cdot (1 - \cos(\delta_f)) \end{aligned}$$

[4.10]

4.2.10 Steering effort *

*Function definition: **Steering effort at low speed** is the steering wheel torque needed to turn the steering wheel a certain angle at a certain angular speed at vehicle stand-still on high road friction.*

*Function definition: **Steering effort at high speed** is the steering wheel torque (or subjectively assessed effort) needed to perform a certain avoidance manoeuvre at high road friction.*

At low or zero vehicle speed, it is often difficult to make steering wheel torque low enough. This has mainly two reasons:

See the Caster offset in Figure 4-5. It gives the wheel a side slip when steering and hence a tyre lateral force is developed. Tyre lateral forces times the caster offset is one part that steering efforts has to overcome.

Additionally, there is a spin moment in the contact patch, M_{ZT} in Figure 2-2. (M_{ZT} does not influence very much, except for at very low vehicle speed, which is why quantitative models for M_{ZT} are not presented in this compendium.) The spin moment also has to be overcome by steering efforts.

A critical test for steering effort at low speed is to steer a parked vehicle with a certain high steering wheel rotational speed, typically some hundred deg/s. The steering wheel torque is then required to stay under a certain design target value, normally a couple of Nm. The torque needed will be dependent on lateral force, spin moment and steering geometry (which is not steering speed dependent) and dependent on the capability of the power steering system (which is dependent on steering, due to delays in the steering assistance actuator). A failure in this test is called “catch-up”, referring to that driver catches up with the power steering system. It can be felt as a soft stop and measured as a step in steering wheel torque.

At higher vehicle speeds, the steering effort is normally less of a problem since unless really high steering wheel rate. Hence, steering wheel torque in avoidance manoeuvres in e.g. 70 km/h can be a relevant requirement. In these situations, the subjective assessment of steering effort can also be the measure. Then, steering effort is probably assessed based on both steering wheel rate and steering wheel torque.

4.2.11 One-track model for low speeds, with non-Ackerman geometry

The model in Figure 4-10 can rather easily be extended to more axles, more units and two-track model, if Ackermann geometry. However, if not Ackermann geometry, one has to do a structural change in the model, because ideal tracking is no longer consistent with geometry. One example is a two-track model of a two-axle vehicle which has parallel steering on one axle. Another example is a one-track model of a truck with three axles, whereof the two last are non-steered, see Figure 4-14.

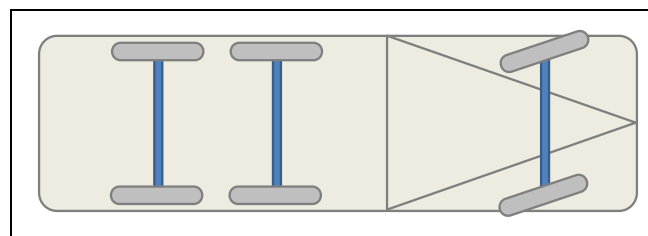


Figure 4-14: Rigid Truck with 3 axles, whereof only the first is steered.

We will go through model changes needed in the latter example. In order to compare the models as closely as possible, we simply split the rear axle into two rear axles, in the example in Section 4.2.6. The physical model becomes as in Figure 4-15. The measures appear in Figure 4-17, and you see that it is not a truck, but a very unconventional passenger size car with two rear axles.

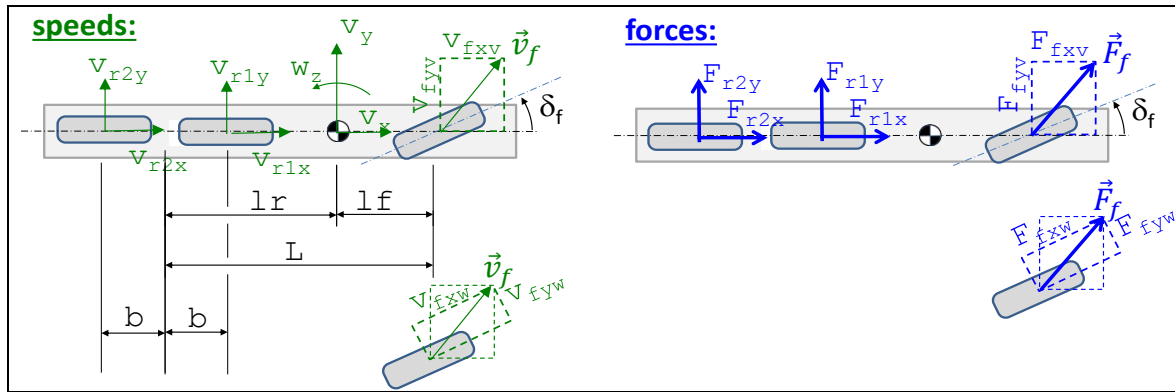


Figure 4-15: One-track model. Not Ackermann geometry, due to un-steered rear axles.

The changes we have to do in the model appear as underlined in Equation [4.11]. There has to be double variables for v_{rx} , v_{ry} , F_{rx} , F_{ry} , denoted 1 and 2 respectively. Also, we cannot use $v_{fyw}=v_{ry}=0$ anymore, but instead we have to introduce a lateral tyre force model, as described in Section 0.

```
//Equilibrium:
0 = Ffxv + Fr1x + Fr2x;
0 = Ffyv + Fr1y + Fr2y;
0 = Ffyv*lf - Fr1y*(lr - b) - Fr2y*(lr + b);

//Constitutive relation, i.e.
Lateral tyre force model (instead of Ideal tracking):
Ffyw = -Cf*sfy;
Fr1y = -Cr1*srly;
Fr2y = -Cr2*sr2y;
sfy = vfyw/vfxw;
srly = vrly/vrlx;
sr2y = vr2y/vr2x;

//Compatibility:
vfxv = vx;
vfyv = vy + lf*wz;
vrlx = vx;
vr2x = vx;
vrly = vy - (lr - b)*wz;
vr2y = vy - (lr + b)*wz;

//Transformation between vehicle and wheel coordinate systems:
Ffxv = Ffxw*cos(df) - Ffyw*sin(df);
Ffyv = Ffxw*sin(df) + Ffyw*cos(df);
vfxv = vfxw*cos(df) - vfyw*sin(df);
vfyv = vfxw*sin(df) + vfyw*cos(df);

//Path with orientation:
der(x) = vx*cos(pz) - vy*sin(pz);
der(y) = vy*cos(pz) + vx*sin(pz);
der(pz) = wz;

// Prescription of steering angle:
df = if time < 4.5 then (35*pi/180)*sin(0.5*2*pi*time) else 35*pi/180;
//Rear axles undriven, which gives drag from roll resistance:
Fr1x = -100/2;
Fr2x = -100/2;
```

[4.11]

The new result is shown in Figure 4-16, which should be compared to Figure 4-11. The radius of the final path radius increases a little. If we read out more carefully, we can draw the different locations of the instantaneous centre for both cases. This is shown, in scale, in Figure 4-17.

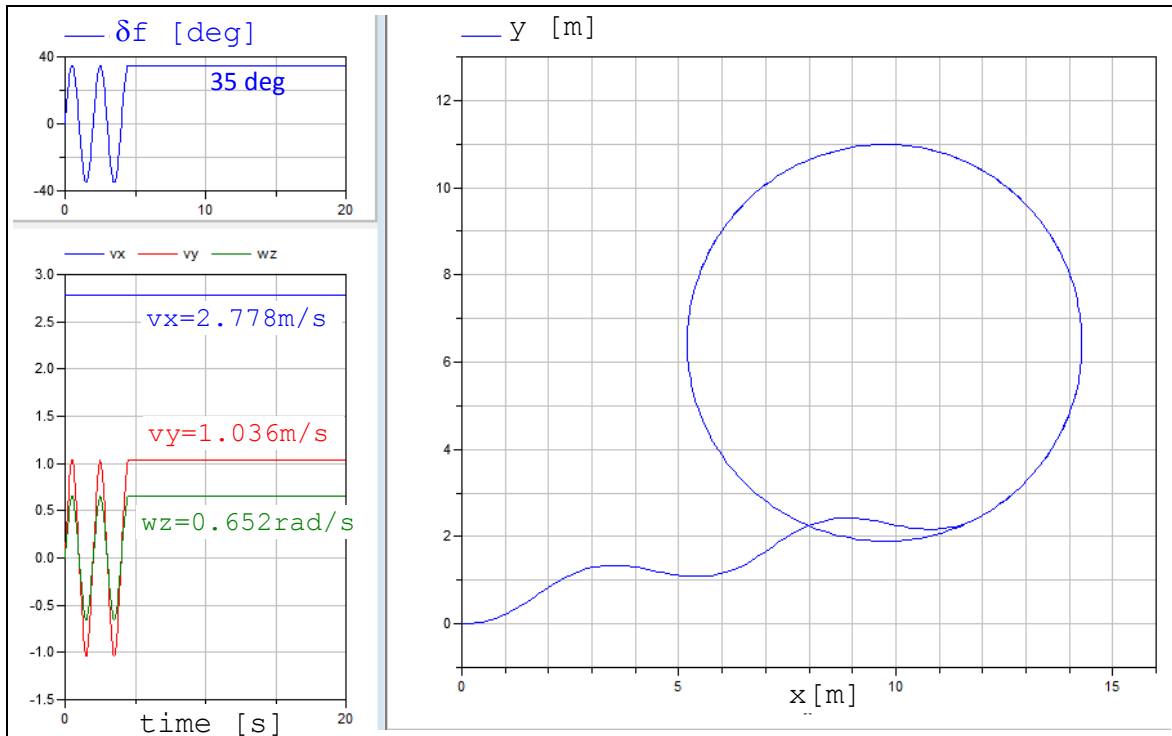


Figure 4-16: Simulation results of one-track model with ideal tracking. Non-Ackermann geometry due to two non-steered rear axles.

We could tune the steering angle required to reach exactly the same path radius as for the 2-axle reference vehicle. Then, we would have to steer a little more than the 35 degrees used, and we could find a new instantaneous centre, and we could identify a so called Equivalent wheelbase. This leads us to a definition: The equivalent wheel base of a multi-axle vehicle is the wheel base of a conventional two-axle vehicle which would exhibit the same turning behaviour as exhibited by the multi-axle vehicle, given same steering angle and similar axle cornering stiffnesses.

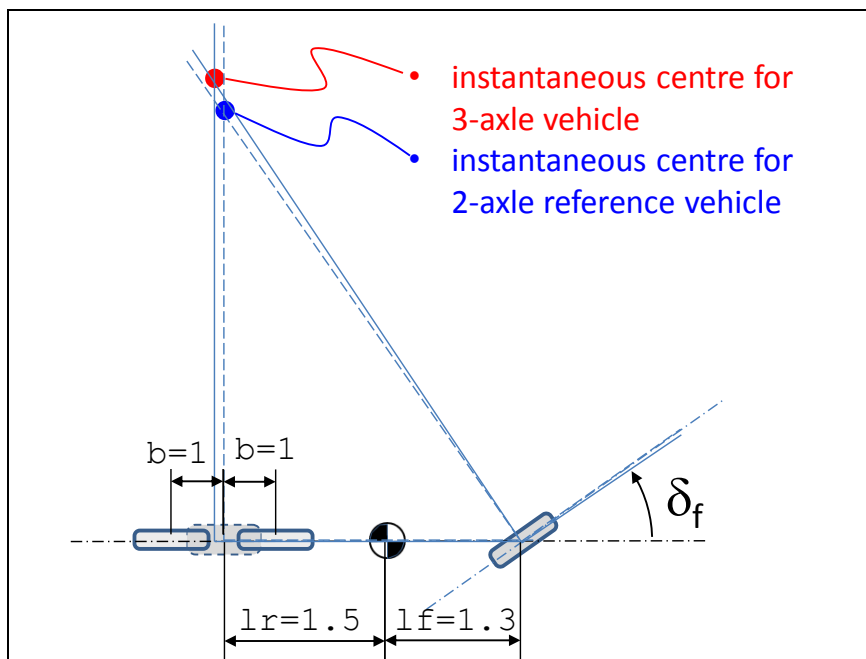


Figure 4-17: Instantaneous centre with a 3-axe vehicle, with the corresponding 2-axe vehicle as reference.

Section 4.2.11 shows that the lateral tyre force model, which is a constitutional relation, can sometimes be needed also at low speed analysis. However, it is always needed in next section about high speed cornering, Section 4.2.12.

4.2.12 One-track model for low speeds, with trailer

When the vehicles has an articulation point, also the low speed case (disregarding inertias) has transients in the sense that the articulation angles changes transiently. Consider the case of instantaneous step steer. For a vehicle without articulation point, a steady state is reached directly, since inertia is not considered. But for an articulated vehicle it takes some travelled distance (not time, since it can be studied independent of speed and time) before a steady state articulation angle is achieved.

So, for articulated vehicles, a scalar requirement on turning radius is not so relevant as for two axle vehicles. But, the function “4.2.8 Swept path width and Swept Area *” and “4.2.9 Off-tracking *” is, if road geometry is reflected, e.g. through outer radius and total angle of turning.

4.3 Steady state cornering at high speed

Steady state cornering refers to that all time derivatives of vehicle speeds (v_x, v_y, ω_z) are zero. The physical understanding is then that the vehicle drives on a circle with constant yaw rate, see Figure 4-18Figure 4-1. Alternatively, this can be described as driving with constant tangential speed (v), on a constant path radius (R) with and with a constant side slip angle (β).

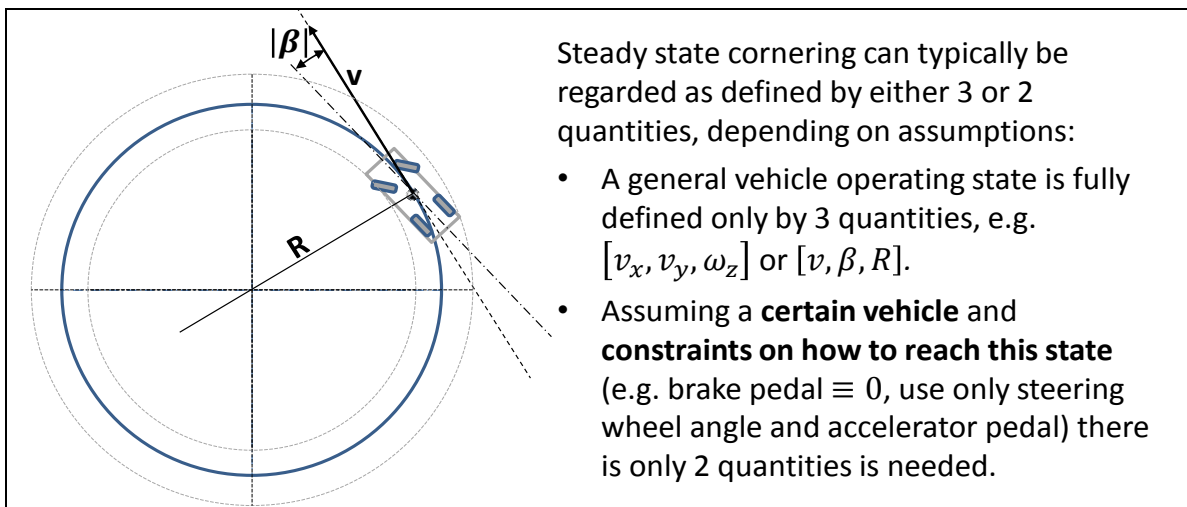


Figure 4-18: Steady state cornering.

4.3.1 Steady state driving manoeuvres

When testing steady state function, one usually runs on a so called “skid-pad” which appears on most test tracks, see Figure 4-8. It is a flat circular surface with typically 100 m diameter and some concentric circles marked. A general note is that tests in real vehicles are often needed to be performed in simulation also, and normally earlier in the product development process.

Typical steady state tests are:

- Constant path radius. Driven for different longitudinal speeds.
- Constant longitudinal speed. Driven for different path radii.

LATERAL DYNAMICS

- Constant steering wheel angle. Then increase accelerator pedal (or apply brake pedal) gently. (If too quick, the test would fall under transient handling instead.)

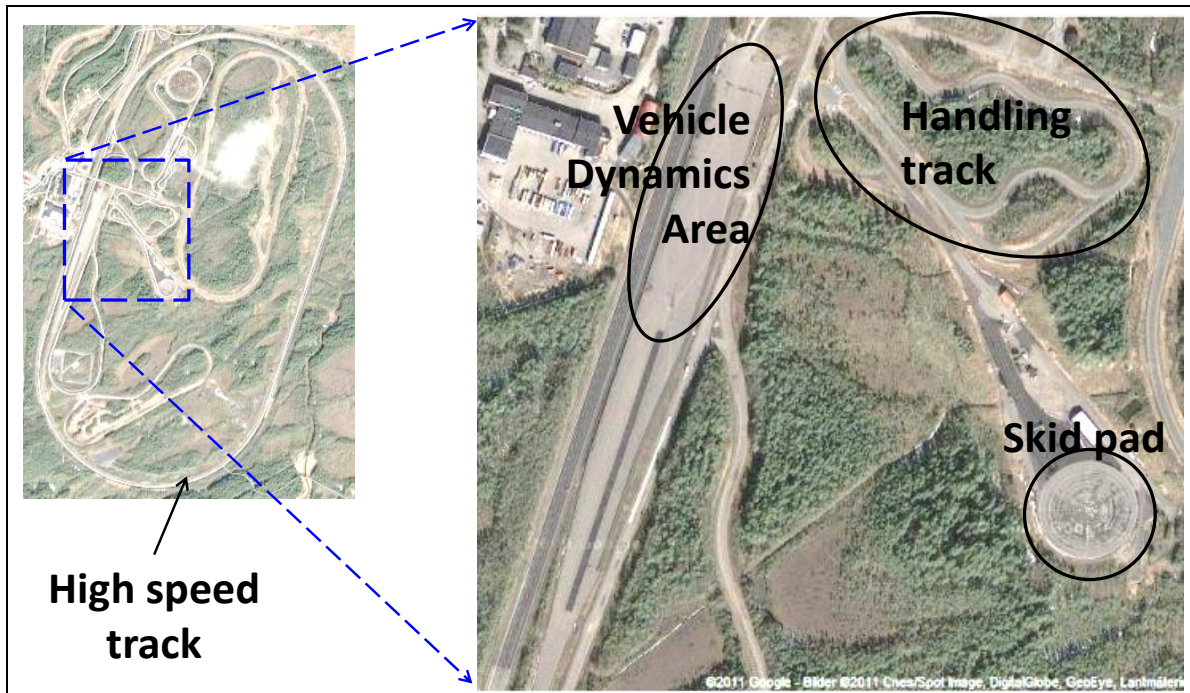


Figure 4-19: An example of test track and some parts with special relevance to Vehicle Dynamics. The example is Hällered Proving Ground, Volvo Car Corporation.

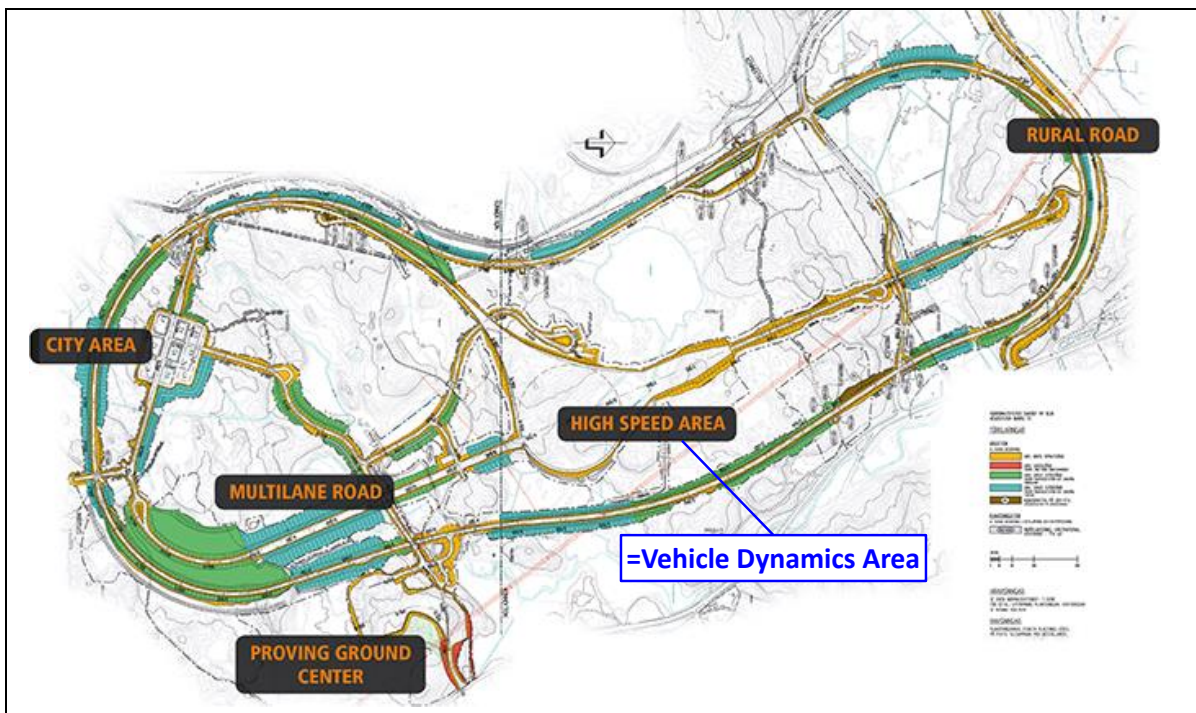


Figure 4-20: An example of test track. The example is AstaZero (Active Safety Test Arena), SP Technical Research Institute of Sweden and Chalmers University of Technology.

Standards which are relevant to these test manoeuvres are, e.g. References (ISO 4138) and (ISO 14792).

4.3.2 Steady state one-track model

In steady state we have neither inertial effects from changing the total vehicle speed ($v = \sqrt{v_x^2 + v_y^2}$ is constant) nor from changing the yaw rate (w_z is constant). However, the inertial “centrifugal” effect of the vehicle must be modelled. The related acceleration is the centripetal acceleration, $a_c = R \cdot \omega_z^2 = v^2/R = \omega_z \cdot v$.

A vehicle model for this is sketched in Figure 4-21. The model is a development of the model for low-speed in Figure 4-10 and Equation [4.9], with the following changes:

- Longitudinal and lateral accelerations are changed from zero to components of centripetal acceleration, a_c , as follows (see Figure 4-21):
 - $a_x = -a_c \cdot \sin(\beta) = -\omega_z \cdot v \cdot \sin(\beta) = -\omega_z \cdot v_y$;
 - $a_y = +a_c \cdot \cos(\beta) = +\omega_z \cdot v \cdot \cos(\beta) = +\omega_z \cdot v_x$;
- The constitutive assumptions for the axles are changed from ideal tracking to a (linear) relation between lateral force and lateral slip. The relations should capture the slip characteristics for the tyres, see Section 0, but they can also capture steering system compliance (see Section 4.3.4.3), roll steering (see Section 4.3.4.5) and side force steering (see Section 4.3.4.4). The total mathematical relations can anyway be written as:
 - $F_{fyw} = -C_f \cdot s_{fy}$; where $s_{fy} = v_{fyw}/v_{fxw}$;
 - $F_{ry} = -C_r \cdot s_{ry}$; where $s_{ry} = v_{ry}/v_{rx}$;

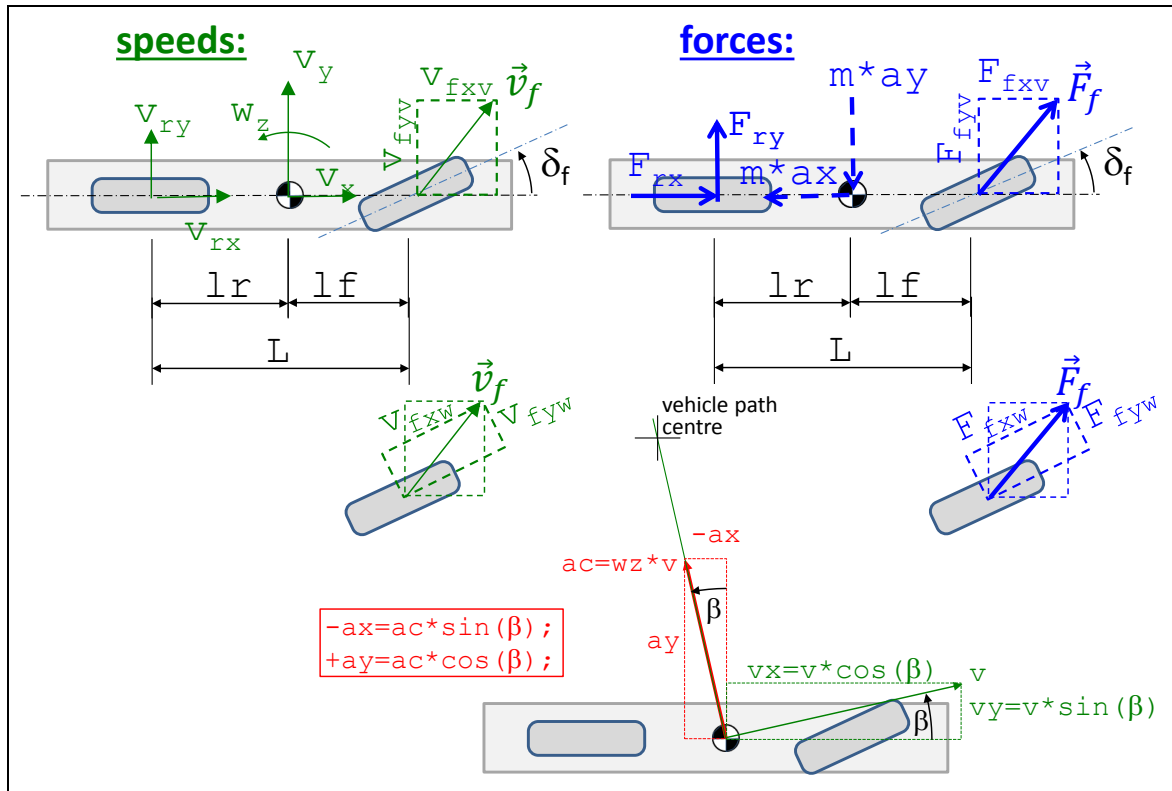


Figure 4-21: One-track model. Dashed forces and moment are fictive forces.

The model in Figure 4-21 is documented in mathematical form in Equation [4.12] (in Modelica format). The subscript v and w refers to vehicle coordinate system and wheel coordinate system, respectively.

```
//Equilibrium:
m*ax = Ffxv + Frx; //Air and grade resistance neglected
m*ay = Ffyv + Fry;
```

[4.12]

LATERAL DYNAMICS

```

J*0 = Ffyv*lf - Fry*lr; // der(wz)=0
-ax = wz*vy;
+ay = wz*vx;

//Constitutive relation, i.e. Lateral tyre force model:
Ffyw = -Cf*sfy;
Fry = -Cr*sry;
sfy = vfyw/vfxw;
sry = vry/vrx;

//Compatibility:
vfxv = vx;
vfyv = vy + lf*wz;
vrx = vx;
vry = vy - lr*wz;

//Transformation between vehicle and wheel coordinate systems:
Ffxv = Ffxw*cos(df) - Ffyw*sin(df);
Ffyv = Ffxw*sin(df) + Ffyw*cos(df);
vfxv = vfxw*cos(df) - vfyw*sin(df);
vfyv = vfxw*sin(df) + vfyw*cos(df);

//Path with orientation:
der(x) = vx*cos(pz) - vy*sin(pz);
der(y) = vy*cos(pz) + vx*sin(pz);
der(pz) = wz;

// Prescription of steering angle:
df = if time < 2.5 then (5*pi/180)*sin(0.5*2*pi*time) else 5*pi/180;
// Rear axle undriven, which gives drag from roll resistance:
Frx = -100; // =10000; //
//Ffxw=0;

```

The longitudinal speed is a parameter, $v_x=100$ km/h. A simulation result from the model is shown in Figure 4-11. It shows the assumed steering angle function of time, which is an input. It also shows the resulting path, $y(x)$.

A driving resistance of 100 N is assumed on the rear axle ($F_{rx}=-100$). This is to exemplify that longitudinal forces does not need to be zero, even if longitudinal forces normally are not so interesting for steady state high speed manoeuvres.

The variables x, y, p_z are the only “state variables” of this simulation. If not including the path model (Equation [4.1]), the model would actually not be a differential equation problem at all, just an algebraic system of equations. That system of equations could be solved isolated for any value of steering angle without knowledge of time history. These aspects are the same for the low speed model in section 4.2.6.

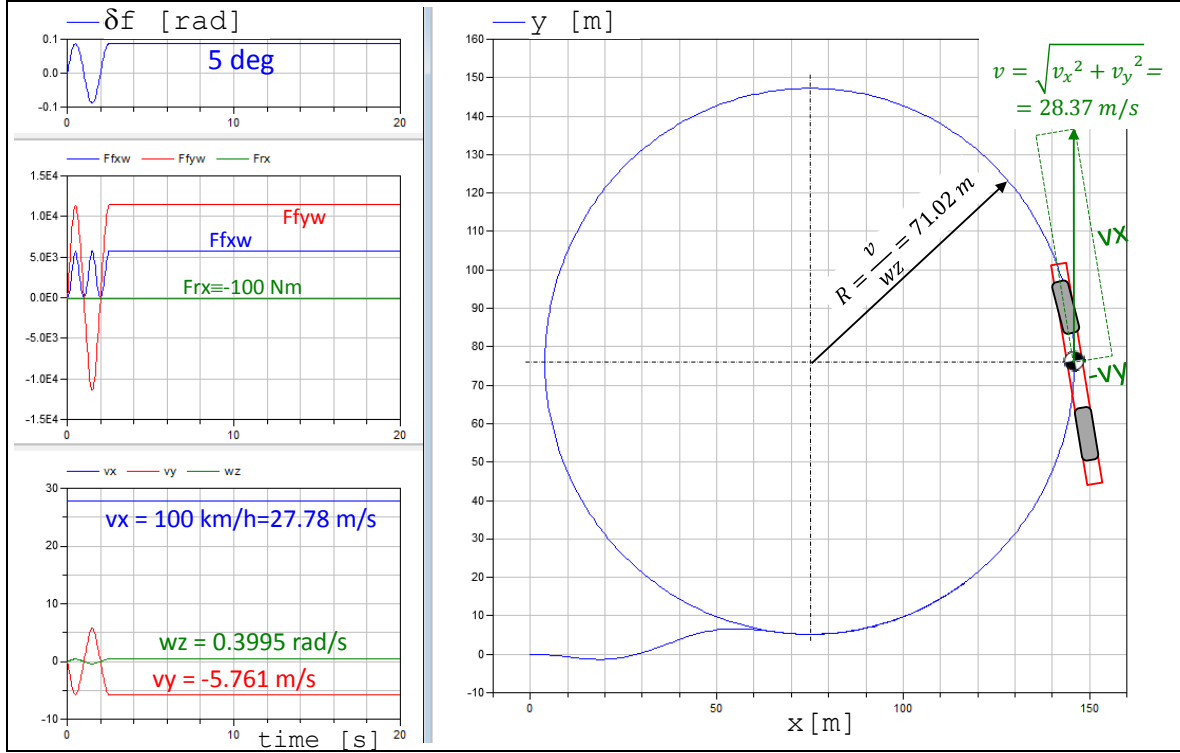


Figure 4-22: Simulation results of steady state one-track model. The vehicle sketched in the path plot is not in scale, but correctly oriented.

Equation [4.12] is a complete model suitable for simulation, but it does not facilitate understanding very well. We will reformulate it assuming small δ_f (i.e. $\cos(\delta_f) = 1$, $\sin(\delta_f) = 0$, and $\delta_f^2 = 0$). Eliminate slip, all forces that are not wheel longitudinal, and all velocities that are not CoG velocities:

$$\begin{aligned}
 & -m \cdot \omega_z \cdot v_y \cdot (v_x + (v_y + l_f \cdot \omega_z) \cdot \delta_f) = \\
 & = F_{fxw} \cdot (v_x + (v_y + l_f \cdot \omega_z) \cdot \delta_f) + C_f \cdot (v_y + l_f \cdot \omega_z) \cdot \delta_f + F_{rx} \cdot (v_x + (v_y + l_f \cdot \omega_z) \cdot \delta_f); \\
 & m \cdot \omega_z \cdot v_x \cdot (v_x + (v_y + l_f \cdot \omega_z) \cdot \delta_f) = \\
 & = -C_f \cdot (-v_x \cdot \delta_f + (v_y + l_f \cdot \omega_z)) + F_{fxw} \cdot \delta_f \cdot v_x - C_r \cdot \frac{v_x}{v_x} \cdot (v_x + (v_y + l_f \cdot \omega_z) \cdot \delta_f); \\
 & C_f \cdot (-v_x \cdot \delta_f + (v_y + l_f \cdot \omega_z)) \cdot l_f - F_{fxw} \cdot \delta_f \cdot l_f \cdot v_x = C_r \cdot \frac{v_x}{v_x} \cdot l_r \cdot (v_x + (v_y + l_f \cdot \omega_z) \cdot \delta_f);
 \end{aligned}
 \tag{4.13}$$

Equation [4.13] is a complete model, which we can see as a dynamic system without state variables.

- Actuation: Steering and wheel torque on each axle: $\delta_f, F_{fxw}, F_{rx}$.
- Motion quantities: v_x, v_y, ω_z

For example, we can chose δ_f, F_{fxw}, v_x and use the 3 equations to calculate F_{rx}, v_y, ω_z . In steady state analysis one often disregard the longitudinal equilibrium, which means to skip 1st equation and the unknown F_{rx} :

$$\begin{aligned}
 \omega_z & = \frac{C_f \cdot C_r \cdot L + (C_r \cdot l_f + C_r \cdot l_r) \cdot F_{fxw}}{C_f \cdot C_r \cdot L^2 + (C_r \cdot l_r - C_f \cdot l_f) \cdot m \cdot v_x^2} \cdot v_x \cdot \delta_f; \\
 v_y & = \frac{C_f \cdot (C_r \cdot L \cdot l_r - l_f \cdot m \cdot v_x^2) + (C_r \cdot L \cdot l_r - l_f \cdot m \cdot v_x^2) \cdot F_{fxw}}{C_f \cdot C_r \cdot L^2 + (C_r \cdot l_r - C_f \cdot l_f) \cdot m \cdot v_x^2} \cdot v_x \cdot \delta_f;
 \end{aligned}
 \tag{4.14}$$

4.3.2.1 Relation δ_f, v_x and R

Solving the first equation in Equation [4.14] yields:

$$\begin{aligned}
 \delta_f &= \frac{C_f \cdot C_r \cdot L^2 + (C_r \cdot l_r - C_f \cdot l_f) \cdot m \cdot v_x^2}{C_f \cdot C_r \cdot L + (C_r \cdot l_f + C_r \cdot l_r) \cdot F_{fxw}} \cdot \frac{\omega_z}{v_x} \approx \\
 &\approx \{ \text{assume: } F_{fxw} \approx 0 \} \approx \left(L + \frac{C_r \cdot l_r - C_f \cdot l_f}{C_f \cdot C_r \cdot L} \cdot m \cdot v_x^2 \right) \cdot \frac{\omega_z}{v_x} = \\
 &= \left\{ \text{define: } K_u = \frac{C_r \cdot l_r - C_f \cdot l_f}{C_f \cdot C_r \cdot L} = \frac{l_r}{C_f \cdot L} - \frac{l_f}{C_r \cdot L} \right\} = L \cdot \frac{\omega_z}{v_x} + K_u \cdot m \cdot a_y \approx \\
 &= \{ \text{use steady state: } a_y = \omega_z \cdot v_x \} = L \cdot \frac{\omega_z}{v_x} + K_u \cdot m \cdot \omega_z \cdot v_x \approx \\
 &\approx \left\{ \text{assume small } v_y \Rightarrow \frac{\omega_z}{v_x} \approx \frac{1}{R} \right\} \approx \frac{L}{R} + K_u \cdot \frac{m \cdot v_x^2}{R};
 \end{aligned}
 \tag{4.15}$$

The coefficient K_u is the *understeer gradient* and it will be explained in next section.

4.3.2.2 Relation δ_f, v_x and β

Solving the second equation in Equation [4.14] yields:

$$\begin{aligned}
 \delta_f &= \frac{C_f \cdot C_r \cdot L^2 + (C_r \cdot l_r - C_f \cdot l_f) \cdot m \cdot v_x^2}{C_f \cdot (C_r \cdot L \cdot l_r - l_f \cdot m \cdot v_x^2) + (C_r \cdot L \cdot l_r - l_f \cdot m \cdot v_x^2) \cdot F_{fxw}} \cdot \frac{v_y}{v_x} \approx \\
 &\approx \{ \text{use: } F_{fxw} = 0 \} \approx \frac{C_f \cdot C_r \cdot L^2 - (C_f \cdot l_f - C_r \cdot l_r) \cdot m \cdot v_x^2}{C_f \cdot C_r \cdot l_r \cdot L - C_f \cdot l_f \cdot m \cdot v_x^2} \cdot \frac{v_y}{v_x} \approx \\
 &\Rightarrow \begin{cases} \delta_f \xrightarrow{v_x \rightarrow 0} \frac{L}{l_r} \cdot \frac{v_y}{v_x}; \\ \delta_f \xrightarrow{v_x \rightarrow \infty} \frac{C_f \cdot l_f - C_r \cdot l_r}{C_f \cdot l_f} \cdot \frac{v_y}{v_x} = -K_u \cdot C_r \cdot \frac{L}{l_f} \cdot \frac{v_y}{v_x}; \end{cases}
 \end{aligned}
 \tag{4.16}$$

We can see that there is a speed dependent relation between steering angle and side slip, $\frac{v_y}{v_x}$. The side slip can also be expressed as a side slip angle, $\beta = \arctan\left(\frac{v_y}{v_x}\right)$. Since normally $K_u > 0$, the side slip changes sign, when increasing speed from zero to sufficient high enough. This should feel intuitively correct, if agreeing on the conceptually different side slip angles at low and high speed, as shown in Figure 4-23. We will come back to this equation in context of Figure 4-33.

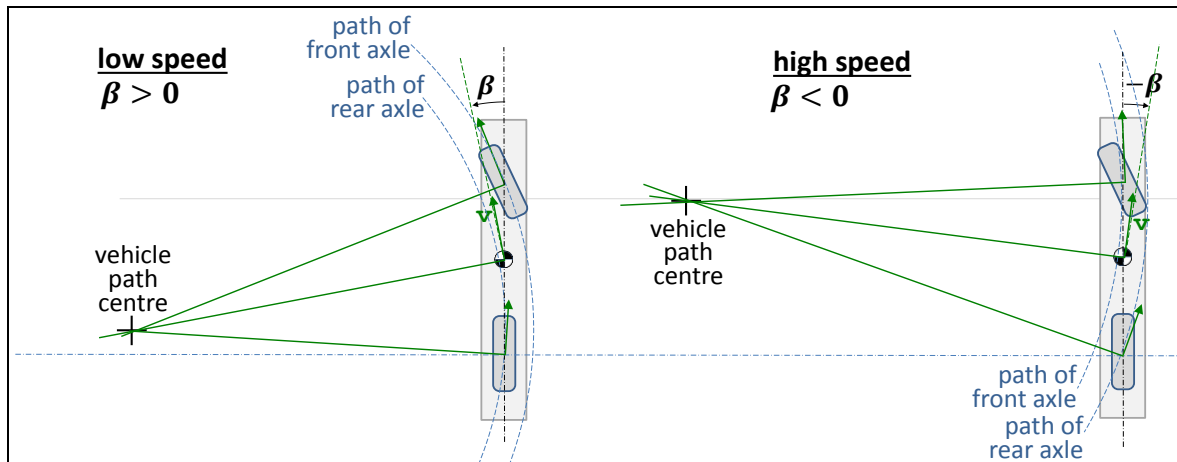


Figure 4-23: Body Slip Angle for Low and High Speed Steady State Curves

4.3.2.3 Relation v_x , R and β

If we approximate $F_{fxw} = 0$ and use both equations in Equation [4.14] to eliminate δ_f we get:

$$\frac{C_r \cdot L \cdot l_r - l_f \cdot m \cdot v_x^2}{C_r \cdot L} = l_r - \frac{l_f \cdot m \cdot v_x^2}{L \cdot C_r} = \frac{v_y}{\omega_z} = \frac{v_x}{\omega_z} \cdot \frac{v_y}{v_x} \approx R \cdot \tan(\beta); \Rightarrow$$

$$\Rightarrow \frac{v_y}{v_x} = \tan(\beta) = \left(l_r - \frac{l_f \cdot m \cdot v_x^2}{L \cdot C_r} \right) \cdot \frac{1}{R};$$

[4.17]

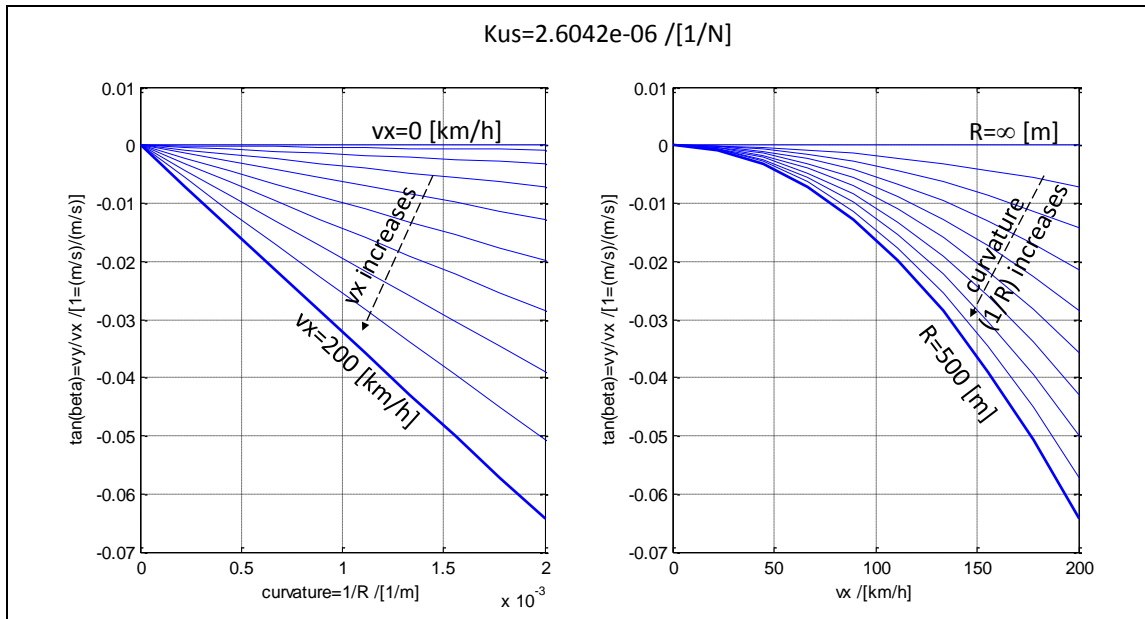


Figure 4-24: How side slip varies with curvature and longitudinal vehicle speed.

4.3.2.4 Simpler model

A simpler way to reach the final expression is given in Figure 4-25. Here, the simplifications are introduced earlier, already in physical model, which means e.g. that the influence of F_{fxw} is not identified.

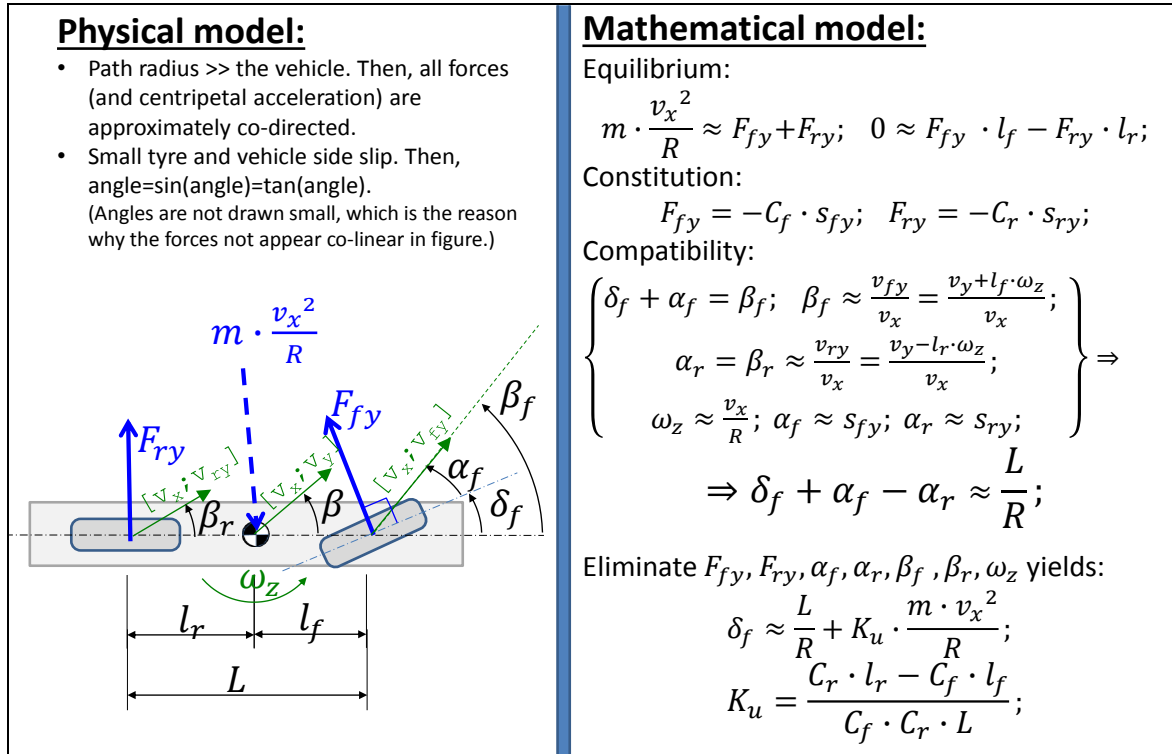


Figure 4-25: Simpler derivation final step in Equation [4.15].

The validity of the steady state model described in this section, section 4.3.2, is of course limited by if the manoeuvre is transient which would mean that steady state is not reached. But it is also limited by if the assumption of linear tyre characteristics, $F_y = -C \cdot s_y$, is violated. Therefore, one should check if some axle (or wheel) is calculated to use more than some certain fraction of available friction, $F = \sqrt{F_x^2 + F_y^2} > fraction \cdot \mu \cdot F_z$; In many cases, one can argue for this limiting fraction to be in the order of 0.5.

4.3.3 Under-, Neutral- and Over-steering *

4.3.3.1 Understeering as built-in measure

Function definition: Understeering (gradient) is the additional steering angle needed per increase of lateral force (or lateral acceleration) when driving in high speed steady state cornering on level ground and high road friction. Additional refers to low speed. The gradient is defined at certain high speed steady state cornering conditions, including straight-line driving. Steering angle can be either road wheel angle or steering wheel angle.

K_u in Equation [4.15] is called “understeer gradient” and has hence the unit rad/N or 1/N. Sometimes one can see slightly other definitions of what to include in definition of understeer gradient, which have different units, see K_{u2} and K_{u3} in Equation [4.18]. (When defined as K_{u3} , one can sometimes see the unit “rad/g” used, which present compendium recommended to not use.)

$$\delta_f = \frac{L}{R} + \frac{C_r \cdot l_r - C_f \cdot l_f}{C_f \cdot C_r \cdot L} \cdot \frac{m \cdot g \cdot v_x^2}{g \cdot R} =$$

$$= \left\{ \text{use: } K_{u2} = m \cdot g \cdot \frac{C_r \cdot l_r - C_f \cdot l_f}{C_f \cdot C_r \cdot L} [1 \text{ or rad}] \right\} = \frac{L}{R} + K_{u2} \cdot \frac{v_x^2}{g \cdot R}; \quad [4.18]$$

$$\begin{aligned}\delta_f &= \frac{L}{R} + \frac{C_r \cdot l_r - C_f \cdot l_f}{C_f \cdot C_r \cdot L} \cdot \frac{m \cdot v_x^2}{R} = \\ &= \left\{ \text{use: } K_{u3} = m \cdot \frac{C_r \cdot l_r - C_f \cdot l_f}{C_f \cdot C_r \cdot L} \left[\frac{1}{m/s^2} \text{ or } \frac{\text{rad}}{m/s^2} \right] \right\} \\ &= \frac{L}{R} + K_{u3} \cdot \frac{v_x^2}{R};\end{aligned}$$

The first term in the final expression in Equation [4.15], L/R , can be seen as a reference steering angle. This is referred to as either “low speed steering angle” or “Ackermann steering angle”. The understanding of this steering angle can be expanded to cover more general vehicles: It is the angle required for low speed turning. For a general vehicle, e.g. with other steering geometry than Ackermann, the angle cannot be calculated as simple as L/R , but with some specific derived formula, or it can be measured on a real vehicle. It is common to use the subscript A. It can be defined for front axle road wheel steering angle, δ_{fA} . It can also be defined for steering wheel angle, δ_{swA} .

The understeering gradient, K_u , is normally positive, which means that most vehicles require more steering angle for a given curve, the higher the speed is. Depending on the sign of K_u a vehicle is said to be oversteered (if $K_u < 0$), understeered (if $K_u > 0$) and neutral steered (if $K_u = 0$). In practice, all vehicles are designed as understeered, because over steered vehicle would become instable very easily.

The understeering gradient K_u can be understood as how much additionally to the Ackermann steering angle one have to steer, in relation to centrifugal force, F_c :

$$\delta_f = \delta_{fA} + K_u \cdot \frac{m \cdot v_x^2}{R} = \delta_{fA} + K_u \cdot F_c; \Rightarrow K_u = \frac{\delta_f - \delta_{fA}}{F_c} = \frac{\Delta\delta_f}{F_c};$$

Or, using the steering ratio, $\delta_f = \delta_{sw}/r_{ste}$:

$$\begin{aligned}\delta_{sw} &= \delta_{swA} + K_u \cdot \frac{r_{ste} \cdot m \cdot v_x^2}{R} = \delta_{fA} + K_u \cdot r_{ste} \cdot F_c; \Rightarrow \\ &\Rightarrow K_u = \frac{\delta_{sw} - \delta_{swA}}{r_{ste} \cdot F_c} = \frac{\Delta\delta_{sw}}{r_{ste} \cdot F_c};\end{aligned}$$

[4.19]

4.3.3.2 Understeering as varying with steady state lateral acceleration

So far, the understeering gradient is presented as a fix built-in vehicle parameter. There is nothing that says that a real vehicle behaves linear, so in order to get a well-defined value of K_u , the $\Delta\delta_f$ and the F_c should be small when using Eq [4.20]. However, if we accept that K_u can change with F_c , K_u can be defined as a differential quantity:

K_u can also be understood as how much the additional steering angle, $\Delta\delta_f$, has to increase per increased centrifugal force, F_c , or per lateral acceleration, a_y :

$$K_u = \frac{\partial(\Delta\delta_f)}{\partial F_c} = \frac{\partial}{\partial F_c} (\delta_f - \delta_A) = \frac{\partial\Delta\delta_f}{\partial F_c}; \text{ or } K_{u3} = \frac{\partial(\Delta\delta_f)}{\partial a_y} = \frac{\partial}{\partial a_y} (\delta_f - \delta_A) = \frac{\partial\delta_f}{\partial a_y};$$

[4.20]

Equation [4.20] shows the understeering gradient as a (mathematical) function, rather than a scalar parameter. But it is still fix and built-in in the vehicle. If assessing understeering for a lateral forces up to near road friction limit, Equation [4.20] is more relevant than Equation [4.15], because it reflects that understeering gradient changes.

4.3.3.3 Understeering as variable during a transient manoeuvre

A third understanding of the word understeering is quite different and less strictly defined. It is to see the understeering as a variable during a transient manoeuvre. For instance, a vehicle can be said to understeer if tyre side slip is larger on front axle than on rear axle, $|\alpha_f| > |\alpha_r|$, and over-steer if opposite, $|\alpha_r| > |\alpha_f|$. This way of defining understeering and oversteering is not built in, but varies over time through a (transient) manoeuvre. E.g., when braking in a curve a vehicle loses grip on rear axle due to temporary load transfer from rear to front. Then the rear axles can slide outwards significantly and the vehicle can be referred to as over-steering at this time instant, although the built-in understeering gradient is >0 . This “instantaneous” under-/over-steering can be approximately found from log data with this simple approximation:

$$\delta_{neutral} = \frac{L}{R} \approx \{v_x \approx R \cdot \omega_z\} \approx \frac{L \cdot \omega_z}{v_x} \approx \{a_y \approx v_x \cdot \omega_z\} \approx \frac{L \cdot a_y}{v_x^2}; \quad [4.21]$$

If the actual vehicle has $|\delta| > |\delta_{neutral}|$ the vehicle oversteers ($|\alpha_r| > |\alpha_f|$), and vice versa. This is often very practical since it only requires simply logged data, δ , v_x and a_y . Note that when δ and a_x have different signs, neither understeer or oversteers is suitable as classification, but it can sometimes be called “counter-steer”.

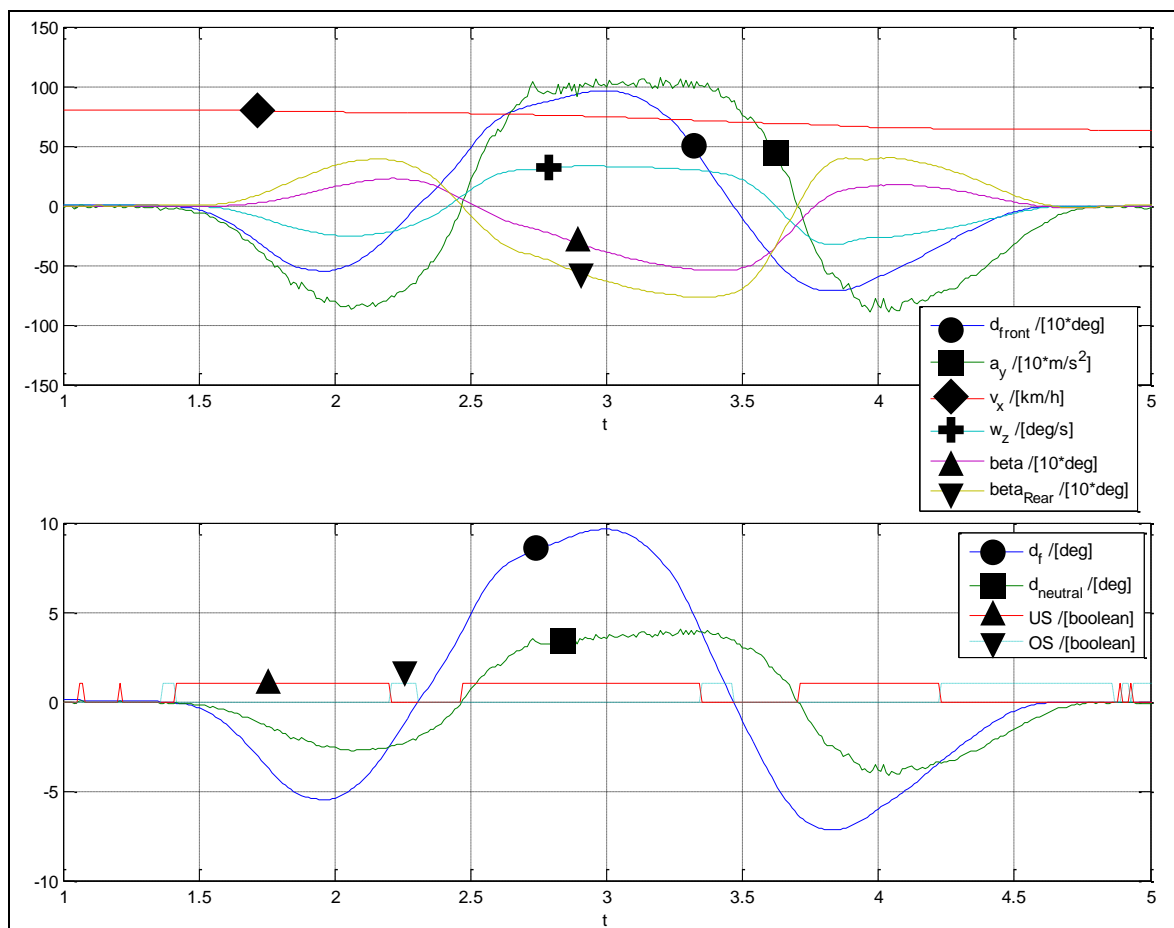


Figure 4-26: Upper: Log data from passenger car with ESC system in a double lane change. Lower: $\delta_{neutral}$ can be used to approximately assess “instantaneous” under-/over-steering (US/OS).

A second look at Equation [4.15] tells us that we have to assume absence of propulsion and braking on front axle, $F_{f_{xw}} = 0$, to get the relatively simple final expression. When propulsion on front axle ($F_{f_{xw}} > 0$), the required steering angle, δ_f , will be smaller; the front propulsion pulls in the front end of the vehicle. When braking on front axle ($F_{f_{xw}} < 0$), the required steering angle, δ_f , will be larger; the front braking hinders the front end to turn in. To keep v_x constant, which is required within definition of steady state, one have to propel the vehicle because there will always be some driving resistance to overcome. Driving fast on a small radius is a situation where the driving resistance from tyre lateral forces becomes significant, which is a part of driving resistance which was only briefly mentioned in Section 3.2.

Above reasoning was made for steady-state both longitudinally and laterally. If longitudinal acceleration, we can still assume lateral steady-state and study under-steering gradient. This is discussed in Section 4.3.4.1.

4.3.3.4 Neutral steering point

An alternative measure to understeering coefficient is the longitudinal position of the *neutral steering point*. The point is defined for lateral force disturbance during steady state **straight-ahead** driving, as opposed to steady state cornering without lateral force disturbance. The point is where a vehicle-external lateral force, such as wind or impact, can be applied on the vehicle without causing a yaw velocity ($\omega_z = 0$), i.e. only causing lateral velocity ($v_y \neq 0$). From this definition we can derive a formula for calculating the position of the neutral steering point, see Figure 4-27.

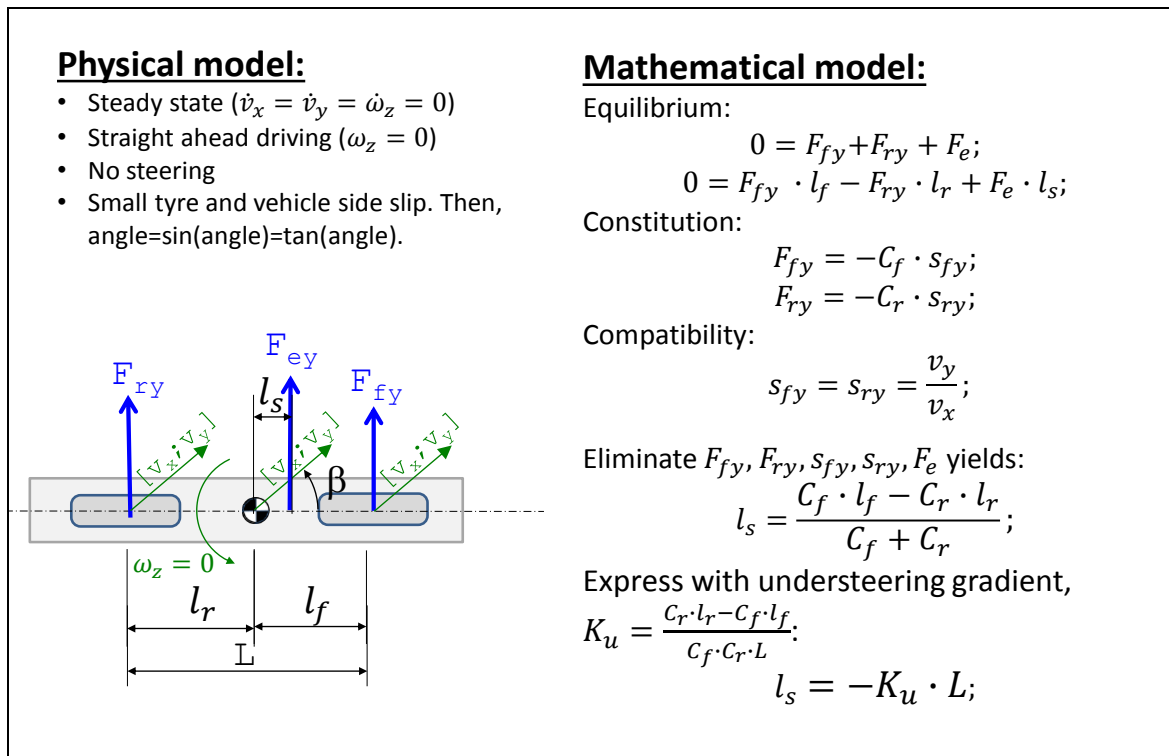


Figure 4-27: Model for definition and calculation of neutral steering point.

The result is condensed in Eq [4.22].

$$l_s = \frac{C_f \cdot l_f - C_r \cdot l_r}{C_f + C_r} = -K_u \cdot L; \quad \text{where } K_u = \frac{C_r \cdot l_r - C_f \cdot l_f}{C_f \cdot C_r \cdot L};$$

[4.22]

We can see that the understeer gradient from steady state cornering model appears also in the formula for neutral steering point position, l_s . This is why l_s (or rather $\frac{l_s}{L}$) and K_u can be said to be alternative measures for the same vehicle function/character, the yaw balance. It also proposes an alternative understanding of the understeering gradient; if $K_u = 0.1$, the neutral steering point is located $0.1 \cdot L$ rear of CoG.

4.3.4 How to design for a desired understeer gradient

The values of cornering stiffness for each axle are design parameters to influence understeer gradient. However, cornering stiffness is an abstract design parameter, in the sense that one cannot put it on a drawing. Instead, cornering stiffness is a combined effect from various, more concrete, design parameters. Such more concrete design parameters are briefly presented in the following.

4.3.4.1 Tyre design, inflation pressure and number of tyres

(This section discusses also influence of longitudinal acceleration, which is no tyre design parameter. However, it is logical in the sense that longitudinal acceleration influence yaw balance via how the tyres cornering stiffness varies with tyre normal load, which is directly influenced by the longitudinal acceleration.)

The cornering stiffness of each tyre is an obvious parameter which influences the axle stiffness. The cornering stiffness of an axle is influence by the sum of cornering stiffness for all tyres. There are normally two tyres per axle, but there are also vehicles with one tyre (e.g. bicycles) or 4 (typically 2 double mounted on each side in heavy trucks).

Tyre design influences, which is geometrical dimensions and material selection. Inflation pressure is in this context very close to a design parameter.

In a first approximation, tyre cornering stiffness is approximately proportional to vertical load: $C_i = k_i \cdot F_{iz}$. For a vehicle with equally many and same tyres front and rear, this means that it will be neutral steered. This is because, in steady state cornering, vertical loads distributes in same relation as lateral loads. Using definition of understeer gradient:

$$\begin{aligned} \frac{K_{u2}}{m \cdot g} &= \frac{l_r}{C_f \cdot L} - \frac{l_f}{C_r \cdot L} = \frac{l_r}{k_f \cdot F_{fz} \cdot L} - \frac{l_f}{k_r \cdot F_{rz} \cdot L} = \left\{ \begin{array}{l} \text{longitudinal} \\ \text{load transfer} \end{array} \right\} \Rightarrow \\ \Rightarrow K_{u2} &= \frac{m \cdot g \cdot l_r}{k_f \cdot \left(m \cdot g \cdot \frac{l_r}{L} - m \cdot a_x \cdot \frac{h}{L} \right) \cdot L} - \frac{m \cdot g \cdot l_f}{k_r \cdot \left(m \cdot g \cdot \frac{l_f}{L} + m \cdot a_x \cdot \frac{h}{L} \right) \cdot L} = \\ &= \frac{l_r/L}{k_f \cdot \left(\frac{l_r}{L} - \frac{a_x}{g} \cdot \frac{h}{L} \right)} - \frac{l_f/L}{k_r \cdot \left(\frac{l_f}{L} + \frac{a_x}{g} \cdot \frac{h}{L} \right)} = \left\{ \begin{array}{l} \text{if } a_x = 0 \\ \text{and} \\ k_f = k_r \end{array} \right\} = 0; \end{aligned} \quad [4.23]$$

Longitudinal load transfer (influence of a_x in the equations) show that braking increases oversteering tendency. It is actually so, that the critical speed $v_{x,crit} = \sqrt{L/(-K_u \cdot m)}$ (see Equation [4.27]) can come down to quite reachable levels when braking hard; i.e. hard braking at high speed may cause instability. This is especially so for front biased CoG location. See Figure 4-28, inspired by Reference (Drenth, 1993).

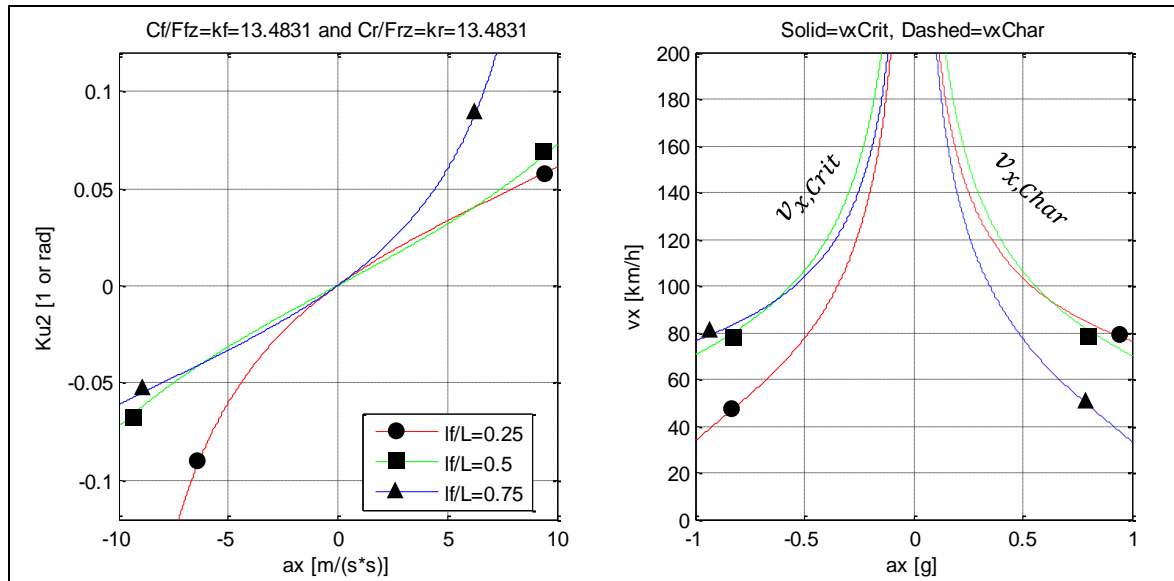


Figure 4-28: Left: Under-steering gradient as function of longitudinal acceleration, ax , and static load distribution, l_f/L . Right: Critical and characteristic velocity as function of acceleration and load distribution.

However, the cornering stiffness varies degressively, e.g. $C_i = k_{ip} \cdot F_{iz} - k_{id} \cdot F_{iz}^2$. This is further studied in Reference (Drenth, 1993).

If taking the degressiveness of tyre cornering stiffness into account, the weight distribution plays a role also without longitudinal load transfer; front biased weight distribution gives under-steered vehicles and vice versa. Also, the number of wheel per axle influence stronger; single wheel front (or double-mounted rear) gives under-steered vehicles and vice versa.

4.3.4.2 Roll stiffness distribution between axles

During cornering, the vertical load is shifted towards the outer wheels. Depending on the roll stiffness of each axle, the axles take differently much of this load shift. Then, the lateral load transfer also influences the yaw balance, see Section 4.3.4.2.

The more roll stiff an axle is, the more of the lateral load shift it takes. Tyre cornering stiffness varies degressively with vertical load. Together, this means that increasing the roll stiffness on the front axle, leads to less front cornering stiffness and consequently more understeered vehicle. Increasing roll stiffness on rear axle makes the vehicle less understeered.

One can change the roll stiffness of an axle by changing roll centre height, wheel stiffness rate and anti-roll bar stiffness. This effect is further described in Section 4.3.9.6.

4.3.4.3 Steering system compliance

A compliant steering system will reduce the effective cornering stiffness on the steered axle. With normal front axle steering, a compliant steering means a more understeered vehicle.

4.3.4.4 Side force steer gradient

Side force steer gradient, c_{iSFS} , is defined for an axle and it is how much the wheels on an axle steers [deg] per lateral force [N]. Also a non-steered axle steers due to side force steering, which depends on the compliance of the suspension bushings.

It can be modelled as an extra compliance, with the constitutional equations: $F_{fy} = -c_{fSFS} \cdot \Delta\delta_f$; and $F_{ry} = -c_{rSFS} \cdot \Delta\delta_r$, where the Δ marks additional steering angle due to the lateral force. These

extra compliances comes into play as series connected with the tyre cornering compliances. If we update Equation [4.15] with side force steering it becomes:

$$\delta_f = \frac{L}{R} + K_u \cdot \frac{m \cdot v_x^2}{R};$$

$$\text{where } K_u = \frac{l_r}{C_{f,tot} \cdot L} - \frac{l_f}{C_{r,tot} \cdot L} = \frac{C_{r,tot} \cdot l_r - C_{f,tot} \cdot l_f}{C_{f,tot} \cdot C_{r,tot} \cdot L};$$

$$\text{where } C_{f,tot} = \frac{1}{\frac{1}{C_f} + \frac{1}{c_{fSFS}}} \quad \text{and} \quad C_{r,tot} = \frac{1}{\frac{1}{C_r} + \frac{1}{c_{rSFS}}};$$

[4.24]

4.3.4.5 Roll steer gradient

Roll steer gradient, c_{iRS} , is defined for an axle and it is how much the wheels on an axle steers [deg] per vehicle roll angle [deg]. Also a non-steered axle steers due to roll-steering, which depends on the suspension linkage geometry. The added steering angle can hence be expressed: $\Delta\delta_i = -c_{iRS} \cdot \varphi_x$;

If one assumes steady state cornering, the vehicle roll angle depends on the vehicle's roll gradient, c_{roll} as: $\varphi_x = c_{roll} \cdot a_y$; For steady state, it is also possible to express $F_{iy} = m \cdot a_y \cdot (L - l_f)/L$; In total: $\Delta\delta_i = -c_{iRS} \cdot c_{roll} \cdot F_{iy} \cdot L / (m \cdot (L - l_f)) = -c_{iRS,F} \cdot F_{iy}$; The parameter $c_{iRS,F}$ comes into the equations in exactly the same way as side force steering gradient, c_{iSFS} , so:

$$\delta_f = \frac{L}{R} + K_u \cdot \frac{m \cdot v_x^2}{R};$$

$$\text{where } K_u = \frac{l_r}{C_{f,tot} \cdot L} - \frac{l_f}{C_{r,tot} \cdot L} = \frac{C_{r,tot} \cdot l_r - C_{f,tot} \cdot l_f}{C_{f,tot} \cdot C_{r,tot} \cdot L};$$

$$\text{where } C_{f,tot} = \frac{1}{\frac{1}{C_f} + \frac{1}{c_{fRS,F}}} \quad \text{and} \quad C_{r,tot} = \frac{1}{\frac{1}{C_r} + \frac{1}{c_{rRS,F}}};$$

[4.25]

Side force steering and roll-steering are very similar. Side force steering does not require a roll angle change, so side-force steering has basically no delay (or at least same magnitude of delay as the tyre cornering forces). However, roll-steering requires that sprung body changes roll angle which takes significantly longer time, typically roll eigen-frequency for a passenger vehicle is around 1.5 Hz. Roll-steering also come into play for one-sided road unevenness, i.e. also without cornering.

Side force steering and roll-steering compliances often represent a significant part of the front axle cornering compliance, e.g. 20-50% on a passenger car.

4.3.4.6 Camber steer

Negative camber (wheel top leaning inwards) increases the cornering stiffness. One explanation to this is that curve outer wheel gets more vertical load than the curve inner wheel. Hence, the inwards directed camber force from outer wheel dominates over outwards directed camber force from the inner wheel. Negative camber is often used at rear axle at passenger cars. Drawback with non-zero camber is tyre wear.

4.3.4.7 Toe angle

Toe has some, but limited effect on an axles cornering stiffness. Non-zero toe increases tyre wear. Toe-angle: When rolling ahead, tyre side forces pre-tension bushes.

If toe (=toe-in) is positive there are tyre-lateral forces on each tyre already when driving straight ahead, even if left and right cancel out each other: $F_{ay} = (C_{left} - C_{right}) \cdot \frac{toe}{2} = 0$. Then, if the axle takes a side force, the vertical load of the wheels are shifted between left and right wheel, which also changes the tyre cornering stiffnesses. The outer wheel will get more cornering stiffness. Due to positive toe, it will also have the largest steering angle. So, the axle will generate larger lateral force than with zero toe. For steady-state cornering vehicle models, this effect comes in as an increased axle cornering stiffness, i.e. a linear effect.

4.3.4.8 Wheel Torque effects

Wheel torque give tyre longitudinal force, directed as the wheel is pointing. If the wheel is steered, the wheel longitudinal forces can influence the yaw balance, see also F_{fx} in Equation [4.15].

Unsymmetrical wheel torques (left/right) will give a **direct yaw moment** in the yaw equilibrium in Equation [4.12]. The actuated yaw moment around CoG is then of the magnitude of wheel longitudinal wheel force times half the track width. ESC and Torque vectoring interventions have such effects.

High longitudinal utilization of friction on an axle leads to that lateral grip is reduced on that axle. The changed yaw moment, compared to what one would have without using friction longitudinally, can be called an **indirect yaw moment**. The actuated change in yaw moment around CoG is then of the magnitude of change in wheel lateral wheel force times half the wheel base. It influences the yaw balance. That is the reason why a front axle driven vehicle may be more understeered than a rear axle driven one. On the other hand, the wheel-longitudinal propulsion force on the front axle does also help the turn-in, which acts towards less understeering.

4.3.4.9 Transient vehicle motion effects on yaw balance

The effects presented here are not so relevant for steady state understeering coefficient. However, they affect the yaw balance in a more general sense, why it is relevant to list them in this section.

- Longitudinal load transfer changes normal forces. E.g. strong deceleration by wheel forces helps against under-steering, since front axle gets more normal load. This effect has some delay. Also, it vanishes after the transient.
(This effect can be compared with the effect described in Section 4.3.4.2, which is caused by tyre cornering stiffness varying degressively with vertical load, while the longitudinal load transfer effect can be explained solely with the proportional variation.)
- Change of longitudinal speed helps later in manoeuvre. E.g. deceleration early in a manoeuvre makes the vehicle easier to manoeuvre later in the manoeuvre. It is the effect of the term $wz \cdot vx$ that is reduced.

4.3.4.10 Some other design aspects

High cornering stiffness is generally desired.

Caster offset gives a self-aligning steering moment, which generally improves the steering feel.

Longer wheel base (with unchanged yaw inertia and unchanged steering ratio) improves the transient manoeuvrability, because the lateral forces have larger levers to generate yaw moment with.

4.3.5 Normalized required steering angle

A fundamental property of the vehicle is what steering angle that is required to negotiate a certain curvature ($=1/\text{path radius} = 1/R_p$). This value can vary with longitudinal speed and it can be normalized with wheel base, L . From Equation [4.15], we can conclude:

$$\begin{aligned} \text{Normalized required steering angle} &= \frac{\delta_f \cdot R}{L} \\ &= 1 + K_u \cdot \frac{m \cdot v_x^2}{L} \end{aligned} \tag{4.26}$$

The normalized required steering angle is plotted for different understeering gradients Figure 4-29. It is the same as the inverted and normalized curvature gain, see 4.3.6.2.

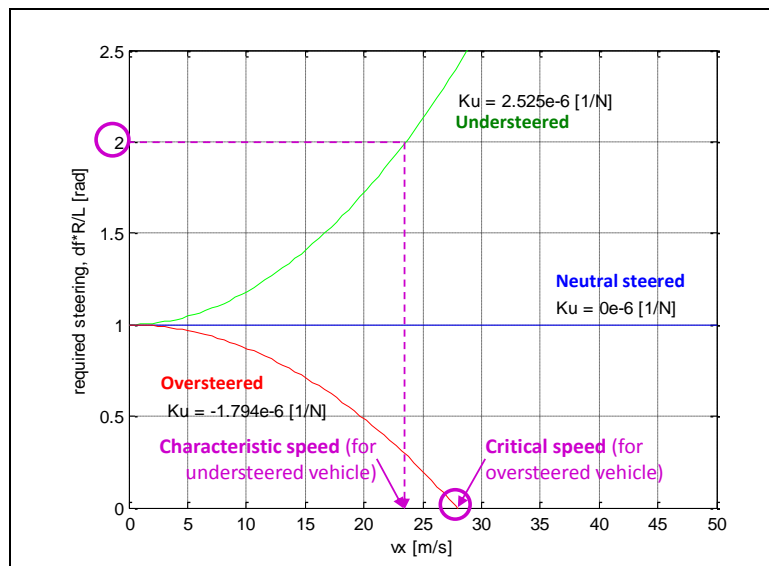


Figure 4-29: Normalized steering angle ($\frac{\delta_f \cdot R}{L}$) for Steady State Cornering

4.3.5.1 Critical and Characteristic speed *

*Function definition: **Critical speed** is the speed above which the vehicle becomes unstable in the sense that the yaw rate grows significantly for a small disturbance in, e.g., steering angle.*

*Function definition: **Characteristic speed** is the speed at which the vehicle requires twice as high steering angle for a certain path radius as required at low speed (Figure 4-29). (Alternative definitions: The speed at which the yaw rate gain reaches maximum (Figure 4-30). The speed at which the lateral acceleration gain per longitudinal speed reaches its highest value. (Figure 4-32).)*

We can identify that zero steering angle is required for the over-steered vehicle at 28 m/s. This is the so called Critical Speed, which is the speed where the vehicle becomes unstable. It should be noted here, that there are stable conditions also above critical speed, but one has to steer in the opposite direction then. Normal vehicles are built understeered, which is why a Critical speed is more of a theoretical definition. However, if studying (quasi-steady state) situations where the rear axle is heavily braked, the cornering stiffness rear is reduced, and a critical speed can be relevant.

For understeered vehicles, we can instead read out another measure, the Characteristic Speed. The understanding of Characteristic Speed is, so far just that required steering increases to over twice what is needed for low speed at the same path radius. A better feeling for Characteristic Speed is easier suggested in a later section, see Section 4.3.6.3.

From Equation [4.15], we can find a formula for critical and characteristic speeds:

$$\begin{aligned} \delta_f = \frac{L}{R} + K_u \cdot \frac{m \cdot v_{x,crit}^2}{R} = 0 &\Rightarrow v_{x,crit} = \sqrt{\frac{L}{-K_u \cdot m}} = \sqrt{\frac{C_f \cdot C_r \cdot L^2}{(C_f \cdot l_f - C_r \cdot l_r) \cdot m}}; \\ \delta_f = \frac{L}{R} + K_u \cdot \frac{m \cdot v_{x,char}^2}{R} = 2 \cdot \frac{L}{R} &\Rightarrow v_{x,char} = \sqrt{\frac{L}{K_u \cdot m}} = \sqrt{\frac{C_f \cdot C_r \cdot L^2}{(C_r \cdot l_r - C_f \cdot l_f) \cdot m}}; \end{aligned} \quad [4.27]$$

4.3.6 Steady state cornering gains *

*Function definition: **Steady state cornering gains** are the amplification from steering angle to certain vehicle response measures for steady state cornering at a certain longitudinal speed.*

From Equation [4.15], we can derive some interesting ratios. We put steering angle in the denominator, so that we get a gain, in the sense that the ratio describes how much of something we get “per steering angle”. If we assume $F_{fxw} = 0$, we get Equation [4.28].

Yaw rate gain =

$$\frac{\omega_z}{\delta_f} = \left\{ \text{use: } \frac{\omega_z}{v_x} \approx \frac{1}{R} \right\} \approx \frac{v_x/R}{\frac{L}{R} + K_u \cdot \frac{m \cdot v_x^2}{R}} = \frac{v_x}{L + K_u \cdot m \cdot v_x^2};$$

Curvature gain =

$$= \frac{\kappa}{\delta_f} = \frac{1/R}{\delta_f} = \frac{1/R}{\frac{L}{R} + K_u \cdot \frac{m \cdot v_x^2}{R}} = \frac{1}{L + K_u \cdot m \cdot v_x^2}; \quad [4.28]$$

Lateral acceleration gain =

$$= \frac{a_y}{\delta_f} = \left\{ \begin{array}{l} \text{use: } a_y = \omega_z \cdot v_x; \\ \text{and } \frac{\omega_z}{v_x} \approx \frac{1}{R}; \end{array} \right\} \approx \frac{\frac{v_x^2}{R}}{\frac{L}{R} + K_u \cdot \frac{m \cdot v_x^2}{R}} = \frac{v_x^2}{L + K_u \cdot m \cdot v_x^2};$$

Yaw rate gain is also derived for $F_{fxw} \neq 0$, and then we get Equation [4.29].

With F_{fxw} taken into account: Yaw rate gain =

$$= \frac{\omega_z}{\delta_f} = \frac{C_f \cdot C_r \cdot L + (C_r \cdot l_f + C_r \cdot l_r) \cdot F_{fxw}}{C_f \cdot C_r \cdot L^2 - (C_f \cdot l_f - C_r \cdot l_r) \cdot m \cdot v_x^2} \cdot v_x \quad [4.29]$$

4.3.6.1 Yaw Rate gain

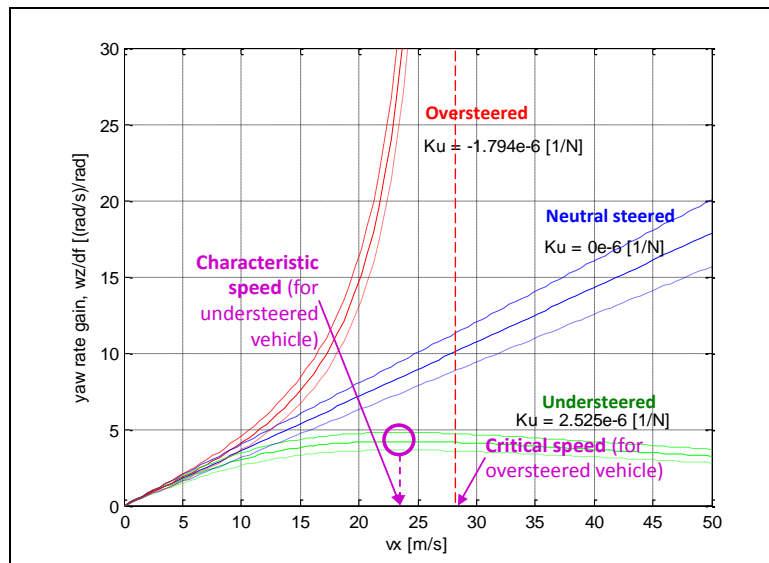


Figure 4-30: Yaw rate gain (ω_z/δ_f) for Steady State Cornering.
 In each “cluster of 3 curves”: Mid curve shows $F_{fxw} = 0$.
 Upper shows $F_{fxw} = +0.25 \cdot F_{fz}$. Lower shows $F_{fxw} = -0.25 \cdot F_{fz}$.

The yaw rate gain gives us a way to understand Characteristic Speed. Normally one would expect the yaw rate to increase if one increases the speed along a circular path. However, the vehicle will also increase its path radius when speed is increased. At the Characteristic Speed, the increase in radius cancel out the effect of increased speed, so that yaw rate in total decrease with increased speed. One can find the characteristic speed as the speed where one senses or measures the highest value of yaw rate increase for a given steering angle step.

The curves for $F_{fxw} = +0.25 \cdot F_{fz}$ and $F_{fxw} = -0.25 \cdot F_{fz}$ in Figure 4-30 are generated using the first stages in Eq [4.15], before assuming $F_{fxw} \approx 0$.

4.3.6.2 Curvature gain

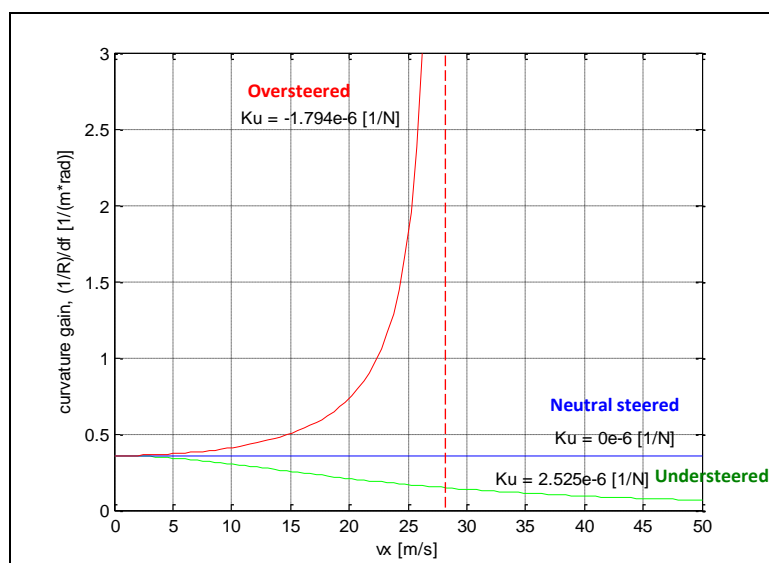


Figure 4-31: Curvature gain ($\frac{1/R}{\delta_f}$) for Steady State Cornering

If driving on a constant path radius, and slowly increase speed from zero, an understeered vehicle will require more and more steering angle (“steer-in”), to stay at the same path radius. For an oversteered vehicle one has to steer less (“open up steering”) when increasing the speed.

4.3.6.3 Lateral Acceleration gain

Figure 4-32 shows the lateral acceleration gain as function of vehicle speed. The characteristic speed is once again identified in this diagram, and now as the speed when lateral acceleration gain per longitudinal speed ($(a_y/\delta_f)/v_x$) reaches its highest value. This is an alternative definition of characteristic speed, cf Section 4.3.5.1.

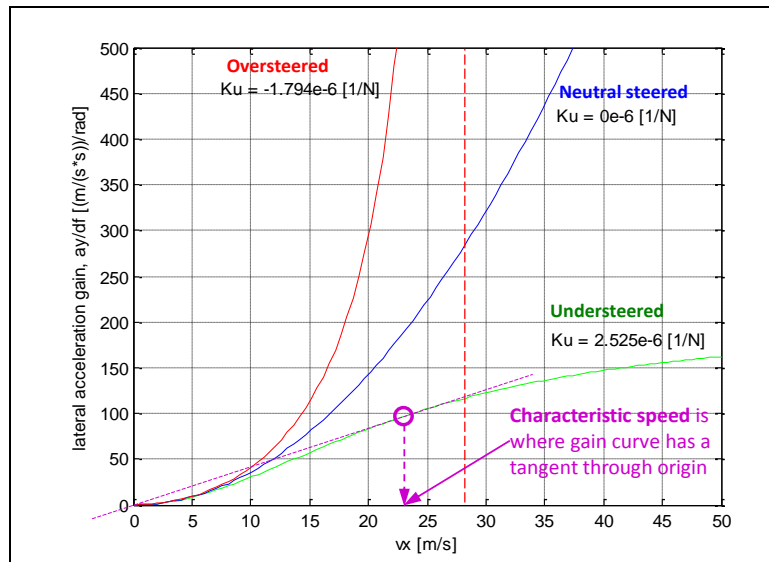


Figure 4-32: Lateral acceleration gain $(\frac{a_y}{\delta_f})$ for Steady State Cornering

From the previous figures the responsiveness of the vehicle can be identified for different understeer gradients. In all cases the vehicle which is understeered is the least responsive of the conditions. Both the yaw rate and lateral acceleration cannot achieve the levels of the neutral steered or oversteered vehicle. The oversteered vehicle is seen to exhibit instability when the critical speed is reached since small changes in the input result in excessive output conditions. In addition, the oversteered vehicle will have a counter-intuitive response for the driver. To maintain a constant radius curve, an increase in speed requires that the driver turns the steering wheel opposite to the direction of desired path. The result of these characteristics leads car manufacturers to produce understeered vehicles that are close to neutral steering to achieve the best stability and driver feedback.

4.3.6.4 Side slip gain as function of speed

All gains above can be found from solving w_z from Equation [4.15]. If instead solving the other unknown, v_y , we can draw “side slip gain” instead. Equation [4.30] shows the formula for this.

$$\frac{v_y}{v_x \cdot \delta_f} = \frac{C_f \cdot C_r \cdot l_r \cdot L - C_f \cdot l_f \cdot m \cdot v_x^2}{C_f \cdot C_r \cdot L^2 - (C_f \cdot l_f - C_r \cdot l_r) \cdot m \cdot v_x^2} \quad [4.30]$$

It is not solely the understeering gradient that sets the curve shape, but we can still plot for the some realistic numerical data, which are under-, neutral and over-steered, see Figure 4-33.

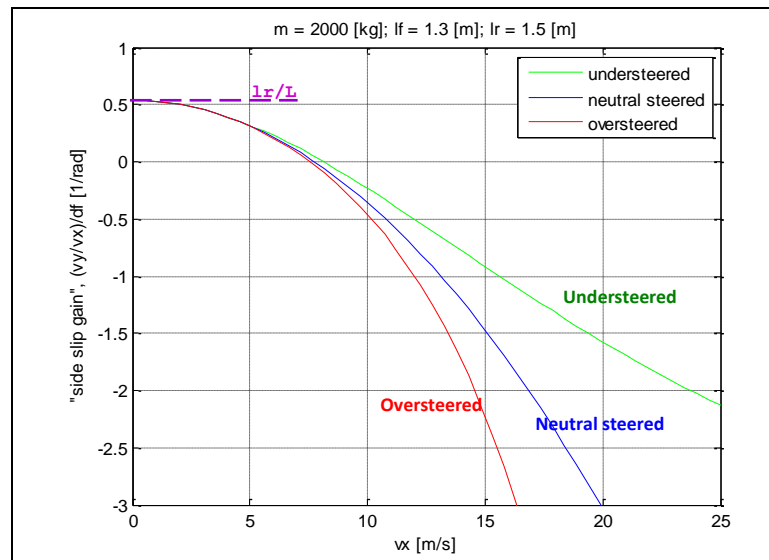


Figure 4-33: “Side slip gain” ($\frac{v_y}{v_x \cdot \delta_f}$) for Steady State Cornering.

All cases in Figure 4-33 goes from positive side slip to negative when speed increases. This is the same as we expected already in Figure 4-23.

4.3.7 Manoeuvrability and Stability

The overall conclusion of previous section is that all gains become higher the more over-steered (or less understeered) the vehicle is. Higher gains are generally experienced as a sportier vehicle and it also improves safety because it improves the manoeuvrability. A higher manoeuvrability makes it easier for the driver to do avoidance manoeuvres. This would motivate a design for low understeering gradient.

However, there is also the effect that a vehicle with too small understeer gradient becomes very sensitive to the steering wheel angle input. In extreme, the driver would not be able to control the vehicle. This limits how small the understeering gradient one can design for.

The overall design rule today is to make the understeering as small as possible, but the neutral steer is a limit which cannot be passed.

It is not impossible for a driver to keep an unstable vehicle ($K_u < 0$ and $v_x > \text{Critical Speed}$) on an intended path, but it requires an active compensation with steering wheel. If adding support systems, such as yaw damping by steering support or differentiated propulsion torques, it can be even easier. If one could rely on a very high up time for such support systems, one could move today’s trade-off between manoeuvrability and stability. This conceptual design step has been taken for some airplanes, which actually are designed so that they would be instable without active control.

4.3.8 Handling diagram

This section gives a brief introduction to handling diagram, which is a useful tool for discussing yaw stability during different steady state cornering situations, as initiated with Equation [4.20].

There are many frequently used graphical tools or diagrams to represent vehicle characteristics. One is the “handling diagram”, which is constructed as follows. Some simplifying assumptions are done as in Figure 4-25, with the exception that we don’t assume linear tyre models.

Equilibrium:

$$\left\{ m \cdot \frac{v_x^2}{R} = m \cdot a_y = F_{fy} + F_{ry}; \quad 0 = F_{fy} \cdot l_f - F_{ry} \cdot l_r; \right\} \Rightarrow F_{fy} = \frac{l_r}{L} \cdot m \cdot a_y; \quad F_{ry} = \frac{l_f}{L} \cdot m \cdot a_y$$

Constitution:

$$F_{fy} = F_{fy}(\alpha_f) \Rightarrow \alpha_f = F_{fy}^{-1}(F_{fy}); \quad F_{ry} = F_{ry}(\alpha_r) \Rightarrow \alpha_r = F_{ry}^{-1}(F_{ry});$$

Solving for $\alpha_r - \alpha_f$ yields:

$$\alpha_r - \alpha_f = F_{ry}^{-1}(F_{ry}) - F_{fy}^{-1}(F_{fy}) = F_{ry}^{-1}\left(\frac{l_f}{L} \cdot m \cdot a_y\right) - F_{fy}^{-1}\left(\frac{l_r}{L} \cdot m \cdot a_y\right);$$

So, we can plot $\alpha_r - \alpha_f$ as function of a_y . This relation is interesting because compatibility ($\delta_f + \alpha_f - \alpha_r = \frac{L}{R}$;) yields $\alpha_r - \alpha_f = \delta_f - \frac{L}{R} = \delta_f - \delta_A$. And $\delta_f - \delta_A$ is connected to one of the understandings of K_u in Equation [4.20], ($K_u = \frac{\partial}{\partial a_y}(\delta_f - \delta_A)$);). If we plot $\alpha_r - \alpha_f = \delta_f - \delta_A$ on abscissa axis and a_y on ordinate axis, we get the most common way of drawing the handling diagram, see Figure 4-34. The axle's constitutive relations can be used as graphical support to construct the diagram, but then the constitutive relations should be plotted as: $a_{yi}(\alpha_i) = \frac{L}{L-l_i} \cdot \frac{1}{m} \cdot F_{iy}(\alpha_i)$;). The quantity a_{yi} can be seen as the lateral force on the axle, but scaled so that both axes' values correspond to the same vehicle lateral acceleration.

Figure 4-34 shows the construction of a handling diagram from axle slip characteristics. Figure 4-35 show examples of handling diagrams constructed via tests with simulation tools. Handling diagrams can be designed from real vehicle tests as well. The slope in the handling diagram corresponds to understeering gradient K_{u3} in Equation [4.18].

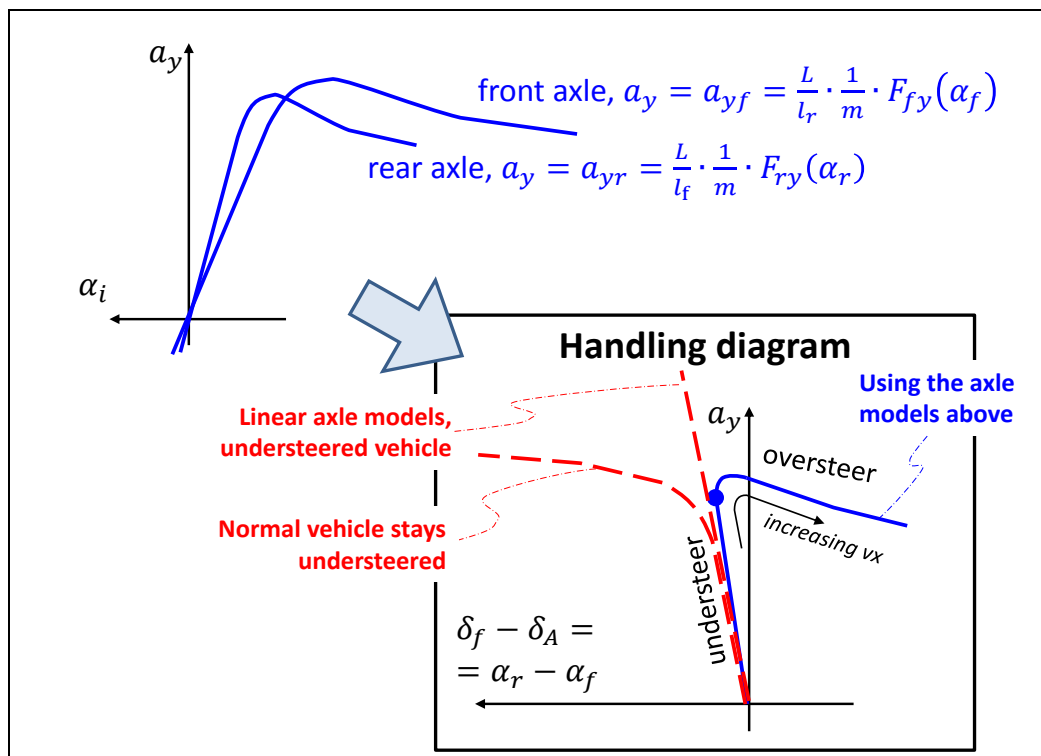


Figure 4-34: Construction of the “Handling diagram”. The axle’s slip characteristics (solid) are chosen so that vehicle transits from understeer to over-steer with increased longitudinal speed, v_x . The dashed shows two other examples.

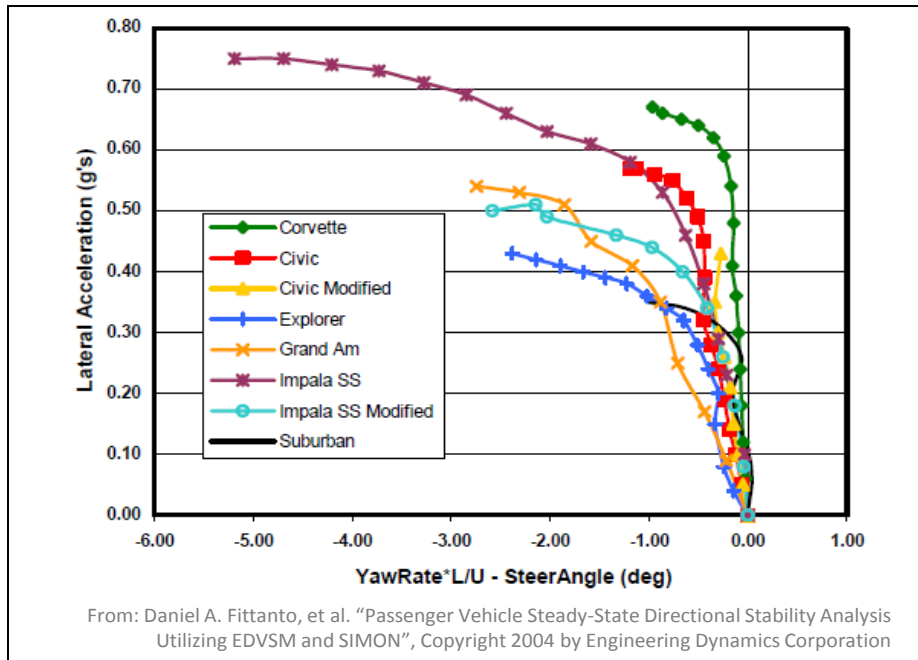


Figure 4-35: Example of handling diagram.

Using a one-track model of a two axle vehicle, there is such curve as drawn in handling diagram, but from a more advanced model, a vehicle with non-Ackermann steering or a real test, the curve becomes an area. This can be understood as if a certain lateral acceleration can be reached at several different longitudinal speeds, using different path radii. One can therefore see handling diagrams with a set of curves, each for a certain longitudinal speed. This is typical for handling diagrams for heavy trucks with several non-steered axles.

4.3.9 Steady state cornering at high speed, with Lateral Load Transfer

In the chapter about longitudinal dynamics we studied (vertical tyre) load transfer between front and rear axle. The corresponding issue for lateral dynamics is load transfer between left and right side of the vehicle. Within the steady state lateral dynamics, we will cover some of the simpler effects, but save the more complex suspension linkage dependent effects to Sections 4.5.

The relevance of analysing the load transfer is the function of limited roll angle in cornering (for comfort) and yaw balance (understeering gradient, see 4.3.9.6). Additionally, the load transfer can influence the transient handling; see Section 4.4 and Section 4.5.

4.3.9.1 Load transfer between vehicle sides

The total load transfer can be found without involving suspension effects.

Moment equilibrium, around left contact with ground:

$$m \cdot g \cdot \frac{w}{2} + m \cdot a_y \cdot h - F_{zr} \cdot w = 0 \Rightarrow F_{zr} = m \cdot \left(\frac{g}{2} + a_y \cdot \frac{h}{w} \right);$$

Moment equilibrium, around right contact with ground: $\Rightarrow F_{zl} = m \cdot \left(\frac{g}{2} - a_y \cdot \frac{h}{w} \right)$

[4.31]

These equations confirm what we know from experience, the left side is off-loaded if turning left. Generally, curve inner side is off-loaded.

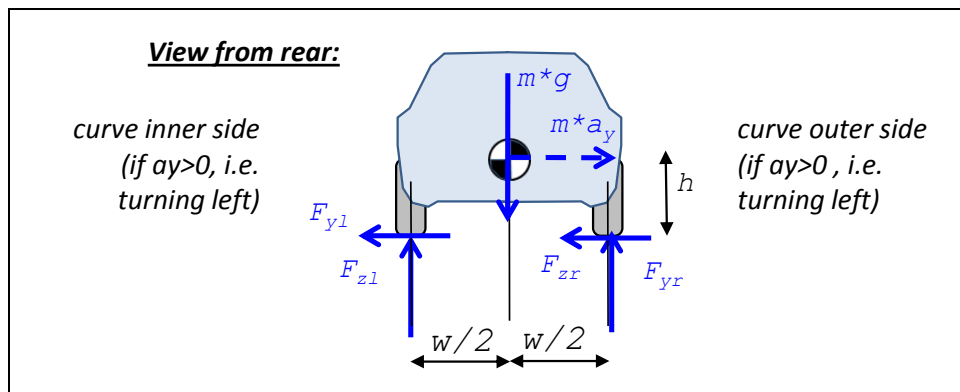


Figure 4-36: Free Body Diagram for cornering vehicle. The force $m \cdot a_y$ is a fictive force. Subscript l and r here means left and right.

4.3.9.2 Body heave and roll due to lateral wheel forces

Now, we shall find out how much the vehicle rolls and heaves during steady state cornering. First, we decide to formulate the model in “effective stiffnesses”, in the same manner as for longitudinal load transfer in previous chapter.

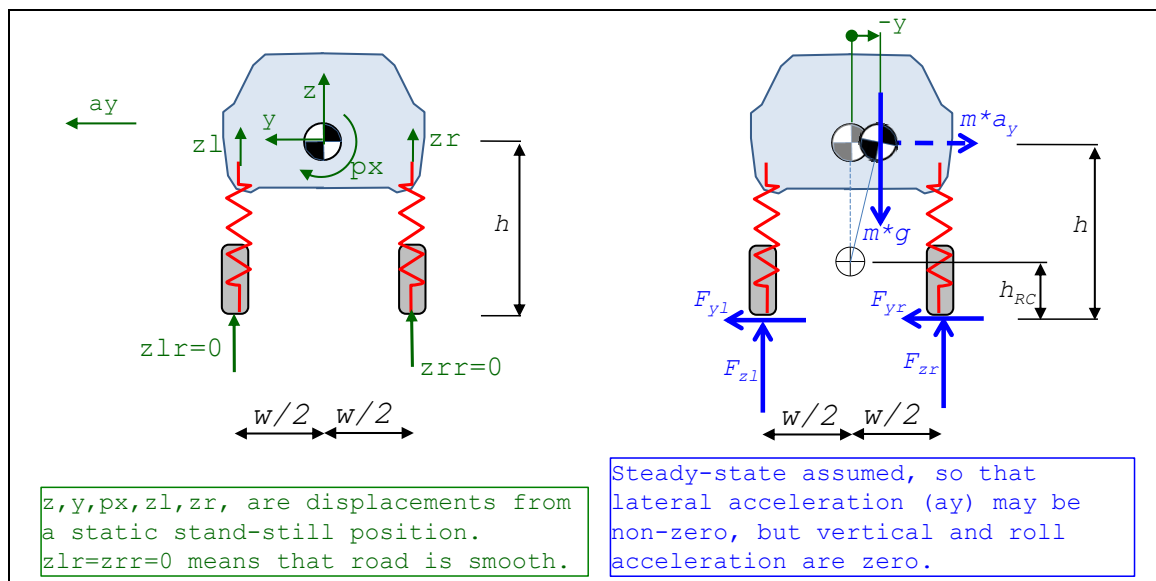


Figure 4-37: Model for steady state heave and roll due to lateral acceleration. Suspension model is no linkage (or “trivial linkage”) and without difference front and rear.

There is no damping included in model, because their forces would be zero, since there is no displacement velocity, due to the “quasi-steady-state” assumption. As constitutive equations for the compliances (springs) we assume that displacements are measured from a static conditions and that the compliances are linear. The road is assumed to be smooth, i.e. $z_l = z_r = 0$.

$$F_{z1} = F_{z10} + c_{side} \cdot (z_{lr} - z_l) \quad \text{and} \quad F_{zr} = F_{zr0} + c_{side} \cdot (z_{rr} - z_r) \quad [4.32]$$

where $F_{z10} + F_{zr0} = m \cdot g$ and $F_{z10} \cdot w/2 - F_{zr0} \cdot w/2 = 0$

The stiffnesses c_f and c_r are the effective stiffnesses at each axle. The physical spring may have different values of stiffness, but its effect is captured in the effective stiffness. Some examples of different physical design are given in Section “Axle suspension system”.

It is especially noted that this model is further developed in next section, to include linkage in the suspension, which allows validity for transient lateral dynamics. Also, the development gives better reflection of steady state levels of displacements, z and p_x .

We see already in free-body diagram that F_{yl} and F_{yr} always act together, so we rename $F_{yl}+F_{yr}=F_{yw}$, where w refers to wheel. This and equilibrium gives:

$$\begin{aligned} F_{yw} - m \cdot a_y &= 0; \\ m \cdot g - F_{zl} - F_{zr} &= 0; \\ F_{zl} \cdot (w/2) - F_{zr} \cdot (w/2) + F_{yw} \cdot h + m \cdot g \cdot (-y) &= 0; \end{aligned} \quad [4.33]$$

The term $m \cdot g \cdot (-y)$ is taken into account, but not corresponding for $m \cdot a_y$, since symmetry of the vehicle motivates that the roll takes place around a point on the vertical symmetry axis. Therefore y is significant but corresponding displacement in vertical direction is not. If we assume a height for the point where the roll takes place, h_{RC} , we can express $-y = (h - h_{RC}) \cdot p_x$. We don't know the value of it, until below where we study the suspension design, but it can be mentioned already here that most vehicles have an $h_{RC} \ll h$. This causes a significant "pendulum effect", especially for heavy trucks.

Compatibility, to introduce body displacements, z and p_x , gives:

$$z_l = z + (w/2) \cdot p_x; \quad \text{and} \quad z_r = z - (w/2) \cdot p_x; \quad [4.34]$$

Combining constitutive relations, equilibrium and compatibility, gives, as Matlab script:

```
clear, syms z_l z_r F_zl F_zr F_zl0 F_zr0 F_yw z p_x
sol=solve( ...
    'F_zl=F_zl0-c_side*z_l', ...
    'F_zr=F_zr0-c_side*z_r', ...
    'F_zl0+F_zr0=m*g', ...
    'F_zl0*w/2-F_zr0*w/2=0', ...
    'F_yw-m*a_y=0', ...
    'm*g-F_zl-F_zr=0', ...
    'F_zl*(w/2)-F_zr*(w/2)+F_yw*h+m*g*(h-h_RC)*p_x=0', ...
    'z_l=z+(w/2)*p_x', ...
    'z_r=z-(w/2)*p_x', ...
    z_l, z_r, F_zl, F_zr, F_zl0, F_zr0, F_yw, z, p_x);
```

The results from the Matlab script in Equation [4.35]:

$$\begin{aligned} F_{yw} &= m \cdot a_y; \\ z &= 0; \\ p_x &= \frac{2 \cdot m \cdot a_y \cdot h}{w^2 \cdot c_{side} - 2 \cdot m \cdot g \cdot (h - h_{RC})}; \\ F_{zl} &= m \cdot \left(\frac{g}{2} - \frac{a_y \cdot h}{w} \cdot \left(\frac{1}{1 + \frac{2 \cdot m \cdot g \cdot (h - h_{RC})}{c_{side} \cdot w^2}} \right) \right); \\ F_{zr} &= m \cdot \left(\frac{g}{2} + \frac{a_y \cdot h}{w} \cdot \left(\frac{1}{1 + m \frac{2 \cdot m \cdot g \cdot (h - h_{RC})}{c_{side} \cdot w^2}} \right) \right); \end{aligned} \quad [4.36]$$

In agreement with intuition and experience the body rolls with positive roll when steering to the left (positive F_{yw}). Further, the body centre of gravity is unchanged in heave (vertical z). The formula uses h_{RC} which we cannot estimate without analysis of the suspension. Since front and rear axle normally are different, we could expect that h_{RC} is expressed in some similar quantities for each of front and rear axle, which also is the case in our further analysis, see Equation [4.43].

4.3.9.2.1 Steady-state roll-gradient *

*Function definition: **Steady state roll-gradient** is the body roll angle per lateral acceleration for the vehicle during steady state cornering with a certain lateral acceleration and certain path radius on level ground.*

4.3.9.3 Lateral load transfer

For longitudinal load transfer, during purely longitudinal dynamic manoeuvres, the symmetry of the vehicle makes it reasonable to split vertical load on each axle equally between the left and right wheel of the axle. For lateral dynamics it is not very realistic to assume symmetry between front and rear axle. Hence, the suspension has to be considered separately for front and rear axle. The properties that are important to model for each axle is not only left and right elasticity (as we modelled the whole vehicle in Figure 4-37). It is also how the lateral tyre forces are transmitted from road contact patches to the vehicle body. We end up with conceptually the same two possible linkage modelling concepts as we found for longitudinal load transfer, see Figure 3-31. Either we can introduce roll centre heights for each axle (c.f. pitch centre in Section 3.4) or we can introduce the pivot point for each wheel (c.f. axle pivot points in Section 3.4). A difference for lateral load transfer, compared to longitudinal load transfer, is that it is significant also at steady state (due to centrifugal force).

The two modelling ways to include the suspension in the load transfer are shown in Figure 4-38. Generally speaking, they can be combined, so that one is used on front axle and the other on rear axle. However, in this compendium we will not combine, but select one of the concepts to describe.

4.3.9.3.1 Load Transfer model with Wheel Pivot Points

This model will not be deeply presented in this compendium. However, it should be mentioned as having quite a few advantages:

- The model has both heave and roll degree of freedom. (Roll centre model is restricted to roll around roll centre.)
- The model does take the distribution of longitudinal wheel forces between left and right side into account. (Roll centre model only uses the sum of lateral forces per axle.)

Generally spoken, this model is more accurate and not much more computational demanding and probably more easy to intuitively understand. (For non-individual, rigid axles or beam axles, the roll centre model is accurate enough and probably more intuitive.)

Cases when this model is recommended as opposed to the model with roll centres are:

- Steady state and transient analysis where heave displacement is important.
- When large differences between lateral load on left and right wheels are present, such as:
- Large load transfer, i.e. high CoG and large lateral accelerations. One example is when studying wheel lift and roll-over tendencies.
 - Large differences between longitudinal slip, while axle skids sideways. Then one wheel might have zero lateral force, due to that friction is used up longitudinally, while the other can have a large lateral force.
 - If individual steering within an axle would be studied. One could think of an extreme case if actuating a sudden toe-in or toe-out, which would cause large but counter-directed lateral forces on left and right wheel.

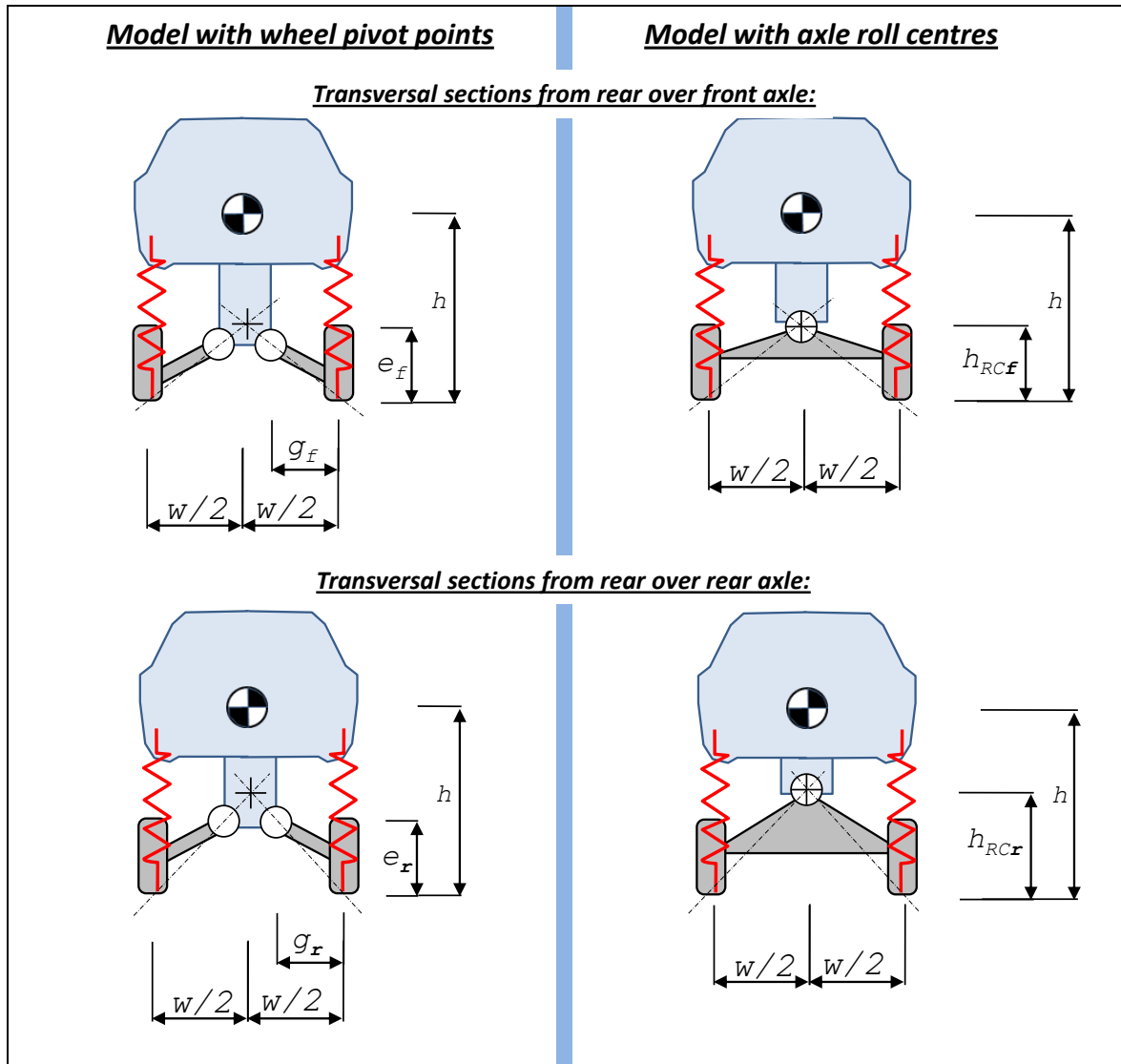


Figure 4-38: Two alternative models for including suspension effects in lateral load transfer

4.3.9.3.2 Load Transfer model with Axle Roll Centres

The model with axle roll centres has some drawback as listen before. To mention some advantages, it is somewhat less computational demanding. However, the main reason why using the roll centre based model in this compendium is that the compendium then cover two different concepts with longitudinal and lateral load transfer.

Behold the free-body diagrams in Figure 4-39. The road is assumed to be flat, $zflr=zfrr=zrlr=zrrr=0$. In free-body diagram for the front axle, Pfz and Pfy are the reaction force in the rear roll-centre. Corresponding reaction forces are found for rear axle. Note that roll centres are free of roll moment, which is the key assumption about roll centres! $Fsfl$, $Fsfr$, $Fsrl$ and $Fsrr$ are the forces in the compliances, i.e. where potential spring energy is stored. One can understand the roll-centres as also unable to take vertical force, as opposed to constraining vertical motion (as drawn). Which of vertically force-free or vertically motion-free depends on how one understand the concept or roll-centre, and it does not influence the equations.

Note carefully that the “pendulum effect” is NOT included here, in section 4.3.9.3, as it was in section 4.3.9.2. The motivation is to get simpler equations for educational reasons.

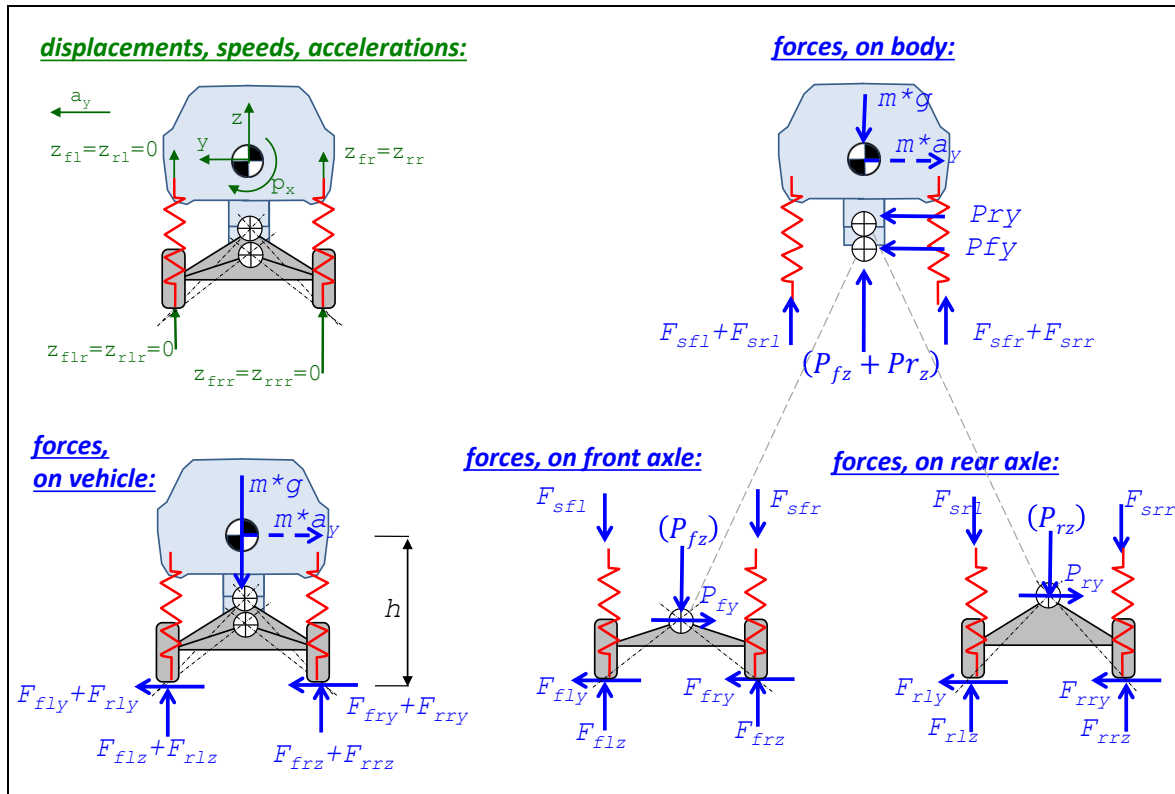


Figure 4-39: Model for steady state heave and roll due to lateral acceleration, using roll centres, which can be different front and rear.

There is no damping included in model, because their forces would be zero, since there is no displacement velocity, due to the steady-state assumption. As constitutive equations for the compliances (springs) we assume that displacements are measured from a static conditions and that the compliances are linear. For simplicity, the anti-roll bars are NOT modelled, but these are generally important and will be added in Section 4.3.9.4. The road is assumed to be smooth, i.e. $z_{flr} = z_{r1r} = z_{flr} = z_{r1r} = z_{flr} = z_{r1r} = 0$.

$$\begin{aligned}
 F_{sfl} &= F_{sf10} + c_{fw} \cdot (z_{flr} - z_{fl}); \\
 F_{sfr} &= F_{sf0} + c_{fw} \cdot (z_{flr} - z_{fr}); \\
 F_{srl} &= F_{sr10} + c_{rw} \cdot (z_{flr} - z_{rl}); \\
 F_{srr} &= F_{sr0} + c_{rw} \cdot (z_{flr} - z_{rr}); \\
 \text{where } F_{sf10} &= F_{sf0} = \frac{m \cdot g \cdot l_r}{2 \cdot L}; \text{ and } F_{sr10} = F_{sr0} = \frac{m \cdot g \cdot l_f}{2 \cdot L};
 \end{aligned}
 \tag{4.37}$$

The stiffnesses c_{fw} and c_{rw} are the effective stiffnesses per wheel at front and rear axle, respectively. The physical spring may have a different value of stiffness, but its effect is captured in the effective stiffness. Some examples of different physical design are given in Section “Axle suspension system”.

It is especially noted that this model is further developed in Section 4.5, to include non-steady state phenomena (damping as well as heave and roll inertial effects), which is needed for model validity for more violent transients lateral dynamics.

We see already in free-body diagram that F_{fly} and F_{fry} always act together, so we rename $F_{fly} + F_{fry} = F_{fy}$ and $F_{rly} + F_{rry} = F_{ry}$.

Equilibrium for whole vehicle (vertical, lateral, yaw, pitch, roll):

$$\begin{aligned}
 F_{flz} + F_{f rz} + F_{rlz} + F_{rrz} &= m \cdot g; \\
 m \cdot a_y &= F_{fy} + F_{ry}; \\
 0 &= F_{fy} \cdot l_f - F_{ry} \cdot l_r; \\
 -(F_{flz} + F_{f rz}) \cdot l_f + (F_{rlz} + F_{rrz}) \cdot l_r &= 0; \\
 (F_{flz} + F_{rlz}) \cdot \frac{w}{2} - (F_{f rz} + F_{rrz}) \cdot \frac{w}{2} + (F_{fy} + F_{ry}) \cdot h &= 0;
 \end{aligned}
 \tag{4.38}$$

Equilibrium for each axle (roll, around roll centre):

$$\begin{aligned}
 (F_{flz} - F_{sfl}) \cdot \frac{w}{2} - (F_{f rz} - F_{sfr}) \cdot \frac{w}{2} + F_{fy} \cdot h_{RCf} &= 0; \\
 (F_{rlz} - F_{srl}) \cdot \frac{w}{2} - (F_{rrz} - F_{srr}) \cdot \frac{w}{2} + F_{ry} \cdot h_{RCr} &= 0;
 \end{aligned}
 \tag{4.39}$$

Compatibility, to introduce body displacements, z, px and py, gives:

$$\begin{aligned}
 z_{fl} &= z + \frac{w}{2} \cdot p_x - l_f \cdot p_y; \\
 z_{fr} &= z - \frac{w}{2} \cdot p_x - l_f \cdot p_y; \\
 z_{rl} &= z + \frac{w}{2} \cdot p_x + l_r \cdot p_y; \\
 z_{rr} &= z - \frac{w}{2} \cdot p_x + l_r \cdot p_y; \\
 z_{fl} + z_{fr} &= 0; \\
 z_{rl} + z_{rr} &= 0;
 \end{aligned}
 \tag{4.40}$$

The measure Δh is redundant and can be connected to the other geometry measures as follows. The geometrical interpretation is given in Figure 4-40.

$$\Delta h = h - \frac{l_r \cdot h_{RCf} + l_f \cdot h_{RCr}}{L};
 \tag{4.41}$$

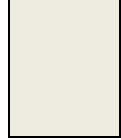
Combining Equations [4.37] to [4.41] gives, as Matlab script and solution:

```

clear, syms zfl zfr zrl zrr Fflz Ffrz Frlz Frrz Fsf1 Fsf2 Fsrl
Fsrr Fsf10 Fsf20 Fsrl0 Fsrr0 Ffy Fry z px py h
sol=solve( ...
    'Fsf1=Fsf10-cfw*zfl', ...
    'Fsf2=Fsf20-cfw*zfr', ...
    'Fsrl=Fsrl0-crw*zrl', ...
    'Fsrr=Fsrr0-crw*zrr', ...
    'Fsf10=(1/2)*m*g*lr/L', ...
    'Fsf20=(1/2)*m*g*lr/L', ...
    'Fsrl0=(1/2)*m*g*lf/L', ...
    'Fsrr0=(1/2)*m*g*lf/L', ...
    'Fflz+Ffrz+Frlz+Frrz=m*g', ...
    'm*ay=Ffy+Fry', ...
    '0=Ffy*lf-Fry*lr', ...
    '-(Fflz+Ffrz)*lf+(Frlz+Frrz)*lr=0', ...
    '(Fflz+Frlz)*w/2-(Ffrz+Frrz)*w/2+(Ffy+Fry)*h=0', ...
    '(Fflz-Fsf1)*w/2-(Ffrz-Fsf2)*w/2+Ffy*hRCf=0', ...
    '(Frlz-Fsrl)*w/2-(Frrz-Fsrr)*w/2+Fry*hRCr=0', ...
    'zfl=z+(w/2)*px-lf*py', ...
    'zfr=z-(w/2)*px-lf*py', ...
    'zrl=z+(w/2)*px+lr*py', ...
    'zrr=z-(w/2)*px+lr*py', ...
    'zfl+zfr=0', ...
    'zrl+zrr=0', ...
    'dh=h-(lr*hRCf+lf*hRCr)/(lf+lr)', ...
)

```

```
zfl, zfr, zrl, zrr, ...
Fsfl, Fsfr, Fsrl, Fsrr, ...
Fsfl0, Fsfr0, Fsrl0, Fsrr0, ...
Fflz, Ffrz, Frlz, Frrz, ...
Ffy, Fry, z, px, py, h);
```



The result from the Matlab script in Equation [4.42], but in a prettier writing format:

$$\begin{aligned}
 F_{fy} &= m \cdot a_y \cdot \frac{l_r}{L}; \\
 F_{ry} &= m \cdot a_y \cdot \frac{l_f}{L}; \\
 z &= 0; \\
 p_x &= \frac{m \cdot a_y \cdot \Delta h}{c_{roll,vehicle}} = \frac{(F_{fy} + F_{ry}) \cdot \Delta h}{c_{roll,vehicle}}; \\
 p_y &= 0; \\
 F_{flz} &= m \cdot \left(\frac{g \cdot l_r}{2 \cdot L} - a_y \cdot \left(\frac{h_{RCf} \cdot l_r}{L \cdot w} + \frac{\Delta h}{w} \cdot \frac{c_{f,roll}}{c_{roll,vehicle}} \right) \right); \\
 F_{frz} &= m \cdot \left(\frac{g \cdot l_r}{2 \cdot L} + a_y \cdot \left(\frac{h_{RCf} \cdot l_r}{L \cdot w} + \frac{\Delta h}{w} \cdot \frac{c_{f,roll}}{c_{roll,vehicle}} \right) \right); \\
 F_{rlz} &= m \cdot \left(\frac{g \cdot l_f}{2 \cdot L} - a_y \cdot \left(\frac{h_{RCr} \cdot l_f}{L \cdot w} + \frac{\Delta h}{w} \cdot \frac{c_{r,roll}}{c_{roll,vehicle}} \right) \right); \\
 F_{rrz} &= m \cdot \left(\frac{g \cdot l_f}{2 \cdot L} + a_y \cdot \left(\frac{h_{RCr} \cdot l_f}{L \cdot w} + \frac{\Delta h}{w} \cdot \frac{c_{r,roll}}{c_{roll,vehicle}} \right) \right);
 \end{aligned}$$

[4.43]

where, roll stiffnesses in [moment/angle], are:

$$\begin{aligned}
 c_{f,roll} &= 2 \cdot c_{fw} \cdot \left(\frac{w}{2} \right)^2 \quad \left[\frac{Nm}{rad} \right]; \\
 c_{r,roll} &= 2 \cdot c_{rw} \cdot \left(\frac{w}{2} \right)^2 \quad \left[\frac{Nm}{rad} \right]; \\
 c_{roll,vehicle} &= c_{f,roll} + c_{r,roll} \quad \left[\frac{Nm}{rad} \right];
 \end{aligned}$$

We should compare Equation [4.43] with Equation [4.36]. Equation [4.36] considers the “pendulum effect”, but not the differentiation between front and rear suspension. Equation [4.43] does the opposite.

Assume $h = h_{RC}$ and look at the sum of vertical force on one side, F_{zl} in Equation [4.36]. Compare F_{zl} in Equation [4.36] and $F_{flz} + F_{rlz}$ in Equation [4.43]; the equations agree if:

$$\begin{aligned}
 F_{flz} + F_{rlz} = F_{zl} &\Rightarrow m \cdot \left(\frac{g}{2} - a_y \cdot \left(\frac{h_{RCf} \cdot l_r + h_{RCr} \cdot l_f}{L \cdot w} + \frac{\Delta h}{w} \right) \right) = m \cdot \left(\frac{g}{2} - a_y \cdot \frac{h}{w} \right) = F_{zl} \Rightarrow \\
 &\Rightarrow \frac{h_{RCf} \cdot l_r + h_{RCr} \cdot l_f}{L \cdot w} + \frac{\Delta h}{w} = \frac{h}{w} \Rightarrow h_{RCf} \cdot l_r + h_{RCr} \cdot l_f = (h - \Delta h) \cdot L;
 \end{aligned}$$

This is exactly in agreement with the definition of the redundant geometric parameter Δh , see Equation [4.41]. This means that a consistent geometric model of the whole model is as drawn in Figure 4-40. Here the artefact roll axis is also defined.

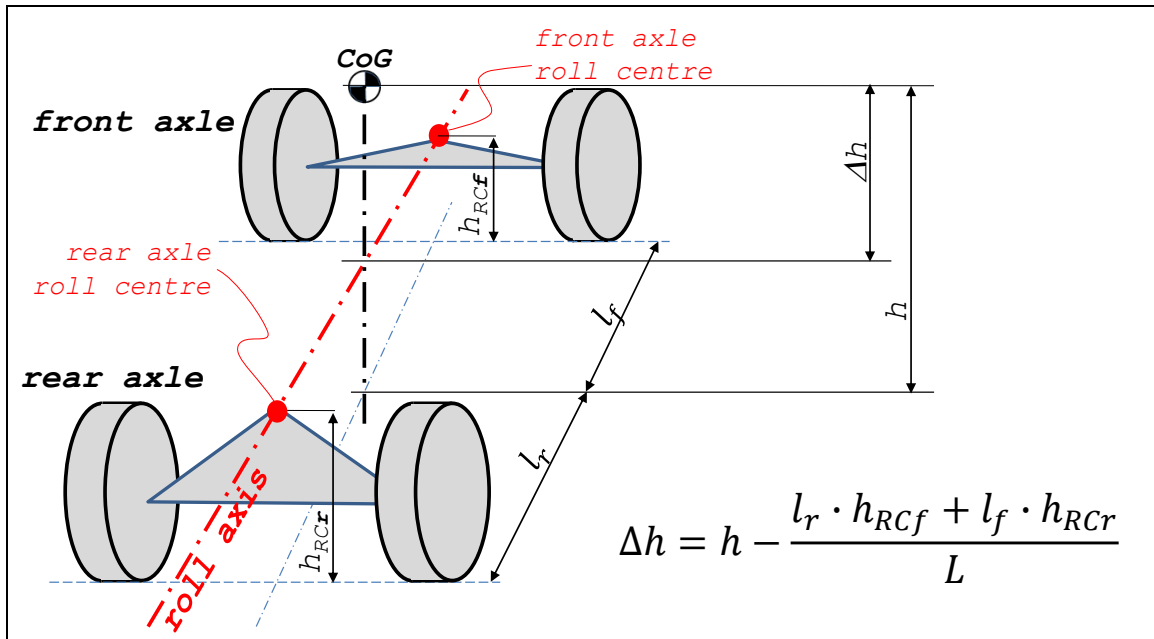


Figure 4-40: Roll axis for a two axle vehicle. (Note that the picture may indicate that the roll centres and roll axis are above wheel centre, but this is normally not the case.)

The terms of type $\frac{h_{RCi} \cdot l_j}{L \cdot w}$ in Equation [4.43] can be seen as the part of the lateral tyre forces that goes via the stiff linkage. The terms of type $\frac{\Delta h}{w} \cdot \frac{c_{iw}}{c_{iw} + c_{jw}}$ in Equation [4.43] can be seen as the part of the lateral tyre forces that goes via the compliance. The latter part is distributed in proportion to roll stiffness of the studied axle, as a fraction of the vehicle roll stiffness. This should be in agreement with intuition and experience from other preloaded mechanical systems (load distributes as stiffness).

Body rolls with positive roll when steering to the left, as long as CoG is above roll axle. Further, the body centre of gravity is unchanged in heave (vertical z) because the model does not allow any vertical displacements, which is a drawback already mentioned.

4.3.9.4 Influence of anti-roll bars

Anti-roll bars will be added to model in this section. Figure 4-41 shows the physical model which includes anti-roll bars. It is an update of Figure 4-39.

Eq [4.37] will remain, and constitutive relation for anti-roll bars is added as in Eq [4.44]. Also here, the road is assumed to be smooth. Note that anti-roll bars are assumed to have no pre-tension. Anti-roll bar stiffnesses for each axle are design parameters, c_{ia} where $i = f, r$.

$$\begin{aligned}
 F_{af} &= c_{fa} \cdot \left((z_{\overline{f\overline{f}}} - z_{fl}) - (z_{\overline{f\overline{r}}} - z_{fr}) \right); \\
 F_{ar} &= c_{ra} \cdot \left((z_{\overline{r\overline{r}}} - z_{rl}) - (z_{\overline{r\overline{f}}} - z_{rr}) \right);
 \end{aligned}
 \tag{4.44}$$

The equilibrium for whole vehicle, Eq [4.38], does not change. The equilibrium for each axle, Eq [4.39], changes to the following:

Equilibrium for each axle (pitch, around roll centre):

$$\begin{aligned} (F_{flz} - F_{sfl} + F_{af}) \cdot \frac{w}{2} - (F_{frz} - F_{sfr} - F_{af}) \cdot \frac{w}{2} + F_{fy} \cdot h_{RCf} &= 0; \\ (F_{rlz} - F_{srl} + F_{ar}) \cdot \frac{w}{2} - (F_{rrz} - F_{srr} - F_{ar}) \cdot \frac{w}{2} + F_{ry} \cdot h_{RCr} &= 0; \end{aligned} \quad [4.45]$$

The compatibility Equation, Eq [4.40], does not change and the definition of Δh , Eq [4.41], can also be kept. It shows that Eq [4.43] is still valid, but with new definitions of the roll stiffnesses as follows:

$$\begin{aligned} c_{f,roll} &= 2 \cdot (c_{fw} + 2 \cdot c_{af}) \cdot \left(\frac{w}{2}\right)^2 \quad \left[\frac{Nm}{rad} \right]; \\ c_{r,roll} &= 2 \cdot (c_{rw} + 2 \cdot c_{ar}) \cdot \left(\frac{w}{2}\right)^2 \quad \left[\frac{Nm}{rad} \right]; \\ c_{roll,vehicle} &= c_{f,roll} + c_{r,roll} \quad \left[\frac{Nm}{rad} \right]; \end{aligned} \quad [4.46]$$

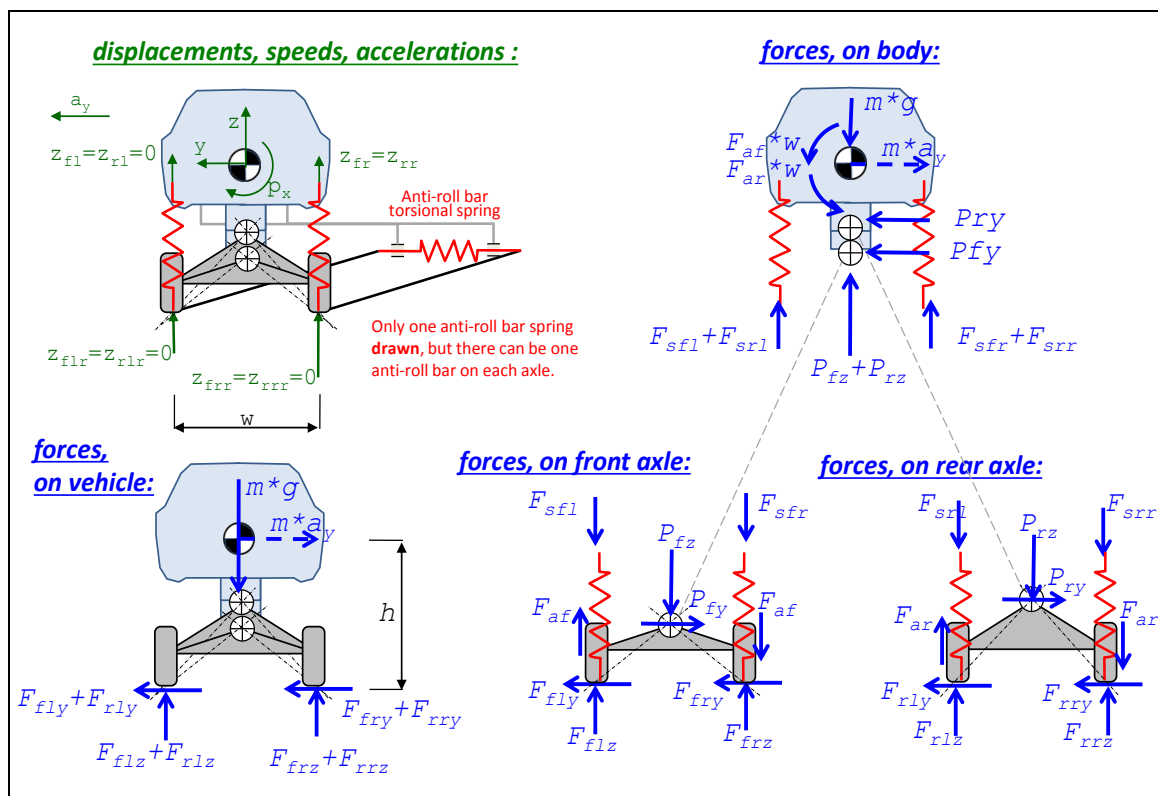


Figure 4-41: Model for steady state heave and roll due to lateral acceleration, using roll centres, which can be different front and rear. Including anti-roll bar on each axle.

4.3.9.5 Axle suspension system

Suspension design is briefly discussed at these places in this compendium: Section 3.4.7, Section 4.3.9.5 and Section 5.2.

There are axles with dependent wheel suspensions, which basically look as the roll centre axle model in Figure 4-38, i.e. that left right wheel are rigidly connected to each other. Then, there are axles with independent wheel suspensions, which look more like the model with wheel pivot points in Figure 4-38. For these, there are no (rigid) connections between left and right wheel.

Many axles have a so called anti-roll bar, which is a elastic connection between left and right side. It is connected such that if the wheel on one side is lifted, it lifts also the wheel on the other side. Note that, if an anti-roll bar is added to an independent wheel suspension it is still called independent, because the connection is not rigid.

Figure 4-42 and Figure 4-43 show design of two axles with independent wheel suspensions. Figure 4-44 shows an axle with dependent wheel suspension. In all these figures it is shown how to find wheel pivot points and roll centre. In the McPherson suspension in Figure 4-43, one should mention that the strut is designed to take bending moments. For the rigid axle in Figure 4-44, one should mention that the leaf spring itself takes the lateral forces. Symmetry between left and right wheel suspension is a reasonable assumption and it places the roll centre symmetrically between the wheels, which is assumed in the previous models and equations regarding roll centre. (Symmetry is not reasonable to assume for pitch centre.)

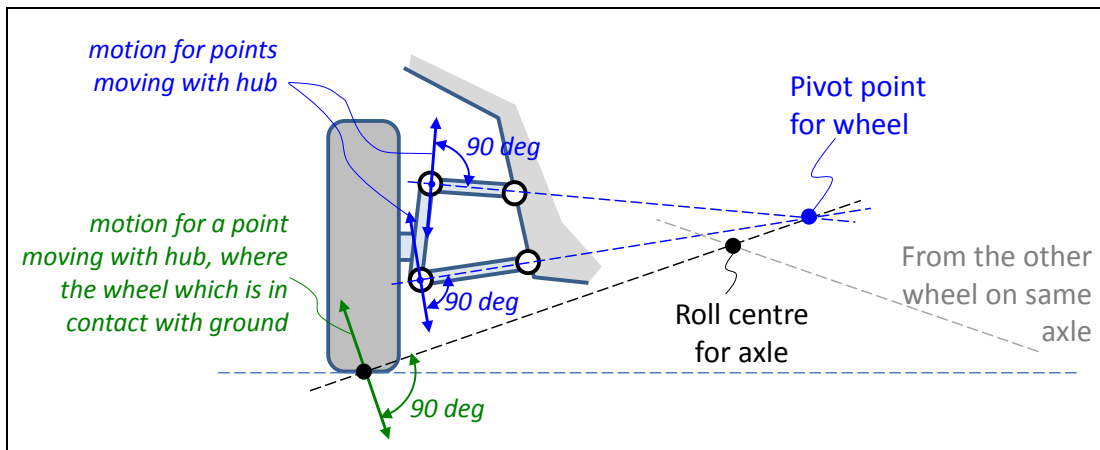


Figure 4-42: Example of how to appoint the pivot point for one wheel and roll centre for axle with double wishbone suspension.

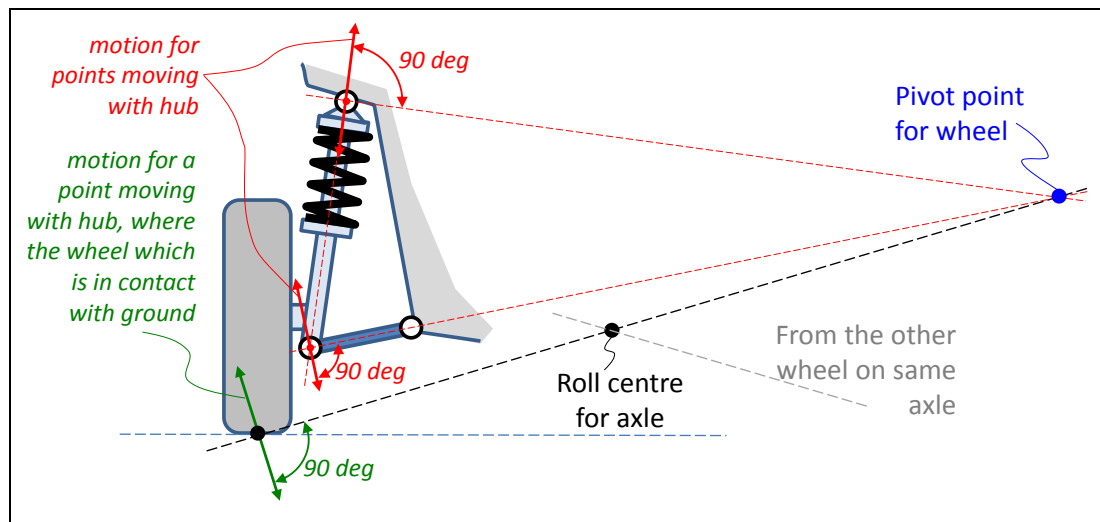


Figure 4-43: Example of how to appoint the pivot point for one wheel and roll centre for axle with double McPherson suspension.

Generally, a "rigid axle" gives roll centre height on approximately the same magnitude as wheel radius, see Figure 4-44. With individual wheel suspension one have much larger flexibility, and typical chosen designs are 30..90 mm front and 90..120 mm rear.

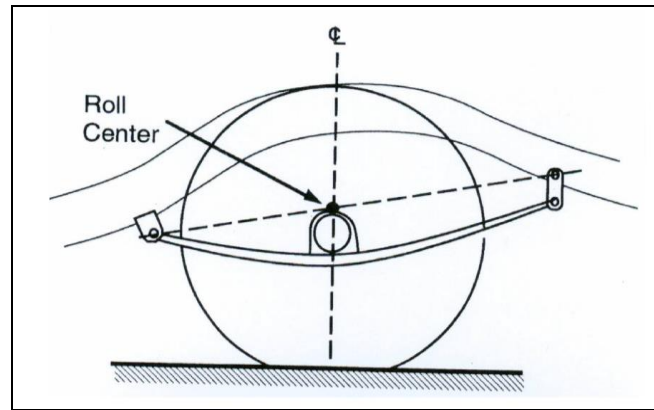


Figure 4-44: Example of how to appoint the pivot point for one wheel and roll centre for axle with rigid axle suspended in leaf springs. From (Gillespie, 1992).

The design of roll centre height is a trade-off. On one side, high roll centre is good because it reduces roll in steady state cornering. On the other side, low roll centre height is good because it gives small track width variations due to vehicle heave variations. Track width variations are undesired, e.g. because it makes the left and right tyre lateral force fight against each other, leaving less available friction for longitudinal and lateral grip. Roll centre is normally higher rear than front. One reason for that is that the main inertia axis leans forward, and parallelism between roll axis and main inertia axis is desired.

4.3.9.6 Lateral load transfer influence on steady state handling

The lateral load transfer will influence the steady state cornering in some different ways. A very fundamental view of a tyre is maybe that forces are proportional to vertical load, and then the cornering stiffness should also vary in this way. This is a good first approximation, but there are actually mechanism that makes the increase degressive, see Figure 2-26. This means that the axle cornering stiffness decrease with increased load transfer.

The total roll stiffness of the vehicle does not influence the understeering gradient, but the distribution of roll stiffness between front and rear axle does. Normally one makes the front axle more roll stiff than the rear axle. This means that vehicle becomes more and more understeered for increased lateral acceleration, e.g. more steering angle is needed to maintain a certain path radius if speed increases.

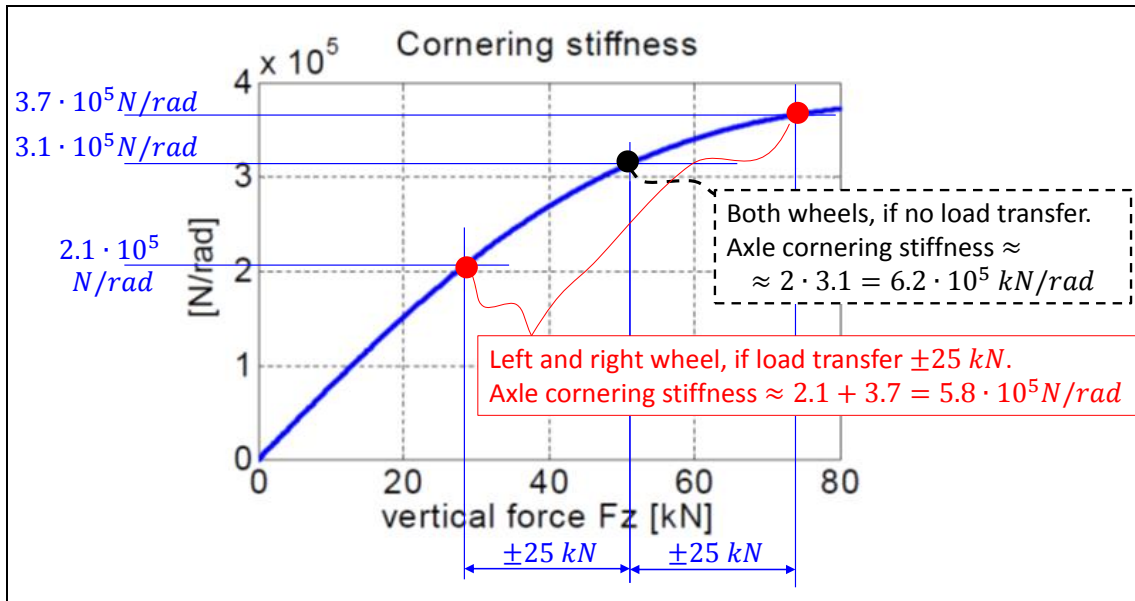


Figure 4-45: The wheels cornering stiffness $\left(\frac{\partial}{\partial \alpha} F_y\right)\bigg|_{s_y=0}$ changes degressively with vertical load.

The axle cornering stiffness therefore decreases with load transfer.

4.3.10 Steering feel *

*Function definition: **Steering feel** is the steering wheel torque response to steering wheel angle. The function is used in a very wide sense; on a high level, it is a measure of steering wheel torque, or its variation, for certain driving situations. Often, it can only be subjectively assessed.*

At steady state driving at high speed, there are basically three aspects of steering feel:

- Lateral steering feel feedback at cornering. The steering wheel torque is normally desired to increase monotonously with lateral forces on the front axle. This is basically the way the mechanics work due to caster trail. Some specifications on steering assistance system is however needed to keep the steering wheel torque low enough for comfort.
- Steering torque drop when cornering at low-friction. It is built into the mechanics of the caster trail and the pneumatic trail that steering wheel torque drops slightly when one approaches the friction limit on front axle. This is normally a desired behaviour because it gives driver feedback that the vehicles is approach the limits.
- On-centre feel in straight line driving. When the vehicle is driven in straight line, the steering wheel is normally desired to return to centre position after small perturbations. This is a comfort function, which OEMs works a lot with and it is often rather subjectively assessed.

4.3.11 Roll-over in steady state cornering

When going in curves, the vehicle will have roll angles of typically some degrees. At that level, the roll is a comfort issue. However, there are manoeuvres which can cause the vehicle to roll-over, which basically means that it rolls at least 90 degrees. So, this is an actual accident event.

Roll-over can be seen as a special event, but if sorting into the chapters of this compendium it probably fits best in present chapter, about lateral dynamics.

One can categorize roll-overs in e.g. 3 different types:

- **Tripped roll-over.** This is when the car skids sideways and hits an edge, which causes the roll-over. It can be an uprising edge, e.g. pavement or refuge. It can be the opposite, a ditch or loose gravel outside road. In both these cases, it is strong lateral forces on the wheels on one side of the vehicle that causes the roll-over.
Tripped roll-over can also be when the vehicle is exposed to large one-sided vertical wheel forces, e.g. by running over a one-sided bump.
A third variant of tripped roll-over is when the vehicle is hit by another vehicle so hard that it rolls over.
- **Un-tripped roll-over** or on-road roll-overs. These happen on the road and triggered by high tyre lateral forces. This is why they require high road friction. For sedan passenger cars these event are almost impossible, since road friction seldom is higher than approximately 1. For SUVs, un-tripped roll-overs can however occur but require dry asphalt roads, where friction is around 1. For trucks, un-tripped roll-over, can happen already at very moderate friction, like 0.4, due to their high CoG in relation to track width. Within un-tripped roll-overs, one can differ between:
 - **Steady state roll-over.** If lateral acceleration is slowly increased, e.g. as running with into a hairpin curve or a highway exit, the vehicle can slowly lift off the inner wheels and roll-over. This is the only case of roll-over for which an analysis model is given in this compendium.
 - **Transient roll-over.** This is when complex manoeuvres, like double lane changes or sinusoidal steering, are made at high lateral accelerations. This can trigger roll eigenmodes, which can be amplified due to unlucky timing between the turns. Analysis models from Section 4.5 can be used as a start, but it is required that load transfer is modelled carefully and includes wheel lifts, suspension end-stops and bump stops.

4.3.11.1 Roll-over threshold definitions

An overall requirement on a vehicle is that the vehicle should not roll-over for certain manoeuvres. Heavy trucks will be possible to roll-over on high- μ conditions. The requirement for those are based on some manoeuvres which not utilize the full road friction. For passenger cars, it is often the intended design that they should be impossible to roll-over, even at high μ . Any requirement need a definition of what exactly roll-over is, i.e. a Roll over threshold definition. Candidates for Roll over threshold definition are:

- **One wheel** lift from ground
- All wheels on **one side** lift from ground
- Vehicle **CoG** passes its **highest point**

Note that:

- It is the 3rd threshold which really is the limit, but other can still be useful in requirement setting. To use the 3rd for requirement setting makes the verification much more complex, of course in real vehicles but also in simulation.
- The 1st is not a very serious situation for a conventional vehicle with 4 wheels. However, for a 3-wheeled vehicle, such as small “tuc-tucs” or a 3-wheel moped, it is still a relevant threshold.
- The 2nd threshold is probably the most useful threshold for two-tracked vehicles, because it defines a condition from which real roll-over is an obvious risk, and still it is relatively easy to test and simulate. For 3-wheeled vehicle, 2nd and 3rd threshold generally coincide.

Figure 4-46 shows how the inner wheels lift off subsequently during a slowly increasing lateral force (or lateral acceleration) build-up. Before any wheel is lifted, the load transfer is proportional to roll-centre heights and roll stiffnesses, as shown in Equation [4.43]. But everytime a wheel lifts, the distribution changes, so that a “knee” on the curves appears, see Figure 4-46. So, the relation of type

as Equation [4.43] is no longer valid. For instance, it is not physically motivated to keep the roll-centre model for an axle which has lifted one side. So, the analysis is not trivial, especially for heavy vehicles which has many axles, and often also a fifth wheel which can transfer roll-moment to a certain extent. There are approximate standards for how to calculate steady state roll-over thresholds for such vehicle, e.g. UN ECE 111 (<http://www.unece.org/fileadmin/DAM/trans/main/wp29/wp29regs/r111e.pdf>).

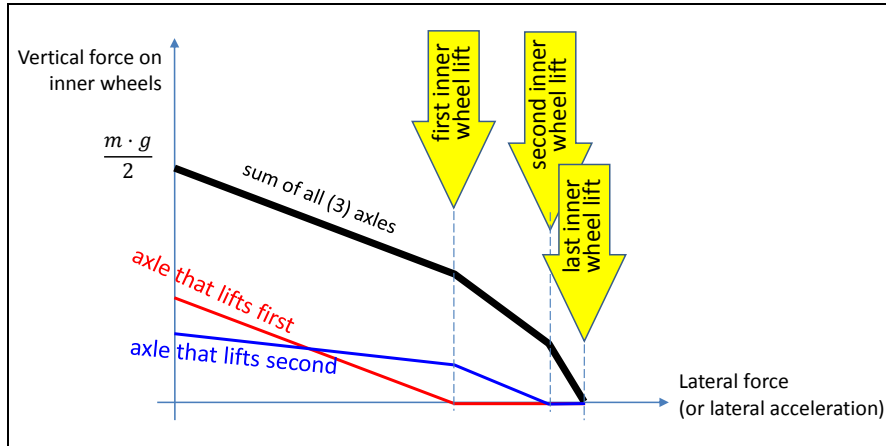


Figure 4-46: Example of 3-axle vehicle steady state roll-over wheel lift diagram.

In the following, 2-axled and 4-wheeled vehicles will be assumed. The 2nd threshold will be used.

4.3.11.2 Static Stability Factor, SSF

One very simple measure of the vehicles tendency to roll-over is the Static Stability Factor, SSF. It is proposed by NHTSA, http://www.nhtsa.gov/cars/rules/rulings/roll_resistance/, and it is simply defined as:

$$SSF = \frac{\text{Half TrackWidth}}{\text{HeightOfCoG}} = \frac{w/2}{h}; \quad [4.47]$$

A requirement which requires $SSF > \text{number}$ cannot be directly interpreted in terms of certain manoeuvre and certain roll-over threshold. It is not a *performance based requirement*, but a *design based requirement*. However, one of many possible performance based *interpretations* is that the vehicle shall not roll-over for steady-state cornering on level ground with a certain friction coefficient, using one-sided wheel lift as threshold. Since the requirement is not truly performance based, each interpretation will also stipulate a certain verification method; here it would be theoretical verification using a rigid suspension model. Such model and threshold is shown in Figure 4-47.

The derivation of the SSF based requirement looks as follows:

$$\text{Model: } \left\{ \begin{array}{l} F_{iz} \cdot w + m \cdot a_y \cdot h = m \cdot g \cdot \frac{w}{2}; \\ F_{iz} + F_{oz} = m \cdot g; \\ m \cdot a_y = F_y = \mu \cdot (F_{iz} + F_{oz}); \end{array} \right\} \Rightarrow F_{iz} = m \cdot g \cdot \left(\frac{1}{2} - \frac{h \cdot \mu}{w} \right); \Rightarrow$$

Requirement: $F_{iz} \geq 0;$ [4.48]

$$\Rightarrow \text{Requirement: } \frac{1}{2} > \frac{h \cdot \mu}{w} \Rightarrow \frac{w}{2 \cdot h} = SSF > \mu;$$

Maximum road friction, μ , is typically 1, which is why $SSF > \mu = 1$ would be a reasonable. However, typical values of SSF for passenger vehicles are between 0.95 and 1.5. For heavy trucks, it can be much lower, maybe 0.3..0.5, much depending on how the load is placed. There are objections to use SSF as a measure, because SSF ignores suspension compliance, handling characteristics, electronic stability control, vehicle shape and structure.

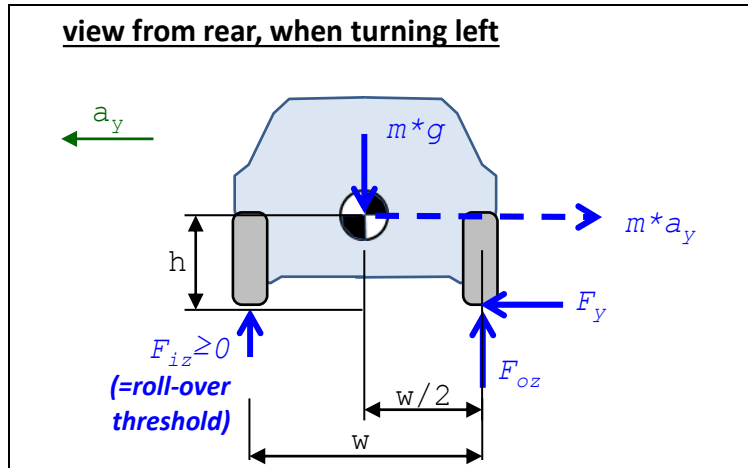


Figure 4-47: Model for verification of requirement based on Static Stability Factor, SSF.

4.3.11.3 Steady-state cornering roll-over

A function defined for requirement setting can be:

*Function definition: **Steady state roll-over resistance** is the maximum lateral acceleration the vehicle can take in steady state cornering without lifting all inner wheels. On level ground with enough road friction and certain weight and position of payload.*

For a long combination-vehicle with several articulation points, one often need to drive a long distance after a steering angle change before steady state values on articulation angles are reached. Hence, it can be more relevant to formulate a corresponding roll-over function in terms of curvature to follow, total yaw angle for turn and longitudinal speed. A common way is also the, somewhat artificial, tilt-table test, which means that one measure steady-state roll-over with a (real or virtual) tilt-table where the maximum road pitch angle before wheel lift on one side is the measure to set requirement on.

4.3.11.3.1 Model with fore/aft symmetry

The model in Figure 4-47 and Equation [4.48] assumes fore/aft symmetry. One can derive this **requirement** on design: $\frac{w}{2 \cdot h} > \mu$, and this interpretation of **performance** (a_y) limitation due to roll-over: $\frac{a_y}{g} < \frac{w}{2 \cdot h}$. In the following, we will elaborate with 4 additional effects and derive how they affects this: $\frac{a_y}{g} < \frac{w}{2 \cdot h} > \mu$. The 4 effects are each connected to one measure, which is marked in Figure 4-48.

- The tyre will take the vertical load on its **outer edge** in a roll-over situation. This suggests a change of performance and requirement to: $\frac{a_y}{g} < \frac{w + w_{tyre}}{2 \cdot h} > \mu$. This effect is accentuated when low tyre profile and/or high inflation pressure. This effect **decreases** the risk for roll-over.
- Due to suspension and tyre **lateral deformation**, the body will translate laterally outwards, relative to the tyre. This could motivate $\frac{a_y}{g} < \frac{w - Def_y}{2 \cdot h} > \mu$. This effect **increases** the risk for roll-over.

- Due to suspension linkage and compliances, the **body will roll**. Since the CoG height above roll axis, Δh , normally is positive, this could motivate $\frac{a_y}{g} < \frac{w - \Delta h \cdot \phi_x}{2 \cdot h} > \mu$. This effect **increases** the risk for roll-over. At heavy vehicle this “pendulum effect” is large.
- Due to suspension linkage and compliances, the body will also heave. This requires a suspension model with pivot points per wheel, as opposed to roll-centre per axle, to be taken into account. The heave is normally positive. This could motivate $\frac{a_y}{g} < \frac{w}{2 \cdot (h+z)} > \mu$. The effect is sometimes called “jacking” and it **increases** the risk for roll-over.
- Road leaning left/right (road banking), or driving with one side on a different level (e.g. outside road or on pavement) also influence the roll-over performance.

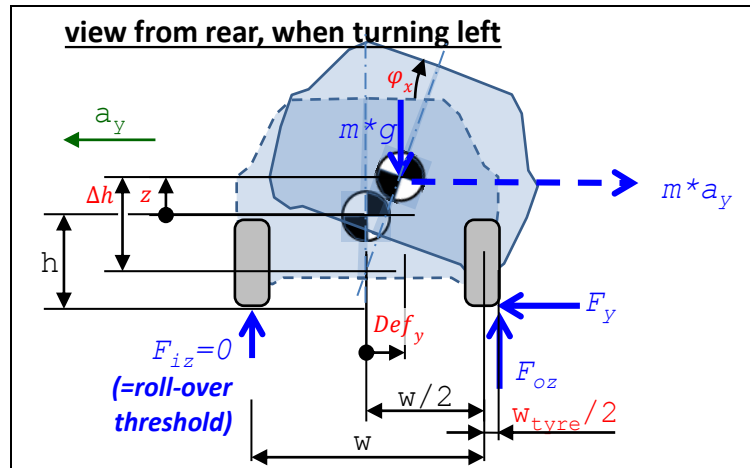


Figure 4-48: Steady-state roll-over model, with fore/aft symmetry. The measures w_{tyre} , Def_y , $\Delta h \cdot \phi_x$ and z mark effects additional to what is covered with a simple SSF approach.

4.3.11.3.2 Model without fore/aft symmetry

As steady state roll-over threshold which takes into account the differences between front and rear suspension is shown in Equation [4.43]. If assuming roll-over in left curve, the wheels to observe would be the front left and rear left. Hence, the vehicle will roll-over when:

$$\left. \begin{aligned}
 F_{flz} &= m \cdot \left(\frac{g \cdot l_r}{2 \cdot L} - a_y \cdot \left(\frac{h_{RCf} \cdot l_r}{L \cdot w} + \frac{\Delta h}{w} \cdot \frac{c_{fw}}{c_{fw} + c_{rw}} \right) \right) < 0; \text{ AND} \\
 F_{rlz} &= m \cdot \left(\frac{g \cdot l_f}{2 \cdot L} - a_y \cdot \left(\frac{h_{RCr} \cdot l_f}{L \cdot w} + \frac{\Delta h}{w} \cdot \frac{c_{rw}}{c_{fw} + c_{rw}} \right) \right) < 0;
 \end{aligned} \right\} \Rightarrow$$

$$\Rightarrow a_y > \frac{g}{2 \cdot L} \cdot \max \left(\frac{l_r}{\frac{h_{RCf} \cdot l_r}{L \cdot w} + \frac{\Delta h}{w} \cdot \frac{c_{fw}}{c_{fw} + c_{rw}}}; \frac{l_f}{\frac{h_{RCr} \cdot l_f}{L \cdot w} + \frac{\Delta h}{w} \cdot \frac{c_{rw}}{c_{fw} + c_{rw}}} \right);$$

[4.49]

It should be noted that this roll-over condition is approximate, in that the effects in section 4.3.11.3.1, are NOT taken into account. Furthermore, the end-stop of the inner wheel which lifts first is NOT taken into account, i.e. it is NOT modelled that the wheel that have lifted takes no more vertical forces.

4.3.11.3.3 Using a transient model for steady-state roll-over

Another work-around to avoid complex algebra is to run a fully transient model, including suspension, and run it until a steady state cornering conditions occur. If then, the lateral acceleration is slowly increased, one can identify when or if the roll-over threshold is reached. Lateral acceleration

increase can be through either increase of longitudinal speed or steering angle. It should be noted that the model should reasonably be able to manage at least lift of one wheel from the ground. This way of verifying steady state cornering roll-over requirements has the advantage that, if using tyre models with friction saturation, the limitation discussed in Section 0 does not have to be checked separately.

4.3.11.4 Roll-over and understeering/propulsion

With the above formulas for roll-over there will always be a certain lateral acceleration that leads to roll-over, because neither limitation due to road friction nor propulsion power modelled yet. Since vehicles generally are understeered, they are limited to develop lateral acceleration, see Figure 4-32. For propulsion-weak vehicles, there is also the limitation of lateral acceleration due to limited longitudinal speed, which in turn is due to driving resistance from the steered wheels (=wheel lateral force * sin(steering angle)) and loosing propulsion power due to longitudinal wheel slip. However, one should take into account that the propulsion limitation is less in down-hill driving, which increases the roll-over risk again. Also, if the vehicles goes relatively quickly into steady state cornering, the longitudinal speed will not have time to decelerate to its real (longitudinal) steady state value.

For heavy trucks, the critical lateral acceleration is typically 0.3..0.4 g, which is quite possible to reach during normal road conditions, because road friction is there around 1. For passenger cars, the critical lateral acceleration is typically in the region of 1, so it is not obvious that it is possible to reach the roll-over-critical lateral acceleration. This is also the case for heavy trucks on low road friction.

4.4 Stationary oscillating steering

In between steady state and transient manoeuvres, one can identify stationary oscillations as an intermediate step.

Generally, a mechanical system can be excited with a stationary oscillating disturbance. The response of the system is, after possible transients are damped out, a stationary oscillation. If staying within the linear region for the system and the excitation is harmonic (sinus and cosine), the ratio between the response amplitude and the excitation amplitude is only dependent of the frequency. The ratio is called transfer function.

For lateral vehicle dynamics, the excitation is typically steering wheel angle and the response is amplitudes of yaw rate, curvature or lateral acceleration. The corresponding transfer functions are a frequency version of the gains defined in Equation [4.28].

Also, there will be a delay between excitation and response. This is another important measure, beside the amplitude ratio.

4.4.1 Stationary oscillating steering tests

When testing Stationary oscillating steering functions, one usually drives on a longer part of the test track. It might be a high speed track, see Figure 4-8, because one generally need to find the response at high speeds, rather than driving close to lateral limits. So the track rather needs to be long than wide. If the available Vehicle Dynamics Area, see Figure 4-8, is long enough this can be a safer option. A Vehicle Dynamics Area is a flat surface with typically 100..300 m diameter. It normally has entrance roads for accelerating up to a certain speed.

Typical tests in this part of lateral vehicle dynamics are:

- Sweeping frequency and/or amplitude
- Random frequency and amplitude

There are ISO standards for both these tests. The response will be very dependent of the vehicle longitudinal speed, why the same tests are typically done at different such speeds.

4.4.2 Transient one-track model

The model needed for stationary oscillation is only a linearization of the model needed for fully transient handling, in Section 4.5. However, a rather complete model will be derived already in present section, to capture the physical assumptions in a proper way. (If the reader is satisfied with the linearized model, it can be found directly in Equation [4.54], and a less general derivation of this equation in Figure 4-53.)

The vehicle model is sketched in Figure 4-51. The model is a development of the model for steady state cornering in Figure 4-21, with the following changes:

- Longitudinal and lateral accelerations don't only have the components of centripetal acceleration ($\omega_z \cdot v_y$ and $\omega_z \cdot v_x$), but also the derivatives of v_x and v_y :

$$\begin{aligned} a_x &= \text{der}(v_x) - \omega_z \cdot v_y = \dot{v}_x - \omega_z \cdot v_y; \\ a_y &= \text{der}(v_y) + \omega_z \cdot v_x = \dot{v}_y + \omega_z \cdot v_x; \end{aligned} \quad [4.50]$$

- The yaw acceleration, $\text{der}(\omega_z)$, is no longer zero.
- The speed v_x is no longer defined as a parameter, but a variable. Then, one more prescription is needed to be a consistent model. For this purpose, an equation that sets front axle propulsion torque to 1000 Nm is added.

The difference between acceleration $\vec{a} = [a_x; a_y]$ and $[\text{der}(v_x); \text{der}(v_y)] = [\dot{v}_x; \dot{v}_y]$ can be confusing. A way to understand those could be to think of \vec{a} as the (geometric vector) acceleration in the inertial coordinate system and $[\dot{v}_x; \dot{v}_y]$ as a (mathematical) vector, with derivatives of the scalar mathematical variables v_x and v_y , which are the velocities in the vehicle fix (and moving) coordinate system. A graphical derivation of Equation [4.50] is found below, in Figure 4-54.

The model in Figure 4-51 is documented as mathematical model in Equation [4.51]. The equation is given in Modelica format. The subscript v and w refers to vehicle coordinate system and wheel coordinate system, respectively. The model is a development of the model for low-speed in Equation [4.12], with the changes marked with underlined text:

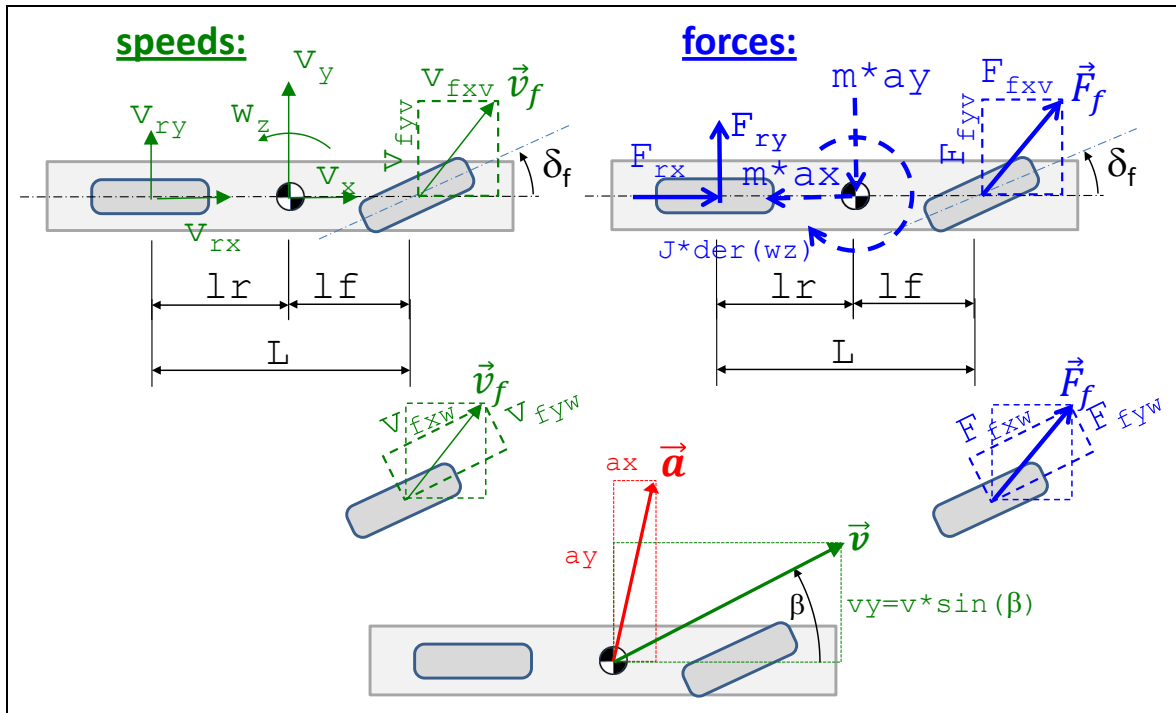


Figure 4-51: One-track model for transient dynamics. Dashed forces and moment are fictive forces. Compare to Figure 4-21.

```

// (Dynamic) Equilibrium:
m*ax = Ffxv + Frx;
m*ay = Ffyv + Fry;
J*der(wz) = Ffyv*lf - Fry*lr;
ax=der(vx)-wz*vy;
ay=der(vy)+wz*vx;

// Constitutive relation (Lateral tyre force model):
Ffyw=-Cf*sfy;
Fry=-Cr*sry;
sfy=vfyw/vfxw;
sry=vry/vrx;

// Compatibility:
vfxv = vx;
vfyv = vy + lf*wz;
vrx = vx;
vry = vy - lr*wz;

// Transformation between vehicle and wheel coordinate systems:
Ffxv = Ffxw*cos(df) - Ffyw*sin(df);
Ffyv = Ffxw*sin(df) + Ffyw*cos(df);
vfxv = vfxw*cos(df) - vfyw*sin(df);
vfyv = vfxw*sin(df) + vfyw*cos(df);

// Path with orientation:
der(x) = vx*cos(pz) - vy*sin(pz);
der(y) = vy*cos(pz) + vx*sin(pz);
der(pz) = wz;

// Prescription of steering angle:
df = if time < 2.5 then (5*pi/180)*sin(0.5*2*pi*time) else 5*pi/180;
// Shaft torques:
Ffxw = +1000; // Front axle driven.
Frx = -100; // Rolling resistance on rear axle.
    
```

[4.51]

The initial longitudinal speed is a parameter, $v_x=100$ km/h. A simulation result from the model is shown in Figure 4-52. The manoeuvre selected is same steering wheel function of time as in Figure 4-22, for better comparison of the different characteristics of the models.

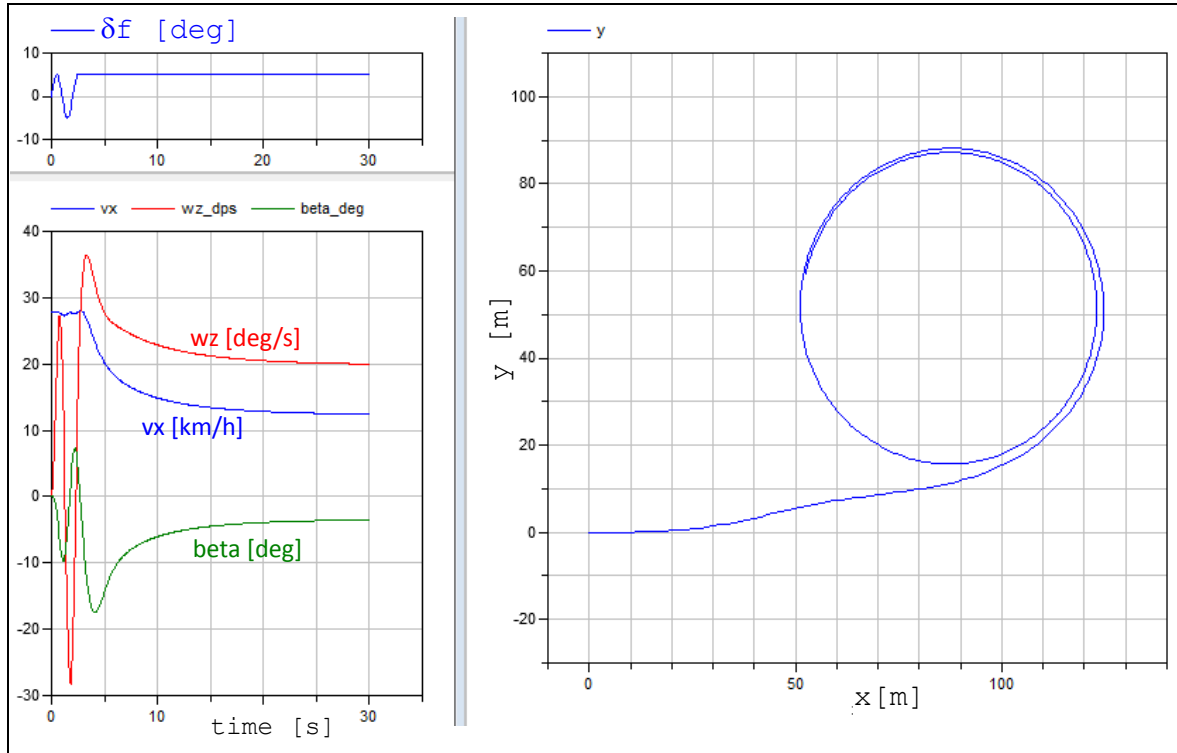


Figure 4-52: Simulation results of one-track model for transient dynamics.

Both position variables x , y , p_z and speed variables v_x , v_y and w_z are “state variables” of this simulation. For each continuation from one time instant, the future solution requires knowledge of the previous states. This means that in the beginning, initial values were needed on the state variable. The only non-zero initial value was for v_x , which was given to 100 km/h.

Equation [4.51] is a complete model suitable for simulation. Eliminating some variable and rewrite in prettier format gives:

Equilibrium:

$$\begin{aligned} m \cdot (\dot{v}_x - \omega_z \cdot v_y) &= F_{f_{xw}} \cdot \cos(\delta_f) - F_{f_{yw}} \cdot \sin(\delta_f) + F_{rx}; \\ m \cdot (\dot{v}_y + \omega_z \cdot v_x) &= F_{f_{xw}} \cdot \sin(\delta_f) + F_{f_{yw}} \cdot \cos(\delta_f) + F_{ry}; \\ J \cdot \dot{\omega}_z &= (F_{f_{xw}} \cdot \sin(\delta_f) + F_{f_{yw}} \cdot \cos(\delta_f)) \cdot l_f - F_{ry} \cdot l_r; \end{aligned}$$

Constitution:

$$F_{f_{yw}} = -C_f \cdot s_{fy}; \quad \text{and} \quad F_{ry} = -C_r \cdot s_{ry};$$

Compatibility:

$$s_{fy} = \frac{v_{fyw}}{v_{fxw}}; \quad \text{and} \quad s_{ry} = \frac{v_y - l_r \cdot \omega_z}{v_x};$$

Transformation from vehicle to wheel coordinate system on front axle:

$$\begin{aligned} v_{f_{xw}} &= (v_y + l_f \cdot \omega_z) \cdot \sin(\delta_f) + v_x \cdot \cos(\delta_f); \\ v_{f_{yw}} &= (v_y + l_f \cdot \omega_z) \cdot \cos(\delta_f) - v_x \cdot \sin(\delta_f); \end{aligned}$$

[4.52]

Typically, this model is used for simulation, where δ_f , F_{fxw} and F_{rx} are input variables. Suitable state variables are then v_x , v_y and ω_z . It is a model suitable for arbitrary transient manoeuvres and we will come back to this in Section 4.5. It is non-linear with respect to angles, but linear with respect to tyre slip model. It is also non-linear with respect to that the states appear as multiplied with each other, e.g. $\omega_z \cdot v_x$.

For the stationary oscillation events, this compendium will be limited to manoeuvres where far from saturating tyre grip and at constant v_x ($\Rightarrow \dot{v}_x = 0$). We assume:

- Low usage of lateral tyre force, i.e. small tyre slip angle (α_f): $s_{fy} = \tan(\alpha_f) \approx \alpha_f$;
- Low level of cornering, i.e.
 - small steering angle: $\sin(\delta_f) \approx \delta_f$; $\cos(\delta_f) \approx 1$;
 - small front body slip angle (β_f): $\alpha_f = \beta_f - \delta_f$;
 where $\beta_f = \arctan\left(\frac{v_{fyv}}{v_{fxv}}\right) \approx \frac{v_{fyv}}{v_{fxv}} = \frac{v_y + l_f \cdot \omega_z}{v_x}$;

We then rewrite the two last equations in Equation [4.52]:

$$\left\{ \begin{array}{l} m \cdot (\dot{v}_y + \omega_z \cdot v_x) = F_{fxw} \cdot \delta_f - C_f \cdot \left(\frac{v_y + l_f \cdot \omega_z}{v_x} - \delta_f \right) - C_r \cdot \frac{v_y - l_r \cdot \omega_z}{v_x}; \\ J \cdot \dot{\omega}_z = \left(F_{fxw} \cdot \delta_f - C_f \cdot \left(\frac{v_y + l_f \cdot \omega_z}{v_x} - \delta_f \right) \right) \cdot l_f + C_r \cdot \frac{v_y - l_r \cdot \omega_z}{v_x} \cdot l_r; \end{array} \right\} \quad [4.53]$$

$$\Rightarrow \left\{ \begin{array}{l} -m \cdot \omega_z \cdot v_y = F_{fxw} + F_{rx} + C_f \cdot \left(\frac{v_y + l_f \cdot \omega_z}{v_x} - \delta_f \right) \cdot \delta_f; \\ m \cdot \dot{v}_y + \frac{C_f + C_r}{v_x} \cdot v_y + \left(\frac{C_f \cdot l_f - C_r \cdot l_r}{v_x} + m \cdot v_x \right) \cdot \omega_z = (C_f + F_{fxw}) \cdot \delta_f; \\ J \cdot \dot{\omega}_z + \frac{C_f \cdot l_f - C_r \cdot l_r}{v_x} \cdot v_y + \frac{C_f \cdot l_f^2 + C_r \cdot l_r^2}{v_x} \cdot \omega_z = (C_f + F_{fxw}) \cdot l_f \cdot \delta_f; \end{array} \right\}$$

This equation is written on matrix form (for the two state variables, v_y and ω_z) and one algebraic equation for the longitudinal equilibrium. Then:

$$\begin{bmatrix} m & 0 \\ 0 & J \end{bmatrix} \cdot \begin{bmatrix} \dot{v}_y \\ \dot{\omega}_z \end{bmatrix} + \begin{bmatrix} \frac{C_f + C_r}{v_x} & \frac{C_f \cdot l_f - C_r \cdot l_r}{v_x} + m \cdot v_x \\ \frac{C_f \cdot l_f - C_r \cdot l_r}{v_x} & \frac{C_f \cdot l_f^2 + C_r \cdot l_r^2}{v_x} \end{bmatrix} \cdot \begin{bmatrix} v_y \\ \omega_z \end{bmatrix} = \begin{bmatrix} C_f + F_{fxw} \\ (C_f + F_{fxw}) \cdot l_f \end{bmatrix} \cdot \delta_f; \quad [4.54]$$

Neglecting the longitudinal equilibrium and assuming that propulsion forces can be neglected for lateral and yaw equilibrium:

$$\begin{bmatrix} m & 0 \\ 0 & J \end{bmatrix} \cdot \begin{bmatrix} \dot{v}_y \\ \dot{\omega}_z \end{bmatrix} + \begin{bmatrix} \frac{C_f + C_r}{v_x} & \frac{C_f \cdot l_f - C_r \cdot l_r}{v_x} + m \cdot v_x \\ \frac{C_f \cdot l_f - C_r \cdot l_r}{v_x} & \frac{C_f \cdot l_f^2 + C_r \cdot l_r^2}{v_x} \end{bmatrix} \cdot \begin{bmatrix} v_y \\ \omega_z \end{bmatrix} = \begin{bmatrix} 1 \\ l_f \end{bmatrix} \cdot C_f \cdot \delta_f; \quad [4.55]$$

It should be noted that the assumption about small front body slip angle (β_f) makes the linearization questionable at high curvature, i.e. at small path radii.

The longitudinal equilibrium (first equation in Equation [4.52]) is often not mentioned, because the longitudinal dynamics is prescribed as a constant speed, v_x . However, this equation can be used to calculate required propulsion on the axles to maintain the constant longitudinal speed. Note that it is complemented with air and grade resistance force.

$$F_{fxw} \cdot \cos(\delta_f) + F_{rx} = F_{air} + F_{grade} - m \cdot \omega_z \cdot v_y - C_f \cdot \frac{(v_y + l_f \cdot \omega_z) \cdot \cos(\delta_f) - v_x \cdot \sin(\delta_f)}{(v_y + l_f \cdot \omega_z) \cdot \sin(\delta_f) + v_x \cdot \cos(\delta_f)} \cdot \sin(\delta_f);$$

[4.56]

If $\delta_f, \alpha_f, \beta_f$ are small and $\beta_f \cdot \delta_f \approx 0; \delta_f \cdot \delta_f \approx 0;$

$$F_{fxw} + F_{rx} = F_{air} + F_{grade} - m \cdot \omega_z \cdot v_y;$$

4.4.2.1 Simpler model

A simpler way to reach this final expression is given in Figure 4-53. Here, the simplifications are introduced earlier, already in physical model, which means e.g. that the influence of F_{fxw} is not found.

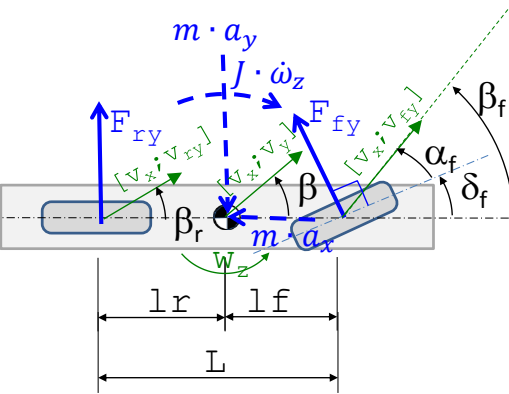
<p>Physical model:</p> <ul style="list-style-type: none"> • Path radius \gg the vehicle. Then, all forces (and centripetal acceleration) are approximately co-directed. • Small tyre and vehicle side slip. Then, angle=$\sin(\text{angle})=\tan(\text{angle})$. (Angles are not drawn small, which is the reason why the forces not appear co-linear in figure.)  <p style="text-align: center;"> $a_x = (\dot{v}_x - \omega_z \cdot v_y);$ $a_y = (\dot{v}_y + \omega_z \cdot v_x);$ </p>	<p>Mathematical model:</p> <p>Equilibrium:</p> $m \cdot (\dot{v}_x - \omega_z \cdot v_y) \approx F_{fx} + F_{rx}; \text{ where } \dot{v}_x = 0;$ $m \cdot (\dot{v}_y + \omega_z \cdot v_x) \approx F_{fy} + F_{ry};$ $J \cdot \dot{\omega}_z \approx F_{fy} \cdot l_f - F_{ry} \cdot l_r;$ <p>Constitution: $F_{fy} = -C_f \cdot s_{yf}; \quad F_{ry} = -C_r \cdot s_{yr};$</p> <p>Compatibility:</p> $\left\{ \begin{array}{l} \delta_f + \alpha_f = \beta_f; \quad \beta_f \approx \frac{v_{fy}}{v_x} = \frac{v_y + l_f \cdot \omega_z}{v_x}; \\ \alpha_r = \beta_r \approx \frac{v_{ry}}{v_x} = \frac{v_y - l_r \cdot \omega_z}{v_x}; \\ \alpha_f \approx s_{yf}; \quad \alpha_r \approx s_{yr}; \end{array} \right\}$ <p>Eliminate $F_{fy}, F_{ry}, \alpha_f, \alpha_r, \beta_f, \beta_r$ yields:</p> $m \cdot \dot{v}_y + \frac{C_f + C_r}{v_x} \cdot v_y + \left(\frac{C_f \cdot l_f - C_r \cdot l_r}{v_x} + m \cdot v_x \right) \cdot \omega_z \approx C_f \cdot \delta_f;$ $J \cdot \dot{\omega}_z + \frac{C_f \cdot l_f - C_r \cdot l_r}{v_x} \cdot v_y + \frac{C_f \cdot l_f^2 + C_r \cdot l_r^2}{v_x} \cdot \omega_z \approx C_f \cdot l_f \cdot \delta_f;$ $F_{fx} + F_{rx} \approx -m \cdot \omega_z \cdot v_y;$
--	---

Figure 4-53: Simpler derivation final step in Equation [4.55].

4.4.2.2 Relation between accelerations in inertial system and velocity derivatives in vehicle fix system

See Equation [4.50]. The relation between accelerations in inertial system, $\vec{a} = [a_x; a_y]$, and velocity derivatives in vehicle fix system, $[\text{der}(v_x); \text{der}(v_y)] = [\dot{v}_x; \dot{v}_y]$, is further explained in Figure 4-54.

We can express the velocity in direction of the x axis at time t, at the two time instants:

Velocity at time = t : \mathbf{v}_x

$$\begin{aligned} \text{Velocity at time } = t + \Delta t: & (v_x + \Delta v_x) \cdot \cos(\Delta\psi) - (v_y + \Delta v_y) \cdot \sin(\Delta\psi) = \\ & (v_x \cdot \cos(\Delta\psi) + \Delta v_x \cdot \cos(\Delta\psi)) - (v_y \cdot \sin(\Delta\psi) + \Delta v_y \cdot \sin(\Delta\psi)) \approx \{\Delta\psi \text{ small}\} \approx \\ & (v_x + \Delta v_x) - (v_y \cdot \Delta\psi + \Delta v_y \cdot \Delta\psi) \approx \{\Delta v_y \cdot \Delta\psi \text{ small}\} \approx (v_x + \Delta v_x) - v_y \cdot \Delta\psi \end{aligned}$$

[4.57]

Using these two expressions, we can express a_x as the change of that speed per time unit:

$$\begin{aligned} \text{Change per time} = \mathbf{a}_x &= \frac{\{(v_x + \Delta v_x) - v_y \cdot \Delta\psi\} - v_x}{\Delta t} = \frac{\Delta v_x - v_y \cdot \Delta\psi}{\Delta t} = \frac{\Delta v_x}{\Delta t} - v_y \frac{\Delta\psi}{\Delta t} \approx \\ & \approx \dot{v}_x - v_y \cdot \dot{\psi} = \dot{v}_x - \mathbf{v}_y \cdot \boldsymbol{\omega}_z \end{aligned}$$

[4.58]

Corresponding for the lateral direction gives, in total, the Equation [4.50].

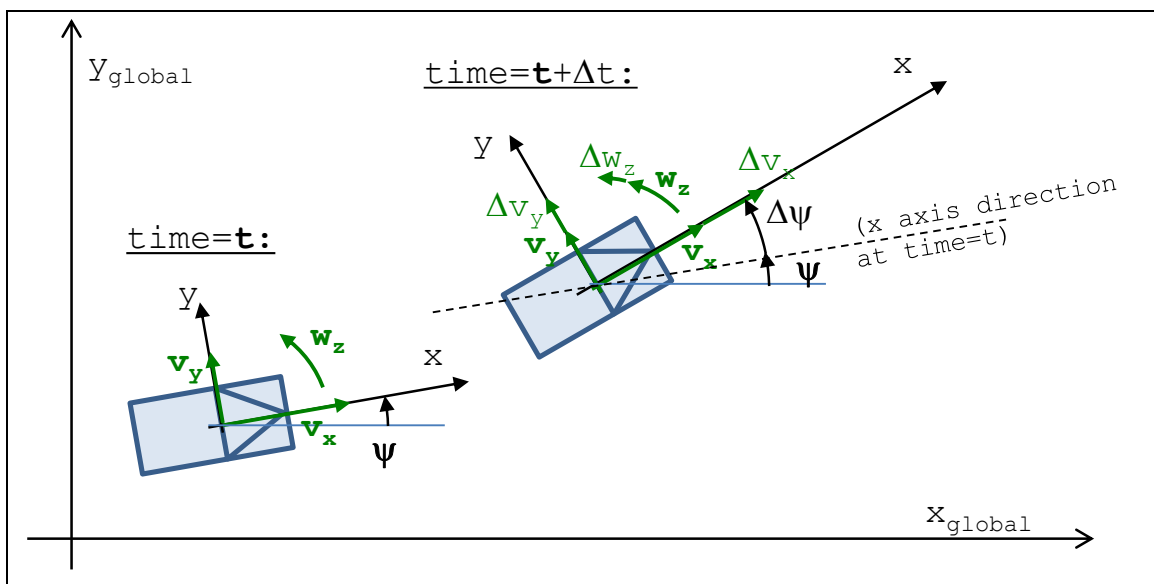


Figure 4-54: Vehicle motion in ground plane

4.4.2.3 Validity of solution

When only studying the response as yaw rate and curvature response, it is easy to forget that one very easily comes into manoeuvres where road friction is limited, i.e. where the linear tyre model is not valid. Hence it is good to look at lateral acceleration response, because we can roughly say that for $|a_y|$ in the same magnitude as $\mu \cdot m \cdot g$, it is doubtful if the model is valid. If the wheel torques are significant, the validity limit is even lower. For high CoG vehicles, another invalidating circumstance is wheel lift, which can be approximately checked by checking that $|a_y| \ll SSF = \frac{g \cdot w}{2 \cdot h}$.

If one really wants to include nonlinear tyre models in stationary oscillation response, one can simulate using time integration (same method as usually used for transient handling) over several excitation cycles, until the response shows a clear stationary oscillation. This consumes more computational efforts and the solutions become approximate and numerical.

4.4.3 Steering frequency response gains *

Function definition: **Steering frequency response gains** are the amplifications from steering angle amplitude to certain vehicle response measure's amplitudes for stationary oscillating harmonic steering at a certain longitudinal speed.

Equation [4.55] (or resulting eq in Figure 4-53) can be seen as a state-space-model:

$$\text{State space form: } \begin{cases} \begin{bmatrix} \dot{v}_y \\ \dot{\omega}_z \end{bmatrix} = \mathbf{A} \cdot \begin{bmatrix} v_y \\ \omega_z \end{bmatrix} + \mathbf{B} \cdot \delta_f; \\ \begin{bmatrix} \omega_z \\ a_y \end{bmatrix} = \mathbf{C} \cdot \begin{bmatrix} v_y \\ \omega_z \end{bmatrix} + \mathbf{D} \cdot \delta_f; \end{cases}$$

$$\text{where } \mathbf{A} = - \begin{bmatrix} m & 0 \\ 0 & J \end{bmatrix}^{-1} \cdot \begin{bmatrix} \frac{C_f + C_r}{v_x} & \frac{C_f \cdot l_f - C_r \cdot l_r}{v_x} + m \cdot v_x \\ C_f \cdot l_f - C_r \cdot l_r & \frac{C_f \cdot l_f^2 + C_r \cdot l_r^2}{v_x} \end{bmatrix};$$

$$\text{and } \mathbf{B} = \begin{bmatrix} m & 0 \\ 0 & J \end{bmatrix}^{-1} \cdot \begin{bmatrix} 1 \\ l_f \end{bmatrix} \cdot C_f;$$

$$\text{and } \mathbf{C} = \begin{bmatrix} 0 & 0 \\ 1 & 0 \end{bmatrix} \cdot \mathbf{A} + \begin{bmatrix} 0 & 1 \\ 0 & v_x \end{bmatrix};$$

$$\text{and } \mathbf{D} = \mathbf{B};$$

[4.59]

When studying “stationary oscillating steering”:

$$\begin{bmatrix} \dot{v}_y \\ \dot{\omega}_z \end{bmatrix} = \mathbf{A} \cdot \begin{bmatrix} v_y \\ \omega_z \end{bmatrix} + \mathbf{B} \cdot \delta(t) = \mathbf{A} \cdot \begin{bmatrix} v_y \\ \omega_z \end{bmatrix} + \mathbf{B} \cdot \hat{\delta} \cdot \cos(\omega \cdot t)$$

(Note similar notation for vehicle yaw rate, ω_z , and steering angular frequency, ω .) Knowing $\hat{\delta}$ and ω , it is possible to calculate the responses \hat{v}_y , $\hat{\omega}_z$, φ_y and φ_z :

$$\begin{bmatrix} v_y \\ \omega_z \end{bmatrix} = \begin{bmatrix} \hat{v}_y \\ \hat{\omega}_z \end{bmatrix} \cdot \cos\left(\omega \cdot t - \begin{bmatrix} \varphi_{v_y} \\ \varphi_{\omega_z} \end{bmatrix}\right);$$

$$\begin{bmatrix} \omega_z \\ a_y \end{bmatrix} = \begin{bmatrix} \hat{\omega}_z \\ \hat{a}_y \end{bmatrix} \cdot \cos\left(\omega \cdot t - \begin{bmatrix} \varphi_{\omega_z} \\ \varphi_{a_y} \end{bmatrix}\right);$$

Different methods are available for calculation of the responses:

- **Real trigonometry**, using $\cos(\omega \cdot t + phase)$, $\sin(\omega \cdot t + phase)$ or $\cos(\omega \cdot t) + \sin(\omega \cdot t)$.
- **Complex mathematics**, using $e^{j \cdot \omega \cdot t}$
- **Fourier transform**

For each of these, one can also work with scalar or matrix algebra. Matrix based Fourier transform is generally the most efficient, especially if Matlab is available and numerical solutions can be accepted.

4.4.3.1 Single frequency response

4.4.3.1.1 Solution with Fourier transform

Equation [4.59] can be transformed to the frequency domain (where the Fourier transform of a function, $\xi(t)$, is denoted $\mathcal{F}(\xi(t)) = \int_0^\infty e^{-j \cdot \omega \cdot t} \cdot \xi(t) \cdot dt$):

$$\begin{cases} j \cdot \omega \cdot \mathcal{F} \left(\begin{bmatrix} v_y \\ \omega_z \end{bmatrix} \right) = \mathbf{A} \cdot \mathcal{F} \left(\begin{bmatrix} v_y \\ \omega_z \end{bmatrix} \right) + \mathbf{B} \cdot \mathcal{F}(\delta_f); \\ \mathcal{F} \left(\begin{bmatrix} \omega_z \\ a_y \end{bmatrix} \right) = \mathbf{C} \cdot \mathcal{F} \left(\begin{bmatrix} v_y \\ \omega_z \end{bmatrix} \right) + \mathbf{D} \cdot \mathcal{F}(\delta_f); \end{cases} \quad [4.60]$$

Solving for states and outputs:

$$\begin{cases} \begin{bmatrix} v_y \\ \omega_z \end{bmatrix} = \mathcal{F}^{-1} \left(\mathcal{F} \left(\begin{bmatrix} v_y \\ \omega_z \end{bmatrix} \right) \right) = \mathcal{F}^{-1} \left((j \cdot \omega \cdot \mathbf{I} - \mathbf{A})^{-1} \cdot \mathbf{B} \cdot \mathcal{F}(\delta_f) \right); \\ \begin{bmatrix} \omega_z \\ a_y \end{bmatrix} = \mathcal{F}^{-1} \left(\mathcal{F} \left(\begin{bmatrix} \omega_z \\ a_y \end{bmatrix} \right) \right) = \mathcal{F}^{-1} \left(\mathbf{C} \cdot \mathcal{F} \left(\begin{bmatrix} v_y \\ \omega_z \end{bmatrix} \right) + \mathbf{D} \cdot \mathcal{F}(\delta_f) \right); \end{cases} \quad [4.61]$$

Expressed as transfer functions:

$$\begin{cases} H_{\delta_f \rightarrow [v_y]} = \frac{\mathcal{F} \left(\begin{bmatrix} v_y \\ \omega_z \end{bmatrix} \right)}{\mathcal{F}(\delta_f)} = \frac{(j \cdot \omega \cdot \mathbf{I} - \mathbf{A})^{-1} \cdot \mathbf{B} \cdot \mathcal{F}(\delta_f)}{\mathcal{F}(\delta_f)} = (j \cdot \omega \cdot \mathbf{I} - \mathbf{A})^{-1} \cdot \mathbf{B}; \\ H_{\delta_f \rightarrow [a_y]} = \frac{\mathcal{F} \left(\begin{bmatrix} \omega_z \\ a_y \end{bmatrix} \right)}{\mathcal{F}(\delta_f)} = \mathbf{C} \cdot H_{\delta_f \rightarrow [v_y]} + \mathbf{D} = \mathbf{C} \cdot (j \cdot \omega \cdot \mathbf{I} - \mathbf{A})^{-1} \cdot \mathbf{B} + \mathbf{D}; \end{cases} \quad [4.62]$$

We have derived the transfer functions. The subscript tells that the transfer function is for the vehicle operation with excitation=input= δ_f and response=output= $\begin{bmatrix} v_y \\ \omega_z \end{bmatrix}$ and output= $\begin{bmatrix} \omega_z \\ a_y \end{bmatrix}$. The transfer functions has dimension 2x1 and it is complex. They operate as follows:

$$\begin{aligned} \text{Amplitudes: } & \begin{cases} \begin{bmatrix} \hat{v}_y \\ \hat{\omega}_z \end{bmatrix} = \left| H_{\delta_f \rightarrow [v_y]} \right| \cdot \hat{\delta}_f; \\ \begin{bmatrix} \hat{\omega}_z \\ \hat{a}_y \end{bmatrix} = \left| H_{\delta_f \rightarrow [a_y]} \right| \cdot \hat{\delta}_f; \end{cases} \\ \text{Phase delays: } & \begin{cases} \begin{bmatrix} \varphi_{v_y} \\ \varphi_{\omega_z} \end{bmatrix} = \begin{bmatrix} \arg(v_y) \\ \arg(\omega_z) \end{bmatrix} - [1] \cdot \arg(\delta_f) = \begin{cases} \arg(\delta_f) \\ = 0 \end{cases} = \arg \left(H_{\delta_f \rightarrow [v_y]} \right); \\ \begin{bmatrix} \varphi_{\omega_z} \\ \varphi_{a_y} \end{bmatrix} = \begin{bmatrix} \arg(\omega_z) \\ \arg(a_y) \end{bmatrix} - [1] \cdot \arg(\delta_f) = \begin{cases} \arg(\delta_f) \\ = 0 \end{cases} = \arg \left(H_{\delta_f \rightarrow [a_y]} \right); \end{cases} \end{aligned} \quad [4.63]$$

4.4.3.1.2 Solution with complex mathematics

This section avoids requiring skills in Fourier transform. This makes the derivation quite long to reach the final results Equation [4.68] and Equation [4.67]. With Fourier Transform, the expression for the Transfer Function, H, can be reached with less algebra. Knowing H, it can be used in Equation [4.67].

The fundamental situation for steering frequency response is that the excitation is: $\delta_f = \hat{\delta}_f \cdot \cos(2 \cdot \pi \cdot f \cdot t) = \{e^{j \cdot a} = \cos(a) + j \cdot \sin(a)\} = \text{Re}(\hat{\delta}_f \cdot e^{j \cdot 2 \cdot \pi \cdot f \cdot t})$, where f is the (time) frequency in Hz and j is the imaginary unit. We rewrite $2 \cdot \pi \cdot f$ as ω (angular frequency), which has to be carefully distinguished from ω_z (yaw rate). Insert this in Equation [4.54] and neglecting the longitudinal force $F_{f_{xw}}$. The full (complex) equation is used:

$$\operatorname{Re} \left[\begin{bmatrix} m & 0 \\ 0 & J \end{bmatrix} \cdot \begin{bmatrix} \dot{v}_{yc} \\ \dot{\omega}_{zc} \end{bmatrix} + \begin{bmatrix} \frac{C_f + C_r}{v_x} & \frac{C_f \cdot l_f - C_r \cdot l_r}{v_x} + m \cdot v_x \\ \frac{C_f \cdot l_f - C_r \cdot l_r}{v_x} & \frac{C_f \cdot l_f^2 + C_r \cdot l_r^2}{v_x} \end{bmatrix} \cdot \begin{bmatrix} v_{yc} \\ \omega_{zc} \end{bmatrix} = \begin{bmatrix} C_f \\ C_f \cdot l_f \end{bmatrix} \cdot \delta_f \cdot e^{j\omega t} \right]; \quad [4.64]$$

We intend to solve the complex equation, and then find the solutions as real parts: $v_y = \operatorname{Re}[v_{yc}]$; and $\omega_z = \operatorname{Re}[\omega_{zc}]$. (Subscript c means complex.)

If only interested in the stationary solution, which is valid after possible initial value dependent transients are damped out, we can assume a general form for the solution.

$$\begin{bmatrix} v_{yc} \\ \omega_{zc} \end{bmatrix} = \begin{bmatrix} \hat{v}_{yc} \\ \hat{\omega}_{zc} \end{bmatrix} \cdot e^{j\omega t} \Rightarrow \begin{bmatrix} \dot{v}_{yc} \\ \dot{\omega}_{zc} \end{bmatrix} = j \cdot \omega \cdot \begin{bmatrix} \hat{v}_{yc} \\ \hat{\omega}_{zc} \end{bmatrix} \cdot e^{j\omega t}; \quad [4.65]$$

Inserting the assumption in the differential equation gives:

$$\begin{aligned} & \begin{bmatrix} m & 0 \\ 0 & J \end{bmatrix} \cdot j \cdot \omega \cdot \begin{bmatrix} \hat{v}_{yc} \\ \hat{\omega}_{zc} \end{bmatrix} \cdot e^{j\omega t} + \\ & + \begin{bmatrix} \frac{C_f + C_r}{v_x} & \frac{C_f \cdot l_f - C_r \cdot l_r}{v_x} + m \cdot v_x \\ \frac{C_f \cdot l_f - C_r \cdot l_r}{v_x} & \frac{C_f \cdot l_f^2 + C_r \cdot l_r^2}{v_x} \end{bmatrix} \cdot \begin{bmatrix} \hat{v}_{yc} \\ \hat{\omega}_{zc} \end{bmatrix} \cdot e^{j\omega t} = \begin{bmatrix} 1 \\ l_f \end{bmatrix} \cdot C_f \cdot \delta_f \cdot e^{j\omega t} \Rightarrow \\ & \Rightarrow \begin{bmatrix} \hat{v}_{yc} \\ \hat{\omega}_{zc} \end{bmatrix} = \\ & = \left(\begin{bmatrix} m & 0 \\ 0 & J \end{bmatrix} \cdot j \cdot \omega + \begin{bmatrix} \frac{C_f + C_r}{v_x} & \frac{C_f \cdot l_f - C_r \cdot l_r}{v_x} + m \cdot v_x \\ \frac{C_f \cdot l_f - C_r \cdot l_r}{v_x} & \frac{C_f \cdot l_f^2 + C_r \cdot l_r^2}{v_x} \end{bmatrix} \right)^{-1} \cdot \begin{bmatrix} 1 \\ l_f \end{bmatrix} \cdot C_f \cdot \delta_f = \\ & = H_{\delta_f \rightarrow \begin{bmatrix} v_y \\ \omega_z \end{bmatrix}} \cdot \delta_f; \end{aligned} \quad [4.66]$$

Then, we can assume we know \hat{v}_{yc} and $\hat{\omega}_{zc}$ from Equation [4.66], and consequently we know v_{yc} and ω_{zc} from Equation [4.65]. We have derived the transfer function, $H_{\delta_f \rightarrow \begin{bmatrix} v_y \\ \omega_z \end{bmatrix}}$. The subscript tells that the transfer function is for the vehicle operation with excitation=input= δ_f and response=output= $\begin{bmatrix} v_y \\ \omega_z \end{bmatrix}$ case. This transfer function has dimension 2x1 and it is complex. It operates as follows:

$$\begin{aligned} \text{Amplitudes: } & \begin{bmatrix} \hat{v}_y \\ \hat{\omega}_z \end{bmatrix} = \begin{bmatrix} |v_y| \\ |\omega_z| \end{bmatrix} = \left| H_{\delta_f \rightarrow \begin{bmatrix} v_y \\ \omega_z \end{bmatrix}} \right| \cdot |\delta_f|; \\ \text{Phase delays: } & \begin{bmatrix} \arg(v_y) \\ \arg(\omega_z) \end{bmatrix} - \begin{bmatrix} 1 \\ 1 \end{bmatrix} \cdot \arg(\delta_f) = \{ \arg(\delta_f) = 0 \} = \arg \left(H_{\delta_f \rightarrow \begin{bmatrix} v_y \\ \omega_z \end{bmatrix}} \right) \end{aligned} \quad [4.67]$$

However, we can derive expressions for v_{yc} and ω_{zc} on a real (non-complex) form, *amplitude* · *cos(angular frequency · t – phase delay)*, without involving transfer function. That is done in the following:

$$v_y = \operatorname{Re}(v_{yc}) = \operatorname{Re}(\hat{v}_{yc} \cdot e^{j\omega t}) = \dots = |\hat{v}_{yc}| \cdot \cos(\omega \cdot t + \arg(\hat{v}_{yc}));$$

The same rewriting can be done with ω_z , so that in total:

$$\begin{bmatrix} v_y \\ \omega_z \end{bmatrix} = \begin{bmatrix} \hat{v}_y \cdot \cos(\omega \cdot t - \varphi_{vy}) \\ \hat{\omega}_z \cdot \cos(\omega \cdot t - \varphi_{\omega z}) \end{bmatrix} = \begin{bmatrix} |\hat{v}_{yc}| \cdot \cos(\omega \cdot t - (-\arg(\hat{v}_{yc}))) \\ |\hat{\omega}_{zc}| \cdot \cos(\omega \cdot t - (-\arg(\hat{\omega}_{zc}))) \end{bmatrix} \quad [4.68]$$

Equation [4.66] and Equation [4.68] now gives us the possibility to find vehicle response amplitude and phase delay. The ratios between amplitude of responses and amplitude of excitation, $\hat{v}_y/\hat{\delta}_f$ and $\hat{\omega}_z/\hat{\delta}_f$, are called gains. The difference in argument is the phase delay.

4.4.3.2 Lateral Velocity and Yaw Rate response

The frequency response for the two states, Lateral Velocity and Yaw Rate, can be plotted for given vehicle data, see Equation [4.66], Equation [4.68] and Figure 4-55. The curves show response for same vehicle, but different speed.

See Figure 4-55. The yaw rate gain curve has a knee at 0.5..1 Hz. The decrease after that is a measure of yaw damping. The curve for high speed actually has a weak peak just before the knee. This is not desired, because the vehicle might feel a bit nervous. Yaw damping can also be how fast yaw rate decays after a step response, see Section 4.5.

From Equation [4.27] we can calculate that characteristic speed for the vehicle is 120 km/h. With another understeering coefficient, we could have calculated a critical speed. With analysis as in Figure 4-55 to Figure 4-58, one can find these special speeds in another appearance:

- For an understeered vehicle, speeds above the characteristic speed gives a negative yaw rate delay for low steering frequencies will be negative.
- For over-steered vehicles, speeds above the critical speed gives a yaw rate delay larger than 180 deg and yaw rate amplitudes which are very large for low steering frequencies.

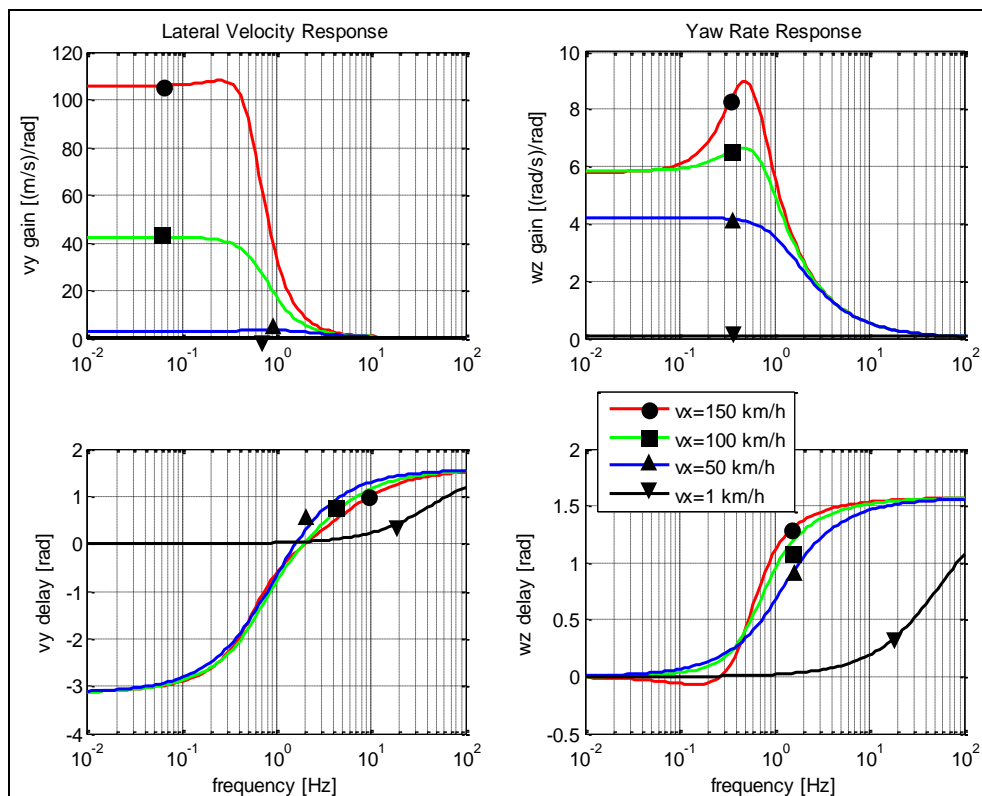


Figure 4-55: Vehicle response to harmonically oscillating steering angle. Vehicle data: $m=2000$ kg; $J=3000$ kg*m²; $l_f=1.3$ m; $l_r=1.5$ m; $C_f=81400$ N/rad; $C_r=78000$ N/rad; $(K_u = 1.26$ rad/MN).

LATERAL DYNAMICS

From Equation [4.27] we can calculate that characteristic speed for the vehicle is 120 km/h.

In Figure 4-56 the curves are for same speed and constant understeering gradient, but they show the response for different sums of cornering stiffness (C_f+C_r). Increasing the stiffness increases the yaw rate gain (agility) at high frequencies.

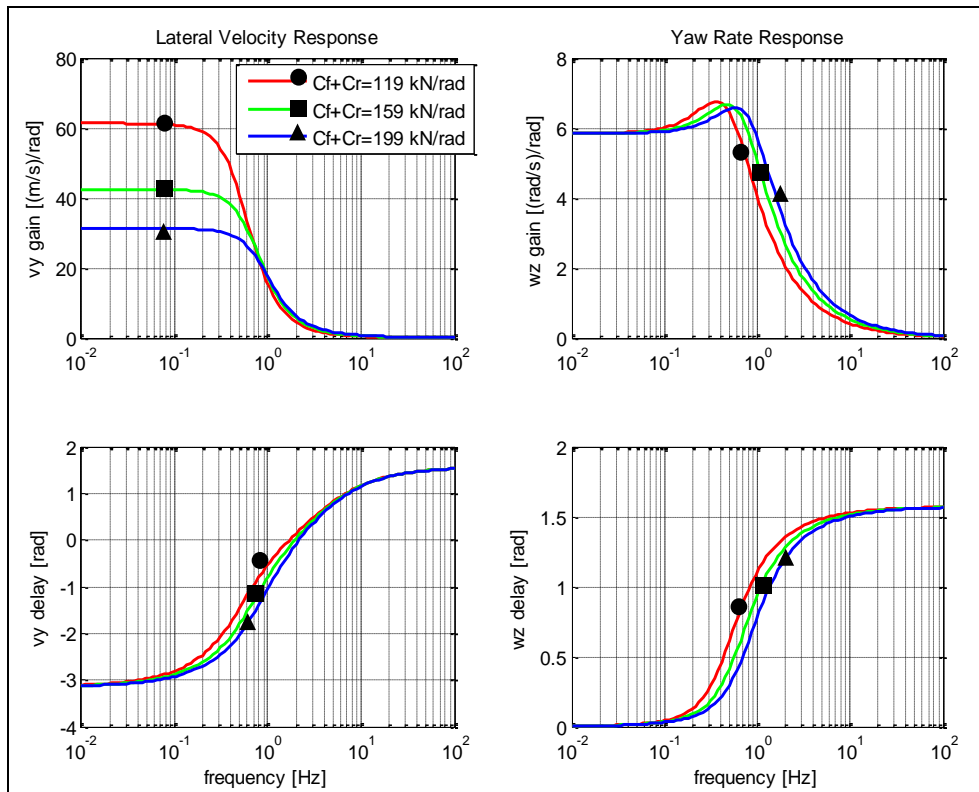


Figure 4-56: Vehicle response to harmonically oscillating steering angle. Same vehicle data as in Figure 4-55, except varying C_f and C_r but keeping understeering gradient K_u constant. Vehicle speed = 100 km/h.

In Figure 4-57 the curves are for same speed and constant sum of cornering stiffness (C_f+C_r), but they show the response for different values of understeering gradient (K_u). Increasing understeer gradient decreases the yaw rate gain (agility) at low frequencies.

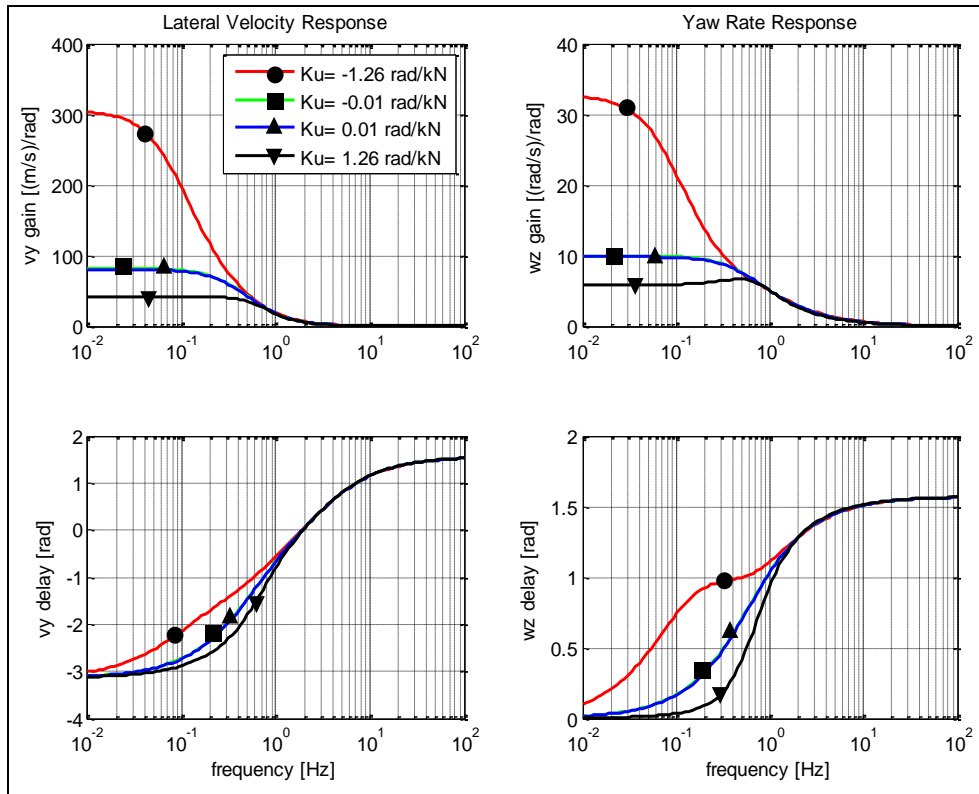


Figure 4-57: Vehicle response to harmonically oscillating steering angle. Same vehicle data as in Figure 4-55, except varying understeering gradient K_u but keeping C_f+C_r constant. Vehicle speed = 100 km/h.

4.4.3.3 Lateral Acceleration response

The lateral acceleration response is another useful response to study and set requirements on. Actually, yaw rate and lateral acceleration are the most frequently used response variables, since they are easily measured, e.g. from ESC sensors in most vehicles.

The transfer function is found (here using Fourier transform and previous results):

$$\begin{aligned}
 \text{Amplitude: } \hat{a}_y &= |a_{yc}| = \left\{ \text{use: } a_y = \frac{\dot{v}_y + \omega_z \cdot v_x}{m} \right\} = \left| \frac{j \cdot \omega \cdot v_{yc} + \omega_{zc} \cdot v_x}{m} \right| = \\
 &= \left| \frac{1}{m} \cdot [j \cdot \omega \quad v_x] \cdot H_{\delta_f \rightarrow [v_y]} \cdot \delta_f \right| = \left| [j \cdot \omega \quad v_x] \cdot H_{\delta_f \rightarrow [v_y]} \right| \cdot \frac{\delta_f}{m}; \\
 \text{Phase delay: } \arg(a_y) - \arg(\delta_f) &= \left\{ \text{use: } \arg(\delta_f) = 0 \right\} \\
 &= \arg \left([j \cdot \omega \quad v_x] \cdot H_{\delta_f \rightarrow [v_y]} \right);
 \end{aligned}
 \tag{4.69}$$

Lateral acceleration response is plotted for different vehicle speeds in Figure 4-58.

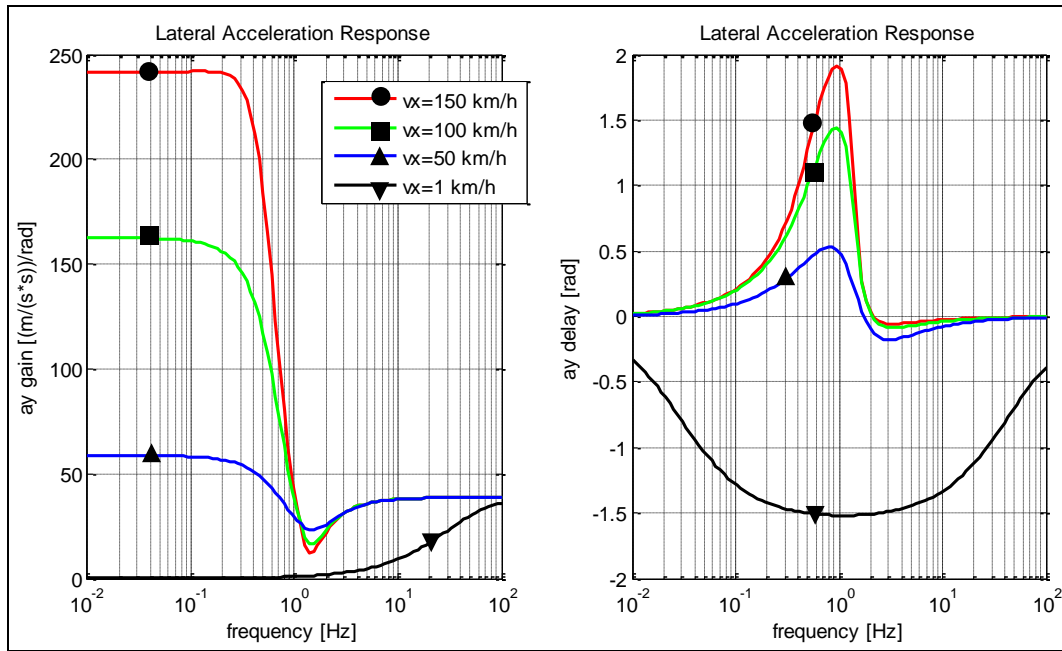


Figure 4-58: Vehicle lateral acceleration response to harmonically oscillating steering angle. Vehicle data: $m=2000$ kg; $J=3000$ kg*m²; $l_f=1.3$ m; $l_r=1.5$ m; $C_f=81400$ N/rad; $C_r=78000$ N/rad; ($K_u=1.26$ rad/MN).

4.4.3.4 Other responses to oscillating steering

In principle, it is possible to study a lot of other responses, such as Path Curvature response, Side slip response and Lateral Path Width response etc. These are not very standardized in requirement setting, but can be used as such or generally used for comparing different designs during the development work. For combination-vehicles it is common to plot Rearward amplification (RWA) as function of frequency. RWA can be either $RWA_{ay} = \max_{i=2,3,4,\dots} \left(\frac{\hat{a}_i}{\hat{a}_1} \right)$; where i denotes vehicle units or axles, or $RWA_{ay} = \max_{i=2,3,4,\dots} \left(\frac{\hat{\omega}_{zi}}{\hat{\omega}_{z1}} \right)$; where i denotes vehicle units.

4.4.3.5 Random frequency response

Solutions to harmonic excitation of linear dynamic systems are superimposable. This is also why the response from a mixed frequency excitation can be spliced into separate frequencies, e.g. using Fourier transformation. Hence, a common way to measure the frequency response diagrams is to log data from a random steering excitation. The frequency response diagram can then be extracted from this test.

4.5 Transient handling

Transient handling in general vehicle dynamics is when the vehicle is manoeuvred in an arbitrary, but not constant or cyclic, way. Generally, this can be turning and braking/accelerating at the same time through a manoeuvre. In this chapter, we only cover transient handling within lateral dynamics. This should be understood as that we assume a reasonably constant longitudinal vehicle speed and modest longitudinal forces on the wheels. The latter assumptions make it possible to base most of the content in this chapter on the model derived in Section 4.4.

4.5.1 Transient driving manoeuvres

When testing Transient driving manoeuvres, the typical part of the test track is the Vehicle Dynamics Area or a Handling Track, see Figure 4-8. A Handling Track is a normal width road, intentionally curved and with safety areas beside the curves for safety in case of run-off road during tests.

Typical transient tests are:

- Step steer, where one can measure transient versions of
 - Yaw rate response
 - Lateral acceleration response
 - Curvature response
 - Yaw damping
- Lateral avoidance manoeuvres:
 - Single lane change in cone track
 - Double lane change in cone track, see example in Figure 4-26
 - Lane change while full braking
 - Sine with dwell
 - Steering effort in evasive manoeuvres
- Tests from steady state cornering
 - Brake or accelerate in curve
 - Lift throttle and steer-in while cornering
 - Over-speeding into curve
- Handling type tests
 - Slalom between cones
 - Handling track, general driving experience
- Roll-over tests

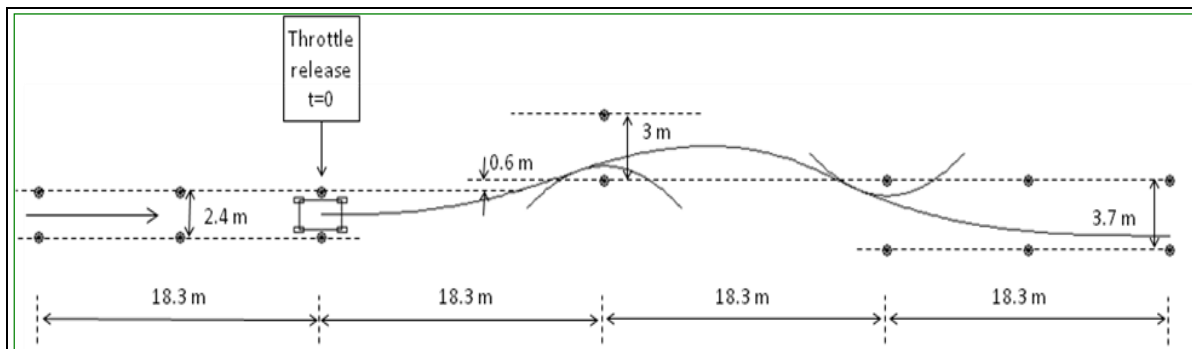


Figure 4-60: Cone track for one standardized Double lane change

Standards which are relevant to these test manoeuvres are, e.g. References (ISO 3888), (ISO 7401), (ISO 7975, 2006), (ISO 11026), (ISO 14791), (ISO 14793), (ISO 14794, 2011) and (NHTSA).

A general note is that tests in real vehicles are often needed to be performed in simulation also, and normally earlier in the product development process.

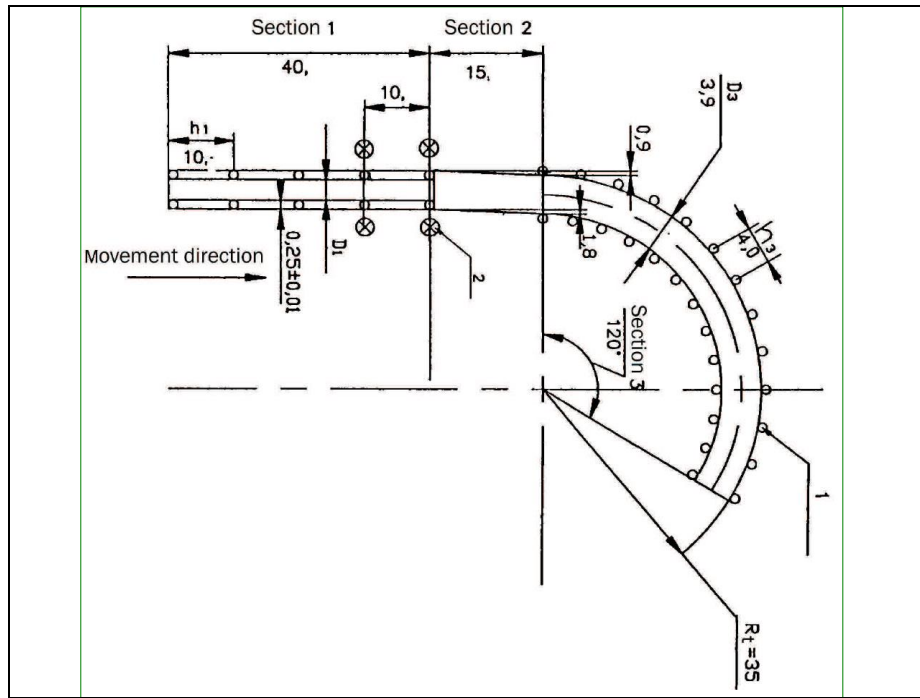


Figure 4-61: Cone track for one standardized test of Over-speeding into curve

4.5.2 Transient one-track model, without Lateral load transfer

Transient handling within lateral vehicle dynamics should be understood as that we assume a reasonably constant longitudinal vehicle speed and modest longitudinal forces on the wheels. The latter assumptions makes it possible to base most of the content in this chapter on the model derived in Figure 4-51 and Equations [4.51] and [4.52]. However, in the context of transient dynamics it is more relevant to use the model for more violent manoeuvres, and also active control such as ESC interventions. Hence, we extend the model in two ways:

- The constitutive relation is saturated, to reflect that each axle may reach friction limit, friction coefficient times normal load on the axle. See max functions in Equation [4.70].
- To be able to do mentioned limitation, the load transfer is modelled, but only in the simplest possible way using stiff suspension models. Basically it is the same model as given in Equation [3.16].
- A yaw moment representing (left/right) unsymmetrical braking/propulsion. See the term $M_{act,z}$ in yaw equilibrium in Equation [4.70].

It should be noted that the model still lacks some: Transients in load transfer and the reduced cornering stiffness and reduced max friction due to load transfer and utilizing friction for wheel longitudinal forces.

Equilibrium in road plane (longitudinal, lateral, yaw):

$$\begin{aligned}
 m \cdot (\dot{v}_x - \omega_z \cdot v_y) &= F_{fxw} \cdot \cos(\delta_f) - F_{fyw} \cdot \sin(\delta_f) + F_{rx}; \\
 m \cdot (\dot{v}_y + \omega_z \cdot v_x) &= F_{fxw} \cdot \sin(\delta_f) + F_{fyw} \cdot \cos(\delta_f) + F_{ry}; \\
 J \cdot \dot{\omega}_z &= (F_{fxw} \cdot \sin(\delta_f) + F_{fyw} \cdot \cos(\delta_f)) \cdot l_f - F_{ry} \cdot l_r + M_{act,z};
 \end{aligned}$$

[4.70]

Equilibrium out of road plane (vertical, pitch):

$$-F_{fz} \cdot l_f + F_{rz} \cdot l_r - (F_{fxw} \cdot \cos(\delta_f) - F_{fyw} \cdot \sin(\delta_f) + F_{rx}) \cdot h = 0;$$

Constitution:

$$F_{fyw} = -\text{sign}(s_{fy}) \cdot \min(C_f \cdot |s_{fy}|; \mu \cdot F_{fz});$$

$$F_{ry} = -\text{sign}(s_{ry}) \cdot \min(C_r \cdot |s_{ry}|; \mu \cdot F_{rz});$$

Compatibility:

$$s_{fy} = \frac{v_{fyw}}{v_{fxw}}; \quad \text{and} \quad s_{ry} = \frac{v_y - l_r \cdot \omega_z}{v_x};$$

Transformation from vehicle to wheel coordinate system on front axle:

$$v_{fxw} = (v_y + l_f \cdot \omega_z) \cdot \sin(\delta_f) + v_x \cdot \cos(\delta_f);$$

$$v_{fyw} = (v_y + l_f \cdot \omega_z) \cdot \cos(\delta_f) - v_x \cdot \sin(\delta_f);$$

The model in Modelica format is given in Equation [4.71]. Changes compared to Equations [4.51] are marked as underlined code.

```
//Equilibrium, in road plane:
m*(der(vx)-wz*vy) = Ffxv + Frx;
m*(der(vy)+wz*vx) = Ffyv + Fry;
J*der(wz) = Ffyv*lf - Fry*lr + Mactz;
//Equilibrium, out of road plane:
Ffz + Frz - m*g = 0;
-Ffz*lf + Frz*lr - (Ffxv + Frx)*h = 0;

//Compatibility:
vfxv = vx;
vfyv = vy + lf*wz;
vrx = vx;
vry = vy - lr*wz;

//Lateral tyre force model:
Ffyw = -sign(sfy)*min(Cf*abs(sfy), mu*Ffz);
Fry = -sign(sry)*min(Cr*abs(sry), mu*Frz);
sfy = vfyw/vfxw;
sry = vry/vrx;

//Transformation between vehicle and wheel coordinate systems:
Ffxv = Ffxw*cos(df) - Ffyw*sin(df);
Ffyv = Ffxw*sin(df) + Ffyw*cos(df);
vfxv = vfxw*cos(df) - vfyw*sin(df);
vfyv = vfxw*sin(df) + vfyw*cos(df);

//Shaft torques
Ffxw = +1000; // Front axle driven.
Frx = -100; // Rolling resistance on rear axle.
Mactz=0;
```

[4.71]

A simulation of this model, with same steering input as used in Figure 4-52. $M_{act,z}$ is zero. Cornering stiffnesses are chosen so that the vehicle is understeered in steady state. Road friction coefficient is 1. We can see that the vehicle now gets instable and spins out with rear to the right. This is mainly because longitudinal load transfer unloads the rear axle, since the kept steering angle decelerates the vehicle. In this manoeuvre, it would have been reasonable to model also that the rear cornering stiffness decreases with the decreased rear normal load, and opposite on front. Such addition to the model would make the vehicle spin out even more. On the other hand, the longitudinal load shift is modelled to take place immediately. With a suspension model, this load shift would require some more time, which would calm down the spin-out. In conclusion, the manoeuvre is violent enough to trigger a spin-out, so a further elaboration with how to control $M_{act,z}$ could be of interest. However, it is beyond the scope of this compendium.

The vehicle reaches zero speed already after 7 seconds, because the wide side slip decelerates the vehicle a lot. The simulation is stopped at time=7 seconds, because the model cannot handle zero speed. That vehicle models become singular at zero speed is very usual, since the slip definition becomes singular due to zero speed in the denominator. The large difference compared to Figure 4-52 is due to the new constitutive equation used, which shows the importance of checking validity region for any model one uses.

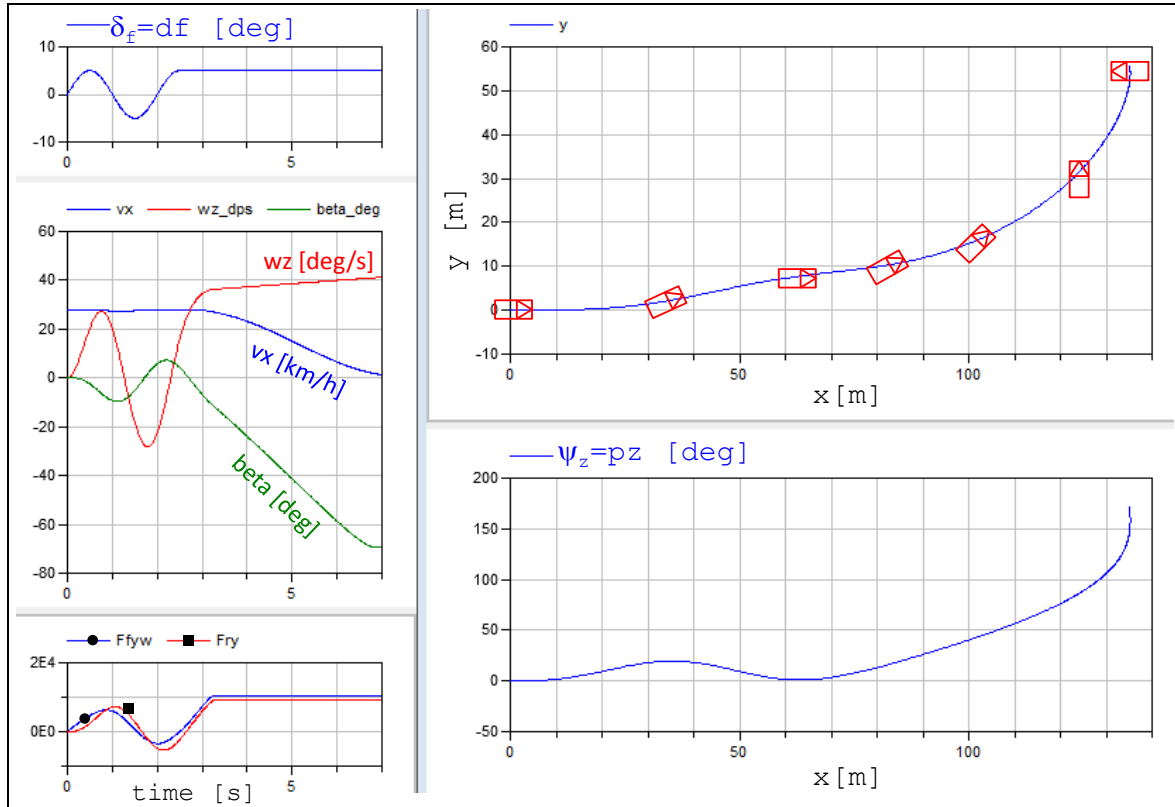


Figure 4-62: Simulation results of one-track model for transient dynamics. The vehicle drawn in the path plot is not in proper scale, but the orientation is approximately correct.

4.5.3 Transient model, with Lateral load transfer

In model of longitudinal load transfer in Section 3.3.10, we assumed instantaneous load transfer. In present chapter we aim to capture the transients better.

4.5.3.1 (Example of) Mathematical model

Compared to the model presented in Figure 4-39 and Equations [4.37]..[4.43], we add the following:

- Inertial term for roll rotation, i.e. $J_{sx} \cdot \dot{\omega}_x$. Note that sprung body roll inertia ($J_{s,x}$), not whole vehicle roll inertia (J_x), is used in roll equilibrium because the unsprung parts does not participate in roll motion.
- Inertial term for lateral acceleration need to capture the lateral acceleration, $a_y = \dot{v}_y + v_x \cdot \omega_z$, **not** only the centripetal acceleration, $a_y = v_x \cdot \omega_z$.
- Damping forces in parallel to each spring force, i.e. adding F_{dfl} , F_{dfr} , F_{drl} , and F_{drr} .

Due to the axle roll centre model, as opposed to wheel pivot point model, the heave acceleration is zero. Hence, no inertial force $m \cdot a_z$ needs to be introduced.

The free-body diagrams are given in Figure 4-63, which should be compared to Figure 4-39.

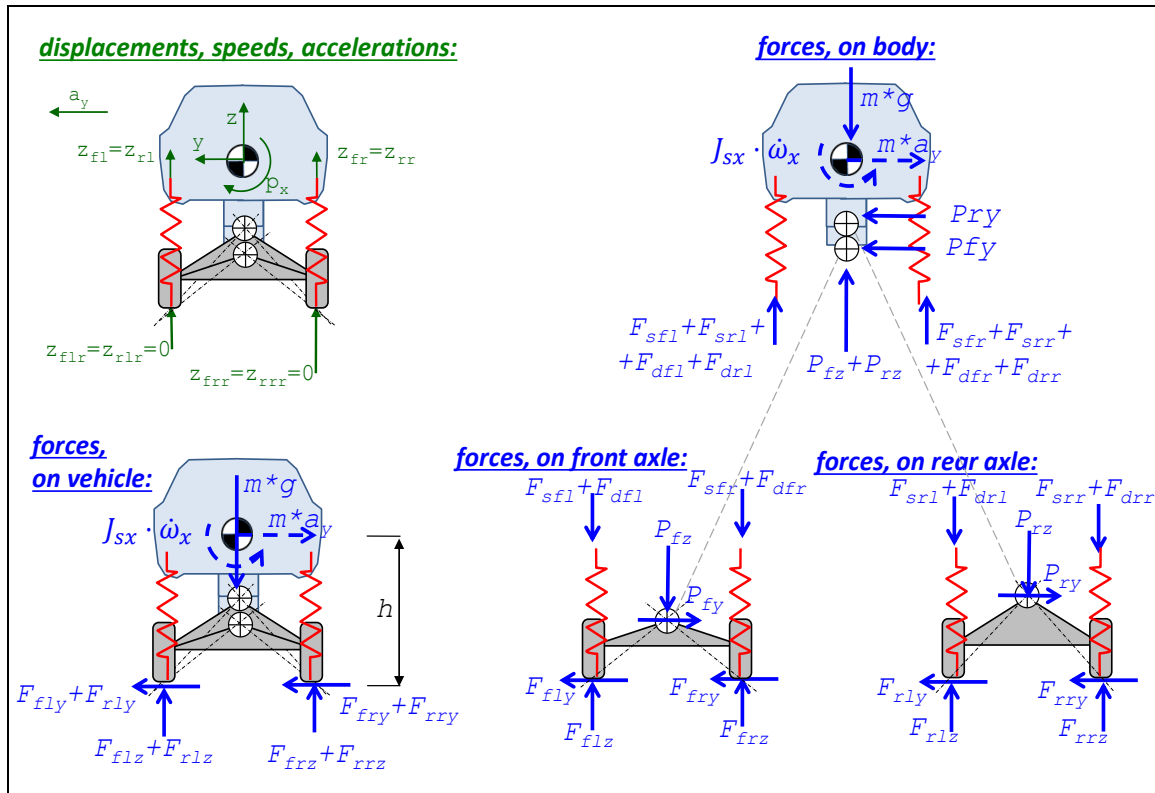


Figure 4-63: Model for transient load transfer due to lateral acceleration, using axle roll centres.

The constitutive equations for the compliances (or springs) are as follows, cf Equation [4.36]. Note that the anti-roll bars are not modelled. Note also that we differentiate, since we will later use the spring forces as state variables in a simulation.

$$\begin{aligned}
 F_{sfl} &= F_{sfl0} + c_{fw} \cdot (z_{flr} - z_{fl}); \Rightarrow \dot{F}_{sfl} = -c_{fw} \cdot \dot{z}_{fl} = -c_{fw} \cdot v_{flz}; \\
 F_{sfr} &= F_{sfr0} + c_{fw} \cdot (z_{frr} - z_{fr}); \Rightarrow \dot{F}_{sfr} = -c_{fw} \cdot \dot{z}_{fr} = -c_{fw} \cdot v_{frz}; \\
 F_{srl} &= F_{srl0} + c_{rw} \cdot (z_{rlr} - z_{rl}); \Rightarrow \dot{F}_{srl} = -c_{rw} \cdot \dot{z}_{rl} = -c_{rw} \cdot v_{rlz}; \\
 F_{srr} &= F_{srr0} + c_{rw} \cdot (z_{rrr} - z_{rr}); \Rightarrow \dot{F}_{srr} = -c_{rw} \cdot \dot{z}_{rr} = -c_{rw} \cdot v_{rrz}; \\
 \text{where } F_{sfl0} &= F_{sfr0} = \frac{m \cdot g \cdot l_r}{2 \cdot L}; \text{ and } F_{srl0} = F_{srr0} = \frac{m \cdot g \cdot l_f}{2 \cdot L};
 \end{aligned}
 \tag{4.72}$$

The constitutive equations for the dampers have to be added:

$$\begin{aligned}
 F_{dfl} &= -d_{fw} \cdot v_{flz}; \\
 F_{dfr} &= -d_{fw} \cdot v_{frz}; \\
 F_{drl} &= -d_{rw} \cdot v_{rlz}; \\
 F_{drr} &= -d_{rw} \cdot v_{rrz};
 \end{aligned}
 \tag{4.73}$$

As comparable with Equation [4.37], we get the next equation to fulfil the equilibrium. The change compared to Equation [4.37] is that we also have a roll and lateral inertia terms and 4 damper forces, acting in parallel to each of the 4 spring forces. Actually, when setting up equations, we also understand that a model for longitudinal load transfer is needed, which is why the simplest possible such, which is the stiff suspension on in Equation [3.16].

In-road-plane: Equilibrium for vehicle (longitudinal, lateral, yaw):

$$\begin{aligned} m \cdot a_x &= m \cdot (\dot{v}_x - \omega_z \cdot v_y) = F_{fx} + F_{rx}; \\ m \cdot a_y &= m \cdot (\dot{v}_y + \omega_z \cdot v_x) = F_{fy} + F_{ry}; \\ J_z \cdot \dot{\omega}_z &= F_{fy} \cdot l_f - F_{ry} \cdot l_r; \end{aligned}$$

Out-of-road-plane: Equilibrium for vehicle (vertical, pitch, roll):

$$\begin{aligned} F_{flz} + F_{frz} + F_{rlz} + F_{rrz} - m \cdot g &= 0; \\ -(F_{flz} + F_{frz}) \cdot l_f + (F_{rlz} + F_{rrz}) \cdot l_r - (F_{fx} + F_{rx}) \cdot h &= 0; \\ J_{s,x} \cdot \dot{\omega}_x &= (F_{flz} + F_{rlz}) \cdot \frac{w}{2} - (F_{frz} + F_{rrz}) \cdot \frac{w}{2} + (F_{fy} + F_{ry}) \cdot h; \end{aligned} \quad [4.74]$$

Equilibrium for each axle (pitch, around roll centre):

$$\begin{aligned} (F_{flz} - (F_{sfl} + F_{dfl})) \cdot \frac{w}{2} - (F_{frz} - (F_{sfr} + F_{dfr})) \cdot \frac{w}{2} + F_{fy} \cdot h_{RCf} &= 0; \\ (F_{rlz} - (F_{srl} + F_{drl})) \cdot \frac{w}{2} - (F_{rrz} - (F_{srr} + F_{drr})) \cdot \frac{w}{2} + F_{ry} \cdot h_{RCr} &= 0; \end{aligned}$$

Compatibility gives, keeping in mind that ω_x is the only non-zero out-of road plane velocity (i.e. $\dot{z} = \omega_y = 0$):

$$\begin{aligned} \dot{z}_{fl} = v_{flz} &= +\frac{w}{2} \cdot \omega_x; \quad \text{and} \quad \dot{z}_{fr} = v_{frz} = -\frac{w}{2} \cdot \omega_x; \\ \dot{z}_{rl} = v_{rlz} &= +\frac{w}{2} \cdot \omega_x; \quad \text{and} \quad \dot{z}_{rr} = v_{rrz} = -\frac{w}{2} \cdot \omega_x; \end{aligned} \quad [4.75]$$

Equations [4.72]..[4.75] give a model very similar to the one in Equation [4.71]. Only the additional equations from this new model are shown in Equation [4.76]. Note especially the new lateral tyre force model equations, which now have one term per wheel, because one wheel on an axle can saturate independent of the other on the same axle.

```
//Equilibrium, roll
Jsx*der(wx) = (Fflz + Frlz)*w/2 - (Ffrz + Frrz)*w/2 + (Ffyv + Fry)*h;
//Equilibrium for each axle (pitch, around roll centre):
(Fflz - (Fsfl + Fdfl))*w/2 - (Ffrz - (Fsfr + Fdfr))*w/2 + Ffy*hRCf = 0;
(Frlz - (Fsrl + Fdrl))*w/2 - (Frrz - (Fsrr + Fdrr))*w/2 + Fry*hRCr = 0;

//Constitutive relation for tyres (Lateral tyre force model):
Ffyw = -
sign(sfy) * (min((Cf/2)*abs(sfy), mu*Fflz) + min((Cf/2)*abs(sfy), mu*Ffrz));
Fry = -
sign(sry) * (min((Cr/2)*abs(sry), mu*Frlz) + min((Cr/2)*abs(sry), mu*Frrz));
sfy = vfyw/vfxw;
sry = vry/vrx;

//Constitution for springs:
der(Fsfl) = -cfw*vflz;
der(Fsfr) = -cfw*vfrz;
der(Fsrl) = -crw*vrlz;
der(Fsrr) = -crw*vrrz;

//Constitution for dampers:
Fdf1 = -dfw*vflz;
Fdfr = -dfw*vfrz;
Fdr1 = -drw*vrlz;
Fdr2 = -drw*vrrz;

//Compatibility, out of road plane:
vflz = +w/2*wx;
vfrz = -w/2*wx;
vrlz = +w/2*wx;
```

[4.76]

$$v_{rrz} = -w/2 * wx;$$



A simulation of this model should be compared with the simulation in Figure 4-52. When comparing these, we see a slight difference, which is that the axles saturate gradually during $3 < \text{time} < 3.5$, instead of both at once at $\text{time} = 3.25$.

Even if the load transfer model does not influence the vehicle path a lot in this case, it may be important to include it to validity check the model through checking wheel lift. Wheel lift can be identified as negative vertical wheel forces, which are why we plot some vertical wheel forces, see Figure 4-65. In this case we see that we have no wheel lift (which would disqualify the simulation). In the right part of the figure we can also see the separate contribution from spring (F_{srr}), damper (F_{drr}) and linkage ($F_{link}, f_{l,z} = F_{flz} - F_{sfl} - F_{dfl}$).

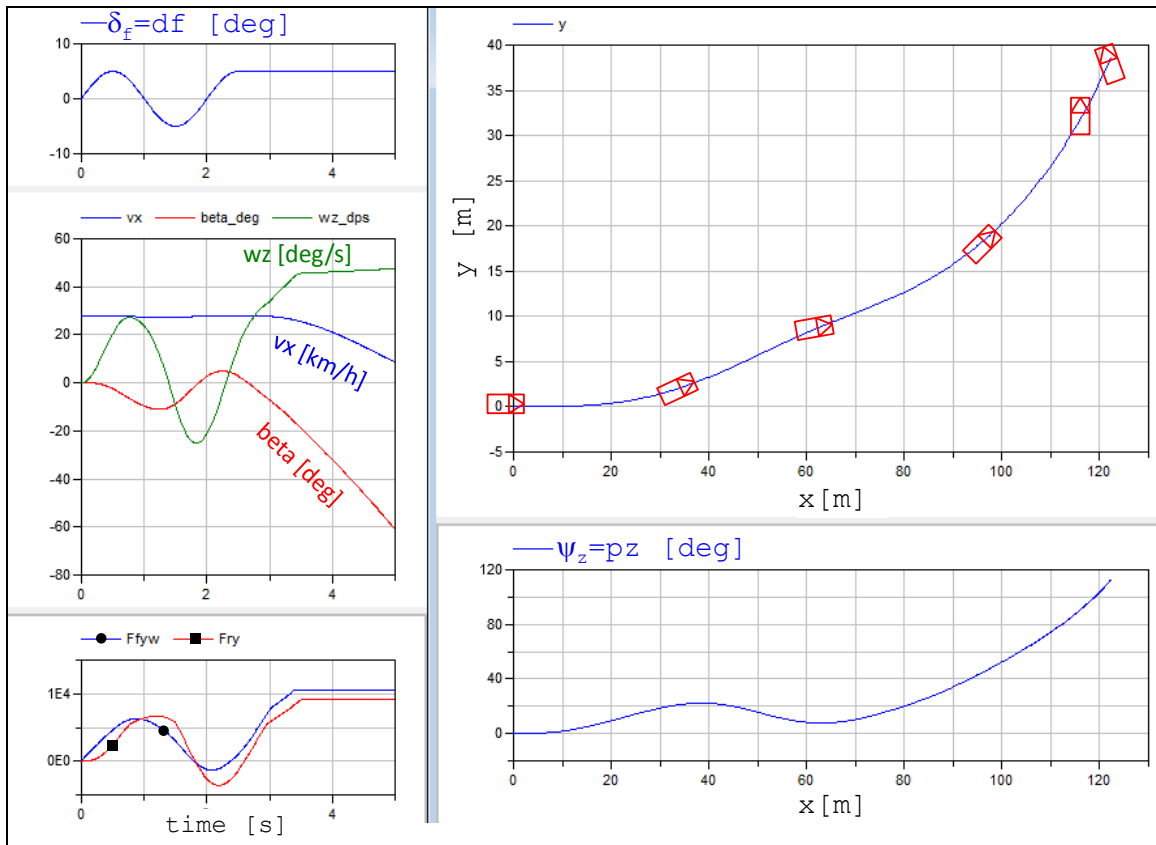


Figure 4-64: Simulation results of one-track model for transient dynamics with lateral load transfer dynamics. The vehicle drawn in the path plot is not in proper scale, but the orientation is approximately correct.

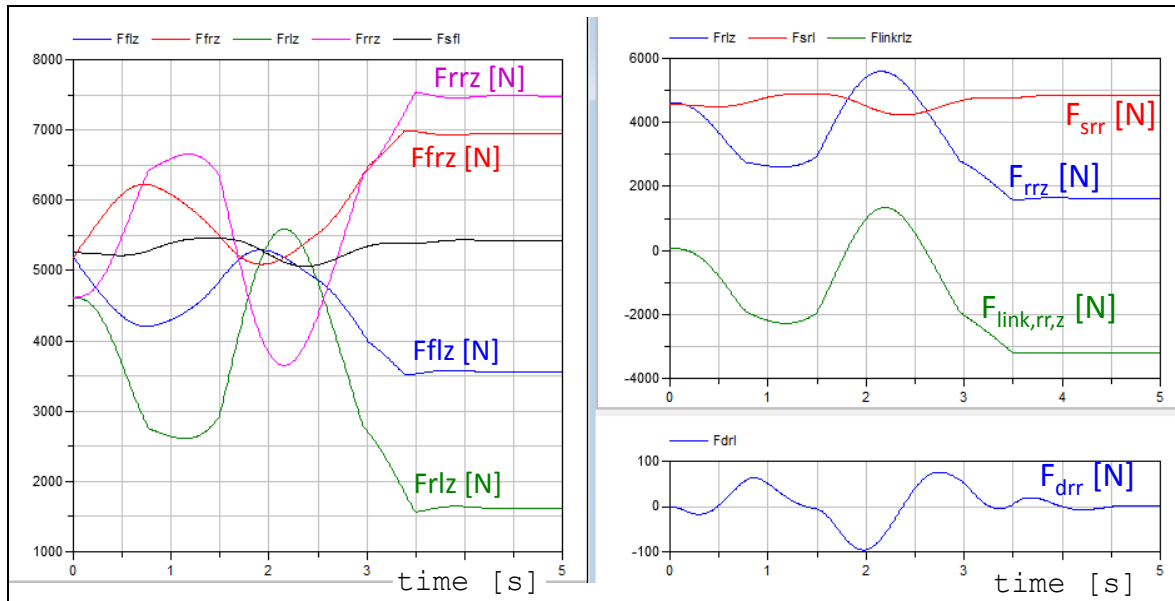


Figure 4-65: Suspension vertical force plots from simulation with one-track model for transient dynamics with lateral load transfer dynamics (same simulation as in Figure 4-64). Left: Road contact forces for all wheels. Right: Different forces for one wheel, rear left.

4.5.3.1.1 Additional phenomena

It is relevant to point out the following, which are not modelled in this compendium:

- Same as pointed out as missing for longitudinal load transfer, see Section 3.4.8.5.
- Additionally, anti-roll arrangements (elastic connections between left and right wheel on one axle, often built as torsion bar) are not modelled in this compendium. With same modelling concept as used above, each such would be treated as a separate spring with one state variable, e.g. F_{af} (Force-antiroll-front). This force will act in parallel with F_{sf} and F_{df} on each side. Note that it will be added on one side and subtracted on the other.

4.5.3.2 (Example of) Explicit form model

A disclaimer to readers which only read the compendium, without following the course: This section might appear incomplete, while the course lectures and hand-out of model is more complete. Still, the description in compendium is regarded as relevant to give general feeling for an Explicit form model.

The implementation of the model in Section 4.5.3 is done in Modelica. A Modelica tool (such as Dymola) automatically transforms the model to explicit form and automatically generates simulation code, which is very efficient. But, as mentioned in Section 1.3.7.5, explicit form models can sometimes facilitate the understanding of the vehicle's dynamics. This is why the following model is presented. It is implemented in the data flow diagram tool Simulink. This section explains how the **states** (or state variables) together with **inputs** (or input variables), influence the **derivatives** (or state derivatives).

The example model in this section is similar, but not identical, to the model in Section 4.5.3. The aim is to model in-road-plane motion, due to transient actuation (wheel torques and wheel steering angles). Limitations in this example model are:

- Influence from vertically uneven road is NOT modelled.
- Influence from varying road friction is NOT modelled.
- Wheel lift from ground is NOT modelled
- Hitting bump stop is NOT modelled

- Control functions (such as ABS, TC and ESC) are NOT modelled
- The pendulum effect is NOT modelled
- Wheel camber angle change with suspension travel is NOT modelled (Camber \equiv 0).
- Wheel steering angle change with suspension travel is NOT modelled (change \equiv 0).

The model is a typical two axle vehicle with interface to driver and environment, see Figure 4-66. The driver interface is the normal, 2 pedals and one steering wheel. The additional discrete request from driver, *LongDir* (= -1 or +1), is also needed to reflect whether driver requests forward or reverse longitudinal actuation. The interface to environment is motion (variable position) in surrounding world. To try out the vehicle model, driver and environment is also modelled. This includes also the interface between them, which is motion of obstacles in environment, relative to subject vehicle. The suspension is exemplified with wheel-individual suspension on both axles.

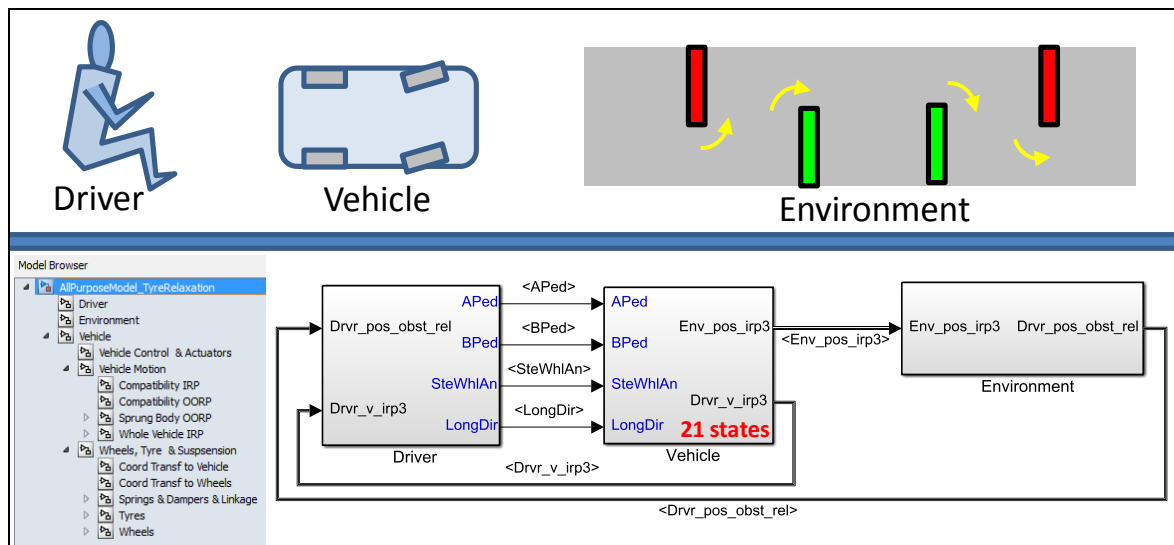


Figure 4-66: Top level of model with model tree structure. The Environment is a track test with cone walls to go left and right around. Notation “irp” and “oorp” refers to in-road-plane and out-of-road-plane, respectively.

As an initial overview, the states are presented. There are **21 states** in total, and distributed:

- Driver: 0 states
- Vehicle:
 - Vehicle Control & Actuation: 0 states
 - **Wheels, Tyres & Suspension: 12 states** (4 wheel rotational speed, 4 Elastic part of vertical wheel forces, 4 Magnitude of tyre force in road plane)
 - **Vehicle Motion: 9 states** (6 velocities and 3 positions)
- Environment: 0 states

One should also mention that 4 “memories” (on vertical tyre forces) are added in one part of the Tyre model to resolve an algebraic loop. Using memory blocks are generally a dangerous way of modelling, see more in Section 4.5.3.2.4.

4.5.3.2.1 Submodel Driver

The driver model is here very sparsely described and the intention is not that it should be a state of the art model. However, in a nut-shell: Driver model is divided into two parts:

- Driver planning (perception): Based on position of obstacles relative to the vehicle, one of the objects is selected to be aim. Basically, the nearest obstacle ahead of vehicle is selected as aim.

- Driver operation (motorics): This should output the steering wheel angle. In the example, it is simply an inverse model of an ideally tracking two-axle vehicle which calculates which constant steering wheel angle that would be needed to make front axle run over the aim obstacle.

4.5.3.2.2 Submodel Environment

The environment model is here very sparsely described and the intention is not that it should be a state of the art model. It captures only stand-still point obstacles with pre-determined whether it should be passed as obstacle left or right of the vehicle. Inputs to environment model is the vehicles position, including orientation in global coordinates. Outputs are the relative position (x,y) to each obstacle, in vehicle coordinate system.

4.5.3.2.3 Submodel Vehicle

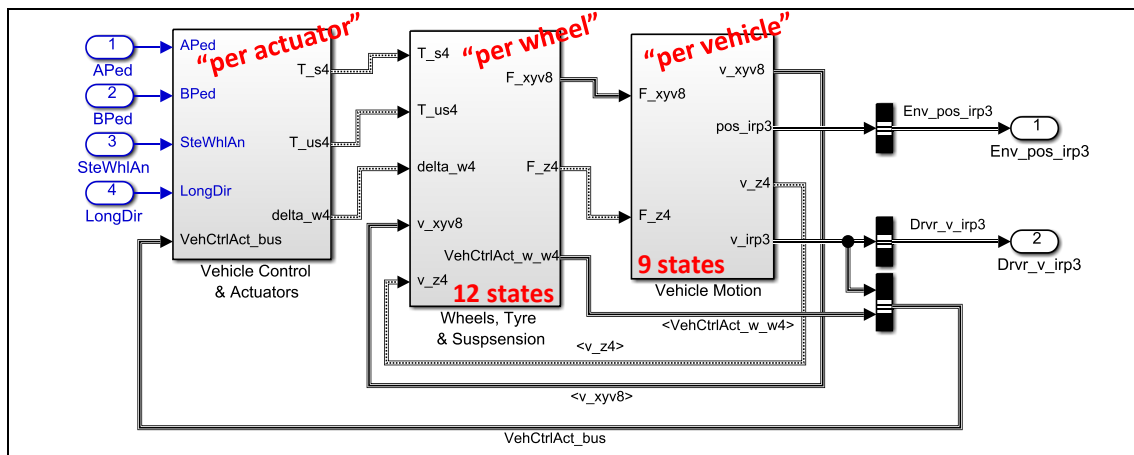


Figure 4-67: Vehicle submodel.

The figure shows the decomposition of the vehicle into 3 parts:

- Submodel **“Vehicle Control & Actuation”** models the actuators (Propulsion system, Brake system and Steering system, including “control functions”) that respond on requests from the driver with wheel torques (T_s and T_{us}) and wheel steering angles (δ_w). The notation ending “4” refers to that the quantities are vectors with 4 components, one per wheel. T_s is shaft torque and T_{us} is torque applied from unsprung parts, e.g. friction brake torque from brake calliper. One can think of very advanced models of these actuator systems, including e.g. propulsion system dynamics and control functions (ABS, ESC, TC, ...). However, in this example model it is only modelled very simple:
 - Propulsion system outputs a fraction (determined by $APed$) of a certain maximum power, distributed equally on front left and front right wheel. If brake pedal is applied, the propulsion system outputs zero torque.
 - Brake system outputs a fraction (determined by $BPed$) of a maximum brake torque ($\mu \cdot m \cdot g / R_w$), distributed in a certain fix fraction between front and rear axle (70/30). The distribution within each axle is equal on left and right wheel.
 - There are **no states** modelled in the vehicle Control & Actuator submodel.
- Submodel **“Wheels, Tyre & Suspension”** models the part which pushes the tyres towards the ground and consequently transforms the wheel torques and wheel steering angles, via the tyre, to forces on the whole vehicle. F_{xyv8} is the x and y forces in each of the 4 wheels, $2 \times 4 = 8$. F_{z4} is the 4 vertical forces under each wheel. Submodel “Wheels, Tyre & Suspension” is **further explained** in Section 4.5.3.2.4.
- Submodel **“Vehicle Motion”** models motion of whole vehicle in-road-plane and motion of sprung body out-of-road-plane. The inertial effects (mass·acceleration) of the unsprung parts

are taken into account for in-road-plane but not for out-of-road-plane. This submodel includes integrators for the 3+3+3=9 **states**:

- Velocities in-road-plane, v_x, v_y, ω_z : **v_irp3** (which is transformed to x- and y- velocities of each wheel and then fed back as v_irpv8)
- Position in-road-plane, x, y, φ_z : **pos_irp3** (which is only fed forward to “Environment”)
- Velocities out-of-road-plane, v_z, ω_x, ω_y : **v_oorp3** (which is transformed to z- velocities of sprung body over each wheel and then fed back as v_z4)

4.5.3.2.4 Submodel Wheels, Tyres & Suspension

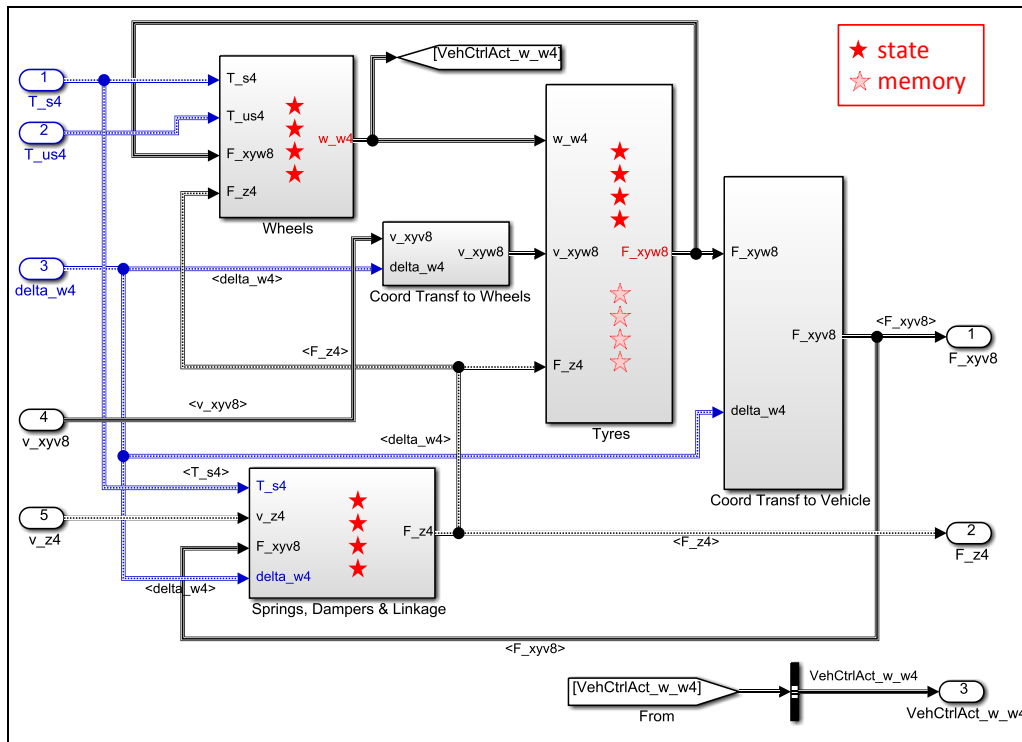


Figure 4-68: Wheels, Tyres & Suspension submodel.

- The two submodels “**Coord Transf ...**” are straight-forward coordinate transformations, using Eq [4.3].
- The submodel “**Wheels**” is also relatively straight-forward. For each wheel, the rotational equilibrium is used as model: $J \cdot \dot{\omega} = T_{us} + T_s - F_x \cdot R_w - \text{sign}(\omega) \cdot RRC \cdot F_z \cdot R_w$; where R_w is wheel radius and RRC is rolling resistance coefficient. The submodel will hence contain the 4 **states**:
 - Rotational speeds of each wheel: **w_w4**.
- The submodel “**Springs, Dampers & Linkage**” models the springs (incl. anti-rollbars) and dampers and the linkage. For each wheel:
 - Four **states**: Elastic part of vertical tyre force under each wheel: **F_s4**
 - The derivatives are governed by the differentiated constitution of the springs: Conceptually $\dot{F}_s = -c \cdot v_z$; but involving both wheel spring and anti-roll-bar.
 - The force in damper is governed by the dampers constitutive relation: $F_d = -d \cdot v_z$;
 - The contact forces F_z are calculated in submodel “Suspension Equilibrium” in Figure 4-69. They are calculated from moment equilibrium of unsprung parts around a 3-dimensional pivot axis. The pivot axis is defined by two points, the pivot point in longitudinal load transfer (see Figure 3-31) and the pivot point in longitudinal load transfer (see Figure 4-38). The scalar equilibrium equation for one wheel can be

expressed, with vector (cross) and scalar (dot) products, in F_{xv} , F_{yv} , F_s , F_d , T_s , F_z and point coordinates. From this, F_z can be solved.

- The submodel “**Tyres**” models the tyre mechanics, very much like the combined slip model in Equation [2.31] and the relaxation model in Equation [2.36]. For each wheel:
 - Four **states**: Magnitudes of tyre forces in ground plane (F_{xy}) for each wheel: **F_xyw4**
 - Unfortunately, the tyre mechanics are such that F_x and F_y depends on F_z . This creates an algebraic loop, see Figure 4-69. The loop can almost be resolved by using F_{xy} as state, but there is a weak dependency left because F_z is needed for small total slip (s_{xy}) to find out the direction of F_{xy} . This dependency of F_z is seen in Equation [2.32]. Since this dependency is weak, we allow ourselves to resolve it using “memories”, mentioned in Section 4.5.3.2.
 - The algebraic loop is resolved by introducing 4 so called “memories”. “Memories” are such that value from last time instant is used to calculate derivatives in present time instant. This is generally NOT a recommended way of modelling, but it works relatively well in this case. To involve full two-dimensional relaxation (both F_x and F_y as states) would avoid the algebraic loop without using memories, but it seems to result in smaller time steps, meaning slower or non-converging simulations.

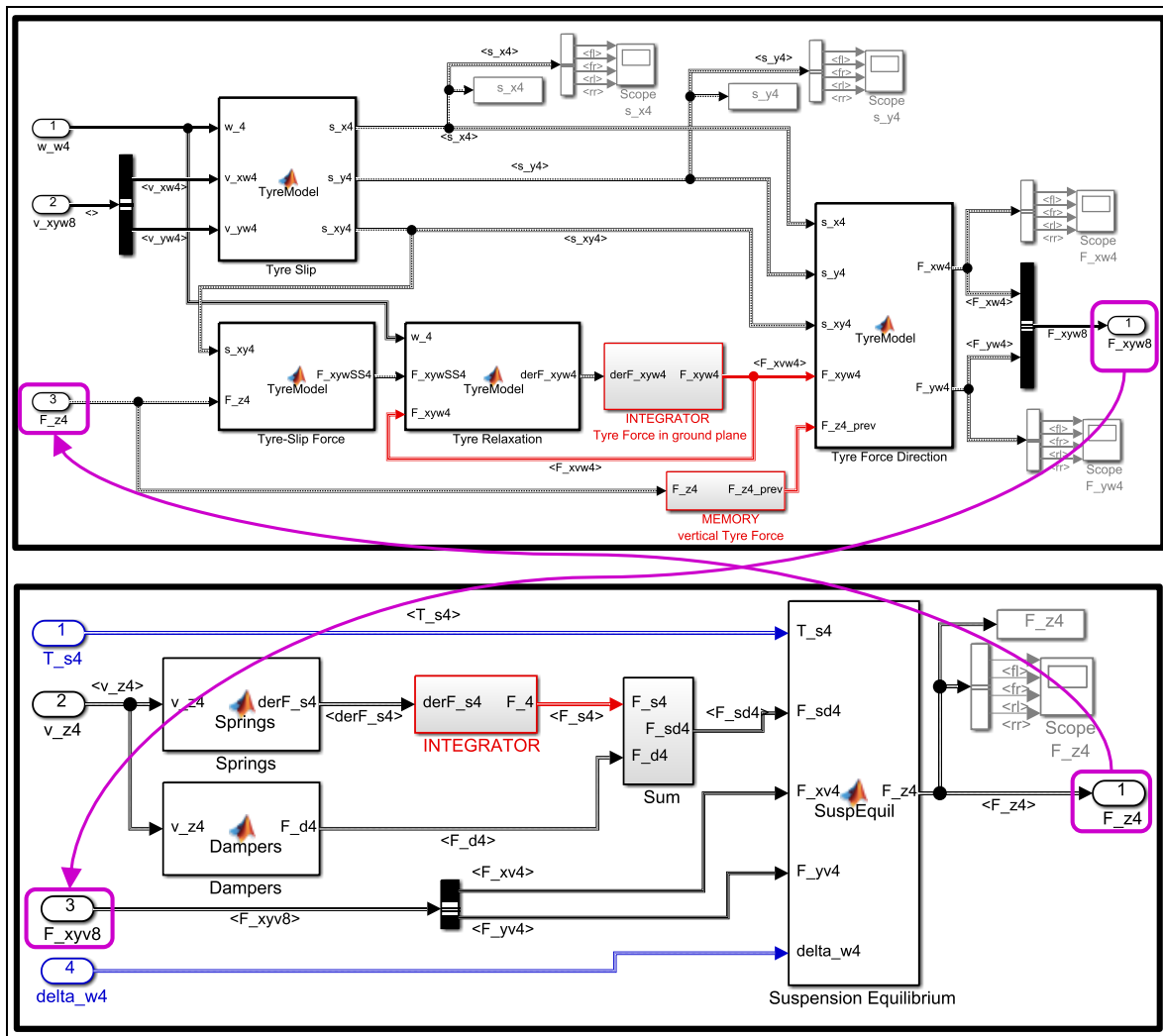


Figure 4-69: Submodel “Tyres” on top and submodel “Springs, Dampers & Linkage” below. The arrows between shows the algebraic loop which appears when they are connected.

4.5.3.2.5 Submodel Vehicle Motion

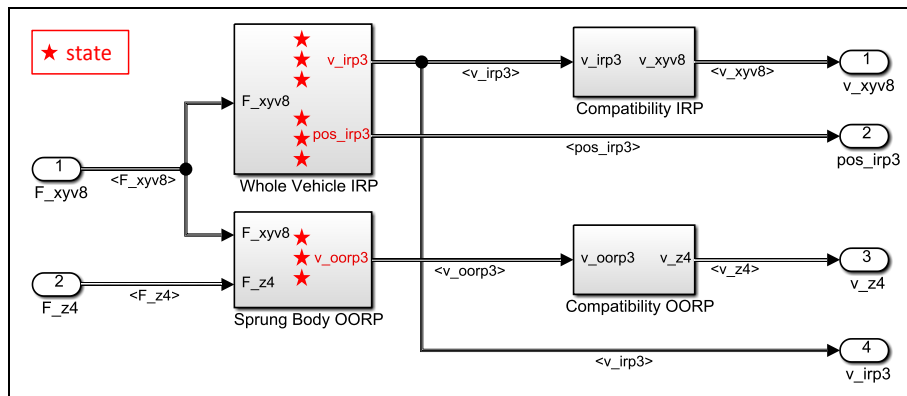


Figure 4-70: Vehicle Motion.

4.5.3.2.6 Simulation example

A double lane change between cones is used as simulation example, see Figure 4-71. The cones are run over and even passed on the wrong side because the driver model is very simple.

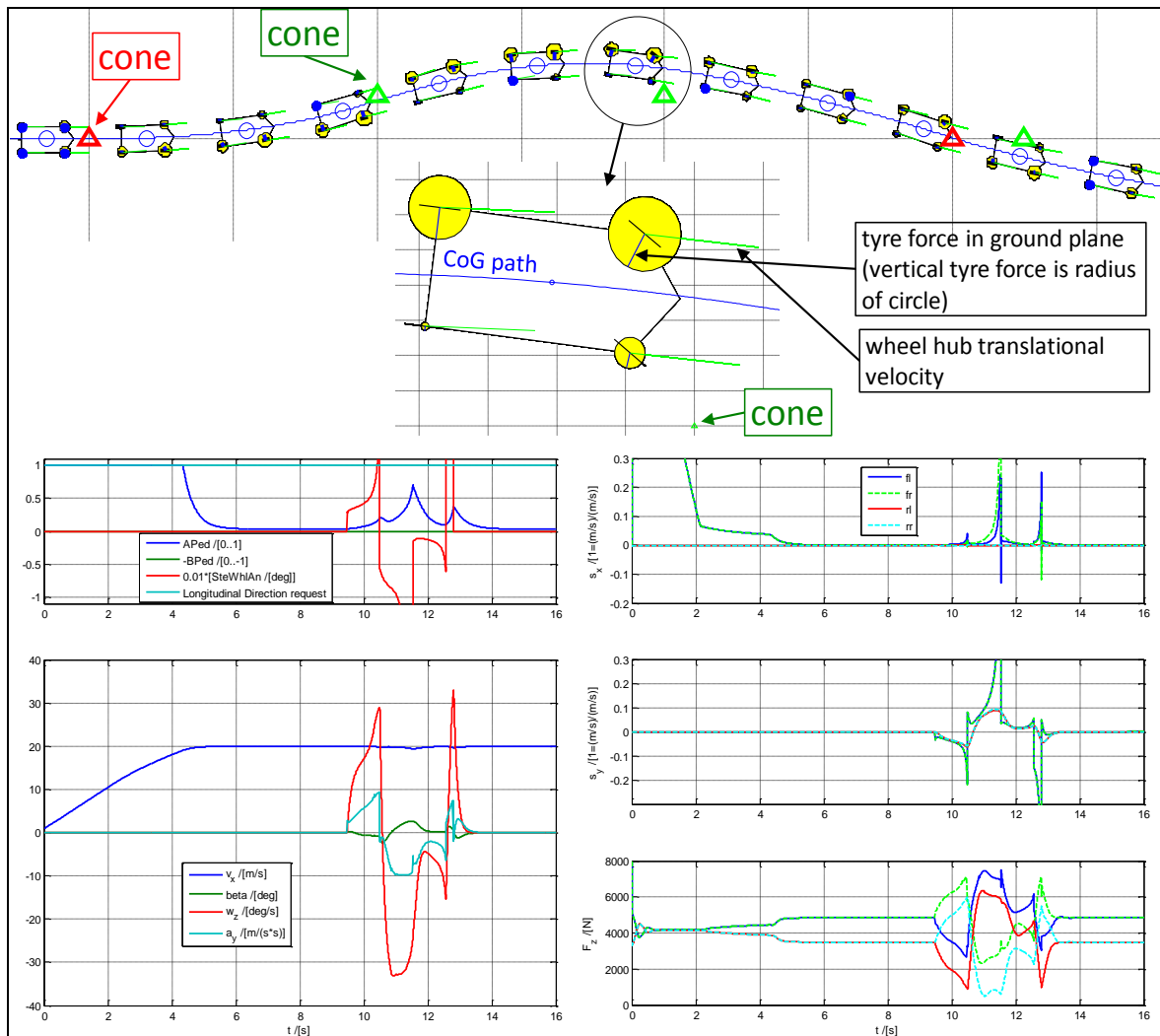


Figure 4-71: Simulation results of a double lane change between cones.

4.5.4 Step steering response *

*Function definition: **Step steering response** is the response to a step in steering wheel angle measured in certain vehicle measures. The step is made from a certain steady state cornering condition to a certain steering wheel angle. The response can be the time history or certain measures on the time history, such as delay time and overshoot.*

4.5.4.1 Mild step steering response

This section is to be compared with section 4.5.4.2, which uses a more advanced model. In present section a less advanced model will be used, which is enough for small steering steps.

The model used for single frequency stationary oscillating steering can also be used for other purposes, as long as limited lateral accelerations.

Most common interpretation is to make the steering step from an initial straight line driving. In reality, the step will be a quick ramp. In simulations an ideal step can be used.

Equation [4.59] allows an easy analysis of stationary oscillating steering, but also an easy analysis of step response:

Start from **Equation [4.59]**: $\begin{bmatrix} \dot{v}_y \\ \dot{\omega}_z \end{bmatrix} = \mathbf{A} \cdot \begin{bmatrix} v_y \\ \omega_z \end{bmatrix} + \mathbf{B} \cdot \delta_f$;

With **initial conditions**: $\begin{bmatrix} v_y(0) \\ \omega_z(0) \end{bmatrix} = \begin{bmatrix} v_{y0} \\ \omega_{z0} \end{bmatrix}$; or $\begin{bmatrix} v_{y0} \\ \omega_{z0} \end{bmatrix} = -\mathbf{A}^{-1} \cdot \mathbf{B} \cdot \delta_{f0}$; where δ_{f0} is before step.

Assume: $\begin{bmatrix} v_y \\ \omega_z \end{bmatrix} = \begin{bmatrix} v_{y\infty} \\ \omega_{z\infty} \end{bmatrix} + \begin{bmatrix} \hat{v}_{y1} & \hat{v}_{y2} \\ \hat{\omega}_{z1} & \hat{\omega}_{z2} \end{bmatrix} \cdot \begin{bmatrix} e^{\lambda_1 \cdot t} & 0 \\ 0 & e^{\lambda_2 \cdot t} \end{bmatrix} \cdot \begin{bmatrix} a_1 \\ a_2 \end{bmatrix}$; \Rightarrow
 $\Rightarrow \begin{bmatrix} \dot{v}_y \\ \dot{\omega}_z \end{bmatrix} = \begin{bmatrix} \hat{v}_{y1} & \hat{v}_{y2} \\ \hat{\omega}_{z1} & \hat{\omega}_{z2} \end{bmatrix} \cdot \begin{bmatrix} \lambda_1 \cdot e^{\lambda_1 \cdot t} & 0 \\ 0 & \lambda_2 \cdot e^{\lambda_2 \cdot t} \end{bmatrix} \cdot \begin{bmatrix} a_1 \\ a_2 \end{bmatrix}$;

Insert: $\begin{bmatrix} \hat{v}_{y1} & \hat{v}_{y2} \\ \hat{\omega}_{z1} & \hat{\omega}_{z2} \end{bmatrix} \cdot \begin{bmatrix} \lambda_1 \cdot e^{\lambda_1 \cdot t} & 0 \\ 0 & \lambda_2 \cdot e^{\lambda_2 \cdot t} \end{bmatrix} \cdot \begin{bmatrix} a_1 \\ a_2 \end{bmatrix} =$
 $= \mathbf{A} \cdot \left(\begin{bmatrix} v_{y\infty} \\ \omega_{z\infty} \end{bmatrix} + \begin{bmatrix} \hat{v}_{y1} & \hat{v}_{y2} \\ \hat{\omega}_{z1} & \hat{\omega}_{z2} \end{bmatrix} \cdot \begin{bmatrix} e^{\lambda_1 \cdot t} & 0 \\ 0 & e^{\lambda_2 \cdot t} \end{bmatrix} \cdot \begin{bmatrix} a_1 \\ a_2 \end{bmatrix} \right) + \mathbf{B} \cdot \delta_f$;

Solve for each time function term (constant, $e^{\lambda_1 \cdot t}$ and $e^{\lambda_2 \cdot t}$ terms):

$$\begin{bmatrix} v_{y\infty} \\ \omega_{z\infty} \end{bmatrix} = -\mathbf{A}^{-1} \cdot \mathbf{B} \cdot \delta_f; \text{ and } \left[\begin{bmatrix} \hat{v}_{y1} & \hat{v}_{y2} \\ \hat{\omega}_{z1} & \hat{\omega}_{z2} \end{bmatrix}, \begin{bmatrix} \lambda_1 & 0 \\ 0 & \lambda_2 \end{bmatrix} \right] = \text{eig}(\mathbf{A});$$

The function "eig" is identical to function "eig" in Matlab. It is defined as eigenvalues and eigenvectors for the matrix input argument.

Initial conditions: $\begin{bmatrix} v_{y0} \\ \omega_{z0} \end{bmatrix} = \begin{bmatrix} v_{y\infty} \\ \omega_{z\infty} \end{bmatrix} + \begin{bmatrix} \hat{v}_{y1} & \hat{v}_{y2} \\ \hat{\omega}_{z1} & \hat{\omega}_{z2} \end{bmatrix} \cdot \begin{bmatrix} a_1 \\ a_2 \end{bmatrix}$; \Rightarrow
 $\Rightarrow \begin{bmatrix} a_1 \\ a_2 \end{bmatrix} = \begin{bmatrix} \hat{v}_{y1} & \hat{v}_{y2} \\ \hat{\omega}_{z1} & \hat{\omega}_{z2} \end{bmatrix}^{-1} \cdot \left(\begin{bmatrix} v_{y0} \\ \omega_{z0} \end{bmatrix} - \begin{bmatrix} v_{y\infty} \\ \omega_{z\infty} \end{bmatrix} \right)$;

The solution in summary:

$$\begin{cases} \begin{bmatrix} v_y \\ \omega_z \end{bmatrix} = \begin{bmatrix} v_{y\infty} \\ \omega_{z\infty} \end{bmatrix} + \begin{bmatrix} \hat{v}_{y1} & \hat{v}_{y2} \\ \hat{\omega}_{z1} & \hat{\omega}_{z2} \end{bmatrix} \cdot \begin{bmatrix} e^{\lambda_1 \cdot t} & 0 \\ 0 & e^{\lambda_2 \cdot t} \end{bmatrix} \cdot \begin{bmatrix} a_1 \\ a_2 \end{bmatrix}; \\ a_y = \dot{v}_y + v_x \cdot \omega_z = \lambda_1 \cdot \hat{v}_{y1} \cdot e^{\lambda_1 \cdot t} \cdot a_1 + \lambda_2 \cdot \hat{v}_{y2} \cdot e^{\lambda_2 \cdot t} \cdot a_2 + v_x \cdot \omega_z; \end{cases}$$

where: $\begin{bmatrix} v_{y\infty} \\ \omega_{z\infty} \end{bmatrix} = -\mathbf{A}^{-1} \cdot \mathbf{B} \cdot \delta_f$;

and $\begin{bmatrix} \begin{bmatrix} \hat{v}_{y1} & \hat{v}_{y2} \\ \hat{\omega}_{z1} & \hat{\omega}_{z2} \end{bmatrix}, \begin{bmatrix} \lambda_1 & 0 \\ 0 & \lambda_2 \end{bmatrix} \end{bmatrix} = \text{eig}(\mathbf{A})$;

and $\begin{bmatrix} a_1 \\ a_2 \end{bmatrix} = \begin{bmatrix} \hat{v}_{y1} & \hat{v}_{y2} \\ \hat{\omega}_{z1} & \hat{\omega}_{z2} \end{bmatrix}^{-1} \cdot \left(\begin{bmatrix} v_{y0} \\ \omega_{z0} \end{bmatrix} - \begin{bmatrix} v_{y\infty} \\ \omega_{z\infty} \end{bmatrix} \right)$;

[4.77]

Results from this model for step steer to +3 deg are shown in Figure 4-72. Left diagram shows step steer from straight line driving, while right diagram shows a step from steady state cornering with -3 deg steering angle.

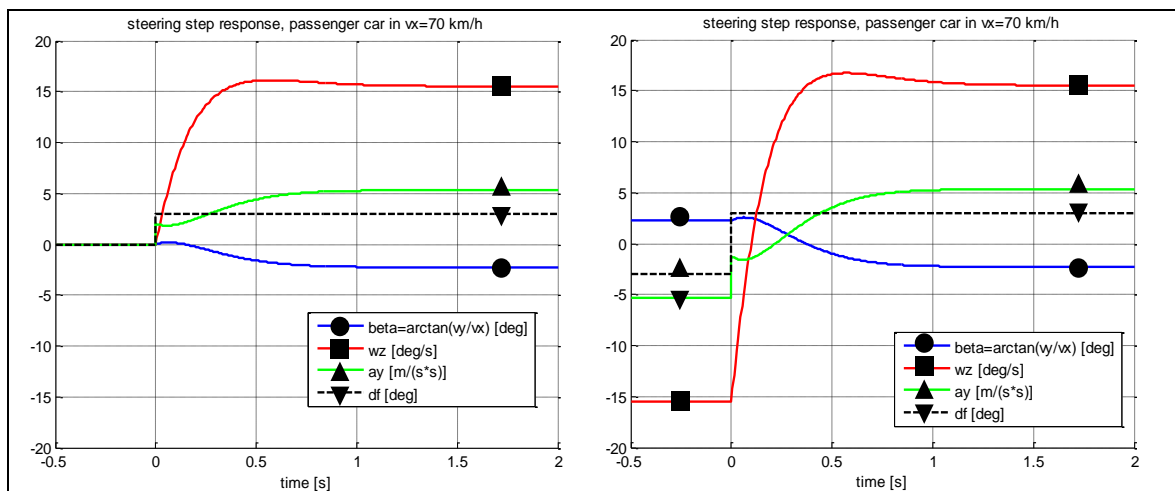


Figure 4-72: Steering step response. Simulation with model from Equation [4.77].

4.5.4.2 Violent step steering response

This section is to be compared with section 4.5.4.1 Mild step steering response, which uses a model with linear tyre models without saturation. In present section a more advanced model will be used, which might be needed when the step steering is more violent.

Most common interpretation is to make the steering step from an initial straight line driving. In reality, the step will be a quick ramp. In simulations an ideal step can be used.

The transients can easily be that violent that a model as Equations [4.72]..[4.76] is needed. If ESC is to be simulated, even more detailed models are needed (full two-track models, which are not presented in this compendium). Anyway, if we apply a step steer to the model in Equations [4.72]..[4.76], we can simulate as in Figure 4-73.

4.5.5 Long heavy vehicle combinations manoeuvrability measures

It is sometimes irrelevant (or difficult) to apply functions/measures from two axle vehicles on combinations of units. This can be the case for passenger cars with a trailer, but it is even more obvious for long combinations of heavy vehicles.

Some typical measures for multi-unit vehicle combination are given in Figure 4-74, Figure 4-75 and Figure 4-76.

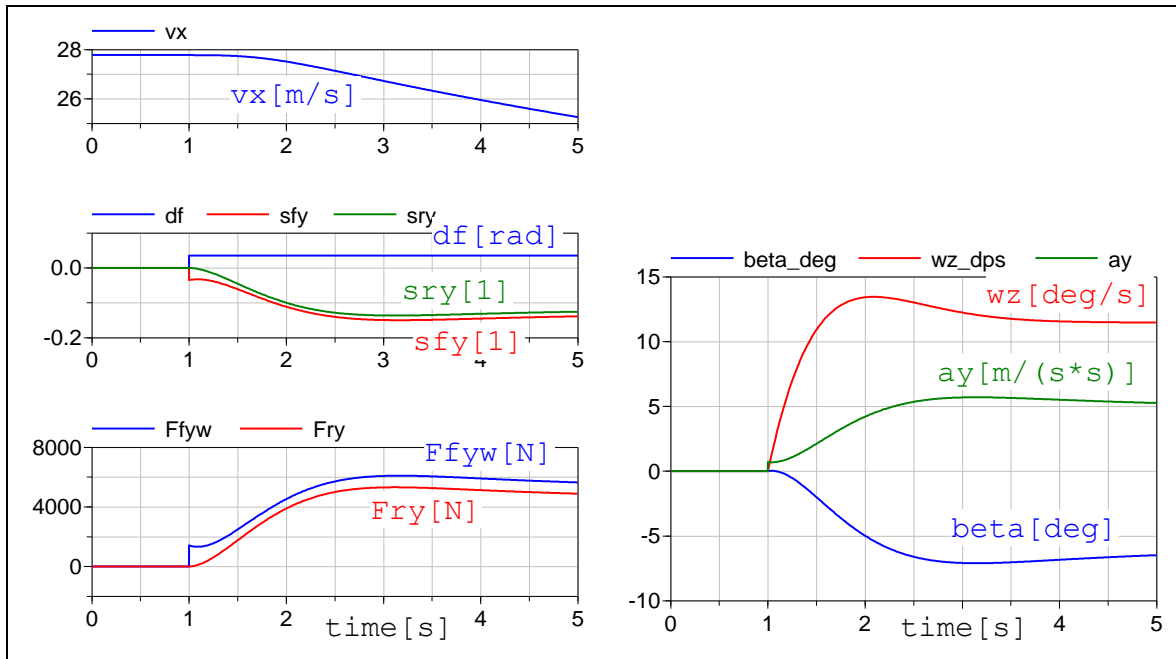


Figure 4-73: Step steer with 2 deg on road wheels at vx=100 km/h. Simulated with model in Equations [4.72]..[4.76].

4.5.5.1 Rearward Amplification *

Function definition: **Rearward Amplification for long heavy vehicle combinations** is the ratio of the maximum value of the motion variable of interest (e.g. yaw rate or lateral acceleration of the centre of gravity) of the worst excited following vehicle unit to that of the first vehicle unit during a specified manoeuvre at a certain friction level and constant speed. From Reference [(Kati, 2013)].

Figure 4-74 illustrates Rearward Amplification, RWA. RWA is defined for a special manoeuvre, e.g. a certain lane change or step steer. RWA is the ratio of the peak value of yaw rate or lateral acceleration for the rearmost unit to that of the lead unit. This performance measure indicates the increased risk for a swing out or rollover of the last unit compared to what the driver is experiencing in the lead unit.

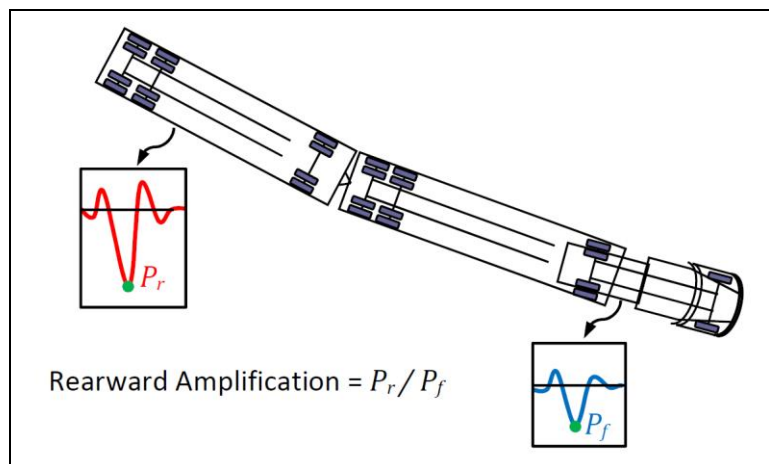


Figure 4-74: Illustration of rearward amplification, P denotes peak value of the motion variable of interest. From (Kharrazi, 2012).

4.5.5.2 Off-tracking *

Function definition: High speed transient off-tracking for long heavy vehicle combinations is the overshoot in the lateral distance between the paths of the centre of the front axle and the centre of the most severely off-tracking axle of any unit in a specified manoeuvre at a certain friction level and a certain constant longitudinal speed. From Reference [(Kati, 2013)].

Function definition: High speed steady-state off-tracking for long heavy vehicle combinations is the lateral offset between the paths of the centre of the front axle and the centre of the most severely off-tracking axle of any unit in a steady turn at a certain friction level and a certain constant longitudinal speed. From Reference [(Kati, 2013)].

Figure 4-75 illustrates Off-tracking. Off-tracking was also mentioned in Section 4.2. The measure is, as RWA, a comparison between the lead and last unit, but in terms of the additional road space required for the last unit manoeuvring. High speed Off-tracking, which is an outboard off-tracking, can be either determined in a steady state turn or in a transient manoeuvre such as lane change; the latter is termed as high speed transient off-tracking.

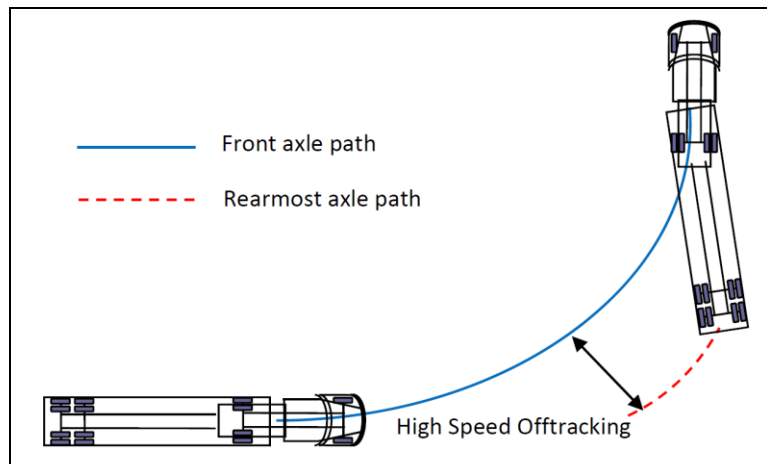


Figure 4-75: Illustration of high speed steady-state off-tracking. From (Kharrazi , 2012).

4.5.5.3 Yaw Damping *

Function definition: Yaw Damping for long heavy vehicle combinations is the damping ratio of the least damped articulation joint's angle of the vehicle combination during free oscillations excited by actuating the steering wheel with a certain pulse or a certain sine-wave steer input at a certain friction level. From Reference [(Kati, 2013)].

Figure 4-76 illustrates Yaw Damping. It is the damping ratio of the least damped articulation joint of the vehicle combination during free oscillations. Yaw damping ratio of an articulation joint is determined from the amplitudes of the articulation angle of subsequent oscillations.

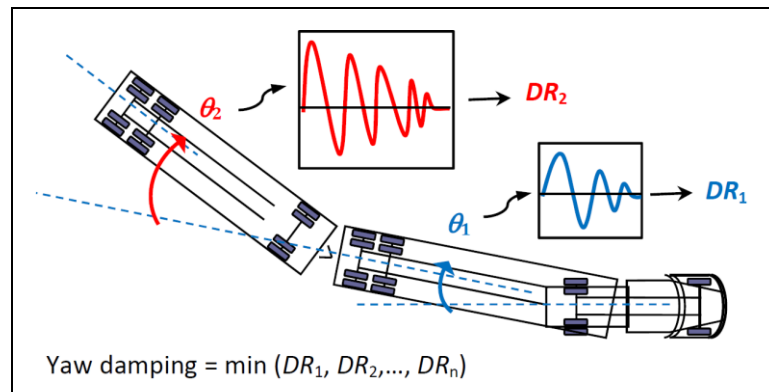


Figure 4-76: Illustration of yaw damping for multi-unit vehicle combination, DR denotes damping ratio of the articulation joint. From (Kharrazi, 2012).

4.6 Lateral Control Functions

Some control functions involving lateral vehicle dynamics will be presented briefly. There are more, but the following are among the most well-established ones. But initially, some general aspects of lateral control is given.

4.6.1 Lateral Control Design

Sensors available and used for lateral control are, generally those mentioned as available for Longitudinal Control, see Section 3.5 plus some more:

Steering wheel sensors gives at least steering wheel angle, if the vehicle is equipped with ESC (which is a legal requirement on many markets). Additionally, if the steering assistance is electrical, the steering wheel torque can be sensed.

High specification modern vehicles also have environment sensors (camera, radar, etc) that can give laterally interesting information, such as: Subject vehicle lateral position versus lane markers ahead and other vehicles to the side or rear of subject vehicle.

As general considerations for actuators, one can mention that interventions with friction brake normally have to have thresholds, because interventions are noticed by driver and also generate energy loss. Interventions with steering are less sensitive, and can be designed without thresholds.

4.6.2 Lateral Control Functions

4.6.2.1 Lane Keeping Aid, LKA *

*Function definition: **Lane Keeping Aid** steers the vehicle without driver having to steer, when probability for lane departure is predicted as high. It is normally actuated as an additional steering wheel torque. Conceptually, it can also be actuated as a steering wheel angle offset.*

Lane Keeping Aid (or Lane Departure Prevention) has the purpose to guide the driver to keep in the lane. Given the lane position from a camera, the function detects whether vehicle tends to leave the lane. If so, the function requests a mild steering wheel torque (typically 1..2 Nm) in appropriate direction. Driver can easily overcome the additional torque. Function does not intervene if too low speed or turning indicator (blinker) is used. There are different concepts whether the function continuously should aim at keeping the vehicle in centre of lane, or just intervene when close to leaving the lane, see Figure 4-77.

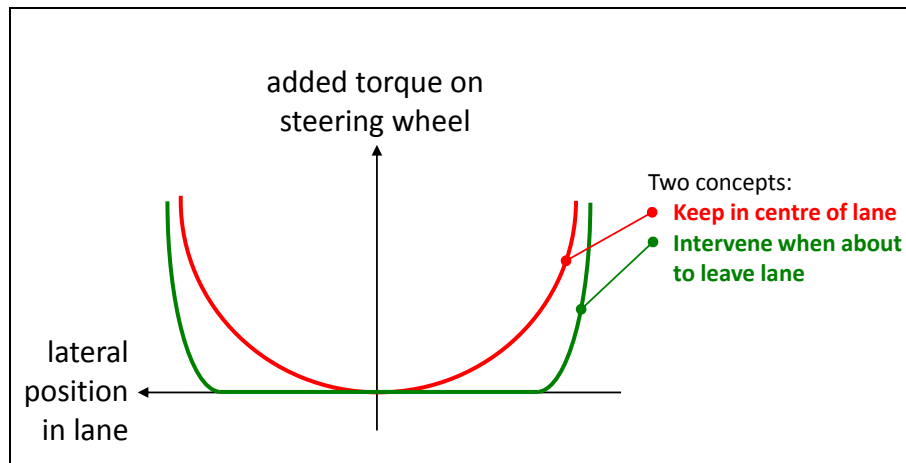


Figure 4-77: Two concepts for Lane Keeping Aid.

4.6.2.2 Electronic Stability Control, ESC *

*Function definition: **Electronic Stability Control** directs the vehicle to match a desired yaw behaviour, when the deviation from desired behaviour becomes above certain thresholds. ESC typically monitors vehicle speed, steering angle and yaw rate to calculate a yaw rate error and uses friction brakes as actuator to reduce it.*

There are 3 conceptual parts of ESC: Over-steer control, Under-steer control, Over-speed control. The actual control error that the vehicle reacts on is typically the yaw rate error between sensed yaw rate and desired yaw rate. Desired yaw rate is calculated from a so called reference model. Some of today's advanced ESC also intervenes on sensed/estimated side slip.

Desired yaw rate (and side-slip) is calculated using a reference model. The reference model requires at least steering angle and longitudinal velocity as input. The reference model can be either of steady state type (approximately as Equation [4.28]) or transient (approximately as Equation [4.55]). The vehicle modelled by the reference model should rather be the desired vehicle than the actually controlled vehicle. But, in order to avoid too much friction brake interventions; the reference model cannot be too different. Also, in order to avoid that vehicle yaws more than its path curvature; the reference model has to be almost as understeered as the controlled vehicle, which typically can be fixed by saturating lateral tyre forces on the front axle of the reference model. This requires some kind of friction estimation, especially for low- μ driving.

When controlling yaw via wheel torques, one can identify some different concepts such as direct and in-direct yaw moment, see Section 4.3.4.8. For ESC there is also a "pre-cautious yaw control" which aims at reducing speed, see Section 4.6.2.2.3.

4.6.2.2.1 Over-steer Control

Over-steer control was the first and most efficient concept in ESC. When a vehicle over-steers, ESC will brake the outer front wheel. It can brake to deep slip levels (typically -50%) since losing side grip on front axle is positive in an over-steer situation. More advanced ESC variants also brakes outer rear, but less and not to same deep slip level.

For multi-unit vehicle combinations with trailers that have controllable brakes, also the trailer is braked to avoid jack-knife effect, see Figure 4-75, or swing-out of the towed units.

4.6.2.2.2 Under-steer Control

Under-steer control means that inner rear is braked when vehicle under-steers. This helps the vehicle turn-in. This intervention is most efficient on low μ , because on high μ the inner rear wheel normally has very little normal load. Also, the slip levels are not usually as deep as corresponding

over-steer intervention, but rather -10%. This is because there is always a danger in braking too much on rear axle, since it can cause over-steering. More advanced ESC variants also brakes inner front, which makes the function very similar to the function in Section 4.6.2.2.3.

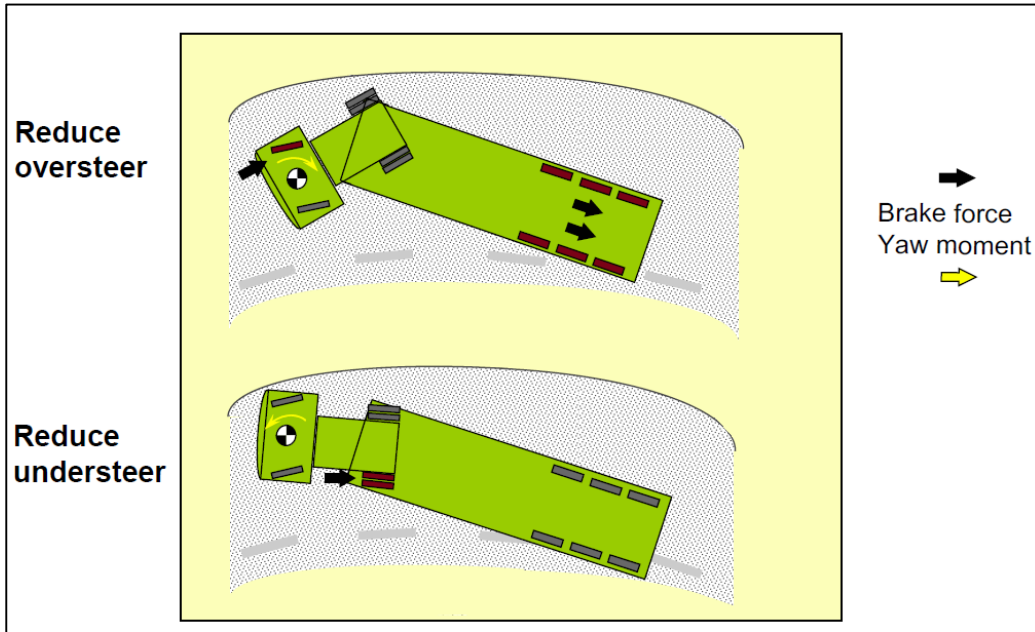


Figure 4-78: ESC when over-steer and understeer, on a truck with trailer

4.6.2.2.3 Over-speed Control

Over-speed control is not always recognised as a separate concept, but a part of under-steer control. It means that more than just inner rear wheels are braked. In this text, we identify this as done to decrease speed, which has a positive effect later in the curve.

4.6.2.2.4 Wheel-level control

A pre-requisite for all controls mentioned above in Section 4.6.2.2 is that the wheel torque actuator respond to a torque request, but it is a normal design that it is also responding to a longitudinal slip request. The slip request is generally used as a sort of “safety net” to not lock-up the wheel more than 10-20%, but at RSC interventions (see Section 4.6.2.3) the lateral grip should be braked away, so a deeper slip request is then used.

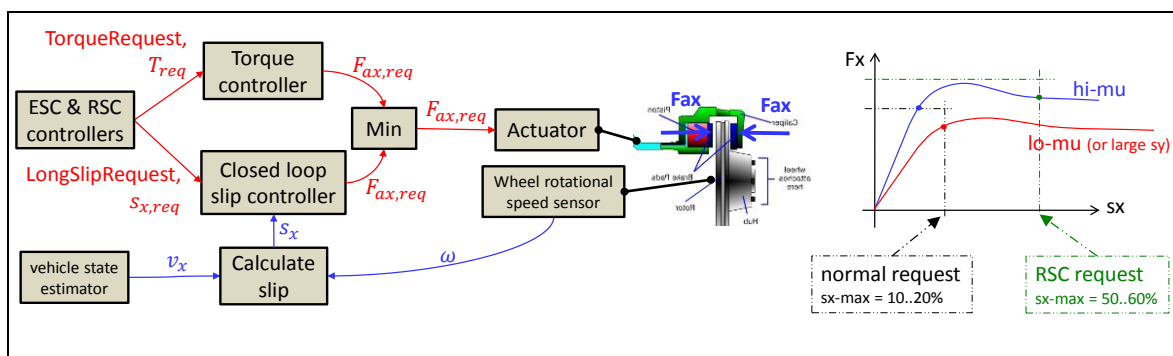


Figure 4-79: Individual wheel control by friction brakes for ESC-type functions

4.6.2.2.5 Other intervention than individual wheel brakes

4.6.2.2.5.1 Balancing with Propulsion per axle

For vehicles with controllable distribution of propulsion torque between the axles, ESC can intervene also with a request for redistribution of the propulsion torque. If over-steering, the propulsion should be redistributed towards front and opposite for understeering.

4.6.2.2.5.2 Torque Vectoring

For vehicles with controllable distribution of propulsion torque between the left and right, ESC can intervene also with a request for redistribution of the propulsion torque. If over-steering, the propulsion should be redistributed towards inner side and opposite for understeering.

4.6.2.2.5.3 Steering guidance

For vehicles with controllable steering wheel torque, ESC can intervene also with a request for additional steering wheel torque. The most obvious functions is to guide driver to open up steering (counter-steer) when the vehicle over-steers. Such functions are on market in passenger cars today. Less obvious is how to guide the driver when vehicle is under-steering.

4.6.2.3 **Roll Stability Control, RSC ***

*Function definition: **Roll Stability Control, RSC**, prohibits vehicle to roll-over due to lateral wheel forces from road friction. RSC uses friction brake as actuator.*

The purpose of RSC is to avoid un-tripped roll-overs. The actuator used is the friction brake system. When roll-over risk is detected, via lateral acceleration sensor (or in some advanced RSC implementations, also roll rate sensor), the outer front wheel is braked. RSC can brake to deep slip levels (typically -70%..-50%) since losing side grip on front axle is positive in this situation.

On heavy vehicles, RSC intervenes earlier and similar to function described in Section 4.6.2.2.3 Over-speed Control.

In future, RSC could be developed towards also using steering.

4.6.2.4 **Lateral Collision Avoidance, LCA ***

*Function definition: **Lateral Collision Avoidance** support the driver when he has to do late lateral obstacle avoidance, when probability for forward collision is predicted as high.*

There are systems on the market for Automatic Emergency Brake, see Section 3.5. If these are seen as Longitudinal Collision Avoidance, one could also think of Lateral Collision Avoidance functions, which would automatically steer away laterally from an obstacle ahead of subject vehicle. There are not yet any such functions on market. One possible first market introduction could be that triggering requires driver to initiate steering. Another would be to trigger on a first collision impact, see Reference (Yang, 2013).

5 VERTICAL DYNAMICS

5.1 Introduction

The vertical dynamics are needed since vehicles are operated on real roads, and real roads are not perfectly smooth. Also, vehicle can be operated off-road, where the ground unevenness is even larger.

The irregularities of the road can be categorized. A **transient** disturbance, such as a pothole or object on the road, can be represented as a step input. Undulating surfaces like grooves across the road may be a type of sinusoidal or other **stationary** (or periodic) input. More natural input like the random surface texture of the road may be a **random** noise distribution. In all cases, the same mechanical system must react when the vehicle travels over the road at varying speeds including doing manoeuvres in longitudinal and lateral directions.

The chapter is organised with one group of functions in each section as follows:

- 5.2 Suspension System
- 5.3 Stationary oscillations theory
- 5.4 Road models
- 5.5 One-dimensional vehicle models
- 5.6 Ride comfort
- 5.7 Fatigue life
- 5.8 Road grip
- 5.9 Variation of stiffness and damping
- 5.10 Two dimensional oscillations
- 5.11 Transient vertical dynamics
- 5.12 Other excitation sources

This chapter is, to a larger extent than Chapters **3** and **4**, organised so that all theory (knowledge) comes first and the vehicle functions comes after. In Figure 5-1 shows the 3 main functions, Ride comfort, Fatigue life and Road grip. It is supposed to explain the importance of the vehicle's dynamic structure. The vehicle's dynamic structure calls for a pretty extensive theory base, described mainly in Section 5.3.

Models in this chapter focus the disturbance from vertical irregularities from the road, i.e. only the vertical forces on the tyre from the road and **not** the forces in road plane. This enables the use of simple models which are independent of exact wheel and axle suspension, such as pivot axes and roll centres. Only the wheel stiffness rate (effective stiffness) and wheel damping rate (effective damping), see Figure 3-30, has to be given. This has the benefit that the chapter becomes relatively independent of previous chapters, but it has the drawback that the presented models are **not** really suitable for studies of steep road irregularities (which have longitudinal components) and sudden changes in wheel torque or tyre side forces.

A vehicle function which is not covered in this compendium is noise.

5.1.1 References for this chapter

- *"Chapter 21 Suspension Systems" in Reference (Ploechl, 2013).*
- *"Chapter 29 Ride Comfort and Road Holding" in Reference (Ploechl, 2013).*

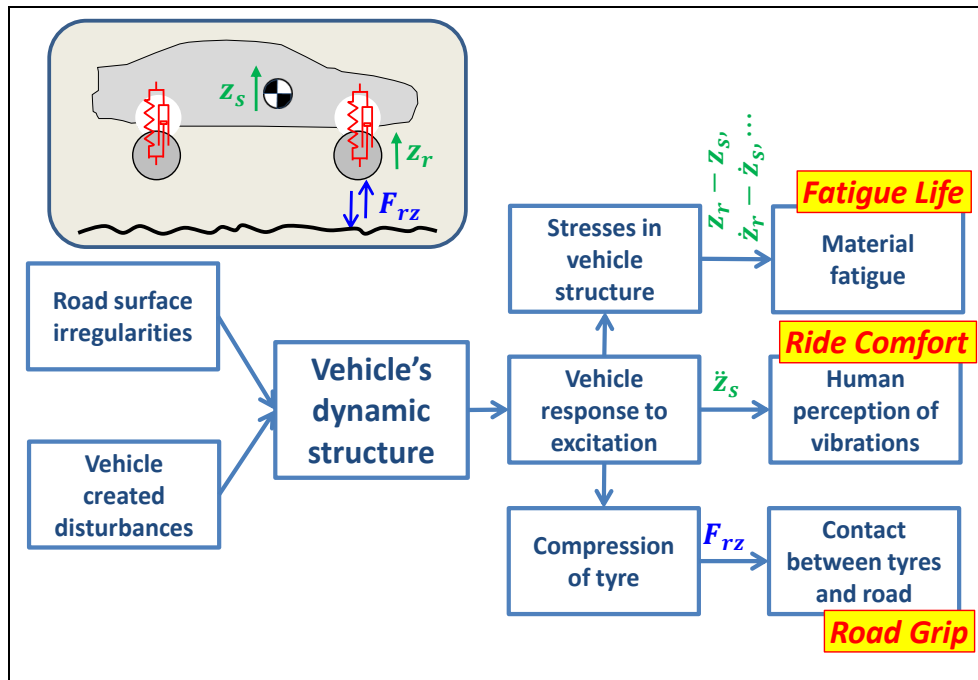


Figure 5-1: Different types of knowledge and functions in the area of vertical vehicle dynamics, organised around the vehicle's dynamic structure.

5.2 Suspension System

Suspension design is briefly discussed at these places in this compendium: Section 3.4.7, Section 4.3.9.5 and Section 5.2.

Suspension design influence ride comfort, load on suspension and road grip through how **vertical forces** and **camber and steering angles** on each wheel changes with **body motion** (heave, roll, pitch), **road unevenness** (bumps, potholes, waviness) and **wheel forces in ground plane** (from Propulsion, Braking and Steering subsystems).

Suspension in a vehicle may refer to suspension wheels (or axles), suspension of sub-frame and drivetrain and suspension of cabin (for heavy trucks). In present section, only wheel (or axle) suspension is considered.

A wheel suspension has the purpose to constrain the wheel from 6 degrees of freedom, dofs, relative the body, to 2 or 3 dofs. A steered wheel needs 3 dofs (pitch rotation, vertical translation and yaw rotation). For an un-steered wheel, also the yaw rotation should be constrained. For most steering, left and right wheels on an axle have dependent steering angles, which could be seen as 2.5 dofs/wheel.

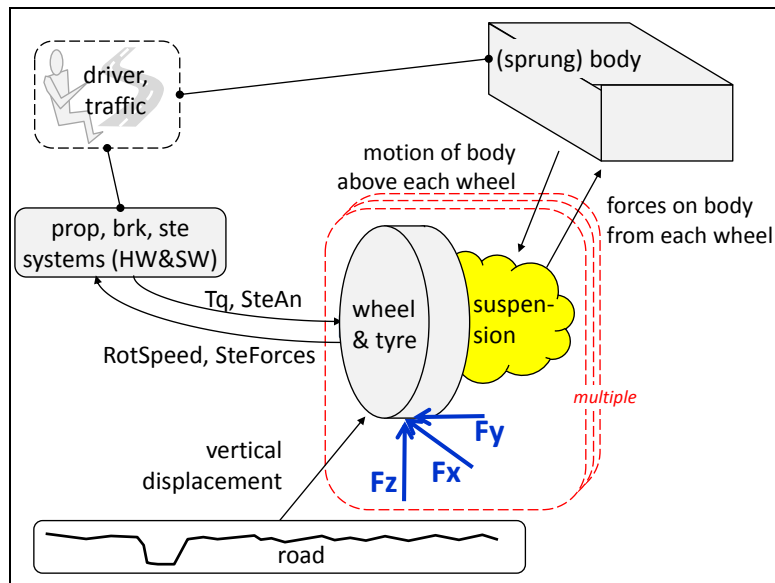


Figure 5-2: Individual wheel suspension described as one modular sub-model per wheel. It may be noted that a both wheel model (main geometry such as wheel radius) and tyre model (how F_x and F_y vary with tyre slip and F_z) is a part of each such sub-model.

An (axle) suspension system mainly consists of:

- **Linkage**, which has the purpose to constrain the relative motion between wheel and body. An alternative way to express this is that the linkage defines how longitudinal and lateral wheel forces are brought into the body (body = sprung mass). Effective pivot points and roll/pitch centres, mentioned earlier in this compendium, are defined through the linkage. In the real pivot points in the linkage, there are **bushings** with stiffness and damping. The bushings stiffness is much larger than the stiffness of the compliances mentioned below. For steered wheels, the linkage also has the purpose to allow steering. There are two main concepts: Individual wheel suspension and rigid axle suspension.
- **Compliances** (or springs), which has the purpose to allow temporary vertical displacement of the wheels relative to the body. There are often one spring per wheel but also a spring per axle. The second is called anti-roll bar and connects left and right wheel to each other to reduce body roll. Compliances often have a rather linear relation between the vertical displacement and force of each wheel, but there are exceptions:
 - **Anti-roll bars** make two wheels dependent of each other (still linear). Anti-roll bars can be used on both individual wheel suspensions and rigid axle suspensions.
 - The compliances can be intentionally designed to be non-linear in the outer end of the stroke, e.g. **bump stops**.
 - The compliances can be non-linear during the whole stroke, e.g. **air-springs** and **leaf-springs**.
 - The compliances can be intentionally designed to be **controllable** during operation of the vehicle. This can be to change the pre-load level to adjust for varying roads or varying weight of vehicle cargo or to be controllable in a shorter time scale for compensating in each oscillation cycle. The latter is very energy consuming and no such “active suspension” is available on market.
- **Dampers**, which has the purpose to dissipate energy from any oscillations of the vertical displacement of the wheel relative to the body. Dampers often has a rather linear relation between the vertical deformation speed and force of each wheel, but there are exceptions:

- The dampers can be intentionally designed to be different in different deformation direction. This is actually the normal design for dampers of **hydraulic piston type**, and it means that damping coefficient is different in compression and rebound.
- Damping in **leaf springs** is non-linear since they work with dry friction.
- Damping in **air-springs** is non-linear due to the nature of compressing gas.
- The dampers can be intentionally designed to be **controllable** during operation of the vehicle. This can be to change the damping characteristics to adjust for varying roads or varying weight of vehicle cargo or to be controllable in a shorter time scale for compensating in each oscillation cycle. The latter is called “semi-active suspension” and is available on some high-end vehicles on market.

The simplest view we can have of a suspension system is that there is an individual suspension between the vehicle body and each wheel. Each such suspension is a parallel arrangement of one linear spring and one linear damper. Chapter 5 uses this simple view for analysis models, because it facilitates understanding and it is enough for a first order evaluation of the functions studied (comfort, road grip and fatigue load) during normal driving on normal roads.

5.3 Stationary oscillations theory

Many vehicle functions in this chapter will be studied using stationary oscillations (cyclic repeating), as opposed to transiently varying. An example of transiently varying quantity is a single step function or single square pulse. A stationary oscillation can always be expressed as a sum of several harmonic terms, a so called multiple frequency harmonic stationary oscillation. The special case that only one frequency is contained can be called single frequency harmonic stationary oscillation. See Figure 5-3 and Equation [5.1].

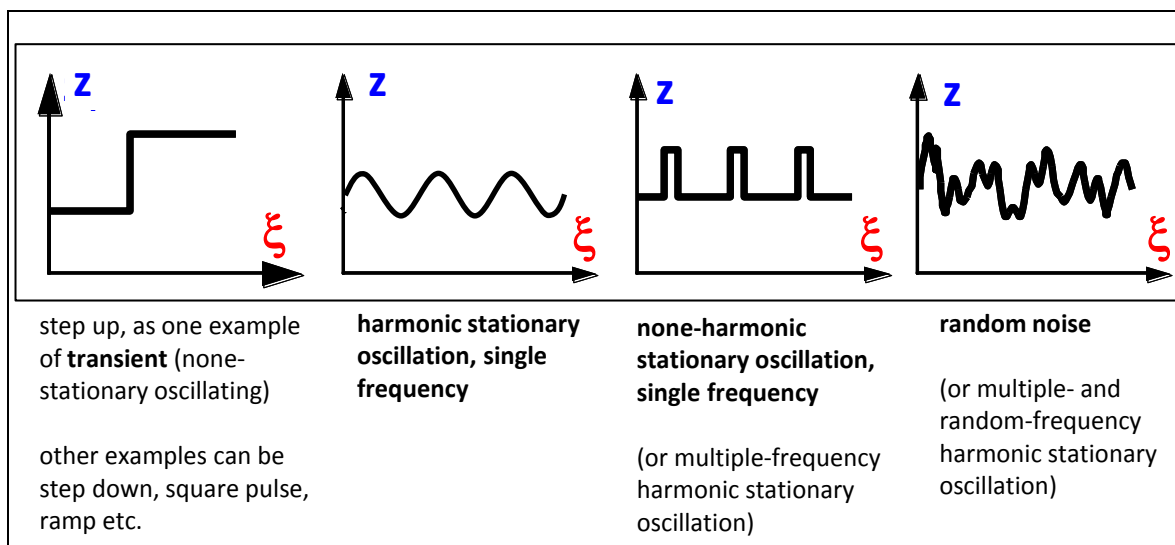


Figure 5-3: Different types of variables, both transient and stationary oscillating. The independent variable ξ can, typically, be either time or distance.

Harmonic stationary oscillations:

Single frequency : $z(\xi) = \hat{z} \cdot \cos(\omega \cdot \xi + \varphi)$;

Multiple frequencies : $z(\xi) = \sum_{i=1}^N \hat{z}_i \cdot \cos(\omega_i \cdot \xi + \varphi_i)$;

where ξ is the independent variable.

[5.1]

The most intuitive is probably to think of time as the independent variable, i.e. that the variation takes place as function of time. This would mean that $\xi = t$ in Equation [5.1]. However, for one specific road, the vertical displacement varies with longitudinal position, rather than with time. This is why we can either do analysis in **time domain** ($\xi = t$) and **space domain** ($\xi = x$).

Since the same oscillation can be described either as a function of ξ ($z = z(\xi)$) or as a function of frequency ω ($\hat{z} = \hat{z}(\omega)$), we can do analysis either in the **independent variable domain** (ξ) or in **frequency domain** (ω).

The four combinations of domains are shown in Figure 5-4.

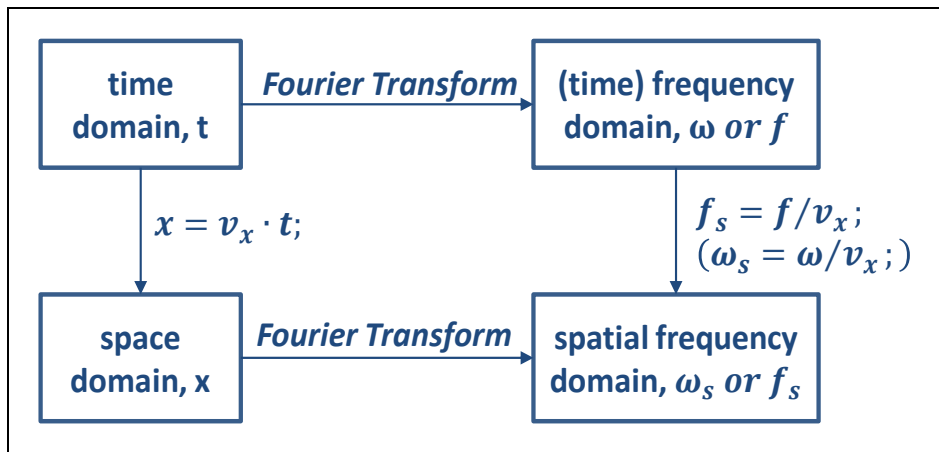


Figure 5-4: Four combinations of domains

Time and space domains are treated in section 5.3.1 and 0. In addition to the domains, we also need to differ between discrete and continuous representations in the frequency domains, see 5.3.1.2 and 5.3.2.2.

5.3.1 Time domain and time frequency domain

In time domain, the frequency has the common understanding of “how often per time”. Even so, there are two relevant ways to measure frequency: angular (time) frequency, and (time) frequency.

$$\omega = 2 \cdot \pi \cdot f;$$

where $\omega \left[\frac{rad}{s} \right] = \text{angular frequency};$

and $f \left[\frac{1}{s} = \frac{\text{oscillations}}{s} \right] = \text{(time) frequency};$

[5.2]

The time for one oscillation is called the period time. It is denoted T :

$$T = \frac{1}{f} = \frac{2 \cdot \pi}{\omega};$$

[5.3]

5.3.1.1 Mean Square (MS) and Root Mean Square (RMS) of variable

For a variable, z , we can define MS and RMS values as follows:

$$\begin{aligned}
 \text{Variable:} \quad z &= z(t); \\
 \text{MeanSquare:} \quad MS(z) &= \frac{\int_0^{t_{end}} z^2 \cdot dt}{t_{end}}; \\
 \text{RootMeanSquare:} \quad RMS(z) &= \sqrt{\frac{\int_0^{t_{end}} z^2 \cdot dt}{t_{end}}};
 \end{aligned}
 \tag{5.4}$$

If the variable is written as a single frequency harmonic stationary oscillation, these values becomes as follows:

$$\begin{aligned}
 \text{Variable:} \quad z &= \hat{z} \cdot \cos(\omega \cdot t + \varphi); \\
 \text{MeanSquare:} \quad MS(z) &= \frac{\int_0^{t_{end}} z^2 \cdot dt}{t_{end}} = \frac{\int_0^{t_{end}} (\hat{z} \cdot \cos(\omega \cdot t + \varphi))^2 \cdot dt}{t_{end}} = \\
 &= \frac{\hat{z}^2 \cdot \left[\frac{t}{2} + \frac{\sin(2 \cdot \omega \cdot t)}{4 \cdot \omega} \right]_{t=0}^{t=t_{end}}}{t_{end}} = \frac{\hat{z}^2 \cdot \left(\frac{t_{end}}{2} + \frac{\sin(2 \cdot \omega \cdot t_{end})}{4 \cdot \omega} \right)}{t_{end}} \xrightarrow{t_{end} \rightarrow \infty} \frac{\hat{z}^2}{2}; \\
 \text{RootMeanSquare:} \quad RMS(z) &= \sqrt{\frac{\int_0^{t_{end}} z^2 \cdot dt}{t_{end}}} = \sqrt{MS(z)} = \frac{|\hat{z}|}{\sqrt{2}};
 \end{aligned}
 \tag{5.5}$$

If the variable is written as a multiple frequency harmonic stationary oscillation, these values becomes as follows:

$$\begin{aligned}
 \text{Variable:} \quad z &= \sum_{i=1}^N z_i = \sum_{i=1}^N \hat{z}_i \cdot \cos(\omega_i \cdot t + \varphi_i); \\
 \text{MeanSquare:} \quad MS(z) &= \frac{\int_0^{t_{end}} z^2 \cdot dt}{t_{end}} = \frac{\int_0^{t_{end}} (\sum_{i=1}^N z_i)^2 \cdot dt}{t_{end}} = \\
 &= \frac{\int_0^{t_{end}} (\sum_{i=1}^N \hat{z}_i \cdot \cos(\omega_i \cdot t + \varphi_i))^2 \cdot dt}{t_{end}} \xrightarrow{t_{end} \rightarrow \infty} \\
 \xrightarrow{t_{end} \rightarrow \infty} &\frac{\int_0^{t_{end}} \sum_{i=1}^N \hat{z}_i^2 \cdot (\cos(\omega_i \cdot t + \varphi_i))^2 \cdot dt}{t_{end}} = \sum_{i=1}^N MS(z_i) = \sum_{i=1}^N \frac{\hat{z}_i^2}{2}; \\
 \text{RootMeanSquare:} \quad RMS(z) &= \sqrt{MS(z)} = \sqrt{\sum_{i=1}^N \frac{\hat{z}_i^2}{2}} = \sqrt{\sum_{i=1}^N MS(z_i)} = \\
 &= \sqrt{\sum_{i=1}^N (RMS(z_i))^2};
 \end{aligned}
 \tag{5.6}$$

5.3.1.2 Power Spectral Density and Frequency bands

So far, the frequency has been a discrete number of frequencies, $\omega_1, \omega_2, \dots, \omega_N$. There are reasons to treat the frequency as a continuous variable instead. The discrete amplitudes, $\hat{z}_1, \hat{z}_2, \dots, \hat{z}_N$, should then be thought of as integrals of a "continuous amplitude curve", \hat{z}_c , where the integration is done over a small frequency interval, centred around a each mid frequency, ω_i :

$$\hat{z}_i = \int_{\omega = \frac{\omega_{i-1} + \omega_i}{2}}^{\omega = \frac{\omega_i + \omega_{i+1}}{2}} \hat{z}_c \cdot d\omega = \hat{z}_c(\omega_i) \cdot \frac{\omega_{i+1} - \omega_{i-1}}{2} = \hat{z}_c(\omega_i) \cdot \Delta\omega_i; \Rightarrow \hat{z}_c(\omega_i) = \frac{\hat{z}_i}{\Delta\omega_i}; \quad [5.7]$$

We realize that the unit of \hat{z}_c has to be same as for z , but per [rad/s]. So, if z is a displacement in [m], \hat{z}_c has the unit [m/(rad/s)]. Now, \hat{z}_c is a way to understand the concept of a spectral density. A similar value, but more used, is the Power Spectral Density, PSD (also called Mean Square Spectral Density).

$PSD(\omega)$ is a continuous function, while \hat{z}_i is a discrete function. That means that $PSD(\omega)$ is fully determined by a certain measured or calculated variable $z(t)$, while \hat{z}_i depends on which discretization (which ω_i or which $\Delta\omega$) that is chosen.

$$PSD(z(t), \omega, \Delta\omega) = \frac{MS(filter(z(t), \omega, \Delta\omega))}{\Delta\omega} = G(\omega); \quad [5.8]$$

where filter is a bandpass filter centered around ω and with band width $\Delta\omega$;

PSD can also be defined with band width in time frequency instead of angular frequency. The Equation [5.8] is the same but replacing $\Delta\omega$ with Δf .

When the variable to study (z) is known and the band width is known, one often write simply $PSD(\omega)$ or $G(\omega)$. G has the same unit as z^2 , but per [rad/s] or per [oscillations/s]. So, if z is a displacement in [m], G has the unit $[\frac{m^2}{rad/s}]$ or $[\frac{m^2}{1/s} = m^2 \cdot s]$.

The usage of the PSD is, primarily, to easily obtain the RMS via integration:

$$RMS(z) = \sqrt{\sum_{i=1}^N MS(z_i)} = \sqrt{\sum_{i=1}^N G(\omega_i) \cdot \Delta\omega_i} = \sqrt{\int_{\omega=0}^{\infty} G(\omega) \cdot d\omega}; \quad [5.9]$$

RMS is square root of the area under the PSD curve.

5.3.1.2.1 Differentiation of PSD

Knowing the PSD of a variable, we can easily obtain the PSD for the derivative of the same variable:

$$G_{\dot{z}}(\omega) = \omega^2 \cdot G_z(\omega); \quad [5.10]$$

5.3.1.3 Transfer function

In a minimum model for vertical dynamics there is at least one excitation, often road vertical displacement, z_r , and one response, e.g. vertical displacement of sprung mass (=vehicle body), z_s . A Transfer function, $H = H(j \cdot \omega)$, is the function which we can use to find the response, given the excitation:

$$Z_s(\omega) = H(\omega) \cdot Z_r(\omega); \Leftrightarrow \mathcal{F}(z_s(t)) = H(\omega) \cdot \mathcal{F}(z_r(t));$$

where \mathcal{F} is the Fourier operator: $Z(\omega) = \mathcal{F}(z(t))$

$$= \int_0^{\infty} e^{-j \cdot \omega \cdot t} \cdot z(t) \cdot dt; \quad [5.11]$$

H is complex, which is why it has a magnitude, $|H| = \sqrt{(\text{Re}(H))^2 + (\text{Im}(H))^2}$, and phase, $\arg(H(\omega)) = \arctan(\text{Im}(H)/\text{Re}(H))$.

$$\begin{aligned} \text{Amplitude: } \hat{z}_s(\omega) &= |H(\omega)| \cdot \hat{z}_r(\omega); \\ \text{Phase: } \varphi_s(\omega) - \varphi_r(\omega) &= \arg(H(\omega)); \\ \text{where } z &= \sum_{i=1}^N \hat{z}(\omega_i) \cdot \cos(\omega_i \cdot t + \varphi_i); \end{aligned}$$

[5.12]

Since there can be different excitations and responses in a system, there are several transfer functions. To distinguish between those, a subscripting of H is often used: $H_{\text{excitation} \rightarrow \text{response}}$, which would be $H_{z_r \rightarrow z_s} = H_{\text{road displacement} \rightarrow \text{sprung mass displacement}}$ in the example above. Other examples of relevant transfer functions in vertical vehicle dynamics are:

- $H_{\text{road displacement} \rightarrow \text{sprung mass acceleration}}$ [$\frac{m/s^2}{m}$], see Section 5.6
- $H_{\text{road displacement} \rightarrow \text{suspension deformation}}$ [$\frac{m}{m}$], see Section 5.7
- $H_{\text{road displacement} \rightarrow \text{tyre force}}$ [$\frac{N}{m}$], see Section 5.8

When transfer function for one derivative is found, it is often easy to convert it to another:

$$\begin{aligned} H_{z_1 \rightarrow \dot{z}_2} &= j \cdot \omega \cdot H_{z_1 \rightarrow z_2}; \\ H_{z_1 \rightarrow \ddot{z}_2} &= j \cdot \omega \cdot j \cdot \omega \cdot H_{z_1 \rightarrow z_2} \\ &= -\omega^2 \cdot H_{z_1 \rightarrow z_2}; \\ H_{z_1 \rightarrow z_2 - z_3} &= H_{z_1 \rightarrow z_2} - H_{z_1 \rightarrow z_3}; \end{aligned}$$

[5.13]

Note that these relations are valid for the complex transfer function. They corresponding relations can be used with $|H|$ replacing H , in cases where the phase is same for all involve variables, which often can be the case when damping is neglected.

The usage of the transfer function is, primarily, to easily obtain the response from the excitation, as shown in Equation [5.12]. Also, the transfer function can operate on the Power Spectral Density, PSD=G, as shown in the following:

$$\begin{aligned} G_{z_s}(\omega) &= \frac{MS(z_s(t), \omega)}{\Delta\omega} = \frac{(\hat{z}_s(\omega))^2/2}{\Delta\omega} = \frac{(|H(\omega)| \cdot \hat{z}_r(\omega))^2/2}{\Delta\omega} \\ &= |H_{z_r \rightarrow z_s}(\omega)|^2 \cdot \frac{(\hat{z}_r(\omega))^2/2}{\Delta\omega} = |H_{z_r \rightarrow z_s}(\omega)|^2 \cdot G_{z_r}(\omega); \end{aligned}$$

[5.14]

Using Equation [5.9], we can then calculate $RMS(z_s)$ from $G_{z_s}(\omega)$.

5.3.2 Space domain and Space frequency domain

All transformations, in this compendium, between time domain and space domain requires a constant longitudinal speed, v_x , so that:

$$x = v_x \cdot t + x_0;$$

[5.15]

The offset (x_0) is the phase (spatial) offset (x_0) is the correspondence to the phase angle (φ).

The corresponding formulas as given in Equations [5.2]..[5.13] can be formulated when changing to space domain, or spatial domain. It is generally a good idea to use a separate set of notations for the spatial domain. Hence the formulas are repeated with new notations, which is basically what will be done in present section.

There are not relevant to define transfer functions for the spatial domain before a road model is given, see Section 5.4.2.1.

In space domain, the frequency has the common understanding of “how often per **distance**”. Even so, there are two relevant ways to measure frequency: spatial angular frequency and spatial frequency.

$$\begin{aligned} \Omega &= 2 \cdot \pi \cdot f_s; \\ \text{where } \Omega \left[\frac{\text{rad}}{\text{m}} \right] &= \text{spatial angular frequency}; \\ \text{and } f_s \left[\frac{1}{\text{m}} = \frac{\text{oscillations}}{\text{m}} \right] &= \text{spatial frequency}; \end{aligned} \quad [5.16]$$

The correspondence to period time is wave length, denoted λ :

$$\lambda[\text{m}] = \frac{1}{f_s} = \frac{2 \cdot \pi}{\Omega}; \quad [5.17]$$

Now, the basic assumption in Equation [5.15] and definitions of frequencies gives:

$$\omega = v_x \cdot \Omega; \quad \text{and } f = v_x \cdot f_s; \quad [5.18]$$

The relation between the phase (spatial) offset (x_0) and the phase angle (φ) is:

$$x_0 = \frac{\lambda \cdot \varphi}{2 \cdot \pi}; \quad [5.19]$$

5.3.2.1 Spatial Mean Square (MS) and spatial Root Mean Square (RMS) of variable

In space domain, a variable, z , varies with distance, x . We can define Mean Square and Root Mean Square values also in space domain. We subscript these with s for space.

$$\begin{aligned} \text{Variable:} \quad z &= z(x); \\ \text{MeanSquare:} \quad MS_s(z) &= \frac{\int_0^{x_{end}} z^2 \cdot dx}{x_{end}}; \\ \text{RootMeanSquare:} \quad RMS_s(z) &= \sqrt{\frac{\int_0^{x_{end}} z^2 \cdot dx}{x_{end}}}; \end{aligned} \quad [5.20]$$

Because v_x is constant, the Mean Square and Root Mean Square will be the same in time and space domain. If the variable is written as a single frequency harmonic stationary oscillation, these values becomes as follows:

$$\begin{aligned}
 \text{Variable:} \quad z &= \hat{z} \cdot \cos(\Omega \cdot x + x_0); \\
 \text{MeanSquare:} \quad MS_S(z) &= \dots = \frac{\hat{z}^2}{2} = MS(z); \\
 \text{RootMeanSquare:} \quad RMS_S(z) &= \dots = \frac{|\hat{z}|}{\sqrt{2}} = RMS(z);
 \end{aligned}
 \tag{5.21}$$

If the variable is written as a multiple frequency harmonic stationary oscillation, these values becomes as follows:

$$\begin{aligned}
 \text{Variable:} \quad z &= \sum_{i=1}^N z_i = \sum_{i=1}^N \hat{z}_i \cdot \cos(\Omega_i \cdot x + x_{0i}); \\
 \text{MeanSquare:} \quad MS_S(z) &= \sum_{i=1}^N \frac{\hat{z}_i^2}{2} = MS(z); \\
 \text{RootMeanSquare:} \quad RMS_S(z) &= \sqrt{MS_S(z)} = \sqrt{\sum_{i=1}^N (RMS(z_i))^2} \\
 &= RMS(z);
 \end{aligned}
 \tag{5.22}$$

5.3.2.2 Spatial Power Spectral Density and Frequency bands

A correspondence to Power Spectral Density in space domain is denoted PSD_s in the following:

$$PSD_s(z(x), \Omega, \Delta\lambda) = \frac{MS(\text{filter}(z(x), \Omega, \Delta\lambda))}{\Delta\lambda} = \Phi(\Omega);$$

where "filter" is a band pass filter centred around ω and with band width Δf ;

[5.23]

When the variable to study (z) is known and the band width is known, one often write simply $PSD_s(\Omega)$ or $\Phi(\Omega)$. Φ has the same unit as z^2 , but per [rad/m] or per [oscillations/m]. So, if z is a displacement in [m], Φ has the unit [$\frac{m^2}{rad/m} = \frac{m^3}{rad}$] or [$\frac{m^2}{1/m} = m^3$].

5.4 Road models

In general, a road model can include ground properties such as coefficient of friction, damping/elasticity of ground and vertical position. The independent variable is either one, along an assumed path, or generally two, x and y in ground plane. In vertical dynamics in this compendium, we only assume vertical displacement as function of a path. We use x as independent variable along the path, meaning that the road model is: $z_r = z_r(x)$. The function $z_r(x)$ can be either of the types in Figure 5-3. We will concentrate on stationary oscillations, which by Fourier series, always can be expressed as multiple (spatial) frequency harmonic stationary oscillation. This can be specialized to either single (spatial) frequency or random (spatial) frequency. Hence, the general form of the road model is multiple (spatial) frequencies:

$$z_r = z_r(x) = \sum_{i=1}^N \hat{z}_i \cdot \cos(\Omega_i \cdot x + x_{0i});$$
[5.24]

5.4.1 One frequency road model

For certain roads, such as roads built with concrete blocks, a single (spatial) frequency can be a relevant approximation to study a certain single wave length. Also, the single (spatial) frequency road model is good for learning the different concepts. A single (spatial) frequency model is the same as a single wave length model ($\lambda = 2 \cdot \pi/\Omega$, from Equation [5.16]) and it can be described as:

$$z_r = z_r(x) = \hat{z} \cdot \cos(\Omega \cdot x + x_0); \tag{5.25}$$

5.4.2 Multiple frequency road models

Based on the general format in Equation [5.24], we will now specialise to models for different road qualities. In Figure 5-5, there are 4 types of road types defined. Approximately, the 3 upper of those are roads and they are also defined as PSD-plots in Figure 5-6. The mathematical formula is given in Equation [5.26] and numerical parameter values are given in Equation [5.27].

$$\Phi = \Phi(\Omega) = \Phi_0 \cdot \left(\frac{\Omega}{\Omega_0}\right)^{-w} = \frac{MS_s(z_r, \Omega)}{\Delta\Omega};$$

where $\Phi_0 = \text{road severity} \left[\frac{\text{m}^2}{\text{rad/m}} \right];$
 $w = \text{road waviness} [1];$
 $\Omega = \text{spatial angular frequency} [\text{rad/m}];$
 $\Omega_0 = 1 [\text{rad/m}];$

[5.26]

Typical values are

Very good road: $\Phi_0 = 1 \cdot 10^{-6} \left[\frac{\text{m}^2}{\text{rad/m}} \right];$
 Bad road : $\Phi_0 = 10 \cdot 10^{-6} \left[\frac{\text{m}^2}{\text{rad/m}} \right];$
 Very bad road : $\Phi_0 = 100 \cdot 10^{-6} \left[\frac{\text{m}^2}{\text{rad/m}} \right];$

The waviness is normally in the range of $w = 2..3 [1]$, where smooth roads have larger waviness than bad roads.

[5.27]

The decreasing amplitude for higher (spatial) frequencies (i.e. for smaller wave length) can be explained by that height variation over a short distance requires large gradients. On micro-level, in the granular level in the asphalt, there can of course be steep slopes on the each small stone in the asphalt. These are of less interest for vehicle vertical dynamics, since the wheel dimensions filter out wave length \ll tyre contact length, see Figure 2-35.

A certain road can be described with:

- $\Omega_1, \dots, \Omega_N$
- $\hat{z}_1, \dots, \hat{z}_N$
- x_{01}, \dots, x_{0N}



Figure 5-5: Four typical road types, whereof the upper 3 can be considered as road types. From (AB Volvo, 2011).

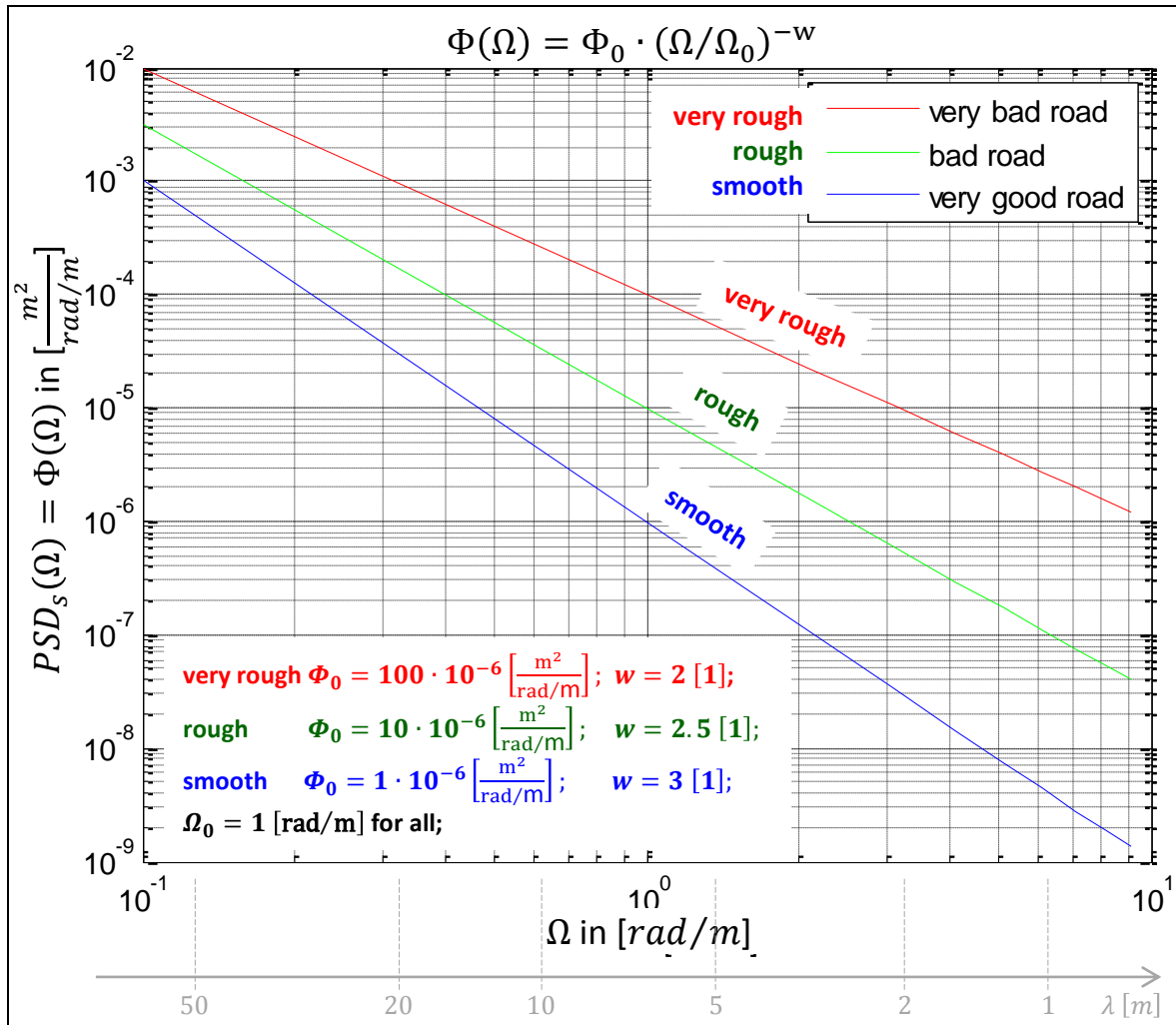


Figure 5-6: PSD spectra for the three typical roads in Figure 5-5.

Number of frequency components, N, to select is a matter of accuracy or experience. The offsets, x_{01}, \dots, x_{0N} , can often be assumed to be zero. If phase is to be studied, as in Figure 5-6, a random generation of offsets is suitable. See also Reference (ISO 8608).

If we generate the actual $z_r(x)$ curves for the 3 road types in Figure 5-6, we can plot as shown in Figure 5-7. To generate those plots, we have to assume different number of harmonic components (N in Equation [5.24]) and also randomly generate the phase for each component (each x_{0i}).

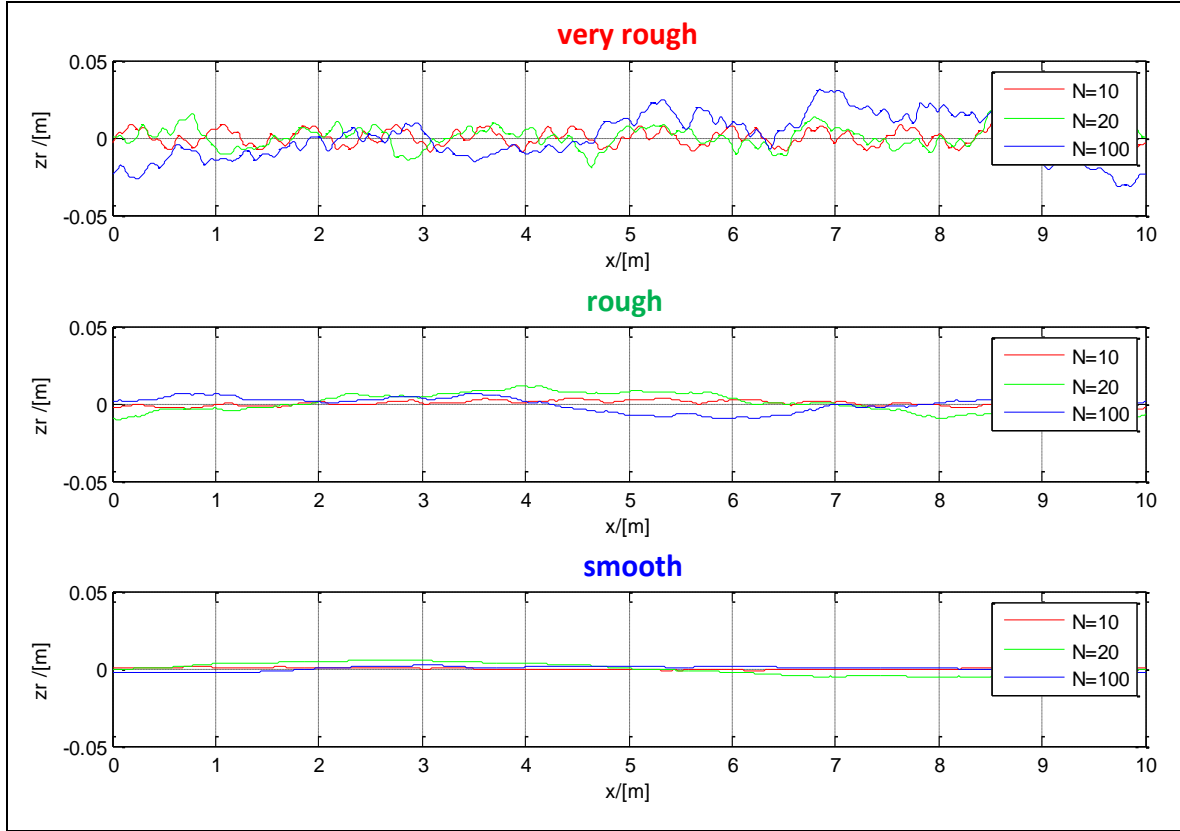


Figure 5-7: Road profiles, $z_r(x)$, for the three typical roads in Figure 5-5.

5.4.2.1 Transfer function from road spectrum in spatial domain to system response in time domain

Since we assume constant longitudinal velocity, v_x , the road spectrum can be transformed to the time-frequency domain:

$$\begin{aligned}
 G_{z_r}(\omega) &= \frac{MS(z_r, \omega)}{\Delta\omega} = \left\{ \text{use: } \omega = v_x \cdot \Omega \right\} = \frac{MS_s(z_r, \Omega)}{v_x \cdot \Delta\Omega} = \\
 &= \left\{ \text{use: } \Phi_0 \cdot \left(\frac{\Omega}{\Omega_0} \right)^{-w} = \frac{MS_s(z_r, \Omega)}{\Delta\Omega} \right\} = \frac{\Phi_0 \cdot \left(\frac{\Omega}{\Omega_0} \right)^{-w}}{v_x} = \\
 &= \frac{\Phi_0 \cdot \Omega^{-w}}{\Omega_0^{-w} \cdot v_x} = \frac{\Phi_0}{\Omega_0^{-w}} \cdot \frac{\left(\frac{\omega}{v_x} \right)^{-w}}{v_x} = \frac{\Phi_0}{\Omega_0^{-w}} \cdot v_x^{w-1} \cdot \omega^{-w};
 \end{aligned}
 \tag{5.28}$$

Then, we can use Equation [5.14] to obtain the response z_s :

$$G_{z_s}(\omega) = |H_{z_r \rightarrow z_s}(\omega)|^2 \cdot G_{z_r}(\omega) = |H_{z_r \rightarrow z_s}(\omega)|^2 \cdot \frac{\Phi_0}{\Omega_0^{-w}} \cdot v_x^{w-1} \cdot \omega^{-w};
 \tag{5.29}$$

Then we can use Equation [5.9] to obtain the RMS of the response z_s :

$$\begin{aligned}
 RMS(z_s) &= \sqrt{\sum_{i=1}^N G_{z_s}(\omega_i) \cdot \Delta\omega} \\
 &= \sqrt{\frac{\Phi_0}{\Omega_0^{-w}} \cdot v_x^{w-1} \cdot \sum_{i=1}^N |H_{z_r \rightarrow z_s}(\omega_i)|^2 \cdot \omega_i^{-w} \cdot \Delta\omega};
 \end{aligned}$$

[5.30]

or

$$RMS(z_s) = \sqrt{\int_{\omega=0}^{\infty} G_{z_s}(\omega) \cdot d\omega} = \sqrt{\frac{\Phi_0}{\Omega_0^{-w}} \cdot v_x^{w-1} \cdot \int_{\omega=0}^{\infty} |H_{z_r \rightarrow z_s}(\omega)|^2 \cdot \omega^{-w} \cdot d\omega};$$

5.5 One-dimensional vehicle models

“One-dimensional” refers to pure vertical motion, i.e. that the vehicle heaves without pitch and without roll. The tyre is stiff and massless.

This can be seen as that the whole vehicle mass, m , is modelled as suspended by the sum of all wheels’ vertical forces, $F_z = F_{flz} + F_{frrz} + F_{rlz} + F_{rrz}$. However, the model can sometimes be referred to as a “quarter-car-model”. That is because one can see the model as a quarter of the vehicle mass, $m/4$, which is suspended by one of the wheel’s vertical force, F_{ijz} . The exact physical interpolation of a quarter car is less obvious, since one can argue whether the fraction $\frac{1}{4}$ of the vehicle mass is the proper fraction or from which point of view it is proper. Using the fraction $\frac{1}{4}$ is at least debatable if the vehicle is completely symmetrical, both left/right and front/rear.

5.5.1 One-dimensional model without dynamic degree of freedom

“Without dynamic degree of freedom” refers to that the (axle) suspension is modelled as ideally stiff. The model can be visualised as in Figure 5-8.

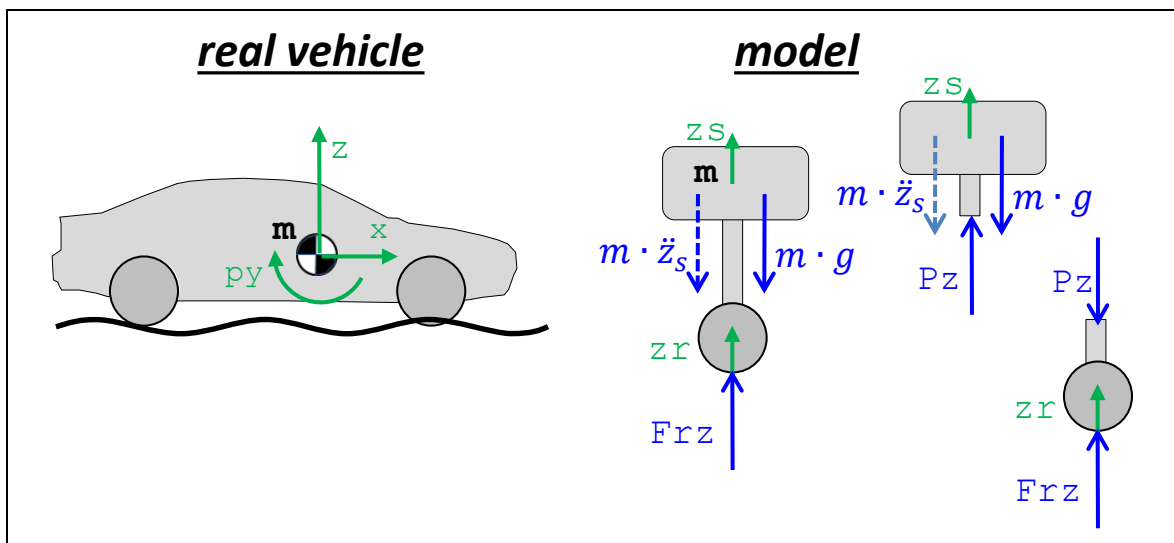


Figure 5-8: One-dimensional model without dynamic degree of freedom

Probably, we could find the equations without very much formalism ($m \cdot \ddot{z}_s = F_{rz}$; and $z_s = z_r(t)$); but the following equations exemplifies a formalism which will be useful when we expand the model later.

$$\begin{aligned}
 \textbf{Equilibrium:} \quad & m \cdot \ddot{z}_s + m \cdot g = P_z; \\
 & F_{rz} - P_z = 0; \\
 \textbf{Compatibility:} \quad & z_r = z_s; \\
 \textbf{Excitation:} \quad & z_r = z_r(t);
 \end{aligned}$$

[5.31]

Note that an alternative model would be to distribute the mass in the model; m_s above P_z and m_u under P_z . However, it would not influence the transfer functions derived later in 5.5.1.1.

5.5.1.1 Response to a single frequency excitation

Assume that the road has only one (spatial) frequency, i.e. one wave length. Then the excitation is as follows:

$$\begin{aligned}
 & \left\{ \begin{aligned} z_r = z_r(x) = \hat{z} \cdot \cos(\Omega \cdot x + x_0) = \hat{z} \cdot \cos\left(\frac{2 \cdot \pi}{\lambda} \cdot x + x_0\right); \\ x = v_x \cdot t; \\ \text{Assume } x_0 = 0; \end{aligned} \right\} \Rightarrow \\
 & \Rightarrow z_r(t) = \hat{z}_r \cdot \cos\left(\frac{2 \cdot \pi \cdot v_x}{\lambda} \cdot t\right) = \hat{z}_r \cdot \cos(\omega \cdot t); \Rightarrow \\
 & \Rightarrow \dot{z}_r(t) = -\frac{2 \cdot \pi \cdot v_x}{\lambda} \cdot \hat{z}_r \cdot \sin\left(\frac{2 \cdot \pi \cdot v_x}{\lambda} \cdot t\right) = -\omega \cdot \hat{z}_r \cdot \sin(\omega \cdot t); \Rightarrow \\
 & \Rightarrow \ddot{z}_r(t) = -\left(\frac{2 \cdot \pi \cdot v_x}{\lambda}\right)^2 \cdot \hat{z}_r \cdot \cos\left(\frac{2 \cdot \pi \cdot v_x}{\lambda} \cdot t\right) = -\omega^2 \cdot \hat{z}_r \cdot \cos(\omega \cdot t);
 \end{aligned}$$

[5.32]

Insertion in the model in Equation [5.31] gives directly the solution:

$$\begin{aligned}
 & \left\{ \begin{aligned} P_z(t) = F_{rz}(t) = m \cdot g + \Delta F(t) = m \cdot g + \hat{F} \cdot \cos(\omega \cdot t); \\ z_r(t) = z_s(t) = \hat{z}_r \cdot \cos(\omega \cdot t); \\ \ddot{z}_r(t) = \ddot{z}_s(t) = \hat{a} \cdot \cos(\omega \cdot t); \end{aligned} \right. \\
 & \text{where } \left\{ \begin{aligned} \hat{F} &= -m \cdot \omega^2 \cdot \hat{z}_r; \\ \hat{a} &= -\omega^2 \cdot \hat{z}_r; \end{aligned} \right.
 \end{aligned}$$

[5.33]

5.5.1.1.1 Analysis of solution

We can identify the magnitude of the transfer functions. The negative sign in Equation [5.33] means 180 degrees phase shift:

$$\begin{aligned}
 H_{z_r \rightarrow z_s} &= \left\{ H_{z_r \rightarrow z_s} = \frac{\mathcal{F}(z_s)}{\mathcal{F}(z_r)} \right\} = 1 + j \cdot 0; \\
 H_{z_r \rightarrow z_r - z_s} &= \{ H_{z_r \rightarrow z_r - z_s} = H_{z_r \rightarrow z_s} - H_{z_s \rightarrow z_s} = H_{z_r \rightarrow z_s} - 1 \} = 0 + j \cdot 0; \\
 H_{z_r \rightarrow \ddot{z}_s} &= \{ H_{z_r \rightarrow \ddot{z}_s} = (j \cdot \omega)^2 \cdot H_{z_r \rightarrow z_s} = -\omega^2 \cdot H_{z_r \rightarrow z_s} \} = -\omega^2 + j \cdot 0; \\
 H_{z_r \rightarrow \Delta F_{rz}} &= \{ H_{z_r \rightarrow \Delta F_{rz}} = m \cdot H_{z_r \rightarrow \ddot{z}_s} \} = -m \cdot \omega^2 + j \cdot 0;
 \end{aligned}$$

[5.34]

The motivation to choose exactly those transfer functions is revealed later, in Section 5.6, 5.7 and 5.8. For now, we simply conclude that various transfer functions can be identified and plotted. The plots are found in Figure 5-9. Numerical values for m and λ has been chosen.

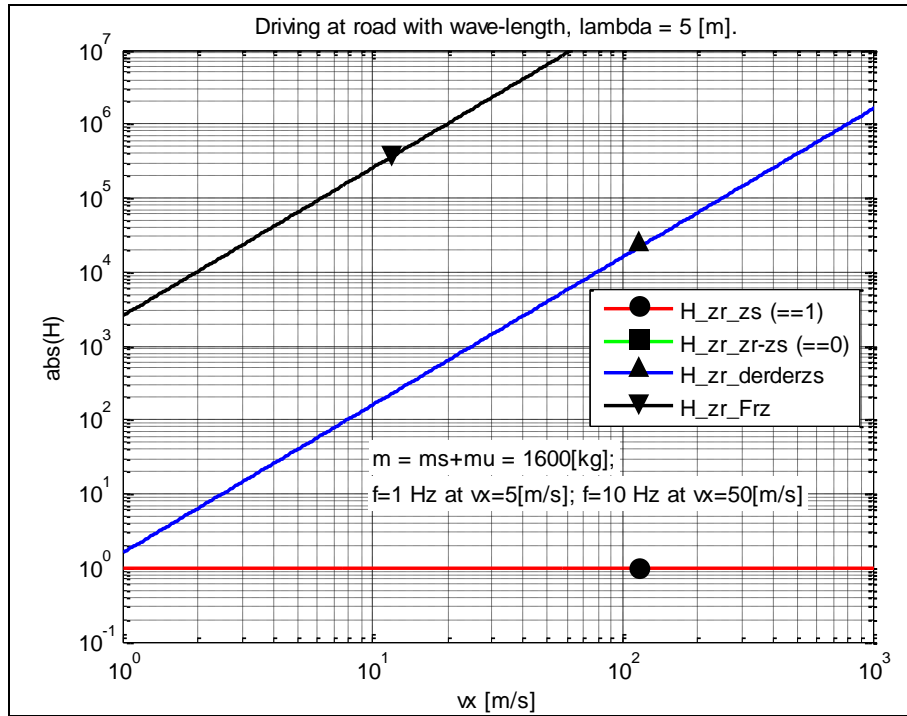


Figure 5-9: Transfer functions from model in Figure 5-8, excited with single frequencies.

So, for example, we can use the transfer function diagram as follows: If we have a road displacement amplitude of 1 cm ($\hat{z}_r = 0.01 \text{ m}$) and a speed of 50 km/h ($v_x \approx 14 \text{ m/s} \hat{=} \approx 2.8\text{Hz}$), we can read out, e.g.:

- $|H_{z_r \rightarrow \ddot{z}_s}(v_x)| \approx 305$; $\Rightarrow |\hat{a}| = 310 \cdot \hat{z}_r = 305 \cdot 0.01 = 3.05 \text{ m/s}^2$; From this we can calculate $RMS(\ddot{z}_s) = |3.05|/\sqrt{2} \approx 2.16 \text{ m/s}^2$. The RMS value of acceleration will later be related to ride comfort, see Section 5.6.
- $|H_{z_r \rightarrow z_r - z_s}(v_x)| = 0$; i.e. no deformation, which is not strange, since model is stiff. The deformation of suspension will later be related to fatigue life, see Section 5.7.
- $|H_{z_r \rightarrow \Delta F_{rz}}(v_x)| \approx 487000$; $\Rightarrow |\hat{F}| = 487000 \cdot \hat{z}_r = 487000 \cdot 0.01 = 4870 \text{ N}$; If $|\hat{F}|$ had been $> m \cdot g \approx 16000 \text{ N}$, the model would have been outside its validity region, because it would require pulling forces between tyre and road, which is not possible. The variation in tyre road contact force will be related to road grip, see Section 5.8.

The phases for the studied variables are seen from the complex transfer functions in Equation [5.34].

5.5.1.2 Response to a multiple frequency excitation

Using Equation [5.30], Equation [5.45] and values for road type “rough” in Figure 5-6, we can conclude:

$$\begin{aligned}
 RMS(z_s) &= \sqrt{\frac{\Phi_0}{\Omega_0^{-w}} \cdot v_x^{w-1} \cdot \int_{\omega=0}^{\infty} |H_{z_r \rightarrow z_s}(\omega)|^2 \cdot \omega^{-w} \cdot d\omega =} \\
 &= \sqrt{\frac{10 \cdot 10^{-6}}{1} \cdot v_x^{2.5-1} \cdot \int_{\omega=0}^{\infty} |H_{z_r \rightarrow z_s}(\omega)|^2 \cdot \omega^{-2.5} \cdot d\omega;}
 \end{aligned}
 \tag{5.35}$$

For now, we simply note that it is possible to calculate this (scalar) RMS value for each vehicle speed over the assumed road. In corresponding way, an RMS value can be calculated for any of the oscillating variables, such as \ddot{z}_s , $z_r - z_s$ and F_{rz} . We will come back to Equation [5.35] in Section 5.6.2.

5.5.2 One dimensional model with one dynamic degree of freedom

“With one dynamic degree of freedom” refers to that the axle suspension is modelled as a linear spring and linear (viscous) damper in parallel. The tyre is still stiff and massless. The model can be visualised as in Figure 5-10.

The corresponding mathematical model becomes as follows:.

Equilibrium:	$m \cdot \ddot{z}_s + m \cdot g = P_z;$	[5.36]
	$F_{rz} - P_z = 0;$	
Constitution:	$P_z = c \cdot (z_r - z_s) + d \cdot (\dot{z}_r - \dot{z}_s) + m \cdot g;$	
Excitation:	$z_r = z_r(t);$	

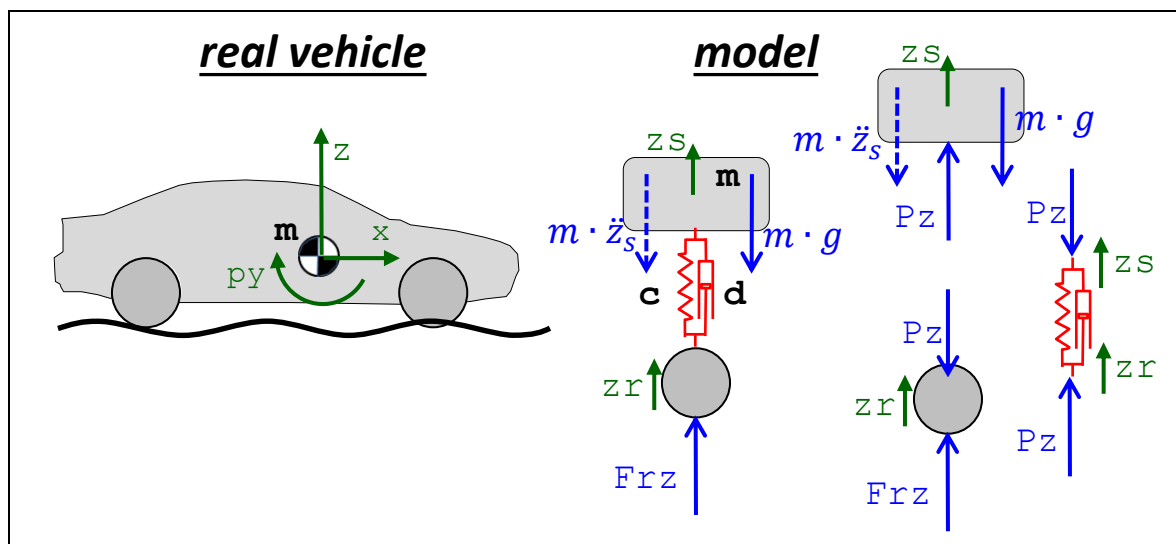


Figure 5-10: One-dimensional model with one dynamic degree of freedom

Note that if we measure z_u and z_s from the static equilibrium, the static load, $m \cdot g$, disappears when constitution is inserted in equilibrium.

Note also that an alternative model would be to distribute the mass in the model; m_s above P_z and m_u under P_z . model lower part as having a mass. Such change would also affect the transfer functions.

5.5.2.1 Response to a single frequency excitation

Eliminating P_z and z_r gives:

$$\begin{aligned}
 m \cdot \ddot{z}_s &= c \cdot (z_r(t) - z_s) + d \cdot (\dot{z}_r(t) - \dot{z}_s); \\
 \Delta F_{rz} &= c \cdot (z_r(t) - z_s) + d \cdot (\dot{z}_r(t) - \dot{z}_s); \\
 \text{where } F_{rz}(t) &= m \cdot g + \Delta F_{rz}(t);
 \end{aligned}$$

[5.37]

Assume that the road has only one (spatial) frequency, i.e. one wave length. Then the excitation is as in Equation [5.25], in which we assume $x_0 = 0$. Insertion in Equation [5.36] yields:

$$\begin{aligned}
 m \cdot \ddot{z}_s &= c \cdot (\hat{z}_r \cdot \cos(\omega \cdot t) - z_s) + d \cdot (-\omega \cdot \hat{z}_r \cdot \sin(\omega \cdot t) - \dot{z}_s); \\
 m \cdot \ddot{z}_s + d \cdot \dot{z}_s + c \cdot z_s &= \hat{z}_r \cdot (c \cdot \cos(\omega \cdot t) - d \cdot \omega \cdot \sin(\omega \cdot t));
 \end{aligned}$$

[5.38]

From here, the system of differential equations can be solved with trigonometry or Fourier transform.

5.5.2.1.1 Solution with Fourier transform

Fourier transform of Equation [5.37] yields:

$$\begin{aligned}
 m \cdot (-\omega^2 \cdot \mathcal{F}(z_s)) &= c \cdot (\mathcal{F}(z_r) - \mathcal{F}(z_s)) + d \cdot (j \cdot \omega \cdot \mathcal{F}(z_r) - j \cdot \omega \cdot \mathcal{F}(z_s)); \\
 \mathcal{F}(\Delta F_{rz}) &= c \cdot (\mathcal{F}(z_r) - \mathcal{F}(z_s)) + d \cdot (j \cdot \omega \cdot \mathcal{F}(z_r) - j \cdot \omega \cdot \mathcal{F}(z_s));
 \end{aligned}$$

[5.39]

From this, we can then solve the transfer functions:

$$\begin{aligned}
 H_{z_r \rightarrow z_s} &= \frac{\mathcal{F}(z_s)}{\mathcal{F}(z_r)} = \frac{c + j \cdot d \cdot \omega}{(c - m \cdot \omega^2) + j \cdot d \cdot \omega}; \\
 H_{z_r \rightarrow \Delta F_{rz}} &= (c + j \cdot d \cdot \omega) \cdot (1 - H_{z_r \rightarrow z_s});
 \end{aligned}$$

[5.40]

5.5.2.1.2 Solution with trigonometry

One way to solve the mathematical model in Equations [5.36] and [5.38] is to assume a real solution, insert it in Equation [5.38]. Then the parameters be solved for. Assume $x_0 = 0$ in Equation [5.25]:

$$m \cdot \ddot{z}_s + d \cdot \dot{z}_s + c \cdot z_s = \hat{z}_r \cdot (c \cdot \cos(\omega \cdot t) - d \cdot \omega \cdot \sin(\omega \cdot t));$$

[5.41]

Assumed solution:

$$\begin{aligned}
 z_s &= \hat{z}_s \cdot \cos(\omega \cdot t - \varphi); \Rightarrow \\
 &\Rightarrow \{\text{use: } \cos(a - b) = \cos a \cdot \cos b + \sin a \cdot \sin b\} \Rightarrow \\
 &\Rightarrow z_s = \hat{z}_s \cdot [\cos(\omega \cdot t) \cdot \cos \varphi + \sin(\omega \cdot t) \cdot \sin \varphi]; \Rightarrow \\
 &\Rightarrow \dot{z}_s = \hat{z}_s \cdot \omega \cdot [-\sin(\omega \cdot t) \cdot \cos \varphi + \cos(\omega \cdot t) \cdot \sin \varphi]; \Rightarrow \\
 &\Rightarrow \ddot{z}_s = -\hat{z}_s \cdot \omega^2 \cdot [\cos(\omega \cdot t) \cdot \cos \varphi + \sin(\omega \cdot t) \cdot \sin \varphi];
 \end{aligned}$$

[5.42]

Insertion:

$$\begin{aligned}
 & -m \cdot \hat{z}_s \cdot \omega^2 \cdot [\cos(\omega \cdot t) \cdot \cos \varphi + \sin(\omega \cdot t) \cdot \sin \varphi] + \\
 & + d \cdot \hat{z}_s \cdot \omega \cdot [-\sin(\omega \cdot t) \cdot \cos \varphi + \cos(\omega \cdot t) \cdot \sin \varphi] + \\
 & + c \cdot \hat{z}_s \cdot [\cos(\omega \cdot t) \cdot \cos \varphi + \sin(\omega \cdot t) \cdot \sin \varphi] = \\
 & = \hat{z}_r \cdot (c \cdot \cos(\omega \cdot t) - d \cdot \omega \cdot \sin(\omega \cdot t)); \Rightarrow \\
 & \Rightarrow \begin{cases} \text{cos terms: } -m \cdot \hat{z}_s \cdot \omega^2 \cdot \cos \varphi + d \cdot \hat{z}_s \cdot \omega \cdot \sin \varphi + c \cdot \hat{z}_s \cdot \cos \varphi = \hat{z}_r \cdot c; \\ \text{sin terms: } -m \cdot \hat{z}_s \cdot \omega^2 \cdot \sin \varphi - d \cdot \hat{z}_s \cdot \omega \cdot \cos \varphi + c \cdot \hat{z}_s \cdot \sin \varphi = -\hat{z}_r \cdot d \cdot \omega; \end{cases} \\
 & \Rightarrow \begin{cases} \varphi = \arctan\left(\frac{m \cdot d \cdot \omega^3}{c^2 - m \cdot c \cdot \omega^2 + d^2 \cdot \omega^2}\right); \\ \frac{\hat{z}_s}{\hat{z}_r} = \frac{d \cdot \omega}{(m \cdot \omega^2 - c) \cdot \sin \varphi + d \cdot \omega \cdot \cos \varphi} = |H_{z_r \rightarrow z_s}|; \end{cases} \\
 & \text{where } \omega = \frac{2 \cdot \pi \cdot v_x}{\lambda};
 \end{aligned} \tag{5.43}$$

We have identified $|H_{z_r \rightarrow z_s}(v_x)|$, which can be compared to $|H_{z_r \rightarrow z_s}(v_x)|$ in Equation [5.34]. The other transfer functions in Equation [5.34] are more difficult to express using the method with real algebra. We leave them to next section.

5.5.2.1.3 Analysis of solution

We can elaborate further with Equation [5.40]:

Amplitude:

$$\begin{aligned}
 |H_{z_r \rightarrow z_s}| &= \frac{\hat{z}_s}{\hat{z}_r} = \left| \frac{c + j \cdot d \cdot \omega}{(c - m \cdot \omega^2) + j \cdot d \cdot \omega} \right| = \\
 &= \left\{ \begin{array}{l} \text{Assume } \frac{c + j \cdot d \cdot \omega}{(c - m \cdot \omega^2) + j \cdot d \cdot \omega} = \text{Re}H + j \cdot \text{Im}H; \\ \text{Solve for Re}H \text{ and Im}H; \\ |H_{z_r \rightarrow z_s}| = \sqrt{\text{Re}H^2 + \text{Im}H^2}; \end{array} \right\} = \dots = \sqrt{\frac{c^2 + d^2 \cdot \omega^2}{(c - m \cdot \omega^2)^2 + d^2 \cdot \omega^2}};
 \end{aligned} \tag{5.44}$$

Phase:

$$\begin{aligned}
 \varphi_s(\omega) - \varphi_r(\omega) &= \arg\left(\frac{c + j \cdot d \cdot \omega}{-m \cdot \omega^2 + c + j \cdot d \cdot \omega}\right) = \\
 &= \left\{ \begin{array}{l} \text{Assume } \frac{c + j \cdot d \cdot \omega}{(c - m \cdot \omega^2) + j \cdot d \cdot \omega} = \text{Re}H + j \cdot \text{Im}H; \\ \text{Solve for Re}H \text{ and Im}H; \\ \tan(\arg(H_{z_r \rightarrow z_s})) = \text{Im}H/\text{Re}H; \end{array} \right\} = \dots = \\
 &= \arctan\left(\frac{m \cdot d \cdot \omega^3}{c^2 - m \cdot c \cdot \omega^2 + d^2 \cdot \omega^2}\right); \quad \text{where } \omega = \frac{2 \cdot \pi \cdot v_x}{\lambda};
 \end{aligned}$$

Equation [5.13] now allows us to get the magnitudes of the other transfer functions as well:

$$\begin{aligned}
 H_{z_r \rightarrow z_s} &= \text{from Equation [5.40]}; \\
 H_{z_r \rightarrow z_r - z_s} &= H_{z_r \rightarrow z_r} - H_{z_r \rightarrow z_s} = 1 - H_{z_r \rightarrow z_s}; \\
 H_{z_r \rightarrow \ddot{z}_s} &= -\omega^2 \cdot H_{z_r \rightarrow z_s}; \\
 H_{z_r \rightarrow \Delta F_{rz}} &= \{\Delta F_{rz} = c \cdot (z_r - z_s) + d \cdot (\dot{z}_r - \dot{z}_s)\} = \\
 &= c \cdot (H_{z_r \rightarrow z_r} - H_{z_r \rightarrow z_s}) + d \cdot (H_{z_r \rightarrow \dot{z}_r} - H_{z_r \rightarrow \dot{z}_s}) = \\
 &= (c + j \cdot d \cdot \omega) \cdot (H_{z_r \rightarrow z_r} - H_{z_r \rightarrow z_s}) = \\
 &= (c + j \cdot d \cdot \omega) \cdot (1 - H_{z_r \rightarrow z_s});
 \end{aligned} \tag{5.45}$$

The motivation to choose exactly those transfer functions is revealed later, in Section 5.6, 5.7 and 5.8. Some of those magnitudes are easily expressed in real (non-complex) mathematics using Equation [5.44]:

$$|H_{z_r \rightarrow z_s}| = \sqrt{\frac{c^2 + d^2 \cdot \omega^2}{(c - m \cdot \omega^2)^2 + d^2 \cdot \omega^2}};$$

$$|H_{z_r \rightarrow \ddot{z}_s}| = \omega^2 \cdot \sqrt{\frac{c^2 + d^2 \cdot \omega^2}{(c - m \cdot \omega^2)^2 + d^2 \cdot \omega^2}};$$

[5.46]

The transfer functions in Equation [5.44] are plotted in Figure 5-11 and Figure 5-12. Numerical values for m and λ has been chosen.

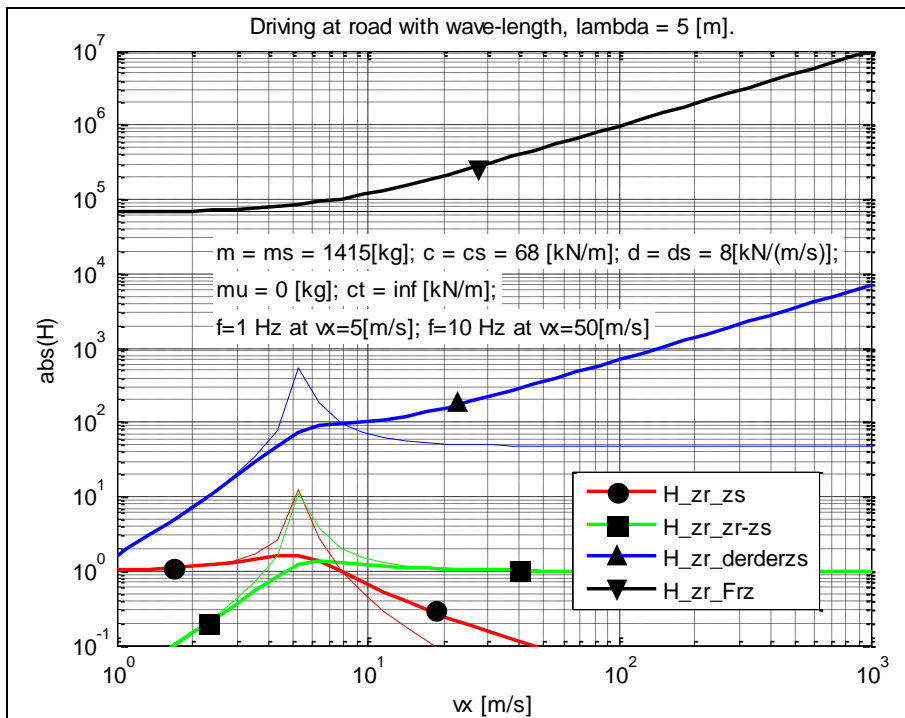


Figure 5-11: Transfer functions for amplitudes from model in Figure 5-10, excited with single frequencies. Thin lines are without damping. Notation: $H_{a \rightarrow b}$ is denoted H_{a_b} .

For example, we can use Figure 5-11 as follows, cf. end of Section 5.5.1.1.1: If we have a certain road, with displacement amplitude of 1 cm ($\hat{z}_r = 0.01 \text{ m}$) and the vehicle should drive on it at a speed of 50 km/h ($v_x \approx 14 \text{ m/s} \hat{=} 2.8 \text{ Hz}$), we can read out, e.g.:

- Ride comfort related: $|H_{z_r \rightarrow \ddot{z}_s}(v_x)| \approx 120$; $\Rightarrow |\hat{a}| = 120 \cdot \hat{z}_r = 120 \cdot 0.01 = 1.20 \text{ m/s}^2$;
From this we can calculate $RMS(\ddot{z}_s) = |1.20|/\sqrt{2} \approx 0.8485 \text{ m/s}^2$.
- Fatigue life related: $|H_{z_r \rightarrow z_r - z_s}(v_x)| \approx 1.11$; $\Rightarrow |\hat{z}_r - \hat{z}_s| = 1.11 \cdot \hat{z}_r = 1.11 \cdot 0.01 = 0.0111 \text{ m} = 1.11 \text{ cm}$;
- Road grip related: $|H_{z_r \rightarrow \Delta F_{rz}}(v_x)| \approx 59795$; $\Rightarrow |\hat{F}_{rz}| = 59795 \cdot \hat{z}_r = 59795 \cdot 0.01 = 598 \text{ N}$;

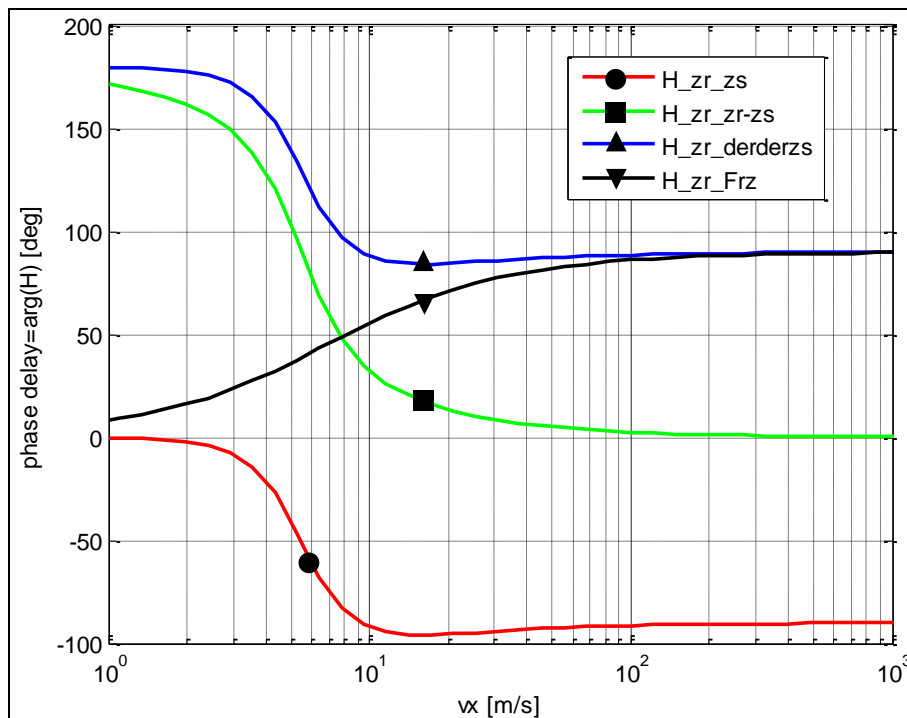


Figure 5-12: Transfer functions for phase delays from model in Figure 5-10, excited with single frequencies.

We compare these numbers with the corresponding numbers for the simpler model, see Sections 5.5.1.1.1. The comfort has been better. The fatigue life and road grip have become more realistic.

Figure 5-11 also shows the curves for the undamped system ($d=0$). The highest peaks appear at approximately $v_x = 5.6$ m/s. This corresponds to the speed where the natural (=undamped) eigen frequency appears ($v_{x,crit} = \lambda \cdot f_{crit} = \lambda \cdot \omega_{crit} / (2 \cdot \pi) = \lambda \cdot \sqrt{c/m} / (2 \cdot \pi) \approx 5.5$ m/s).

Figure 5-12 shows the phase angles for the different responses.

5.5.3 One dimensional model with two degrees of freedom

The expression “two dynamic degree of freedom” in section the heading refers to that both elasticity between road and wheel as well as between wheel and sprung mass is modelled. Alternatively, one can describe the two degrees of freedom as the suspension spring deformation and the tyre spring deformation.

The model can be visualised as in Figure 5-13. No damping is modelled in tyre (in parallel with elasticity c_t) because it is generally relatively low.

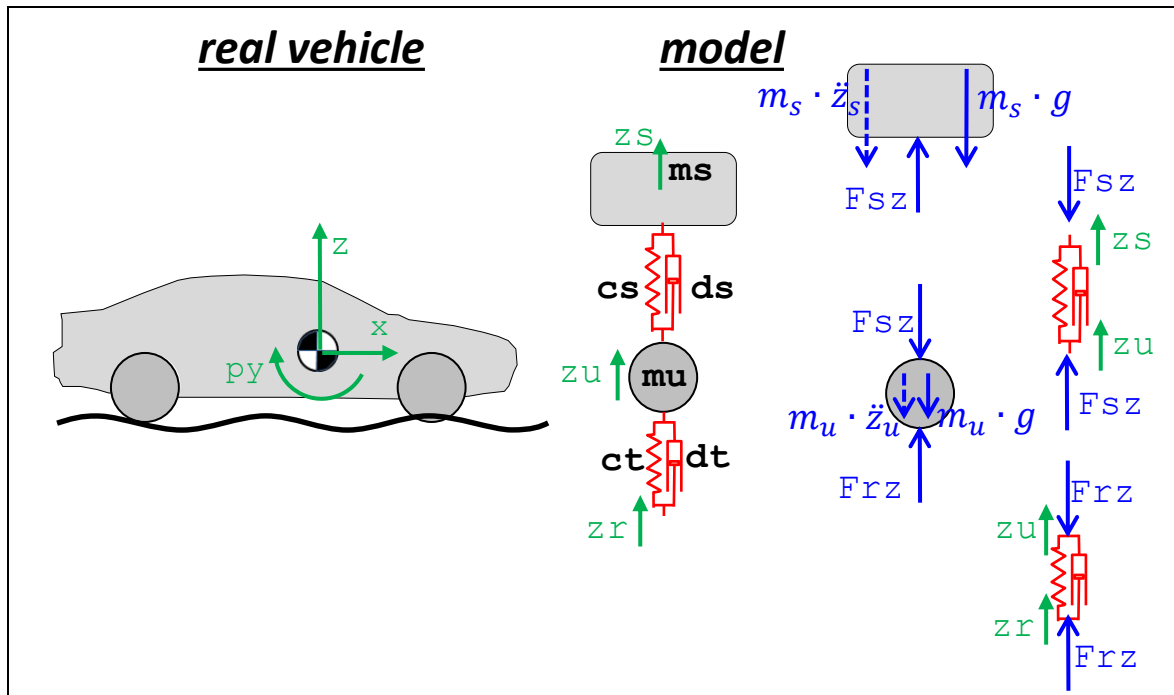


Figure 5-13: One-dimensional model with two dynamic degrees of freedom

The corresponding mathematical model becomes as follows:

Equilibrium:

$$m_s \cdot \ddot{z}_s = F_{sz} - m_s \cdot g;$$

$$m_u \cdot \ddot{z}_u = F_{rz} - F_{sz} - m_u \cdot g;$$

Constitution (displacements counted from static equilibrium):

$$F_{sz} = c_s \cdot (z_u - z_s) + d_s \cdot (\dot{z}_u - \dot{z}_s) + m_s \cdot g;$$

$$F_{rz} = c_t \cdot (z_r - z_u) + d_t \cdot (\dot{z}_r - \dot{z}_u) + (m_s + m_u) \cdot g;$$

Excitation:

$$z_r = z_r(t);$$

[5.47]

The same can be formulated with matrices and Fourier transforms:

$$\begin{bmatrix} m_s & 0 \\ 0 & m_u \end{bmatrix} \cdot \begin{bmatrix} \ddot{z}_s \\ \ddot{z}_u \end{bmatrix} + \begin{bmatrix} d_s & -d_s \\ -d_s & d_s + d_t \end{bmatrix} \cdot \begin{bmatrix} \dot{z}_s \\ \dot{z}_u \end{bmatrix} + \begin{bmatrix} c_s & -c_s \\ -c_s & c_s + c_t \end{bmatrix} \cdot \begin{bmatrix} z_s \\ z_u \end{bmatrix} \\ = \begin{bmatrix} 0 \\ d_t \end{bmatrix} \cdot \dot{z}_r + \begin{bmatrix} 0 \\ c_t \end{bmatrix} \cdot z_r;$$

$$\Rightarrow \mathbf{M} \cdot \begin{bmatrix} \ddot{z}_s \\ \ddot{z}_u \end{bmatrix} + \mathbf{D} \cdot \begin{bmatrix} \dot{z}_s \\ \dot{z}_u \end{bmatrix} + \mathbf{C} \cdot \begin{bmatrix} z_s \\ z_u \end{bmatrix} = \mathbf{D}_r \cdot \dot{z}_r + \mathbf{C}_r \cdot z_r; \Rightarrow$$

$$\Rightarrow \mathbf{M} \cdot (-\omega^2 \cdot Z) + \mathbf{D} \cdot (j \cdot \omega \cdot Z) + \mathbf{C} \cdot Z = \mathbf{D}_r \cdot (j \cdot \omega \cdot Z_r) + \mathbf{C}_r \cdot Z_r; \Rightarrow$$

$$\Rightarrow (-\omega^2 \cdot \mathbf{M} + j \cdot \omega \cdot \mathbf{D} + \mathbf{C}) \cdot Z = (j \cdot \omega \cdot \mathbf{D}_r + \mathbf{C}_r) \cdot Z_r;$$

$$\text{where } Z = \begin{bmatrix} Z_s \\ Z_u \end{bmatrix} = \begin{bmatrix} \mathcal{F}(z_s) \\ \mathcal{F}(z_u) \end{bmatrix}; \text{ and } Z = \mathcal{F}(z_r);$$

[5.48]

The matrix \mathbf{D}_r is zero, but marks a more general form, typical for modelling damping also in the tyre.

5.5.3.1 Response to a single frequency excitation

5.5.3.1.1 Solution with Fourier transform

We can find the transfer functions via Fourier transform, starting from Equation [4.64]:

$$\begin{bmatrix} H_{z_r \rightarrow z_s} \\ H_{z_r \rightarrow z_u} \end{bmatrix} = \begin{bmatrix} Z_s \\ Z_u \end{bmatrix} \cdot \frac{1}{Z_r} = Z \cdot \frac{1}{Z_r} = (-\omega^2 \cdot \mathbf{M} + j \cdot \omega \cdot \mathbf{D} + \mathbf{C})^{-1} \cdot (j \cdot \omega \cdot \mathbf{D}_r + \mathbf{C}_r); \quad [5.49]$$

This format is very compact, since it includes both transfer functions for amplitude and phase. For numerical analyses, the expression in Equation [5.52] is explicit enough, since there are tools, e.g. Matlab, which supports matrix inversion and complex mathematics.

For analytic solution one would need symbolic tools, e.g. Mathematica or Matlab with symbolic toolbox, or careful manual algebraic operations. With $d_t = 0$, the explicit forms becomes as follows:

$$\begin{aligned} H_{z_r \rightarrow z_s} &= \frac{Z_s}{Z_r} \\ &= \frac{(-m_u \cdot \omega^2 + j \cdot d_s \cdot \omega + c_t + c_s) \cdot c_t}{-m_u \cdot \omega^2 + j \cdot d_s \cdot \omega + c_t + c_s - \frac{(c_s + j \cdot d_s \cdot \omega)^2}{-m_s \cdot \omega^2 + j \cdot d_s \cdot \omega + c_s}} - c_t \\ &= \frac{c_t}{c_s + j \cdot d_s \cdot \omega}; \\ H_{z_r \rightarrow z_u} &= \frac{c_t}{-m_u \cdot \omega^2 + j \cdot d_s \cdot \omega + c_t + c_s - \frac{(c_s + j \cdot d_s \cdot \omega)^2}{-m_s \cdot \omega^2 + j \cdot d_s \cdot \omega + c_s}} \\ \text{where } \omega &= \frac{2 \cdot \pi \cdot v_x}{\lambda}; \end{aligned} \quad [5.50]$$

5.5.3.1.2 Analysis of solution

Equation [5.13] now allows us to get the magnitudes of the other transfer functions as well:

$$\begin{aligned} H_{z_r \rightarrow z_s} &= \text{see Equation [5.50]}; \\ H_{z_r \rightarrow z_u} &= \text{see Equation [5.50]}; \\ H_{z_r \rightarrow z_r - z_u} &= H_{z_r \rightarrow z_r} - H_{z_r \rightarrow z_u} = 1 - H_{z_r \rightarrow z_u}; \\ H_{z_r \rightarrow z_u - z_s} &= H_{z_r \rightarrow z_u} - H_{z_r \rightarrow z_s}; \\ H_{z_r \rightarrow \ddot{z}_s} &= -\omega^2 \cdot H_{z_r \rightarrow z_s}; \\ H_{z_r \rightarrow \Delta F_{sz}} &= \{\Delta F_{sz} = c_s \cdot (z_u - z_s) + d_s \cdot (\dot{z}_u - \dot{z}_s)\} = \\ &= c_s \cdot (H_{z_r \rightarrow z_u} - H_{z_r \rightarrow z_s}) + d_s \cdot j \cdot \omega \cdot (H_{z_r \rightarrow z_u} - H_{z_r \rightarrow z_s}) = \\ &= (c_s + j \cdot d_s \cdot \omega) \cdot (H_{z_r \rightarrow z_u} - H_{z_r \rightarrow z_s}); \\ H_{z_r \rightarrow \Delta F_{rz}} &= \{\Delta F_{rz} = c_t \cdot (z_r - z_u)\} = c_t \cdot (H_{z_r \rightarrow z_r} - H_{z_r \rightarrow z_u}) = c_t \cdot (1 - H_{z_r \rightarrow z_u}); \end{aligned} \quad [5.51]$$

Expression in real can be derived, see Equation [5.52]. Note that it is more general than Equation [5.51], having a tyre damper modelled, $d_t \neq 0$. The derivation is not documented in present compendium.

$$\begin{aligned}
 |H_{z_r \rightarrow \ddot{z}_s}| &= \omega^2 \cdot \frac{\sqrt{(c_s \cdot c_t - d_s \cdot d_t \cdot \omega^2)^2 + (\omega \cdot (d_s \cdot c_t + d_t \cdot c_s))^2}}{\sqrt{A^2 + B^2}}; \\
 |H_{z_r \rightarrow z_u - z_s}| &= \frac{m_s \cdot \sqrt{(c_t \cdot \omega^2)^2 + (d_t \cdot \omega^3)^2}}{\sqrt{A^2 + B^2}}; \\
 |H_{z_r \rightarrow z_r - z_u}| &= \frac{\sqrt{(-m_s \cdot m_u \cdot \omega^4 + \omega^2 \cdot (m_s + m_u) \cdot c_s)^2 + (\omega^3 \cdot (m_s + m_u) \cdot d_s)^2}}{\sqrt{A^2 + B^2}}; \\
 A &= \omega^4 \cdot m_s \cdot m_u - \omega^2 \cdot (m_s \cdot c_t + m_s \cdot c_s + d_s \cdot d_t + c_s \cdot m_u) + c_s \cdot c_t; \\
 B &= \omega^3 \cdot (m_s \cdot d_t + m_s \cdot d_s + m_u \cdot d_s) - \omega \cdot (d_s \cdot c_t + d_t \cdot c_s);
 \end{aligned}$$

[5.52]

The transfer functions in Equation [5.51] are plotted in Figure 5-14. If we have a certain road, with displacement amplitude of 1 cm ($\hat{z}_r = 0.01 \text{ m}$) and the vehicle should drive on it at a speed of 50 km/h ($v_x \approx 14 \frac{\text{m}}{\text{s}} \hat{=} \approx 2.8 \text{ Hz}$), we can read out, e.g.:

- Ride comfort related: $|H_{z_r \rightarrow \ddot{z}_s}(v_x)| \approx 123$; $\Rightarrow |\hat{a}| = 123 \cdot \hat{z}_r = 123 \cdot 0.01 = 1.23 \text{ m/s}^2$; From this we can calculate $RMS(\ddot{z}_s) = |1.23|/\sqrt{2} \approx 0.8697 \text{ m/s}^2$.
- Fatigue life related: $|H_{z_r \rightarrow z_u - z_s}(v_x)| \approx 1.14$; $\Rightarrow |\hat{z}_u - \hat{z}_s| = 1.14 \cdot \hat{z}_r = 1.14 \cdot 0.01 = 0.0114 \text{ m} = 1.14 \text{ cm}$;
- Road grip related: $|H_{z_r \rightarrow \Delta F_{rz}}(v_x)| \approx 177470$; $\Rightarrow |\hat{F}_{rz}| = 177470 \cdot \hat{z}_r = 177470 \cdot 0.01 = 1775 \text{ N}$;

This analysis can be compared with the analysis in Section 5.5.2.1.3. Ride comfort and fatigue does not change a lot, but road grip does. This indicates that the more advanced model is only needed for road grip evaluation.

Figure 5-15 shows the phase angles for the different responses.

Figure 5-16, shows the amplitude gains for the corresponding un-damped system. We identify natural frequencies at around 5 m/s and 50 m/s. These two speeds correspond to frequencies $v_{x,crit}/\lambda$, i.e. approximately 1 Hz and 10 Hz. The lower frequency is an oscillation mode where the both masses move in phase with each other, the so called “bounce mode”. The higher frequency comes from the mode where the masses are in counter-phase to each other, the so called “wheel hop mode”. In the wheel hop mode, the sprung mass is almost not moving at all. We will come back to these modes in Section 5.5.3.2.

VERTICAL DYNAMICS

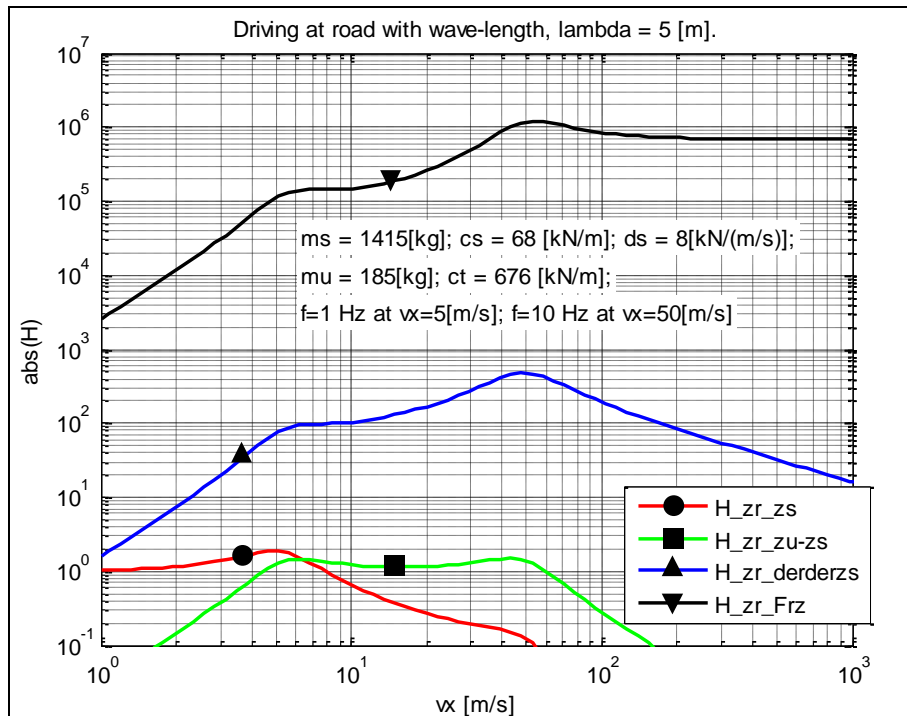


Figure 5-14: Transfer functions for amplitudes from model in Figure 5-13, excited with single frequencies. Notation: $H_{a \rightarrow b}$ is denoted H_a_b .

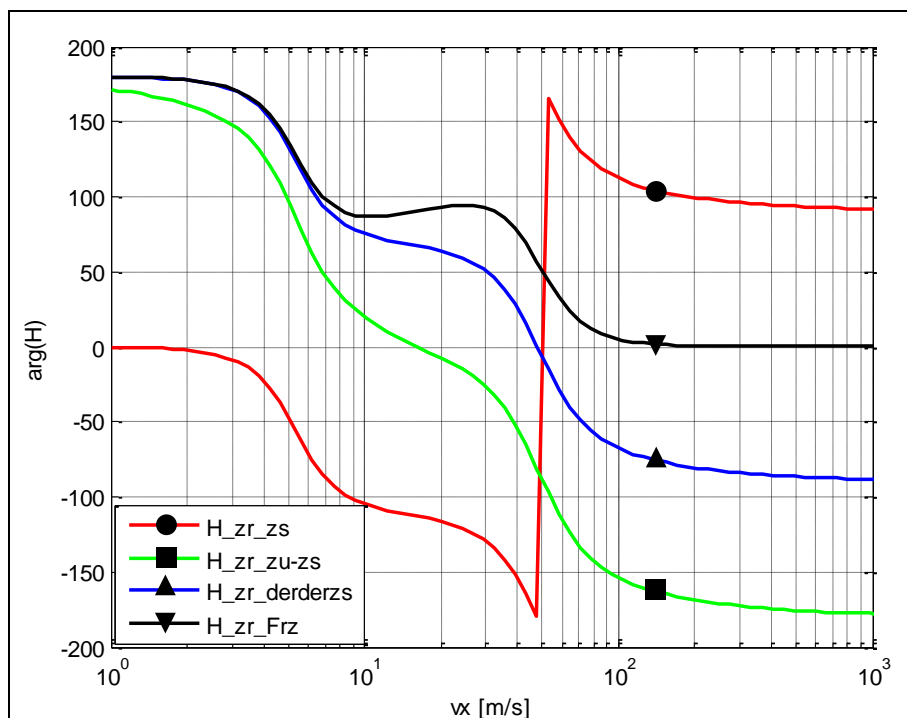


Figure 5-15: Transfer functions for phase delays. Same model and data as in Figure 5-14.

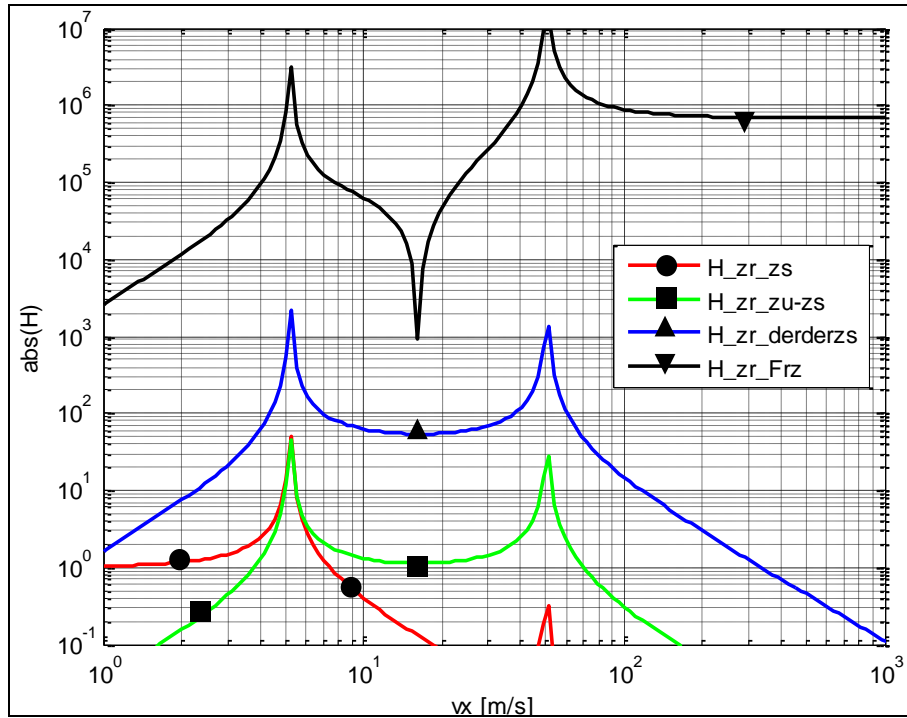


Figure 5-16: Un-damped transfer functions for amplitudes. Same model and data as in Figure 5-14, except $c_s = 0$.

5.5.3.2 Simplified model

A more practical way to approach the system is to consider the properties of the system. The sprung mass is typically an order of magnitude greater than the unsprung mass and the suspension spring is usually an order of magnitude lower than the tyre stiffness. Then, one can split the model in to models, which explains one mode each, see Figure 5-17. The modes were identified already in Section 5.5.3.1.1.

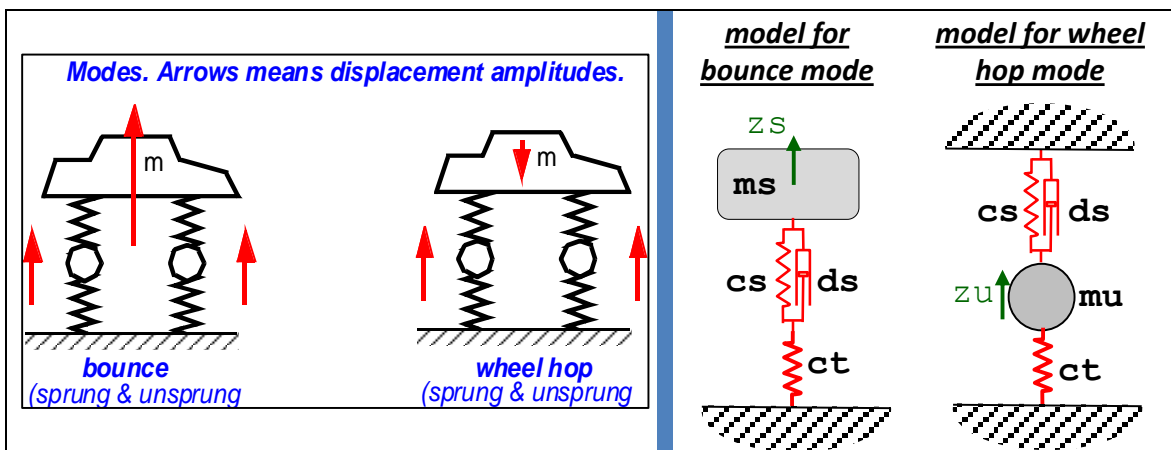


Figure 5-17: Modes and approximate models.

We will now derive the natural frequencies for the two models, and compared with the natural frequencies ($ds=0$) found for the combined model, in Figure 5-16. Both models are one degree of freedom models with mass and spring, why the Eigen frequency is $\sqrt{\text{stiffness}/\text{mass}}$.

For the bounce model, the mass is m_s . Stiffnesses c_s and c_t are series connected, which means that the total stiffness= $1/(1/c_s+1/c_t)$.

For the wheel hop model, the mass is m_u . Stiffnesses c_s and c_t are parallel connected, which means that the total stiffness= c_s+c_t .

$$\omega_{Bounce} = \sqrt{\frac{1/\left(\frac{1}{c_s} + \frac{1}{c_t}\right)}{m_s}} = 15.3 \frac{rad}{s};$$

$$\omega_{WheelHop} = \sqrt{\frac{c_s + c_t}{m_u}} = 86.0 \frac{rad}{s};$$

[5.53]

We see that the numbers match well with the more advanced model, which gave 15.2 rad/s and 86.7 rad/s, respectively.

Bounce refers to the mode where the sprung mass has the greatest amplitude and wheel hop is related to the case when the unsprung mass exhibits the greatest amplitude. For a passenger car, the spring mass has the lowest frequency, typically around 1 Hz while tyre hop is more prevalent at frequencies around 10 Hz.

5.6 Ride comfort *

Function definition: (Stationary) Ride comfort is the comfort that vehicle occupants experience from stationary oscillations when the vehicle travels over a road with certain vertical irregularity in a certain speed. The measure is defined at least including driver (or driver seat) vertical acceleration amplitudes.

Ride comfort is sometimes divided into:

- **Primary Ride** – the vehicle body on its suspension. Bounce(Heave), Pitch and Roll ≈ 0.4 Hz
- **Secondary Ride** – same but above body natural frequencies, i.e. $\approx 4..25$ Hz

5.6.1 Single frequency

It is generally accepted for stationary vibrations, that humans are sensitive to the RMS value of the acceleration. However, the sensitivity is frequency dependent, so that highest discomfort appears for a certain range of frequencies. Some human tolerance curves are shown in Figure 5-18 and Figure 5-19.

The curves can be considered a threshold for acceptance where everything above the line is unacceptable and points below the curve are acceptable. Discomfort is a subjective measure, and this is why the different diagrams cannot be directly compared to each other. The SAE has suggested that frequencies from 4 to 8 Hz are the most sensitive and the accepted accelerations for these are no higher than 0.025 g (RMS).

The curves in Figure 5-18 mostly represent an extended exposure to the vibration. As one can expect, a human can endure exposure to more severe conditions for short periods of time. The SAE limits presented are indicative of 8 hours of continuous exposure. Curves for different exposure times can also be obtained from ISO, (ISO2631). The ISO curves are from the first version of ISO 2631 and were later modified, see Figure 5-19.

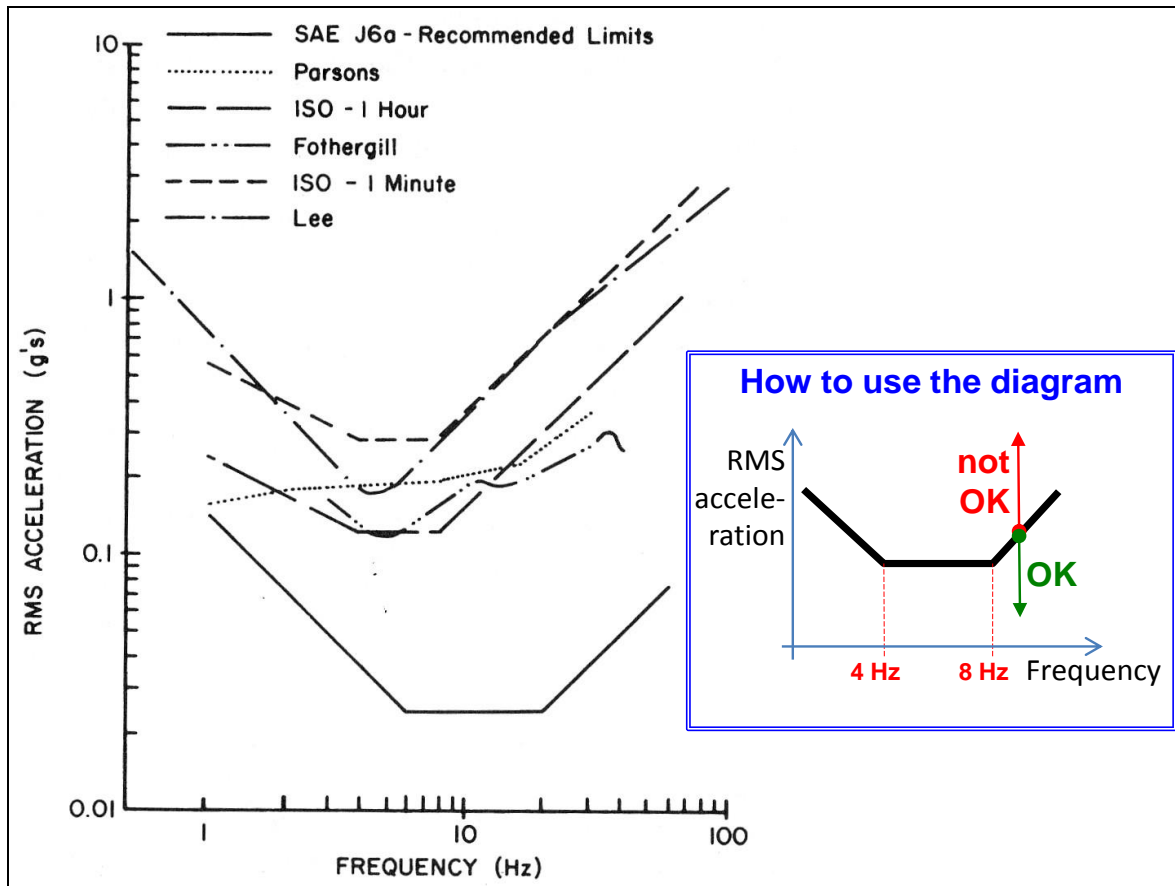


Figure 5-18: Various Human Sensitivity Curves to Vertical Vibration, (Gillespie, 1992)

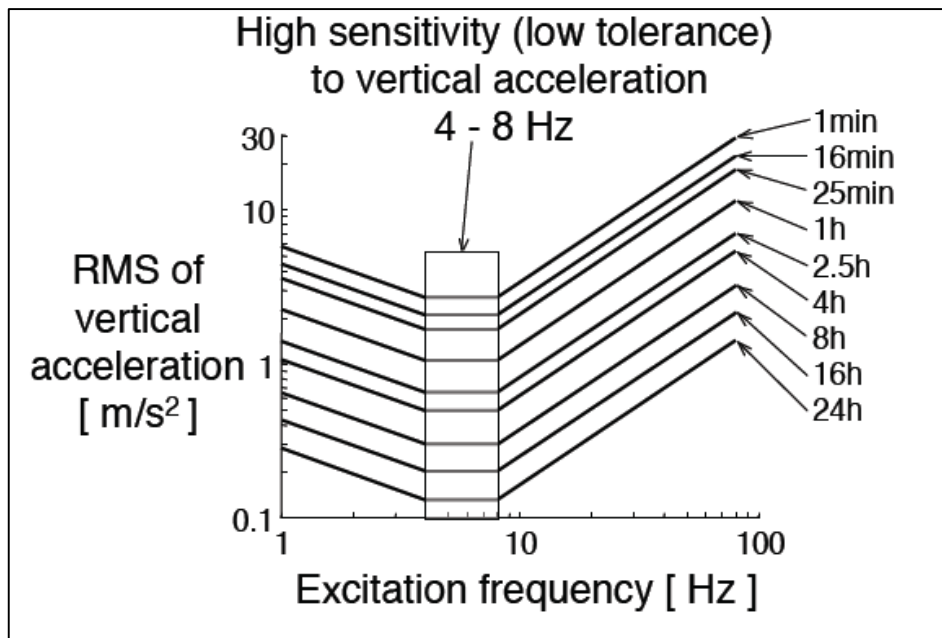


Figure 5-19: ISO 2631 Tolerance Curves

5.6.2 Multiple frequencies

The curves in Figure 5-18 and Figure 5-19 can be interpreted as a filter, where the response of the human is influenced by the frequencies they are exposed to. This leads to the concept of a Human

Filter Function $W_k(f)$. (W_k refers to vertical whole human body vibration sensitivity, while there are other for sensitivities for other directions and human parts.) This approach uses the concept of a transfer function from driver seat to somewhere inside the drivers brain, where discomfort is perceived.

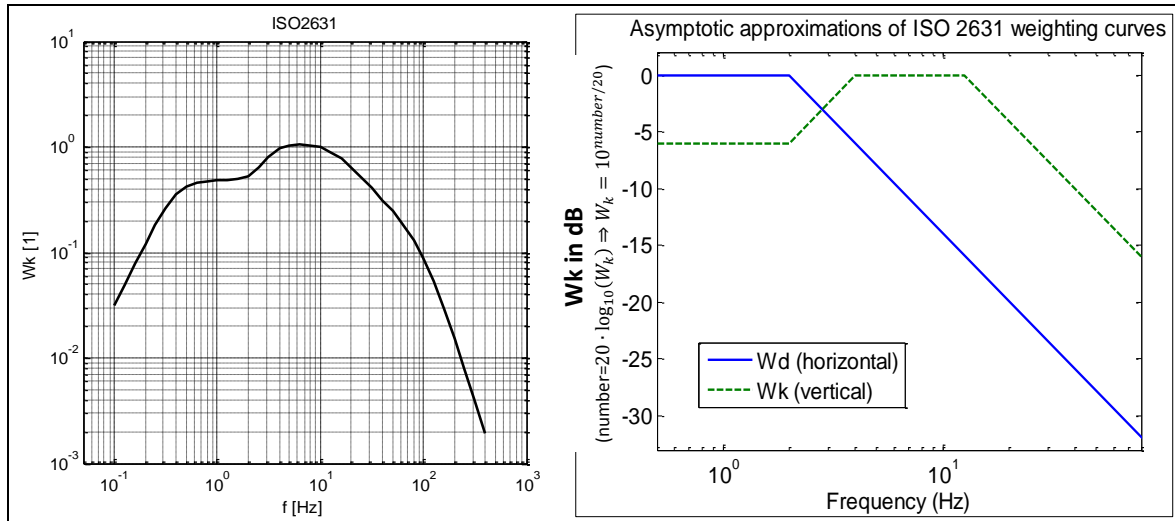


Figure 5-20: Human Filter Function. From (ISO2631). Right: Asymptotic approximation

Frequency f Hz	W_k	
	factor $\times 1\ 000$	dB
0,02		
0,025		
0,031 5		
0,04		
0,05		
0,063		
0,08		
0,1	31,2	- 30,11
0,125	48,6	- 26,26
0,16	79,0	- 22,05
0,2	121	- 18,33
0,25	182	- 14,81
0,315	263	- 11,60
0,4	352	- 9,07
0,5	418	- 7,57
0,63	459	- 6,77
0,8	477	- 6,43
1	482	- 6,33
1,25	484	- 6,29
1,6	494	- 6,12
1,6	494	- 6,12
2	531	- 5,49
2,5	631	- 4,01
3,15	804	- 1,90
4	967	- 0,29
5	1 039	0,33
6,3	1 054	0,46
8	1 036	0,31
10	988	- 0,10
12,5	902	- 0,89
16	768	- 2,28
20	636	- 3,93
25	513	- 5,80
31,5	405	- 7,86
40	314	- 10,05
50	246	- 12,19
63	186	- 14,61
80	132	- 17,56
100	88,7	- 21,04
125	54,0	- 25,35
160	28,5	- 30,91
200	15,2	- 36,38
250	7,90	- 42,04
315	3,98	- 48,00
400	1,95	- 54,20

Figure 5-21: Human Filter Function for vertical vibrations. Table from (ISO2631).

With formulas from earlier in this chapter we can calculate an RMS value of a signal with multiple frequencies, see Equation [5.6]. Consequently, we can calculate RMS of multiple frequency acceleration. Since humans are sensitive to acceleration, it would give one measure of human discomfort. However, to get a measure which is useful for comparing accelerations with different frequency content, the measure have to take the human filter function into account. The Weighted RMS Acceleration, a_w , in the following formula is such measure:

$$a_w = a_w(\ddot{z}(t)) = \left\{ \text{use: } RMS(\ddot{z}(t)) = \sqrt{\sum_{i=1}^N \frac{\hat{z}_i^2}{2}} \right\} = \sqrt{\sum_{i=1}^N \frac{(W_k(\omega_i) \cdot \hat{z}_i)^2}{2}};$$

or

$$a_w = a_w(\ddot{z}(t)) = \left\{ \text{use: } RMS(\ddot{z}(t)) = \sqrt{\int_{\omega=0}^{\infty} G_{\ddot{z}}(\omega) \cdot d\omega} \right\} =$$

$$= \sqrt{\int_{\omega=0}^{\infty} (W_k(\omega))^2 \cdot G_{\ddot{z}}(\omega) \cdot d\omega};$$

[5.54]

Equation [5.54] is written for a case with only vertical vibrations, hence W_k and $G_{\ddot{z}}$. If vibrations in several directions, a total a_w can still be calculated, see (ISO2631).

In (ISO2631) one can also find the following equation, which weights together several time periods, with different vibrations spectra. The a_w is the time averaged whole-body vibration exposure value.

$$a_w = \sqrt{\frac{\sum_i a_{wi}^2 \cdot T_i}{\sum_i T_i}};$$

[5.55]

The a_w in Eq [5.55] is used both for vehicle customer requirement setting at OEMs and governmental legislation. One example of legislation is (DIRECTIVE 2002/44/EC, 2002). This directive stipulates that a_w in Eq [5.55] in any direction, normalized to 8 hours, may not exceed 1.15 m/s², and if the value exceeds 0.5 m/s² action must be taken.

5.6.2.1 Certain combination of road, vehicle and speed

Now we can use Equation [5.35] without assuming road type. However, we have to identify \hat{z}_s and multiply it with $W_k(\omega)$, according to Equation [5.54]. Then we get [5.56].

Using Equation [5.56], we can calculate the weighted RMS value for the different models in Sections 5.5.1, 5.5.2 and 5.5.3. For each model, it will vary with speed, v_x . A plot, assuming a certain road type ("Rough" from Figure 5-6) is shown in Figure 5-28. We can see that the simplest model "*stiff tyre, no unsprung mass*" gives much different comfort value than the two other, so the simplest is not good to estimate comfort. However, the two other models give approximately same result, which indicates that the medium model, "*stiff tyre, no unsprung mass*", is enough for comfort evaluation. This is no general truth but an indication that the most advanced model, "*two masses, elastic tyre*", is not needed for comfort on normal roads. The advanced model is more needed for road grip.

We can also see that the comfort decreases, the faster the vehicle drives. If we read out at which speed we reach $a_w = 1 \text{ m/s}^2$ (which is a reasonable value for long time exposure) we get around $v_x \approx 70 \text{ m/s} \approx 250 \text{ km/h}$ on this road type ("Rough") with the medium (and advanced) model. With the simplest model we get $v_x \approx 1 \text{ m/s} \approx 3.4 \text{ km/h}$.

$$\begin{aligned}
 RMS(\ddot{z}_s) &= \sqrt{\frac{\Phi_0}{\Omega_0^{-w}} \cdot v_x^{w-1} \cdot \int_{\omega=0}^{\infty} |H_{z_r \rightarrow \ddot{z}_s}(\omega)|^2 \cdot \omega^{-w} \cdot d\omega = \left\{ \begin{array}{l} \text{use: } H_{z_r \rightarrow \ddot{z}_s} = \\ = -\omega^2 \cdot H_{z_r \rightarrow z_s} \end{array} \right\}} \\
 &= \sqrt{\frac{\Phi_0}{\Omega_0^{-w}} \cdot v_x^{w-1} \cdot \int_{\omega=0}^{\infty} |\omega^2 \cdot H_{z_r \rightarrow z_s}(\omega)|^2 \cdot \omega^{-w} \cdot d\omega =} \\
 &= \sqrt{\frac{\Phi_0}{\Omega_0^{-w}} \cdot v_x^{w-1} \cdot \int_{\omega=0}^{\infty} |H_{z_r \rightarrow z_s}(\omega)|^2 \cdot \omega^{4-w} \cdot d\omega; \Rightarrow \left\{ \begin{array}{l} \text{use:} \\ \text{Equation} \\ [5.54] \end{array} \right\} \Rightarrow} \\
 \Rightarrow a_w &= \sqrt{\frac{\Phi_0}{\Omega_0^{-w}} \cdot v_x^{w-1} \cdot \int_{\omega=0}^{\infty} (W_k(\omega))^2 \cdot |H_{z_r \rightarrow z_s}(\omega)|^2 \cdot \omega^{4-w} \cdot d\omega =} \\
 &= \sqrt{\frac{\Phi_0}{\Omega_0^{-w}} \cdot v_x^{w-1} \cdot \int_{\omega=0}^{\infty} (W_k(\omega))^2 \cdot |H_{z_r \rightarrow z_s}(\omega)|^2 \cdot \omega^{4-w} \cdot d\omega;
 \end{aligned}$$

[5.56]

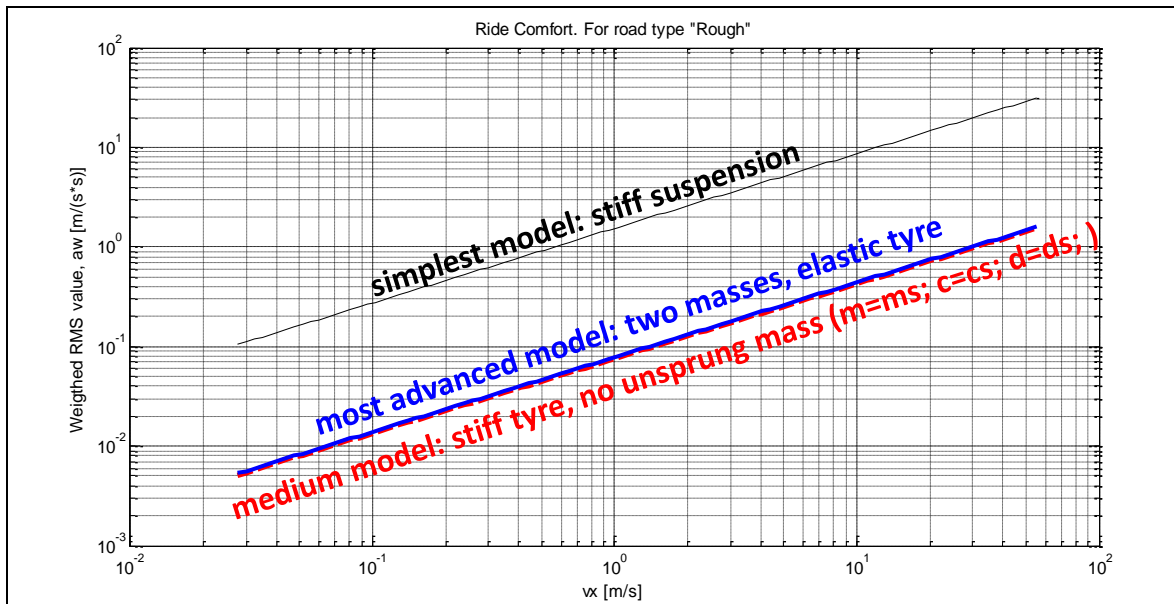


Figure 5-22: Weighted RMS values for road type “Smooth” from Figure 5-6. The 3 curves show 3 different models: Simplest (from Sections 1.5.1), Medium (from Section 1.5.2) and Most advanced (from Section 1.5.3).

5.7 Fatigue life *

Function definition: (Vehicle) Fatigue life is the life that the vehicle, mainly suspension, can reach due to stationary oscillations when vehicle travels over a road with certain vertical irregularity in a certain speed. The measure is defined at least including suspension vertical deformation amplitudes.

Beside human comfort, the fatigue of the vehicle structure itself is one issue to consider in vertical vehicle dynamics.

5.7.1 Single frequency

5.7.1.1 Loads on suspension spring

In particular, the suspension spring may be subject to fatigue. The variation in spring material stress is dimensioning, which is why the force variation or amplitude in the springs should be under observation. Since spring force is proportional to deformation, the suspension deformation amplitude is proposed as a good measure. This is the explanation to why the amplitude of $z_u - z_s$ is plotted in Figure 5-11.

Beside fatigue loads, $z_u - z_s$ is also relevant for judging whether suspension bump-stops become engaged or not. At normal driving, that limit should be far from reached, except possibly at maximum loads (many persons and much luggage).

5.7.1.2 Fatigue of other components

Fatigue of other parts may require other amplitudes.

One other relevant example can be the damper fatigue. Damper fatigue would be more relevant to judge from amplitude of $\dot{z}_u - \dot{z}_s$, which determines the force level and hence the stress level.

Another example is the load of the road itself. For heavy trucks it is important to consider how much they wear the road. At some roads with legislated maximum (static) axle load, one can be allowed to exceed that limit if the vehicle has especially road friendly suspensions. For these judgements, it is the contact force between tyre and road, \hat{F}_{rz} , which is the most relevant variable to study.

5.7.2 Multiple frequencies

If the excitation is of one single frequency, the stress amplitude can be used when comparing two designs. However, for spectra of multiple frequencies, one cannot look at amplitudes solely, $[\hat{z}_1, \hat{z}_2, \dots, \hat{z}_N]$, because the amplitudes will depend on how the discretization is done, i.e. the number N . Some kind of integral of a spectral density is more reasonable. In this compendium it is proposed that a very approximate measure of fatigue load is calculated as follows, exemplified for the case of fatigue of the spring:

$$\begin{aligned}
 \text{Measure for spring fatigue life} &= \text{RMS}(z_u(t) - z_s(t)) = \\
 &= \sqrt{\frac{\Phi_0}{\Omega_0^{-w}} \cdot v_x^{w-1} \cdot \int_{\omega=0}^{\infty} |H_{z_r \rightarrow z_u - z_s}(\omega)|^2 \cdot \omega^{-w} \cdot d\omega} = \left\{ \begin{array}{l} \text{use: } H_{z_r \rightarrow z_u - z_s} = \\ = H_{z_r \rightarrow z_u} - H_{z_r \rightarrow z_s} \end{array} \right\} = \\
 &= \sqrt{\frac{\Phi_0}{\Omega_0^{-w}} \cdot v_x^{w-1} \cdot \int_{\omega=0}^{\infty} |H_{z_r \rightarrow z_u}(\omega) - H_{z_r \rightarrow z_s}(\omega)|^2 \cdot \omega^{-w} \cdot d\omega};
 \end{aligned}
 \tag{5.57}$$

Equation is written for application to a known road spectra (Φ_0, w) and vehicle dynamic structure ($H_{z_r \rightarrow z_u}, H_{z_r \rightarrow z_s}$), but the first expression ($\text{RMS}(z_u(t) - z_s(t))$) is applicable on a measured or simulated time domain solution.

Road grip *

*Function definition: **Road grip (on undulated roads)** is how well the longitudinal and lateral grip between tyres and road is retained due to stationary oscillations when the vehicle travels over a road with certain vertical irregularity in a certain speed.*

Sections 3.3 and 3.4 show the brush model explain how the tyre forces in the ground plane appears. It is a physical model where the contact length influences how stiff the tyre is for longitudinal and lateral slip. There is also a brief description of relaxation models for tyres. This together motivates that a tyre have more difficult to build up forces in ground plane if the vertical force varies. We can understand it as when contact length varies, the shear stress build up has to start all over again. As an average effect, the tyre will lose more and more grip, the more the vertical force varies.

5.8.1 Multiple frequencies

If the excitation is of one single frequency, the stress amplitude can be used when comparing two designs. However, for spectra of multiple frequencies, one cannot look at amplitudes solely, $[\hat{z}_1, \hat{z}_2, \dots, \hat{z}_N]$, because the amplitudes will depend on how the discretization is done, i.e. the number N. Some kind of integral of a spectral density is more reasonable. In this compendium it is proposed that a very approximate measure of road grip is calculated as follows:

$$\begin{aligned}
 \text{Measure for (bad)road grip} &= \text{RMS}(\Delta F_{rz}(t)) = \\
 &= \sqrt{\frac{\Phi_0}{\Omega_0^{-w}} \cdot v_x^{w-1} \cdot \int_{\omega=0}^{\infty} |H_{z_r \rightarrow \Delta F_{rz}}(\omega)|^2 \cdot \omega^{-w} \cdot d\omega} = \\
 &= \left\{ \text{use: } H_{z_r \rightarrow z_u - z_s} = c_t \cdot (1 - H_{z_r \rightarrow z_u}) \right\} = \\
 &= \sqrt{\frac{\Phi_0}{\Omega_0^{-w}} \cdot v_x^{w-1} \cdot \int_{\omega=0}^{\infty} |c_t \cdot (1 - H_{z_r \rightarrow z_u})|^2 \cdot \omega^{-w} \cdot d\omega};
 \end{aligned}
 \tag{5.58}$$

Equation is written for application to a known road spectra (Φ_0, w) and vehicle dynamic structure ($H_{z_r \rightarrow z_u}$), but the first expression ($\text{RMS}(\Delta F_{rz}(t))$) is applicable on a measured or simulated time domain solution.

5.9 Variation of stiffness and damping

The influence of design parameters on vehicle functions Ride comfort, Suspension fatigue and Road grip can now be made. E.g., it is important to not only use the transfer function, but also take the road and human sensitivity into account, which calls for different weighting for different frequencies.

Transfer function for the model in Section 5.5.3 is shown as dashed lines in Figure 5-23. Same figure also shows the Road- and Human-weighted versions. Studying how these curves change with design parameters gives a quantitative understanding of how different suspension design parameters influence. Such variations will be done in Sections 5.9.1 to 5.9.4.

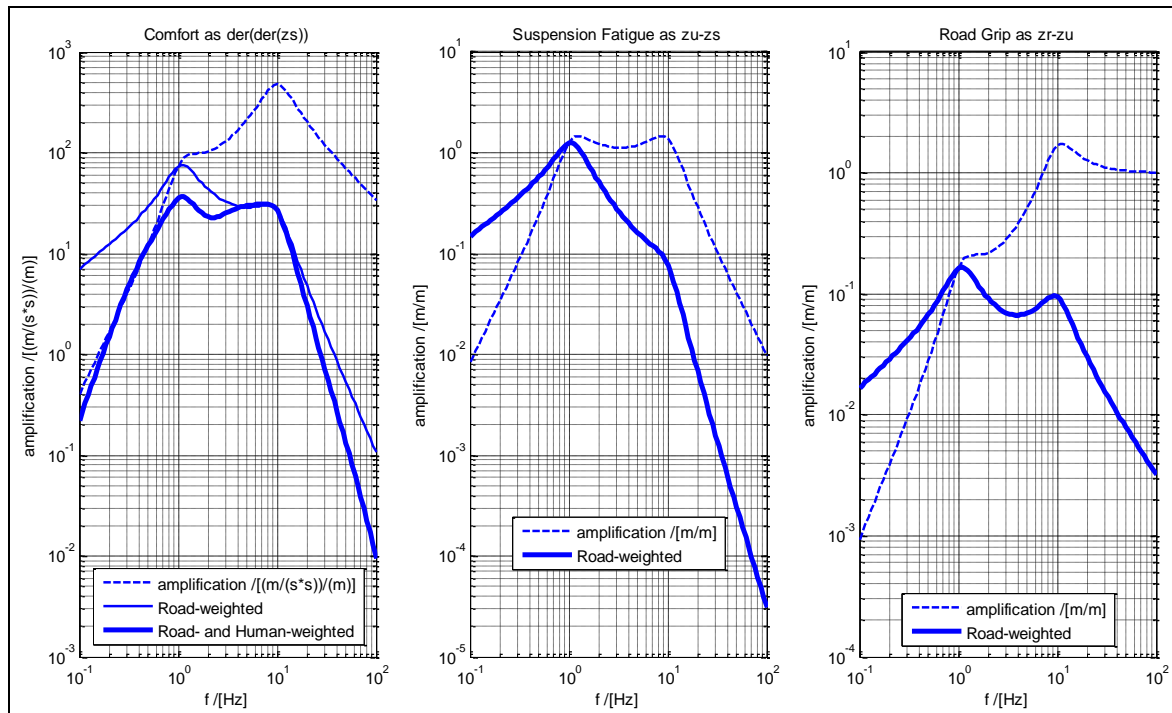


Figure 5-23: For a passenger car with $m_s = 1600$ [kg], $m_u = 200$ [kg], $c_s = 76$ [kN/m], $d_s = 9$ [kN/(m/s)], $c_t = 764$ [kN/m], $d_t = 0$. Left is vertical acceleration (amplitude) of sprung mass for Ride Comfort. Middle is relative displacement (amplitude) between sprung and unsprung mass for Suspension Fatigue. Right is deformation (amplitude) of tyre spring for Road Grip. Weightings for typical road and for human sensitivity is shown.

There are two particular frequency intervals of the graphs to observe. These are the 2 peaks around the two the natural frequencies of the sprung and unsprung masses, the peak at lower frequency is mainly a resonance in bounce mode, while the higher one is in wheel hop mode.

5.9.1 Varying suspension stiffness

In Figure 5-24 the benefits of the low suspension stiffness (1 Hz) is seen for suspension travel and comfort without much change in the road grip performance.

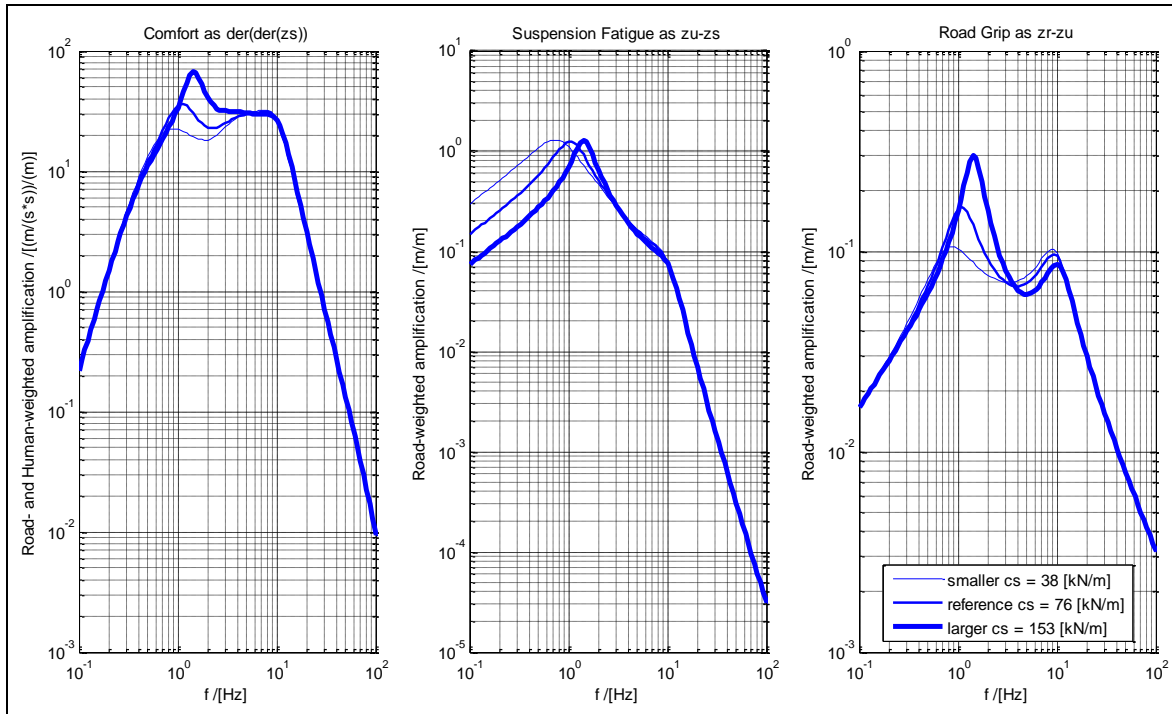


Figure 5-24: Result from varying suspension stiffness, cs

Regarding Figure 5-24 and Figure 5-25 we see that there is a large influence of the acceleration gain at low frequencies with little change at the wheel hop and higher frequencies. The suspension stiffness and damping was seen to have little influence on the ride comfort / road grip response around 10 Hz.

5.9.2 Varying suspension damping

In Figure 5-25, we see that the changes in suspension damping have opposite effects for the bounce and wheel hop frequency responses. High damping is good for reducing bounce, but not so effective for wheel hop.

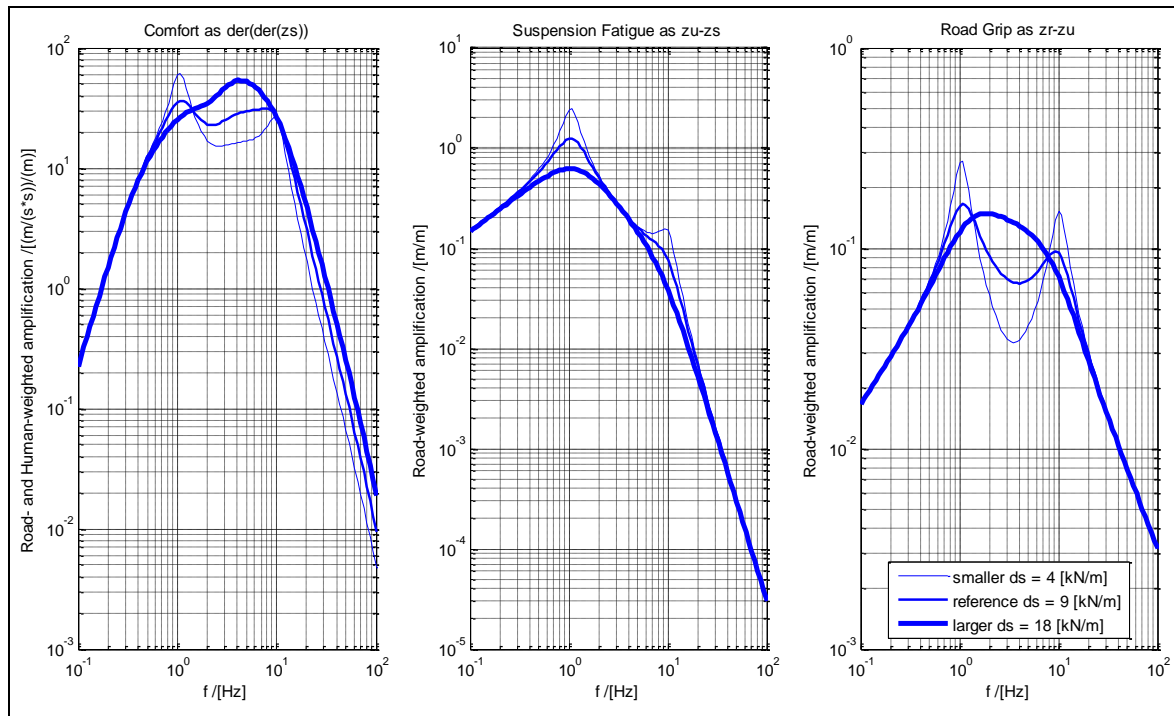


Figure 5-25: Result from varying suspension damping, d_s

5.9.3 Varying unsprung mass

In Figure 5-26, we see that if the response around the wheel hop frequency is to be changed, the unsprung mass is one of the most influential parameters. The unsprung mass is usually in the range of 10% of the sprung mass. Opposite to the suspension parameters, the unsprung mass influences frequencies around the wheel hop frequency with little influence around the bounce frequency.

In Figure 5-26, the case with $m_u = 0$ is added. This is to demonstrate what a model with neglected mass gives and can be nearly compared with the model in Section 5.5.2.

5.9.4 Varying tyre stiffness

In Figure 5-27 a general observation is that low sprung mass natural frequencies are preferred for comfort considerations. Another parameter that has a strong affect near the wheel hop frequency is the tyre stiffness. The strongest response is noticed for the road grip function. (Note that, since c_t is now varying, we have to express road grip as $c_t \cdot (z_r - z_u)$; only $z_r - z_u$ does not give a fair comparison.)

VERTICAL DYNAMICS

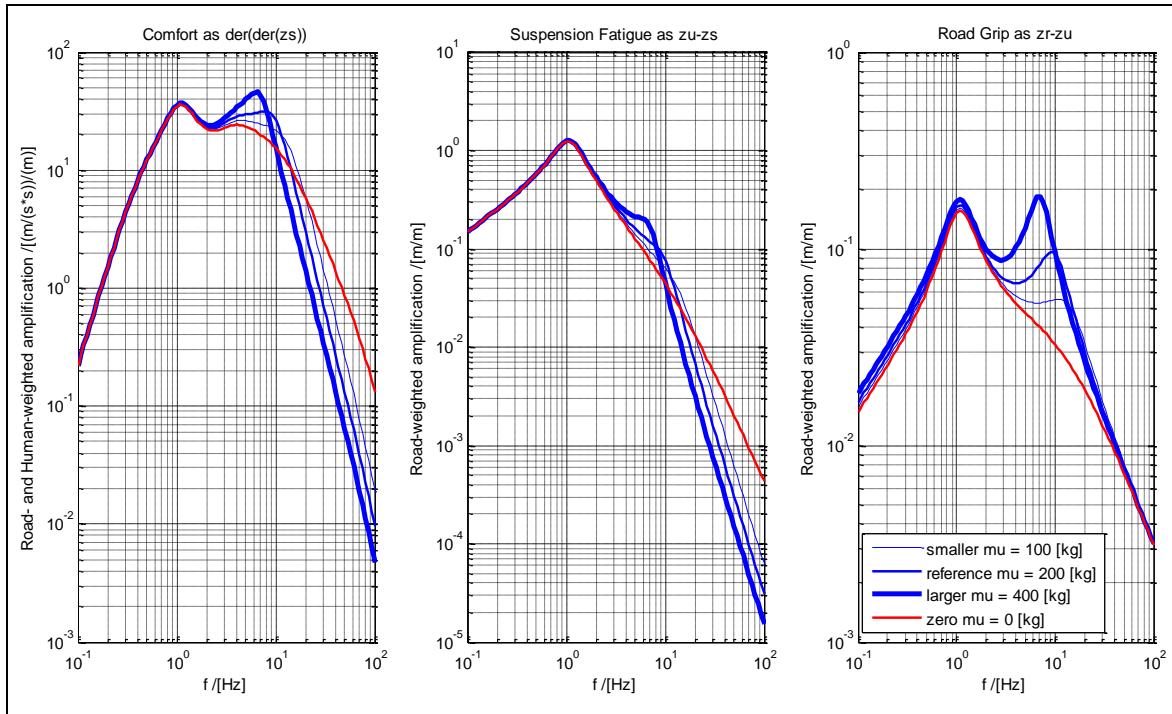


Figure 5-26: Result from varying unsprung mass, μ

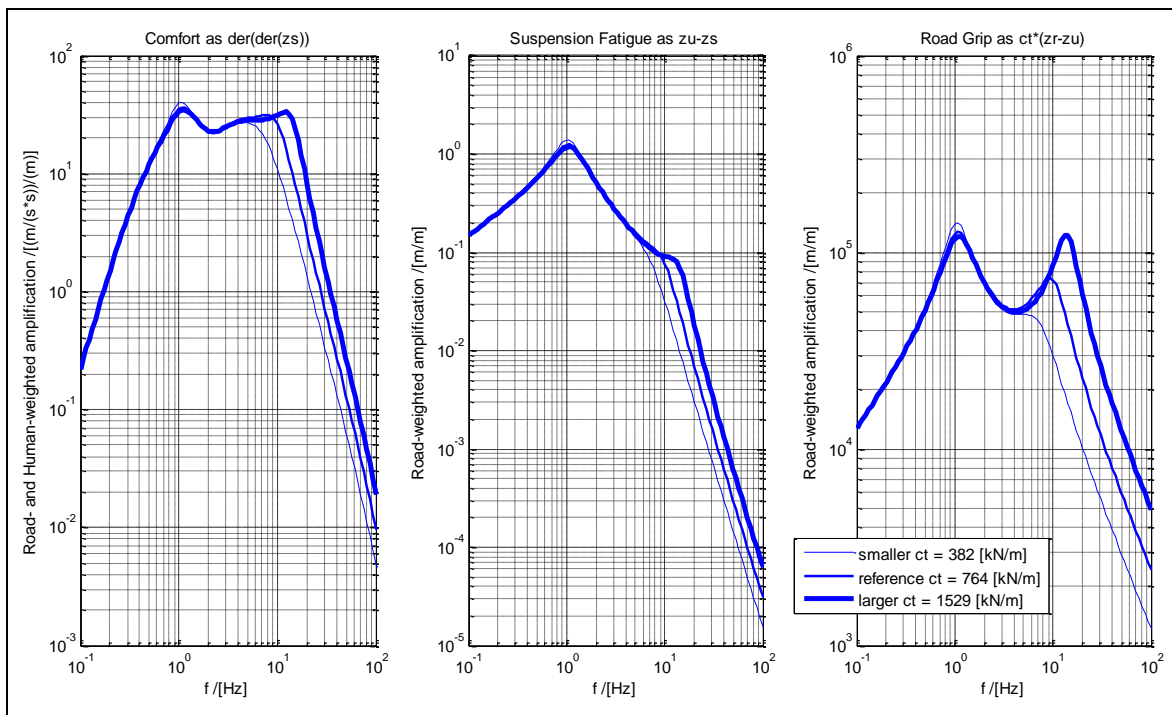


Figure 5-27: Result from varying Tyre Stiffness, ct

5.10 Two dimensional oscillations

The one-dimensional model is useful for analysing the response of one wheel/suspension assembly. Some phenomena do connect other vehicle body motions than the vertical translation, especially pitch and roll. Here, other models are needed, such as Figure 5-28 and Figure 5-32.

5.10.1 Bounce (heave) and pitch

A model like in Figure 5-28 is proposed. We have been studying bounce and pitch before, in Section 3.4.8. Hence compare with corresponding model in Figure 3-32. In Chapter 3, the excitation was longitudinal tyre forces, while the vertical displacement of the road was assumed to be zero. In vertical vehicle dynamics, it is the opposite. The importance of model with linkage geometry (pitch centre or axle pivot points above ground level) is that tyre forces are transferred correctly to the body. That means that the linkage geometry is not so relevant for vertical vehicle dynamics in Chapter 5. So the model can be somewhat simpler.

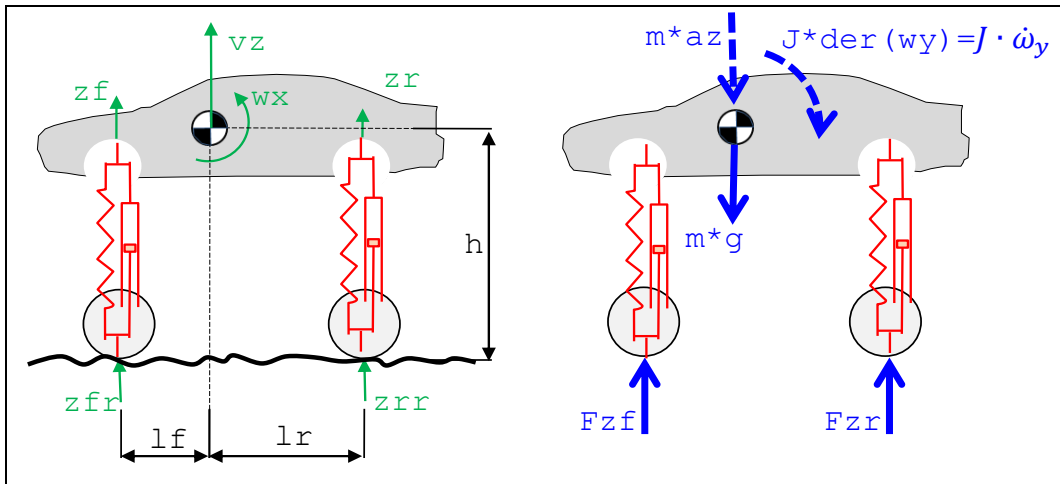


Figure 5-28: Bounce (heave) and pitch model.

No equations will be formulated for this model. The model would typically show two different modes, see Figure 5-29. The bounce eigen-frequency is typically 1-1.5 Hz for a passenger car. The pitch frequency is somewhat higher.

We should reflect on that if we are analysis the same vehicle with the models in Section 5.5 and 5.10.1, we are actually talking about the same bounce mode. But the models will most likely give different numbers of, e.g. Eigen frequency. A total model, with all motion degrees of freedom, would align those values, but the larger a model is the more data it produces which often leads to less easy design decisions.

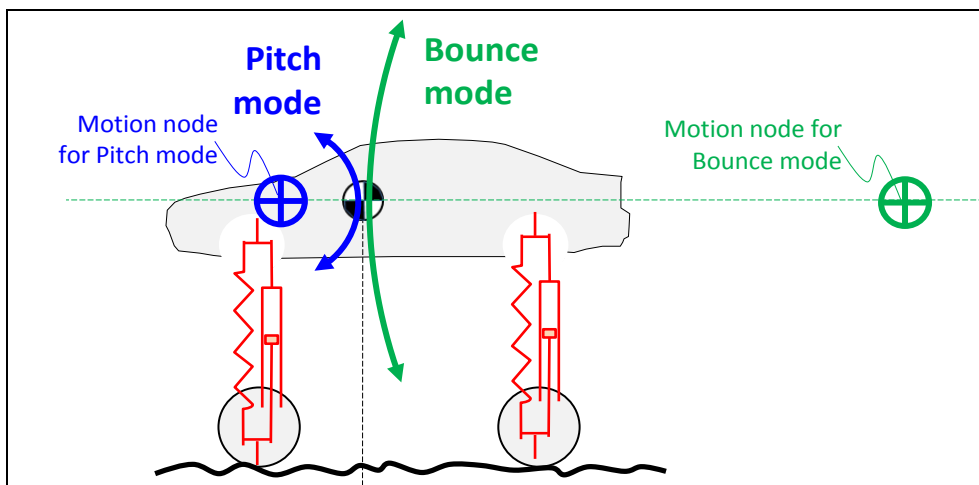


Figure 5-29: Oscillation modes of a Bounce and Pitch model.

5.10.1.1 Wheel base filtering

The response of the vehicle to road irregularities can be envisioned as in Figure 5-30. The vehicle can be excited in a pure bounce motion if the road wavelength is exciting each axle identically. In a similar analysis, the pure pitch motion can be excited with the road displacing the axles out of phase with each other. So, at some frequencies, one mode is not excited at all, which is called “wheel base filtering”.

Figure 5-31 gives an example of spectrum for vertical and pitch accelerations. It compares the accelerations for the correlated and uncorrelated excitation.

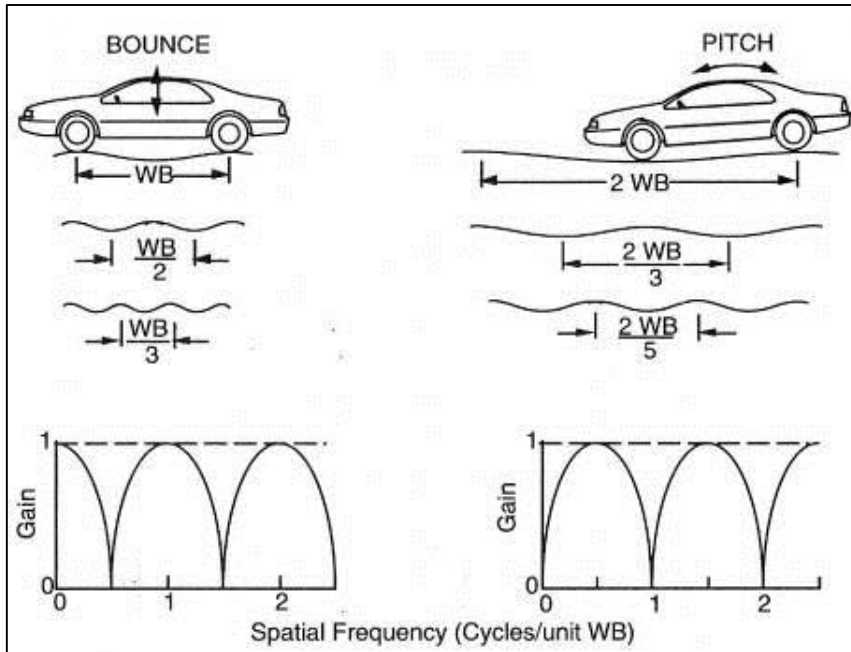


Figure 5-30: Response of the Vehicle to Different Road Wavelengths. (Gillespie, 1992)

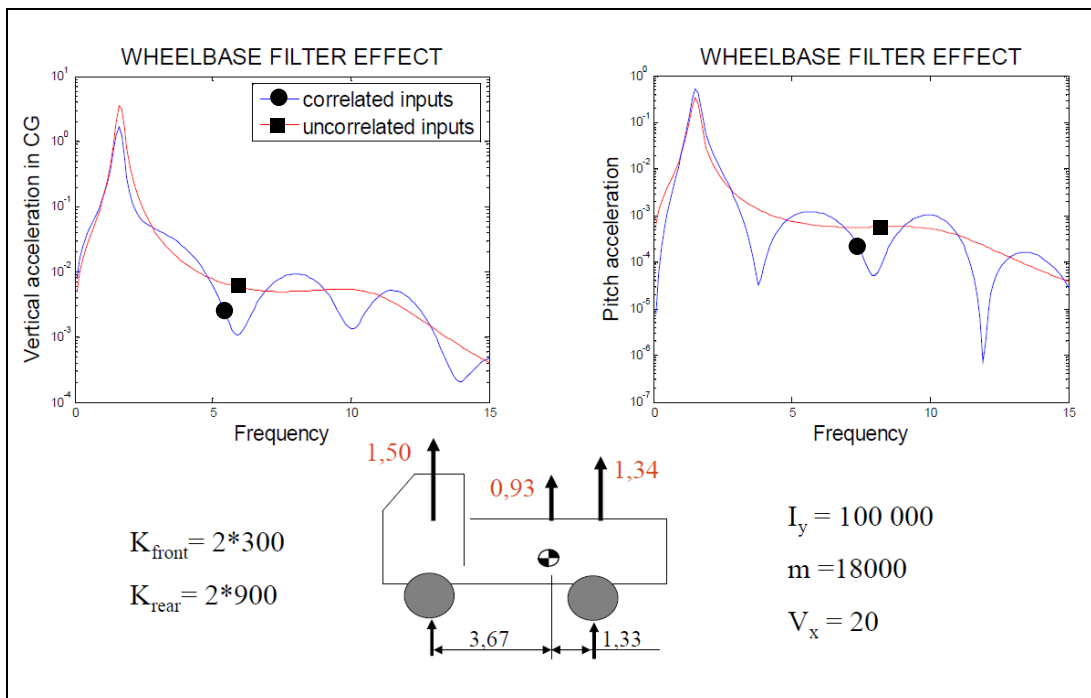


Figure 5-31: Example of wheelbase filter effect

5.10.2 Bounce (heave) and roll

A model like in Figure 5-32 is proposed. We have been studying bounce and pitch before, in Sections 4.3.9 and 4.5.3. Hence compare with corresponding model in Figure 4-63. In Chapter 4, the excitation was lateral tyre/axle forces, while the vertical displacement of the road was assumed to be zero. In vertical vehicle dynamics, it is the opposite. That means that the linkage geometry (roll centre or wheel pivot points) is not so relevant here. So the model can be somewhat simpler.

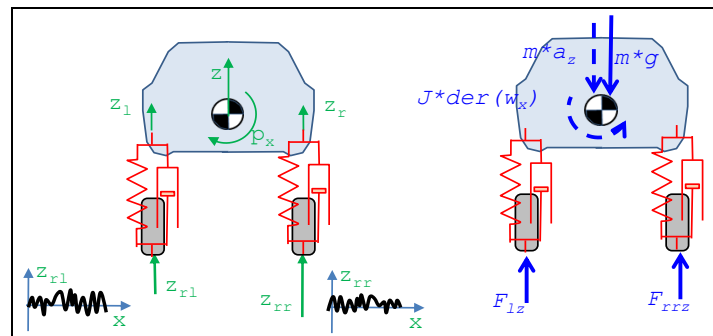


Figure 5-32: Bounce (heave) and roll model.

No equations will be formulated for this model.

The model will typically show two different modes, the bounce and roll. Bounce Eigen frequency is typically 1-1.5 Hz for a passenger car, as mentioned before. The roll frequency is similar or somewhat higher.

5.11 Transient vertical dynamics

The majority of the chapter you read now, considers normal driving which is how the vehicle is driven for during long time periods. Functions are then suitably analysed using theory for stationary oscillations.

Vertical vehicle dynamics also have transient disturbances to consider. Test cases can be one-sided or two sides road bumps or pot-holes. Two sided bump is envisioned in Figure 5-33. It can represent driving over a speed bump or an object/low animal on a road.

Models from earlier in this chapter are all relevant for two-sided bumps/pot-holes, but one might need to consider non-linearities such as bump stops or wheel lift as well as different damping in compression and rebound. For one-sided bumps/potholes, the models from earlier in this chapter are generally not enough.

The evaluation criteria should be shifted somewhat:

- Human **comfort** for transients are often better described as time derivative of acceleration (called “jerk”).
- The material **loads** are more of maximum load type than fatigue life dimensioning, i.e. higher material stress but fewer load cycles during vehicle life time.
- **Road grip** studies over road bumps and pot-holes are challenging. Qualitatively, the tyre models have to include relaxation, because that is the mechanism which reduces road grip when vertical load shifts. To get quantitatively correct tyre models is beyond the goal of the compendium you presently read.
- **Roll-over** can be tripped by large one sided bumps. This kind of roll-overs is unusual and requires complex models.

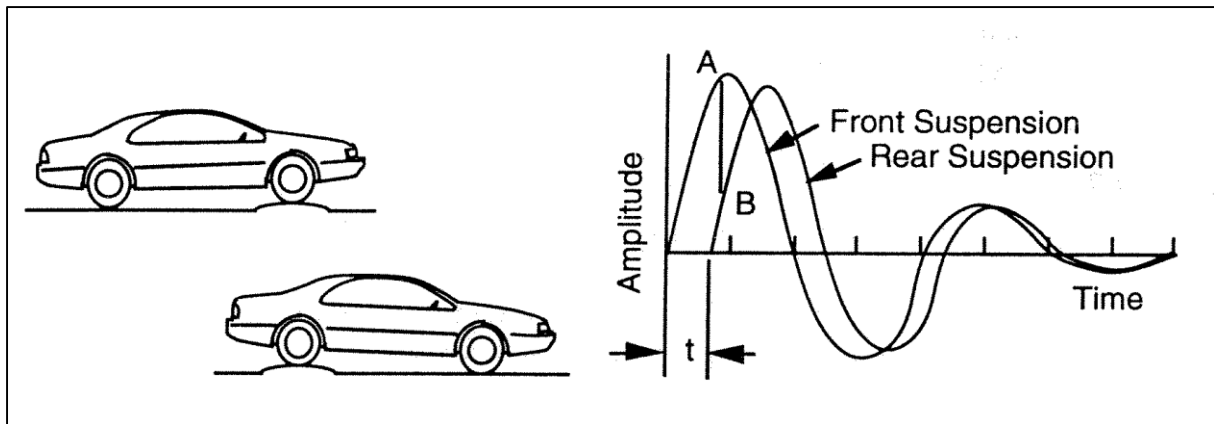


Figure 5-33: Response of Vehicle for Front and Rear Axle Impulses, (Gillespie, 1992)

5.12 Other excitation sources and functions

5.12.1.1 Other excitation sources

The chapter you read now have analysed the influence of excitation from vertical displacement of the road. Examples of other, but often co-operating, excitation sources are:

- Powertrain vibrations, non-uniform rotation in engine. Frequencies will be proportional to engine speed
- Wheel vibrations, e.g. due to non-round wheels or otherwise unbalanced wheels. Frequencies will be proportional to vehicle speed.
- Special machineries mounted on vehicles (e.g. climate systems or concrete mixers)

5.12.1.2 Other functions

The chapter you read now have analysed some functions. Examples of other, but related, functions are:

- An area of functions that encompasses the vertical dynamics is **Noise, Vibration, and Harshness – NVH**. It is similar to ride comfort, but the frequencies are higher, stretching up to sound which is heard by humans.
- **Ground clearance** (static and dynamic) between vehicle body and ground. Typically important for off-road situations.
- **Longitudinal comfort**, due to drive line oscillations and/or vertical road displacements. Especially critical when driver cabin is separately suspended to the body. This is the case for heavy trucks.
- **Disturbances in steering wheel feel**, due to one-sided bumps. Especially critical for rigid steered axles. This is often the design of the front axle in heavy trucks.
- There are of course an infinite amount of combined manoeuvres, in which functions with requirements can be found. Examples can be **bump during strong cornering** (possibly destabilizing vehicle) or **one-sided bump** (exciting both bounce, pitch and roll modes).

Bibliography

- AB Volvo. 2011.** *Global Transport Application*. 2011.
- Bakker, E., Nyborg, L., Pacejka, H.B. 1987.** *Tyre Modelling for use in Vehicle Dynamics Studies*. 1987. SAE Paper No.870495.
- Barnard, R.H. 2010.** *Road Vehicle Aerodynamic Design*. u.o. : Mechaero Publishing, 2010.
- Boerboom, Max. 2012.** *Electric Vehicle Blended Braking maximizing energy recovery while maintaining vehicle stability and maneuverability*. Göteborg, Sweden : Chalmers University of Technology, 2012. Diploma work - Department of Applied Mechanics. ISSN 1652-8557; no 2012:01.
- Clark, S, (ed). 1971.** *Mechanics of Pneumatic Tires, Monograph 122*. u.o. : National Bureau of Standards, USA, 1971.
- Cooper Tire & Rubber Co. 2007.** Passenger radial tire cutaway. Online Art. [Online] Cooper Tire & Rubber Co., den 16 September 2007. <http://deantires.com/us/en/information/info-construction.asp>.
- DIRECTIVE 2002/44/EC. 2002.** *DIRECTIVE 2002/44/EC OF THE EUROPEAN PARLIAMENT AND OF THE COUNCIL*. 2002.
http://europa.eu/legislation_summaries/employment_and_social_policy/health_hygiene_safety_at_work/c11145_en.htm.
- Drenth, Edo F. 1993.** *Brake Stability of Front Wheel Driven Cars at High Speed*. Delft, Netherlands : Delft University of Technology., 1993. Master thesis.
- Encyclopædia Britannica Online. 2007.** belted tire: tire designs." Online Art. Encyclopædia Britannica Online. [Online] 16 September 2007. <http://www.britannica.com/eb/art-7786>.
- Gillespie, T. 1992.** *Fundamentals of Vehicle Dynamics*. s.l. : Society of Automotive Engineers, 1992.
- Grosch, K.A. and Schallamach, A. 1961.** Tyre wear at controlled slip. *Wear*. September–October 1961, Vol. Volume 4, Issue 5, pp. Pages 356–371.
- Happian-Smith, Julian. 2002.** *An Introduction to Modern Vehicle Design*. u.o. : Butterworth-Heinemann, ISBN 0-7506-5044-3, 2002.
- Hirschberg, W., Rill, G. and Weinfurter, H. 2002.** User-Appropriate Tyre-Modelling for Vehicle Dynamics in Standard and Limit Situations. *Vehicle System Dynamics: International Journal of Vehicle Mechanics and Mobility*. 2002, Vol. 38:2, pp. 103-125.
- Hucho, Wolf-Heinric. 1998.** *Aerodynamics of Road Vehicles*. u.o. : SAE International, 1998. R-177.
- ISO 11026.** *ISO 11026 Heavy commercial vehicles and buses - Test method for roll stability - Closing-curve test*. u.o. : ISO.
- ISO 14791.** *ISO 14791 Road vehicles - Heavy commercial vehicle combinations and articulated buses - Lateral stability test methods*. u.o. : ISO.
- ISO 14792.** *ISO14792 Road vehicles - Heavy commercial vehicles and buses - Steady-state circular tests*. u.o. : ISO. ISO14792.
- ISO 14793.** *ISO 14793 Road vehicles – Heavy commercial vehicles and buses – Lateral transient response test methods*. u.o. : ISO.
- ISO 14794. 2011.** *ISO 14794 Heavy commercial vehicles and buses - Braking in a turn - Open-loop test methods*. u.o. : ISO, 2011. ISO 14794.

ISO 3888. *ISO 3888 Passenger Cars -- Test track for severe lane change manoeuvre -- Part 2: Obstacle Avoidance.* u.o. : ISO. ISO 3888.

ISO 4138. *ISO 4138 Passenger cars – Steady-state circular driving behaviour - Open-loop test methods.* u.o. : ISO. ISO 4138.

ISO 7401. *ISO 7401 Lateral transient response test methods - Open-loop test methods.* u.o. : ISO.

ISO 7975. 2006. *Passenger cars – Braking in a turn – Open-loop test method.* u.o. : ISO, 2006. ISO 7975.

ISO 8608. *ISO 8608 Mechanical vibration - Road surface profiles - Reporting of measured data.* u.o. : ISO.

ISO. 2011. *ISO 14794 Heavy commercial vehicles and buses - Braking in a turn - Open-loop test methods.* u.o. : ISO, 2011. ISO 14794.

— **2006.** *Passenger cars – Braking in a turn – Open-loop test method.* u.o. : ISO, 2006. ISO 7975.

ISO2631. *ISO 2631 – Evaluation of Human Exposure to Whole-Body Vibration.* Genève, Switzerland : International Organization for Standardization.

ISO8855. *ISO 8855 – Road vehicle – Vehicle dynamics and road holding ability – Vocabulary.* s.l. : International Organization for Standardization, Genève, Switzerland.

Kati, Maliheh Sadeghi. 2013. *Definitions of Performance Based Characteristics for Long Heavy Vehicle Combinations.* Signals and Systems. u.o. : Chalmers University of Technology, 2013. ISSN 1403-266x.

Kharrazi , Sogol. 2012. *Steering Based Lateral Performance Control of Long Heavy Vehicle Combinations.* Göteborg, Sweden : Chalmers University of Technology, 2012. ISBN/ISSN: 978-91-7385-724-6.

Kiencke, U. and Nielsen, L. 2005 . *Automotive Control Systems.* 2005 .

NHTSA. *Electronic Stability Control Systems.* u.o. : NHTSA. FMVSS 126.

Pacejka, H. 2005. *Tyre and Vehicle Dynamics, 2nd ed.* u.o. : Elsevier, 2005.

Ploechl, Manfred, [red.]. 2013. *Road and Off-Road Vehicle System Dynamics Handbook.* u.o. : CRC Press, 2013. Print ISBN: 978-0-8493-3322-4; eBook ISBN: 978-1-4200-0490-8; <http://www.crcnetbase.com/isbn/9781420004908>.

Rill, Georg. 2006. *FIRST ORDER TIRE DYNAMICS.* Lisbon, Portugal : III European Conference on Computational Mechanics Solids, Structures and Coupled Problems in Engineering, 5–8 June 2006, 2006.

Robert Bosch GmbH. 2004. *Bosch Automotive Handbook 6th Edition.* s.l. : Bentley Publishes, 2004.

Rösth, Markus. 2007. *Hydraulic Power Steering System Design in Road Vehicles: Analysis, Testing and Enhanced Functionality.* Linköping : Linköping University, Department of Management and Engineering, Fluid and Mechatronic Systems, 2007. Dissertation. Dissertations, ISSN 0345-7524; 1068.

SAEJ670. *SAE J670e - Vehicle Dynamics Terminology.* u.o. : Society of Automotive Engineers, Warrendale, PA, USA.

Svendenius, Jacob. 2007. *Tire Modeling and Friction Estimation.* Lund, Sweden : Department of Automatic Control, Lund University, 2007. Dissertation.

UN ECE 111. 2001. *UNIFORM PROVISIONS CONCERNING THE APPROVAL OF TANK VEHICLES OF CATEGORIES N AND O WITH REGARD TO ROLLOVER STABILITY.* u.o. : UNITED NATIONS, 2001. Regulation No. 111.

Wipke, Keith B, Cuddy, Matthew R. och Burch, Steven D. 1999. ADVISOR 2.1: A User-Friendly Advanced Powertrain Simulation Using a Combined Backward/Forward Approach. *IEEE TRANSACTIONS ON VEHICULAR TECHNOLOGY*. 1999, Vol. 48, 6, ss. 1751-1761.

Wong, J.Y. 2001. *Theory of Ground Vehicles (3rd ed.)*. s.l. : John Wiley and Sons, Inc., New York, 2001.

Yang, Derong. 2013. *Vehicle Dynamics Control after Impacts in Multiple-Event Accidents*. Göteborg : Chalmers University of Technology, 2013. PhD thesis. ISBN 978-91-7385-887-8.

Index

(discrete) state diagram	20	Cornering Compliance	66
Ackermann steering angle	156	counter-steer	157
Ackermann steering geometry	133	Critical Speed	163
Active safety	33	data flow diagram	20
actual toe angle	45	Differential-Algebraic system of Equations, DAE	18
actuation	15, 72	direct yaw moment	162
Advanced Driver Assistance Systems (ADAS)	33	effective damping	114, 117
aerodynamic drag	77	effective stiffness	114
agility	197	Electronic Brake Distribution, EBD	125
aligning torque	70	Electronic Control Units, ECUs	34
angular (time) frequency	225	Electronic Stability Control, ESC	218
Anti-lock Braking System, ABS	124	Engine Drag Torque Control, EDC	126
architecture	34	Equivalent wheelbase	147
Attributes	12	flow charts	20
Automatic Emergency Brake, AEB	126	Forward Collision Warning (FCW)	15
axle rate	114	Friction Circle	71
bicycle model	137	Functions	14
Blind Spot Detection (BSD)	15	handling diagram	167
bounce mode	245	Human Filter Function	250
brush model	56	ideal tracking	139
Cambering Vehicle	37	indirect yaw moment	162
castor offset at ground	135	inertial coordinate system	30
Castor offset at wheel center	135	internal combustion engine (ICE)	84
Characteristic Speed	163	kinematic models	139
Closed-loop Manoeuvres	79	Kingpin axis	135
coefficient of rolling resistance	51	Lane Departure Prevention	217
combined (tyre) slip	71	Lane Departure Warning (LDW)	15
Continuous Variable ratio Transmission, CVT	90	Lane Keeping Aid, LKA	217
Controller Area Network, CAN	34	Lateral Collision Avoidance, LCA	220
Cornering	131	lateral slip	64
cornering coefficient	67	Leaning vehicle	37
		longitudinal (tyre) slip	50

low speed steering angle	156	Scrub radius	135
Magic Formula	61	Secondary Ride	248
Mean Square Spectral Density	227	side slip	64
neutral steered vehicle.....	156	single-track model	137
Normal steering axis offset at wheel centre	135	slip angle	64
object vehicle.....	33	spectral density.....	227
Off-tracking.....	216	sprung mass.....	113
one-track model	137	static toe angle	45
Open-loop Manoeuvres	79	Steering axis.....	135
Ordinary Differential Equations, ODE.....	27	steering axis offset at ground	135
oversteered vehicle	156	subject vehicle	33
overturning moment	69	TM-Easy	61
parallell steering geometry	134	Traction Control, TC.....	126
pendulum effect	185	Traction diagram.....	87
physical stiffness.....	114	turning circle.....	142
platform.....	34	turning diameter.....	142
pneumatic trail	70	tyre slip	50
Power Spectral Density, PSD	227	understeer gradient.....	153, 155
Primary Ride	248	understeered vehicle.....	156
Rearward Amplification, RWA.....	215	unsprung mass.....	113
roll axis.....	176	vehicle fixed coordinate systems.....	29
Roll Stability Control, RSC.....	220	Weighted RMS Acceleration.....	250
rolling radius.....	43	wheel base filtering	260
rolling resistance	51	wheel hop mode	245
Roll-stiff Vehicle.....	37	wheel rate.....	114
		yaw damping.....	216